



**Earth Resources**  
A Continuing  
Bibliography  
with Indexes

NASA SP-7041 (56)  
February 1988

National Aeronautics and  
Space Administration

(NASA-SP-7041 (56)) EARTH RESOURCES: A  
CONTINUING BIBLIOGRAPHY WITH INDEXES  
(SUPPLEMENT 56) (NASA) 151 p CSCL 05B

N88-18051

Unclas  
00/43 0126005

es Earth Resources  
s Earth Resources  
Earth Resources E  
th Resources Ear  
Resources Earth  
Resources Earth R  
sources Farth Re

## ACCESSION NUMBER RANGES

Accession numbers cited in this Supplement fall within the following ranges.

STAR (N-10000 Series)    N87-25267 — N87-30248

IAA (A-10000 Series)    A87-42685 — A87-54377

# **EARTH RESOURCES**

## **A CONTINUING BIBLIOGRAPHY WITH INDEXES**

### **Issue 56**

A selection of annotated references to unclassified reports and journal articles that were introduced into the NASA scientific and technical information system and announced between October 1 and December 31 in

- *Scientific and Technical Aerospace Reports (STAR)*
- *International Aerospace Abstracts (IAA).*



Scientific and Technical Information Division 1988  
National Aeronautics and Space Administration  
Washington, DC

This bibliography was prepared by the NASA Scientific and Technical Information Facility operated for the National Aeronautics and Space Administration by RMS Associates.



# INTRODUCTION

The technical literature described in this continuing bibliography may be helpful to researchers in numerous disciplines such as agriculture and forestry, geography and cartography, geology and mining, oceanography and fishing, environmental control, and many others. Until recently it was impossible for anyone to examine more than a minute fraction of the Earth's surface continuously. Now vast areas can be observed synoptically, and changes noted in both the Earth's lands and waters, by sensing instrumentation on orbiting spacecraft or on aircraft.

This literature survey lists 547 reports, articles, and other documents announced between October 1 and December 31, 1987 in *Scientific and Technical Aerospace Reports (STAR)*, and *International Aerospace Abstracts (IAA)*.

The coverage includes documents related to the identification and evaluation by means of sensors in spacecraft and aircraft of vegetation, minerals, and other natural resources, and the techniques and potentialities of surveying and keeping up-to-date inventories of such riches. It encompasses studies of such natural phenomena as earthquakes, volcanoes, ocean currents, and magnetic fields; and such cultural phenomena as cities, transportation networks, and irrigation systems. Descriptions of the components and use of remote sensing and geophysical instrumentation, their subsystems, observational procedures, signature and analyses and interpretive techniques for gathering data are also included. All reports generated under NASA's Earth Resources Survey Program for the time period covered in this bibliography are also included. The bibliography does not contain citations to documents dealing mainly with satellites or satellite equipment used in navigation or communication systems, nor with instrumentation not used aboard aerospace vehicles.

The selected items are grouped in nine categories. These are listed in the Table of Contents with notes regarding the scope of each category. These categories were especially chosen for this publication, and differ from those found in *STAR* and *IAA*.

Each entry consists of a standard bibliographic citation accompanied by an abstract. The citations include the original accession numbers from the respective announcement journals.

Under each of the nine categories, the entries are presented in one of two groups that appear in the following order:

- IAA* entries identified by accession number series A87-10,000 in ascending accession number order;

- STAR* entries identified by accession number series N87-10,000 in ascending accession number order.

After the abstract section, there are seven indexes:

- subject, personal author, corporate source, foreign technology, contract number, report/ accession number, and accession number.

# TABLE OF CONTENTS

<b>Category 01     Agriculture and Forestry</b>	<b>Page</b>
Includes crop forecasts, crop signature analysis, soil identification, disease detection, harvest estimates, range resources, timber inventory, forest fire detection, and wildlife migration patterns.	<b>1</b>
<b>Category 02     Environmental Changes and Cultural Resources</b>	<b>17</b>
Includes land use analysis, urban and metropolitan studies, environmental impact, air and water pollution, geographic information systems, and geographic analysis.	
<b>Category 03     Geodesy and Cartography</b>	<b>21</b>
Includes mapping and topography.	
<b>Category 04     Geology and Mineral Resources</b>	<b>23</b>
Includes mineral deposits, petroleum deposits, spectral properties of rocks, geological exploration, and lithology.	
<b>Category 05     Oceanography and Marine Resources</b>	<b>28</b>
Includes sea-surface temperature, ocean bottom surveying imagery, drift rates, sea ice and icebergs, sea state, fish location.	
<b>Category 06     Hydrology and Water Management</b>	<b>50</b>
Includes snow cover and water runoff in rivers and glaciers, saline intrusion, drainage analysis, geomorphology of river basins, land uses, and estuarine studies.	
<b>Category 07     Data Processing and Distribution Systems</b>	<b>55</b>
Includes film processing, computer technology, satellite and aircraft hardware, and imagery.	
<b>Category 08     Instrumentation and Sensors</b>	<b>68</b>
Includes data acquisition and camera systems and remote sensors.	
<b>Category 09     General</b>	<b>80</b>
Includes economic analysis.	
<b>Subject Index .....</b>	<b>A-1</b>
<b>Personal Author Index .....</b>	<b>B-1</b>
<b>Corporate Source Index .....</b>	<b>C-1</b>
<b>Foreign Technology Index .....</b>	<b>D-1</b>
<b>Contract Number Index .....</b>	<b>E-1</b>
<b>Report Number Index .....</b>	<b>F-1</b>
<b>Accession Number Index .....</b>	<b>G-1</b>

## TYPICAL REPORT CITATION AND ABSTRACT

**NASA SPONSORED**  
↓  
ON MICROFICHE

**ACCESSION NUMBER** → **N87-13900\*** # Pennsylvania State Univ., University Park. Dept. of Meteorology. ← **CORPORATE SOURCE**

**TITLE** → **ANALYSIS OF THE INFLOW AND AIR-SEA INTERACTIONS IN HURRICANE FREDERIC (1979) Final Report**

**AUTHORS** → J. KAPLAN and W. M. FRANK Dec. 1986 119 p ← **PUBLICATION DATE**

**CONTRACT NUMBER** → (Contract NAG5-398)

**REPORT NUMBERS** → (NASA-CR-180014; NAS 1.26:180014) Avail: NTIS HC A06/MF ← **AVAILABILITY SOURCE**

**COSATI CODE** → A01 CSCL 55C

An unusually large amount of aircraft, rawinsonde, satellite, ship and buoy data from hurricane Frederic (1979) are composited over a 40 hr period. These are combined with Frank's (1984) analysis of Frederic's core and Powell's (1982) surface wind analysis to analyze Frederic's three dimensional low level structure between the storm center and a radius of 10 deg. latitude. The analysis is improved significantly by determining the levels at which low level cloud motion winds (CMW's) are in the best agreement with verification wind data and then adjusting the winds to uniform analysis levels. Due to the unusually good low level wind resolution afforded by this data set, it is possible to obtain kinematically derived fields of vorticity, divergence and vertical velocity. These analyses are observed to be internally consistent and should prove useful for future analysis. Analysis of Frederic's surface to 560 m angular momentum budget beyond 2 deg. radius indicates that surface drag coefficients increase slightly with increasing radius and decreasing wind speed. Estimates of storm rainfall obtained by performing a moisture budget between the surface and the top of the inflow layer show that most storm rainfall falls inside about 4 deg. radius and that substantial underestimation of storm rainfall occurs when all low level CMW's are assigned to 560 m. Author

## TYPICAL JOURNAL ARTICLE CITATION AND ABSTRACT

**NASA SPONSORED**  
↓  
ON MICROFICHE

**ACCESSION NUMBER** → **A87-14176\*** # National Aeronautics and Space Administration. Langley Research Center, Hampton, Va.

**TITLE** → **VARIABILITY OF EARTH-EMITTED RADIATION FROM ONE YEAR OF NIMBUS-6 ERB DATA**

**AUTHOR** → T. D. BESS (NASA, Langley Research Center, Hampton, VA) ← **AUTHOR'S AFFILIATION**

**JOURNAL TITLE** → Journal of the Atmospheric Sciences (ISSN 0022-4928), vol. 43, July 15, 1986, p. 1445-1453. refs

Outgoing longwave radiation (OLR) measurements from the Nimbus-6 ERB wide field-of-view instrument are used to study daytime and nighttime radiation variability on a 15 deg regional, zonal, and global scale. An analysis of components of variance is used to determine how much of the total variability is due to between-region and within-region variance. Most of the analysis is on July and January data from one year of Nimbus-6 ERB. Different geographical scales are considered: regions within latitude zones and latitude zones within hemispheres. Results show that much of the variability is spatial, peaks in the tropics and subtropics, and is concentrated in the Northern Hemisphere. Daytime variability is generally larger than nighttime variability for July but not for January. Variance in OLR in the tropics and subtropics is largely a function of cloud variability. Author

# EARTH RESOURCES

*A Continuing Bibliography (Issue 56)*

FEBRUARY 1988

01

## AGRICULTURE AND FORESTRY

Includes crop forecasts, crop signature analysis, soil identification, disease detection, harvest estimates, range resources, timber inventory, forest fire detection, and wildlife migration patterns.

**A87-40944\*** Scranton Univ., Pa.

### REMOTE SENSING OF COASTAL WETLANDS

M. A. HARDISKY (Scranton, University, PA), V. KLEMAS (Delaware, University, Newark), and M. F. GROSS BioScience (ISSN 0006-3568), vol. 36, July-Aug. 1986, p. 453-460. Research supported by the Tinker Foundation and University of Delaware. refs

(Contract NOAA-NA-85AADSG033; NAGW-374; NSF DAR-80-17836)

Various aircraft and satellite sensors for detecting and mapping wetlands properties are examined. The uses of color IR photography to map coastal vegetation, and of Landsat MSS and TM and SPOT data to quantify biomass and productivity for large wetland areas are discussed. For spectral estimation of biomass and productivity, the relation between radiance and biomass needs to be studied; the quantity and orientation of dead biomass and the amount of soil reflectance in comparison with vegetation reflectance in a given target area affect the spectral estimation of biomass. The radiometric evaluation of brackish wetland, and remote sensing in mangroves are described. The collection of images in narrow, contiguous spectral band using imaging spectrometry is considered. i.F.

**A87-42936**

### RADAR OBSERVATIONS OF TERRESTRIAL VEGETATION COVERS IN THE 3-CM RANGE [OPYT RADIOLOKATSIONNYKH NABLIUDENII ZEMNYKH POKROVOV V 3-SANTIMETROVOM DIAPAZONE RADIOVOLN]

A. S. GAVRILENKO, A. I. KALMYKOV, and A. P. PICHUGIN (AN USSR, Institut Radiofiziki i Elektroniki, Kharkov, Ukrainian SSR) Issledovanie Zemli iz Kosmosa (ISSN 0205-9614), Jan.-Feb. 1987, p. 85-92. In Russian. refs

The possibility of the accurate assessment of vegetation covers by means of airborne sidelooking radar were studied using data on the scattering of 3-cm waves by forests and cultivated fields in April and September. The methodological details of the experiment and the treatment of the radar spectra are discussed. Special consideration is given to the correlations between the scattering characteristics of agricultural areas and the conditions of these areas at different phases of cultivation. The conditions optimal for the identification of different vegetation covers are summarized. i.S.

**A87-43263\*#** National Aeronautics and Space Administration. National Space Technology Labs., Bay Saint Louis, Miss.

### POTENTIAL APPLICATION OF MULTIPOLARIZATION SAR FOR PINE-PLANTATION BIOMASS ESTIMATION

SHIH-TSENG WU (NASA, National Space Technology Laboratories, Bay Saint Louis, MS) IEEE Transactions on Geoscience and Remote Sensing (ISSN 0196-2892), vol. GE-25, May 1987, p. 403-409. refs

This paper presents the technique and the potential utility of multipolarization Synthetic Aperture Radar (SAR) data for pine-plantation biomass estimation. Three channels of SAR data, one from the Shuttle Imaging Radar SIR-A and the other two from the aircraft SAR, were acquired over the Baldwin County, Alabama, study area. The SIR-A data were acquired with HH polarization and the aircraft SAR data with VV and VH polarizations. Linear regression techniques are used to estimate the pine-plantation biomass, tree height, and age using 21 test plots. The results indicate that the multipolarization data are highly related to the plantation biomass. The results suggest a potential application of multipolarization SAR for pine-plantation biomass estimation. Author

**A87-45046**

### USE OF RICE RESPONSE CHARACTERISTICS IN CLASSIFICATION USING LANDSAT MSS DIGITAL DATA

K. R. MCCLOY (New South Wales Department of Agriculture, Haymarket, Australia) International Journal of Remote Sensing (ISSN 0143-1161), vol. 8, May 1987, p. 735-740. refs

**A87-45047**

### MONITORING RICE AREAS USING LANDSAT MSS DATA

K. R. MCCLOY, F. R. SMITH, and M. R. ROBINSON (New South Wales Department of Agriculture, Haymarket, Australia) International Journal of Remote Sensing (ISSN 0143-1161), vol. 8, May 1987, p. 741-749.

A specialized system to monitor the rice growing areas of New South Wales has been developed. The monitor has been run for 2 years with accurate and consistent results. The monitor system starts with a land-cover mask. Each image is classified and the result used to update the mask using agronomic criteria. The criteria can, and often will, be changed between the different phenological stages of the crop. The system, with incremental revision of a land-cover mask, is quite different in approach to that adopted in multitemporal image classification as utilized in LACIE and AgRISTARS. Author

**A87-45100**

### COLOR AERIAL PHOTOGRAPHY IN THE PLANT SCIENCES AND RELATED FIELDS; PROCEEDINGS OF THE TENTH BIENNIAL WORKSHOP, UNIVERSITY OF MICHIGAN, ANN ARBOR, MAY 21-24, 1985

CHARLES E. OLSON, JR., ED. (Michigan, University, Ann Arbor) Workshop sponsored by the American Society for Photogrammetry and Remote Sensing. Falls Church, VA, American Society for Photogrammetry and Remote Sensing, 1987, 101 p. No individual items are abstracted in this volume.

Research concerned with the use of color aerial photography in the plant sciences is examined. Papers are presented on the use of digitized color IR photographs to detect, map, and evaluate spruce budworm defoliation; densitometric separation of forest

species on color IR transparencies; the use of low-altitude aerial photography to identify submersed aquatic macrophytes; detailed forest mapping with color IR aerial photographs; and land use cover classification using large-, medium-, and small-scale photographs in South Carolina. Consideration is given to a comparison of small- and medium-scale color IR photographs for forest cover classification; applications of aerial photography to new and unusual vegetation pest problems; aerial observations of citrus groves with color video tape and color 35-mm film; spectral sliced video for the detection of stress and disease; and the evaluation of false color video imagery for assessing ecological characteristics of grasslands. i.F.

**A87-46543\*** National Aeronautics and Space Administration. Ames Research Center, Moffett Field, Calif.

**DETECTING FOREST STRUCTURE AND BIOMASS WITH C-BAND MULTIPOLARIZATION RADAR - PHYSICAL MODEL AND FIELD TESTS**

WALTER E. WESTMAN (NASA, Ames Research Center, Moffett Field, CA) and JACK F. PARIS (California Institute of Technology, Jet Propulsion Laboratory, Pasadena) Remote Sensing of Environment (ISSN 0034-4257), vol. 22, July 1987, p. 249-269. refs

The ability of C-band radar (4.75 GHz) to discriminate features of forest structure, including biomass, is tested using a truck-mounted scatterometer for field tests on a 1.5-3.0 m pygmy forest of cypress (*Cupressus pygmaea*) and pine (*Pinus contorta* ssp. *Bolanderi*) near Mendocino, CA. In all, 31 structural variables of the forest are quantified at seven sites. Also measured was the backscatter from a life-sized physical model of the pygmy forest, composed of nine wooden trees with 'leafy branches' of sponge-wrapped dowels. This model enabled independent testing of the effects of stem, branch, and leafy branch biomass, branch angle, and moisture content on radar backscatter. Field results suggested that surface area of leaves played a greater role in leaf scattering properties than leaf biomass per se. Tree leaf area index was strongly correlated with vertically polarized power backscatter ( $r = 0.94$ ;  $P$  less than 0.01). Field results suggested that the scattering role of leaf water is enhanced as leaf surface area per unit leaf mass increases; i.e., as the moist scattering surfaces become more dispersed. Fog condensate caused a measurable rise in forest backscatter, both from surface and internal rises in water content. Tree branch mass per unit area was highly correlated with cross-polarized backscatter in the field ( $r = 0.93$ ;  $P$  less than 0.01), a result also seen in the physical model. Author

**A87-46744**

**UPDATING MAPS OF CLIMAX VEGETATION COVER WITH LANDSAT MSS DATA IN QUEENSLAND, AUSTRALIA**

GAIL D. KELLY and GREG J. E. HILL (Queensland, University, Brisbane, Australia) Photogrammetric Engineering and Remote Sensing (ISSN 0099-1112), vol. 53, June 1987, p. 633-637. Research supported by the Department of Mapping and Surveying and the University of Queensland. refs

**A87-47582**

**REMOTE-SENSING EVALUATION OF MOISTURE SUPPLY TO CROPS ACCORDING TO THE LEAF-SURFACE THERMAL REGIME [DISTANTSIONNYE OTSENKI VLAGOOBESPECHENNOSTI POSEVOV PO TERMICHESKOMU REZHIMU LISTOVOI POVERKHNOSTI]**

D. R. IOKICH, S. F. KOCHGAROV, V. A. PISARENKO, and B. L. SHINBEROV IN: Remote sensing techniques for the study of hydrological elements. Moscow, Izdatel'stvo VINITI, 1986, p. 84-88. In Russian. refs

A technique for the aerial remote-sensing evaluation of the degree of the moisture supply to irrigated crops according to the leaf-surface temperature is examined. The technique involves: (1) the examination of data on reference regions with a known soil temperature and (2) remote measurements of the leaf-surface absolute temperature, with allowance for correlations with

solar-radiation intensity. The results can be used to regulate the irrigation process. B.J.

**A87-48190**

**MONTE CARLO CALCULATION OF THE DEPENDENCE OF THE SPECTRAL RADIANCE OF VEGETATION COVER ON THE ILLUMINATION CONDITIONS [RASHCHET METODOM MONTE-KARLO ZAVISIMOSTI KOEFFITSIENTA SPEKTRAL'NOI IAR-KOSTI RASTITEL'NOGO POKROVA OT USLOVII OS-VESHCHENIIA]**

IU. K. ROSS and A. L. MARSHAK (AN ESSR, Institut Astrofiziki i Fiziki Atmosfery, Tartu, Estonian SSR) issledovanie Zemli iz Kosmosa (ISSN 0205-9614), Mar.-Apr. 1987, p. 96-105. In Russian. refs

**A87-48360\*** National Aeronautics and Space Administration. Goddard Space Flight Center, Greenbelt, Md.

**THE EFFECT OF SUBPIXEL CLOUDS ON REMOTE SENSING**

YORAM J. KAUFMAN (NASA, Goddard Space Flight Center, Greenbelt, MD; Technion - Israel Institute of Technology, Haifa) International Journal of Remote Sensing (ISSN 0143-1161), vol. 8, June 1987, p. 839-857. refs

A method for estimating the cloud effect on remote sensing is described, and it is applied to cloudiness in several climatological conditions. The algorithm is based on the Haurwitz (1948) measurements of the cloud layer transmission of solar radiation for an overcast sky and on an empirical interpolation of data for broken cloudiness by Pochop et al. (1968). Radiances for a sunny area observed directly from space and through a cloud, and for a shady area observed from space and through a cloud are computed. Methods for detecting the cloud effect from satellite images are discussed. The relation between cloud reflectance and cloud size is studied. It is observed that the subpixel clouds affect the detected radiance and vegetation index, and the effect depends on the cloud types and the dependence of the cloud transmissivity on cloud fraction. Procedures for decreasing or eliminating cloud effect are examined. I.F.

**A87-48668**

**SPECTRAL DISCRIMINATION OF GEOBOTANICAL ANOMALIES USING LANDSAT THEMATIC MAPPER DATA**

C. BANNINGER (Graz, Technische Universitaet und Forschungszentrum, Austria) IN: Earth remote sensing using the Landsat Thematic Mapper and SPOT sensor systems; Proceedings of the Meeting, Innsbruck, Austria, Apr. 15-17, 1986. Bellingham, WA, Society of Photo-Optical Instrumentation Engineers, 1986, p. 118-122. Research supported by the Scientific Research Office of Styria, ESA, and BMFWF.

**A87-48673\*** International Business Machines Corp., Palo Alto, Calif.

**DISCRIMINATION OF NATURAL AND CULTIVATED VEGETATION USING THEMATIC MAPPER SPECTRAL DATA**

STEPHEN D. DEGLORIA (Resource Survey Institute, Benicia, CA), RALPH BERNSTEIN (IBM Palo Alto Scientific Center, CA), and SILVANO DIZENZO IN: Earth remote sensing using the Landsat Thematic Mapper and SPOT sensor systems; Proceedings of the Meeting, Innsbruck, Austria, Apr. 15-17, 1986. Bellingham, WA, Society of Photo-Optical Instrumentation Engineers, 1986, p. 144-150. Research supported by the University of California, Centro di Studi ed Applicazioni in Tecnologie Avanzate, the Resource Survey Institute, and IBM Corp. refs (Contract NAS5-27377)

The availability of high quality spectral data from the current suite of earth observation satellite systems offers significant improvements in the ability to survey and monitor food and fiber production on both a local and global basis. Current research results indicate that Landsat TM data when used in either digital or analog formats achieve higher land-cover classification accuracies than MSS data using either comparable or improved spectral bands and spatial resolution. A review of these quantitative results is presented for both natural and cultivated vegetation. Author

A87-48809#

**LANDSAT-BASED WILDLIFE HABITAT MAPPING - A STUDY OF COLLABORATION BETWEEN ANALYST AND USER**

T. J. ELLIS, D. B. WHITE (Ontario Centre for Remote Sensing, Toronto, Canada), and K. COLEMAN (Ministry of National Resources, Toronto, Canada) IN: Canadian Symposium on Remote Sensing, 10th, Edmonton, Canada, May 5-8, 1986, Proceedings. Volume 1. Ottawa, Canadian Aeronautics and Space Institute, 1987, p. 65-72.

From a pilot project to map land cover over two townships in Eastern Ontario, the Ontario Centre for Remote Sensing demonstrated that the digital analysis of Landsat data provided valuable input into the determination of a general rating of township-sized areas as deer habitat. On the basis of that finding, the Centre undertook an operational project to map land cover types suitable for deer habitat over an area encompassing 17 townships (approximately 427,000 hectares), also in Eastern Ontario. Both summer and winter imagery was used, in order to provide information on both summer and winter range, including coniferous stands and forest clearings as well as early successional forest. This paper describes both the pilot and operational projects, the methodology employed and the problems encountered at various stages of the program. An examination is made of areas of concern on the final maps which resulted from a difference between the perspectives of the analyst and the user. The close cooperation between the analyst and user needed to avoid such problems is discussed. Finally, a brief assessment is made of the value of the habitat maps in the user's deer management program.

Author

A87-48811#

**OPERATIONAL, PROVINCE WIDE CROP AREA ESTIMATION FOR MANITOBA**

H. POKRANT (Department of National Resources, Manitoba Remote Sensing Centre, Winnipeg, Canada) and L. MAGAHAY (Statistics Canada, Remote Sensing Unit, Ottawa) IN: Canadian Symposium on Remote Sensing, 10th, Edmonton, Canada, May 5-8, 1986, Proceedings. Volume 1. Ottawa, Canadian Aeronautics and Space Institute, 1987, p. 83-89.

Based on the success of a pilot project conducted on three crop districts in 1983 to determine crop area estimates from Landsat satellite data, a yearly, operational program has evolved for all of agro Manitoba. The program is jointly conducted by the Manitoba Remote Sensing Centre, Statistics Canada and the Manitoba Department of Agriculture. The primary goal of the program is to generate accurate, real-time area estimates for canola, summerfallow and cereal grains on a crop district basis. Each year approximately 300 National Farm Survey (NFS) ground segments each measuring three square miles are field enumerated. All crop types and sown acreages are plotted on 1:15,840 photo mosaics which are used for supervised classification of eight satellite images. The crop classification for each new tape is registered to a master archival satellite image which contains the boundary lines for all crop districts, enumerative areas and segments. Non-agricultural areas are removed from the classification via theme file masks. Area calculations from the classification are extracted for each segment and compared to the actual field acreages. A linear regression is performed using these two variables to obtain a regression estimator for each of the twelve crop districts.

Author

A87-48813#

**APPLICATION OF IMAGE SEGMENTATION ALGORITHMS TO THE INVENTORY OF CROPS IN CANADA [APPLICATION D'ALGORITHMES DE SEGMENTATION D'IMAGES A L'INVENTAIRE DES CULTURES AU CANADA]**

G. P. BENIE, K. P. B. THOMSON, M. FILLON (Universite Laval, Saint-Foy, Canada), and M. GOLDBERG (Ottawa, University, Canada) IN: Canadian Symposium on Remote Sensing, 10th, Edmonton, Canada, May 5-8, 1986, Proceedings. Volume 1.

Ottawa, Canadian Aeronautics and Space Institute, 1987, p. 101-108. In French. refs

Three segmentation algorithms, Jeansoulin's (1982) multiband fuzzy segmentation, Beaulieu's (1984) hierarchical segmentation of optimization by stages, and Chen's (1984) automatic spatial clustering method, were evaluated for their application to agricultural inventory using remote sensing data. A new algorithm for the correction of segmentation or classification results using contextual parameters is also presented. The algorithms were tested using simulated TM data collected over Melfort, Saskatchewan in 1983. The modified Beaulieu algorithm provided the best results, and the context-based correction technique was found to produce geometrically precise segmented images. R.R.

A87-48815#

**LARGE-SCALE BLACK AND WHITE AND NATURAL COLOR PHOTOGRAPHS FOR THE MEASUREMENT OF TREE CROWN AREAS**

R. J. MORTON (Silvacom, Ltd., Edmonton, Canada), R. J. HALL (Canadian Forestry Service, Edmonton, Canada), R. K. NESBY (Alberta Energy and Natural Resources, Edmonton, Canada), and I. SUTHERLAND (Alberta Remote Sensing Centre, Edmonton, Canada) IN: Canadian Symposium on Remote Sensing, 10th, Edmonton, Canada, May 5-8, 1986, Proceedings. Volume 1. Ottawa, Canadian Aeronautics and Space Institute, 1987, p. 133-140. Research supported by Alberta Environment. refs

Tree crown area, measured on large-scale aerial photographs, is a frequently estimated forest inventory variable. There is uncertainty, however, regarding the accuracy to which crown area can be measured on various scale and film types. In order to address this question, a controlled factorial experiment was conducted to test differences in performance between two film types (color, black and white panchromatic), four scales (1:500, 1:1000, 1:2000, 1:3000) and two experienced interpreters. Crown area targets were specially constructed to resemble typical tree crown outlines. The accuracy response variable used in this analysis was the absolute deviation between the known crown target area and the photoestimate of that target area. Major differences in accuracy were observed between scales, with minor differences evident between films and interpreters. There were no significant differences between the photo estimates and known target areas using any of the 1:500 or 1:1000 photography, however, the minimum differences were encountered on the black and white 1:1000 photographs.

Author

A87-48817#

**INVENTORY OF WETLANDS WITH LANDSAT'S THEMATIC MAPPER**

G. T. KOELN, D. E. WESLEY, J. E. JACOBSON (Ducks Unlimited, Inc., Long Grove, IL), and P. CALDWELL (Ducks Unlimited Canada, Winnipeg, ) IN: Canadian Symposium on Remote Sensing, 10th, Edmonton, Canada, May 5-8, 1986, Proceedings. Volume 1. Ottawa, Canadian Aeronautics and Space Institute, 1987, p. 153-162. refs

The use of Landsat TM data for wetland habitat inventories is studied. The steps for processing the TM data of the Great Plains region are described. Maps at 1:24,000, 1:50,000, 1:100,000, and 1:250,000 were produced, and statistical tables representing each wetland complex were generated and incorporated into six data bases. The data bases developed are: a wetland basin file, quarter section land use file, basin identification/land key cross index file, basin identification/project cross index, map sheet summary file, and management unit analysis file. Total acres, acres of open water, acres of deep marsh, acres of shallow marsh, and shoreline

length for each wetland area in the Great Plain region were estimated. It is noted that the information derived from the TM data is very accurate and can be applied to wetland reconnaissance, selection of wetlands for protection of enhancement, change detection, and strategic planning. I.F.

**A87-48819#****COMPARISON OF SPACE AND AIRBORNE L-HH RADAR IMAGERY IN AN AGRICULTURAL ENVIRONMENT**

C. A. HUTTON (F.G. Bercha and Associates, Ltd., Ottawa, Canada) and R. J. BROWN (Canada Centre for Remote Sensing, Ottawa) IN: Canadian Symposium on Remote Sensing, 10th, Edmonton, Canada, May 5-8, 1986, Proceedings. Volume 1. Ottawa, Canadian Aeronautics and Space Institute, 1987, p. 171-181.

The effects of ground features on radar returns are investigated using SIR-B data obtained on October 7, 1984 and SAR data collected on October 25, 1984 of an area south of Montreal, Canada. The images were separated into three regions based on field/row orientation: parallel, orthogonal, and diagonal to sensor look direction. The visual and digital classification analyses applied to the images are described. It is observed that where the row/field/ditch orientation is orthogonal to the sensor look direction of both the space and airborne radars, the radar returns are affected by the ditch orientation, and where the orientation is parallel or diagonal, ground cover type influences the radar returns. Based on the airborne images, it is detected that corn, pasture, and ploughed fields can be distinguished, but harvested corn can not be accurately defined; and the classification accuracy from the spaceborne images is poor. This radar response data are compared with images from Saskatchewan, and the differences observed are discussed. I.F.

**A87-48820#****COMPARISON OF C-BAND SYNTHETIC APERTURE RADAR (SAR) DATA ACCORDING TO TWO DIFFERENT DEPRESSION ANGLES FOR AGRICULTURAL APPLICATIONS [COMPARAISON DES DONNEES RADAR A OUVERTURE SYNTHETIQUE /ROS/ EN BANDE C, SELON DEUX ANGLES DE DEPRESSION DIFFERENTS POUR LE DOMAINE AGRICOLE]**

S. POIRIER, K. P. B. THOMSON (Universite Laval, Sainte-Foy, Canada), and R. J. BROWN (Canada Centre for Remote Sensing, Ottawa) IN: Canadian Symposium on Remote Sensing, 10th, Edmonton, Canada, May 5-8, 1986, Proceedings. Volume 1. Ottawa, Canadian Aeronautics and Space Institute, 1987, p. 185-196. In French. Research supported by NSERC and Fond pour la Formation de Chercheurs et l'Aide a la Recherche. refs

C-band SAR data collected over Melfort, Saskatchewan at two depression angles during June, July, and August 1983 are analyzed. Of the 246 experimental fields analyzed, only three correspond to a theoretically Gaussian distribution. The 60-deg depression angle data are found to approach more closely a normal frequency distribution than the 37-deg data, and it is suggested that the difference between the two sets of images is due principally to the influence of the vegetation on the backscatter. Results indicate that classification by fields is more appropriate for the present data set than classification by pixels. The analysis permits a detailed comparison of the intraclass and interclass variance for the principal crops in this region. R.R.

**A87-48821#****COMPARISON OF CLASSIFICATION AND ENHANCEMENT TECHNIQUES USING LANDSAT IMAGERY FOR THE NORTHERN CONIFEROUS FOREST**

R. L. MORIN, E. E. DERENYI, R. W. WEIN, and R. YAZDANI (New Brunswick, University, Fredericton, Canada) IN: Canadian Symposium on Remote Sensing, 10th, Edmonton, Canada, May 5-8, 1986, Proceedings. Volume 1. Ottawa, Canadian Aeronautics and Space Institute, 1987, p. 197-206. Research supported by NSERC, and Donner Canadian Foundation. refs

Satellite imagery has been used for many studies in the commercial coniferous forest but few studies have been conducted in the northern coniferous forest to differentiate forest cover and/or

fuel types. Available vegetation inventories have usually been developed from aerial photography; these inventories are time consuming and expensive and therefore cannot be up-dated on a short interval basis. These applications are soon rendered obsolete, especially if fire is a major force such as in Wood Buffalo National Park. To develop the most effective means of up-dating the existing vegetation cover data base two digital classifications were compared. The first of these was based on standard Landsat MSS data while the second use data enhanced using a principal component transformation. Aerial photography and large-scale maps were used as references. Results indicated that satellite imagery provided data at resolutions larger than those of currently compiled vegetation mass. Cover types of jack pine, trembling aspen and alder were readily differentiated as were two bog types (dry palsas bogs and wet bogs). Classifications based on enhanced data were found most efficient in terms of time and effort. Certain classes, such as regenerating enhanced data. Classification accuracies were, in general, increased using enhanced data.

Author

**A87-48822#****USE OF THEMATIC MAPPER SATELLITE IMAGES FOR DISTURBANCE UPDATING OF TIMBER/RANGE MAPS**

J. E. HILTON (British Columbia Ministry of Forests, Williams Lake, Canada) IN: Canadian Symposium on Remote Sensing, 10th, Edmonton, Canada, May 5-8, 1986, Proceedings. Volume 1. Ottawa, Canadian Aeronautics and Space Institute, 1987, p. 209-214.

**A87-48828#****USING AVHRR DATA TO EVALUATE THE GREENNESS VARIABILITY WITHIN MONITORING POLYGONS**

F. C. WESTIN (Fred Westwin, Inc., Brookings, SD), D. O. OHLEN (TGS Technology, Inc., Sioux Falls, SD), and D. G. MOORE (USGS, Washington, DC) IN: Canadian Symposium on Remote Sensing, 10th, Edmonton, Canada, May 5-8, 1986, Proceedings. Volume 1. Ottawa, Canadian Aeronautics and Space Institute, 1987, p. 265-271. refs

A project was initiated at the U.S. Geological Survey's (USGS) Earth Resources Observation Systems (EROS) Data Center (EDC) to evaluate the potential for using satellite data for monitoring production of food and fiber on range and agricultural land. The basic concept of monitoring is to assess changes within a data base of land potential monitoring units where remote sensing spectral data are used to measure the dynamics of the vegetation and relate the spectral measures to production parameters. The objective of this first-year effort was to use Advanced Very High Resolution Radiometer (AVHRR) data within a soil-derived spatial data base to evaluate the spectral variability within various monitoring polygons. The state of Montana was the study area. The soil 1:500,000 scale association map of Montana was used to construct the data base since these map polygons can provide a means for estimating productivity. Four dates of AVHRR data acquired by the NOAA-8 meteorological satellite during the 1983 growing season were converted to greenness indices using the normalized difference (ND) transformation. Three stratification designs, each based on existing soil maps, were used to establish monitoring strata. The standard deviation of ND for each strata within the three designs was computed and compared. Soil association polygons had the least spectral variance of nearly all the factors evaluated. This, plus the fact that soil associations can be linked to soil taxonomic units which are rated for agricultural production, makes them the most desirable monitoring units of those tested. Author

A87-48830#

**EXTENT OF SALINE/WATERLOGGED LANDS WITHIN IRRIGATED ALBERTA. I - INVENTORY AND PRELIMINARY EVALUATION OF EXISTING MAPPING DATA**

D. B. HARKER, F. HECKER, T. G. SOMERFELDT, C. CHANG, L. LEWKI (Alberta Agriculture Research Centre, Lethbridge, Canada) et al. IN: Canadian Symposium on Remote Sensing, 10th, Edmonton, Canada, May 5-8, 1986, Proceedings. Volume 1. Ottawa, Canadian Aeronautics and Space Institute, 1987, p. 281-289. refs

Considerable disagreement exists about the extent, location and severity of saline/waterlogged lands within irrigated Alberta. Mapping projects have differed markedly in their terms of reference and coverage, making inter-study comparisons and final acreage compilations difficult. An inventory of previous studies has been completed. Several recent projects (Saline/Wetland, PFRA, Landsat) alone or in combination provide complete coverage of all irrigation districts. In a pilot project analysis, information from a scattered detailed data base (Level II) has been compared to Saline/Wetland and indirectly to Landsat mapping. Significant differences exist between Saline/Wetland and Level II mapping, and between Saline/Wetland and Landsat mapping in terms of extent and location of saline lands. Further detailed multiple parcel comparisons are required (Phase II) to establish the specific accuracies of individual data bases in order to compile final affected acreage estimates and clarify their potential limitations/applications.

Author

A87-48831#

**SPECTRAL AND TEXTURAL SEGMENTATION OF MULTISPECTRAL AERIAL IMAGES**

F. A. GOUGEON (Canadian Forestry Service, Chalk River, Canada) and A. K. C. WONG IN: Canadian Symposium on Remote Sensing, 10th, Edmonton, Canada, May 5-8, 1986, Proceedings. Volume 1. Ottawa, Canadian Aeronautics and Space Institute, 1987, p. 291-300. refs

In this paper, a spectral signature is represented by reflectance distributions in various spectral bands considered at different artificially created resolution levels. A textural signature is represented by gradient event distributions based on the reflectance gradient magnitudes and directions of the same features. Based on these representations, two distance measures between the probability distributions, an information measure and a region-growing segmentation process, are introduced. The potential of this approach to the segmentation of multispectral aerial images is demonstrated on a Multidetector Electrooptical Imaging Scanner image of forest stands.

Author

A87-48834#

**THE USE OF MULTI-SPECTRAL AND RADAR REMOTE SENSING DATA FOR MONITORING FOREST CLEARCUT AND REGENERATION SITES ON VANCOUVER ISLAND**

D. WERLE (FG Bercha and Associates (Ontario), Ltd., Ottawa, Canada), Y. J. LEE (Pacific Forest Research Centre, Victoria, Canada), and R. J. BROWN (Canada Centre for Remote Sensing, Ottawa, Canada) IN: Canadian Symposium on Remote Sensing, 10th, Edmonton, Canada, May 5-8, 1986, Proceedings. Volume 1. Ottawa, Canadian Aeronautics and Space Institute, 1987, p. 319-329. refs

Landsat multispectral scanner (MSS) and Thematic Mapper (TM) data as well as SEASAT and airborne radar data were collected over the Sooke Lake Watershed Forest on Vancouver Island, British Columbia, between 1975 and 1984 and have been evaluated for use in forest depletion monitoring. Registered multiband MSS and TM data provided the best results in identifying up to five forest regeneration stages. Visual interpretation of digitally processed SEASAT radar imagery provided poor results and indicated that a small incidence angle operational mode is not very suitable for forest cover mapping in mountainous terrain. Only 20 percent of the sites were identified. Larger incidence angles, as obtained from a digitally processed and integrated set of X-HH and L-HH/HV airborne SAR imagery provided improved results.

Almost 80 percent of all clearcut and regeneration sites were identified.

Author

A87-48840#

**STRATIFICATION OF SATELLITE IMAGERY BY UNIFORM PRODUCTIVITY AREAS**

A. R. MACK, D. BAIN (Agriculture Canada, Land Resource Research Institute, Ottawa), and C. PREVOST (Canada Centre for Remote Sensing, Energy, Mines and Resources, Ottawa) IN: Canadian Symposium on Remote Sensing, 10th, Edmonton, Canada, May 5-8, 1986, Proceedings. Volume 1. Ottawa, Canadian Aeronautics and Space Institute, 1987, p. 377-384. refs

A series of agricultural maps of Uniform Productivity Areas (UPAs) were prepared at a scale of one to a million for the prairie provinces of Canada, using multitemporal Landsat transparencies and generalized soil landscape maps. The UPA maps outline areas delineated by permanent soil landscape boundaries (in terms of soil-climatic region, soil texture, and physiographic features) and possessing a uniformity of agricultural productivity and cropping practices discernible by spectral uniformity. Criteria were established to have the UPAs applicable to large-crop estimation but small enough to minimize seasonal weather patterns. The overlay of the UPA maps and the Land Use Maps (based on maps prepared by the Canada Land Inventory) onto satellite imagery quickly locates and 'masks out' unwanted features which may confuse crop classification or the assessment of crop conditions when subtle changes in spectra convey critically important information.

I.S.

A87-48845#

**LANDSAT THEMATIC MAPPER DATA IN WILDLIFE HABITAT MANAGEMENT - REFERENCE TO DEER WINTERING HABITAT**

J. SIROIS and F. BONN (Sherbrooke, Université, Canada) IN: Canadian Symposium on Remote Sensing, 10th, Edmonton, Canada, May 5-8, 1986, Proceedings. Volume 1. Ottawa, Canadian Aeronautics and Space Institute, 1987, p. 423-430. In French. Research supported by the Fond pour la Formation de Chercheurs et l'Aide à la Recherche du Québec. refs

A87-48846#

**EFFECTS OF SURFACE GEOMETRY OF AGRICULTURAL FIELDS ON RADAR AIRBORNE IMAGERY IN X- AND C-BANDS [EFFETS DE LA GEOMETRIE DE SURFACE DES CHAMPS AGRICOLES SUR DES IMAGES RADAR AEROPORTEES EN BANDE-X ET -C]**

G. DUMOULIN, Q. H. J. GWYN, and F. BONN (Sherbrooke, Université, Canada) IN: Canadian Symposium on Remote Sensing, 10th, Edmonton, Canada, May 5-8, 1986, Proceedings. Volume 1. Ottawa, Canadian Aeronautics and Space Institute, 1987, p. 431-448. In French. Research supported by the Fond pour la Formation de Chercheurs et l'Aide à la Recherche du Québec. refs

(Contract NSERC-A-4201)

Variations in the radar signal in X and C bands (SAR-580) have been evaluated as a function of the incidence angle and the azimuth of row crops. Two parallel flight lines with opposing look directions were recorded over the study area. Using linear, multiple and polynomial regression models, it is demonstrated that the azimuth angle and the incidence angle contribute up to 30 to 50 percent of the variance in the radar data. The best models were found using second and third degree regressions.

Author



A87-48850#

**EFFECTIVENESS OF THE THEMATIC MAPPER FOR THE RANGE CONDITION ASSESSMENT IN FESCUE GRASSLANDS OF SOUTHWESTERN ALBERTA**

B. W. ADAMS (Alberta Forestry, Public Lands Div., Lethbridge, Canada), M. BERNIER (Canada Centre for Remote Sensing, Ottawa), J. C. MCLEOD (Alberta Remote Sensing Centre, Edmonton, Canada), and O. DUPONT (Intera Technologies, Ltd., Ottawa, Canada) IN: Canadian Symposium on Remote Sensing, 10th, Edmonton, Canada, May 5-8, 1986, Proceedings. Volume 1. Ottawa, Canadian Aeronautics and Space Institute, 1987, p. 481-483. refs

A87-48855#

**THE DETECTION OF WETLANDS ON RADAR IMAGERY**

J. HARRIS and S. DIGBY-ARGUS (F.G. Bercha and Associates, Ltd., Ottawa, Canada) IN: Canadian Symposium on Remote Sensing, 10th, Edmonton, Canada, May 5-8, 1986, Proceedings. Volume 1. Ottawa, Canadian Aeronautics and Space Institute, 1987, p. 529-543. refs

Anomalous bright areas have been detected on Seasat-SAR satellite imagery over much of central Ontario. These areas comprise specific wetland regions, namely the Low Boreal and Eastern Temperate regions, classified by Environment Canada. Field work has revealed that these areas, which fall into the Marsh-Swamp-Shallow water categories of the Environment Canada wetland classification system, consist of a base of standing water and emergent vegetation in the form of drowned trees and, in some cases, aquatic vegetation (bullrushes, shrubs). It is thought that the very high backscatter results from a dihedral (corner) reflecting surface consisting of the water surface (specular reflector) and the trunks of the dead trees. The signatures of these areas are visually compared to airborne SAE 580 (X + L) imagery to determine if a frequency/polarization/incidence angle relationship exists. Initial analysis indicates that the frequency of the radar is an important parameter in that these areas appear to be more sensitive to longer wavelengths. The detection and mapping of such areas is important as they may offer good habitats for certain types of wildlife (i.e., beavers) and waterfowl, a possible source of peat and a source of bullrushes and cattails that could be used as an economic source of cattle feed. Author

A87-48859#

**AN EVALUATION OF LANDSAT TM AND MSS DATA FOR CROP IDENTIFICATION IN MANITOBA**

R. STEFFENSEN (Geostudio Consultants, Ltd., Ottawa, Canada) and A. R. MACK (Agriculture Canada, Land Resource Research Institute, Ottawa) IN: Canadian Symposium on Remote Sensing, 10th, Edmonton, Canada, May 5-8, 1986, Proceedings. Volume 2. Ottawa, Canadian Aeronautics and Space Institute, 1987, p. 579-589. refs

A87-48863#

**COMPARISON OF LANDSAT THEMATIC MAPPER AND MULTISPECTRAL SCANNER INFORMATION CONTENT FOR AGRICULTURAL APPLICATIONS IN WESTERN CANADA**

H. VICKERS (Intera Technologies, Ltd., Ottawa, Canada) and R. J. BROWN (Canada Centre for Remote Sensing, Ottawa) IN: Canadian Symposium on Remote Sensing, 10th, Edmonton, Canada, May 5-8, 1986, Proceedings. Volume 2. Ottawa, Canadian Aeronautics and Space Institute, 1987, p. 623-636. refs

A87-48864#

**COLOUR INFRARED AERIAL PHOTOGRAPHY FOR HERBICIDE DRIFT DAMAGE ASSESSMENT**

R. V. DAMS (Intera Technologies, Ltd., Calgary, Canada), L. J. D. FITZE (McCartney and Reavil Adjusters (Alberta), Ltd., Edmonton, Canada), and E. M. LANE (Lane, Allen, Barristers and Solicitors, Toronto, Canada) IN: Canadian Symposium on Remote Sensing, 10th, Edmonton, Canada, May 5-8, 1986, Proceedings. Volume 2. Ottawa, Canadian Aeronautics and Space Institute, 1987, p. 639-642. refs

A87-48867#

**LANDSAT THEMATIC MAPPER DATA - A USEFUL TOOL FOR MAPPING AGRICULTURAL AREAS IN QUEBEC**

M. BERNIER (Canada Centre for Remote Sensing, Ottawa), M. THERRIEN (Ministere de l'Agriculture, des Pêcheries et de l'Alimentation du Québec, Canada), and O. DUPONT (Intera Technologies, Ltd., Ottawa, Canada) IN: Canadian Symposium on Remote Sensing, 10th, Edmonton, Canada, May 5-8, 1986, Proceedings. Volume 2. Ottawa, Canadian Aeronautics and Space Institute, 1987, p. 661-671. In French.

A87-48869#

**THEMATIC MAPPER INFORMATION ABOUT CANADIAN FORESTS - EARLY RESULTS FROM ACROSS THE COUNTRY**

F. J. AHERN (Canada Centre for Remote Sensing, Ottawa) and P. D. ARCHIBALD (PAMP Graphics, Ltd., Victoria, Canada) IN: Canadian Symposium on Remote Sensing, 10th, Edmonton, Canada, May 5-8, 1986, Proceedings. Volume 2. Ottawa, Canadian Aeronautics and Space Institute, 1987, p. 683-697. refs

A87-48878#

**TECHNOLOGICAL FEASIBILITY TO MOBILIZATION FOR OPERATIONS - THE NOAA CROP MONITORING CASE**

N. A. PROUT, J. SUTTON, J. WESSELS, M. MANORE (Intera Technologies, Ltd., Ottawa, Canada), and R. J. BROWN (Canada Centre for Remote Sensing, Ottawa, Canada) IN: Canadian Symposium on Remote Sensing, 10th, Edmonton, Canada, May 5-8, 1986, Proceedings. Volume 2. Ottawa, Canadian Aeronautics and Space Institute, 1987, p. 787-796. refs

A great effort has gone into developing applications of remotely sensed data; however, only some of these which are technically feasible, have also become operationally or economically feasible. Years of background research have been carried out in Canada and the United States on the processing and analysis of NOAA AVHRR data leading toward potential operational use in crop monitoring for domestic and international yield forecasting. Government remote sensing and agricultural agencies and industry have all been involved in the development process. Currently a cooperative program sponsored by the Canada Center for Remote Sensing, the Canadian Wheat Board and Agriculture Canada is being conducted by Intera Technologies, Ltd. to move technology from the research stage to design, develop, mobilize, demonstrate, and evaluate the feasibility of processing and application of NOAA image products for an operational context. This paper discusses the need for such a program as an essential part of the technology transfer process. The discussion includes the impact and relevance of operational feasibility in the context of this technology and its routine application in crop monitoring programs. The parameters include products, timeliness, cost and value. Author

A87-48882#

**REMOTE SENSING AS A TOOL FOR ALBERTA AGRICULTURAL WETLANDS DRAINAGE INVENTORY**

M. D. THOMPSON and R. V. DAMS (Intera Technologies, Ltd., Calgary, Canada) IN: Canadian Symposium on Remote Sensing, 10th, Edmonton, Canada, May 5-8, 1986, Proceedings. Volume 2. Ottawa, Canadian Aeronautics and Space Institute, 1987, p. 829-840. Research supported by the Interdepartmental Steering Committee on Drainage. refs

The use of remote sensing data to map wetlands in Alberta, Canada is evaluated. Color, color-IR, and panchromatic photographs and Landsat MSS data were collected for seven areas in Alberta in 1983, and a wetland classification and mapping system was developed. Maps were derived from the data and the areas for each wetland class were calculated from these maps and ground survey data. The accuracies of the data sets are analyzed in terms of wetland type, permanency, vegetation, position in the watershed, type of disturbance to the wetland, and wetland chemistry. It is observed that the accuracy levels for the photography are very good, but varied according to the type of photography, study area, wetland parameters, and general moisture conditions; and the Landsat data are useful in a multistage approach for extrapolating wetlands information from sample sites

mapped with aerial photography, and/or in monitoring wetland changes on a regional scale. I.F.

**A87-48887#**  
**GROUND TARGETS FOR THE RADIOMETRIC CORRECTION OF AVHRR IMAGERY FOR CROP MONITORING**

M. J. MANORE (Intera Technologies, Ltd., Ottawa, Canada) and R. J. BROWN (Canada Centre for Remote Sensing, Ottawa) IN: Canadian Symposium on Remote Sensing, 10th, Edmonton, Canada, May 5-8, 1986, Proceedings. Volume 2. Ottawa, Canadian Aeronautics and Space Institute, 1987, p. 875-884. refs

The use of forest, irrigated areas, and selected agricultural sites as secondary targets for correcting AVHRR imagery for crop monitoring is investigated. The radiometric stability of each of these areas was analyzed over a growing season using AVHRR data of Western Canada acquired from June 17-August 6, 1985. The mean radiance values over all the forest sites is  $64.4 \pm 3.5$  for channel 1 and  $96.6 \pm 3.8$  for channel 2. For the irrigated areas, the mean radiance values were calculated as  $77.0 \pm 6.2$  for channel 1 and  $129.7 \pm 7.5$  for channel 2; and at the agricultural sites, the mean radiance values for channel 1 were estimated as  $79.6 \pm 9.4$  and  $116.0 \pm 11.3$  for channel 2. Forest radiances are examined in terms of forest class. The use of the normalized difference vegetation index to reduce the multiplicative effects of atmosphere and illumination on image interpretability is discussed. I.F.

**A87-48888#**  
**INTERPRETATION OF PRAIRIE LAND COVER TYPES FROM SIR-B DATA**

J. CIHLAR, C. PREVOST (Canada Centre for Remote Sensing, Ottawa), and H. VICKERS (Intera Technologies, Ltd., Ottawa) IN: Canadian Symposium on Remote Sensing, 10th, Edmonton, Canada, May 5-8, 1986, Proceedings. Volume 2. Ottawa, Canadian Aeronautics and Space Institute, 1987, p. 885-894. refs

A study was carried out to evaluate the feasibility of discriminating among various land cover categories on Shuttle Imaging Radar (SIR-B) L-band data. The data were acquired over agricultural areas in south-western Saskatchewan in October 1984. The entire area was quite dry at this time, thus limiting the potential influence of soil moisture on radar backscatter. Land cover types were interpreted with the aid of nearly coincident Thematic Mapper images, as well as airborne and ground data from similar sites. It was found that general land cover categories could be differentiated on the SIR-B images, but contextual information is needed to reduce ambiguities due to overlapping image tones. Similar trends were observed in data collected at two incidence angles, 15 deg and 34 deg. It was concluded that soil surface roughness was a dominant factor influencing radar backscatter. The extrapolation of these findings to other areas or SAR sensors should take into consideration the suboptimum SIR-B performance during the Shuttle mission. Author

**A87-48891#**  
**PRELIMINARY RESULTS FROM MODELLING VEGETATION SPECTRA DERIVED FROM MEIS DATA, ALGONQUIN PARK, ONTARIO**

A. N. RENCZ, G. F. BONHAM-CARTER, C. VAN DER GRIENT (Geological Survey of Canada, Mineral Resources Div., Ottawa), J. R. MILLER, and E. W. HARE (York University, North York, Canada) IN: Canadian Symposium on Remote Sensing, 10th, Edmonton, Canada, May 5-8, 1986, Proceedings. Volume 2. Ottawa, Canadian Aeronautics and Space Institute, 1987, p. 909-917. refs

Analysis of airborne data using the multidetector electrooptical Imaging Scanner (MEIS) and the programmable multispectral imager (PMI) and ground spectroradiometer data was conducted in Allan Lake, Ontario. The objective was to compare results from the data sets and to establish the relationship between spectral features of vegetation and a carbonatite showing. Samples of leaf tissue from sugar maple were collected on a grid to include sampling over the known anomaly, samples in the zone 'upglacier' of the deposit (background), and samples in the dispersal zone.

MEIS was configured with eight narrow-band filters concentrated over the region of the red edge. The PMI was flown in a spatial and spectral mode, covering the 430-800 nm range. Reflectance values in the anomalous regions were identified and statistically compared to background regions. Reflectance values were also related to tissue trace elements and to content of elements in till. Author

**A87-48892#**  
**A TRIAL OF OBLIQUE IMAGERY FROM A LOW COST VIDEO CAMERA SYSTEM FOR DEFOLIATION ASSESSMENT**

D. G. LECKIE and I. D. KNEPPECK (Canadian Forestry Service, Petawawa National Forestry Institute, Chalk River, Canada) IN: Canadian Symposium on Remote Sensing, 10th, Edmonton, Canada, May 5-8, 1986, Proceedings. Volume 2. Ottawa, Canadian Aeronautics and Space Institute, 1987, p. 919-926. refs

Aerial observation surveys from light aircraft or helicopter are the most common technique for mapping and assessing insect and disease damage to the forest. Interpretation of oblique video camera imagery taken in continuous strips during aerial observation may provide a practical method of augmenting aerial observation surveys and increasing their capability for providing more accurate and detailed information when required. An experiment was conducted to determine if imagery from a low cost video system could provide sufficient defoliation information to be useful under operational conditions. Spruce budworm defoliation, both cumulative defoliation and the red discolouration of current defoliation was used to test the interpretation capabilities of video imagery. Imagery was acquired at three altitudes (90, 180 and 490 meters) above ground level with a hand-held consumer quality image tube color video camera system. Interpretation tests were conducted to quantify the ability to assess defoliation level. The capability to assess current defoliation was very poor. Poor results were also obtained for assessing cumulative defoliation; with a best accuracy of 69 percent for the assessment of two defoliation levels (light and heavy). The information content of the imagery was insufficient for practical use in defoliation assessment. Author

**A87-48894#**  
**THE ROLE OF LANDSAT MULTI-SPECTRAL SCANNER DATA IN THE ANALYSIS OF NORTHERN SPOTTED OWL HABITAT**

M. J. HEWITT, III, J. R. EBY, and L. W. BREWER (Washington State Dept. of Game, Olympia) IN: Canadian Symposium on Remote Sensing, 10th, Edmonton, Canada, May 5-8, 1986, Proceedings. Volume 2. Ottawa, Canadian Aeronautics and Space Institute, 1987, p. 937-942. refs

The northern spotted owl requires large forested areas for its home range; a substantial portion of it must be old-growth forest (more than 200 years). In order to assess potential timber harvest impacts on this species, a computational program was combined with observational and radio-telemetry data to determine the home range for 15 owls. Program Home Range was used to develop convex and harmonic mean polygonal plots and vector files representing home range variations. Using the VICAR/IBIS image processing system, the vector files were converted into home range polygon raster images. Preclassified Landsat MSS data were ground checked and used to supply vegetation cover data. The Landsat data and home range polygon images were registered and overlaid in the VICAR system, allowing a map output showing the vegetation distribution over the home range and a tabular summary of vegetation types. Using these procedures it was found that an average of 2309 ha were required per bird with 53 percent in old growth and 3077 ha per mating pair with 68 percent in old growth. Author

**A87-48897#**

**THERMOGRAPHIC REMOTE SENSING OF NORTHERN FOREST AREAS IN REGENERATION AFTER CLEAR OR STRIP CUTTING - PRELIMINARY OBSERVATIONS [LA TELEDTECTION THERMOGRAPHIQUE DES ESPACES FORESTIERS BOREALS EN REGENERATION APRES COUPE A BLANC ET COUPE PAR BANDES - PREMIERES OBSERVATIONS]**

G. H. LEMIEUX, S. PERRON (Laboratoire de Teledetection, Chicoutimi, Canada), M. LABONTE, and F. BONN (Sherbrooke, Universite, Canada) IN: Canadian Symposium on Remote Sensing, 10th, Edmonton, Canada, May 5-8, 1986, Proceedings. Volume 2 . Ottawa, Canadian Aeronautics and Space Institute, 1987, p. 971-979. In French. Research supported by the Ministere de l'Energie et des Ressources du Quebec, CRSNG and Universite de Sherbrooke. refs

**A87-48899#**

**REMOTE SENSING AND THE AGRICULTURAL RESOURCE INVENTORY**

G. JACKSON (Ontario Ministry of Agriculture and Food, Toronto, Canada) IN: Canadian Symposium on Remote Sensing, 10th, Edmonton, Canada, May 5-8, 1986, Proceedings. Volume 2 . Ottawa, Canadian Aeronautics and Space Institute, 1987, p. 985-990.

**A87-48900#**

**TM AND MEIS DATA FOR FUTURE ALBERTA FOREST INVENTORIES**

S. L. ROBERTSON and R. K. NESBY (Alberta Forestry, Resource Evaluation and Planning Div., Edmonton, Canada) IN: Canadian Symposium on Remote Sensing, 10th, Edmonton, Canada, May 5-8, 1986, Proceedings. Volume 2 . Ottawa, Canadian Aeronautics and Space Institute, 1987, p. 997-1000. refs

The extent to which remote sensing technology can be incorporated into a forest inventory is being investigated in a pilot project focused in the Whitecourt area (NTS map sheet 83J). Rapidly advancing remote sensing technologies are being evaluated for operational use in two activity areas - Phase 3 forest inventory enhancements and future inventory development. Investigations in support of Phase 3 enhancements include updates for fires and logging activities, mapping hardwood volumes in areas outside the existing inventory, and mapping of regeneration in burned and cutover areas. Landsat Thematic Mapper (TM) and Multispectral Scanner (MSS) imagery will be evaluated for appreciation in Phase 3 inventory enhancements. Investigations in support of future inventories include the stratification and measurement of forest stand parameters (species, density, height, slope and disturbance) using TM and multispectral electrooptical imaging scanner (MEIS) imagery. These activities will be carried out and assessed during the next two years so that an efficient integrated system could become operational as soon as possible.

Author

**A87-48901#**

**SPECTRAL STUDIES OF DRYLAND AGRICULTURAL SALINITY IN WESTERN AUSTRALIA**

P. T. HICK, W. A. REA, W. G. R. RUSSELL, C. LENDON (CSIRO, Div. of Groundwater Research, PBM Wembley, Australia), and P. H. CROWN (Alberta, University, Edmonton, Canada) IN: Canadian Symposium on Remote Sensing, 10th, Edmonton, Canada, May 5-8, 1986, Proceedings. Volume 2 . Ottawa, Canadian Aeronautics and Space Institute, 1987, p. 1001-1007. Research supported by the Australian National Soil Conservation Program and CSIRO. refs

Remotely sensed data are being evaluated to map and monitor dryland agricultural secondary salinization. An estimated 264,000 ha of formerly productive farm land, in Western Australia, has been debilitated by salinity encroachment resulting from rising saline groundwater as a consequence of the clearing, for agriculture, the perennial native vegetation, and its replacement with annual crops and pastures. Farmer questionnaires, and aerial photographic and Landsat based surveys have been instituted. Questions relating to the most appropriate spectral, spatial and temporal resolutions

have been addressed, and the findings of this study should provide a basis for developing a cost effective logistical planning method for a state wide survey of agricultural salinity. This study evaluates the use of laboratory and field spectrometers and a 15 channel airborne multispectral scanner to determine the optimum resolutions. The spectral regions between 400-2600 nanometers have been analyzed, using multivariate techniques, for optimum discrimination of field study sites throughout a full annual cycle. These data are presented. Author

**A87-50231**

**THE DETECTION OF VEGETATIVE STRESS UTILIZING REMOTELY SENSED DATA AND SOIL SAMPLING**

M. S. AKHAVI (Nova Scotia College of Geographic Sciences, Lawrencetown, Canada) Geocarto International (ISSN 1010-6049), vol. 2, June 1987, p. 57-59.

The soil and salinity conditions in the Granville Marsh of Nova Scotia are analyzed using color IR, normal color, and thermal IR images from aerial photography and soil samples collected at 0.0-0.5 m, 0.5-1.0 m, 1.0-1.5 m, and 1.5-2.0 m. The color, texture, odor, apparent water content, conductivity, and pH of the soil samples are examined. The data reveal that conductivity increases with depth; however, the conductivity measurements are low and do not affect plant growth. It is observed that areas containing excessive moisture have a dark tone on the thermal IR data. It is noted that remote sensing and soil sample data are useful for stress detection. I.F.

**A87-53017\*** National Aeronautics and Space Administration. Ames Research Center, Moffett Field, Calif.

**RELATIONSHIP OF THEMATIC MAPPER SIMULATOR DATA TO LEAF AREA INDEX OF TEMPERATE CONIFEROUS FORESTS**

DAVID L. PETERSON (NASA, Ames Research Center, Moffett Field, CA), MICHAEL A. SPANNER (NASA, Ames Research Center; TGS Technology, Inc., Moffett Field, CA), STEVEN W. RUNNING (Montana, University, Missoula), and KURT B. TEUBER (USDA, Southern Forest Experimental Station, Starkville, MS) Remote Sensing of Environment (ISSN 0034-4257), vol. 22, Aug. 1987, p. 323-341. refs

(Contract NCA2-OR-475-301)

Regional relationships between remote sensing data and the leaf area index (LAI) of coniferous forests were analyzed using data acquired by an Airborne Thematic Mapper. Eighteen coniferous forest stands with a range of projected leaf area index of 0.6-16.1 were sampled from an environmental gradient in moisture and temperature across west-central Oregon. Spectral radiance measurements to account for atmospheric effects were acquired above the canopies from a radiometer mounted on a helicopter. A strong positive relationship was observed between LAI of closed canopy forest stands and the ratio of near-infrared and red spectral bands. A linear regression based on LAI explained 83 percent of the variation in the ratio of the atmospherically corrected bands. A log-linear equation fit the asymptotic characteristic of the relationship better, explaining 91 percent of the variance. The positive relationship is explained by a strong asymptotic inverse relationship between LAI and red radiation and a relatively flat response between LAI and near-infrared radiation.

Author

**A87-53019**

**MONITORING WHEAT CANOPIES WITH A HIGH SPECTRAL RESOLUTION RADIOMETER**

F. BARET, I. CHAMPION, G. GUYOT (Institut National de la Recherche Agronomique, Montfavet, France), and A. PODAIRE (CNES, Toulouse, France) Remote Sensing of Environment (ISSN 0034-4257), vol. 22, Aug. 1987, p. 367-378. Research supported by the Institut National de Recherche Agronomique, CNES, CNRS, and IFREMER. refs

The evolution of reflectance factors of 16 wheat plots was monitored during the growing cycle using a high spectral resolution radiometer. The position of the inflexion point on the red edge of the reflectance curves of plants and the 'red slope' give specific information on the leaf area state and percent ground coverage.

Results also show that a spectral resolution of 5 nm is adequate to observe the described phenomena. Spectra have also been used to simulate and interrelate different broad spectral bands. The possibility of estimating the reflected photosynthetic active radiation, from SPOT visible channels, is discussed. It is concluded that high spectral resolution gives additional information compared with classical measurements performed with broad band radiometers.

Author

#### A87-53023

##### USING AIRBORNE MIDDLE-INFRARED (1.45-2.0 MICRONS) VIDEO IMAGERY FOR DISTINGUISHING PLANT SPECIES AND SOIL CONDITIONS

J. H. EVERITT, D. E. ESCOBAR, M. A. ALANIZ, and M. R. DAVIS (USDA, Agricultural Research Service, Weslaco, TX) Remote Sensing of Environment (ISSN 0034-4257), vol. 22, Aug. 1987, p. 423-428. refs

This paper describes the use of a black-and-white visible/infrared (0.4-2.4 microns) sensitive video camera, filtered to record radiation within the 1.45-2.0 microns middle-infrared water absorption region, for discriminating among plant species and soil conditions. The camera provided adequate quality airborne imagery that distinguished the succulent plant species onions and aloe vera from nonsucculent plant species. Moreover, wet soil, dry crusted soil, and dry fallow soil could be differentiated in middle-infrared video images. Succulent plants, however, could not be distinguished from wet soil or water. These results show that middle-infrared video imagery has potential use for remote sensing research and applications.

Author

A87-53024\* Jet Propulsion Lab., California Inst. of Tech., Pasadena.

##### MEASUREMENT OF LEAF RELATIVE WATER CONTENT BY INFRARED REFLECTANCE

E. RAYMOND HUNT, JR. (California Institute of Technology, Jet Propulsion Laboratory, Pasadena; California, University, Los Angeles), BARRETT N. ROCK (California Institute of Technology, Jet Propulsion Laboratory, Pasadena), and PARK S. NOBEL (California, University, Los Angeles) Remote Sensing of Environment (ISSN 0034-4257), vol. 22, Aug. 1987, p. 429-435. refs

(Contract DE-AC03-76SF-00012; NSF BSR-84-14455)

From basic considerations and Beer's law, a leaf water content index incorporating reflectances of wavelengths from 0.76 to 0.90 microns and from 1.55 to 1.75 microns was developed that relates leaf reflectance to leaf relative water content. For the leaf succulent, *Agave deserti*, the leaf water content index was not significantly different from the relative water content for either individual leaves or an entire plant. Also, the relative water contents of intact plants of *Encelia farinosa* and *Hilaria rigida* in the field were estimated by the leaf water content index; variations in the proportion of living to dead leaf area could cause large errors in the estimate of relative water content. Thus, the leaf water content index may be able to estimate average relative water content of canopies when TM4 and TM5 are measured at a known relative water content and fraction of dead leaf material.

Author

#### A87-53093

##### THE CLOSED ECOLOGY PROJECT - AGRICULTURAL AND LIFE SCIENCES BACKGROUND

CARL N. HODGES (Arizona, University, Tucson) IN: The human quest in space; Proceedings of the Twenty-fourth Goddard Memorial Symposium, Greenbelt, MD, Mar. 20, 21, 1986. San Diego, CA, Univelt, Inc., 1987, p. 255-271. (AAS PAPER 86-120)

Some of the research that was applied to the development of Biosphere II is discussed. Consideration is given to the use of solar energy to desalt sea water; a desert agricultural environment; animal production inside a controlled environment; and the Land Pavilion project depicting the history of agriculture. Attention is also given to temperature control for the agricultural area of the greenhouse, recycling, and maintaining a clean atmosphere. I.F.

#### A87-53109

##### CLUSTER BASED SEGMENTATION OF MULTI-TEMPORAL THEMATIC MAPPER DATA AS PREPARATION OF REGION-BASED AGRICULTURAL LAND-COVER ANALYSIS

JOACHIM HILL and JACQUES MEGIER (CEC, Joint Research Centre, Ispra, Italy) IN: IGARSS '87 - International Geoscience and Remote Sensing Symposium, Ann Arbor, MI, May 18-21, 1987, Digest, Volume 1. New York, Institute of Electrical and Electronics Engineers, Inc., 1987, p. 91-96. refs

A range of classification approaches currently used in remote sensing application programs suffer from drawbacks related to the per-pixel image treatment. Structural approaches to image analysis are commonly considered superior, but will also not allow an adequate identification of agricultural crop types when only single date imagery is used. This stems from the fact that the most significant information for a correct identification of cover types in diverse agricultural systems can only be derived from the combination of images taken during the growing season. The segmentation of a multitemporal data set, which facilitates the combined use of structural image description and optimized radiometric information for a subsequent interpretation in terms of agricultural land-cover categories, is described.

Author

#### A87-53111

##### EFFECT OF RESOLUTION ON TEXTURE APPLICATION TO NEARLY SIMULTANEOUS AVHRR AND MSS IMAGES OF AN AGRICULTURAL REGION

XIANG-NING KONG and DANIEL VIDAL-MADJAR (CNRS and CNET, Centre de Recherches en Physique de l'Environnement Terrestre et Planetaire, Issy-les-Moulineaux, France) IN: IGARSS '87 - International Geoscience and Remote Sensing Symposium, Ann Arbor, MI, May 18-21, 1987, Digest, Volume 1. New York, Institute of Electrical and Electronics Engineers, Inc., 1987, p. 103-109. refs

The effect of degradation on textural features is investigated using a degradation-correlation image registration method. The linear correlation between MSS and AVHRR images is studied. The linear registration of the images was performed, and the MSS images were degraded to AVHRR images using the methods of linear transformation effecting in image space and of linear transformation by spatial filter. The spatial gray level dependence method, gray level run length method, gray level difference method, and power spectral method were applied to MSS images being degraded from 50 m to 8 km. The basic characteristics of the three matrix methods and the power spectral method are described. It is observed that the size of the image is unchanged as the image is degraded and the resolution effect does not influence the image direction property for MSS leaf area index images.

I.F.

#### A87-53120

##### SATELLITE MICROWAVE RADIOMETRY OF FOREST AND SURFACE TYPES

MARTTI HALLIKAINEN and PETRI JOLMA (Helsinki University of Technology, Espoo, Finland) IN: IGARSS '87 - International Geoscience and Remote Sensing Symposium, Ann Arbor, MI, May 18-21, 1987, Digest, Volume 1. New York, Institute of Electrical and Electronics Engineers, Inc., 1987, p. 193-197.

10.7-GHz, 18-GHz, and 37-GHz data from the Nimbus-7 SMMR were used to investigate the microwave response to different surface and forest types. SMMR data for the falls of 1978 through 1981 were compared against a digital surface type map that shows seven different surface types for southern Finland and six for northern Finland. For each land-cover category, the brightness temperature behavior as a function of frequency and polarization was determined.

Author

A87-53122

**AIRBORNE MULTISPECTRAL OBSERVATIONS OVER BURNED AND UNBURNED PRAIRIES**

T. J. SCHMUGGE (USDA, Agricultural Research Service, Beltsville, MD), E. T. KANEMASU, and G. ASRAR (Kansas State University, Manhattan) IN: IGARSS '87 - International Geoscience and Remote Sensing Symposium, Ann Arbor, MI, May 18-21, 1987, Digest. Volume 1. New York, Institute of Electrical and Electronics Engineers, Inc., 1987, p. 203-207. refs

The effects of periodic burning on the native grassland ecosystem of the Konza Prairie Natural Area, Kansas, are investigated. Watersheds were burned at intervals from one year to ten years or not at all, and the multispectral responses of the burned and unburned watersheds, obtained in June 1985 using radiometer and microwave scatterometers, are analyzed. The normalized difference vegetation index (NDVI) using TM band 3 and 4 are calculated. It is observed that for the unburned watershed that contained a mixture of senescent and green vegetation, the NDVI values are less than 0.5; for burned watersheds that contained only green vegetation, the NDVI values are greater than 0.6. In the thermal IR, a 3 to 4 C temperature difference between the two treatments are detected with the burned watershed being cooler. The data also reveal large differences between the microwave emissivities for the two watersheds. I.F.

**A87-53123\*** National Aeronautics and Space Administration. National Space Technology Labs., Bay Saint Louis, Miss.  
**DIGITAL IMAGE CLASSIFICATION APPROACH FOR ESTIMATING FOREST CLEARING AND REGROWTH RATES AND TRENDS**

STEVEN A. SADER (NASA, National Space Technology Laboratories, Bay Saint Louis, MS) IN: IGARSS '87 - International Geoscience and Remote Sensing Symposium, Ann Arbor, MI, May 18-21, 1987, Digest. Volume 1. New York, Institute of Electrical and Electronics Engineers, Inc., 1987, p. 209-213. refs

A technique is presented to monitor vegetation changes for a selected study area in Costa Rica. A normalized difference vegetation index was computed for three dates of Landsat satellite data and a modified parallelepiped classifier was employed to generate a multitemporal greenness image representing all three dates. A second-generation image was created by partitioning the intensity levels at each date into high, medium, and low and thereby reducing the number of classes to 21. A sampling technique was applied to describe forest and other land cover change occurring between time periods based on interpretation of aerial photography that closely matched the dates of satellite acquisition. Comparison of the Landsat-derived classes with the photo-interpreted sample areas can provide a basis for evaluating the satellite monitoring technique and the accuracy of estimating forest clearing and regrowth rates and trends. Author

A87-53124

**USING REMOTELY SENSED LANDSAT MSS DATA TO ASSESS GROUNDWATER INFLUENCE ON THE BARMAH-MILLEWA FOREST**

DAVID P. ALEXANDER (Department of Conservation, Forest and Lands, Victoria, Australia) IN: IGARSS '87 - International Geoscience and Remote Sensing Symposium, Ann Arbor, MI, May 18-21, 1987, Digest. Volume 1. New York, Institute of Electrical and Electronics Engineers, Inc., 1987, p. 215-220. refs

Visual interpretation of satellite imagery is often overlooked in favor of computerized digital image analysis. Using a groundwater exploration technique developed by the United States Geological Survey, Landsat MSS data are visually interpreted to establish the relationship between spectral response and near surface groundwater in the complex riverine Barmah-Millewa Forest ecosystem. This paper briefly describes the techniques applied in the study and the field survey initiated to verify the interpretation. Having established a correlation between groundwater levels and spectral response, potential aquifer recharge areas are identified within the Forest using the USGS method and the results of previous research. Additional field investigations required to confirm the extent and suitability of the identified aquifer recharge areas

are recommended. It is concluded that there is still a place for visual interpretation of satellite imagery in the analysis of complex earth-science related systems. Author

A87-53125

**A MULTI-SOURCE IMAGE SET FOR THE STUDY OF SOIL TEXTURE AND DRAINAGE AS OBSERVED FROM THEMATIC MAPPER DATA IN NORTHERN BELGIUM**

L. VAN CAMP (Copenhagen, University, Denmark) and R. GOOSSENS (Gent, Rijksuniversiteit, Ghent, Belgium) IN: IGARSS '87 - International Geoscience and Remote Sensing Symposium, Ann Arbor, MI, May 18-21, 1987, Digest. Volume 1. New York, Institute of Electrical and Electronics Engineers, Inc., 1987, p. 221-225. refs

The potential of a Landsat-4 Thematic Mapper winter image for the study of two soil properties, namely texture and natural drainage, was investigated for an agricultural area in Northern Belgium. An aligned image set was created containing a land use image, a soil image, and a Landsat-4 Thematic Mapper (TM) image. The results show that the TM channels 3, 4, and 5 reflect soil drainage and texture for both bare soils as well as soils on pasture. TM channel 3 reflects strongly both the soil texture and drainage for bare soils. Author

A87-53126

**CROP INVENTORYING OF SMALL-PARCELLED AREAS USING SPOT- AND TM-DATA IN CONJUNCTION WITH FIELD RADIOMETRIC MEASUREMENTS**

H. EERENS, M. ROEKAERTS, and R. GOMBEER (Leuven, Katholieke Universiteit, Louvain, Belgium) IN: IGARSS '87 - International Geoscience and Remote Sensing Symposium, Ann Arbor, MI, May 18-21, 1987, Digest. Volume 1. New York, Institute of Electrical and Electronics Engineers, Inc., 1987, p. 227-232.

Target discrimination by means of remotely sensed data is essentially based on the varying reflective behavior of different targets. A linear, but channel-, scene- and platform-dependent relation is observed between satellite-recorded relative radiances and ground-measured reflectances. A method is discussed for converting these CCT-digital values into target-reflectances, which form a better base for direct comparison between different channels and scenes, and also facilitate the link to plant health and biomass estimates in agricultural research. A first (and single) trial on a CCT of Landsat-TM showed promising results. Author

A87-53130\* Computer Sciences Corp., Beltsville, Md.

**RETRIEVAL OF SURFACE ROUGHNESS PARAMETERS FROM DUAL-FREQUENCY MEASUREMENTS OF RADAR BACKSCATTERING COEFFICIENTS**

TSAN MO (Computer Sciences Corp., Beltsville, MD), JAMES R. WANG (NASA, Goddard Space Flight Center, Greenbelt, MD), and THOMAS J. SCHMUGGE (USDA, Agricultural Research Service, Beltsville, MD) IN: IGARSS '87 - International Geoscience and Remote Sensing Symposium, Ann Arbor, MI, May 18-21, 1987, Digest. Volume 1. New York, Institute of Electrical and Electronics Engineers, Inc., 1987, p. 269-272. refs

The use of dual-frequency data of backscattering coefficients at a fixed angle to estimate surface roughness parameters is evaluated. Radar backscattering coefficients at 1.5 and 4.25 GHz are calculated using a model based on Kirchhoff approximation of electromagnetic wave scattering from a rough soil surface. Plots of the calculated backscattering coefficients for Kansas soil moisture contents at the C- and L-band frequencies and HH polarization are analyzed. The effects of changes in correlation length on the backscattering coefficients are investigated. The calculated backscattering coefficients are compared with scatterometer data collected at 1.5 and 4.25 GHz, and it is detected that the model and field data correlate well. The data reveal that it is possible to retrieve the surface roughness parameters from measured radar data. I.F.

A87-53136

**A SYSTEM FOR KNOWLEDGE-BASED SEGMENTATION OF REMOTELY-SENSED IMAGES**

A. TAILOR, D. G. CORR (Systems Designers, Ltd., Camberley, England), P. COSOLI (CSATA, Italy), A. CROSS (NERC, Unit for Thematic Information Systems, Reading, England), D. C. HOGG (Sussex, University, Brighton, England) et al. IN: IGARSS '87 - International Geoscience and Remote Sensing Symposium, Ann Arbor, MI, May 18-21, 1987, Digest. Volume 1. New York, Institute of Electrical and Electronics Engineers, Inc., 1987, p. 111-116. refs

The current status of a system for the automatic segmentation of remotely sensed data which uses knowledge of the expected regions to resolve ambiguity is described. Particular attention is given to land use applications such as crop and environmental monitoring. It is concluded that the present knowledge-based segmentation system is potentially better than a traditional segmentation by clustering. The two are comparable in terms of classification accuracy. K.K.

A87-53151\* Joint Research Centre of the European Communities, Ispra (Italy).

**THE CONTRIBUTION OF AVHRR DATA FOR MEASURING AND UNDERSTANDING GLOBAL PROCESSES - LARGE-SCALE DEFORESTATION IN THE AMAZON BASIN**

J. P. MALINGREAU (CEC, Joint Research Centre, Ispra, Italy) and C. J. TUCKER (NASA, Goddard Space Flight Center, Greenbelt, MD) IN: IGARSS '87 - International Geoscience and Remote Sensing Symposium, Ann Arbor, MI, May 18-21, 1987, Digest. Volume 1. New York, Institute of Electrical and Electronics Engineers, Inc., 1987, p. 443-448. NASA-supported research. refs

A87-53153

**THE USE OF OLD-FIELD STANDS OF LOBLOLLY PINE IN STUDIES OF THE POTENTIAL USE OF ACTIVE MICROWAVE REMOTE SENSORS FOR MONITORING FOREST ECOSYSTEMS**

NORMAN C. CHRISTENSEN, JR. (Duke University, Durham, NC) and ERIC S. KASISCHKE (Michigan, Environmental Research Institute, Ann Arbor) IN: IGARSS '87 - International Geoscience and Remote Sensing Symposium, Ann Arbor, MI, May 18-21, 1987, Digest. Volume 1. New York, Institute of Electrical and Electronics Engineers, Inc., 1987, p. 457-466. refs

A87-53155\* National Aeronautics and Space Administration, Goddard Space Flight Center, Greenbelt, Md.

**LANDSCAPE PATTERN AND SUCCESSIONAL DYNAMICS IN THE BOREAL FOREST**

FORREST G. HALL (NASA, Goddard Space Flight Center, Greenbelt, MD), DONALD E. STREBEL, SCOTT J. GOETZ (Science Applications Research, Lanham, MD), KERRY D. WOODS (Bennington College, VT), and DANIEL B. BOTKIN (California, University, Santa Barbara) IN: IGARSS '87 - International Geoscience and Remote Sensing Symposium, Ann Arbor, MI, May 18-21, 1987, Digest. Volume 1. New York, Institute of Electrical and Electronics Engineers, Inc., 1987, p. 473-482. refs

The landscape-scale community dynamics of a boreal forest ecosystem was investigated using the Landsat MSS data record from 1973 to 1983 to generate a stochastic description of the key life cycle states of the community landscape elements. Such descriptions can provide input and verification for models of community development and landscape dynamics. It is anticipated that the proposed approach may be extended to measure, monitor, and model ecosystems at continental and planetary scales.

Author

A87-53201

**POLARIZATION UTILIZATION IN THE MICROWAVE INVERSION OF LEAF ANGLE DISTRIBUTIONS**

N. S. CHAUHAN and R. H. LANG (George Washington University, Washington, DC) IN: IGARSS '87 - International Geoscience and Remote Sensing Symposium, Ann Arbor, MI, May 18-21, 1987, Digest. Volume 2. New York, Institute of Electrical and Electronics Engineers, Inc., 1987, p. 807-812. refs

In the present investigation of the inverse problem for deducing the inclination angle distributions of leafy vegetation on the basis of horizontal, vertical, and cross-polarized backscattered data, the vegetation is modeled by a layer of circular dielectric disks of specified area and inclination angle distribution. The reconstruction of the distribution of leaf inclination angle leads to a linear Fredholm integral equation of the first kind. It is found that inversions with too few data points do not yield a good estimate of the inverted parameters; parameter accuracies can be improved by inverting the combined three-polarization data. O.C.

A87-53202\* Jet Propulsion Lab., California Inst. of Tech., Pasadena.

**RADAR POLARIZATION SIGNATURES OF VEGETATED AREAS**

JAKOB J. VAN ZYL and HOWARD A. ZEBKER (California Institute of Technology, Jet Propulsion Laboratory, Pasadena) IN: IGARSS '87 - International Geoscience and Remote Sensing Symposium, Ann Arbor, MI, May 18-21, 1987, Digest. Volume 2. New York, Institute of Electrical and Electronics Engineers, Inc., 1987, p. 835-837. refs

A simple model is presented for the prediction of the full polarization signature of vegetation resembling tall grass. This polarization signature can be used to detect the presence of vegetation even in those cases in which the vegetation layers are comparatively thin. Also presented is a model which predicts the polarization dependence of different tree types. Attention is given to the cases of pine and deciduous forest model predictions; both types of forest can be expected to contain terms representing the scatter from the ground, as well as forward, double reflections from the ground and limbs/trunk. O.C.

A87-53205

**THE DETECTION OF SOIL DRAINAGE BY USING LANDSAT MSS AND TM (BELGIAN TEST ZONES)**

H. GOOSSENS (Gent, Rijksuniversiteit, Ghent, Belgium) and L. VAN CAMP (CEC, Joint Research Centre, Ispra, Italy) IN: IGARSS '87 - International Geoscience and Remote Sensing Symposium, Ann Arbor, MI, May 18-21, 1987, Digest. Volume 2. New York, Institute of Electrical and Electronics Engineers, Inc., 1987, p. 871-875. refs

A87-53206\* Department of Agriculture, Beltsville, Md.  
**RESULTS FROM THE PUSHBROOM MICROWAVE RADIOMETER FLIGHTS OVER THE KONZA PRAIRIE IN 1985**

T. J. SCHMUGGE (USDA, Hydrology Laboratory, Beltsville, MD), J. R. WANG (NASA, Goddard Space Flight Center, Greenbelt, MD), and R. W. LAWRENCE (NASA, Langley Research Center, Hampton, VA) IN: IGARSS '87 - International Geoscience and Remote Sensing Symposium, Ann Arbor, MI, May 18-21, 1987, Digest. Volume 2. New York, Institute of Electrical and Electronics Engineers, Inc., 1987, p. 877-881.

Four flights were conducted by the NASA C-130 aircraft sensor platform bearing the 'pushbroom' microwave radiometer (PBM) over the Konza Prairie in central Kansas in 1985, in order to monitor soil surface variations. When the brightness temperature maps thus obtained were analyzed, a striking difference was noted between burned and unburned watersheds; the latter had a very high emissivity despite having saturated soils, while the former had low values that increased with the gradual drying of the soils. The lack of sensitivity for the unburned watershed is tentatively attributed to the build-up of a thatch layer by the decaying vegetation, which serves as a good microwave absorber when wet. O.C.



**A87-53211****AUTOMATIC CLASSIFICATION OF FORESTAL AREAS BY REMOTE SENSING TECHNIQUES**

C. CONESE, G. MARACCHI, and F. MASELLI (CNR, Istituto di Analisi Ambientale e Telerilevamento Applicati all' Agricoltura, Florence, Italy) IN: IGARSS '87 - International Geoscience and Remote Sensing Symposium, Ann Arbor, MI, May 18-21, 1987, Digest. Volume 2. New York, Institute of Electrical and Electronics Engineers, Inc., 1987, p. 919-925. CNR-supported research. refs

**A87-53214\*** Jet Propulsion Lab., California Inst. of Tech., Pasadena.

**SCIENCE SYNERGISM STUDY FOR EOS ON EVOLUTION OF DESERT SURFACES**

TOM G. FARR (California Institute of Technology, Jet Propulsion Laboratory, Pasadena)\* IN: IGARSS '87 - International Geoscience and Remote Sensing Symposium, Ann Arbor, MI, May 18-21, 1987, Digest. Volume 2. New York, Institute of Electrical and Electronics Engineers, Inc., 1987, p. 947, 948.

The effectiveness of EOS data as a basis for the study of desert surfaces' evolution is presently evaluated for both long and short term geomorphic evolution. Attention is given to the usefulness of such sensor systems planned for EOS as MODIS for regional vegetation distribution/variability monitoring, HIRIS for visible-near IR observations, TIMS for lithological identification, HMMR and SSMI for soil characteristics, LASA for atmospheric profiles, SAR for surface roughness, ALT for two-dimensional topography, ACR for the calibration of imaging sensors, and ERBE for climate modeling and regional surface albedo variation determinations. O.C.

**A87-53217\*** Commission of the European Communities, Ispra (Italy).

**THE GLOBAL FOREST ECOSYSTEM AS VIEWED BY ERS-1, SIR-C AND EOS**

A. J. SIEBER (CEC, Joint Research Centre, Ispra, Italy), J. B. CIMINO, J. FORD, J. PARIS, B. ROCK (California Institute of Technology, Jet Propulsion Laboratory, Pasadena), R. BROWN, J. CHILAR (Canada Centre for Remote Sensing, Ottawa), C. DOBSON, D. GATES (Michigan, University, Ann Arbor), M. IMHOFF (NASA, Goddard Space Flight Center, Greenbelt, Md) et al. IN: IGARSS '87 - International Geoscience and Remote Sensing Symposium, Ann Arbor, MI, May 18-21, 1987, Digest. Volume 2. New York, Institute of Electrical and Electronics Engineers, Inc., 1987, p. 967-974. refs

A program is presented to perform coordinated global experiments designed to use the unique features of synthetic aperture radar (SAR) sensors such as the ones on ERS-1, SIR-C and EOS to characterize the physical nature of forest stands as input to global ecosystem and climatology models. Details about the objectives, program and expected results are presented.

Author

**A87-53218\*** National Aeronautics and Space Administration, Washington, D.C.

**THE FIRST ISLSCP FIELD EXPERIMENT (FIFE)**

ROBERT E. MURPHY (NASA, Washington, DC), FORREST G. HALL (NASA, Goddard Space Flight Center, Greenbelt, MD), and PIERS J. SELLERS (Maryland, University, College Park) IN: IGARSS '87 - International Geoscience and Remote Sensing Symposium, Ann Arbor, MI, May 18-21, 1987, Digest. Volume 2. New York, Institute of Electrical and Electronics Engineers, Inc., 1987, p. 975-979.

In 1987, the International Satellite Land Surface Climatology Project (ISLSCP) will conduct a major field experiment aimed at the development of superior methods for relating satellite remote sensing to biological and physical parameter and exchange process data obtained during simultaneous ground truth measurements. This, the First ISLSCP Field Experiment, will attempt to arrive at a better understanding of the role of the land surface in the behavior of the global climate system, as required by next-generation global circulation models and general biospheric models. The field

experiment will be conducted in the Konza Prairie of Kansas.

O.C.

**A87-53245\*** Wisconsin Univ., Madison.

**ESTIMATING KEY FOREST ECOSYSTEM PARAMETERS THROUGH REMOTE SENSING**

CAROL A. WESSMAN, JOHN D. ABER (Wisconsin, University, Madison), and DAVID L. PETERSON (NASA, Ames Research Center, Moffett Field, CA) IN: IGARSS '87 - International Geoscience and Remote Sensing Symposium, Ann Arbor, MI, May 18-21, 1987, Digest. Volume 2. New York, Institute of Electrical and Electronics Engineers, Inc., 1987, p. 1189-1193. refs

Forest canopy chemistry and biomass indicators of ecosystem photosynthesis and decomposition processes are presently studied in view of Airborne Imaging Spectrometer data, which generated spectra from averaged 3 x 3 pixel areas for each of 20 sites for mutual qualitative comparison. Vegetation spectra were strongly differentiated from other cover types by an apparent absorption feature at 1500-1700 nm. Preliminary work with stepwise regression suggests that lignin may play a role in canopy reflectance, and that there is potential for remote detection of forest canopy lignin. O.C.

**A87-53246\*** National Aeronautics and Space Administration, Ames Research Center, Moffett Field, Calif.

**VEGETATION MAPPING AND STRESS DETECTION IN THE SANTA MONICA MOUNTAINS, CALIFORNIA**

CURTIS V. PRICE (NASA, Ames Research Center; Technicolor Government Services, Inc., Moffett Field, CA) and WALTER E. WESTMAN (NASA, Ames Research Center, Moffett Field, CA) IN: IGARSS '87 - International Geoscience and Remote Sensing Symposium, Ann Arbor, MI, May 18-21, 1987, Digest. Volume 2. New York, Institute of Electrical and Electronics Engineers, Inc., 1987, p. 1195-1200. refs

(Contract NASA TASK 677-21-35-08; NASA TASK 199-30-72-05)

Thematic Mapper (TM) simulator data have been used to map coastal sage scrub in the mountains near Los Angeles by means of supervised classification. Changes in TM band radiances and band ratios are examined along an east-west gradient in ozone pollution loads. While the changes noted are interpretable in terms of ozone- and temperature-induced premature leaf drop, and consequent exposure of a dry, grassy understory, TM band and band ratio reflectances are influenced by a variety of independent factors which require that pollution stress interpretations be conducted in the context of the greatest possible ecological system comprehension. O.C.

**A87-53247****METHOD DEVELOPMENT AND EXPERIENCES IN APPLICATION OF AIRBORNE MSS DATA FOR FOREST DAMAGE DETECTION**

CHOEN KIM (Freiburg, Universitaet, Freiburg im Breisgau, West Germany) IN: IGARSS '87 - International Geoscience and Remote Sensing Symposium, Ann Arbor, MI, May 18-21, 1987, Digest. Volume 2. New York, Institute of Electrical and Electronics Engineers, Inc., 1987, p. 1213-1216. Research supported by the Projekt Europaeisches Forschungszentrum fuer Massnahmen zur Luftreinhaltung. refs

**A87-53248****THEMATIC MAPPER RESPONSE TO HEAVY METAL RELATED CHANGES IN CANOPY LAI OF A MIXED FOREST**

C. BANNINGER (Graz, Technische Universitaet und Forschungszentrum, Austria) IN: IGARSS '87 - International Geoscience and Remote Sensing Symposium, Ann Arbor, MI, May 18-21, 1987, Digest. Volume 2. New York, Institute of Electrical and Electronics Engineers, Inc., 1987, p. 1217-1221. refs

The spectral response of a coniferous-broadleaved forest subjected to metal stress exhibits only a fair correspondence with soil copper, lead, and zinc content and canopy leaf density. Major changes in canopy reflectance appear to be related to both the toxic effects of metals on canopy structure and the presence of broadleaved trees within a predominately coniferous tree stand.

This likely reduces the usefulness of rather low spatial resolution sensor systems, such as the Landsat Thematic Mapper, for detecting low levels of stress in mixed forest stands. Author

**A87-53249****THE EUROPEAN CAMPAIGN 'AGRISAR '86'**

G. FRAYSSE and A. J. SIEBER (CEC, Joint Research Centre, Ispra, Italy) IN: IGARSS '87 - International Geoscience and Remote Sensing Symposium, Ann Arbor, MI, May 18-21, 1987, Digest. Volume 2. New York, Institute of Electrical and Electronics Engineers, Inc., 1987, p. 1223-1228. refs

The European 'AGRISAR '86' project attempted to analyze the potential of multitemporal SAR images taken from the same test sites during the crop-growing period for crop identification and growth monitoring. SAR data taken from the same sites at different measurement times were then cross-calibrated. The first results of this multitemporal campaign, which include track-mounted scatterometer measurements and ground truth data collections, are presently documented. O.C.

**A87-53250\*** Woods Hole Oceanographic Institution, Mass.  
**ANALYSIS OF FOREST AND FOREST CLEARINGS IN AMAZONIA WITH LANDSAT AND SHUTTLE IMAGING RADAR-A DATA**

THOMAS A. STONE and GEORGE M. WOODWELL (Woods Hole Oceanographic Institution, MA) IN: IGARSS '87 - International Geoscience and Remote Sensing Symposium, Ann Arbor, MI, May 18-21, 1987, Digest. Volume 2. New York, Institute of Electrical and Electronics Engineers, Inc., 1987, p. 1229-1235. NASA-supported research. refs

Landsat and Shuttle Imaging Radar-A L band (23.5 cm wavelength) data from 1981 were used to analyze areas of intact tropical forest and areas recently cleared from forest for agriculture and pasture in Mato Grosso, Brazil. Portions of SIR-A Data Takes #24C and #31 film were digitized using a microdensitometer. Landsat MSS data of July 1981 were also examined. The digital values from SIR-A DT 31 were compared with the normalized difference vegetation index values (NDVI) from the Landsat data for the same sites. Contrary to expectations some cleared areas had brighter radar responses than surrounding forest. The explanation seems to be that a recently cleared forest (cut and burned during the dry season) is texturally very rough as the exposed standing and fallen boles and woody litter may function as effective corner or dihedral reflectors. Combining radar data with NDVI data may help to assess the relative age of forest clearings and determine differences in both woody and green leaf biomass of primary and secondary tropical forests. Author

**A87-53252**

**EVALUATION OF MOMS (MODULAR OPTOELECTRONIC MULTISPECTRAL SCANNER) DATA FOR LAND USE/LAND COVER STUDIES - TEST SITE: PIRACICABA REGION, SAO PAULO STATE, BRAZIL**

HERMANN J. H. KUX (Instituto de Pesquisas Espaciais, Sao Jose dos Campos, Brazil), PEDRO LUIZ DONZELI (Instituto Agronomico, Campinas, Brazil), and MARTIN HAUCK (DFVLR, Cologne, West Germany) IN: IGARSS '87 - International Geoscience and Remote Sensing Symposium, Ann Arbor, MI, May 18-21, 1987, Digest. Volume 2. New York, Institute of Electrical and Electronics Engineers, Inc., 1987, p. 1251-1253. refs

**A87-53269****AIRCRAFT MICROWAVE RADIOMETRY OF LAND**

R. BONSIGNORI (Officine Galileo S.p.A., Florence, Italy), L. CHIARANTINI (Segnalamento Marittimo ed Aereo S.p.A., Florence, Italy), S. PALOSCIA, P. PAMPALONI (CNR, Istituto di Ricerca sulle onde Elettromagnetiche, Florence, Italy), P. FERRAZZOLI (Roma II, Università, Italy) et al. IN: IGARSS '87 - International Geoscience and Remote Sensing Symposium, Ann Arbor, MI, May 18-21, 1987, Digest. Volume 2. New York, Institute of Electrical and Electronics Engineers, Inc., 1987, p. 1429-1433. CNR-supported research. refs

A sensor package composed of two radiometers at 10 and 36 GHz, a thermal IR sensor, and a color TV camera has been arranged to fly on a small aircraft. The system, designed to be chiefly employed for the study of vegetation emission, was tested in summer 1986 during the 'Agrisar Campaign' on the Italian test site 'Oltrepo Pavese'. Since the 10-GHz antenna angular resolution was somewhat coarse with respect to the scale of emissivity variations, an enhancement of spatial resolution has been achieved by using a retrieval algorithm based on singular function analysis. Crop emissivities, retrieved by measurements on agricultural fields, have been compared with ground-truth data and are reported in this paper. Author

**A87-53275**

**A STATISTICAL AND GEOMETRICAL EDGE DETECTOR FOR SAR IMAGE SEGMENTATION**

R. TOUZI, A. LOPES, and P. BOUSQUET (Centre d'Etude Spatiale des Rayonnements, Toulouse, France) IN: IGARSS '87 - International Geoscience and Remote Sensing Symposium, Ann Arbor, MI, May 18-21, 1987, Digest. Volume 2. New York, Institute of Electrical and Electronics Engineers, Inc., 1987, p. 1469-1474.

**A87-53276\*** Hunter Coll., New York.

**MODELING GAP PROBABILITY IN DISCONTINUOUS VEGETATION CANOPIES**

XIAOWEN LI and ALAN H. STRAHLER (Hunter College, New York) IN: IGARSS '87 - International Geoscience and Remote Sensing Symposium, Ann Arbor, MI, May 18-21, 1987, Digest. Volume 2. New York, Institute of Electrical and Electronics Engineers, Inc., 1987, p. 1483-1491. CNR-supported research. refs

(Contract NAGW-735)

In the present model for the gap probability of a discontinuous vegetation canopy, the assumption of a negative exponential attenuation within individual plant canopies will yield a problem involving the distribution distances within canopies through which a ray will pass. If, however, the canopies intersect and/or overlap, so that foliage density remains constant within the overlap area, the problem can be approached with two types of approximations. Attention is presently given to the case of a comparison of modeled gap probabilities with those observed for a stand of Maryland pine, which shows good agreement for zenith angles of illumination up to about 45 deg. O.C.

**A87-53277\*** National Aeronautics and Space Administration, Lyndon B. Johnson Space Center, Houston, Tex.

**ESTIMATION OF X-BAND SCATTERING PROPERTIES OF TREE COMPONENTS**

D. E. PITTS, G. D. BADHWAR (NASA, Johnson Space Center, Houston, TX), E. REYNA (Lockheed Engineering and Management Services Co., Inc., Houston, TX), R. ZOUGHBI, L. K. WU (University of Kansas Center for Research, Lawrence) et al. IN: IGARSS '87 - International Geoscience and Remote Sensing Symposium, Ann Arbor, MI, May 18-21, 1987, Digest. Volume 2. New York, Institute of Electrical and Electronics Engineers, Inc., 1987, p. 1493-1498. refs

An X-band FM-CW very fine range resolution scatterometer was used to acquire backscattering data for a number of tree species. Using a model to describe the scattering source function and an experimental procedure for selected removal of plant parts allows the estimation of the volume backscatter coefficient and the volume extinction coefficient. It is found that: (1) leaves are



strong attenuators as well as scatterers; (2) the albedo at a given angle of incidence is nearly independent of the tree type; (3) the tree limbs are good attenuators but rather poor scatterers; and (4) the albedo changes as a function of the angle of incidence and for deciduous trees is also a function of the season. Author

**A87-53278\*** National Aeronautics and Space Administration. National Space Technology Labs., Bay Saint Louis, Miss.  
**INTEGRATION OF TOPOGRAPHIC DATA WITH SYNTHETIC APERTURE RADAR DATA FOR DETERMINING FOREST PROPERTIES IN MOUNTAINOUS TERRAIN**

SHIH-TSENG WU (NASA, National Space Technology Laboratories, Bay Saint Louis, MS) IN: IGARSS '87 - International Geoscience and Remote Sensing Symposium, Ann Arbor, MI, May 18-21, 1987, Digest. Volume 2. New York, Institute of Electrical and Electronics Engineers, Inc., 1987, p. 1495-1503. refs

The elevation gradients affecting tropical forest stand characteristics are presently studied in light of multipolarization airborne SAR data. A 'rubber sheeting' computer code was used to georeference the SAR data sets to the digital elevation data. The TOPO code from NASA's NSTL generated the terrain slope and aspect angle data from the terrain elevation data set; computed local incidence angles were used to delete those data areas that were shadowed, and to produce local incidence angle data that were not shadowed. The results obtained demonstrate that the SAR data are related to the elevation gradient. O.C.

**A87-53741**  
**SAMPLING SEMIARID VEGETATION WITH LARGE-SCALE AERIAL PHOTOGRAPHY**

PETER L. WARREN and CHRISTOPHER DUNFORD (Arizona, University, Tucson) ITC Journal (ISSN 0303-2434), no. 4, 1986, p. 273-279. refs  
 (Contract USDA-59-2041-1-2-086-0)

The effects of photograph scale, measurement method, and camera format on the accuracy of plant cover measurements are investigated. Fifteen semiarid vegetation sites in southeastern Arizona were photographed using 70 and 35 mm cameras from 122, 212, and 305 m above ground level. Cover measurements were obtained with the line-intercept and point methods, and the influence of photography scale and format is evaluated for scales ranging from 1:2000 to 1:3000. It is detected that the measurements of total vegetation cover and tree cover correlate well with ground measurements for all the scales; measurements of shrub and grass cover differ from ground data at scales less than or equal to 1:1000; the point method is less accurate than the line-intercept method, but has better general use for photography measurements; and up to a scale of 1:1500, the 35 and 70 mm film formats are interchangeable. I.F.

**A87-53996**  
**SMOOTHING VEGETATION INDEX PROFILES - AN ALTERNATIVE METHOD FOR REDUCING RADIOMETRIC DISTURBANCE IN NOAA/AVHRR DATA**

ALBERT VAN DIJK, WAYNE L. DECKER (Missouri-Columbia, University, Columbia), SUSAN L. CALLIS, and CLARENCE M. SAKAMOTO (NOAA, National Environmental Satellite, Data, and Information Service, Columbia, MO) Photogrammetric Engineering and Remote Sensing (ISSN 0099-1112), vol. 53, Aug. 1987, p. 1059-1067. Research supported by the Agency for International Development and NOAA. refs

The NOAA satellites are becoming an increasingly important source of information for crop condition assessments. However, the data collected by sensors onboard the NOAA-N satellites are seriously disturbed radiometrically due to complex radiative interactions between atmosphere, sensor view angle, solar zenith angle, and vegetation canopy structure. Correction procedures for radiometric disturbances are still being developed and, as of yet, have not been quantified. Therefore, a method has been devised to reduce the effects of radiometric disturbances on remotely-sensed data without quantitative knowledge of the variable interactions that cause them. The method involves deriving composite weekly vegetation index values from the daily values

for the area to be assessed followed by a 'smoothing' of the weekly values over a selected period of time. Author

**A87-53997**  
**COMPARISON OF NOAA AVHRR DATA TO METEOROLOGIC DROUGHT INDICES**

STEPHEN J. WALSH (North Carolina, University, Chapel Hill) Photogrammetric Engineering and Remote Sensing (ISSN 0099-1112), vol. 53, Aug. 1987, p. 1069-1074. refs

Evaluation of the AVHRR sensor on the NOAA-6 satellite shows that the spatial and temporal variations in drought conditions as defined by the crop moisture index (CMI), drought severity index (DSI), and the hydrologic deficit (HD) can be estimated by a combination of remote sensing vegetation indices. Multiple regression analysis explains 80, 57, and 44 percent of the variation in the CMI, DSI, and the HD, respectively, when regressed against AVHRR spectral channels and derived vegetation indices for four study periods extending from June through August, 1980. Regression R-squared values for a single selected study period range from 62 to 90 percent, 68 to 91 percent, and 51 to 88 percent of the variation in each of the nine Oklahoma climatic divisions for the CMI, DSI, and the HD, respectively. Author

**A87-53998\*** National Aeronautics and Space Administration. Goddard Space Flight Center, Greenbelt, Md.

**WHITETAIL DEER FOOD AVAILABILITY MAPS FROM THEMATIC MAPPER DATA**

JAMES P. ORMSBY (NASA, Goddard Space Flight Center, Greenbelt, MD) and ROSS S. LUNETTA (U.S. Army, Corps of Engineers, Detroit, MI) Photogrammetric Engineering and Remote Sensing (ISSN 0099-1112), vol. 53, Aug. 1987, p. 1081-1085. refs

**A87-54089**  
**HOW USEFUL IS LANDSAT MONITORING?**

B. CURREY (Winrock International Institute for Agricultural Development, Dhaka, Bangladesh), A. S. FRASER, and K. L. BARDSLEY (Flinders University, Bedford Park, Australia) Nature (ISSN 0028-0836), vol. 328, Aug. 13, 1987, p. 587-589. refs

The effect of cloudiness on the availability of useful Landsat images for critical dates in the cropping calendars at 58 rice nurseries in monsoon Asia is discussed. It is concluded that the images produced from the satellite are of doubtful value for monitoring rice production in southern Asia. After 1990, the benefits of radar for penetrating cloud cover may provide useful imagery from the Canadian Radar Satellite. C.D.

**N87-23136#** Joint Publications Research Service, Arlington, Va.  
**INVESTIGATION OF CAUSES OF HYDROGEN SULFIDE FORMATION IN RECLAIMED WATER**

I. G. POPOV, V. V. VLODAVETS, S. V. CHIZHOV, YU. YE. SINYAK, M. I. SHIKINA, L. A. VINOGRADOVA, and N. B. KOLESINA In its USSR Report: Space Biology and Aerospace Medicine, Volume 20, No. 5, September - October 1986 p 108-111 16 Dec. 1986 Transl. into ENGLISH from Kosmicheskaya Biologiya i Aviakosmicheskaya Meditsina (Moscow, USSR), v. 20, no. 5, Sep. - Oct. 1986 p 75-78

Avail: NTIS HC A07/MF A01

The factors responsible for the formation of hydrogen sulphide in the water reclaimed from the atmospheric condensate were investigated. It was found that hydrogen sulphide developed in reclaimed water due to microorganisms which in the presence of inorganic sulphur acquired the capacity to produce hydrogen sulphide, although normally they are not sulphur reducing. Among the microorganisms studied, E. coli showed the highest capacity (100%) and Streptococcus faecalis and Citrobacter freundii showed the lowest capacity (10 to 20%) to produce hydrogen sulphide.

Author

**N87-27312#** Colorado Univ., Boulder. Inst. of Arctic and Alpine Research.

**VEGETATION AND A LANDSAT-DERIVED LAND COVER MAP OF THE BEECHY POINT QUADRANGLE, ARCTIC COASTAL PLAIN, ALASKA**

DONALD A. WALKER and WILLIAM ACEVEDO Apr. 1987

72 p

(Contract DACA89-81-K-0006)

(AD-A180931; CRREL-87-5) Avail: NTIS HC A04/MF A01

CSC 08B

This report presents a LANDSAT-derived land cover classification of the Beechy Point, Alaska, 1:250,000-scale quadrangle with descriptions of the major vegetation units. Eight LANDSAT-level units derived from multispectral scanner data, eleven photo-interpreted units, and eight common vegetation complexes are described. The region is divided into four landscape units: flat thaw-lake plains, gently rolling thaw-lake plains, hill, and flood plains. Area analysis of the quadrangle was done according to townships and nine small study areas. The map uses a modified version of the hierarchical tundra mapping classification of Walker (1983). Area-measurement data from geobotanical maps at eight study sites are compared with similar data from LANDSAT maps of the same sites. The results indicate that LANDSAT maps yield area measurements corresponding to broad geobotanical categories. GRA

**N87-27862#** Digim (1983), Inc. Montreal (Quebec).

**STUDY ON THE USE OF SAR DATA FOR AGRICULTURE AND FORESTRY**

G. ROCHON, C. GOSSELIN, M. RHEAULT, P. VINCENT, K. P. B. THOMSON, B. GOZEBERTIN, S. POIRIER, and F. CAVAYAS *In* ESA Proceedings of the SAR Applications Workshop p 81-93 Dec. 1986 Prepared in cooperation with Laval Univ., Quebec and Montreal Univ., Quebec

Avail: NTIS HC A06/MF A01

Modeling of radar backscatter from vegetation canopies using existing ground measurements; processing techniques required to facilitate information extraction from noisy SAR data; and the increase in information content brought about by the integration of optical data with SAR data are considered with respect to agriculture and the forestry applications of ERS-1 (ESA satellite). Lack of data on ground parameters and on the geometrical configuration of the SAR system restricts conclusions, but the potential of ERS-1 in agricultural applications is confirmed. ESA

**N87-28109#** Du Pont de Nemours (E. I.) and Co., Aiken, S.C.  
**COLOR INFRARED VIDEO MAPPING OF UPLAND AND WETLAND COMMUNITIES**

H. E. MACKEY, JR., J. R. JENSEN, M. E. HODGSON, and K. W. OCULINN 1987 15 p Presented at the 11th Biennial Workshop on Color Aerial Photography in the Plant Sciences, Weslaco, Tex., 27 Apr. 1987 Prepared in cooperation with South Carolina Univ., Columbia and Coyote (E.) Enterprises, Inc., Mineral Wells, Tex. (Contract DE-AC09-76SR-00001)

(DE87-010202; DP-MS-86-210; CONF-8704136-1) Avail: NTIS HC A02/MF A01

Color infrared images were obtained using a video remote sensing system at 3000 and 5000 feet over a variety of terrestrial and wetland sites on the Savannah River Plant near Aiken, SC. The terrestrial sites ranged from secondary successional old field areas to even aged pine stands treated with varying levels of sewage sludge. The wetland sites ranged from marsh and macrophyte areas to mature cypress-tupelo swamp forests. The video data were collected in three spectral channels, 0.5-0.6 microns, 0.6-0.7 microns, and 0.7-1.1 microns at a 12.5 mm focal length. The data were converted to digital form and processed with standard techniques. Comparisons of the video images were made with aircraft multispectral scanner (MSS) data collected previously from the same sites. The analyses of the video data indicated that this technique may present a low cost alternative for evaluation of vegetation and landcover types for environmental monitoring and assessment. DOE

**N87-28127#** Joint Research Centre of the European Communities, Ispra (Italy). Remote Sensing Div.

**RURAL LAND USE INVENTORY AND MAPPING IN THE ARDECHE AREA (FRANCE). IMPROVEMENT OF AUTOMATIC CLASSIFICATION BY MULTITEMPORAL ANALYSIS OF TM DATA**

JOACHIM HILL and JACQUES MEGIER *In* ESA Proceedings of the ESA/EARSeL Europe from Space Symposium p 75-85 Dec. 1986

Avail: NTIS HC A14/MF A01

A set of four Thematic Mapper scenes (LANDSAT-5) was examined. The images can be rectified to map projection with excellent accuracy, but superposition of four TM subframes is affected by relief induced distortions and residual rotations. A systematic compensation of the relief dependent dislocations is not possible due to the lack of a digital terrain model. Further image analysis included the generation of multitemporal normalized vegetation index, image enhancement by edge preserving smoothing, verification and refinement of ground truth information, and supervised classification (maximum likelihood). Best results are achieved when classification output from 2 different data sets (multitemporal vegetation index, multitemporal combination of TM 3, 4, and 5) are combined. ESA

**N87-28128#** Florence Univ. (Italy).

**CROP DISCRIMINATION BY MEANS OF RADAR AND INFRARED IMAGES**

G. BENELLI, V. CAPPELLINI, L. NIGRO, S. PALOSCIA, and P. PAMPALONI (Consiglio Nazionale delle Ricerche, Florence, Italy) *In* ESA Proceedings of the ESA/EARSeL Europe from Space Symposium p 87-91 Dec. 1986

Avail: NTIS HC A14/MF A01

Filtering techniques, developed by Lee and Frost (1981, 1981) were used for noise reduction of X and C band images collected during the SAR 580 campaign. Using filtered images a crop classification on a pixel by pixel basis was carried out as an indirect test of two algorithms. Results show that the filters give almost the same performance, while crop classification is better pursued by using a Bayes classifier and multiband data. ESA

**N87-28129#** Ghent Univ. (Belgium). Lab. voor Regionale Geografie en Landschapkunde.

**DETECTION OF SOIL DRAINAGE IN PAYS DE HERVE, BELGIUM, ON LANDSAT MSS IMAGERY**

R. GOOSSENS *In* ESA Proceedings of the ESA/EARSeL Europe from Space Symposium p 93-99 Dec. 1986

Avail: NTIS HC A14/MF A01

The detection of soil drainage conditions in a grassland region, with different classes of soil drainage, using LANDSAT MSS images enhanced by using high gamma films is described. For the interpretation, the composite -4/-5 (enhanced) was used. Densitometric analysis shows a differentiation between well drained, poorly drained soils, and soils with perched water. Visual image analysis leads to photomorphologic unit maps. The maps were compared with soil map and field data. A map of the soil drainage conditions was made. ESA

**N87-28136#** Valencia Univ. (Spain). Dept. of Thermology.

**THERMAL INFRARED IMAGES FROM SATELLITES COMPARED TO SHELTER TEMPERATURE. APPLICATION TO FROST NOWCASTING IN A CITRUS ORCHARD**

V. CASELLES, J. A. SOBRINO, and J. MELIA *In* ESA Proceedings of the ESA/EARSeL Europe from Space Symposium p 145-150 Dec. 1986 Sponsored by the Comision Asesora para la Investigacion Cientifica y Tecnica

Avail: NTIS HC A14/MF A01

The effective parameters of emissivity and temperature in a citrus orchard were determined and the significance of the shelter temperature measured among the trees was studied. The emissivity and temperature values of the different parts of the radiative system were calculated using a manual scanning system and the box method. During clear cloudless night without wind, when radiative frost may be produced, the effective values are almost identical

## 01 AGRICULTURE AND FORESTRY

to the orange tree ones. Air temperature significance depends on the atmospheric situation and the time, being more representative for clear cloudless nights without wind and less for the maximum heating period on clear days. ESA

**N87-28138#** Technische Univ., Munich (West Germany). Lehrstuhl fuer Landschaftstechnik.

### **MONITORING AND INVENTORING OF FOREST DAMAGES BY USE OF LANDSAT TM DATA**

B. KOCH, R. HAYDN, H. KAUFMANN, and S. KRAUSE-RABE / In ESA Proceedings of the ESA/EARSeL Europe from Space Symposium p 163-168 Dec. 1986

Avail: NTIS HC A14/MF A01

Forest damage field investigations based on processed TM data, in which display ratios of near infrared against short wave infrared channels are described. To display subtle spectral variations and to improve visual interpretation the Intensity Hue and Saturation approach was applied with ratio techniques. The results show that a differentiation of stands due to age classes is possible but the assessment of damage is not definite. ESA

**N87-28140#** Instituto Nacional de Investigaciones Agrarias, Madrid (Spain). Seccion de Proceso de Datos.

### **ERAFIS: A COMPUTER INFORMATION SYSTEM FOR AGRICULTURE AND FORESTRY IN SPAIN**

J. M. CUEVAS, F. GONZALEZ-ALONSO, and J. MORO / In ESA Proceedings of the ESA/EARSeL Europe from Space Symposium p 183-188 Dec. 1986 Sponsored by the Comision Asesora para la Investigacion Cientifica y Tecnica

Avail: NTIS HC A14/MF A01

A system for processing remote sensing data and its integration with geographical and ecological data in an agricultural context was designed. The system is mainly oriented towards the recognition and superficial evaluation of crops using supervised classification techniques. The system was applied to an agricultural land use surface estimation study in the Toledo province (Spain) and the results demonstrate the viability of the adopted methodology to discriminate land uses. ESA

**N87-28148#** Technical Univ. of Denmark, Lyngby. Inst. of Electromagnetics.

### **LARGE SCALE SEA ICE STUDIES BASED ON SCANNING MULTICHANNEL MICROWAVE RADIOMETERS (SMMR) DATA**

PETER SLOTH and LEIF TOUDAL PEDERSEN / In ESA Proceedings of the ESA/EARSeL Europe from Space Symposium p 235-238 Dec. 1986 Sponsored by the Danish Space Research, the Commission for Scientific Research in Greenland, and IBM-Denmark

Avail: NTIS HC A14/MF A01

Large scale ice edge variations in the Greenland Sea were investigated through analysis of time series of data from the NIMBUS-7 Scanning Multichannel Microwave Radiometer (SMMR). Using a simple model for the relation between microwave radiances and sea ice concentration, a period from January to March was studied. Difficulties in interpreting variations in the ice edge position as observed by SMMR are discussed and illustrated through examples of the correspondence of the observed ice edge variations to different wind conditions. ESA

**N87-28149#** Roskilde Univ. (Denmark).

### **MAPPING OF VEGETATION TYPES IN SW GREENLAND**

S. FOLVING / In ESA Proceedings of the ESA/EARSeL Europe from Space Symposium p 239-243 Dec. 1986

Avail: NTIS HC A14/MF A01

To help plan sheep farming in Greenland, and to get a tool with which the impact on vegetation can be monitored, general thematic maps on vegetational surface cover types were made from LANDSAT multispectral data. The climate and the poorly developed soils cause the vegetation cover to be very patchy; most often the signal recorded per pixel originates in various surface cover types. Thus traditional classifications of the data give very insufficient results. It is shown that a combination of principal

component analysis and the normalized vegetation index is best suited to extract the needed information from satellite data. ESA

**N87-28151#** Valencia Univ. (Spain). Dept. of Thermology.

### **A MODEL OF THERMAL INERTIA FOR FROST FORECASTING IN AGRICULTURAL AREAS**

V. CASELLES, M. J. SALOM, J. DELEGIDO, and S. GANDIA / In ESA Proceedings of the ESA/EARSeL Europe from Space Symposium p 253-257 Dec. 1986

Avail: NTIS HC A14/MF A01

The Valentian region (Spain) was classified into different thermally homogeneous zones, to carry out frost forecasting for these small zones. The classifying parameter is thermal inertia because it is considered to be a good index of the system ground-vegetation when its temperature changes. For managing frost forecasting, Price's (1977) model for thermal inertia estimate was modified by adding the evapotranspiration term. Since evapotranspiration in irrigated lands mainly depends on crops, this forecasting is made from the maximum temperature image obtained by remote sensing and the crop image. ESA

**N87-28160#** Instituto de Pesquisas Espaciais, Sao Jose dos Campos (Brazil).

### **EVALUATION OF THE RANGE AND DEGRADATION OF MANGROVES IN SOUTHERN SERGIPE WITH REMOTE SENSING TECHNIQUES [AVALIACAO DA EXTENSAO E DEGRADACAO DE MANGUEZAIS NO SUL DE SERGIPE ATRAVES DE SENSORIAMENTO REMOTO]**

MYRIAN DEMOURAABDON, ERNESTO GETULIOMVIEIRA, and CARMEN REGINA S. ESPINDOLA Jun. 1987 26 p In PORTUGUESE; ENGLISH summary

(INPE-4196-PRE/1080) Avail: NTIS HC A03/MF A01

The purpose of this report is to estimate the mangrove population at the estuary of the rivers Piaui and Real (SE) with remote sensing techniques, and also to evaluate any degradation of these areas associated with the growing industrialization in the region. Aerial panchromatic photos in the 1:25,000 scale from 20 December 1987 were used to produce ground truth maps where mangrove areas were identified from other ground cover features. Digital multispectral and multitemporal analysis of MSS/LANDSAT (26 March 1979) and TM/LANDSAT (19 July 1984) imagery produced thematic maps of the region. The field work conducted in the area under study furnished data that confirm the efficacy of the method used in the identification and classification of the mangrove areas. Author

**N87-28190#** Oak Ridge National Lab., Tenn.

### **EFFECTS OF OZONE ON FORESTS IN THE NORTHEASTERN UNITED STATES**

M. B. ADAMS and G. E. TAYLOR, JR. 1987 51 p Presented at the Ozone Risk Communication Conference, Amherst, Mass., 21 Apr. 1987

(Contract DE-AC05-84OR-21400)

(DE87-010887; CONF-8704155-1) Avail: NTIS HC A04/MF A01

Methodologies for characterizing O<sub>3</sub> air quality are reviewed, with particular reference to forests in the northeastern United States. It is proposed that analyses be more ecologically and physiologically based. In particular, exposure statistics are recommended that (1) capture the temporal and spatial characteristics of O<sub>3</sub> air quality, (2) incorporate an understanding of the ecological properties of the pollutant and the physiological sensitivity of forest trees, and (3) recognize the pollutant's unique chemical attributes that make it distinct from other pollutants. With respect to forest ecosystems in the Northeast, the most distinctive feature of O<sub>3</sub> air quality is the dynamics of episodically high O<sub>3</sub> concentrations during the growing season. O<sub>3</sub> concentrations of 50 ppB or greater for a 28-day exposure period were found to affect growth and yield of sensitive forest species. However, the majority of species require substantially longer exposure or higher concentrations before growth reductions occur. In mixed stands, the most probable effects of O<sub>3</sub> stress will be subtle, long-term shifts in species composition, due to impacts on sensitive individuals or species. DOE

**N87-28195\*** Washington State Univ., Pullman. Dept. of Agronomy and Soils.

**SPECTRAL CHARACTERISTICS AND THE EXTENT OF PALEOSOLS OF THE PALOUSE FORMATION** Semiannual Progress Report No. 4

B. E. FRAZIER, ALAN BUSACCA, YAAN CHENG, DAVID WHERRY, JUDY HART, and STEVE GILL Aug. 1987 23 p (Contract NAS5-28758)

(NASA-CR-181208; NAS 1.26:181208) Avail: NTIS HC A02/MF A01 CSCL 08G

Three spectral models defining the spatial distribution of soil areas by levels of amorphous iron, organic carbon, and the ratio of amorphous iron to organic carbon were developed and field verification studies were conducted. The models used particular Thematic Mapper band ratios selected by statistical correlation with soil chemical data. The ability of the models to indicate erosion severity and to differentiate between iron enriched and carbonate paleosols is discussed. In addition, the effect of vegetation cover on paleosols is addressed. M.G.

## 02

### ENVIRONMENTAL CHANGES AND CULTURAL RESOURCES

Includes land use analysis, urban and metropolitan studies, environmental impact, air and water pollution, geographic information systems, and geographic analysis.

**A87-46309**

**SMALL FORMAT AERIAL PHOTOGRAPHY FOR ANALYZING URBAN HOUSING PROBLEMS - A CASE STUDY IN THE BANGKOK METROPOLITAN REGION**

CHANTANA CHANOND and CHAMNIAN LEEKBHAI (National Housing Authority, Bangkok, Thailand) (International Society for Photogrammetry and Remote Sensing, Commission VII Symposium, Enschede, Netherlands, Aug. 25-29, 1986) ITC Journal (ISSN 0303-2434), no. 3, 1986, p. 197-205. refs

**A87-46310**

**REMOTE SENSING IN INDONESIA - A REVIEW OF THE AVAILABLE TECHNOLOGY AND ITS APPLICATIONS FOR RESOURCES SURVEYS**

JEAN-PAUL MALINGREAU (Commission of the European Communities, Joint Research Centre, Ispra, Italy) and SUTANTO (Gadjah Mada University, Yogyakarta, Indonesia) ITC Journal (ISSN 0303-2434), no. 3, 1986, p. 206-216. refs

The current status of the Indonesian remote sensing program is considered. The use of aerial photography and Landsat images in Indonesia is examined; particular attention is given to the access to information about the Landsat data; the availability of the Landsat data; and access to the data. The Landsat data are applicable for such uses as land cover/land use inventories, vegetation surveys, and water resources monitoring. The methods of visual and digital analyses of images are described. Other remote sensing systems utilized in Indonesia are: microwave systems, the Spot satellite, the tropical earth observation satellite, and environmental satellites. A list of the national institutions, research institutions, universities, and government agencies and departments involved in remote sensing in Indonesia is presented. The education and training of personnel to use remote sensing equipment and analyze the satellite data are discussed. I.F.

**A87-48671**

**SIGNIFICANCE OF TM DATA AS A TOOL TO SUPPORT REGIONAL PLANNING ACTIVITIES**

R. HAYDN, P. VOLK (Gesellschaft fuer angewandte Fernerkundung mbH, Munich, West Germany), and J. BRAEDT (Bayerisches Staatsministerium fuer Landesentwicklung und Umweltfragen, Munich, West Germany) IN: Earth remote sensing using the Landsat Thematic Mapper and SPOT sensor systems; Proceedings of the Meeting, Innsbruck, Austria, Apr. 15-17, 1986. Bellingham, WA, Society of Photo-Optical Instrumentation Engineers, 1986, p. 139-141.

Landsat MSS data (and formerly ERTS) have initialized a euphoric boom to obtain excellent and specific information for the use in regional planning and environmental tasks. Nevertheless, in many cases those expectations have been proven to be overemphasized due to concrete problems in this field of application. With some of the first results of a pilot project in southern Bavaria using TM-data, it is now possible to support the expectation of providing very detailed and geometrically accurate planning base data. An object-oriented presentation of spectral features for microclimatic investigations, hydrological sealing, land use, and indicators of the vitality of vegetation canopies confirms the high potential for much more differentiated land information analysis. In this context, not only the high-resolution capabilities but especially the properties of the NIR and SWIR channels of TM should be emphasized.

Author

**A87-48802#**

**AIRBORNE VIDEO - APPLIED TO ROUTE LOCATION STUDIES FOR ELECTRICAL POWER TRANSMISSION FACILITIES**

R. N. PIERCE (Ontario Hydro, Land Use and Environmental Planning Dept., Toronto, Canada) IN: Canadian Symposium on Remote Sensing, 10th, Edmonton, Canada, May 5-8, 1986, Proceedings. Volume 1. Ottawa, Canadian Aeronautics and Space Institute, 1987, p. 1, 2. refs

The Land Use and Environmental Planning Department of Ontario Hydro has successfully used color aerial video imagery for various aspects of route location planning. Imagery has been used to update existing maps and photography; provide ground control for data interpretation; monitor changes in land cover and land use throughout the course of a project. The nature of video technology produces advantages in terms of cost of acquisition, accessibility, adaptability, and convenience of handling and reproduction. The suitability of aerial video imagery for illustration and presentation has greatly assisted in public participation and assessment hearing procedures. Methods of acquisition, application, and presentation are discussed. The future direction in this field is also considered.

Author

**A87-48838#**

**MONITORING THE FIRE-DANGER HAZARD OF NEBRASKA RANGELANDS WITH AVHRR DATA**

F. G. SADOWSKI (TGS Technology, Inc., Sioux Falls, SD) and D. E. WESTOVER (Nebraska Forest Service, Lincoln) IN: Canadian Symposium on Remote Sensing, 10th, Edmonton, Canada, May 5-8, 1986, Proceedings. Volume 1. Ottawa, Canadian Aeronautics and Space Institute, 1987, p. 355-365. refs

**A87-48858#**

**NATIONAL LAND USE MAPPING - THE APPLICATION OF LOW ALTITUDE SAMPLE PHOTOGRAPHY**

R. S. KIMANGA (Manitoba, University, Winnipeg, Canada) IN: Canadian Symposium on Remote Sensing, 10th, Edmonton, Canada, May 5-8, 1986, Proceedings. Volume 2. Ottawa, Canadian Aeronautics and Space Institute, 1987, p. 571-577. refs

A national program is under way to map land use and land cover in Kenya for the rationalization of resource development planning and monitoring. For various reasons a low altitude photographic sampling method has been chosen for the data acquisition. And, for ease of administration and user information dissemination the surveys are being done by administrative units. In this paper the methodology and results of a survey carried out in Meru District of Kenya in 1985 are discussed. The survey

attempted to use a standardized land use and land cover classification which was a basis for assessing photointerpretation accuracy and consistency measurements. Possible alternative mapping techniques of the data are briefly discussed. Author

### A87-48868#

#### RURAL LAND USE CLASSIFICATION USING LANDSAT THEMATIC MAPPER DATA

R. G. BRAMM (Alberta Environment, Land Use Branch, Edmonton, Canada) and G. C. REICHERT (Alberta Environment, Remote Sensing, Centre, Edmonton, Canada) IN: Canadian Symposium on Remote Sensing, 10th, Edmonton, Canada, May 5-8, 1986, Proceedings, Volume 2. Ottawa, Canadian Aeronautics and Space Institute, 1987, p. 675-682. refs

### A87-48886#

#### AN APPLICATION FOR THE TESTING AND USE OF THE STANDARD DATA TRANSFER FORMAT

K. D. KORPORAL (Statistics Canada, Geocartographics Subdiv., Ottawa) and M. J. MANORE (Intera Technologies, Ltd., Ottawa, Canada) IN: Canadian Symposium on Remote Sensing, 10th, Edmonton, Canada, May 5-8, 1986, Proceedings, Volume 2. Ottawa, Canadian Aeronautics and Space Institute, 1987, p. 867-873. refs

Cooperative projects to transfer remotely sensed classified data from the Canada Centre for Remote Sensing (CCRS) to geographic information systems at the Geocartographics Subdivision (GCGC), Statistics Canada, have been ongoing since 1982. The transfers utilize an ad-hoc 'Standard Format for the Transfer of Geocoded Information in Spatial Data Polygon Files' (SDTF), which was developed in 1979 by a committee of federal government departments. Recent modifications to the SDTF, coupled with an increasing requirement to utilize existing spatial data files resident at both agencies, has prompted further testing and the development of new interfaces. This paper will discuss an application requiring the classification of urban concentrations from Landsat MSS data processed at CCRS, their transfer via the SDTF to GCGC, and their subsequent use in a geographic information and mapping system (GIMMS). The remotely sensed data was georeferenced and integrated with spatial data files such as a Census enumeration areas and street networks. It is thought that the addition of these data could provide a timely, cost-efficient supplementary data source for a variety of applications including the delineation of Census urban area boundaries. Author

### A87-48895#

#### THE ROLE OF REMOTE SENSING IN THE CANADA LAND USE MONITORING PROGRAM (CLUMP)

D. A. WILSON (Environment Canada, Lands Directorate, Dartmouth) IN: Canadian Symposium on Remote Sensing, 10th, Edmonton, Canada, May 5-8, 1986, Proceedings, Volume 2. Ottawa, Canadian Aeronautics and Space Institute, 1987, p. 947-956. refs

Remote sensing technology is an essential part of the operational Canada Land Use Monitoring Program (CLUMP). Examples of the evolving use of airborne and orbital sensor output in the collection of land-use-change information are described. Present program plans call for the replacement of conventional aerial photography with satellite imagery as the chief CLUMP data (along with standard geographic information) to meet the 1991 goal. Author

### A87-48898#

#### ENVIRONMENTAL MONITORING OF ALPINE MEADOWS WITH LARGE SCALE AERIAL PHOTOGRAPHY IN BANFF NATIONAL PARK

A. WESTHAVER (Banff National Park, Canada) and A. KLAR (Lakeland College, Vermilion, Canada) IN: Canadian Symposium on Remote Sensing, 10th, Edmonton, Canada, May 5-8, 1986, Proceedings, Volume 2. Ottawa, Canadian Aeronautics and Space Institute, 1987, p. 981-984.

### A87-48903#

#### THE EVALUATION OF TM ANALYSIS AS A TOOL IN MONITORING LAND USE AND AGRICULTURAL STRESS IN EGYPT

N. A. PROUT and J. F. SUTTON (Intera Technologies, Ltd., Ottawa, Canada) IN: Canadian Symposium on Remote Sensing, 10th, Edmonton, Canada, May 5-8, 1986, Proceedings, Volume 2. Ottawa, Canadian Aeronautics and Space Institute, 1987, p. 1017-1027. Research supported by the Centre International de Developpement de l'Aluminium. refs

The use of Landsat imagery for land use inventory, evaluation, and change detection in the NE part of the Nile Delta in Egypt is examined. Landsat MSS and TM data were analyzed in terms of land use, salinity, and vegetation stress. It is observed that both MSS and TM data are useful for delineating vegetated areas, bare ground, probable water logged or salinity stressed areas, and rural and urban infrastructures. The MSS data are more useful for regional monitoring at scales in the 1:75,000 and 1:250,000 range, and urban areas, some rural infrastructure, irrigated fields, drying fields, emergent vegetation, and vigorous crop growth are identifiable in the images. The TM permits more detailed analysis and class separation, and provides information on rural infrastructure, agricultural land and urban area estimation, and crop separation. I.F.

### A87-48907#

#### COMPUTER-ASSISTED MAP ANALYSIS - EXTENDING THE UTILITY OF GIS TECHNOLOGY

J. K. BERRY (Yale University, New Haven, CT) IN: Canadian Symposium on Remote Sensing, 10th, Edmonton, Canada, May 5-8, 1986, Proceedings, Volume 2. Ottawa, Canadian Aeronautics and Space Institute, 1987, p. 1057-1066. refs

The growing use of computers in land management is profoundly changing data collection procedures, analytic processes and even the decision making environment itself. Use of word processing systems, data base management systems and spreadsheets have become commonplace in the contemporary office. The emerging technology of Geographic Information Systems (GIS) is expanding this revolution to fully integrate spatial information into research, planning and management of land. In one sense, this technology is similar to conventional map processing involving traditional maps and drafting aids, such as pens, rub-on shading, rulers, planimeters, dot grids and acetate sheets for light-table overlays. In another sense, these systems provide advanced analytic capabilities, which enable managers to address complex issues in entirely new ways. This paper discusses spatial statistics and cartographic modeling, as extensions of the current computer mapping and data base management capabilities of GIS technology. The mathematical structure described consists of a set of primitive operators which may be flexibly combined to address a wide variety of applications. All of the procedures discussed are currently available as Mainframe and microcomputer software. Author

### A87-50227

#### LAND COVER CLASSIFICATION USING SPOT DATA

RYUTARO TATEISHI and YUJI MUKOUYAMA (Chiba University, Japan) Geocarto International (ISSN 1010-6049), vol. 2, June 1987, p. 17-29.

SPOT multispectral data were compared statistically with 10-m mesh numerical land use data in the study area near Tokyo. The numerical land use data have 16 categories and were produced from color aerial photographs by the Geographical Survey Institute of Japan. This statistical analysis shows the poor possibility of 'land use' classification from SPOT data, and it suggests the establishment of 'land cover' categories. Six types of land cover categories were established based on the above statistical analysis and aerial photographs for ground truth, and they were defined mainly by dividing two-dimensional SPOT feature space into regions. The study area is classified into these land cover categories by the decision tree method and is examined with numerical land use data. The conclusions of this study are: (1) numerical geographical information is highly useful for analysis of

remotely sensed data; (2) new methods of defining land cover categories were proposed; (3) six types of land cover classes can be extracted from SPOT data and they indicate well the degree of vegetation and nonvegetation; and (4) the difference between land use and land cover were found out statistically. Author

**A87-52241****MONITORING THE BACKGROUND POLLUTION OF NATURAL ENVIRONMENTS, NO. 3 [MONITORING FONOVOGO ZAGRIAZNENIYA PRIRODNYKH SRED, NO.3]**

IU. A. IZRAEL', ED. and F. IA. ROVINSKII, ED. Leningrad, Gidrometeoizdat, 1986, 256 p. In Russian. No individual items are abstracted in this volume.

This collection of papers examines such topics as the background content of lead, mercury, arsenic, and cadmium in the environment; the background content of organochlorine pesticides and polycyclic aromatic hydrocarbons in the environment; the background content of sulfur compounds in the atmospheric surface layer; the global distribution of lead in the atmosphere; and the pollution of fauna of natural ecosystems by organochlorine compounds. Consideration is also given to the submicron component of heavy metals in the atmosphere; the background content of ozone in the atmospheric surface layer; dissolved trace elements in lake waters; the element composition of Lake Baikal snow cover; heavy metals in Baltic Sea sediments; aerosol concentrations over Lithuania; and the background content of minerals in air, snow cover, and natural waters. B.J.

**A87-52242****PROBLEMS IN THE BACKGROUND MONITORING OF THE ENVIRONMENT, NO. 4 [PROBLEMY FONOVOGO MONITORINGA SOSTOIANIYA PRIRODNOI SREDY, NO. 4]**

F. IA. ROVINSKII, ED. Leningrad, Gidrometeoizdat, 1986, 304 p. In Russian. No individual items are abstracted in this volume.

This collection of papers (reflecting research carried out in the framework of the Global Environmental Monitoring System) covers such topics as background pollution monitoring, the modeling of the transborder transport of air pollutants, the assessment of the contribution of pollutants to long-range atmospheric transport, and the evaluation and prediction of environmental conditions. Particular papers are presented on the background pollution of snow cover on Soviet territory; sulfur concentration in precipitation; a dispersion model for air-pollutant transport over medium distances; the remote sensing of emission plumes; and the measurement of polycyclic aromatic hydrocarbons in water bodies. B.J.

**A87-53187****ANALYSIS OF ENVIRONMENTAL INFORMATION OF URBAN AREAS USING LANDSAT TM DATA**

IKUO SAITOU (Yatsushiro National College of Technology, Hirayamashin, Japan), OSAMU ISHIHARA, and SHIGEYOSHI IMAIZUMI (Kumamoto University, Japan) IN: IGARSS '87 - International Geoscience and Remote Sensing Symposium, Ann Arbor, MI, May 18-21, 1987, Digest. Volume 1. New York, Institute of Electrical and Electronics Engineers, Inc., 1987, p. 709-714.

Irradiance is uneven in urban areas where shade is created due to unevenness of ground surface. Therefore, remote sensing data obtained by earth observation satellites exhibit both the reflection characteristics of the ground surface coverage and the spatial characteristics of urban areas. In this paper, the effects of the form of the urban space on the Landsat TM data were investigated using both actual data and simulation. First, the spatial characteristics of urban areas and the statistics of CCT counts for the same area were investigated, and their relationship was examined. Then, on the basis of simulation results regarding shade distribution, the effects of the form of the urban space on the Landsat TM data were investigated. Author

**N87-25634#** Environmental Protection Agency, Research Triangle Park, N.C. Monitoring and Data Analysis Div.

**REVIEW OF CONTROL STRATEGIES FOR OZONE AND THEIR EFFECTS ON OTHER ENVIRONMENTAL ISSUES**

E. L. MEYER Nov. 1986 117 p  
(PB87-171195; EPA-450/4-85-011) Avail: NTIS HC A06/MF A01 CSCL 13B

The review summarizes theoretical, experimental, field and modeling data related to effects of reducing volatile organic compounds (VOC), oxides of nitrogen (NOx) or both for meeting the ambient air quality standard for ozone (O3). Implications are reviewed for several environmental concerns. These include O3 levels within and immediately downwind of major sources of precursors (i.e., cities), O3 concentrations in rural/remote areas, ambient levels of nitrogen dioxide (NO2), acidic species formation and visibility attenuation. GRA

**N87-26463#** Environmental Research Lab., Gulf Breeze, Fla. **CHARACTERIZING THE CHESAPEAKE BAY ECOSYSTEM AND LESSONS LEARNED**

D. A. FLEMER, V. K. TIPPIC, G. B. MACKIERNAN, R. B. BIGGS, and W. NEHLSSEN Mar. 1987 34 p Sponsored by EPA Prepared in cooperation with National Marine Fisheries Service, Washington, D.C., Maryland Univ., College Park, Delaware Univ., Newark and Delaware Univ., Lewes  
(PB87-166930; EPA/600/D-87/071) Avail: NTIS HC A03/MF A01 CSCL 13B

During the scientific study phase, the U.S. EPA Chesapeake Bay Program examined the complex ecological structure and processes of the Bay estuary in a coherent and manageable framework. The historic geological, physical, chemical (water quality), and biological data were analyzed within this framework to determine trends, correlations and, where appropriate, causal relationships. The overall process resulted in a synthesis or statement on the environmental condition of the Chesapeake Bay ecosystem. GRA

**N87-26464#** Butler Univ., Indianapolis, Ind. **BIOMONITORING PLOTS AT THE OZONE MONITORING STATIONS AT GREAT SMOKY MOUNTAINS NATIONAL PARK, 1985 SURVEY RESULTS Final Report**

P. J. SANCHINI and S. J. STEIN Oct. 1986 48 p Prepared in cooperation with Utah State Univ., Logan and Sanchini BioResearch, Inc., Aurora, Colo.  
(Contract NPS-PX-0001-5-0823)  
(PB87-172078; HRI-93) Avail: NTIS HC A03/MF A01 CSCL 13B

High ambient ozone levels recorded in Great Smoky Mountains National Park and the continued development in the valleys north and east of the Park have prompted concern about air-quality-related values in the Park. The goal of this research was to establish biomonitoring plots near four ozone monitoring stations in Great Smoky Mountains National Park. A total of seven plots was established, using four tree species known to be sensitive to air pollution. Foliar injury was evaluated on 115 trees in August and September 1985. No symptoms of ozone injury were observed. This report provides a detailed summary of the data collected in 1985, descriptions of the procedures used in evaluating trees, and directions to the study sites. GRA

**N87-28115#** European Space Agency, Paris (France). **PROCEEDINGS OF THE ESA-EARSEL EUROPE FROM SPACE SYMPOSIUM**

OLGA MELITA, comp. Dec. 1986 325 p Symposium held in Lyngby, Denmark, 25-27 Jun. 1986  
(ESA-SP-258; ISSN-0379-6566; ETN-87-90155) Avail: NTIS HC A14/MF A01

Spaceborne remote sensing for cartography and geoinformation; environmental monitoring; economic factors in satellite remote sensing; inventory and monitoring of renewable resources; and disaster management were discussed.

ESA



**N87-28117#** Technische Univ., Munich (West Germany). Lehrstuhl fuer Geographie und Geogr. Fernerkundung.  
**URBAN DEVELOPMENT PLANNING USING THEMATIC MAPPER DATA OF MUNICH (FRG)**  
 F.-W. STRATHMANN and H. KAUFMANN (Karlsruhe Univ., West Germany ) *In* ESA Proceedings of the ESA-EARSeL Europe from Space Symposium p 9-14 Dec. 1986  
 Avail: NTIS HC A14/MF A01

With regard to the requirements of thematic mapping and development planning in urban areas, multitemporal datasets of LANDSAT Thematic Mapper (TM) were investigated to demonstrate the possibilities and limitations of high resolution satellite imagery. An image improvement concept, based on combined filtering and color-coding algorithms was developed. It guarantees an optimized presentation of structural and spectral image contents. A catalog of band combinations for the enhancement of different land use categories and urban details was elaborated. Results of the image analysis provide information about basic building features and typical land use patterns. Because the multitemporal use offers an actual data base for change detection in urban areas, TM mapping and monitoring can be useful for the extension of urban/regional information systems. For needs of urban development planning TM data can only have a supplementary function. ESA

**N87-28130#** National Aeronautics and Space Administration. Goddard Space Flight Center, Greenbelt, Md.  
**CONTRIBUTION OF SPACE TECHNOLOGY TO DISASTER PREPAREDNESS, WARNING, AND RELIEF**  
 L. WALTER *In* ESA Proceedings of the ESA-EARSeL Europe from Space Symposium p 103-107 Dec. 1986  
 Avail: NTIS HC A14/MF A01

Use of remote sensing for disaster control and vulnerability analysis, disaster prevention, and disaster relief is discussed. ESA

**N87-28135#** Dundee Univ. (Scotland). Physics Lab.  
**ON THE USE OF AVHRR CHANNEL-3 DATA FOR ENVIRONMENTAL STUDIES**  
 A. P. CRACKNELL and M. C. DOBSON *In* ESA Proceedings of the ESA/EARSeL Europe from Space Symposium p 137-144 Dec. 1986  
 Avail: NTIS HC A14/MF A01

It is shown that NOAA AVHRR channel-3 data enable more discrimination to be achieved between different types of clouds than can be achieved with data from other channels. Channel-3 data can also be used, from night-time passes, in multichannel algorithms for calculating sea surface temperatures. The use of channel-3 data in monitoring gas flares at oil exploration and production platforms in the North Sea, and in monitoring agricultural straw burning is described. Results for Denmark are presented. ESA

**N87-28137#** Joint Research Centre of the European Communities, Ispra (Italy).  
**THE ROLE AND PERSPECTIVE OF REMOTE SENSING FOR DISASTER MANAGEMENT IN THE EUROPEAN COMMUNITY**  
 S. R. GALLIDEPARATESI *In* ESA Proceedings of the ESA/EARSeL Europe from Space Symposium p 151-162 Dec. 1986  
 Avail: NTIS HC A14/MF A01

A reconnaissance map derived from a representation matrix of the degree of application of a specific type of remote sensing system to a specific type of hazard/disaster for a specific type of management activity is described. Satellite options for disaster management application are discussed in terms of feasibility of the expected applications, timeliness and continuity of data delivery, reliability, and operation continuity of space platforms. It emerges that further priorities and allocation resources could be usefully applied to disaster management phases when supported by advanced space technologies. ESA

**N87-28141#** North East London Polytechnic, Dagenham (England). Dept. of Land Surveying.  
**ENVIRONMENTAL INFORMATION AND CARTOGRAPHY**  
 RICHARD K. BULLARD and ROBERT W. DIXON-GOUGH *In* ESA Proceedings of the ESA/EARSeL Europe from Space Symposium p 189-194 Dec. 1986  
 Avail: NTIS HC A14/MF A01

Factors fundamental to the implementation of an environmental impact analysis investigation, in particular the acquisition of remotely sensed environmental data together with the means by which data can be brought together in a compatible format are discussed. Much of the data will be either raster or vector format and available in digital or analog form so the need to bring these sets of data together for their joint analysis is considered. The classification of data, its display, and reproduction to ensure that the best use is made of the analysis under consideration are looked at in respect of the environmental impact. ESA

**N87-28145#** Joint Research Centre of the European Communities, Ispra (Italy).  
**MEASUREMENT OF SPECTRAL SIGNATURES IN LESS FAVORED AREAS (LFA): A CONTRIBUTION TO THE DEFINITION OF A REMOTE SENSING MULTITEMPORAL EXPERIMENT**  
 G. MARACCI, G. ANDREOLI, and B. HOSGOOD *In* ESA Proceedings of the ESA/EARSeL Europe from Space Symposium p 215-218 Dec. 1986  
 Avail: NTIS HC A14/MF A01

A multitemporal analysis criterion for classification based on ground measured spectral reflectances by means of the vegetation index was established. The possibility to express LANDSAT Thematic Mapper (TM) data in terms of spectral reflectances, once atmospheric effects are taken into account is proved and these are comparable with those measured at ground level. This step requires knowledge of the reflective properties of a reference target in the scene or the measurement of the incoming irradiance. It is possible to compare TM data of different seasons, in an objective way, for multitemporal analysis. This might be a significant contribution to the definition of a remote sensing project for less favored area management. The effect of an unidentified cause which results in too high a value of radiance in TM band 4 is noted. ESA

**N87-28147#** Ludwig-Maximilians-Universitaet, Munich (West Germany). Inst. fuer Allgemeine und Angewandte Geologie.  
**THE IMPACT OF LANDSAT THEMATIC MAPPER DATA FOR ECOLOGICAL MAPPING PURPOSES. A CASE STUDY AT THE NORTHERN MARGIN OF THE ALPS**  
 F. JASKOLLA *In* ESA Proceedings of the ESA/EARSeL Europe from Space Symposium p 225-230 Dec. 1986  
 Avail: NTIS HC A14/MF A01

The suitability of the model CORINE for ecological mapping on the European level is discussed. By an example of LANDSAT-TM data of a test site south of Munich, their high significance is demonstrated. Results show that thematic mapping scaled up to 1:50 000 is possible; the depiction of land descriptors is improved significantly; and the crucial point for use of the information content is digital image processing. ESA

## GEODESY AND CARTOGRAPHY

Includes mapping and topography.

**A87-42938**

**A METHOD FOR THE OPTIMIZATION OF ORBITS AND STRUCTURES OF SATELLITE SYSTEMS FOR THE PERIODIC ROUND-THE-CLOCK SURVEY OF THE EARTH [METOD OPTIMIZATSII ORBIT I STRUKTURY SISTEM ISZ DLIA PERIODICHESKOGO KRUGLOSUTOCHNOGO OBZORA ZEMLI]**  
V. K. SAUL'SKII Issledovanie Zemli iz Kosmosa (ISSN 0205-9614), Jan.-Feb. 1987, p. 111-121. In Russian. refs

A quick-response algorithm is presented for optimizing the circular orbits and positions relative to each other of satellites which make up a space system for the periodic round-the-clock monitoring of the earth surface. The method helps to minimize the repetition period of the continuous scanning of a given global zone. The application of the method to a multisatellite system is demonstrated. I.S.

**A87-42939**

**NEW POSSIBILITIES FOR THE USE OF GRAVITY DATA IN THE REALIZATION OF GEODETIC COORDINATE SYSTEMS [NOVYE VOZMOZHNOСТИ ISPOL'ZOVANIYA GRAVITATSION-NYKH DANNYKH PRI REALIZATSII GEODEZICHESKIKH SISTEM KOORDINAT]**

L. P. PELLINEN Geodeziia i Kartografiia (ISSN 0016-7126), March 1987, p. 10-13. In Russian. refs

Radio-altimeter observations from GEOS-3 and Seasat as well as laser-tracking observations of Lageos have opened new possibilities for the realization of geodetic coordinate systems by the joint processing of ground measurements and satellite observations. This paper proposes a method for the processing of geodetic data which makes it possible to use height anomalies that are completely free of the indirect effect of geodetic-coordinate errors. B.J.

**A87-44352**

**GEOID ANOMALIES ACROSS ASCENSION FRACTURE ZONE AND THE COOLING OF THE LITHOSPHERE**

DOMINIQUE GIBERT, CHRISTIAN CAMERLYNCK (Institut Francais de Recherche pour l'Exploitation de la Mer, Brest, France), and VINCENT COURTILOT (Paris VI, Universite, France) Geophysical Research Letters (ISSN 0094-8276), vol. 14, June 1987, p. 603-606. CNRS-supported research. refs

Twenty-three Seasat altimeter profiles crossing the Ascension fracture zone are used together with sea-floor ages inferred from a kinematic model to estimate a geoid slope-age relation between ages of 5 and 50 Ma. The data do not definitely contradict a half space cooling model (slope =  $-9.5 \pm 3$  cm/Ma) if biases are accepted, resulting in large scatter. However, the data would seem to support a puzzling explanation in terms of a plate cooling model involving two distinct thermal thicknesses, one of about 70 km for ages less than 35 Ma, the other of at least 100 km for ages greater than 35 Ma. Although preliminary, this result is similar to that found in the Pacific with a much larger data set. Author

**A87-45743**

**SEASAT ALTIMETRY AND THE SOUTH ATLANTIC GEOID. I - SPECTRAL ANALYSIS**

DOMINIQUE GIBERT (Institut Francais de Recherche pour l'Exploitation de la Mer, Brest, France) and VINCENT COURTILOT (Paris, Institut de Physique du Globe, France) Journal of Geophysical Research (ISSN 0148-0227), vol. 92, June 10, 1987, p. 6235-6248. CNRS-supported research. refs

The spectral characteristics of geoid profiles for seven provinces in the South Atlantic, derived from Seasat altimetry in the South Atlantic, are analyzed. The provinces studied include: the Mid-Atlantic Ridge and flanks, the Rio Grande rise, the Walvis

Ridge, and the Argentine and Cape basins. Three distinct wavebands were detected in all the spectra with boundaries at 35 km and 250-300 km. Impedance is estimated for each province using bathymetric spectral estimates and an extended simple power law extrapolated from longer wavelengths. The elastic and crustal thicknesses are calculated; the elastic thickness ranges from 2-5 km for the ridge and flanks and the crustal thickness from 4-13 km. It is noted that despite insufficient bathymetric data, the geoid data can be used at the scale of the entire South Atlantic to provide data on thermochemical compensation in the various provinces. I.F.

**A87-45817**

**EARTH GRAVITY MODEL IMPROVEMENT - AN ALTERNATIVE METHOD FOR DOPPLER-TRACKED SATELLITES**

E. LANSARD (CNES, Groupe de Recherche de Geodesie Spatiale, Toulouse, France) and R. BIANCALE (COSPAR, International Association of Geodesy, and Inter-Union Commission on the Lithosphere, Plenary Meeting, 26th, Symposium on Solid Earth Geophysics and Satellite Orbits, 2nd, and Topical Meeting, Toulouse, France, June 30-July 11, 1986) Advances in Space Research (ISSN 0273-1177), vol. 6, no. 9, 1986, p. 103-106. refs

A new method of earth gravity model improvement based on an analytical formulation of Doppler residuals is presented here in prospect of future geodetic and altimetric missions (DORIS < TOPEX/POSEIDON, ERS1). After an intermediate step of orbit improvement, disturbing forces due to gravity field mismodeling are recovered above tracking stations at satellite altitude. Some significant simulation results for Seasat and DORIS are presented. Author

**A87-46139**

**THE DETERMINATION OF LOVE NUMBERS FROM THE RESULTS OF EARTH-TIDE OBSERVATIONS IN THE DNEIPER-DONETS BASIN (DDB) REGION [OPREDELENIE CHISEL LIAVA PO REZULTATAM ZEMNOPRILIVNYKH NAB-LIUDENII V REGIONE DNEPROVSKO-DONETSKOI VPADINY /DDV/]**

V. G. BALENKO (Poltavskaia Gravimetricheskaia Observatoriia, Poltava, Ukrainian SSR) and B. P. PERTSEV (AN SSSR, Institut Fiziki Zemli, Moscow, USSR) Kinematika i Fizika Nebesnykh Tel (ISSN 0233-7665), vol. 3, May-June 1987, p. 45-48. In Russian. refs

The Love numbers are determined from the results of earth-tide observations in the DDB region and their accuracies are assessed. The present determinations are compared with values previously obtained from measurements of the earth's rotational velocity, laser observations of artificial satellites, and extensometric investigations. K.K.

**A87-46688#**

**RADIO INTERFEROMETRY**

DOUGLAS S. ROBERTSON (NOAA, National Geodetic Survey, Rockville, MD) Reviews of Geophysics (ISSN 8755-1209), vol. 25, June 1987, p. 867-870. refs

The progress made during the period of 1983-1986 in the application of VLBI techniques in the fields of geodesy and geophysics is described. During this period three major observing campaigns were devoted to applications in these fields: (1) the IRIS project, with stations in U.S., Sweden, and FRG; (2) the NASA's Crustal Dynamics Project, with stations in North America, Europe, and across the Pacific; and (3) the JPL's project Time and Earth Motion Precision Observations, using antennas in California, Spain, and Australia. Data taken during this period have contributed to understanding the interactions between the earth's mantle and its fluid core and the atmosphere and to the knowledge of lithospheric deformation. The determination of the earth tide Love numbers was improved, and a new standard of accuracy was established for the determination of variations in the earth's orientation. Finally, new information was obtained on the celestial reference coordinate frame which is of fundamental importance for determining the motions of the earth. I.S.



A87-46692#

**NEW INSTRUMENTATION TECHNIQUES IN GEODESY**

CHRISTOPHER JEKELI (USAF, Geophysics Laboratory, Hanscom AFB, MA) Reviews of Geophysics (ISSN 8755-1209), vol. 25, June 1987, p. 889-894. refs

New instrumentation techniques for geodetic studies, developed during the period of 1983-1986 are discussed. Special attention is given to the Global Positioning System of satellites that has virtually revolutionized geodesy, yielding data on precise positioning and baseline determination, time dissemination, geoid computations, earth rotation monitoring, and navigation and satellite tracking. Consideration is also given to improvements in inertial positioning systems and gravimetry instrumentation, radar altimetry from satellites, and the laser ranging from aircraft. In addition, geodetic applications of active and passive optical inertial rotation sensors, the tethered satellite-subsatellite system, and VLBI methodology are discussed. I.S.

A87-51964\*# National Aeronautics and Space Administration. Goddard Space Flight Center, Greenbelt, Md.

**SNOW LOAD EFFECT ON EARTH'S ROTATION AND GRAVITATIONAL FIELD, 1979-1985**

B. FONG CHAO, WILLIAM P. O'CONNOR, ALFRED T. C. CHANG, DOROTHY K. HALL, and JAMES L. FOSTER (NASA, Goddard Space Flight Center, Greenbelt, MD) Journal of Geophysical Research (ISSN 0148-0227), vol. 92, Aug. 10, 1987, p. 9415-9422. refs

A global, monthly snow depth data set has been generated from the Nimbus 7 satellite observations using passive microwave remote-sensing techniques. Seven years of data, 1979-1985, are analyzed to compute the snow load effects on the earth's rotation and low-degree zonal gravitational field. The resultant time series show dominant seasonal cycles. The annual peak-to-peak variation in  $J_2$  is found to be  $2.3 \times 10^{-10}$ , that in  $J_3$  to be  $1.1 \times 10^{-10}$ , and believed to decrease rapidly for higher degrees. The corresponding change in the length of day is 41 micro-s. The annual wobble excitation is (4.9 marc sec, -109 deg) for the prograde motion component and (4.8 marc sec, -28 deg) for the retrograde motion component. The excitation power of the Chandler wobble due to the snow load is estimated to be about 25 dB less than the power needed to maintain the observed Chandler wobble. Author

A87-52507

**PRELIMINARY RESULTS FROM THE PROCESSING OF A LIMITED SET OF GEOSAT RADAR ALTIMETER DATA**

DENNIS H. VAN HEE (DMA, Aerospace Center, Saint Louis, MO) Johns Hopkins APL Technical Digest (ISSN 0270-5214), vol. 8, Apr.-June 1987, p. 201-205. refs

The representation of the mean sea surface and the accurate computation of anomalous aspects of the earth's gravitational field are problems that are uniquely addressed by data obtained during the geodetic phase of Geosat. Statistics from comparisons of mean gravity anomalies that were computed on the basis of Gerosat data, and corresponding values obtained on the basis of the best survey data extant, are presented together with a discussion of the possibilities for future processing and exploitation of these data. Attention is given to an interim Geosat geoid-height data set, the computation of mean gravity anomalies, and noteworthy oceanographic and bathymetric characteristics. O.C.

A87-52766

**A PROGRAM FOR THE COMBINED ADJUSTMENT OF VLBI OBSERVING SESSIONS**

WILLIAM H. DILLINGER and DOUGLAS S. ROBERTSON (NOAA, Geodetic Research and Development Laboratory, Rockville, MD) Manuscripta Geodaetica (ISSN 0340-8825), vol. 11, Dec. 1986, p. 278-281.

As Very Long Baseline Interferometry (VLBI) observing sessions increase in number and complexity, the need for efficient computer software to process large amounts of VLBI data increases. This paper describes a new system of programs developed at the National Geodetic Survey for this purpose. This system, called

SOLVE3, computes a least squares adjustment of VLBI data to estimate polar motion, UT1, site and source coordinates, as well as certain other geophysical parameters. This system is now being used routinely to process the observations collected regularly under project IRIS, and for analytical studies that are expected to play a key role in the future of VLBI research efforts. Author

A87-53146\*

National Aeronautics and Space Administration. Goddard Space Flight Center, Greenbelt, Md.

**SPACEBORNE LASER RANGING FROM EOS**

STEVEN C. COHEN and JOHN J. DEGNAN (NASA, Goddard Space Flight Center, Greenbelt, MD) IN: IGARSS '87 - International Geoscience and Remote Sensing Symposium, Ann Arbor, MI, May 18-21, 1987, Digest. Volume 1. New York, Institute of Electrical and Electronics Engineers, Inc., 1987, p. 373-378. refs

High precision laser ranging measurements from an Earth Observing System (EOS) platform would provide data for conducting a variety of basic geoscience investigations. For example, range data to retroreflectors arranged in grids located at tectonic plate boundaries could be used to study the spatial and temporal distribution of the crustal movements associated with stress accumulation and release in an earthquake cycle. The Geodynamics Laser Ranging System (GLRS) is a proposed facility instrument for EOS that can perform the ranging function as well as simple height-measurement altimetry over ice sheets. This instrument is the derivative of several generations of ground-based laser trackers and prototype laboratory systems. The Geoscience Laser Altimetry/Ranging System (GLARS) is an advanced laser ranging system which would provide higher accuracy ranging observations and detailed altimetric mapping of surface height distributions over land and ice sheets. Author

A87-54325

**ESTIMATION AND MODELLING OF THE LOCAL EMPIRICAL COVARIANCE FUNCTION USING GRAVITY AND SATELLITE ALTIMETER DATA**

PER KNUDSEN (Geodaetisk Institut, Charlottenlund, Denmark) Bulletin Geodesique (ISSN 0007-4632), vol. 61, no. 2, 1987, p. 145-160. Research supported by the Danish Space Board. refs

Gravity measurements and Seasat altimetry for the Faroe Islands are analyzed to determine LECF, the local empirical covariance function defined by Goad et al. (1984), and the problems involved in modeling the LECF and calculating the spectral density from it are discussed. Both space-domain and frequency-domain (Fourier-transform) methods are applied, and a Tscherring-Rapp (1974) degree-variance model is fit to the estimated LECFs for free-air anomalies and geoid heights (simultaneously) by iterative least-squares inversion; good accuracy is obtained in two or three iterations. The results are presented in graphs, and it is shown that the smoothing produced by the gridding procedure of the Fourier technique must be compensated for (in this case, by deconvolution with a filter representing the smoothing). T.K.

N87-25652# National Geodetic Survey, Rockville, Md.

**GEODETIC GLOSSARY**

Sep. 1986 283 p  
(PB87-181210; LC-86-61105) Avail: NTIS HC A13/MF A01  
CSCL 08G

This glossary is a revision of Definitions of Terms Used in Geodetic and Other Surveys (U.S. Coast and Geodetic Survey Special Publication 242) by Hugh C. Mitchell, published in 1948 by the U.S. Government Printing Office. Since this book appeared, the standards, instruments, theory, and procedures of that time have been markedly changed, complemented, reduced in importance, or completely replaced by new ones. In addition, the interaction of geodesy with other disciplines has greatly increased, which demands that these relationships be covered also. Such a variety of changes and additions has swelled the number of definitions from 800 to almost 5000. GRA

## GEOLOGY AND MINERAL RESOURCES

Includes mineral deposits, petroleum deposits, spectral properties of rocks, geological exploration, and lithology.

A87-42937

**STEREOSCOPIC VISUALIZATION OF AERIAL AND SPACE PHOTOGRAPHS IN THEMATIC MAPPING [STEREOSKOPICHESKAIA VIZUALIZATSIIA AERO- I KOSMICHESKIKH SNIMKOV PRI TEMATICHESKOM KARTIROVANII]**

R. I. VITKUS, V. E. GENDLER, V. A. IL'IN, and L. P. IAROSLAVSKII (AN SSSR, Institut Problem Peredachi Informatsii; Proizvodstvenno-Geologicheskoe Ob'edinenie Aerogeol Issledovanie Zemli iz Kosmosa (ISSN 0205-9614), Jan.-Feb. 1987, p. 102-110. In Russian.

The paper presents a method for space-photograph interpretation in which the results obtained by the interpretation of space images containing different parameters are presented as a single stereoscopic image. The method, termed stereovision or stereoscopic visualization, uses pairs of images in which one is a brightness image (for which an original space photograph can be used) and the other determines conventional topography to synthesize artificial stereoscopic images for stereoscopic visualization. Application of the stereovision to the geological interpretation of space images is demonstrated. I.S.

A87-43353#

**CHARACTERISTICS OF THE GREGORY RIFT (KENYA) DYNAMICS, GROUND STRUCTURAL ANALYSIS, AND REMOTE SENSING**

GERARD F. VIDAL AIAA Student Journal (ISSN 0001-1460), vol. 25, Spring 1987, p. 4-9. refs

The use of satellite imagery in structural geology is discussed. The Gregory Rift in Africa, which is 600-km long and 40-km wide, is examined in terms of plate tectonics. The dynamics of the rift are studied using synoptic data obtained from literature, satellite images, and field observations. The N-S pattern of the main faults is revealed by the structural map produced from the data. The number of normal, dextral strike-slip, and sinistral strike-slip faults is estimated. I.F.

A87-45048

**REMOTE SENSING OF THE GEOMORPHOLOGIC FORMATIONS AND VEGETATION IN THE EASTERN HIGH ATLAS REGION OF MOROCCO FROM SPOT SATELLITE DATA [TELEDTECTION DES FORMATIONS GEOMORPHOLOGIQUES ET DE LA VEGETATION DANS UN TERRITOIRE DU HAUT ATLAS ORIENTAL MAROCAIN A PARTIR DES DONNEES DU SATELLITE SPOT]**

BERNARD LACAZE (CNRS, Centre L. Emberger, Montpellier, France) and LAHCEN LAHRAOUI (Institut Agronomique et Veterinaire, Rabat, Morocco) International Journal of Remote Sensing (ISSN 0143-1161), vol. 8, May 1987, p. 751-763. In French. Research supported by the Ministere de la Cooperation. refs (Contract CNES-85-1264)

A87-48185

**SPACE PHOTOGRAPHS OF THE ONEGA-LADOGA ISTHMUS AND THE PREDICTION OF MINERAL FINDS [KOSMICHESKIE SNIMKI ONEZHNSKO-LADOZHNSKOGO PERESHEIKA I PROGNOZIROVANIE POLEZNYKH ISKOPAEMYKH]**

Z. A. BAGROVA and I. B. ANTONOVA (Proizvodstvenno-Geologicheskoe Ob'edinenie Sevzapgeologii, Leningrad, USSR) Issledovanie Zemli iz Kosmosa (ISSN 0205-9614), Mar.-Apr. 1987, p. 66-72. In Russian. refs

The paper considers the geological-structural characteristics of the Onega-Ladoga isthmus as interpreted from space imagery. Fault systems and ring structures were identified. This information along with available geological and geophysical data makes it

possible to recognize signs of explosive magmatism and to predict the occurrence of bauxites and other minerals. B.J.

A87-48186

**APPLICATION OF SPACE PHOTOGRAPHS TO GEOMORPHOLOGICAL INVESTIGATIONS IN SOUTHWESTERN TADZHIKISTAN [PRIMENENIE KOSMICHESKIKH FOTOSNIMKOV PRI GEOMORFOLOGICHESKIKH ISSLEDOVANIYAKH V IUGO-ZAPADNOM TADZHIKISTANE]**

V. P. LOZIEV and M. S. SAIDOV (Gosudarstvennyi Nauchno-Issledovatel'skii i Proizvodstvennyi Tsentr Priroda, USSR) Issledovanie Zemli iz Kosmosa (ISSN 0205-9614), Mar.-Apr. 1987, p. 73-80. In Russian. refs

A87-48187

**APPLICATION OF SPACE PHOTOGRAPHS TO PALEOSEISMOLOGICAL INVESTIGATIONS (WITH REFERENCE TO THE MONGOLIAN ALTAI) [PRIMENENIE KOSMICHESKIKH SNIMKOV PRI PALEOSEISMOLOGICHESKIKH ISSLEDOVANIYAKH/NA PRIMERE MONGOL'SKOGO ALTAIA]**

A. L. STROM (Institut Gidroprom, Moscow, USSR) Issledovanie Zemli iz Kosmosa (ISSN 0205-9614), Mar.-Apr. 1987, p. 81-84. In Russian. refs

It is demonstrated that, in Central Asia, young faults observed on space photographs can be reliably interpreted as paleoseismodislocations. Such faults are characterized by their manifestation as scarps and the presence of displacements of river beds or deluvial/proluvial cones. B.J.

A87-48188

**INVESTIGATION OF THE RELIEF OF ORE-CONTAINING REGIONS ON THE BASIS OF SPACE PHOTOGRAPHS (WITH REFERENCE TO EASTERN IAKUTIA) [ISSLEDOVANIE REL'EF A RUDNYKH RAIONOV PO KOSMICHESKIM SNIMKAM /NA PRIMERE VOSTOCHNOI IAKUTII/]**

V. A. BALANDIN (AN SSSR, Institut Gornogo Dela, Yakutsk, USSR) Issledovanie Zemli iz Kosmosa (ISSN 0205-9614), Mar.-Apr. 1987, p. 85-89. In Russian. refs

A87-48358

**LITHOLOGICAL DISCRIMINATION IN CENTRAL SNOWDONIA USING AIRBORNE MULTISPECTRAL SCANNER IMAGERY**

D. GREENBAUM (British Geological Survey, Nottingham, England) International Journal of Remote Sensing (ISSN 0143-1161), vol. 8, June 1987, p. 799-816. NERC-supported research. refs

A87-48666

**EVALUATION OF LANDSAT THEMATIC MAPPER - IMAGERY FOR GEOLOGICAL EXPLORATION**

JOHN R. EVERETT (Earth Satellite Corp., Chevy Chase, MD) IN: Earth remote sensing using the Landsat Thematic Mapper and SPOT sensor systems; Proceedings of the Meeting, Innsbruck, Austria, Apr. 15-17, 1986. Bellingham, WA, Society of Photo-Optical Instrumentation Engineers, 1986, p. 106-111.

The potential value of the broader spectral coverage and higher resolution of digitally processed Thematic Mapper data to geologic exploration is enormous. Already there are reported successes in improved geologic mapping and the detection of spectral anomalies associated with mineralization and hydrocarbon microseepage.

Author

A87-48667\* Dartmouth Coll., Hanover, N.H.

**LITHOLOGIC DISCRIMINATION USING GEOBOTANICAL AND LANDSAT TM SPECTRAL DATA**

RICHARD W. BIRNIE, NANCY J. DEFEO, and CURTIS PRICE, V. (Dartmouth College, Hanover NH) IN: Earth remote sensing using the Landsat Thematic Mapper and SPOT sensor systems; Proceedings of the Meeting, Innsbruck, Austria, Apr. 15-17, 1986. Bellingham, WA, Society of Photo-Optical Instrumentation Engineers, 1986, p. 112-117. refs (Contract NASW-4049)

**A87-48803#**

**INTEGRATION OF RADIOMETRIC AND LANDSAT DIGITAL DATA FOR GEOLOGIC INVESTIGATION AND EXPLORATION, GUYSBOROUGH AREA, NOVA SCOTIA**

T. R. MCINNIS and M. S. AKHAVI (Nova Scotia Land Survey Institute, Lawrencetown, Canada) IN: Canadian Symposium on Remote Sensing, 10th, Edmonton, Canada, May 5-8, 1986, Proceedings. Volume 1. Ottawa, Canadian Aeronautics and Space Institute, 1987, p. 11-17. Sponsorship: Department of Energy, Mines, and Resources of Canada. refs  
(Contract DEMR-247)

A multilayer database is formed by digitizing, resampling, overlaying and registering airborne radiometric data, Landsat imagery, and geologic boundaries for the Guysborough area, Nova Scotia. The database is utilized to depict and map the distribution and coalescence of radioelements eU, eTh, and percent K as well as U/Th, U/K and Th/K ratios. The analysis of radioelements and ratios suggest a distinct eastern and western domain as well as the occurrence of various granitic phases. A circular radiometric high is selected as a target for detailed geologic field work. This locality coincides with a contact metamorphic aureole and a network of intersecting lineaments. Author

**A87-48804#**

**ANALYSIS OF AIRBORNE INFRARED DATA FOR INTERPRETATIVE GEOLOGICAL MAPPING OF THE BROOKFIELD AREA, NOVA SCOTIA**

K. D. KALICHARRAN (Ontario Ministry of Northern Affairs and Mines, Kirkland Lake, Canada) and M. S. AKHAVI (Nova Scotia Land Survey Institute, Lawrencetown, Canada) IN: Canadian Symposium on Remote Sensing, 10th, Edmonton, Canada, May 5-8, 1986, Proceedings. Volume 1. Ottawa, Canadian Aeronautics and Space Institute, 1987, p. 19-26. refs

This paper reports on the use of airborne infrared data in locating previously unmapped lithologic contacts and lineaments, and in providing interpretive data on the local hydrology and geomorphology. Selective analog processing and image enhancement of thermal infrared data (3-5 and 8-14 microns) enable the recognition of lithologic contacts and lineaments within the gold bearing Meguma Group. Enhancement of color infrared images enable the mapping of zones and metasomatic contact of the Westfield granitic cupola, and area of greisenization. It is believed that this area may harbor mineralization. The mapping of lithological contacts, surface expression of buried intrusive, intersection of joint systems and bedding, and the offset produced by intersecting fault systems, as located from the infrared data, may be indicators of associated mineral deposits. Author

**A87-48816#**

**EVALUATION OF MEIS-II MULTISPECTRAL SCANNER DATA FOR QUATERNARY GEOLOGICAL MAPPING IN THE CHATHAM AREA, SOUTHWESTERN ONTARIO**

H. GEORGE, M. B. DUSSEAU, A. B. KESIK (Waterloo, University, Canada), and E. V. SADO (Ministry of Northern Development and Mines, Ontario Geological Survey, Toronto, Canada) IN: Canadian Symposium on Remote Sensing, 10th, Edmonton, Canada, May 5-8, 1986, Proceedings. Volume 1. Ottawa, Canadian Aeronautics and Space Institute, 1987, p. 141-151. Research supported by the Ontario Geoscience Research Fund. refs

Multispectral imagery collected using the MEIS-II scanner fitted with the 1985 'TM + SPOT' filter set has been studied in order to evaluate its usefulness for surficial geologic mapping. Results show that the eight-band digital data contains three inherent principal factors with the first three ordered principal components accounting for approximately 99.3 percent of the total scene variance. Spectral ranges of the three bands comprising the optimal band triplet for visually discriminating surficial deposits when viewing color composites were: 456-518nm, 522-735nm, and 793-893nm. Several digital enhancements (including principal components transformation, contrast stretching, band ratioing) were of varying utility. Color composites formed using the three histogram-equalized contrast-stretched bands which comprise the optimal band triplet provide very good discrimination of deposits with a minimum

expenditure of processing time. Many subtle tonal and textural variations evident on 1:26,000 color infrared transparencies appear sharper on the digitally enhanced color composites, allowing easier delineation of geologic boundaries. Comparatively, 1:15,840 black-and-white Summer panchromatic airphotographs currently being used routinely for the preparation of standard 1:50,000 surficial geologic maps provide the least amount of information for geologic discrimination. Author

**A87-48827#**

**A STUDY OF THE POTENTIAL APPLICATION OF SPOT IMAGERY IN STRUCTURAL GEOLOGY [ETUDE DE L'APPLICATION POTENTIELLE DES IMAGES SPOT A LA GEOLOGIE STRUCTURALE]**

M. RHEAULT, P. ST-JULIEN (Universite Laval, Sainte-Foy, Canada), and G. ROCHON (Digim, Inc., Montreal, Canada) IN: Canadian Symposium on Remote Sensing, 10th, Edmonton, Canada, May 5-8, 1986, Proceedings. Volume 1. Ottawa, Canadian Aeronautics and Space Institute, 1987, p. 253-262. In French. refs

Simulations of SPOT imagery were carried out using airborne data from the CCRS Multidetector Electrooptical Imaging Scanner II for an area of approximately 300 sq km in the Gaspé Peninsula in Quebec. Each of the multiband images from three flight lines covering the study area was radiometrically and geometrically corrected and then mosaicked. First, a digital terrain model (DTM) was created by the interpolation of lines of equal altitude. This DTM was then used with the simulated SPOT imagery to simulate imagery acquired at an angle of 27 deg from nadir, which is equal to the maximum pointing angle of SPOT. This makes it possible to have a stereoperception of the terrain. An evaluation was carried out of information available from SPOT imagery, Landsat imagery, and the DTM, taken individually or combined. Author

**A87-48832#**

**APPLICATION OF REMOTE SENSING DATA TO BEDROCK GEOLOGICAL INTERPRETATION, BLACK RIVER-MATHESON AREA, NORTHERN ONTARIO, CANADA**

K. D. KALICHARRAN and A. C. BATH (Ontario Ministry of Northern Development and Mines, Kirkland Lake, Canada) IN: Canadian Symposium on Remote Sensing, 10th, Edmonton, Canada, May 5-8, 1986, Proceedings. Volume 1. Ottawa, Canadian Aeronautics and Space Institute, 1987, p. 301-308. refs

Computer-enhanced Landsat MSS data and black and white aerial photography over the Black River-Matheson area (Canada) were used to identify regional and semiregional basement structural trends (including the location of the Porcupine-Destor Fault Zone) and to differentiate between different basement lithologic and volcano-stratigraphic domains of this area. The results of the analysis for this area, which contains up to 90 percent glacial overburden cover, demonstrate the applicability of remote sensing analysis to the bedrock geologic interpretation and to regional and semiregional geological mapping and/or exploration programs. I.S.

**A87-48853#**

**DIGITAL SAR-LANDSAT COMBINATION FOR GEOLOGIC MAPPING**

W. C. JEFFERIES and G. R. LAWRENCE (Intera Technologies, Ltd., Ottawa, Canada) IN: Canadian Symposium on Remote Sensing, 10th, Edmonton, Canada, May 5-8, 1986, Proceedings. Volume 1. Ottawa, Canadian Aeronautics and Space Institute, 1987, p. 505-512. refs

Digital data obtained by the airborne Sea-Ice and Terrain Assessment Radar (STAR)-1 X-band H-H radar imagery over a large area in central Pennsylvania were combined with corresponding Landsat MSS data registered to a subset of the STAR-1 data, and the resulting image was in turn registered to ground control points. A series of band combinations were then created at both the maximum Landsat and maximum radar resolutions, and standard feature-enhancements were performed individually and in conjunction with one another in order to evaluate a range of products useful to the exploration geologist.

Comparisons with regional geologic maps and ground truth data have shown that the product of the combined satellite MSS and airborne radar data can be useful in exploration mapping. By maintaining a digital data base, processing techniques can be varied, producing a series of output images, rather than a single scene, and accentuating the particular features of interest. I.S.

**A87-48854#****SHUTTLE IMAGING RADAR-A (SIR-A) SCENES FROM IRAN AND CHINA**

D. F. GRAHAM (Radarsat Project Office, Ottawa, Canada) and J. HARRIS (F. G. Bercha and Associates, Ltd., Ottawa, Canada) IN: Canadian Symposium on Remote Sensing, 10th, Edmonton, Canada, May 5-8, 1986, Proceedings. Volume 1. 1987, p. 513-527. refs

Five of the SIR-A images obtained over Iran and central China on the Shuttle mission of November 12, 1981, were selected for geological analysis of the area and for comparing the SIR-A and Landsat imageries with respect to their value for geological mapping. It is shown that SIR-A imagery offers fairly detailed structural information that should be useful in a general reconnaissance geological survey; it offers information complementary to that of Landsat. Vegetated areas and water bodies are more easily delineated on the Landsat imagery, while SIR-A offers good discrimination of surface materials based on distinct roughness properties. A summary table is presented, describing those geological features that are most emphasized in each of the five SIR-A images analyzed, indicating the benefits of using radar imaging for geological interpretation. I.S.

**A87-48860#****A GEOBOTANIC APPROACH TO THE STUDY OF THE GEOLOGY OF CAPE SMITH USING LANDSAT-MSS DATA**

C. SEUTHE (Centre Quebecoise de Coordination de la Teledetection, Sainte-Foy, Canada), L. DION (Canadian Institute of Surveying, Centre Forestier des Laurentides, Edmonton, Canada), and J. BEAUBIEN IN: Canadian Symposium on Remote Sensing, 10th, Edmonton, Canada, May 5-8, 1986, Proceedings. Volume 2. Ottawa, Canadian Aeronautics and Space Institute, 1987, p. 591-600. In French. refs

**A87-48861#****REGIONAL GEOBOTANY WITH TM - A SUDBURY CASE STUDY**

J. K. HORNSBY (Intera Technologies, Ltd., Ottawa, Canada) and B. BRUCE (Canada Centre for Remote Sensing, Ottawa, Canada) IN: Canadian Symposium on Remote Sensing, 10th, Edmonton, Canada, May 5-8, 1986, Proceedings. Volume 2. Ottawa, Canadian Aeronautics and Space Institute, 1987, p. 601-609. refs

The use of the Landsat TM to study the relation between geology and vegetation is examined. The effects of topography, surficials, lithology, and structure on the nature and patterns of vegetation cover are investigated in the Levack area of the Sudbury Basin in Ontario. The four stage analysis of the TM data involves: (1) preliminary processing, (2) field investigations, (3) detailed image processing, and (4) data integration and analysis. A regional geobotanical model which integrates image, map, and field data is developed. It is noted that the TM is applicable for the study of mineral-induced stress in vegetation cover. I.F.

**A87-48862#****GEOLOGICAL INTERPRETATIONS FROM LANDSAT OF THE TROODOS MASSIVE, CYPRUS**

B. BRUCE (Canada Centre for Remote Sensing, Ottawa), J. HORNSBY (Intera Technologies, Ltd., Ottawa, Canada), A. ZUNIGA (Direccion General de Geologia y Minas Carrion, Ecuador), and J. HALL (Dalhousie University, Halifax, Canada) IN: Canadian Symposium on Remote Sensing, 10th, Edmonton, Canada, May 5-8, 1986, Proceedings. Volume 2. Ottawa, Canadian Aeronautics and Space Institute, 1987, p. 611-621. refs

A 30 x 40 km region of the Cyprus Troodos Massif was analyzed using Landsat MSS data in order to examine the structure and lithologic setting of the massif. Logarithmic and linear contrast

stretches, directional convolution filtering, principal component enhancements, and unsupervised classifications were applied to the Landsat data in order to produce enhancements for visual interpretation, and the Procom II was used for interpretation of the data. It is detected that the linears follow a N-S trend that is related to the fracture zones or faults; the E-W trending linears are transform faults; the lineaments are cross-cutting the axis of the Troodos Massif at right angles; and there are upper and lower pillow lavas that form a discontinuous belt around the margin of the massif. Maps of the topology, physiography, geology, linears, and lineaments of the massif are provided. I.F.

**A87-48879#****A STRUCTURAL ANALYSIS OF THE MABOU BASIN, CAPE BRETON ISLAND USING ENHANCED LANDSAT MSS IMAGERY**

J. C. MILFORD (Chevron Canada Resources, Ltd., Calgary), S. M. YATABE (Intera Technologies, Ltd., Ottawa, Canada), and A. G. FABBRI (Canada Centre for Remote Sensing, Ottawa) IN: Canadian Symposium on Remote Sensing, 10th, Edmonton, Canada, May 5-8, 1986, Proceedings. Volume 2. Ottawa, Canadian Aeronautics and Space Institute, 1987, p. 797-806. refs

**A87-51144****CONTRIBUTION OF IMPROVED RESOLUTION TO MORPHOLOGICAL ANALYSIS - THE EXAMPLE OF THE RHONE DELTA [L'APPORT DE LA RESOLUTION AMELIOREE DANS L'ANALYSE MORPHOLOGIQUE - L'EXEMPLE DU DELTA DU RHONE]**

M. GUY (Groupement pour le Developpement de la Teledetection Aerospatiale, Toulouse, France) Photo Interpretation (ISSN 0031-8523), vol. 24, Nov.-Dec. 1985, p. 1-5, 7. In French, English and Spanish.

**A87-51145****GEOMORPHOLOGICAL INTERPRETATION OF THE SPOT IMAGE OF FEBRUARY 23, 1986 CONCERNING DJEBEL AMOUR (ALGERIA) AND ITS BORDER WITH THE SAHARA [INTERPRETATION GEOMORPHOLOGIQUE DE L'IMAGE SPOT DU 23 FEVRIER 1986 CONCERNANT LE DJEBEL AMOUR (ALGERIE) ET SA BORDURE SAHARIENNE]**

F. JOLY, A. SIMONIN (CNRS, Paris, France), and J. GUILLEMOT (Institut Francais du Petrole, Rueil-Malmaison, France) Photo Interpretation (ISSN 0031-8523), vol. 24, Nov.-Dec. 1985, p. 9-13, 15, 17 (5 ff.).

**A87-51146****MORPHOSTRUCTURE AND GEOLOGICAL PATTERNS IN CENTRAL-SOUTHERN NORWAY ACCORDING TO A LANDSAT IMAGE [MORPHOSTRUCTURE ET MODELES EN NORVEGE CENTRE-SUD D'APRES UNE IMAGE LANDSAT]**

J.-P. PEULVAST (Paris VI, Universite, France) Photo Interpretation (ISSN 0031-8523), vol. 25, May-June 1986, p. 19-23, 25. In French, English, and Spanish.

A Landsat MSS 7 image of a high-latitude mountain in central-southern Norway is analyzed in order to relate the morphological and geological features. The importance of taking geomorphological features into consideration in photointerpretation is emphasized. A visual overlay compares tracings of the lineaments and of the principal features with data obtained by conventional methods and field work. It is suggested that the topographical differences and the degree of coverage by in situ or moderately disturbed materials, contributing more than the lithology to the determination of photofeatures, are less indicative of the scale of erosion-resistance of the rocks than of the past and present dynamic differences. In these mountains, good rock outcrop conditions are expected, and the surface formations are shown to modify the signature. R.R.

**A87-51725\*** Arizona State Univ., Tempe.  
**RHEOLOGY OF THE 1983 ROYAL GARDENS BASALT FLOWS, KILAUEA VOLCANO, HAWAII**  
 JONATHAN H. FINK (Arizona State University, Tempe) and JAMES R. ZIMBELMAN (Lunar and Planetary Institute, Houston, TX) Bulletin of Volcanology (ISSN 0258-8988), vol. 48, 1986, p. 87-96. refs  
 (Contract NAGW-529; NASW-3389)

**A87-51875**  
**REMOTE-SENSING AND GEOLOGICAL-GEOPHYSICAL STUDIES OF CLOSED PLATFORM TERRITORIES [AEROKOSMICHESKIE I GEOLOGO-GEOFIZICHESKIE ISSLEDOVANIYA ZAKRYTYKH PLATFORMENNYKH TERRITORII]**  
 DMITRII MIKHAILOVICH TROFIMOV, VADIM ALEKSANDROVICH BOGOSLOVSKII, ELENA BORISOVNA IL'INA, E. N. KUZ'MINA, A. A. OGIL'VI et al. Moscow, Izdatel'stvo Nedra, 1986, 240 p. In Russian. refs

Methods used in aerial and satellite photography, image decoding, and image transformation are discussed, with emphasis on the problems arising in the geological interpretation of these images. Methods used in the integration of geophysical and remote-image data on closed platform territories are considered along with the construction of geophysical-geological models of closed platforms. The results of combined satellite-based and geological-geophysical studies are presented on the closed platform territories of Kursk, Riazan', and the Caspian regions. Special attention is given to the applications of the results of integrated remote imaging and geological-geophysical data to the geological mapping of mineral- and oil-bearing formations. I.S.

**A87-53150**  
**REMOTE SENSING OF DEEP POTENTIAL SOURCES OVER THE NILE DELTA AREA**  
 M. EL-RAEY, E. EL-MOSSELY, and A. EL-SAHARTY (Alexandria, University, Egypt) IN: IGARSS '87 - International Geoscience and Remote Sensing Symposium, Ann Arbor, MI, May 18-21, 1987, Digest. Volume 1. New York, Institute of Electrical and Electronics Engineers, Inc., 1987, p. 429-433. refs

Inherent material properties of deep seated geophysical anomalies, such as their associated magnetic and gravitational fields, are used for the remote sensing of these sources. Aeromagnetic and Bouguer maps of the northwestern area of the Nile Delta, Egypt, are analyzed by digital techniques. Downward continuation of both fields are carried out to subsurface depths at intervals of 2.5 km down to 10 km. Resulting digitized images are considered as equivalent to spectral multiband images providing information on geophysical sources at different subsurface levels. Histograms and scatter plots are obtained for successive depths at intervals of 2.5 km. Correlations among fields at various depths have been discussed in terms of clusters of points in the gravitational-magnetic feature space. Author

**A87-53242**  
**PLEISTOCENE EARTH MOVEMENTS IN PENINSULAR INDIA - EVIDENCES FROM LANDSAT MSS AND THEMATIC MAPPER DATA**  
 S. M. RAMASAMY, S. PANCHANATHAN, and R. PALANIVELU (Anna University, Madras, India) IN: IGARSS '87 - International Geoscience and Remote Sensing Symposium, Ann Arbor, MI, May 18-21, 1987, Digest. Volume 2. New York, Institute of Electrical and Electronics Engineers, Inc., 1987, p. 1157-1161. refs

**A87-53243\*** Carnegie Museum of Natural History, Pittsburgh, Pa.  
**ANALYSIS OF EOCENE DEPOSITIONAL ENVIRONMENTS - PRELIMINARY TM AND TIMS RESULTS, WIND RIVER BASIN, WYOMING**  
 RICHARD K. STUCKY, LEONARD KRISHTALKA, ANDREW D. REDLINE (Carnegie Museum of Natural History, Pittsburgh, PA), and HAROLD R. LANG (California Institute of Technology, Jet Propulsion Laboratory, Pasadena) IN: IGARSS '87 - International Geoscience and Remote Sensing Symposium, Ann Arbor, MI, May 18-21, 1987, Digest. Volume 2. New York, Institute of Electrical and Electronics Engineers, Inc., 1987, p. 1163-1168. Research supported by the Carnegie Museum of Natural History. refs  
 (Contract NSF BSR-84-02051)

Both Landsat TM and aircraft Thermal IR Multispectral Scanner (TIMS) data have been used to map the lithofacies of the Wind River Basin's Eocene physical and biological environments. Preliminary analyses of these data have furnished maps of a fault contact boundary and a complex network of fluvial ribbon channel sandstones. The synoptic view thereby emerging for Eocene fluvial facies clarifies the relationships of ribbon channel sandstones to fossil-bearing overbank/floodplain facies and certain pebbles. The utility of TM and TIMS data is thereby demonstrated. O.C.

**A87-53244**  
**USE OF TM LANDSAT DATA AS A SUPPORT TO CLASSICAL GROUND-BASED METHODOLOGIES IN THE INVESTIGATION OF A VOLCANIC SITE IN CENTRAL ITALY - THE CALDERA OF LATERA**  
 G. ONORATI, M. POSCOLIERI (CNR, Istituto di Astrofisica Spaziale, Frascati, Italy), S. SALVI (Istituto Nazionale di Geofisica, Rome, Italy), and R. TRIGILA (Roma I, Università, Rome, Italy) IN: IGARSS '87 - International Geoscience and Remote Sensing Symposium, Ann Arbor, MI, May 18-21, 1987, Digest. Volume 2. New York, Institute of Electrical and Electronics Engineers, Inc., 1987, p. 1173-1178. refs

**A87-53257**  
**APPLICATION OF TM IMAGERY TO MAPPING VOLCANIC ROCK ASSEMBLAGES AT TERTIARY CALDERAS OF THE BASIN AND RANGE PROVINCE**  
 D. M. SPATZ, J. V. TARANIK, and L. C. HSU (Nevada, University, Reno) IN: IGARSS '87 - International Geoscience and Remote Sensing Symposium, Ann Arbor, MI, May 18-21, 1987, Digest. Volume 2. New York, Institute of Electrical and Electronics Engineers, Inc., 1987, p. 1299-1308. refs

**A87-53733**  
**TIDAL AND SECULAR TILT FROM AN EARTHQUAKE ZONE - THRESHOLDS FOR DETECTION OF REGIONAL ANOMALIES**  
 JOHN PETERS and CHRISTOPHER BEAUMONT (Dalhousie University, Halifax, Canada) Earth and Planetary Science Letters (ISSN 0012-821X), vol. 84, no. 2-3, July 1987, p. 263-276. Research supported by the Geological Survey of Canada. refs  
 (Contract F19628-80-C-0032; F19628-83-K-0023)

Data from a series of borehole tiltmeters located in the Charlevoix seismic region of Quebec were analyzed for evidence of tectonically related signals. Special consideration was given to long-term nontidal tilt and the linear and nonlinear tidal response with emphasis on the time variation of the tidal admittance. Strongly coherent time variations in the tidal admittance among the observations of all the major tidal constituents are shown to be generated by corresponding variations in marine tidal loading in the St. Lawrence estuary. Diurnal band variations are closely correlated with the tide gage data. The level of earthquake activity in the Charlevoix seismic zone throughout the four years of the tiltmeter experiment was low, so that no significant tilt anomalies were expected or were undeniably detected. I.S.

A87-53954

**ELEMENTS OF LINEAMENT TECTONICS [OSNOVY LINEAMENTNOI TEKTONIKI]**

IAKOV GIRSHEVICH KATS, ANATOLII IVANOVICH POLETAEV, and ELIA FEDOROVNA RUMIANTSEVA Moscow, Izdatel'stvo Nedra, 1986, 144 p. In Russian. refs

The evolution of lineament tectonics as an independent branch of geotectonics is discussed together with the methods of lineament analysis, and their interpretation and classification. Consideration is given to the lineament tectonics of ancient and modern continental platforms and folded mountainous zones, as well as to the lineament genesis and to the relationship of lineaments with known disturbances of the earth mantle. Special attention is given to the applications of the lineament tectonics in seismology and metallogeny, and in the search for potential sites of oil and gas deposits.

I.S.

N87-26466# Technische Univ., Graz (Austria). Inst. for Image Processing and Computer Graphics.

**STUDY ON THE USE AND CHARACTERISTICS OF SAR FOR GEOLOGICAL APPLICATIONS. PART 2: RADARGRAMMETRY ASPECTS Final Report**

G. DOMIK, E. KIENEGGER, F. LEBERL, and J. RAGGAM Paris, France ESA Jun. 1985 98 p

(Contract ESOC-5443/83-D-IM(SC))

(ESA-CR(P)-2325-PT-2; ETN-87-99980) Avail: NTIS HC A05/MF A01

The influence of imaging and flight parameters relevant in geological applications, such as the elevation angle and the flight direction, was investigated using radar imagery from experiments and simulated data. A geologically interesting test area was chosen to suggest processing algorithms for the creation of radar ortho images as a step to merge radar images to other data sets (e.g., data from geological maps) and subsequent nonlinear feature extraction. A method to create a digital elevation model from radar stereo images is presented. The influence of elevation angle and flight direction on the data quantity and quality is proved using a simulator.

ESA

N87-26467# Arbeitsgemeinschaft Geowissenschaftliche Fernerkundung, Munich (West Germany).

**STUDY ON THE USE AND CHARACTERISTICS OF SAR SYSTEMS FOR GEOLOGICAL APPLICATIONS Final Report**

Paris, France ESA 1987 301 p

(Contract ESA-5443/03)

(ESA-CR(P)-2342; ETN-87-99993) Avail: NTIS HC A14/MF A01

The history and theory of satellite radar geology are reviewed, and geological surveys using other standard remote sensing data are described. Processing algorithms for synthetic aperture radar (SAR) are discussed. A SAR system for radargrammetric and geological applications is defined.

ESA

N87-28119# Technische Univ., Munich (West Germany). Inst. for General and Applied Geology.

**INTEGRATION OF REMOTE SENSING AND GEOPHYSICAL DATA-APPLICATION TO EXPLORATION OF PYRITE ORE FACIES IN SW SPAIN**

P. VOLK In ESA Proceedings of the ESA/EARSel Europe from Space Symposium p 21-27 Dec. 1986

(Contract BMFT-01-QS-0730)

Avail: NTIS HC A14/MF A01

Information contents of remote sensing and geophysical data sets were assessed for mineral exploration. Aerial photographs and LANDSAT Thematic Mapper data provide a good basis for interpretation-optimized data-combination via an IHS, SST and HLF-Add approach. Two groups of thematic information were extracted: nondirect hints to ore facies (volcanogenic strata under sterile shallow cover); and direct hints to ore facies (anomalies related to physical properties of the ore itself). A field check and data about known mineralizations compared to the results obtained show good correlation.

ESA

N87-28120# Institut fuer Allgemeine und Angewandte Geophysik, Munich (West Germany).

**REQUIREMENTS ON RADAR DATA FOR GEOLOGICAL APPLICATION: A CASE STUDY BY USE OF MULTISTAGE DATA OF THE TESTSITE SARDEGNA/ITALY**

F. JASKOLLA and M. RAST (European Space Agency. European Space Research and Technology Center, ESTEC, Noordwijk, Netherlands) In ESA Proceedings of the ESA/EARSel Europe from Space Symposium p 29-34 Dec. 1986

Avail: NTIS HC A14/MF A01

Multitemporal LANDSAT MSS, Seasat-SAR, and multilook SIR-A and results from field investigations were used to assess the possibilities of radar geology in a Mediterranean site. Results show that radar data is very useful to support geological mapping purposes if it is correlated with other data sources. Structural investigations are limited due to geometric distortions. It is an absolute necessity to apply radargrammetric procedures; by doing this, the restricting factors due to radar geometry can be improved. Optimized results can be obtained by combining corrected radar data digitally with other information sources, e.g., LANDSAT MSS or TM.

ESA

N87-28121# Geological Survey of the Netherlands, Enschede. **SPOT: HOW GOOD FOR GEOLOGY? A COMPARISON WITH LANDSAT MSS**

A. SESOEREN In ESA Proceedings of the ESA/EARSel Europe from Space Symposium p 35-39 Dec. 1986

Avail: NTIS HC A14/MF A01

Geological interpretation possibilities of SPOT MSS and LANDSAT MSS positive prints enlarged to the same scale were compared, using as a test area part of the Jebel Amour (Algeria). The SPOT imagery offers many advantages, filling the gap between remote sensing from space and aerial photography. The best results by visual interpretation are obtained in combining SPOT for the required details with LANDSAT for the synoptic view. Further improvements are expected from the use of SPOT stereo-pairs.

ESA

N87-28200\*# Cornell Univ., Ithaca, N.Y. Dept. of Geological Sciences.

**MECHANISMS OF CRUSTAL DEFORMATION IN THE WESTERN US Final Technical Report, 13 May 1983 - 31 Jul. 1986**

DONALD L. TURCOTTE Jul. 1986 8 p

(Contract NAG5-319)

(NASA-CR-181230; NAS 1.26:181230) Avail: NTIS HC A02/MF A01 CSCL 08G

The deformation processes in the western United States were studied, considering both deterministic models and random or statistical models. The role of the intracrustal delamination and mechanisms of crustal thinning were also examined. The application of fractal techniques to understand how the crust is deforming was studied in complex regions. Work continued on the development of a fractal based model for deformation in the western United States. Fractal studies were also extended to the study of topography and the geoid.

B.G.

N87-28208\*# Jet Propulsion Lab., California Inst. of Tech., Pasadena.

**KINEMATICS AT THE INTERSECTION OF THE GARLOCK AND DEATH VALLEY FAULT ZONES, CALIFORNIA: INTEGRATION OF TM DATA AND FIELD STUDIES. LANDSAT TM INVESTIGATION PROPOSAL TM-019 Progress Report, 15 Jan. - 15 Aug. 1987**

MICHAEL ABRAMS and KEN VEROSUB (California Univ., Davis.) 1987 13 p Sponsored by NASA, Goddard Space Flight Center, Greenbelt, Md.

(NASA-CR-180666; NAS 1.26:180666) Avail: NTIS HC A02/MF A01 CSCL 08G

Processing and interpretation of Thematic Mapper (TM) data, extensive field work, and processing of SPOT data were continued. Results of these analyses led to the testing and rejecting of several of the geologic/tectonic hypotheses concerning the continuation of the Garlock Fault Zone (GFZ). It was determined that the Death



Valley Fault Zone (DVFZ) is the major through-going feature, extending at least 60 km SW of the Avawatz Mountains. Two 5 km wide fault zones were identified and characterized in the Soda and Bristol Mountains, forming a continuous zone of NW trending faulting. Geophysical measurements indicate a buried connection between the Avawatz and the Soda Mountains Fault Zone. Future work will involve continued field work and mapping at key locations, further analyses of TM data, and conclusion of the project. B.G.

## **N87-29574#** Joint Publications Research Service, Arlington, Va. **GEOMAGNETIC INTERSECTION OF TECTONIC STRUCTURES SEEN IN SPACE PHOTOGRAPHS Abstract Only**

M. I. BURLISHIN *In its* JPRS Report: Science and Technology. USSR: Space p 111 19 Aug. 1987 Transl. into ENGLISH from Issledovaniye Zemli iz Kosmosa (Moscow, USSR), no. 6, Nov. - Dec. 1986 p 32-37  
 Avail: NTIS HC A08/MF A01

Interpretation of space photographs yields information on positive tectonic structures in platform territories. Analysis of previous works indicates that positive tectonic structures of widely varied configurations are found by different authors in the same territory. An attempt is made here to analyze the reasons for this variety and to characterize the major types of intersections of tectonic structures. Recommendations are given for increasing the effectiveness of utilization of space photographs in geological structure studies. Author

# 05

## **OCEANOGRAPHY AND MARINE RESOURCES**

Includes sea-surface temperature, ocean bottom surveying imagery, drift rates, sea ice and icebergs, sea state, fish location.

## **A87-42746\*** Canada Centre for Inland Waters, Burlington (Ontario).

### **RADAR SCATTERING AND EQUILIBRIUM RANGES IN WIND-GENERATED WAVES WITH APPLICATION TO SCATTEROMETRY**

MARK A. DONELAN (Canada Centre for Inland Waters, Burlington) and WILLARD J. PIERSON, JR. (City College, New York) *Journal of Geophysical Research* (ISSN 0148-0227), vol. 92, May 15, 1987, p. 4971-5029. refs  
 (Contract NAGW-690)

To provide theoretical basis for the connection between observed radar scattering and wind-generated waves, a model for the response of surface waves in the gravity-capillary equilibrium region of the spectrum is proposed on the basis of a local (in wavenumber) balance between wind input and dissipation. The wind input function was constructed on the basis of laboratory observations of short-wave growth, while the dissipation function was developed from ideas of viscous dissipation and wave breaking in response to local accelerations and modified by kinematic effects of phase and group velocity differences. The model was exercised at L, C, X, and Ka bands to demonstrate the differences in wind speed and water temperature sensitivity. I.S.

## **A87-42748**

### **SOME ASPECTS OF THE SURFACE CIRCULATION SOUTH OF 20 DEG S REVEALED BY FIRST GARP GLOBAL EXPERIMENT DRIFTERS**

ALBERTO R. PIOLA, HORACIO A. FIGUEROA, and ALEJANDRO A. BIANCHI (Servicio de Hidrografia Naval, Departamento de Oceanografia, Buenos Aires, Argentina) *Journal of Geophysical Research* (ISSN 0148-0227), vol. 92, May 15, 1987, p. 5101-5114. Research supported by the Servicio de Hidrografia Naval and CONICET. refs  
 (Contract N0014-85-C-0020)

Daily averaged positions from about 280 satellite-tracked drifting buoys launched during the First GARP Global Experiment

are used to estimate the sea-surface current velocity field south of 20 deg S. The time-averaged surface velocity field based on velocity averages over 4 x 4-deg areas is used to construct the surface stream function. The gross features of the mean circulation are generally in agreement with other representations of the time-averaged circulation although they do differ in details from the climatological relative surface dynamic topographies in the southern hemisphere subtropical gyres. Mean and eddy horizontal momentum fluxes based on a 2 x 2-deg grid are estimated for the region south of 40 deg S. The zonally averaged momentum flux at the sea surface for the region of the Antarctic Circumpolar Current, from 40 to 60 deg S, leads to a momentum flux divergence of 60 sq cm/sq s, indicating a meridional flux of eastward momentum away from the current axis. Given the relatively large errors associated with the zonally averaged momentum fluxes, the sign of the flux divergence remains uncertain. Author

## **A87-42931**

### **STUDIES OF THE WAVELIKE PROCESS IN THE SURFACE TEMPERATURE FIELD OF THE EQUATORIAL PACIFIC USING METEOR-SATELLITE IR MEASUREMENTS [ISSLEDOVANIYE VOLNOOBRASNOGO PROTSESSA V POLE TEMPERATURY POVERKHNOSTI EKVATORIAL'NOI CHASTI TIKHOGO OKEANA PO DANNYM IK - IZMERENII S ISZ'METEOR']**

L. I. KOPROVA (AN SSSR, Institut Okeanologii, Moscow, USSR) and V. V. KALUGIN (AN SSSR, Institut Fiziki Atmosfery, Moscow, USSR) *Issledovanie Zemli iz Kosmosa* (ISSN 0205-9614), Jan.-Feb. 1987, p. 3-13. In Russian. refs

## **A87-43345\*** Texas A&M Univ., College Station.

### **MOISTURE BURSTS OVER THE TROPICAL PACIFIC OCEAN**

JAMES P. MCGUIRK, AYLMEER H. THOMPSON, and NEIL R. SMITH (Texas A&M University, College Station) *Monthly Weather Review* (ISSN 0027-0644), vol. 115, April 1987, p. 787-798. refs  
 (Contract NAS8-35182)

The frequency and location of moisture bursts are examined. A moisture burst is described and defined, and this definition is applied to IR imagery for four six-month cool seasons (November-April) in the eastern North Pacific. It is observed that about ten moisture bursts/month occur during the cool seasons; the bursts last about 2-4 days and no more than 10 days; and they are distributed uniformly across the Pacific to the west of 110 deg W. The relation between the moisture bursts and the El Nino event of 1982-1983, and moisture bursts in the general circulation are analyzed. The analyses reveal that few bursts occur in the region associated with the El Nino event, and the moisture bursts resemble transient intensification of the mean meridional circulation in regions with a weak Hadley cell. Two modes for the behavior of the Hadley cell in the Pacific are proposed. I.F.

## **A87-44289**

### **FOAM ACTIVITY ON THE SEA SURFACE AS A MARKOV RANDOM PROCESS [PENNAIA AKTIVNOST' NA MORSKOI POVERKHNOSTI KAK MARKOVSKII SLUCHAINYI PROTSESS]**

I. V. POKROVSKAIA and E. A. SHARKOV (AN SSSR, Institut Kosmicheskikh Issledovaniy, Moscow, USSR) *Akademiia Nauk SSSR, Doklady* (ISSN 0002-3264), vol. 293, no. 5, 1987, p. 1108-1111. In Russian.

An analysis of multispectral remote sensing data on the Caspian Sea indicates that the integer point process of sea-foam formation belongs to the class of Markov processes with stationary independent increments. The data also point to the existence of stable distribution laws of specific density in the static field of foam activity. In the language of branching processes, foam activity can be described as a random process of the inhomogeneous growth of populations with independent and noninteracting members having a finite lifetime. B.J.

A87-44679

**FROM SATELLITE ORBIT INTO THE EYE OF THE TYPHOON [S ORBITY SPUTNIKA - V GLAZ TAIFUNA]**

SERGEI NIKOLAEVICH BAIBAKOV and ALEKSANDR IVANOVICH MARTYNOV Moscow, Izdatel'stvo Nauka, 1986, 176 p. In Russian. refs

The use of satellites and balloons to study tropical cyclones is described in detail. Particular attention is given to models of tropical cyclones; the detection of cyclones from satellite orbit; and the insertion of probes (e.g. balloons) via descent modules into cyclones. The discussion touches on the use of satellites to study problems of oceanography and environment protection. B.J.

A87-44811\* California Univ., Santa Barbara.

**MULTIPLATFORM SAMPLING (SHIP, AIRCRAFT, AND SATELLITE) OF A GULF STREAM WARM CORE RING**

RAYMOND C. SMITH (California, University, Santa Barbara), OTIS B. BROWN, FRANK E. HOGE (Miami, University, Florida), KAREN S. BAKER (NASA, Wallops Flight Center, Wallops), ROBERT H. EVANS (California, University, San Diego) et al. Applied Optics (ISSN 0003-6935), vol. 26, June 1, 1987, p. 2068-2081. refs (Contract N000-80-C-0042; NAGW-273; NAGW-290-2; NSF OCE-80-16991)

The purpose of this paper is to demonstrate the ability to meet the need to measure distributions of physical and biological properties of the ocean over large areas synoptically and over long time periods by means of remote sensing utilizing contemporaneous buoy, ship, aircraft, and satellite (i.e., multiplatform) sampling strategies. A mapping of sea surface temperature and chlorophyll fields in a Gulf Stream warm core ring using the multiplatform approach is described. Sampling capabilities of each sensing system are discussed as background for the data collected by means of these three dissimilar methods. Commensurate space/time sample sets from each sensing system are compared, and their relative accuracies in space and time are determined. The three-dimensional composite maps derived from the data set provide a synoptic perspective unobtainable from single platforms alone. Author

A87-44812\* National Aeronautics and Space Administration. Wallops Flight Center, Wallops Island, Va.

**RADIANCE-RATIO ALGORITHM WAVELENGTHS FOR REMOTE OCEANIC CHLOROPHYLL DETERMINATION**

FRANK E. HOGE, C. WAYNE WRIGHT (NASA, Wallops Flight Center, Wallops Island, VA), and ROBERT N. SWIFT (FG&G Washington Analytical Services, Inc., Pocomoke City, MD) Applied Optics (ISSN 0003-6935), vol. 26, June 1, 1987, p. 2082-2094. refs

Two-band radiance-ratio in-water algorithms in the visible spectrum have been evaluated for remote oceanic chlorophyll determination. Airborne active-passive (laser-solar) data from coastal, shelf-slope, and blue-water regions were used to generate two-dimensional chlorophyll-fluorescence and radiance-ratio statistical correlation matrices containing all possible two-band ratio combinations from the thirty-two available contiguous 11.25-nm passive bands. The principal finding was that closely spaced radiance-ratio bands yield chlorophyll estimates which are highly correlated with laser-induced chlorophyll fluorescence within several distinct regions of the ocean color spectrum. Band combinations in the yellow, orange-red, spectral regions showed considerable promise for satisfactory chlorophyll pigment estimation in near-coastal Case II waters. Pigment recovery in Case I waters was best accomplished using blue-green radiance ratios in the 490/500-nm region. Author

A87-44866\* Miami Univ., Coral Gables, Fla.

**CALIBRATION REQUIREMENTS AND METHODOLOGY FOR REMOTE SENSORS VIEWING THE OCEAN IN THE VISIBLE**

HOWARD R. GORDON (Miami, University, Coral Gables, FL) Remote Sensing of Environment (ISSN 0034-4257), vol. 22, June 1987, p. 103-126. refs (Contract NAS5-28798; NAGW-273)

The calibration requirements for ocean-viewing sensors are outlined, and the present methods of effecting such calibration are described in detail. For future instruments it is suggested that provision be made for the sensor to view solar irradiance in diffuse reflection and that the moon be used as a source of diffuse light for monitoring the sensor stability. Author

A87-45023

**UPWELLING FILAMENTS AND MOTION OF A SATELLITE-TRACKED DRIFTER ALONG THE WEST COAST OF NORTH AMERICA**

RICHARD E. THOMSON and JOHN E. PAPADAKIS (Institute of Ocean Sciences, Sidney, Canada) Journal of Geophysical Research (ISSN 0148-0227), vol. 92, June 15, 1987, p. 6445-6461. refs

Temperature, pressure, and positional data provided by an Argos-tracked surface buoy during the first 260 days of its course from the Vancouver Island towards Hawaii are analyzed. The buoy followed a mean equatorward course that resembled the expected course based on the climatological geopotential topography but was consistently to the right of the direction expected. The offset is presumably due to the effect of winds associated with the North Pacific High. The flow along the continental margin of the western U.S. was complicated by mesoscale processes. Seaward of the upwelling zone off Oregon and California, the buoy experienced five sinuous fluctuations with an amplitude of 50 km. Buoy temperature records combined with AVHRR imagery showed that these fluctuations were linked to strong surface currents associated with upwelling filaments. The buoy data indicate that these filaments were formed through distortion of the velocity fields by mesoscale eddies. I.S.

A87-45024\* Massachusetts Univ., Amherst.

**A MICROWAVE RADIOMETER WEATHER-CORRECTING SEA ICE ALGORITHM**

J. M. WALTERS, C. RUF, and C. T. SWIFT (Massachusetts, University, Amherst) Journal of Geophysical Research (ISSN 0148-0227), vol. 92, June 15, 1987, p. 6521-6534. refs (Contract NAGW-559)

A new algorithm for estimating the proportions of the multiyear and first-year sea ice types under variable atmospheric and sea surface conditions is presented, which uses all six channels of the SMMR. The algorithm is specifically tuned to derive sea ice parameters while accepting error in the auxiliary parameters of surface temperature, ocean surface wind speed, atmospheric water vapor, and cloud liquid water content. Not only does the algorithm naturally correct for changes in these weather conditions, but it retrieves sea ice parameters to the extent that gross errors in atmospheric conditions propagate only small errors into the sea ice retrievals. A preliminary evaluation indicates that the weather-correcting algorithm provides a better data product than the 'UMass-AES' algorithm, whose quality has been cross checked with independent surface observations. The algorithm performs best when the sea ice concentration is less than 20 percent. I.S.



**A87-45816**

## **SATELLITE ALTIMETER MEASUREMENTS OF THE GEOID IN SEA ICE ZONES**

S. W. LAXON and C. G. RAPLEY (London, University College, Dorking, England) (COSPAR, International Association of Geodesy, and Inter-Union Commission on the Lithosphere, Plenary Meeting, 26th, Symposium on Solid Earth Geophysics and Satellite Orbits, 2nd, and Topical Meeting, Toulouse, France, June 30-July 11, 1986) *Advances in Space Research* (ISSN 0273-1177), vol. 6, no. 9, 1986, p. 99-102. refs

The Seasat radar altimeter provided surface height measurements to a precision better than 10 cm over the open ocean. The data have been used to produce maps of the ocean geoid which reveal details of sub-surface topography such as sea mounts, ocean trenches and mid-ocean ridges 1.. In areas of the ocean covered by sea ice, however, the quasi-specular ice returns which occurred were incorrectly handled by the on-board processor. This resulted in a significant decrease in the precision of the surface height estimates. Consequently, researchers have generally eliminated data from regions where sea ice is suspected to have been present, including large areas of the Antarctic ocean. A technique was developed for significantly improving the height measurements over such areas permitting the mapping of the geoid in such regions. The short wavelength RMS deviation of elevation measurements from collinear passes over such areas has been reduced from 1.032m to 0.632m. The application of the technique to ERS-1 altimeter data will be particularly important, since coverage of a substantial area of the Arctic ocean (up to 82 percent latitude) will be possible for the first time. Author

**A87-46311**

## **CORAL REEF SURVEY METHOD FOR VERIFICATION OF LANDSAT MSS IMAGE DATA**

DEBORAH A. KUCHLER (CSIRO, Div. of Water and Land Resources, Canberra, Australia), CHRISTINE MAGUIRE, ANTHONY MCKENNA (Australian Institute of Marine Science, Townsville, Australia), ROGER PRIEST, and JOHN R. MELLOR (Australian Survey Office, Brisbane, Australia) *ITC Journal* (ISSN 0303-2434), no. 3, 1986, p. 217-223. Research supported by the Great Barrier Reef Marine Park Authority. refs

The use of remote sensing techniques demands some method for checking the accuracy of the data obtained. 'Survey controlled reef assessment' (SCRA) is a survey method developed for the verification of Landsat MSS reef cover classification maps. It utilizes satellite-based ground control, remotely sensed images and visual observation. Data collection and assignment to a quadrat with known geographic coordinates allows its integration with ancillary data. A recent exercise on Hardy Reef, Great Barrier Reef, Australia is used as an example. Author

**A87-46403**

## **CLIMATOLOGICAL IMPLICATIONS OF A SATELLITE-BORNE SAR IMAGING THE SEA SURFACE**

B. FISCELLA, P. P. LOMBARDINI, P. TRIVERO, and C. CAPPA (Torino, Università; CNR, Istituto di Cosmogeofisica, Turin, Italy) *Nuovo Cimento C, Serie 1* (ISSN 0390-5551), vol. 10 C, Mar.-Apr. 1987, p. 162-168. refs

The possibility of deriving meteorological data from SAR images taken in low and strong wind conditions is discussed. In low wind conditions, SAR images of marine data depend on the spatial distribution of wind surface stress. A method for extracting local wind direction and median wavelength of the turbulent spectrum from SAR images is described. The relation between the median wavelength of the mesoscale turbulence and the Reynolds number is studied. Under strong wind conditions, SAR images are characterized by the appearance of arrays parallel equidistant traces revealing the presence of long sea waves; these long sea waves in the SAR images provide data on atmospheric turbulence. It is noted that under low wind conditions the SAR images are useful for the mapping of tropospheric mesoscale eddies, and from high wind SAR images the effects of coastal obstacles in the wind field can be derived. I.F.

**A87-46539**

## **REMOTE OBSERVATIONS OF THE MARINE ENVIRONMENT - SPATIAL HETEROGENEITY OF THE MESOSCALE OCEAN COLOR FIELD IN CZCS IMAGERY OF CALIFORNIA NEAR-COASTAL WATERS**

VITTORIO BARALE (California, University, La Jolla) *Remote Sensing of Environment* (ISSN 0034-4257), vol. 22, July 1987, p. 173-186. refs

**A87-46542\*** Bigelow Lab. for Ocean Sciences, West Boothbay Harbor, Maine.

## **REMOTE SENSING OF SUBMERGED AQUATIC VEGETATION IN LOWER CHESAPEAKE BAY - A COMPARISON OF LANDSAT MSS TO TM IMAGERY**

S. G. ACKLESON (Bigelow Laboratory for Ocean Science, Boothbay Harbor, ME) and V. KLEMAS (Delaware, University, Newark) *Remote Sensing of Environment* (ISSN 0034-4257), vol. 22, July 1987, p. 235-248. refs  
(Contract NAS5-27580; NAGW-374)

Landsat MSS and TM imagery, obtained simultaneously over Guinea Marsh, VA, as analyzed and compares for its ability to detect submerged aquatic vegetation (SAV). An unsupervised clustering algorithm was applied to each image, where the input classification parameters are defined as functions of apparent sensor noise. Class confidence and accuracy were computed for all water areas by comparing the classified images, pixel-by-pixel, to rasterized SAV distributions derived from color aerial photography. To illustrate the effect of water depth on classification error, areas of depth greater than 1.9 m were masked, and class confidence and accuracy recalculated. A single-scattering radiative-transfer model is used to illustrate how percent canopy cover and water depth affect the volume reflectance from a water column containing SAV. For a submerged canopy that is morphologically and optically similar to *Zostera marina* inhabiting Lower Chesapeake Bay, dense canopies may be isolated by masking optically deep water. For less dense canopies, the effect of increasing water depth is to increase the apparent percent crown cover, which may result in classification error. Author

**A87-46690#**

## **OCEANOGRAPHIC AND GEOPHYSICAL APPLICATIONS OF SATELLITE ALTIMETRY**

B. C. DOUGLAS, D. C. MCADOO, and R. E. CHENEY (NOAA, National Geodetic Survey, Rockville, MD) *Reviews of Geophysics* (ISSN 8755-1209), vol. 25, June 1987, p. 875-880. refs

Since the last quadrennial report, new satellite altimeter data have not been generally available. Nevertheless, important progress has been made from analyses of GEOS 3 and Seasat data. The marine gravity field has been determined to an extraordinary resolution and accuracy, and important solid earth geophysical interpretations made. In the area of oceanography, statistical estimates of the variability of dynamic topography have been published, methods for incorporating altimeter data into numerical models have been developed and applied, and tentative, but interesting determinations of the mean circulation have been made. In addition, altimeter waveform analysis has made it possible to use altimeter data to determine elevations of major ice fields. Finally, important new insights into the nature of satellite ephemeris error and its influence on altimetrically derived sea surface topography have been achieved. Author

A87-47291

**MESOSCALE EDDIES IN THE FRAM STRAIT MARGINAL ICE ZONE DURING THE 1983 AND 1984 MARGINAL ICE ZONE EXPERIMENTS**

J. A. JOHANNESSEN, O. M. JOHANNESSEN, E. SVENDSEN (Bergen, Universitetet, Norway), R. SHUCHMAN (Michigan, Environmental Research Institute, Ann Arbor), T. MANLEY (Lamont-Doherty Geological Observatory, Palisades, NY) et al. *Journal of Geophysical Research* (ISSN 0148-0227), vol. 92, June 30, 1987, p. 6754-6772. Research supported by the Bergen Universitetet, Norges Teknisk-Naturvitenskapelige Forskningsrad, Norges Almenvitenskapelige Forskningsrad, Navy, and USGS; Centre National pour l'Exploitation l' Exploitation des Oceans. refs

(Contract CNEXO-83/3147; CNRS-98-1022; CEC-CLI-083-F)

Fourteen mesoscale eddies, in both deep and shallow water, were studied between 78 and 81 deg N during the summer Marginal Ice Zone Experiment (MIZEX) in Fram Strait in 1983 and 1984. To provide a detailed picture of eddies, the MIZEX '83 and MIZEX '84 used a variety of observational techniques, including satellite and aircraft remote sensing, standard conductivity-temperature-depth (CTD) sections from ships and helicopters, the drift of surface and subsurface floats, current meter measurements, and Cyclesonde measurements. Typical scales of the eddies in the marginal ice zone were found to be 20-40 km, and typical lifetimes were at least 20 to 30 days. Rotation was mainly cyclonic with a maximum speed, in some cases subsurface, of up to 40 cm/s. Five generation sources are suggested for these eddies. I.S.

A87-47292\* Geological Survey, Tacoma, Wash.

**VARIATIONS OF MESOSCALE AND LARGE-SCALE SEA ICE MORPHOLOGY IN THE 1984 MARGINAL ICE ZONE EXPERIMENT AS OBSERVED BY MICROWAVE REMOTE SENSING**

W. J. CAMPBELL, E. G. JOSBERGER (USGS, Tacoma, WA), P. GLOERSEN (NASA, Goddard Space Flight Center, Greenbelt, MD), O. M. JOHANNESSEN (Bergen, Universitetet, Norway), P. S. GUEST (U.S. Naval Postgraduate School, Monterey, CA) et al. *Journal of Geophysical Research* (ISSN 0148-0227), vol. 92, June 30, 1987, p. 6805-6824. Research supported by the Institut Geographique National, Canada Centre for Remote Sensing, U.S. Navy, CNES, and NASA. refs

The data acquired during the summer 1984 Marginal Ice Zone Experiment in the Fram Strait-Greenland Sea marginal ice zone, using airborne active and passive microwave sensors and the Nimbus 7 SMMR, were analyzed to compile a sequential description of the mesoscale and large-scale ice morphology variations during the period of June 6 - July 16, 1984. Throughout the experiment, the long ice edge between northwest Svalbard and central Greenland meandered; eddies were repeatedly formed, moved, and disappeared but the ice edge remained within a 100-km-wide zone. The ice pack behind this alternately diffuse and compact edge underwent rapid and pronounced variations in ice concentration over a 200-km-wide zone. The high-resolution ice concentration distributions obtained in the aircraft images agree well with the low-resolution distributions of SMMR images. I.S.

A87-47293\* Environmental Research Inst. of Michigan, Ann Arbor.

**EVOLUTION OF MICROWAVE SEA ICE SIGNATURES DURING EARLY SUMMER AND MIDSUMMER IN THE MARGINAL ICE ZONE**

R. G. ONSTOTT (Michigan Environmental Research Institute, Ann Arbor), T. C. GRENFELL (Washington, University, Seattle), C. MATZLER (Bern, Universitaet, Bern, Switzerland), C. A. LUTHER (U.S. Navy, Washington, DC), and E. A. SVENDSEN (Bergen, Universitetet, Norway) *Journal of Geophysical Research* (ISSN 0148-0227), vol. 92, June 30, 1987, p. 6825-6835. refs (Contract N00014-81-K-0460; N00014-85-K-0200; NAGW-334)

Emissivities at frequencies from 5 to 94 GHz and backscatter at frequencies from 1 to 17 GHz were measured from sea ice in Fram Strait during the marginal Ice Zone Experiment in June and

July of 1983 and 1984. The ice observed was primarily multiyear; the remainder, first-year ice, was often deformed. Results from this active and passive microwave study include the description of the evolution of the sea ice during early summer and midsummer; the absorption properties of summer snow; the interrelationship between ice thickness and the state and thickness of snow; and the modulation of the microwave signature, especially at the highest frequencies, by the freezing of the upper few centimeters of the ice. Author

A87-47294

**USE OF SYNTHETIC APERTURE RADAR-DERIVED KINEMATICS IN MAPPING MESOSCALE OCEAN STRUCTURE WITHIN THE INTERIOR MARGINAL ICE ZONE**

T. O. MANLEY (Lamont-Doherty Geological Observatory, Palisades, NY), R. A. SHUCHMAN, and B. A. BURNS (Michigan, Environmental Research Institute, Ann Arbor) *Journal of Geophysical Research* (ISSN 0148-0227), vol. 92, June 30, 1987, p. 6837-6842. refs (Contract N00014-83-C-0132; N00014-81-C-0295; N00014-83-C-0404)

A87-47295\* Environmental Research Inst. of Michigan, Ann Arbor.

**MULTISENSOR COMPARISON OF ICE CONCENTRATION ESTIMATES IN THE MARGINAL ICE ZONE**

B. A. BURNS (Michigan, Environmental Research Institute, Ann Arbor), D. J. CAVALIERI, P. GLOERSEN (NASA, Goddard Space Flight Center, Greenbelt, MD), M. R. KELLER (U.S. Navy, Naval Research Laboratory, Washington, DC), W. J. CAMPBELL (USGS, Tacoma, WA) et al. *Journal of Geophysical Research* (ISSN 0148-0227), vol. 92, June 30, 1987, p. 6843-6856. NASA-Navy-supported research. refs

Aircraft remote sensing data collected during the 1984 summer Marginal Ice Zone Experiment in the Fram Strait are used to compare ice concentration estimates derived from synthetic aperture radar (SAR) imagery, passive microwave imagery at several frequencies, aerial photography, and spectral photometer data. The comparison is carried out not only to evaluate SAR performance against more established techniques but also to investigate how ice surface conditions, imaging geometry, and choice of algorithm parameters affect estimates made by each sensor. Active and passive microwave sensor estimates of ice concentration derived using similar algorithms show an rms difference of 13 percent. Agreement between each microwave sensor and near-simultaneous aerial photography is approximately the same (14 percent). The availability of high-resolution microwave imagery makes it possible to ascribe the discrepancies in the concentration estimates to variations in ice surface signatures in the scene. Author

A87-47296

**BOUNDARY LAYER, UPPER OCEAN, AND ICE OBSERVATIONS IN THE GREENLAND SEA MARGINAL ICE ZONE**

JAMES H. MORISON, GARY A. MAYKUT (Washington, University, Seattle), and MILES G. MCPHEE (McPhee Research Co., Yakima, WA) *Journal of Geophysical Research* (ISSN 0148-0227), vol. 92, June 30, 1987, p. 6987-7011. refs (Contract N00014-84-C-0111; N00014-78-C-0135; N00014-84-C-0028)

A heat and mass balance study of the summer marginal ice zone of the Greenland Sea was conducted during the 1984 Marginal Ice Zone Experiment. The measurements were made at two drifting ice-stations and included ocean boundary layer turbulence observations, water temperature profiles, salinity, wind and ice velocities, ice ablation, ice concentration, solar radiation, and spectral albedos. The ice and upper ocean conditions encountered during the experiment and the magnitude and the importance of inertial motions, tides, eddies, and large-scale currents were evaluated and are discussed in the context of ice-ocean interactions. Vertical fluxes of heat and momentum at the underside of the ice were calculated and used to construct time histories of drag and heat transfer coefficients. Variations of these coefficients are shown to reveal much about the structure of the boundary

layer adjacent to the ice and about processes that impact vertical fluxes. I.S.

**A87-47297\*** National Aeronautics and Space Administration. Goddard Space Flight Center, Greenbelt, Md.

## **SATELLITE COLOR OBSERVATIONS OF SPRING BLOOMING IN BERING SEA SHELF WATERS DURING THE ICE EDGE RETREAT IN 1980**

NANCY G. MAYNARD (NASA, Goddard Space Flight Center, Greenbelt, MD; California, University, La Jolla) and DENNIS K. CLARK (NOAA, National Environmental Satellite, Data, and Information Service, Washington, DC) *Journal of Geophysical Research* (ISSN 0148-0227), vol. 92, June 30, 1987, p. 7127-7139. refs

The temporal and spatial development of the ice-edge bloom and the spring open-water bloom on the eastern Bering Sea shelf was studied using CZCS images of the eastern Bering Sea between April 27 and July 22, 1980. Images of the Norton Sound area taken during the period of ice breakup show that the influence of ice melt on phytoplankton growth is particularly significant where the ice is actively melting. Significant levels (5-30 mg/cu m) of chlorophyll could be seen trailing the ice pack as it melted and moved northward and westward in late April and early May. In the ice-free eastern Bering Sea midsummer image, a northwesterly oriented band of high pigment concentration was seen in the area of the outer domain, suggesting periodic offshore movements of shelf waters. I.S.

**A87-47298\*#** National Aeronautics and Space Administration. Goddard Space Flight Center, Greenbelt, Md.

## **ON THE RELATIONSHIP BETWEEN ATMOSPHERIC CIRCULATION AND THE FLUCTUATIONS IN THE SEA ICE EXTENTS OF THE BERING AND OKHOTSK SEAS**

D. J. CAVALIERI and C. L. PARKINSON (NASA, Goddard Space Flight Center, Greenbelt, MD) *Journal of Geophysical Research* (ISSN 0148-0227), vol. 92, June 30, 1987, p. 7141-7162. refs

The influence of the hemispheric atmospheric circulation on the sea ice covers of the Bering Sea and the Sea of Okhotsk is examined using data obtained with the Nimbus 5 electrically scanning microwave radiometer for the four winters of the 1973-1976 period. The 3-day averaged sea ice extent data were used to establish periods for which there is an out-of-phase relationship between fluctuations of the two ice covers. A comparison of the sea-level atmospheric pressure field with the seasonal, interannual, and short-term sea ice fluctuations reveal an association between changes in the phase and the amplitude of the long waves in the atmosphere and advance and retreat of Arctic ice covers. I.S.

**A87-47299\*** Jet Propulsion Lab., California Inst. of Tech., Pasadena.

## **BEAUFORT-CHUKCHI ICE MARGIN DATA FROM SEASAT - ICE MOTION**

FRANK CARSEY and BENJAMIN HOLT (California Institute of Technology, Jet Propulsion Laboratory, Pasadena) *Journal of Geophysical Research* (ISSN 0148-0227), vol. 92, June 30, 1987, p. 7163-7172. refs

The motion of sea ice in the summer and fall marginal zone of the Beaufort and Chukchi seas is observed by tracking ice features in sequential Seasat synthetic aperture radar images. Four examples of ice motion fields are shown and discussed with translation observation density finer than one observation per 5 km for the most part. In this region the components of proportional relative motion are shown to commonly have values in the range 0.1 to 0.25/day throughout the marginal zone, which itself has a scale of the order of 100 km. Author

**A87-47300\*** Washington Univ., Seattle.

## **SHUTTLE IMAGING RADAR B (SIR-B) WEDDELL SEA ICE OBSERVATIONS - A COMPARISON OF SIR-B AND SCANNING MULTICHANNEL MICROWAVE RADIOMETER ICE CONCENTRATIONS**

SEELYE MARTIN (Washington, University, Seattle), BENJAMIN HOLT (California Institute of Technology, Jet Propulsion Laboratory, Pasadena), DONALD J. CAVALIERI (NASA, Goddard Space Flight Center, Greenbelt, MD), and VERNON SQUIRE (Cambridge University, England) *Journal of Geophysical Research* (ISSN 0148-0227), vol. 92, June 30, 1987, p. 7173-7179. Research supported by British Petroleum, Ltd., U.S. Navy, and NERC. refs (Contract NAGW-700)

Ice concentrations over the Weddell Sea were studied using SIR-B data obtained during the October 1984 mission, with special attention given to the effect of ocean waves on the radar return at the ice edge. Sea ice concentrations were derived from the SIR-B data using two image processing methods: the classification scheme at JPL and the manual classification method at Scott Polar Research Institute (SPRI), England. The SIR ice concentrations were compared with coincident concentrations from the Nimbus-7 SMMR. For concentrations greater than 40 percent, which was the smallest concentration observed jointly by SIR-B and the SMMR, the mean difference between the two data sets for 12 points was 2 percent. A comparison between the JPL and the SPRI SIR-B algorithms showed that the algorithms agree to within 1 percent in the interior ice pack, but the JPL algorithm gives slightly greater concentrations at the ice edge (due to the fact that the algorithm is affected by the wind waves in these areas). I.S.

**A87-48176**

## **ANALYSIS OF COSMOS-1500 RADAR IMAGES OF THE OCEAN SURFACE IN A ZONE OF CYCLONES AND MESOSCALE CLOUD FORMATIONS [ANALIZ RADIOLOKATSIONNYKH IZOBRAZHENII POVERKHNOSTI OKEANA V ZONE DEISTVIA TSIKLONOV I MEZOMASSHTABNYKH OBLACHNYKH OBRAZOVANII PO DANNYM ICZ 'KOSMOS-1500']**

O. V. SHUL'GIN (AN USSR, Morskoi Gidrofizicheskii Institut, Sevastopol, Ukrainian SSR) *Issledovanie Zemli iz Kosmosa* (ISSN 0205-9614), Mar.-Apr. 1987, p. 3-11. In Russian. refs

An analysis of the Cosmos-1500 radar imagery shows that the ocean surface in a zone of cyclones and mesoscale cloud formations has a specific pattern which depends on the wind-field characteristics. Sidelooking-radar imagery of Hurricane Diana off the coast of Florida in September 1984 is considered as an example. It is noted that a better understanding of the typical occurrence of atmospheric formations can reduce errors in the identification of brightness contrasts on radar images which appear to be due to hydrodynamic processes in the ocean. B.J.

**A87-48177**

## **MEASUREMENT OF CURRENTS ACCORDING TO THE DRIFT OF SUBSATELLITE BUOYS [IZMERENIE TECHENII PO DREIFU PODSPUTNIKOVYKH BUEV]**

S. V. MOTYZHEV, I. I. BEKHTEREV, N. I. KIIASHCHENKO, V. L. KOTLIAROV, and A. G. KARASEV (AN USSR, Morskoi Gidrofizicheskii Institut, Sevastopol; L'vovskii Politekhnikheskii Institut, Lvov, *Issledovanie Zemli iz Kosmosa* (ISSN 0205-9614), Mar.-Apr. 1987, p. 12-16. In Russian. refs

Specific applications of subsatellite drift buoys in the study of ocean surface currents are described. The least squares method is used to calculate the mean buoy drift velocity vector according to navigation-satellite data. Attention is given to measurements of tropical Atlantic currents performed in the framework of the Razrezy program by LOBAN drift buoys with COSPAS instrumentation. It is shown that the countercurrent in the northwestern part of the tropical Atlantic has a nonzonal nature in the winter and can break up into a system of eddies in the spring. B.J.

A87-48178

**ESTIMATION OF ERRORS IN THE DETERMINATION OF SEA SURFACE TEMPERATURE AND ATMOSPHERIC MOISTURE CONTENT FROM SATELLITE MEASUREMENTS OF OUTGOING IR RADIATION IN THE 10.5-12.5 MICRON RANGE [OTSENKA POGRESHNOSTEI OPREDELENIYA TEMPERATURY POVERKHNOSTI OKEANA I VLAGOSODERZHANIYA ATMOSFERY PO DANNYM SPUTNIKOVYKH IZMERENII UKHODIASHCHEGO IKIZLUCHENIYA V DIAPAZONE 10,5-12,5 MKM]**

V. M. SUTOVSKII, A. B. USPENSKII, and E. I. ROZANOVA (Gosudarstvennyi Nauchno-Issledovatel'skii Tsentr Izucheniya Prirodnykh Resursov, Moscow, USSR) *Issledovanie Zemli iz Kosmosa* (ISSN 0205-9614), Mar.-Apr. 1987, p. 17-23. In Russian. refs

Statistical and regression algorithms for the remote sensing of the sea surface temperature and the integral moisture content of the atmosphere are applied to NOAA-7 data on outgoing radiation in the 10.5-12.5-micron range. The accuracy of these procedures is estimated on the basis of archival data comprising concurrent satellite, radio balloon, and ship measurements. The temperature estimation error is close to predicted error limits, while the moisture-content estimation error is less accurate, which may be attributed to a relatively low moisture content in the environment considered. B.J.

A87-48180

**DIVERGENT REDISTRIBUTION OF ICE IN THE ARCTIC OCEAN (ANALYSIS OF SPACE IMAGERY) [DIVERGENTNOE PERERASPREDELENIE L'DOV V SEVERNOM LEDOVITOM OKEANE /K ANALIZU KOSMICHESKIKH IZOBRAZHENII/]**

M. NAZIROV (Gosudarstvennyi Nauchno-Issledovatel'skii Tsentr Izucheniya Prirodnykh Resursov, Moscow, USSR) *Issledovanie Zemli iz Kosmosa* (ISSN 0205-9614), Mar.-Apr. 1987, p. 30-36. In Russian. refs

An analysis of Meteor-satellite imagery shows that the divergence of tidal currents is the main factor responsible for the formation of the spatial structure of the Arctic ice cover. The analysis reveals regular patterns in the generation and development of trans-Arctic passages suitable for navigation. B.J.

A87-48181

**EVALUATION OF THE EFFECT OF HYDROMETEORS ON THE CHARACTERISTICS OF RADAR IMAGES OF SEA ICE [OTSENKA VLIYANIYA GIDROMETEOROV NA KHA RAKTERISTIKI RADIOLOKATSIONNYKH IZOBRAZHENII MORSKIKH L'DOV]**

V. I. ALEKSANDROV (Arkticheskii i Antarkicheskii Nauchno-Issledovatel'skii Institut, Leningrad, USSR) *Issledovanie Zemli iz Kosmosa* (ISSN 0205-9614), Mar.-Apr. 1987, p. 37-43. In Russian. refs

The effect of hydrometeors on the features of aerial and space sidelooking-radar images of sea ice is calculated, and the results are correlated with aerial observations of Arctic sea ice in the presence of precipitation. It is shown that the effects of clouds (without precipitation), fog, and snow on the image characteristics are negligible. The power of the received signal is reduced somewhat when the precipitation zone is located over the entire survey band; the reduction is 1 dB for satellite imagery and 6 dB for aerial imagery. When the precipitation zone has a frontal location with respect to the radar, intense precipitation can completely mask the ice-cover image. B.J.

A87-48184

**MAXIMUM ACCURACY OF SATELLITE-BORNE SCATTEROMETER MEASUREMENTS OF WIND VELOCITY ABOVE THE OCEAN [O PREDEL'NOI TOCHNOSTI SKATTEROMETRICHESKOGO OPREDELENIYA SO SPUTNIKA SKOROSTI VETRA NAD OKEANOM]**

G. N. KHRISTOFOROV, A. S. ZAPEVALOV, and V. E. SMOLOV (AN USSR, Morskoi Gidrofizicheskii Institut, Sevastopol, Ukrainian SSR) *Issledovanie Zemli iz Kosmosa* (ISSN 0205-9614), Mar.-Apr. 1987, p. 57-65. In Russian. refs

Errors in determining wind velocities from scatterometer measurements are assessed, and it is shown that the highest accuracy of wind-field determination is about  $\pm 1$  m/s over the 4-17 m/s range. It is found that the velocity of weak winds cannot be accurately determined from remote measurements of sea ripple, while for velocities higher than 4 m/s the accuracy of scatterometer measurements is limited by a statistical spread of  $\pm 1-2$  m/s. B.J.

A87-48362

**THE VARIABILITY OF THE NORTH ATLANTIC MARINE ATMOSPHERE AND ITS RELEVANCE TO REMOTE SENSING**

P. J. MINNETT (SERC, Rutherford Appleton Laboratory, Chilton, England), J. R. EYRE, and R. W. PESCOD (Meteorological Office, Oxford, England) *International Journal of Remote Sensing* (ISSN 0143-1161), vol. 8, June 1987, p. 871-880. refs

Results are presented describing the seasonal changes in the marine atmosphere of variables relevant to infrared remote sensing from satellites and aircraft. The area is restricted to that of the north-eastern Atlantic Ocean and adjacent seas. The description has been derived from a large number of radiosonde profiles from the archive of the U.K. Meteorological Office. Author

A87-48363

**OCEAN WAVE PARAMETER MEASUREMENT USING A DUAL-RADAR SYSTEM - A SIMULATION STUDY**

LUCY R. WYATT (Birmingham, University, England) *International Journal of Remote Sensing* (ISSN 0143-1161), vol. 8, June 1987, p. 881-891. SERC-supported research. refs

The accurate measurement of ocean wave parameters using a single narrow-beam HF radar has been shown to be limited to particular wave field/radar beam configurations. In addition, because of symmetries in the scattering process, it is not possible to determine whether estimated wave directions are to the left or right of the radar beam. Measurement of the long-wave directional spectrum has also been limited by a requirement for at least 50 dB dynamic range in the Doppler spectrum of the backscattered radar signal. This paper describes the application of a model-fitting technique to a dual-radar system which overcomes the limitations found for a single system. Author

A87-48829#

**OPERATIONAL USE OF REMOTE SENSING FOR COMMERCIAL ARCTIC CLASS VESSEL NAVIGATION**

A. R. SNEYD, M. P. LUCE, R. W. GORMAN, D. DEER, and D. MILLER (Canarctic Shipping Co., Ltd., Ottawa, Canada) IN: Canadian Symposium on Remote Sensing, 10th, Edmonton, Canada, May 5-8, 1986, Proceedings. Volume 1. Ottawa, Canadian Aeronautics and Space Institute, 1987, p. 273-280. refs

A shipboard ice navigation support system (SINSS), developed in Canada for the needs of commercial Arctic-class vessels for navigation in ice-covered waters, is described. The SINSS uses remotely sensed data obtained from the STAR-1 SAR and an on-board computer-enhanced radar image display system. The SAR imagery was found to provide information of the quality required for confident decision making in the hazardous ice environments of the Arctic. The work efforts during the 1986 shipping season will involve the assessment of the SINSS subsystems in the thick first-year ice of the northern Baffin Bay in May, old ice and decayed first-year ice in the central Parry Channel in August, and the highly dynamic old ice and developing first-year ice in the Lancaster Sound during the October-January period. I.S.

**A87-48837#**

**INTEGRATED MULTI-TEMPORAL AERIAL PHOTOGRAPHY AND DIGITAL MAPPING FOR COASTAL MONITORING, CAPE BRETON ISLAND, NOVA SCOTIA**

B. R. BOWLEY, M. L. MCCOURT, and C. A. SPEIGHT (Maritime Resource Management Service, Inc., Amherst, Canada) IN: Canadian Symposium on Remote Sensing, 10th, Edmonton, Canada, May 5-8, 1986, Proceedings. Volume 1. Ottawa, Canadian Aeronautics and Space Institute, 1987, p. 349-354.

**A87-48842#**

**USING NOAA AVHRR IN STUDIES OF SEA ICE MOTION IN THE BEAUFORT SEA**

J. Y. CHERNIAWSKY, J. F. R. GOWER (G.A. Borstad Associates, Ltd., Sidney, Canada), H. MELLING, D. N. TRUAX (Institute for Ocean Sciences, Sidney, Canada), and R. C. KERR (Apocalypse Enterprises, Ltd., Victoria, Canada) IN: Canadian Symposium on Remote Sensing, 10th, Edmonton, Canada, May 5-8, 1986, Proceedings. Volume 1. Ottawa, Canadian Aeronautics and Space Institute, 1987, p. 395-403. Research sponsored by Institute of Ocean Sciences.

**A87-48843#**

**REMOTE SENSING IN SUPPORT OF ECOLOGICAL STUDIES OF THE BOWHEAD WHALE**

G. A. BORSTAD (G.A. Borstad Associates, Ltd., Sidney, Canada) IN: Canadian Symposium on Remote Sensing, 10th, Edmonton, Canada, May 5-8, 1986, Proceedings. Volume 1. Ottawa, Canadian Aeronautics and Space Institute, 1987, p. 405-412. refs

Airborne and satellite remote sensing of water color and temperature in the Beaufort Sea suggest that to a large extent, the movements and congregations of the bowhead whale (*Balaena mysticetus*) are related to variability in its oceanic environment. Large numbers of plankton-eating bowheads are often found in the vicinity of oceanographic fronts which are remotely detectable as abrupt changes in temperature or color. This paper outlines the remote sensing methods used in several related studies between 1983 and 1985, including a real-time spectrometer system used in aerial surveys of the north Alaskan coast in September 1985. An example of satellite data is presented, and the distributions of bowhead whales obtained through separate but coincident visual surveys are compared. Author

**A87-48849#**

**THE INFLUENCE OF MELTING CONDITIONS ON THE INTERPRETATION OF RADAR IMAGERY OF SEA ICE**

R. T. LOWRY (Intera Technologies, Ltd., Calgary, Canada), D. J. LAPP (Norland Science and Engineering, Ltd., Ottawa, Canada), and A. R. SNEYD (Canarctic Shipping Co., Ltd., Ottawa, Canada) IN: Canadian Symposium on Remote Sensing, 10th, Edmonton, Canada, May 5-8, 1986, Proceedings. Volume 1. Ottawa, Canadian Aeronautics and Space Institute, 1987, p. 473-480.

Airborne radar imagery has become one of the principle sources of both strategic and tactical ice information in the Arctic. However, important interpretation clues are lost when the radar data are collected over melting ice. This problem has been studied during the course of several studies and operational missions associated with the sailings of the M.V. Arctic in the High Arctic. The associated data set consists of SAR imagery taken with the STAR-1 radar over the same ice during the winter and later during melting conditions. Detailed analysis of first-year and old ice has shown that the melt dramatically reduces contrast between ice types. Later, some contrast between ice types returns, which is significant as later in the melt season, the older ice gets much softer and less hazardous, whereas earlier it still has the properties of winter ice. Author

**A87-48851#**

**MANAGING CORAL REEFS - OPERATIONAL BENEFITS OF REMOTE SENSING IN MARINE PARK PLANNING**

A. VAN R. CLAASEN, R. A. KENCHINGTON, and T. S. SHEARN (Great Barrier Reef Marine Park Authority, Townsville, Australia) IN: Canadian Symposium on Remote Sensing, 10th, Edmonton, Canada, May 5-8, 1986, Proceedings. Volume 1. Ottawa, Canadian Aeronautics and Space Institute, 1987, p. 489-496. refs

**A87-48876#**

**ICEBERG DETECTION USING SLAR**

V. L. SHAW (F.G. Bercha and Associates (Alberta), Ltd., Calgary, Canada) IN: Canadian Symposium on Remote Sensing, 10th, Edmonton, Canada, May 5-8, 1986, Proceedings. Volume 2. Ottawa, Canadian Aeronautics and Space Institute, 1987, p. 767-773. refs

Monitoring of potentially hazardous ice conditions on the Canadian Grand Banks is critical to the safe and efficient operation of offshore petroleum drilling programs. During the 1984 and 1985 Grand Banks ice seasons sea ice and iceberg conditions were monitored using an airborne real aperture side looking radar (SLAR) data acquisition system and a computer assisted interpretation and products generation program. The objective of the service was to determine the extent and location of the sea ice edge and icebergs in the operational area and relay accurate map and digital computer information to the Grand Banks Operators (GBO) and the Ice Data Management Center (IDMC), based in St. John's, Newfoundland, in a timely and efficient manner. The monitoring program was available with limitations imposed largely by weather conditions, providing aircraft could safely operate out of St. John's, Newfoundland. The radar derived ice information was integrated with auxiliary data. digitized and transmitted to the client's computer facilities in a two-phased process involving airborne data transmission followed by post-landing verification and transmission. Author

**A87-48881#**

**OPTIMIZATION OF SEISMIC VESSEL DEPLOYMENT USING SIDE LOOKING AIRBORNE RADAR**

E. D. LEAVITT, P. BOYD, and E. KRAKOWSKI (Intera Technologies, Ltd., Calgary, Canada) IN: Canadian Symposium on Remote Sensing, 10th, Edmonton, Canada, May 5-8, 1986, Proceedings. Volume 2. Ottawa, Canadian Aeronautics and Space Institute, 1987, p. 821-828.

The operational program conducted in 1984, 1985, and 1986, referred to as the Summer Ice Monitoring Program, in which a sidelooking airborne radar (SLAR) and a synthetic aperture radar (SAR) are utilized to provide strategic ice information to geophysical operators is examined. The characteristics of the two airborne radars are described. The data collected with the two radars for the Beaufort and Chukchi Seas in Alaska are analyzed. The data reveal that the SLAR is useful for distinguishing between ice and open water and for determining ice concentrations up to about 0.05; and the SAR offers higher resolution and better ability to distinguish between ice types than the SLAR. I.F.

**A87-50277**

**RESPONSE OF MARINE ATMOSPHERIC BOUNDARY LAYER HEIGHT TO SEA SURFACE TEMPERATURE CHANGES - MIXED-LAYER THEORY**

HOWARD P. HANSON (Cooperative Institute for Research in Environmental Sciences, Boulder, CO) Journal of Geophysical Research (ISSN 0148-0227), vol. 92, July 15, 1987, p. 8226-8230. refs

(Contract N00014-84-K-0405)

The flow of marine atmospheric boundary layer (MABL) air across ocean-surface temperature fronts subjects the MABL to an abrupt change in surface thermal forcing. The MABL responds to this variable forcing by a readjustment of both the MABL heat and moisture content as well as the MABL depth. This note addresses questions raised in recent publications in this journal with a rigorous theoretical analysis for the simplest case, an equilibrated MABL crossing a very abrupt front at right angles.

The MABL's adjustment is found by a solution to the mixed-layer budget of buoyancy and the entrainment closure based on turbulent energetics of the MABL. Since the solution is analytic, this simple case can be easily extended to circumstances of more realistic forcing. The solution discussed here establishes a firm theoretical basis for previous, partly heuristic and partly empirical, work; highlights weaknesses of that approach; and shows how simplistic engineering solutions to complex geophysical problems can be completely misleading. Author

**A87-50292****ATMOSPHERIC CORRECTION OF DATA MEASURED BY A FLYING PLATFORM OVER THE SEA - ELEMENTS OF A MODEL AND ITS EXPERIMENTAL VALIDATION**

RODOLFO GUZZI, GIUSEPPE ZIBORDI (Modena, Università, Italy), and ROLANDO RIZZI (Bologna, Università, Italy) Applied Optics (ISSN 0003-6935), vol. 26, Aug. 1, 1987, p. 3043-3051. refs (Contract CEC-2359/84/05-PP-ISP-I)

A model for the atmospheric correction of data remotely sensed over the sea at different altitudes is proposed on the basis of an approximate solution of the radiative transfer equation. The model includes atmospheric and surface effects, and takes into account the altitude of the sensor above the sea surface. Good agreement is found between the computed data and data measured by a modular multispectral scanner mounted in a plane flying over the North Adriatic Sea during the Adria 83 campaign. Corrected data obtained from measurements carried out in different atmospheric conditions are also discussed. R.R.

**A87-51147****THE DYNAMICS OF THE NORTHERN BORDER OF THE GULF STREAM REVEALED BY A TIROS-N AVHRR IMAGE FROM OCTOBER 22, 1980 [LA DYNAMIQUE DE LA BORDURE NORD DU GULF STREAM REVELEE PAR L'IMAGE AVHRR DE TIROS-N DU 22 OCTOBRE 1980]**

D. DE BRUM FERREIRA (Centro de Estudos Geograficos, Lisbon, Portugal) Photo Interpretation (ISSN 0031-8523), vol. 25, May-June 1986, p. 45-49, 51. In French, English, and Spanish.

A thermal image of the ocean surface at the northern edge of the Gulf Stream, obtained by Tiros-N on October 22, 1980 at the time of a powerful influx of polar cold water associated with the Labrador Current, is analyzed. The present AVHRR thermograph shows the dynamics of the ocean in synoptic form, and reveals the complexity of the structures which result from the turbulence at the contact point of the water masses. Turbulent phenomena, corresponding to structures on the surface which are clear enough to be visualized, are isolated, suggesting the presence of the surface flows with which they are associated. The presence of cloud cover poses a serious limitation to the use of IR images and to their multitemporal analysis. R.R.

**A87-51487\*** Minnesota Univ., Minneapolis.**AZIMUTHAL DEPENDENCE IN THE GRAVITY FIELD INDUCED BY RECENT AND PAST CRYOSPHERIC FORCINGS**

DAVID A. YUEN (Minnesota, University, Minneapolis), PAOLO GASPERINI (Istituto Nazionale di Geofisica, Rome, Italy), ROBERTO SABADINI (Bologna, Università, Italy), and ENZO BOSCHI (Istituto Nazionale di Geofisica, Rome; Bologna, Università, Italy) Geophysical Research Letters (ISSN 0094-8276), vol. 14, Aug. 1987, p. 812-815. refs (Contract CNR-PSN-86-060; NAG5-770; NSF EAR-85-11200)

Present-day glacial activities and the current variability of the Antarctic ice volume can cause variations in the long-wavelength gravity field as a consequence of transient viscoelastic responses in the mantle. The azimuthal dependence of the secular variations of the gravitational potential are studied and it is found that the nonaxisymmetric contributions are more important for recent glacial retreats than for Pleistocene deglaciation. Changes in land-based ice covering Antarctica can be detected by monitoring satellite orbits and their sensitivity to variations in gravitational harmonic for degree  $l$  greater than 3. Resonances in satellite orbits may be useful for detecting these azimuthally-dependent gravity signals. Author

**A87-51532****MEISSNER EFFECT IN HIGH-TC SUPERCONDUCTIVE THIN FILMS**

SHIN-ICHIRO HATTA, HIDETAKA HIGASHINO, and KIYOTAKA WASA (Matsushita Electric Industrial Co., Ltd., Central Research Laboratories, Moriguchi, Japan) Japanese Journal of Applied Physics, Part 2 (ISSN 0021-4922), vol. 26, May 1987, p. L724, L725. refs

The Meissner effect of superconductive thin films was measured by the simple technique, which is the observation of the change in the sensing inductance with respect to the superconductive plane. By using this method, slight and gradual exclusion of magnetic flux was found below the perfect conductivity temperature in Y-Ba-Cu oxide films. Author

**A87-51552****OBSERVING SYSTEMS EXPERIMENTS FOR THE ONSET VORTEX DURING SUMMER MONEX**

FREDERICK H. CARR, MOHAN RAMAMURTHY (Oklahoma, University, Norman), and B. M. CHHABRA (Oklahoma, University, Norman; Indian Meteorological Department, New Delhi, India) IN: National Conference on the Scientific Results of the First GARP Global Experiment, Miami, FL, Jan. 14-17, 1986, Preprints. Boston, MA, American Meteorological Society, 1986, p. 6-9. refs (Contract NSF ATM-79-23918; NSF ATM-81-19321)

The effect of Monex/FGGE data sets on a four-dimensional data assimilation initialization scheme for a limited-area model in the tropics is investigated. A 10-level, semi-Lagrangian primitive equation model using data from June 17, 1979 was used in the experiments. The impact of the conventional observing network on numerical prediction over the monsoon region is examined. The influences of dropwindsonde and satellite derived cloud-tracked wind data on observing networks are studied. It is observed that the dropwindsonde data has the largest effect on the onset vortex vorticity center, and it is suggested that the dropwindsonde data could produce an improvement in the intensity and track of forecasts. I.F.

**A87-51553****SEA SURFACE TEMPERATURE RETRIEVAL FROM THE TIROS-N AVHRR INSTRUMENT FOR THE FGGE PERIOD (DEC. 1978-NOV. 1979)**

Z. AHMAD, J. SUTTON, W. MITCHELL (SASC Technologies, Inc., Lanham, MD), and A. STRONG (NOAA, Suitland, MD) IN: National Conference on the Scientific Results of the First GARP Global Experiment, Miami, FL, Jan. 14-17, 1986, Preprints. Boston, MA, American Meteorological Society, 1986, p. 10-13. refs

A method for reducing noise and retrieving multichannel sea surface temperature data from the AVHRR of the Tiros-N satellite is described. The composition and capabilities of the AVHRR instrument are discussed. The space, blackbody, and earth view noises, and the use of a 25-point triangular filter to reduce the noise are analyzed. The reduction and validation of the sea surface temperature data are examined, and the data are compared with climatology. The equations for removing bias from the retrievals are presented. It is noted that this procedure is useful for providing accurate sea surface temperature data. I.F.

**A87-51559\*** Texas A&M Univ., College Station.**COMPARISONS OF FGGE IIB AND IIIB WINDS IN A TROPICAL SYNOPTIC SYSTEM**

J. P. MCGUIRK, A. H. THOMPSON, and B. A. SNYDER (Texas A & M University, College Station) IN: National Conference on the Scientific Results of the First GARP Global Experiment, Miami, FL, Jan. 14-17, 1986, Preprints. Boston, MA, American Meteorological Society, 1986, p. 40-43. refs (Contract NAS8-35182)

The ECMWF wind analysis of a moisture burst over the NE Pacific Ocean occurring during a 9-day period in January 1979 is discussed. The availability of the data in synoptically active regions, and the horizontal, vertical, and temporal correlations of the data are considered. The accuracy of the wind data and the divergence in the tropics are examined. It is noted that it is necessary to



maximize wind accuracy, and procedures for relating divergence to synoptic activity and satellite imagery to data correction are needed. I.F.

**A87-51560\*** Texas A&M Univ., College Station.  
**WINTERTIME DISTURBANCES IN THE TROPICAL PACIFIC - FGGE IIIB AND SATELLITE COMPARISONS**

J. P. MCGUIRK, A. H. THOMPSON, and L. L. ANDERSON, JR. (Texas A & M University, College Station) IN: National Conference on the Scientific Results of the First GARP Global Experiment, Miami, FL, Jan. 14-17, 1986, Preprints . Boston, MA, American Meteorological Society, 1986, p. 44-47. (Contract NAS8-35182)

The synoptic development of moisture fields associated with moisture bursts near the ITCZ is described. Dropsonde and satellite (Tiros and GOES) data for the moisture structure along the winter ITCZ North Pacific are presented and examined. These observations were compared with ECMWF analysis along the ITCZ; consideration is given to relative humidity and burst dynamics. It is observed that the ECMWF analysis reproduces the synoptic variations reasonably well. I.F.

**A87-51579\*** National Aeronautics and Space Administration. Goddard Space Flight Center, Greenbelt, Md.  
**CLOUD AND MOISTURE FIELDS DERIVED FROM THE GLA RETRIEVALS OF HIRS2/MSU DATA**

D. REUTER and J. SUSSKIND (NASA, Goddard Space Flight Center, Greenbelt, MD) IN: National Conference on the Scientific Results of the First GARP Global Experiment, Miami, FL, Jan. 14-17, 1986, Preprints . Boston, MA, American Meteorological Society, 1986, p. 130-133.

The GLA retrieval scheme for the analysis of HIRS and MSU radiances is applied to derive cloud and humidity fields from the HIRS2/MSU data for June 1979. For the retrieval of cloud fraction and cloud top pressure, the original algorithm of Susskind et al. (1983) and Susskind et al. (1984) was improved. The derived profiles of the monthly mean fields of cloud fraction and cloud top pressure clearly show the intertropical convergence zone, with the most intense convection in the monsoonal region of the southern Asia and over Central America, which show up as containing the highest cloud top levels and largest cloud amount. For the retrieval of humidity profiles, which are not one of the products of the original processing system, a new algorithm was derived. I.S.

**A87-51580\*** National Aeronautics and Space Administration. Marshall Space Flight Center, Huntsville, Ala.  
**USE OF IR SATELLITE RAINFALL ESTIMATES IN DIAGNOSING THERMALLY FORCED CIRCULATIONS IN THE PACIFIC DURING FGGE SOP-1**

FRANKLIN R. ROBERTSON (NASA, Marshall Space Flight Center, Huntsville, AL) IN: National Conference on the Scientific Results of the First GARP Global Experiment, Miami, FL, Jan. 14-17, 1986, Preprints . Boston, MA, American Meteorological Society, 1986, p. 134-137. refs (Contract NAS8-35187)

**A87-51585**  
**LARGE SCALE OCEAN-ATMOSPHERE INTERACTION IN THE SUMMER MONSOON - THE INFLUENCE OF OCEANIC UPWELLING AND ADVECTION ON EASTERN ARABIAN SEA OFFSHORE CONVECTION**

ROBERT L. GROSSMAN (Cooperative Institute for Research in Environmental Sciences, Boulder, CO) IN: National Conference on the Scientific Results of the First GARP Global Experiment, Miami, FL, Jan. 14-17, 1986, Preprints . Boston, MA, American Meteorological Society, 1986, p. 164-168. NOAA-supported research. refs (Contract NSF ATM-82-069004)

The factors which are responsible for the differences in the pattern of changes in the deep convection in the Arabian Sea (with a maximum in June) and close to the western coast of India (with a maximum in July) are discussed. The emphasis is placed

on determining the thermodynamic conditions which influence the intraseasonal variation in offshore convection, such as changes in midtropospheric moisture, seasonal advance of sea surface temperature (SST), and cooling mechanisms. A highly positive correlation was found between the occurrence of deep convection and the seasonal march of SST and boundary-layer equivalent potential temperature. Physical mechanism are examined supporting a hypothesis that upwelling due to the wind stress and advection of cool water from the western Arabian Sea affect the central Arabian Sea, while upwelling associated with a southward-directed current system is mainly responsible for the cooling along the west India coastal zone. I.S.

**A87-51587**  
**SATELLITE OBSERVATIONS OF CONVECTION DURING THE SUMMER MONSOON OF 1979**

STEVEN A. ACKERMAN and STEPHEN K. COX (Colorado State University, Fort Collins) IN: National Conference on the Scientific Results of the First GARP Global Experiment, Miami, FL, Jan. 14-17, 1986, Preprints . Boston, MA, American Meteorological Society, 1986, p. 175-177. (Contract NSF ATM-84-18472)

IR measurements from the Tiros-N and GOES-1 satellites are used to investigate regions of convective activity associated with the 1979 summer monsoon. Tiros-N observations show day-to-day changes in the convective cloud systems for the May-July 1979 period. GOES-1 data for the preonset, onset, and postonset phases of the monsoon season show the diurnal variations in convective type clouds. The daytime-nighttime high cloud analyses reveal a phase difference between the maxima over the land and the ocean, suggesting interactions between continental and oceanic convection. R.R.

**A87-51593\*** Texas A&M Univ., College Station.  
**MOISTURE TRANSPORTS AND BUDGETS OF 'MOISTURE BURSTS'**

A. H. THOMPSON and J. P. MCGUIRK (Texas A & M University, College Station) IN: National Conference on the Scientific Results of the First GARP Global Experiment, Miami, FL, Jan. 14-17, 1986, Preprints . Boston, MA, American Meteorological Society, 1986, p. 212-215. refs (Contract NAS8-35182)

The paper discusses moisture fluxes and budgets associated with a pair of 'moisture bursts' in the eastern North Pacific Ocean area, described by Smith et al. (1985). The moisture fluxes were calculated using data obtained during the first Special Observing Period (SOP-1) of the FGGE. The area specifically examined extended from the equator to the latitude 20 deg N and from longitude 180 deg to 100 deg W, with concentration on the region south and southeast of the Hawaiian Islands. From the comparison of the calculations based on dropwindsonde and radiosonde data and reports from commercial and military aircraft, it is concluded that the calculations of water vapor flow across latitude lines probably provide a fair representation of reality, especially when based on the dropwindsonde data. However, water vapor flow out of small volumes is not well represented by the results from either data. I.S.

**A87-51594**  
**A COMPARISON OF THE SIGNIFICANT FEATURES OF THE MARINE BOUNDARY LAYERS OVER THE ARABIAN SEA AND THE BAY OF BENGAL DURING MONEX 79**

TEDDY HOLT and SETHU RAMAN (North Carolina State University, Raleigh) IN: National Conference on the Scientific Results of the First GARP Global Experiment, Miami, FL, Jan. 14-17, 1986, Preprints . Boston, MA, American Meteorological Society, 1986, p. 218-221. refs (Contract NSF ATM-82-17960)

The characteristic features of the mean structure and the flux and turbulence structures of marine boundary layers observed over two Indian southwest monsoon regions, the Arabian Sea and the Bay of Bengal are compared, using aircraft data collected during Monex 79. Dropwindsonde data were obtained at strategic locations

along the flight tracks of the NCAR Electra aircraft. Ships made surface measurements of pressure, height, and dry-bulb and dew-point temperatures; radiosonde soundings were taken every 6 h with a resolution of 50 mb. The primary difference observed in the mean structure between the Arabian Sea and the Bay of Bengal boundary layers is the presence/absence of a strong low-level jet in the wind field. Both the turbulence and the flux profiles were dependent on location, i.e., varying synoptic or mesoscale conditions occurring in these areas. I.S.

**A87-51603\*** Purdue Univ., West Lafayette, Ind.

## **LATENT HEAT AND CYCLONE ACTIVITY IN THE SOUTH PACIFIC, 10-18 JANUARY 1979**

B. L. MILLER, D. G. VINCENT, D. M. KANN (Purdue University, West Lafayette, IN), and FRANKLIN R. ROBERTSON (NASA, Marshall Space Flight Center, Huntsville, AL) IN: National Conference on the Scientific Results of the First GARP Global Experiment, Miami, FL, Jan. 14-17, 1986, Preprints. Boston, MA, American Meteorological Society, 1986, p. 260-263. NOAA-sponsored research. refs  
(Contract NSF ATM-85-05748; NAS8-35187)

This paper examines the heat budget of the tropical South Pacific for the period of January 10-18, 1979 and compares precipitation estimates obtained from the budget equation with those derived from GOES-IR satellite imagery, using data that were part of the total FGGE package. In addition, the relationship between latent heat release and the baroclinic energy conversion is examined for the life cycles of two cyclones which propagated along the South Pacific Convection Zone in that period. It is shown that latent heat plays an important role in the baroclinic energy conversion between potential and kinetic energy through diabatically-induced vertical circulations. For a cyclone where latent heat stays at a high level both spatially and with regard to intensity, there appears to be ample fuel for its intensification. On the other hand, for a filling cyclone, the latent heat impact decreased and the baroclinic conversion fell off rapidly, due to the lack of both potential energy generation and diabatically-induced thermally-direct circulations. I.S.

**A87-51943**

## **ANTARCTIC ICE STREAMS - A REVIEW**

CHARLES R. BENTLEY (Wisconsin, University, Madison) Journal of Geophysical Research (ISSN 0148-0227), vol. 92, Aug. 10, 1987, p. 8843-8858. refs  
(Contract NSF DPP-84-12404)

Present understanding of Antarctic ice streams is reviewed. Physiographic aspects of these streams are discussed, taking into account the surface profiles and driving stresses of various Antarctic ice streams. Dynamic models that have been applied to the Ross ice streams are addressed, emphasizing models for the fast sliding of glaciers. Sliding speed values for ice streams obtained with various models are compared. C.D.

**A87-51944**

## **RECENT GLACIAL HISTORY AND RAPID ICE STREAM RETREAT IN THE AMUNDSEN SEA**

THOMAS B. KELLOGG and DAVIDA E. KELLOGG (Maine, University, Orono) Journal of Geophysical Research (ISSN 0148-0227), vol. 92, Aug. 10, 1987, p. 8859-8864. refs  
(Contract NSF DPP-80-20000)

**A87-51945**

## **THE MORPHOLOGY OF ICE STREAMS A, B, AND C, WEST ANTARCTICA AND THEIR ENVIRONS**

SION SHABTAIE, CHARLES R. BENTLEY (Wisconsin, University, Madison), and IAN M. WHILLANS (Ohio State University, Columbus) Journal of Geophysical Research (ISSN 0148-0227), vol. 92, Aug. 10, 1987, p. 8865-8883. refs  
(Contract NSF DPP-81-20332; NSF DPP-84-12404)

The results of mapping efforts over West Antarctica made by airborne radar soundings are reported for surface elevations of ice streams A, B, and C, the intervening ridges, and the interior regions. Ice thickness profiles across the ice streams and the

intervening ridges are also presented. The basal reflection coefficient and the basal hydrological potential gradient for the catchment region are calculated. C.D.

**A87-51946\*** National Aeronautics and Space Administration. Goddard Space Flight Center, Greenbelt, Md.

## **ICE DYNAMICS AT THE MOUTH OF ICE STREAM B, ANTARCTICA**

R. A. BINDSCHADLER (NASA, Goddard Space Flight Center, Greenbelt, MD), S. N. STEPHENSON (Science Applications Research, Lanham, MD), D. R. MACAYEAL (Chicago, University, IL), and S. SHABTAIE (Wisconsin, University, Madison) Journal of Geophysical Research (ISSN 0148-0227), vol. 92, Aug. 10, 1987, p. 8885-8894. refs  
(Contract NSF DPP-82-07320; NSF DPP-84-05287; NSF DPP-85-14543; NSF DPP-84-14402)

Data collected in the region of the mouth of ice stream B, West Antarctica, during three field seasons are presented. The physical characteristics of the mouth of ice stream B are described, and the dynamics in the vicinity of the DNB network are discussed. The dynamics of ice stream B from DNB to the grounding line is briefly considered, and a force analysis of the grounding line region is made. The results demonstrate that the dynamic situation of the region at the mouth of ice stream B is distinctly different from either the greater portion of the ice stream upstream or the Ross ice shelf downstream. C.D.

**A87-51947**

## **VELOCITY OF ICE STREAMS B AND C, ANTARCTICA**

I. M. WHILLANS, J. BOLZAN (Ohio State University, Columbus), and S. SHABTAIE (Wisconsin, University, Madison) Journal of Geophysical Research (ISSN 0148-0227), vol. 92, Aug. 10, 1987, p. 8895-8902. refs  
(Contract NSF DPP-81-17235)

The essential difference between ice stream and inland ice and the cause of ice streaming are not known. In order to study these problems, velocities have been measured on and near ice streams B and C by repeated tracking of TRANSIT satellites. The results confirm the difference in mode of flow between fast on ice stream B and slow on the interstream ice ridges. Also as expected, ice stream C is nearly stagnant, which with other evidence of formerly fast flow confirms its recent slowing and current thickening. The drainage of ice stream B has a negative balance equivalent to thinning by 0.15 m or - 0.05 m/yr over the entire catchment. The lower portion of the ice stream is thickening at about 2 m/yr, but the overall behavior is thinning. This general thinning is probably partly due to progressive extension of the ice stream into inland ice. The transition from inland ice to ice stream seems to occur irregularly both spatially and in time, with rafts of inland ice being carried into the ice stream and slowly incorporated. Author

**A87-51948**

## **TILL BENEATH ICE STREAM B. I - PROPERTIES DERIVED FROM SEISMIC TRAVEL TIMES. II - STRUCTURE AND CONTINUITY. III - TILL DEFORMATION - EVIDENCE AND IMPLICATIONS. IV - A COUPLED ICE-TILL FLOW MODEL**

D. D. BLANKENSHIP, C. R. BENTLEY, S. T. ROONEY, and R. B. ALLEY (Wisconsin, University, Madison) Journal of Geophysical Research (ISSN 0148-0227), vol. 92, Aug. 10, 1987, p. 8903-8940. refs  
(Contract NSF DPP-81-20322; NSF DPP-84-12404)

Seismic studies of the till beneath West Antarctic ice stream B are reported. Seismic travel times imply that the material in the layer is highly porous and is saturated with water at a high pore pressure. Other data show that the till layer varies in thickness but is continuous over almost the entire length of the profiles with an average thickness of 6.5 km. The upper surface of the till layer is smooth, but the lower boundary is fluted parallel to flow. Nowhere on the profiles can any feature be discerned to penetrate more than a few m into the ice from the bed. The entire thickness of the till layer is deforming and is eroding subjacent bedrock into flutes parallel to ice flow and hundreds of m across. The erosion



rate suggests that till deltas tens of km long have been deposited at the grounding line during the Holocene. A simple one-dimensional time-dependent model for flow of an ice stream on deforming till is developed. Steady-state solutions are obtained for till viscosity, thickness, and generation rate. C.D.

#### A87-51950

##### GLACIOLOGICAL STUDIES ON RUTFORD ICE STREAM, ANTARCTICA

C. S. M. DOAKE, R. M. FROLICH, D. R. MANTRIPP, A. M. SMITH, and D. G. VAUGHAN (NERC, British Antarctic Survey, Cambridge, England) *Journal of Geophysical Research* (ISSN 0148-0227), vol. 92, Aug. 10, 1987, p. 8951-8960. refs

Velocities at five sites on the Rutford ice stream have been calculated using Doppler satellite position measurements. The characteristics of the accumulation area are summarized, and the findings on the surface morphology, ice thickness, bedrock profiles, and movement of the ice stream are described. The results for the grounding zone are also considered. C.D.

#### A87-51963

##### INVESTIGATIONS OF RELATIVE PLATE MOTIONS IN THE SOUTH ATLANTIC USING SEASAT ALTIMETER DATA

PETER R. SHAW (Woods Hole Oceanographic Institution, MA) *Journal of Geophysical Research* (ISSN 0148-0227), vol. 92, Aug. 10, 1987, p. 9363-9375. refs  
(Contract NSF OCE-85-00874)

An inverse method for estimating poles of opening of an ocean basin from the trajectories of fracture zones (FZs) is derived. The method analyzes the trajectory of each FZ in terms of the appropriate set of stage poles. The method is applied to a set of 17 FZs in the South Atlantic. Seven finite poles describing relative motion between the South American and African plates between approximately 72 My B.P. and the present are included in the estimation. The solution poles converge rapidly to a set of stable locations, which are relatively insensitive to the precise starting choice of poles. In particular, the method converges even if the starting flow lines are modeled simply as small circles about a common pole. Synthetic flow lines computed using the solution poles follow the observed FZ trajectories to 6 km rms, indicating that FZs closely follow flow lines of relative plate motion. The solution documents a marked change in relative motion between approximately 20 and 50 My B.P. C.D.

#### A87-52501

##### THE NAVY GEOSAT MISSION - AN OVERVIEW

CHARLES C. KILGUS (Johns Hopkins University, Laurel, MD) and DONALD R. MCCONATHY (Johns Hopkins APL Technical Digest (ISSN 0270-5214), vol. 8, Apr.-June 1987, p. 170-175. Navy-DMA-sponsored research.

The Geosat radar altimeter is able to measure the distance between a point in orbit and the subsatellite point on the ocean surface with a precision of the order of a few cm, allowing the shape of the ocean's surface to be determined. Oceanographic features can be removed from the altimeter data by subtracting the long-term mean surface. These functions directly support: (1) improved map compensations for geoid height, vertical deflections, and in-flight gravity; (2) the definition of specific geophysical/geological areas for more detailed ship surveys; and (3) the detection of possible bathymetric hazards to submerged navigation. O.C.

#### A87-52502

##### THE GEOSAT RADAR ALTIMETER

JOHN L. MACARTHUR, PAUL C. MARTH, JR., and JOSEPH G. WALL (Johns Hopkins University, Laurel, MD) *Johns Hopkins APL Technical Digest* (ISSN 0270-5214), vol. 8, Apr.-June 1987, p. 176-181.

The Geosat radar altimeter is an improved version of the one flown on Seasat. The characteristics of the return signal from the ocean surface are discussed as a basis for understanding the altimetry process. The primary measurements provided by the altimeter are listed along with a description of altimeter hardware

implementation. The processing and corrections to the raw measurements to yield the end-user data products are presented, followed by a summary of the altimeter's in-orbit performance.

Author

#### A87-52503

##### PRELIMINARY DETERMINATION OF THE GEOSAT RADAR ALTIMETER NOISE SPECTRUM

RICHARD V. SAILOR and A. RICHARD LESCHACK (Analytic Sciences Corp., Reading, MA) *Johns Hopkins APL Technical Digest* (ISSN 0270-5214), vol. 8, Apr.-June 1987, p. 182, 183. Research supported by Johns Hopkins University.

The noise component of Geosat altimeter observations of sea-surface topography encompasses contributions from orbit errors, radar propagation effects, tides, oceanography, and any electronic noise in the altimeter itself. An analysis of the total noise allows quantification of the precision with which Geosat can measure geoid height. To determine how the noise varies as a function of spatial wavenumber, along-track noise power spectral density (PSD) functions must be computed; attention is presently given to the derivation of Geosat average noise PSDs on the basis of a rather small data set. It is found that the instrument white noise component has been reduced in Geosat below the level of the earlier Seasat altimeter. O.C.

#### A87-52506

##### DETERMINATION OF OCEAN GEODETIC DATA FROM GEOSAT

SAMUEL L. SMITH, III, GLADYS B. WEST, and CAROL W. MALYEVAC (U.S. Navy, Naval Surface Weapons Center, Dahlgren, VA) *Johns Hopkins APL Technical Digest* (ISSN 0270-5214), vol. 8, Apr.-June 1987, p. 197-200. DMA-supported research. refs

The more than 360 million observations gathered from more than 6000 Geosat orbits have been reduced to along-track geodetic data encompassing geoid heights and vertical reflections, using a system of computer programs. These data will furnish operational support to USN and other Department of Defense missions. The major inputs to the observation-reduction procedure are sensor data record tapes, Doppler precise orbits, climatology constants, coastline coordinates, and sunspot numbers. Attention is given to the role played by an adaptive Kalman smoother. O.C.

#### A87-52508

##### INTRODUCTION TO SEA-SURFACE TOPOGRAPHY FROM SATELLITE ALTIMETRY

JACK CALMAN (Johns Hopkins University, Laurel, MD) *Johns Hopkins APL Technical Digest* (ISSN 0270-5214), vol. 8, Apr.-June 1987, p. 206-211. Research supported by Johns Hopkins University.

In addition to surface waves and tides, ocean phenomena that influence sea surface shape vary on different scales of length and time; these include the large current systems, their eddies and rings, El Nino, storm response, and other open-ocean processes. Attention is presently given to the theoretical basis of satellite-borne radar altimetry, its achievements in sea surface topography, and its future applications. GEOS-3, Geosat, and Seasat ocean surface altimetry results are compared, and the combined use of satellite-derived sea surface heights and a numerical ocean-circulation model for ocean forecasting is discussed. O.C.

#### A87-52509

##### COMPARISON OF GEOSAT AND GROUND-TRUTH WIND AND WAVE OBSERVATIONS - PRELIMINARY RESULTS

JOSEPH L. SHUHY, MITCHELL R. GRUNES, ENZO A. ULIANA, and LAWRENCE W. CHOY (U.S. Navy, Naval Research Laboratory, Washington, DC) *Johns Hopkins APL Technical Digest* (ISSN 0270-5214), vol. 8, Apr.-June 1987, p. 219-221.

Problems associated with the comparison of satellite data, which are spatially variable, to ground-truth station data, which are temporally variable, are well appreciated and inherent in the present comparison of Geosat and ground-truth data. The Naval Research

Laboratory's preliminary evaluation of Geosat radar altimeter windspeed and wave-height data indicates that the Geosat windspeeds are slightly higher than the ground-truth data below 6 m/sec, and slightly lower than the ground-truth data for wind speeds greater than 6 m/sec. Wave-height values, on the other hand, compare well with ground truth. O.C.

**A87-52510  
VALIDATION OF GEOSAT ALTIMETER-DERIVED WIND SPEEDS AND SIGNIFICANT WAVE HEIGHTS USING BUOY DATA**

ELLA DOBSON, FRANK MONALDO, JULIUS GOLDBIRSH (Johns Hopkins University, Laurel, MD), and JOHN WILKERSON (NOAA, Rockville, MD) Johns Hopkins APL Technical Digest (ISSN 0270-5214), vol. 8, Apr.-June 1987, p. 222-233. NOAA-supported research. refs

Geosat radar altimeter-derived wind speeds and significant wave heights are compared with those measured by buoys in the National Data Buoy Center network. Measurements from a subset of 43 buoys moored in coastal regions and deep within the North Pacific, North Atlantic, and Gulf of Mexico were examined. Altimeter comparisons were obtained during the Geosat geodetic mission from May through August and October through December 1985. Only Geosat data within 150 kilometers of buoy locations were accessed, resulting in 1166 wind-speed and significant-wave-height pairs. An error analysis was performed to better understand the differences between altimeter- and buoy-derived results and to establish consistency between the two data sets. Four algorithms relating altimeter radar cross section to ocean-surface wind speed were investigated. Measurement goals for Geosat were 1.8 meters per second rms for wind speeds of 1 to 18 meters per second and 0.5 meter rms for significant wave height, or 10 percent, whichever was greater. These goals were met. Author

**A87-52511  
REX AND GEOSAT - PROGRESS IN THE FIRST YEAR**

JIM L. MITCHELL, ZACHARIAH R. HALLOCK, and J. DANA THOMPSON (U.S. Navy, Naval Ocean Research and Development Activity, Bay Saint Louis, MS) Johns Hopkins APL Technical Digest (ISSN 0270-5214), vol. 8, Apr.-June 1987, p. 234-244. Navy-sponsored research. refs

The major objectives, plans, and some preliminary progress of the Northwest Atlantic Regional Energetics Experiment (REX) in which sea-surface topography from Geosat plays a major role are presented. In addition, a description is provided of those facets of the Geosat missions and hardware that have significant impact on the use of this satellite system for the measurement of sea-surface topography, particularly mesoscale topography. Some preliminary comparisons of REX-collected in-situ data and Geosat altimetry are included. Author

**A87-52512  
MONITORING EQUATORIAL PACIFIC SEA LEVEL WITH GEOSAT**

ROBERT E. CHENEY, LAURY L. MILLER, BRUCE C. DOUGLAS, and RUSSELL W. AGREEN (NOAA, National Ocean Service, Rockville, MD) Johns Hopkins APL Technical Digest (ISSN 0270-5214), vol. 8, Apr.-June 1987, p. 245-250. refs

Observations of sea levels and their changes over time furnish valuable information about the ocean's dynamic interactions with the atmosphere. It is presently demonstrated that Geosat sea surface altimeter data can be used to construct sea level time series at discrete locations with an accuracy of the order of a few cm, for time-scales of 10 days or longer. Geosat data are therefore equivalent to the possession of island tide gages every few deg in position throughout the ocean. NOAA researchers are currently engaged in the use of Geosat data to uncover relationships between sea level variability in the tropical Pacific Ocean and El Nino. O.C.

**A87-52513\*** National Aeronautics and Space Administration. Goddard Space Flight Center, Greenbelt, Md.

**ICE MEASUREMENTS BY GEOSAT RADAR ALTIMETRY**

H. JAY ZWALLY, ROBERT A. BINDSCHADLER (NASA, Goddard Space Flight Center, Greenbelt, MD), JUDY A. MAJOR, and ANITA C. BRENNER (EG&G Washington Analytical Services Center, Inc., Lanham, MD) Johns Hopkins APL Technical Digest (ISSN 0270-5214), vol. 8, Apr.-June 1987, p. 251-254. refs

Radar altimetry for ice-covered ocean and land is more complex and variable than open ocean radar altimetry; attention is presently given to Geosat ice-sheet topography for the Greenland and Antarctic ice sheets between 72 deg N and 72 deg S which owes its excellent accuracy to the well separated spacing of the orbital tracks and an 18-month geodetic mission duration. A surface elevation map of southern Greenland, produced from 110 days of retracked Geosat data, is presented in color-coded three-dimensional perspective. Comparisons are made between Seasat and Geosat data for ice mass elevations in Greenland. O.C.

**A87-52514\*** National Aeronautics and Space Administration. Wallops Flight Center, Wallops Island, Va.

**WAVEFORM ANALYSIS FOR GEOSAT DAY 96**

GEORGE S. HAYNE and DAVID W. HANCOCK, III (NASA, Goddard Space Flight Center, Wallops Island, VA) Johns Hopkins APL Technical Digest (ISSN 0270-5214), vol. 8, Apr.-June 1987, p. 255-259. refs

A detailed model waveform function has been least-squares-fitted to 10-second averages of waveform sampler data from selected over-ocean portions of day 96 of the Geosat mission. The results confirm that the height corrections already applied in the routine Geosat data processing are generally good to well within 10 centimeters. Additional height corrections are provided that can refine height estimates to within the several-centimeter level. Author

**A87-52515  
DESIGN OF GEOSAT EXACT REPEAT MISSION**

GEORGE H. BORN (Colorado, University, Boulder), JIM L. MITCHELL (U.S. Navy, Naval Ocean Research and Development Activity, Bay Saint Louis, MS), and GENE A. HEYLER (Johns Hopkins University, Laurel, MD) Johns Hopkins APL Technical Digest (ISSN 0270-5214), vol. 8, Apr.-June 1987, p. 260-266. refs

At the inception of its Exact Repeat Mission, the Geosat satellite was maneuvered into a 17-day, exact-repeat 'frozen' orbit. In order to minimize the effect of geoid uncertainty on the determination of ocean variability derived from Geosat altimetry, the ground tracks from each repeat cycle must deviate by no more than 1 km from the mean ground tracks in all other repeat cycles. The collection of sea-level data from the 17-day exact repeat orbit of this mission will represent a very valuable data set for the study of global oceanic mesoscale variability. O.C.

**A87-52516  
ALTIMETRIC DATA ASSIMILATION FOR OCEAN DYNAMICS AND FORECASTING**

ALLAN R. ROBINSON and LEONARD J. WALSTAD (Harvard University, Cambridge, MA) Johns Hopkins APL Technical Digest (ISSN 0270-5214), vol. 8, Apr.-June 1987, p. 267-271. refs

The prediction of oceanic mesoscale variability is now possible by means of a systematic approach in which observations are combined with dynamical model outputs in four-dimensional data assimilation. Attention is presently given to the Gulf Stream region, which generates strong mesoscale signals as well as interesting dynamical phenomena. Weekly forecasts and 'nowcasts' in real time are being generated for the Gulf Stream on the basis of dedicated air-expendable bathythermography flights, the Harvard open ocean model, and Geosat altimeter sea-surface height data. O.C.

A87-53020

**SATELLITE OBSERVATIONS OF SURFACE TEMPERATURES AND FLOW PATTERNS, SEA OF JAPAN AND EAST CHINA SEA, LATE MARCH 1979**

OSCAR K. HUH and TAEBO SHIM (Louisiana State University, Baton Rouge) Remote Sensing of Environment (ISSN 0034-4257), vol. 22, Aug. 1987, p. 379-393. Navy-supported research. refs

Unusually cloud-free NOAA thermal IR images of the Sea of Japan reveal patterns of surface temperature (ST) important to understanding surface circulation. A March 26 image of almost the entire ocean basin, cloud-free, shows the appropriate ST structure of the expected classical surface circulation as formulated by Uda (1934). A March 28 image is supportive of the conclusions of Lim (1971), that the Tsushima Current waters are formed in the outer East China Sea by mixing of Kuroshio waters with outer-shelf and slope waters. Satellite-measured STs differed from surface ship measurements by 1-2 C. Author

A87-53113

**POSEIDON RADAR ALTIMETER OCEANOGRAPHIC REMOTE SENSING**

P. DE CHATEAU-THIERRY (Alcatel Thomson Espace, Toulouse, France) IN: IGARSS '87 - International Geoscience and Remote Sensing Symposium, Ann Arbor, MI, May 18-21, 1987, Digest. Volume 1. New York, Institute of Electrical and Electronics Engineers, Inc., 1987, p. 147-151.

The TOPEX/Poseidon mission is a joint mission of the NASA experiment TOPEX (Ocean Topography Experiment) and the CNES Poseidon program. The main purpose of the scientific mission is the accurate measurement of sea surface topography. This makes it possible to assess the oceanic currents in order to improve the knowledge of the general circulation of the ocean and its variability in mesoscale. The TOPEX/Poseidon radar altimeter is a new design that mixes the advantage of the Seasat architecture, the potential of advanced technology, and the knowledge of operational requirements that comes out of the Seasat results. Author

A87-53114

**POSEIDON RADAR ALTIMETER DESCRIPTION AND SIGNAL PROCESSING**

J. ABADIE, M. LAMBOLEY, P. RAIZONVILLE (CNES, Toulouse, France), and J. P. DUMONT (Groupeement pour le Developpement de la Teledetection Aerospaciale, Toulouse, France) IN: IGARSS '87 - International Geoscience and Remote Sensing Symposium, Ann Arbor, MI, May 18-21, 1987, Digest. Volume 1. New York, Institute of Electrical and Electronics Engineers, Inc., 1987, p. 153-160.

The principles and design of the Poseidon radar altimeter, proposed for measuring sea level altitude, are described. The altimeter operates at a pulse repetition frequency of 1700 Hz, has a central frequency of 13.65 GHz, a bandwidth of 320 MHz, a pulse duration of 100 microsec, a pulse compression ratio of 320 MHz/10kHz, emitted power of 5 W, and an antenna gain of about 42 dB. A diagram of the altimeter and its functions is presented. The altimeter's microprocessor performs altitude and amplitude tracking and waveform parameter precise estimation. The altimeter signal processing system which estimates sea level altitude data from waveforms is examined. The objectives of the signal acquisition and calibration modes are discussed. The performance of a breadboard model of the altimeter is evaluated. I.F.

A87-53115\* National Aeronautics and Space Administration. Wallops Flight Center, Wallops Island, Va.

**AIRBORNE MULTIBEAM RADAR ALTIMETRY**

CHESTER L. PARSONS (NASA, Wallops Flight Center, Wallops Island, VA) IN: IGARSS '87 - International Geoscience and Remote Sensing Symposium, Ann Arbor, MI, May 18-21, 1987, Digest. Volume 1. New York, Institute of Electrical and Electronics Engineers, Inc., 1987, p. 161-165.

A study of the components of the ocean's circulation using radar altimetry is discussed. The use of a wide-swath radar altimeter to investigate the dynamics of the ocean is examined. The design

and operation of the Aircraft Multibeam Altimeter are described. I.F.

A87-53119

**A SPACEBORNE LFM SCATTEROMETER FOR OCEAN SURFACE WIND VECTOR MEASUREMENT - A TIME DOMAIN APPROACH**

N. S. PILLAI, A. M. JHA, and TAPAN MISRA (Indian Space Research Organization, Space Applications Centre, Ahmedabad, India) IN: IGARSS '87 - International Geoscience and Remote Sensing Symposium, Ann Arbor, MI, May 18-21, 1987, Digest. Volume 1. New York, Institute of Electrical and Electronics Engineers, Inc., 1987, p. 185-190. refs

Spaceborne scatterometers utilize the concept of cell segmentation either by range gating or by Doppler filtering. The three-beam ERS-1 scatterometer to be launched by ESA during 1989 is proposed to have a time domain processing aspect. Doppler processing was implemented for Seasat, while the more advanced three-beam scatterometer NSCAT, which is to be flown around 1990, is proposed to have digital implementation of the frequency domain processing approach. Both approaches utilize a cw pulse and pose problems for smaller cell size and wider swath achievement. This paper proposes a modified scheme where the pulse transmitted is linearly frequency-modulated and the processing is carried out in the time domain. The proposed scheme takes care of limitations imposed by cw-pulse transmission. Author

A87-53127

**WIND AND WAVE STATISTICS AS DERIVED FROM THE GEOSAT RADAR ALTIMETER AND WITH COMPARISONS WITH IN SITU MEASUREMENTS**

ELLA B. DOBSON (Johns Hopkins University, Laurel, MD) IN: IGARSS '87 - International Geoscience and Remote Sensing Symposium, Ann Arbor, MI, May 18-21, 1987, Digest. Volume 1. New York, Institute of Electrical and Electronics Engineers, Inc., 1987, p. 245-249. refs

Measurements of wind speed and significant waveheight over the world's oceans have been provided by the Geosat altimeter since March 1985. These measurements comprise a unique data base which is expanding as the altimeter continues to collect data in the Exact Repeat Mission which began in November 1986. In order to properly interpret research results which utilize these data, it is necessary to know the accuracies which can be associated with the measurements. This paper evaluates these accuracies by comparing altimeter and buoy measurements. These studies have shown that the altimeter is performing within the required specifications in measuring both wind speed and significant waveheight. There is evidence that a more refined wind speed algorithm may even improve present accuracies. Author

A87-53144\* National Aeronautics and Space Administration. Goddard Space Flight Center, Greenbelt, Md.

**MODIS - ADVANCED FACILITY INSTRUMENT FOR STUDIES OF THE EARTH AS A SYSTEM**

V. V. SALOMONSON, W. BARNES, H. MONTGOMERY, and H. OSTROW (NASA, Goddard Space Flight Center, Greenbelt, MD) IN: IGARSS '87 - International Geoscience and Remote Sensing Symposium, Ann Arbor, MI, May 18-21, 1987, Digest. Volume 1. New York, Institute of Electrical and Electronics Engineers, Inc., 1987, p. 361-365. refs

The Moderate Resolution Imaging Spectrometer (MODIS), a key part of the Earth Observing System planned for the 1990's, is described. The complementary MODIS-T (64 channels) and MODIS-N (40 channels) instruments provide a multispectral observing capability that has application to land, ocean, and atmospheric research. The modules have a 500-1000 meter spatial resolution to accompany a swath width sufficient to provide two-day repeat coverage from a polar-orbiting, sun-synchronous, space-station serviceable platform. High signal-to-noise capability (500/1 or better) and 10-12 bit quantization over the dynamic ranges of the various spectral bands will be provided by the two modules. R.R.

A87-53189

**INVERSE SYNTHETIC APERTURE RADAR IMAGING TECHNIQUES FOR SEA-SURFACE TARGETS**

YIN-WU CHEN and RAYMOND S. BERKOWITZ (Pennsylvania, University, Philadelphia) IN: IGARSS '87 - International Geoscience and Remote Sensing Symposium, Ann Arbor, MI, May 18-21, 1987, Digest. Volume 1. New York, Institute of Electrical and Electronics Engineers, Inc., 1987, p. 723-728. Research supported by IBM Corp. refs

For a short time interval the motion of the target can be linearized and represented by a constant angular velocity (rotation) and a constant linear velocity (translation). The former motion can be utilized to obtain an image. A general geometric formulation of range-Doppler imaging, based on a point-scatterer model and short observation time, is derived in this paper. Range variation and uncertainties of phase measurements are incorporated in the equations in order to exemplify range-alignment and dominant reflector phase compensation techniques. Some simulation results demonstrate the importance of these techniques. Superresolution spectral estimation techniques are proposed to obtain high resolution images from a short time record of signal samples. Comparison of two superresolution spectral estimation techniques, Burg's algorithm and a linear prediction extrapolation method, with conventional FFT processing are presented. Author

A87-53191

**OBSERVATION OF OIL SLICKS ON THE OCEAN BY X-BAND SLAR**

TOSHIAKI KOZU, TOSHIHIKO UMEHARA, TAKEYUKI OJIMA, TAKESHI SUITSU, HARUNOBU MASUKO (Ministry of Posts and Telecommunications, Radio Research Laboratories, Koganei, Japan) et al. IN: IGARSS '87 - International Geoscience and Remote Sensing Symposium, Ann Arbor, MI, May 18-21, 1987, Digest. Volume 1. New York, Institute of Electrical and Electronics Engineers, Inc., 1987, p. 735-740. Research supported by the Environmental Agency of Japan. refs

The oil slick observation was carried out in the Pacific Ocean with an X-band real aperture SLAR. The feature of the SLAR is the capability of quantitative radar cross-section measurement which is useful for microwave remote sensing study. The purpose of the experiment was to clarify the microwave radar signatures of ocean slicks and to obtain information for choosing the observation parameters most suitable for oil spill monitoring by SLAR and spaceborne SAR. In the experiment, slicks of three different sizes were made with oleyl alcohol discharged from a ship. From straight flight observations, results were obtained on the reduction in normalized radar cross section due to slicks. Author

A87-53192

**RADAR SIGNATURES OF OIL FILMS FLOATING ON THE SEA SURFACE**

WERNER ALPERS (Bremen, Universitaet, West Germany) and HEINRICH HUEHNERFUSS (Hamburg, Universitaet, West Germany) IN: IGARSS '87 - International Geoscience and Remote Sensing Symposium, Ann Arbor, MI, May 18-21, 1987, Digest. Volume 1. New York, Institute of Electrical and Electronics Engineers, Inc., 1987, p. 741-745. refs  
(Contract BMFT-01-QS-86174; DFG-WA-124/12-1)

Airborne radar backscattering experiments carried out recently by Singh et al. (1986) at C- and Ku-band over sea surfaces covered with mineral oil films show that the radar cross section depression has a maximum as a function of incidence angle. In this paper, this phenomenon is explained by the Marangoni effect which causes a resonance-type wave damping in the short gravity wave region when the sea surface is covered with a viscoelastic film. Maximum wave damping was observed by Singh et al. (1986) at frequencies around 8 Hz. It is argued that the Marangoni damping arises from surface active compounds, which are always encountered in mineral oil as 'impurities'. This surface active material tends to spread from the thick oil spill centers over the surrounding sea surface. Author

A87-53194

**SPOT, A SATELLITE FOR OCEANOGRAPHY?**

A. WADSWORTH and P. PIAU (Institut Francais de Petrole, Rueil-Malmaison, France) IN: IGARSS '87 - International Geoscience and Remote Sensing Symposium, Ann Arbor, MI, May 18-21, 1987, Digest. Volume 1. New York, Institute of Electrical and Electronics Engineers, Inc., 1987, p. 757-759.

The application of SPOT data to oceanography is examined. The ocean features detected on the SPOT images of the area around Madras, India, obtained on March 22, 1986, which include internal waves, a swell, an oil slick, and coastal processes, are described. It is noted that SPOT images obtained when the satellite sensor operates in the tilt mode are useful for oceanic studies. I.F.

A87-53196\* Jet Propulsion Lab., California Inst. of Tech., Pasadena.

**THE EFFECTS OF WIND-WAVE COUPLING ON SCATTEROMETER WIND MEASUREMENT ACCURACY**

ROMAN E. GLAZMAN (California Institute of Technology, Jet Propulsion Laboratory, Pasadena) IN: IGARSS '87 - International Geoscience and Remote Sensing Symposium, Ann Arbor, MI, May 18-21, 1987, Digest. Volume 2. New York, Institute of Electrical and Electronics Engineers, Inc., 1987, p. 769-771. refs

The recent study of the effects of large-scale waves on scatterometer wind-measurement accuracy provides evidence of the important role played by the degree of wind-wave coupling. This degree is quantified by means of a generalized wind fetch introduced by definition. As a result, the fetch-induced bias in the SASS wind speeds is found to be as high as 2 m/s per 100 km of the fetch. An explanation of the bias is suggested based on the consideration of an additional component of surface scattering caused by EM wave diffraction at the crests of individual, sufficiently steep wavelets. Author

A87-53197\* Jet Propulsion Lab., California Inst. of Tech., Pasadena.

**A COMPARATIVE STUDY OF SEVERAL WIND ESTIMATION ALGORITHMS FOR SPACEBORNE SCATTEROMETERS**

CHONG-YUNG CHI and FUK K. LI (California Institute of Technology, Jet Propulsion Laboratory, Pasadena) IN: IGARSS '87 - International Geoscience and Remote Sensing Symposium, Ann Arbor, MI, May 18-21, 1987, Digest. Volume 2. New York, Institute of Electrical and Electronics Engineers, Inc., 1987, p. 773-777. refs

The paper presents a comparison study for the performances of seven wind estimation algorithms for spaceborne scatterometers. These algorithms are weighted least square in log domain, maximum-likelihood, least square weighted least square, adjustable weighted least square, L1 norm, and least wind speed square algorithms using radar scatterometer measurements. For each algorithm, the system performance simulation results are presented for the NASA scatterometer system planned to be launched in the 1990's. Author

A87-53198\* Jet Propulsion Lab., California Inst. of Tech., Pasadena.

**DECONVOLUTION OF SEA STATE PARAMETERS FROM ALTIMETER WAVEFORMS**

ERNESTO RODRIGUEZ, BRUCE CHAPMAN, CHONG-YUNG CHI, and ERIC LIU (California Institute of Technology, Jet Propulsion Laboratory, Pasadena) IN: IGARSS '87 - International Geoscience and Remote Sensing Symposium, Ann Arbor, MI, May 18-21, 1987, Digest. Volume 2. New York, Institute of Electrical and Electronics Engineers, Inc., 1987, p. 779-782. refs

The paper reports on an on-going effort at the JPL to estimate the accuracy of ocean state parameters which have been obtained from the specular point probability density function (pdf) of the ocean surface. This pdf is obtained by the deconvolution of the return waveform of oceanographic altimeters such as Seasat, Geosat, or Topex. Author

**A87-53199\*** National Aeronautics and Space Administration. National Space Technology Labs., Bay Saint Louis, Miss.  
**AN OPERATIONAL MULTISPECTRAL SCANNER FOR BATHYMETRIC SURVEYS - THE ABS NORDA SCANNER**  
 STEPHEN P. HAIMBACH, RICHARD T. JOY, and G. DANIEL HICKMAN (NASA, National Space Technology Laboratories; U.S. Navy, Naval Ocean Research and Development Activity, Bay Saint Louis, MS) IN: IGARSS '87 - International Geoscience and Remote Sensing Symposium, Ann Arbor, MI, May 18-21, 1987, Digest. Volume 2. New York, Institute of Electrical and Electronics Engineers, Inc., 1987, p. 785-790. refs

The Naval Ocean Research and Development Activity (NORDA) is developing the Airborne Bathymetric Survey (ABS) system, which will take shallow water depth soundings from a Navy P-3 aircraft. The system combines active and passive sensors to obtain optical measurements of water depth. The ABS NORDA Scanner is the systems passive multispectral scanner whose design goal is to provide 100 percent coverage of the seafloor, to depths of 20 m in average coastal waters. The ABS NORDA Scanner hardware and operational environment is discussed in detail. The optical model providing the basis for depth extraction is reviewed and the proposed data processing routine discussed. Author

**A87-53212**  
**MODELING OF FOCUS EFFECTS IN SAR IMAGES OF THE OCEAN SURFACE**

DAVID R. LYZENGA and CHRISTOPHER C. WACKERMAN (Michigan, Environmental Research Institute, Ann Arbor) IN: IGARSS '87 - International Geoscience and Remote Sensing Symposium, Ann Arbor, MI, May 18-21, 1987, Digest. Volume 2. New York, Institute of Electrical and Electronics Engineers, Inc., 1987, p. 933-936. refs  
 (Contract N00014-81-C-0692)

The present numerical simulation model for the phase and magnitude modulation of SAR signals by ocean surface waves is used to investigate the effects of radial accelerations, azimuthal scatterer velocities, and modulation pattern velocities on SAR-image focusing properties while ocean wavelengths, directions, and amplitudes are varied. While scatterers with constant radial acceleration or constant azimuthal velocity are smeared by the nominally focused SAR image, refocusing is obtainable through adjustment of the quadratic phase coefficient in the SAR processor. A modulation pattern moving in the azimuth direction can generate a smearing effect that is partially removable by means of a quadratic phase correction. O.C.

**A87-53219**  
**MODULATION TRANSFER FUNCTION OF RADAR RETURN POWER FROM THE OCEAN**

VAHID HESANY and RICHARD K. MOORE (University of Kansas Center for Research, Inc., Radar Systems and Remote Sensing Laboratory, Lawrence) IN: IGARSS '87 - International Geoscience and Remote Sensing Symposium, Ann Arbor, MI, May 18-21, 1987, Digest. Volume 2. New York, Institute of Electrical and Electronics Engineers, Inc., 1987, p. 993-998. refs  
 (Contract N00014-79-C-0533)

The linear 'modulation transfer function' (MTF) concept has been used to describe the modulation of the backscattered power of large-scale ocean waves under remote radar sensing. Attention is given to the MTF concept's shortcomings: MTF assumes (1) a linear relation between long-wave slope and radar backscatter and (2) the adequacy of linear ocean wave theory for the determination of slopes from velocity measurements. Here it is shown that the relation of long-wave slope and backscatter is often nonlinear, as presently treated in the case of horizontally polarized backscatterers. O.C.

**A87-53224**  
**THE PRODUCTION OF REAL TIME WAVE SPECTRA FROM THE SIR-C SAR**

FRANK M. MONALDO (Johns Hopkins University, Laurel, MD) IN: IGARSS '87 - International Geoscience and Remote Sensing Symposium, Ann Arbor, MI, May 18-21, 1987, Digest. Volume 2. New York, Institute of Electrical and Electronics Engineers, Inc., 1987, p. 1049-1052.

The analysis of ocean imagery from the synthetic aperture radars (SARs) aboard the Seasat satellite and the Shuttle imaging radar (SIR-B) mission has demonstrated that two-dimensional image spectra can be used to generate estimates of two-dimensional ocean wave spectra. The production of such spectra does not require as high a spatial resolution and swath width as was generally available for Seasat and SIR-B imagery. This, combined with the higher radar frequency available on SIR-C make possible the real time production of SAR imagery and image spectra on SIR-C. It is the purpose of this paper to show that spectra produced by the planned, on-board SIR-C wave image processor can provide useful estimates of wave spectra. Author

**A87-53234**  
**REAL TIME GLOBAL OCEAN WAVE SPECTRA FROM SIR-C - SYSTEMS DESIGN**

J. L. MACARTHUR and S. F. ODEN (Johns Hopkins University, Laurel, MD) IN: IGARSS '87 - International Geoscience and Remote Sensing Symposium, Ann Arbor, MI, May 18-21, 1987, Digest. Volume 2. New York, Institute of Electrical and Electronics Engineers, Inc., 1987, p. 1105-1108.

A processing system is being designed that will operate in conjunction with the SIR-C C-band Synthetic Aperture Radar (SAR) to produce real-time, on-board wave directional spectra. An all-digital design will be used for range and azimuth compression, clutter-locking, range-walk correction, and the transformation to two-dimensional spectra. The processor will require that the SAR be in the 10 MHz pulse bandwidth mode, but will accommodate pulse rates between 1250 and 1800 Hz. The spectra will be formed from 256 x 256 cell images with an overall dimension of approximately 7.7 x 7.7 km. This process may be repeated continuously with a small gap between images. The basic output spectra will consist of 16 x 32 pixels of 8 bits each, having an upper cut-off of 1/120 cycles/meter. The resulting data rate will be approximately 4 Kbps. Author

**A87-53236\*** Massachusetts Inst. of Tech., Cambridge.  
**THEORETICAL MODELS FOR MICROWAVE REMOTE SENSING OF SNOW-COVERED SEA ICE**

F. C. LIN, J. A. KONG, and R. T. SHIN (MIT, Cambridge, MA) IN: IGARSS '87 - International Geoscience and Remote Sensing Symposium, Ann Arbor, MI, May 18-21, 1987, Digest. Volume 2. New York, Institute of Electrical and Electronics Engineers, Inc., 1987, p. 1121-1125. refs  
 (Contract N00014-83-K-0528; NAG5-270; NSF ECS-85-04381)

The volume scattering effects of snow-covered sea ice are studied with a three-layer random medium model for microwave remote sensing. Theoretical results are illustrated by matching experimental data for dry snow-covered thick first-year sea ice at Point Barrow. The radar backscattering cross sections are seen to increase with snow cover for snow-covered sea ice, due to the increased scattering effects in the snow layer. The results derived can also be applied to passive remote sensing. Author

**A87-53237\*** Environmental Research Inst. of Michigan, Ann Arbor.

**THEORETICAL AND EXPERIMENTAL STUDY OF THE RADAR BACKSCATTER OF ARCTIC SEA ICE**

ROBERT G. ONSTOTT (Michigan, Environmental Research Institute, Ann Arbor) IN: IGARSS '87 - International Geoscience and Remote Sensing Symposium, Ann Arbor, MI, May 18-21, 1987, Digest. Volume 2. New York, Institute of Electrical and Electronics Engineers, Inc., 1987, p. 1127-1129. refs  
(Contract N00014-85-K-0200; NAGW-334)

The present theoretical model for sea ice radar backscatter has supported parametric studies of radar signature sensitivity to changes in salinity, temperature, brine volume, density, air bubble size, and surface roughness. Parametric study results indicate that first-year and multiyear ice may be confused when first-year ice is very rough and has exceptionally high salinity, as well as being only a few degrees C from the melting point. Confusion also arises when multiyear ice is slightly more saline, the temperature is a few degrees C from the melting point, surface is moderately rough, and air bubbles are small but still typical of multiyear ice. O.C.

**A87-53238**

**PROGRESS ON DIGITAL ALGORITHMS FOR DERIVING SEA ICE PARAMETERS FROM SAR DATA**

R. A. SHUCHMAN, B. A. BURNS, C. C. WACKERMAN, R. G. ONSTOTT, and J. D. LYDEN (Michigan, Environmental Research Institute, Ann Arbor) IN: IGARSS '87 - International Geoscience and Remote Sensing Symposium, Ann Arbor, MI, May 18-21, 1987, Digest. Volume 2. New York, Institute of Electrical and Electronics Engineers, Inc., 1987, p. 1131-1133. refs  
(Contract N00014-81-C-0295)

**A87-53239\*** Stanford Univ., Calif.

**OBSERVING ROTATION AND DEFORMATION OF SEA ICE WITH SYNTHETIC APERTURE RADAR**

J. F. VESECKY, R. SAMADANI, J. M. DAIDA, M. P. SMITH, and R. N. BRACEWELL (Stanford University, CA) IN: IGARSS '87 - International Geoscience and Remote Sensing Symposium, Ann Arbor, MI, May 18-21, 1987, Digest. Volume 2. New York, Institute of Electrical and Electronics Engineers, Inc., 1987, p. 1137-1145. refs  
(Contract NAGW-419)

The ESA's ERS-1 satellite will carry SARs over the polar regions; an important component in the use of these data is an automated scheme for the extraction of sea ice velocity fields from a sequence of SAR images of the same geographical region. The image pyramid area-correlation hierarchical method is noted to be vulnerable to uncertainties for sea ice rotations greater than 10-15 deg between SAR observations. Rotation-invariant methods can successfully track isolated floes in the marginal ice zone. Hu's (1962) invariant moments are also worth considering as a possible basis for rotation-invariant tracking methods. Feature tracking is inherently robust for tracking rotating sea ice, but is limited when features are floe-lead boundaries. A variety of techniques appears necessary. O.C.

**A87-53240**

**OPTIMUM USE OF DUAL FREQUENCY PASSIVE MICROWAVE MEASUREMENTS FOR ICE/OCEAN INTERACTIONS**

I. G. RUBINSTEIN and R. O. RAMSEIER (York University, Downsview, Canada) IN: IGARSS '87 - International Geoscience and Remote Sensing Symposium, Ann Arbor, MI, May 18-21, 1987, Digest. Volume 2. New York, Institute of Electrical and Electronics Engineers, Inc., 1987, p. 1147-1149. refs

Passive microwave measurements from Nimbus-7 SMMR, interpreted by sea ice and ocean surface wind models, provide simultaneous observations on the extent of the sea ice and ocean surface wind speeds. The information on atmospheric conditions over open ocean areas is also derived from the same sets of SMMR data. The potential application of these results for driving ice/ocean interaction models and to serve as one of the inputs for wave models is discussed. Author

**A87-53241\*** National Aeronautics and Space Administration. Goddard Space Flight Center, Greenbelt, Md.

**INVESTIGATION OF MULTI-DIMENSIONAL ALGORITHMS USING ACTIVE AND PASSIVE MICROWAVE DATA FOR ICE CONCENTRATION DETERMINATION**

DONALD J. CAVALIERI (NASA, Goddard Space Flight Center, Greenbelt, MD), BARBARA A. BURNS, and ROBERT G. ONSTOTT (Michigan, Environmental Research Institute, Ann Arbor) IN: IGARSS '87 - International Geoscience and Remote Sensing Symposium, Ann Arbor, MI, May 18-21, 1987, Digest. Volume 2. New York, Institute of Electrical and Electronics Engineers, Inc., 1987, p. 1151-1153. NASA-supported research.  
(Contract N00014-81-C-0295)

A discussion is presented concerning the effect of variations in ice surface characteristics on the concentration calculations, in order to ascertain how active and passive microwave data can be optimally combined. Attention is given to dual-polarized, multifrequency passive microwave sensors and to single-channel SAR, in virtue of their availability in the near future. An examination of SAR intensity data at both 1 and 10 GHz indicates that the latter are much less sensitive to ice type and surface condition variations such as wetness and ridging. The Advanced Multichannel Microwave Radiometer is discussed. O.C.

**A87-53263\*** National Aeronautics and Space Administration. Wallops Flight Center, Wallops Island, Va.

**OBSERVATIONS OF AND A NEW MODEL FOR FETCH-LIMITED WAVE GROWTH**

E. J. WALSH, D. W. HANCOCK, III, D. E. HINES (NASA, Wallops Flight Center, Wallops Island, VA), R. N. SWIFT, and J. F. SCOTT (EG&G Washington Analytical Services Center, Inc., Pocomoke City, MD) IN: IGARSS '87 - International Geoscience and Remote Sensing Symposium, Ann Arbor, MI, May 18-21, 1987, Digest. Volume 2. New York, Institute of Electrical and Electronics Engineers, Inc., 1987, p. 1367-1373. refs

The Surface Contour Radar (SCR) is a 36-GHz computer-controlled airborne radar which generates a false-color coded elevation map of the sea surface below the aircraft in real time. In the present paper, SCR observations are discussed which demonstrate the existence of a full developed sea state. These observations are used to judge the validity of growth rates for fetch-limited wave spectrum development and lead to new refinements in the modeling of wave generation by wind. It is noted that the observations have resolved an apparent paradox in the JONSWAP and Donelan et al (1985) fetch-limited algorithms. B.J.

**A87-53264**

**PROCESSING OF AIRBORNE SAR IMAGES OF OCEAN WAVES**

P. PIAU (Institut Francais du Petrole, Rueil-Malmaison, France) IN: IGARSS '87 - International Geoscience and Remote Sensing Symposium, Ann Arbor, MI, May 18-21, 1987, Digest. Volume 2. New York, Institute of Electrical and Electronics Engineers, Inc., 1987, p. 1375-1380. refs

**A87-53265**

**THE COMPARISON OF OCEAN-WAVE SPECTRA RECOVERED FROM SIR-B AND SEASAT OBSERVATIONS WITH SIMULTANEOUS BUOY DATA**

J. T. MACKLIN and R. A. CORDEY (General Electric Co., PLC; Marconi Research Centre, Chelmsford, England) IN: IGARSS '87 - International Geoscience and Remote Sensing Symposium, Ann Arbor, MI, May 18-21, 1987, Digest. Volume 2. New York, Institute of Electrical and Electronics Engineers, Inc., 1987, p. 1381-1386. Research supported by the Royal Aircraft Establishment. refs

The current understanding of how ocean waves are imaged by SAR is tested by comparing wave spectra recovered from SIR-B and Seasat observations with simultaneous buoy measurements. Velocity bunching was expected to be the dominant imaging mechanism on the second SIR-B pass and on the Seasat pass



studied. Here SAR estimates of the wave amplitudes were much lower than the buoy-derived values. Author

**A87-53266**

## **AIRBORNE SAR IMAGING OF AZIMUTHALLY TRAVELLING OCEAN SURFACE WAVES - THE LEWEX EXPERIMENTAL PLAN**

N. G. FREEMAN, P. W. VACHON, and C. E. LIVINGSTONE (Canada Centre for Remote Sensing, Ottawa) IN: IGARSS '87 - International Geoscience and Remote Sensing Symposium, Ann Arbor, MI, May 18-21, 1987, Digest. Volume 2. New York, Institute of Electrical and Electronics Engineers, Inc., 1987, p. 1393-1398. refs

**A87-53286\*** Johns Hopkins Univ., Laurel, Md.

## **THE RESPONSE OF SAR IMAGERY TO AZIMUTH TRAVELLING OCEAN SURFACE WAVES AS DETERMINED FROM SHUTTLE SAR IMAGERY**

FRANK M. MONALDO (Johns Hopkins University, Laurel, MD) and FREDERICK C. JACKSON (NASA, Goddard Space Flight Center, Greenbelt, MD) IN: IGARSS '87 - International Geoscience and Remote Sensing Symposium, Ann Arbor, MI, May 18-21, 1987, Digest. Volume 2. New York, Institute of Electrical and Electronics Engineers, Inc., 1987, p. 1565-1568. refs

Comparisons between two-dimensional ocean wave spectra, derived from synthetic aperture radar (SAR) imagery, and two-dimensional wave spectra from independent instruments have shown good agreement. The procedure by which raw SAR image intensity-variance spectra are converted to estimates of wave spectra is dependent upon models of how a SAR is able to image ocean waves. The greatest uncertainty exists about the mechanism by which azimuth (along track) traveling waves are imaged. In this paper, independent wave spectra from an airborne, radar ocean wave spectrometer (ROWS) are systematically compared with spatially and temporally coincident shuttle SAR image intensity-variance spectra to determine an optimum description of the relationship between the two. The result of these comparisons is to demonstrate that a SAR image intensity-variance spectrum is nearly proportional to the ocean wave slope-variance spectrum for azimuth traveling waves. Author

**A87-53287\*** Environmental Research Inst. of Michigan, Ann Arbor.

## **COMPARISON OF NUMERICAL SIMULATIONS WITH SAR IMAGES OF OCEAN SURFACE WAVES IN THE NEW YORK BIGHT**

DAVID R. LYZENGA and JOHN R. BENNETT (Michigan, Environmental Research Institute, Ann Arbor) IN: IGARSS '87 - International Geoscience and Remote Sensing Symposium, Ann Arbor, MI, May 18-21, 1987, Digest. Volume 2. New York, Institute of Electrical and Electronics Engineers, Inc., 1987, p. 1575-1580. refs

(Contract NASA ORDER W-15085)

**A87-53288\*** Johns Hopkins Univ., Laurel, Md.

## **APPROXIMATING SIR-B RESPONSE CHARACTERISTICS AND ESTIMATING WAVE HEIGHT AND WAVELENGTH FOR OCEAN IMAGERY**

DAVID G. TILLEY (Johns Hopkins University, Laurel, MD) IN: IGARSS '87 - International Geoscience and Remote Sensing Symposium, Ann Arbor, MI, May 18-21, 1987, Digest. Volume 2. New York, Institute of Electrical and Electronics Engineers, Inc., 1987, p. 1581-1586. NASA-supported research. refs

NASA Space Shuttle Challenger SIR-B ocean scenes are used to derive directional wave spectra for which speckle noise is modeled as a function of Rayleigh random phase coherence downrange and Poisson random amplitude errors inherent in the Doppler measurement of along-track position. A Fourier filter that preserves SIR-B image phase relations is used to correct the stationary and dynamic response characteristics of the remote sensor and scene correlator, as well as to subtract an estimate of the speckle noise component. A two-dimensional map of sea

surface elevation is obtained after the filtered image is corrected for both random and deterministic motions. O.C.

**A87-53925#**

## **EUROPEAN DISSEMINATION OF MARINE OBSERVATION SATELLITE (MOS-1) DATA**

M. EGLME (Louvain, Universite Catholique, Louvain-la-Neuve, Belgium) and L. FUSCO (ESA, European Space Research Institute, Frascati, Italy) ESA Bulletin (ISSN 0376-4265), no. 50, May 1987, p. 105-110.

In response to the increasing demand in Europe for remote-sensing products, ESA has entered into an agreement with Japan's National Space Development Agency (NASDA) for the operational acquisition, processing, and distribution of data from the Marine Observation Satellite (MOS-1). Although the satellite is dedicated to marine observation, MOS-1 data will have a wide range of potential applications in a variety of fields. Author

**A87-54107\*** Jet Propulsion Lab., California Inst. of Tech., Pasadena.

## **INTERFEROMETRIC RADAR MEASUREMENT OF OCEAN SURFACE CURRENTS**

R. M. GOLDSTEIN and H. A. ZEBKER (California Institute of Technology, Jet Propulsion Laboratory, Pasadena) Nature (ISSN 0028-0836), vol. 328, Aug. 20, 1987, p. 707-709. Navy-sponsored research. refs

A new method of measuring surface currents using an interferometric synthetic aperture radar is presented. An airborne implementation has been tested over San Francisco Bay near the time of maximum tidal flow, resulting in a map of the east-west component of the current. Only the line-of-sight component of velocity is measured by this technique. Where the SNR ratio was strongest, statistical fluctuations of less than 4 cm/s were observed for ocean patches of 60 x 60 m. C.D.

**A87-54301**

## **THE BAKERIAN LECTURE, 1986 - SHIPS FROM SPACE**

W. H. MUNK (California, University, La Jolla), P. SCULLY-POWER (U.S. Navy, Naval Underwater Systems Center, New London, CT), and F. ZACHARIASEN (California Institute of Technology, Pasadena) Royal Society (London), Proceedings, Series A - Mathematical and Physical Sciences (ISSN 0080-4630), vol. 412, no. 1843, Aug. 8, 1987, p. 231-254. Navy-supported research. refs

Narrow V-shaped wakes extending some 20 km behind surface ships were first found on SAR images from Seasat in 1978. The V-wake geometry differed strikingly from the traditional Kelvin wake geometry consisting of divergent and transverse wave components generated by a traveling pressure point. The SAR images can be accounted for in terms of Bragg scatter from relatively short waves generated by the surface vessel. An essential ingredient of this hypothesis is that the wave generation is by an intermittent rather than a steady point source. Optical images from a hand-held camera on a 1985 Space Shuttle mission revealed many V-like wakes behind surface ships. There is no Bragg scattering from the ocean surface at optical wavelengths, so an alternative hypothesis is called for. The observed features can be interpreted in terms of sun glitter from the tilted facets of a Kelvin wake. An essential ingredient is the generation by complex sources rather than by a single point source. The present study is a step toward the interpretation of many unexplained naturally occurring features at the edge of the sun glitter. Author

**N87-25610#** Texas Univ., Austin. Applied Research Lab.

## **DESIGN STUDY OF REMOTE SENSING FOR OCEAN SURFACE AND INTERIOR ACTIVITY Final Report, 1 Jul. 1985 - 30 Sep. 1986**

NICHOLAS P. CHOTIROS 31 Dec. 1986 116 p

(Contract N00014-85-K-0569)

(AD-A180578) Avail: NTIS HC A06/MF A01 CSCL 08C

This is a study to determine the feasibility of using acoustic instruments to observe upper ocean processes. The processes include surface gravity waves, upper ocean turbulence, Langmuir

cells and near currents, and internal waves. The acoustic surface backscatter and the acoustic volume backscatter from bubbles and suspended matter will allow the processes to be observed and tracked. The main issues are spatial resolution, volume coverage, sampling rate, and velocity measurement or tracking accuracy. The acoustic properties of the scatterers were modeled to determine signal detectability, hence volume coverage and resolution. Existing velocity measurement techniques and a new tracking method were also modeled. From all the submodels, a system performance prediction model was constructed, from which recommendations were made regarding sonar configuration, operating frequencies, and other system specifications. GRA

**N87-26405#** GKSS-Forschungszentrum Geesthacht (West Germany). Inst. fuer Physik.

**REMOTE SENSING OF SUSPENDED MATTER IN THE OCEAN BY AIRBORNE LASERS AND SATELLITE RADIOMETERS**  
Thesis - Kiel Univ., West Germany [FERNERKUNDUNG OZEANISCHER SCHWEBSTOFFE MIT FLUGZEUGGETRAGENEN LASERN UND SATELLITENRADIOMETERN]

A. SCHMITZ-PEIFFER 1986 142 p In GERMAN; ENGLISH summary  
(GKSS-86/E/49; ISSN-0344-9629; ETN-87-99915) Avail: NTIS HC A07/MF A01

The remote sensing of suspended and dissolved matter in the ocean by an airborne lidar and the Coastal Zone Color Scanner was examined using radiative transfer calculations. Phytoplankton, suspended matter, and yellow matter can be detected by Raman scattering and fluorescence measurements using an airborne lidar detecting signals at three wavelengths. Changes in concentration of all three substances are easier to detect with an airborne lidar than with a passive radiometer, even if the radiometer is measuring at sea level. Lidar and satellite measurements show satisfactory agreement. The radiative transfer calculations were compared with measurements from ship, plane, and satellite, for calibration.

ESA

**N87-27696#** Joint Publications Research Service, Arlington, Va.  
**SUCCESSSES OF COSMOS-1500 SATELLITE, SLR SYSTEM**  
YURIY ANDREOTTI In its USSR Report: Space p 100-103 21 Apr. 1986 Transl. into ENGLISH from APN: Advances of Science and Technology (Moscow, USSR), no. 21, 5 Nov. 1985 p 1-5  
Avail: NTIS HC A07/MF A01

Some of the results obtained from the Soviet artificial Earth satellite Cosmos-1500 during its two years in orbit are described.

Author

**N87-27855#** Technical Univ. of Denmark, Lyngby. Inst. of Electromagnetics.

**ACTIVE MICROWAVE OBSERVATIONS OF SEA ICE AND ICEBERGS**

H. SKRIVER, P. GUDMANDSEN, and L. ULANDER (Chalmers Univ. of Technology, Goeteborg, Sweden) In ESA Proceedings of the SAR Applications Workshop p 13-24 Dec. 1986  
Avail: NTIS HC A06/MF A01

Methods of automatic retrieval of sea ice parameters from SAR and radar altimeters were investigated. For classification of ice types and for reidentification of floes in consecutive SAR images, texture measures were assessed. Statistical measures, measures of contrast and homogeneity, and co-occurrence matrix measures were studied. For classification the most simple measure, the ratio between the standard deviation and the mean performs best. Texture measures are correlated. For reidentification of floes the performance of the measures is modest, and more advanced methods must be developed. Parameter retrieval from radar altimeter data based on a model of the backscattering mechanisms was investigated, and consistency is found from a comparison between a Seasat SAR scene and overlapping altimeter data. The capability of a spaceborne SAR to detect icebergs was evaluated.

ESA

**N87-27856#** Innsbruck Univ. (Austria). Inst. fuer Meteorologie und Geophysik.

**THE POTENTIAL OF SAR IN A SNOW AND GLACIER MONITORING SYSTEM**

H. ROTT, C. MAETZER, and D. STROBL (Technische Univ., Graz, Austria) In ESA Proceedings of the SAR Applications Workshop p 25-35 Dec. 1986

Avail: NTIS HC A06/MF A01

The use of SAR for snow and glacier applications as part of a multisensor land application system is investigated. Results on the physical properties and the signatures of backscattering of snow and ice are presented. The capabilities of sensors in the various spectral regions are compared. A synergistic data set was analyzed using rectified airborne SAR and LANDSAT TM data. Investigations with additional data sets are going on for optimum use of SAR in an advanced Earth observation system. ESA

**N87-28077#** Joint Publications Research Service, Arlington, Va.  
**MORPHOMETRIC STUDIES OF WORLD OCEAN Abstract Only.**

K. A. ZVONAREV and YE. G. KAPRALOV In its USSR Report: Earth Sciences p 12 4 Mar. 1987 Transl. into ENGLISH from Vestnik Leningradskogo Universiteta, Seriya 7: Geologiya, Geografiya (Leningrad, USSR), no. 3, Sep. 1986 p 50-57

Avail: NTIS HC A05/MF A01

Literature of morphometric studies of the world ocean is reviewed, with emphasis on the work of E. Kossina, M. Groll, O. Krummel, H. W. Menard, and S. M. Smith. The most recent data indicate that about 16% of the area of the ocean has been studied to such a degree that bottom relief forms can be mapped precisely, another 22% is mappable only with the principal relief forms, whereas the remaining area has been studied only very approximately. Many significant contributions to morphometric study of the ocean have been made during the last decade by specialists at Leningrad State University, Moscow State University and the Oceanology Institute, but also by many other Soviet and foreign authors and organizations. Unfortunately, all these studies have been made using different methods and with unlike accuracy. As the degree of study of the ocean floor increases and its shoreline is plotted more precisely there has been an increase in the number of the principal quantitative characteristics used in describing relief of the ocean floor. More and more studies are appearing which give the statistical characteristics of relief, the indices of vertical and horizontal dissection and orientation of the bottom surface, as well as shoreline length and sinuosity, but most are limited to small areas and the range of initial data used is extremely small.

Author

**N87-28125#** Dundee Univ. (Scotland). Physics Lab.  
**SEA SURFACE TEMPERATURES AND THE DETECTION OF OCEAN CIRCULATION PATTERNS AND FRONTS FROM AVHRR IMAGERY**

R. A. VAUGHAN, I. D. DOWNEY (Salford Univ., England), D. LENG, and J. COKER In ESA Proceedings of the ESA/EARSel Europe from Space Symposium p 59-67 Dec. 1986

Avail: NTIS HC A14/MF A01

Data from the NOAA-8 AVHRR were used to study sea surface temperatures in the North East Atlantic and around the Eastern coast of Scotland. Using in situ temperature data, multichannel sea surface temperature algorithms were tested for their validity in these waters with varying degrees of success, and possible sources of error were considered. The development of circulation patterns in the waters in these areas was examined in relation to data from drifting buoys, and the stability of thermal fronts in the Irish and Celtic Seas was investigated. Cloud cover limits the usefulness of the technique.

ESA



**N87-28132#** Institute of Oceanographic Sciences, Wormley (England).

## **THE DETERMINATION OF SEA-STATE BIAS AND NON-LINEAR WAVE PARAMETERS FROM SATELLITE ALTIMETER DATA**

T. H. GUYMER and M. A. SROKOSZ / In ESA Proceedings of the ESA/EARSeL Europe from Space Symposium p 115-120 Dec. 1986 Sponsored in part by the UK ERS Data Center  
 Avail: NTIS HC A14/MF A01

Data from the repeat track period of SEASAT were analyzed to investigate the variation of mesoscale ocean variability with sea state. Results show that the relationship is not constant but appears to depend on whether the wave field is developing or decaying. This is interpreted in terms of parameters describing the nonlinearities of the surface gravity waves. Implications for the interpretation of mesoscale variability analyses are discussed. Attempts to calculate the sea-state bias theoretically from the shape of the return pulse measured by an altimeter are described. ESA

**N87-28133#** Joint Research Centre of the European Communities, Ispra (Italy).

## **MONITORING AND MODELING OF THE ADRIATIC SEA**

J. A. DEBEKKER / In ESA Proceedings of the ESA/EARSeL Europe from Space Symposium p 121-127 Dec. 1986  
 Avail: NTIS HC A14/MF A01

A program to develop a spaceborne monitoring system to track coastal transport of pollution is outlined. Sensors used include the Coastal Zone Color Scanner on NIMBUS 6, the Advanced Very High Resolution Radiometers on NOAA 6 and 9, and the LANDSAT 5 Thematic Mapper. A model of the northern Adriatic Sea was developed. Image processing, and measuring campaigns are described. ESA

**N87-28134#** Joint Research Centre of the European Communities, Ispra (Italy). Physics Div.

## **EVALUATION OF THE POTENTIAL OF THE THEMATIC MAPPER FOR MARINE APPLICATION**

S. TASSAN / In ESA Proceedings of the ESA/EARSeL Europe from Space Symposium p 129-136 Dec. 1986  
 Avail: NTIS HC A14/MF A01

The potential of the Thematic Mapper (TM) for chlorophyll and suspended sediment determination in the sea was investigated by comparison with the Coastal Zone Color Scanner (CZCS) on NIMBUS-7. A sensitivity analysis, considering error sources as retrieval algorithm sensitivity, atmospheric correction, instrument noise, and signal digitalization, was completed by a TM image analysis. Tests validate the positive conclusions of the theoretical work, indicating that the analysis of TM band 1 to 3 data can yield quantitative information on chlorophyll and sediment concentration in the sea of satisfactory quality, substantially similar to that of CZCS derived values. ESA

**N87-28146#** Copenhagen Univ. (Denmark). Inst. of Geophysics.

## **COASTAL ZONE COLOR SCANNER (CZCS) IMAGES AND OCEAN DYNAMICS. APPLICATION TO THE NORTHWEST AFRICAN UPWELLING AREA**

L. NYKJAER, L. VANCAMP, P. SCHLITTENHARDT (Joint Research Centre of the European Communities, Ispra, Italy), and R. REFK / In ESA Proceedings of the ESA/EARSeL Europe from Space Symposium p 219-223 Dec. 1986  
 Avail: NTIS HC A14/MF A01

Eleven Coastal Zone Color Scanner images covering the northwest African upwelling area were processed to geometrically rectified maps of phytoplankton pigment concentrations. The spatial features visible in the satellite images are interpreted in terms of the dynamics in the area. To support this interpretation wind data were collected and processed to show parameters related to wind induced transport mechanisms in the water. From this it is evident that the differences in pigment patterns in the northern and southern part of the study area are due to differences in wind patterns. Other phenomena are explained using knowledge about the fluid forces occurring in currents and eddies. ESA

**N87-28153#** Joint Research Centre of the European Communities, Ispra (Italy).

## **CORRECTION OF THE SENSOR DEGRADATION OF THE COASTAL ZONE COLOR SCANNER ON NIMBUS-7**

B. STURM / In ESA Proceedings of the ESA/EARSeL Europe from Space Symposium p 263-267 Dec. 1986  
 Avail: NTIS HC A14/MF A01

Sensitivity loss in NIMBUS-7 Coastal Zone Color Scanner (CZCS) channels 443, 520, and 550 on nm the order of 50%, 20% and 10%, respectively, is discussed. The loss is due to a deterioration of optical surfaces positioned before the introduction of the internal calibration light sources. For quantitative determination of chlorophyll-like pigment and total suspended matter concentrations from the CZCS data this sensitivity loss must be corrected. Sensitivity-loss correction factors are evaluated up to Orbit No. 35345 (Oct 10, 1985) by comparing measured and expected sensor aperture radiances for water with low pigment and total suspended matter concentrations (clear water). The water-leaving radiances and the optical parameters of the aerosol are assumed to vary randomly around fixed standard values. The evaluated pigment concentration is little affected by the inaccuracy of the calculated decay compensation factors because compensation for the errors occurs when the aerosol Angstrom exponent is calculated with consistent clear waterleaving radiances. ESA

**N87-28154#** Deutsche Forschungs- und Versuchsanstalt fuer Luft- und Raumfahrt, Oberpfaffenhofen (West Germany).

## **ADRIA 84: AIRBORNE INVESTIGATIONS OF GELBSTOFF BY OPTICAL RADIOMETRY AND FLUORESCENCE LIDAR**

V. AMMANN, R. REUTER, and P. SCHLITTENHARDT (Joint Research Centre of the European Communities, Ispra, Italy) / In ESA Proceedings of the ESA/EARSeL Europe from Space Symposium p 269-273 Dec. 1986  
 Avail: NTIS HC A14/MF A01

Gelbstoff (dissolved organic matter) was used as a natural tracer for the study of transport and mixing, and for the identification of characteristic water masses and frontal systems, in the Adriatic Sea. Airborne lidar measurements with excitation at 308 nm and 450 nm; ocean color data in the visible spectral range collected with airborne sensors (ocean color radiometer and six-channels radiometer); in-situ measurements of gelbstoff, chlorophyll, and suspended matter concentrations are summarized. ESA

**N87-28155#** Technical Univ. of Denmark, Lyngby. Inst. of Electromagnetics.

## **TRACKING OF ICE FLOES**

PETER RANDRUP CHRISTENSEN / In ESA Proceedings of the ESA/EARSeL Europe from Space Symposium p 275-279 Dec. 1986 Sponsored by the Danish Space Research Committee, the Commission for Scientific in Greenland, and IBM-Denmark  
 Avail: NTIS HC A14/MF A01

Future position of a floe was predicted using NOAA AVHRR, from its previous position and the motion of other floes in the area. An interactive program allowing the analyst to track floes in consecutive images was developed. An improvement of the method is possible, if an automatic determination of the new position of the floe is possible. A method in which a spatial correlation technique is employed to determine the new position of the floe is investigated. Since the prediction allows the search region to be small the number of false findings is reduced. The method works well on cloud free or nearly cloud free images. The heuristic method used to pick the floe from the image may be improved by the use of an edge enhancement of an adaptive threshold determined from local values for the brightness levels of ice and water. ESA

**N87-28156#** Technical Univ. of Denmark, Lyngby. Inst. of Electromagnetics.

**SEA ICE OBSERVATIONS BY SAR**

HENNING SKRIVER *In* ESA Proceedings of the ESA/EARSel Europe from Space Symposium p 281-288 Dec. 1986 Sponsored by ESA

Avail: NTIS HC A14/MF A01

Methods for sea ice parameter retrieval from synthetic aperture radar (SAR) data were investigated. Automatic parameter estimation methods are needed to cope with the huge amount of data. A pixel-by-pixel classification scheme for sea ice type determination, and a spatial segmentation scheme for studies of sea ice dynamics were assessed. The SAR data must be corrected before the parameter retrieval is carried out, i.e., radiometrically and geometrically corrected, and speckle reduced. Speckle reduction was investigated and noncoherent averaging and adaptive filtering (Lee and Frost filters) were applied. ESA

**N87-28157#** Roskilde Univ. (Denmark).

**STUDIES OF TIDAL FLAT ENVIRONMENTS WITH LANDSAT MSS DATA**

S. FOLVING *In* ESA Proceedings of the ESA/EARSel Europe from Space Symposium p 289-293 Dec. 1986

Avail: NTIS HC A14/MF A01

Multitemporal LANDSAT data were used to classify and map tidal flats in accordance with the main sediment types found by field work. By combining imagery from 1976 with imagery from 1981 and by means of principal component analysis, it is possible to detect major changes in the sandy tidal flats, whereas changes in the silty and clayey tidal flats seem hard to detect. Multispectral measurements from aircraft, 150 m above the surface, recorded concurrently with collection of water samples were used to calibrate the satellite data. Multivariate statistical analyses were performed, and the results made it possible to map the spatial variation in concentrations of suspended matter. ESA

**N87-28239#** Woods Hole Oceanographic Institution, Mass.

**DATA TELEMETRY, ASSIMILATION AND OCEAN MODELING Semiannual Report, 1 Oct. 1986 - 1 Apr. 1987**

DANIEL E. FRYE Jun. 1987 41 p

(Contract N00014-86-K-0751)

(AD-A181899; WHOI-87-21) Avail: NTIS HC A03/MF A01

CSCL 08C

The objectives of this program are to advance the state of the art in ocean data telemetry, interpretation of remotely sensed data from satellite, and numerical modeling of ocean circulation. Ocean data telemetry is being addressed by several development projects whose aim is to reliably transfer data from in situ oceanographic instruments to laboratory computers on the shore. The satellite oceanography group is developing expertise in analyzing, manipulating, displaying and archiving data from all of the major satellite oceanographic sensors. The numerical modeling initiative is working on a family of circulation models which can be connected at their boundaries to cover the important mesoscale and basin wide flow regimes. These ambitious plans are intended to bring new technologies developed in the communications, electronics, satellite sensing and computer science fields into everyday use in oceanography so that they can be ready for the global science programs planned for the 1990's. GRA

**N87-28242#** Naval Postgraduate School, Monterey, Calif.

**COMPARISON OF SATELLITE-DERIVED OCEAN VELOCITIES WITH OBSERVATIONS IN THE CALIFORNIA COASTAL REGION M.S. Thesis**

JOHN F. OHARA Mar. 1987 42 p

(AD-A182291) Avail: NTIS HC A03/MF A01 CSCL 08C

Satellite derived ocean surface velocity vectors in the California Current System (CCS) are compared with in situ hydrographic and Doppler data. The in situ data were acquired during the April 1981 phase of the Coastal Ocean Dynamics Experiment (CODE) experiment. In general, the satellite derived velocities agreed with the in situ data. Due to the baroclinic nature of the study region, the satellite vectors were found to be representative of the

subsurface geostrophic flow. Although the number and concentration of the satellite vectors was small, these vectors were capable of resolving the mesoscale features located in the study region. Comparison of collocated data revealed that the in situ Doppler velocity measurements were approximately 1.5 times larger than the satellite derived velocity vectors. These results agree with a similar study conducted in an offshore region. GRA

**N87-28471\*#** National Aeronautics and Space Administration. Langley Research Center, Hampton, Va.

**CALCULATION AND ACCURACY OF ERBE SCANNER MEASUREMENT LOCATIONS**

LAWRENCE H. HOFFMAN, WILLIAM L. WEAVER, and JAMES F. KIBLER Sep. 1987 34 p

(NASA-TP-2670; L-16218; NAS 1.60:2670) Avail: NTIS HC

A03/MF A01 CSCL 03B

The Earth Radiation Budget Experiment (ERBE) uses scanning radiometers to measure shortwave and longwave components of the Earth's radiation field at about 40 km resolution. It is essential that these measurements be accurately located at the top of the Earth's atmosphere so they can be properly interpreted by users of the data. Before the launch of the ERBE instrument sets, a substantial emphasis was placed on understanding all factors which influence the determination of measurement locations and properly modeling those factors in the data processing system. After the launch of ERBE instruments on the Earth Radiation Budget Satellite and NOAA 9 spacecraft in 1984, a coastline projection method was developed to assess the accuracy of the algorithms and data used in the location calculations. Using inflight scanner data and the coastline detection technique, the measurement location errors are found to be smaller than the resolution of the scanner instruments. This accuracy is well within the required location knowledge for useful science analysis. Author

**N87-28954#** National Oceanic and Atmospheric Administration, Seattle, Wash. Marine Environmental Lab.

**THEORY OF FLUORESCENT IRRADIANCE FIELDS IN LAKES AND SEAS**

R. W. PREISENDORFER Mar. 1987 256 p

(PB87-196465; NOAA-TM-ERL-PMEL-70) Avail: NTIS HC

A12/MF A01 CSCL 08H

The present work forms the basis for applications of radiative transfer theory to remote sensing of seas and lakes and specifically for optically-based chlorophyll assays within such media. In particular, it is shown how to determine the intrinsic (or specific) optical properties of a natural hydrosol from irradiance measurements in the hydrosol. GRA

**N87-29033#** National Ocean Service, Anchorage, Alaska. Ocean Assessments Div.

**GULF OF ALASKA: PHYSICAL ENVIRONMENT AND BIOLOGICAL RESOURCES**

D. W. HOOD and S. T. ZIMMERMAN Jun. 1987 629 p

Sponsored by Minerals Management Service, Anchorage, Alaska

(PB87-103230; OCS/MMS-86/0095) Avail: NTIS HC A99/MF

A01 CSCL 13B

Gulf of Alaska; Physical Environment and Biological Resources, is a comprehensive treatise (600 pp). The multi-author document contains twenty chapters on a broad spectrum of marine disciplines that consolidate the authors' knowledge of the region into a single document. It is heavily referenced and, in addition, includes a glossary and extensive index. The book is intended for a broad audience: students, researchers, resource managers and the public. GRA

## 05 OCEANOGRAPHY AND MARINE RESOURCES

**N87-29067\*#** Texas A&M Univ., College Station. Coll. of Geosciences.

**APPLICATION OF SATELLITE DATA TO TROPIC-SUBTROPIC MOISTURE COUPLING Final Contractor Report, Apr. 1983 - Jul. 1987**

AYLMER H. THOMPSON and JAMES P. MCGUIRK Washington  
NASA Sep. 1987 119 p  
(Contract NAS8-35182)  
(NASA-CR-4092; NAS 1.26:4092) Avail: NTIS HC A06/MF A01  
CSCL 04B

Common tropical synoptic events, called moisture bursts, have been defined in terms of their appearance in infrared satellite imagery. Their synoptic and climatological behavior over the tropical North Pacific Ocean is described using data from four cool seasons, including the 1982 to 1983 El Nino winter and the January and May of 1979. Author

**N87-29573#** Joint Publications Research Service, Arlington, Va.  
**MAJOR MORPHOLOGIC FEATURES OF THE ATLANTIC OCEAN SURFACE Abstract Only**

R. KH. GREKU *In its* JPRS Report: Science and Technology.  
USSR: Space p 99 19 Aug. 1987 Transl. into ENGLISH from  
Issledovaniye Zemli iz Kosmosa (Moscow, USSR), no. 1, Jan. -  
Feb. 1987 p 20-25  
Avail: NTIS HC A08/MF A01

Satellite altimetry was used to produce new information on the topography of the surface of the Atlantic Ocean. Surface topography anomalies result both from heterogeneities in the geological structure of the Earth and from hydrodynamic phenomena in the ocean. Large scale features of the Atlantic Ocean surface are discussed. These features are compared with known geomorphologic features of the bottom relief. Author

**N87-29907#** Naval Ship Research and Development Center, Bethesda, Md. Ship Performance Dept.

**LABRADOR WIND AND WAVE ENVIRONMENTS Final Report**  
WAH T. LEE May 1987 78 p  
(AD-A183218; DTNSRDC/SPD-1214-01) Avail: NTIS HC  
A05/MF A01 CSCL 08C

The Labrador Extreme Waves Experiment (LEWEX) is designed to evaluate the in situ and remote sensors of the sea surface. This report is a source document for specifying climatological wind and wave data for the Labrador Sea. This report also provides atmospheric qualities such as temperature and sea ice which are known to affect the operation of certain ship systems as well as tactical decision making. GRA

**N87-30009#** Walcoff and Associates, Inc., Alexandria, Va.  
**PROCEEDINGS OF ATLANTIC OUTER CONTINENTAL SHELF REGION INFORMATION TRANSFER MEETING (ITM) (2ND), JANUARY 28-29, 1987**

G. J. GOULD May 1987 103 p Meeting held in Arlington, Va., 28-29 Jan. 1987  
(Contract DI-14-12-0001-30337)  
(PB87-200168; OCS/MMS-87/0033) Avail: NTIS HC A06/MF  
A01 CSCL 08C

The second Information Transfer Meeting (ITM) for the Atlantic Outer Continental Shelf (OCS) included 20 presentations followed by discussions. The purpose of the ITM is to communicate research results of the Environmental Studies Program and programs funded by other organizations which are relevant to OCS environmental management issues to an audience of state and Federal agencies, environmental organizations, industry and other decision-making groups. An overview was given of the Outer Continental Shelf Environmental Studies Program introducing a day of detailed presentations on active and recently completed North, Mid-, and South Atlantic, and Multi-Regional Studies. The second day was devoted to panel discussions on non-energy minerals on the Atlantic OCS and environmental concerns on the Georges Bank. Summaries of all presentations are included. GRA

**N87-30010#** IceCasting, Inc., Seattle, Wash.

**INTERPOLATION, ANALYSIS AND ARCHIVAL OF DATA ON SEA ICE TRAJECTORIES AND OCEAN CURRENTS OBTAINED FROM SATELLITE-LINKED INSTRUMENTS Final Report**

R. S. PRITCHARD and D. J. HANZLICK Apr. 1987 126 p  
Sponsored by NOAA, Anchorage, Alaska and Minerals  
Management Service, Juneau, Alaska  
(PB87-201430; ICI-RPT-87010) Avail: NTIS HC A07/MF A01  
CSCL 08C

Described are the movement of 17 ARGOS buoys deployed on ice floes in the northern Bering and Chukchi Seas. The analysis is based on the geographical position, meteorology and ocean current data obtained from satellite-linked instruments. Ice motion histories showed that diurnal tide oscillations dominated the short-term velocity behavior in Norton Sound. In contrast, there was no significant tidal velocity component in the Chukchi Sea. It was shown that 58-60% of the daily ice velocity variance in Norton Sound was explained by the currents, whereas in Chukchi Sea currents accounted for 44-93% of the ice velocity variance. These differences might be attributed to internal ice stress divergence, non-geostrophic currents, or other unknown factors. GRA

**N87-30011#** Walcoff and Associates, Inc., Alexandria, Va.  
**PROCEEDINGS OF ATLANTIC OUTER CONTINENTAL SHELF REGION INFORMATION TRANSFER MEETING (ITM) (1ST), SEPTEMBER 4-6, 1985**

G. J. GOULD 1986 127 p Meeting held in Crystal City, Va.,  
4-6 Sep. 1985  
(Contract DI-14-12-0001-30337)  
(PB87-194361; OCS/MMS-85/0106) Avail: NTIS HC A07/MF  
A01 CSCL 08C

The first Information Transfer Meeting (ITM) for the Atlantic OCS included 35 presentations over a two-and-a-half day period. The goal of the ITM is to present technical information in a context useful to OCS decision-makers. The results of the Region's Environmental Studies Program were presented as well as reports on Federal and state coastal management activities, petroleum resource estimation, and industry's oil-spill technology. Summaries of all presentations are included in the document. GRA

**N87-30012#** Science Applications International Corp., Newport, R.I.

**STUDY OF PHYSICAL PROCESSES ON THE US MID-ATLANTIC CONTINENTAL SLOPE AND RISE. VOLUME 1: EXECUTIVE SUMMARY Final Report, Sep. 1983 - May 1987**

O. BROWN, R. EVANS, R. WATTS, C. CASAGRANDE, and P. HAMILTON May 1987 53 p  
(Contract DI-14-12-0001-30066)  
(PB87-200515; SAIC-86/7539/129-VOL-1;  
OCS/MMS-87/0024-VOL-1) Avail: NTIS HC A04/MF A01; also  
available in set of 3 reports HC E99 as PB87-200507 CSCL  
08C

Three years of physical oceanographic research in the Mid-Atlantic Slope and Rise (MASAR) Program are described. The data was collected to provide sufficient information to allow assessment of the potential impacts of petroleum exploration and production activities on the outer continental shelf (OCS) of the Mid-Atlantic region. Major tasks undertaken were: determination of the general seasonal circulation features; quantification and description of the processes which produce variability; and determination of the degree to which the slope/rise circulation features influence the physical oceanography of the adjacent Mid-Atlantic continental shelf. The data were collected using instrumented moorings, satellite infrared imagery, and hydrographic sampling. The collected data is being used in models to estimate potential coastal pollution from offshore activities. B.G.

## 05 OCEANOGRAPHY AND MARINE RESOURCES

**N87-30013#** Science Applications International Corp., Newport, R.I.

**STUDY OF PHYSICAL PROCESSES ON THE US MID-ATLANTIC CONTINENTAL SLOPE AND RISE. VOLUME 2: TECHNICAL PRESENTATION Final Report, Sep. 1983 - May 1987**

O. BROWN, R. EVANS, R. WATTS, C. CASAGRANDE, and P. HAMILTON May 1987 326 p

(Contract DI-14-12-0001-30066)

(PB87-200523; SAIC-86/7539/129-VOL-2;

OCS/MMS-87/0024-VOL-2) Avail: NTIS HC A15/MF A01; also available in set of 3 reports HC E99 as PB87-200507 CSCL 08C

Described are three years of physical oceanographic research by Science Applications International Corporation (SAIC) and its subcontractors in the Mid-Atlantic Slope and Rise (MASAR) program. MASAR began in October 1983 and was designed to provide the Department of Interior's Minerals Management Service (MMS) with sufficient information to allow assessment of the potential impacts of petroleum exploration and production activities on the Outer Continental Shelf (OCS) of the Mid-Atlantic region. Several major tasks were undertaken: determining the general seasonal circulation features; quantifying and describing processes which produce variability; and determining the degree to which the slope/rise circulation features influence the physical oceanography of the adjacent Mid-Atlantic continental shelf.

GRA

**N87-30014#** Science Applications International Corp., Newport, R.I.

**STUDY OF PHYSICAL PROCESSES ON THE US MID-ATLANTIC CONTINENTAL SLOPE AND RISE. VOLUME 3: APPENDIX Final Report, Sep. 1983 - May 1987**

O. BROWN, R. EVANS, R. WATTS, C. CASAGRANDE, and P. HAMILTON May 1987 146 p

(Contract DI-14-12-0001-30066)

(PB87-200531; SAIC-86/7539/129-VOL-3;

OCS/MMS-87/0024-VOL-3) Avail: NTIS HC A07/MF A01; also available in set of 3 reports HC E99 as PB87-200507 CSCL 08C

Described are three years of physical oceanographic research by Science Applications International Corporation (SAIC) and its subcontractors in the Mid-Atlantic Slope and Rise (MASAR) program. MASAR began in October 1983 and was designed to provide the Department of Interior's Minerals Management Service (MMS) with sufficient information to allow assessment of the potential impacts of petroleum exploration and production activities on the outer continental shelf (OCS) of the Mid-Atlantic region. Several major tasks were undertaken: determining the general seasonal circulation features; quantifying and describing processes which produce variability; and determining the degree to which the slope/rise circulation features influence the physical oceanography of the adjacent Mid-Atlantic continental shelf.

GRA

**N87-30015#** Florida State Univ. System, St. Petersburg. Inst. of Oceanography.

**PHYSICAL OCEANOGRAPHIC STUDY OF FLORIDA'S ATLANTIC COAST REGION: FLORIDA ATLANTIC COAST TRANSPORT STUDY (FACTS). VOLUME 1: EXECUTIVE SUMMARY Final Report, 9 Jan. 1984 - 18 Feb. 1986**

M. RINKEL, S. VARGO, T. LEE, F. SCHOTT, and R. ZANTOPP 15 Sep. 1986 54 p Sponsored by Minerals Management Service, Vienna, Va.

(Contract DI-14-12-0001-30082)

(PB87-200994; OCS/MMS-86/0079-VOL-1) Avail: NTIS HC

A04/MF A01; also available in set of 3 reports HCE99 as

PB87-200986 CSCL 08C

Information is provided on the eddy structures which were observed to break off from the Florida Current and Gulf Stream along Florida's Atlantic coast from 27 deg N to 30 deg N to aid in assessment of risks from oil and gas activities in the South Atlantic Planning Area. Satellite sea surface temperature (SST) imagery was used as a supplementary tool in the study to help

interpret the data from the field instrumentation. Field sampling was conducted from 12 March 1984 through 19 June 1985. This volume 1 of a 3 volume set contains the executive summary.

GRA

**N87-30016#** Florida State Univ. System, St. Petersburg. Inst. of Oceanography.

**PHYSICAL OCEANOGRAPHIC STUDY OF FLORIDA'S ATLANTIC COAST REGION: FLORIDA ATLANTIC COAST TRANSPORT STUDY (FACTS), VOLUME 2 Final Report, 9 Jan. 1984 - 18 Feb. 1986**

M. RINKEL, S. VARGO, T. LEE, F. SCHOTT, and R. ZANTOPP 15 Sep. 1986 429 p Sponsored by Minerals Management Service, Vienna, Va.

(Contract DI-14-12-0001-30082)

(PB87-201000; OCS/MMS-86/0079-VOL-2) Avail: NTIS HC

A19/MF A01; also available in set of 3 reports HC E99 as

PB87-200986 CSCL 08C

Information is provided on the eddy structures which were observed to break off from the Florida Current and Gulf Stream along Florida's Atlantic coast from 27 deg N to 30 deg N to aid in assessment of risks from oil and gas activities in the South Atlantic Planning Area. The study involved the combined use of moored current meter arrays, PEGASUS current profiler, satellite tracked surface drifters, and inverted echo sounder/bottom pressure gauges (IES/PGs) to directly measure currents and particle trajectories with the Florida Current and Gulf Stream and the adjacent shelf.

GRA

**N87-30017#** Florida State Univ. System, St. Petersburg. Inst. of Oceanography.

**PHYSICAL OCEANOGRAPHIC STUDY OF FLORIDA'S ATLANTIC COAST REGION: FLORIDA ATLANTIC COAST TRANSPORT STUDY (FACTS). VOLUME 3: APPENDICES Final Report, 9 Jan. 1984 - 18 Feb. 1986**

M. RINKEL, S. VARGO, T. LEE, F. SCHOTT, and R. ZANTOPP 15 Sep. 1986 218 p Sponsored by Minerals Management Service, Vienna, Va.

(Contract DI-14-12-0001-30082)

(PB87-201018; OCS/MMS-86/0079-VOL-3) Avail: NTIS HC

A10/MF A01; also available in set of 3 reports HCE99 as

PB87-200986 CSCL 08C

The goal of the study was to provide information on the eddy structures which had been observed to break off from the Florida Current and Gulf Stream along Florida's Atlantic Coast from 27 to 30 degrees N to aid in the assessment of risks from oil and gas activities in the South Atlantic Planning Area. The study involved the combined use of moored current meter arrays, PEGASUS current profiler, satellite tracked surface drifters, and inverted echo sounder/bottom pressure gauges (IES/PGs) to directly measure currents and particle trajectories with the Florida Current and Gulf Stream and the adjacent shelf. Satellite sea surface temperature (SST) imagery was used as a supplementary tool in the study to help interpret the data from the field instrumentation. Field sampling was conducted from March 12, 1984 through June 12, 1985.

GRA

**N87-30018\*#** National Aeronautics and Space Administration. Goddard Space Flight Center, Greenbelt, Md.

**NASA SEA ICE AND SNOW VALIDATION PLAN FOR THE DEFENSE METEOROLOGICAL SATELLITE PROGRAM SPECIAL SENSOR MICROWAVE/IMAGER**

DONALD J. CAVALIERI, ed. and CALVIN T. SWIFT, ed. Sep. 1987 81 p

(NASA-TM-100683; REPT-87B0492; NAS 1.15:100683) Avail:

NTIS HC A05/MF A01 CSCL 08C

This document addresses the task of developing and executing a plan for validating the algorithm used for initial processing of sea ice data from the Special Sensor Microwave/Imager (SSM/I). The document outlines a plan for monitoring the performance of the SSM/I, for validating the derived sea ice parameters, and for providing quality data products before distribution to the research community. Because of recent advances in the application of

passive microwave remote sensing to snow cover on land, the validation of snow algorithms is also addressed. Author

**N87-30019#** Coast Guard Research and Development Center, Groton, Conn.

**ARCTIC DRIFTING BUOY DATA 1979 - 1985 Final Report**

JOSEPH W. ST. MARTIN Apr. 1987 126 p

(AD-A182967; CGR/DC-07/87; USCG-D-10-87) Avail: NTIS HC A07/MF A01 CSCL 13J

As part of an investigation of potential Arctic oil spills, the U.S. Coast Guard Research and Development and Canadian Marine Drilling, Ltd. (CANMAR) released satellite-tracked drifting buoys at two sites in the southern Beaufort Sea during six years (1979 to 1983, 1985). The sites were near Canadian offshore drilling locations off the Tuktoyaktuk Peninsula, Northwest Territories and near Prudhoe Bay, Alaska. An analysis of the trajectories of these buoys indicated that the majority of buoy drift was in an alongshore (east/west) direction. When buoys did move in a north/south direction, their speeds were generally lower and the length of excursions shorter. A comparison of the drift of these buoys to the calculated geostrophic wind (east/west component only) revealed that, over a long term, the buoys drifted, on average, with the mean wind. Buoys had average drift speeds which varied from 1% to 5.5% of the mean wind. When cumulative drift was compared to the cumulative wind, high correlations were noted for those buoys with spar type hulls. This indicates that the cumulative large-scale geostrophic wind plays an important role in the cumulative movement of the upper 1-2 meters of the water column. A comparison of the trajectories of buoys which were released in close spacial and time proximity was conducted. In general, their drifts were variable enough to indicate that the total forcing function on separate buoys was different. Author (GRA)

**N87-30020#** SACLANT ASW Research Center, La Spezia (Italy).

**WAVE-THEORY MODELLING OF CONVERGENCE ZONE PROPAGATION IN THE OCEAN**

GIANCARLO DREINI and FINN B. JENSEN Jun. 1987 28 p

(AD-A183607; SACLANTCEN-SM-194) Avail: NTIS HC A03/MF A01 CSCL 20A

Improved numerical techniques together with advances in computer technology have made it feasible to study sound propagation in the deep ocean with wave-theory models and hence avoid the artifacts and approximations associated with standard ray-theory analysis techniques. We apply a computationally efficient normal-mode code to the problem of convergence zone propagation, which is the repetitive focusing of sound (every 40-60 km) in the upper part of the ocean for an acoustic source near the sea surface. We investigate the structure of the first 3 convergence zones as a function of geographical area (Mediterranean Sea and Atlantic Ocean), season (summer and winter), frequency (25-200 Hz), and source/receiver depth (15-300 m). It is shown that convergence-zone propagation only occurs under summer conditions, and that the focusing of sound is much stronger in the Atlantic than in the Mediterranean. Moreover the convergence zone length is around 60 km in the Atlantic and just 35-40 km in the Mediterranean. GRA

**N87-30021\*#** National Aeronautics and Space Administration, Goddard Space Flight Center, Greenbelt, Md.

**SATELLITE-DERIVED ICE DATA SETS NO. 2: ARCTIC MONTHLY AVERAGE MICROWAVE BRIGHTNESS TEMPERATURES AND SEA ICE CONCENTRATIONS, 1973-1976**

1973-1976

C. L. PARKINSON, J. C. COMISO, and H. J. ZWALLY May 1987 43 p

(NASA-TM-87825; NAS 1.15:87825) Avail: NTIS HC A03/MF A01 CSCL 08L

A summary data set for four years (mid 70's) of Arctic sea ice conditions is available on magnetic tape. The data include monthly and yearly averaged Nimbus 5 electrically scanning microwave radiometer (ESMR) brightness temperatures, an ice concentration parameter derived from the brightness temperatures, monthly

climatological surface air temperatures, and monthly climatological sea level pressures. All data matrices are applied to 293 by 293 grids that cover a polar stereographic map enclosing the 50 deg N latitude circle. The grid size varies from about 32 X 32 km at the poles to about 28 X 28 km at 50 deg N. The ice concentration parameter is calculated assuming that the field of view contains only open water and first-year ice with an ice emissivity of 0.92. To account for the presence of multiyear ice, a nomogram is provided relating the ice concentration parameter, the total ice concentration, and the fraction of the ice cover which is multiyear ice. Author

## HYDROLOGY AND WATER MANAGEMENT

Includes snow cover and water runoff in rivers and glaciers, saline intrusion, drainage analysis, geomorphology of river basins, land uses, and estuarine studies.

**A87-42911**

**FORMATION OF NATURAL UNDERGROUND-WATER RESOURCES IN ARID REGIONS WITH SPECIAL REFERENCE TO THE DOLINOOZERSKII ARTESIAN BASIN IN MONGOLIA [FORMIROVANIE ESTESTVENNYKH RESURSOV PODZEMNYKH VOD ARIDNYKH RAIONOV NA PRIMERE DOLINOOZERSKOGO ARTEZIANSKOGO BASSEINA MNR]**

IURI I. LEONIDOVICH OB'EDKOV Moscow, Izdatel'stvo Nauka, 1986, 152 p. In Russian. refs

The processes that govern formation of natural underground water resources and the spatial distribution of underground drainage in zones of intensive water exchange are examined, with special reference to the Dolinoozerskii intermontane artesian basin in central Mongolia. The geology and hydrogeology of the region are described together with the methodology used in these studies, including satellite photography and gravitation prospecting. Methods for obtaining regional estimates of natural underground water reserves and of the water exchange rates using calculations or maps of water reserves and water drainage are discussed.

I.S.

**A87-44245**

**VISUAL INTERPRETATION OF LANDSAT MSS QUICK-LOOK IMAGES FOR THE STUDY OF THE ANNUAL SWELLING OF THE NIGER RIVER IN ITS INTERIOR DELTA, IN MALI [INTERPRETATION VISUELLE DE QUICK LOOKS D'IMAGES LANDSAT MSS POUR L'ETUDE DE LA CRUE ANNUELLE DE FLEUVE NIGER DANS SON DELTA INTERIEUR, AU MALI]**

LIONEL GUYOT (Institut Geographique National, Paris, France) Societe Francaise de Photogrammetrie et de Teledetection

**A87-44296**

**FEATURES OF THE WATER DYNAMICS OF LAKE LADOGA ACCORDING TO REMOTE SENSING DATA [OSOBENNOSTI DINAMIKI VOD LADOZHSKOGO OZERA PO DANNYM DISTANTSIONNOGO ZONDIROVANIYA]**

K. I. A. KONDRAT'EV, N. N. FILATOV, L. V. ZAITSEV, and F. S. ZUBENKO (AN SSSR, Institut Ozerovedeniia, Leningrad, USSR) Akademiia Nauk SSSR, Doklady (ISSN 0002-3264), vol. 293, no. 5, 1987, p. 1224-1227. In Russian. refs

A87-46538

**A MULTISPECTRAL STUDY OF THE ST. LOUIS AREA UNDER SNOW-COVERED CONDITIONS USING NOAA-7 AVHRR DATA**  
 STANLEY Q. KIDDER (Illinois State Water Survey, Champaign) and HUEY-TZU WU (Illinois, University, Urbana) Remote Sensing of Environment (ISSN 0034-4257), vol. 22, July 1987, p. 159-172. refs

(Contract NSF ATM-83-05502)

Albedos and equivalent blackbody temperatures (EBTs) from the AVHRR on NOAA-7 have been examined for two consecutive passes of the satellite over the St. Louis (SL) area when snow was on the ground. The albedo difference for channel 1 (visible) between SL and a typical rural area was -16 percent, much larger than urban-rural albedo differences found in previous studies under snow-free conditions. The albedo difference between channel 1 and channel 2 (NIR) appears to be a better indicator of the snow boundary than either channel alone. The channel 4 (11-micron) difference between the warmest part of SL and a typical rural area was 3 K during the day and 2.5 K at night, about the same as urban-rural EBT differences found under snow-free conditions. Day-night EBT differences were nearly the same in urban as in rural areas. Largest day-night differences were found in forested portions of the snow-covered area. Slightly larger (about 0.5 K) day-night differences were observed in the commercial-industrial area of SL than in the residential area. This may be caused by residential heating. Finally, hot industrial targets were easily observed in 3.7-micron images. These targets may be useful for accurate registration of AVHRR images. Author

A87-46545

**CALIBRATION OF THEMATIC MAPPER THERMAL DATA FOR WATER SURFACE TEMPERATURE MAPPING - CASE STUDY ON THE GREAT LAKES**

RICHARD G. LATHROP, JR. and THOMAS M. LILLESAND (Wisconsin, University, Madison) Remote Sensing of Environment (ISSN 0034-4257), vol. 22, July 1987, p. 297-307. Research supported by the University of Wisconsin. refs  
 (Contract NOAA-NA-800AAD00086; NOAA PROJECT 144-U824)

The potential utility of Landsat-5 TM thermal IR (band 6) data for measuring and mapping surface water temperatures of the Great Lakes is analyzed. Two contiguous TM scenes were collected on July 18, 1984 over the Green Bay-North Central Lake Michigan and Milwaukee-South Central Lake Michigan regions. The TM thermal IR data were empirically calibrated using surface reference data. The regression model so developed was then used to map surface temperature over the entire TM coverage area. Surface reference data points not used in the original calibration were used to test the predictive capability of the model over a wider geographic area. As part of the Landsat Image Data Quality Analysis effort (LIDQA), Bartolucci et al. (1985) have investigated the absolute calibration of TM thermal IR data. Application of these calibration equations to the present data verified their accuracy, resulting in an rms error of less than 1 C. Author

A87-47576

**REMOTE SENSING TECHNIQUES FOR THE STUDY OF HYDROLOGICAL ELEMENTS [DISTANTSIONNYE METODY IZUCHENIIA ELEMENTOV UVLAZHNIENIIA GEOSISTEM]**

A. M. GHIN, L. G. KUCHMENT, and I. U. N. KULIKOV Moscow, Izdatel'stvo VINITI (Gidrologicheskie Issledovaniia, No. 1), 1986, 115 p. In Russian. For individual items see A87-47577 to A87-47585.

Papers are presented on such topics as the evaluation of reservoir influx from aerial and satellite photographs, the modeling of snowmelt runoff in mountain catchment areas using satellite data, the operational measurement of moisture content in irrigated areas and adjacent territories, and the analysis of suspended-load dynamics in reservoirs in regions with extensive erosion on the basis of aerial and ground data. Consideration is also given to spectral reflectance from water bodies with mineral and biogenic suspensions, the remote-sensing evaluation of moisture supply to crops according to the leaf-surface thermal regime, and the

remote-sensing evaluation of the spatial variability of evaporation.

B.J.

A87-47577

**POSSIBILITY OF EVALUATING RESERVOIR INFLUX FROM AERIAL AND SATELLITE PHOTOGRAPHS [VOZMOZHNOСТИ OTSENKI PRITOCHNOSTI K VODOKHRANILISHCHU PO AEROKOSMICHESKIM SNIMKAM]**

K. G. BAKANOV and A. F. MANDYCH IN: Remote sensing techniques for the study of hydrological elements. Moscow, Izdatel'stvo VINITI, 1986, p. 5-15. In Russian. refs

A method for evaluating reservoir influx is described which is based on a differential equation of nonuniform, continuously changing motion. Attention is given to the possibility of determining the equation parameters (river length, bankline length, and flooded area) on the basis of aerial and satellite photographs in the visible range. It is shown that the proposed method is applicable only if occasional ground work is done: i.e., the selection of a monitoring section and the determination of its morphometric and hydraulic-channel parameters. B.J.

A87-47578

A87-47578

**MODELING THE SNOWMELT RUNOFF IN MOUNTAIN CATCHMENT AREAS USING SATELLITE DATA [MODELIROVANIE TALOGO STOKA NA GORNYKH VODOSBORAKH S ISPOL'ZOVANIEM SPUTNIKOVOI INFORMATSII]**

E. L. MUZYLEV and L. K. POPLAVSKAIA IN: Remote sensing techniques for the study of hydrological elements. Moscow, Izdatel'stvo VINITI, 1986, p. 16-29. In Russian. refs

The proposed model is used to calculate daily values of the snowcover area, heights of the snow-layer borderline, the distribution of snow amount with respect to the height of the catchment area, as well as the daily volume of water inflow into the catchment area. A runoff hydrograph is calculated using a two-capacity model of runoff transformation with distributed parameters. Model adjustment is carried out on the basis of satellite remote-sensing data and field observations in the Gavassay and Kassansay basins in western Tien-Shan. It is noted that the proposed model can be used to predict snowmelt runoff for mountain rivers in the case of insufficient information about the catchment areas. B.J.

A87-47579#

**PARAMETERIZATION OF MODELS OF RUNOFF FORMATION IN SIMPLE CATCHMENT AREAS USING REMOTE-SENSING DATA [K PROBLEME DISTANTSIONNOI PARAMETRIZATSII MODELEI FORMIROVANIIA STOKA ELEMENTARNYKH VODOSBOROV]**

I. U. N. KULIKOV and S. V. IASINSKII IN: Remote sensing techniques for the study of hydrological elements. Moscow, Izdatel'stvo VINITI, 1986, p. 30-36. In Russian. refs

The advantages and limitations of various remote-sensing techniques for the parameterization of runoff formation models are considered. Based on work done on the Kursk test area, an algorithm is developed for the investigation of snowmelt and runoff processes, making it possible to analyze the spatial distribution of snowcover and filtering coefficients. B.J.

A87-47580

**WATER-CYCLE PROCESSES IN GEOSYSTEMS AND THE POSSIBILITY OF THE REMOTE SENSING OF THE MOISTURE CONTENT OF THE UNDERLYING SURFACE [PROTSESSY VODOOBMENA V GEOSISTEMAKH I VOZMOZHNOСТИ DISTANTSIONNOI INDIKATSII UVLAZHNIENIIA PODSTILAIUSHCHEI POVERKHNOSTI]**

A. F. MANDYCH, I. G. MESHCHENIN, and A. V. SKORIK IN: Remote sensing techniques for the study of hydrological elements. Moscow, Izdatel'stvo VINITI, 1986, p. 45-55. In Russian. refs

Field observations were carried out during 1980-1981 in the Nanay region of the Khabarovsk territory with the aim of investigating water-cycle processes in geosystems of land improvement, bogs, and minor catchment areas. The overall

objective was to develop techniques for the remote sensing of moisture content in geosystems according to the water quantity in the subsurface layers. The relationship between water contents in the upper and lower layers characterizes the soil absorption of precipitation, drainage, and ground-water evaporation. These data allow the interpretation of aerial photographs in terms of the moisture content of the underlying surface. B.J.

## A87-47583

### REMOTE-SENSING EVALUATION OF THE SPATIAL VARIABILITY OF EVAPORATION [ISSLEDOVANIE PROSTRANSTVENNOI IZ-MENCHIVOSTI ISPARENIIA S POMOSHCH'U DISTANTSION-NOGO ZONDIROVANIIA]

I. P. ANAN'EV IN: Remote sensing techniques for the study of hydrological elements. Moscow, Izdatel'stvo VINITI, 1986, p. 89-96. In Russian. refs

Intergeosystemic differences in reflected and long-wave radiation have been investigated in the Tiumen region using an airborne pyranometer/IR radiometer system. Based on this study, a difference model for the remote evaluation of a geosystem's thermal and radiation characteristics was developed which can be used to assess variations in the evaporation conditions. The spatial variability of evaporation in bog areas of the Tiumen region is examined. B.J.

## A87-47584

### REMOTE-SENSING TECHNIQUES FOR INVESTIGATING THE STRUCTURE OF RADIATION-HEAT FLUXES AND THE MOISTURE CONTENT OF GEOSYSTEMS IN CONNECTION WITH THE PROBLEM OF MONITORING THE WATER COMPONENT [DISTANTSIONNYE METODY VISSLEDOVANIYAKH STRUKTURY RADIATSIONNO-TEPLOVYKH POTOKOV I UVLA-ZHNENIIA GEOSISTEM V SVIAZI S PROBLEMOI MONITORINGA VODNOI KOMPONENTY]

IU. N. KULIKOV IN: Remote sensing techniques for the study of hydrological elements. Moscow, Izdatel'stvo VINITI, June 1986, p. 97-106. In Russian. refs

## A87-48670

### SHALLOW WATER BATHYMETRY AND BOTTOM CLASSIFICATION BY MEANS OF THE LANDSAT AND SPOT OPTICAL SCANNERS

D. SPITZER and R. W. J. DIRKS (Nederlands Instituut voor Onderzoek der Zee, Texel, Netherlands) IN: Earth remote sensing using the Landsat Thematic Mapper and SPOT sensor systems; Proceedings of the Meeting, Innsbruck, Austria, Apr. 15-17, 1986. Bellingham, WA, Society of Photo-Optical Instrumentation Engineers, 1986, p. 136-138.

## A87-48823#

### SATELLITE MICROWAVE RADIOMETRY OF SNOW WATER EQUIVALENT

M. HALLIKAINEN and P. JOLMA (Helsinki University of Technology, Espoo, Finland) IN: Canadian Symposium on Remote Sensing, 10th, Edmonton, Canada, May 5-8, 1986, Proceedings. Volume 1. Ottawa, Canadian Aeronautics and Space Institute, 1987, p. 215-220. refs

## A87-48841#

### OPERATIONAL WATER QUALITY SURVEILLANCE IN SWEDEN USING LANDSAT MSS DATA

L. T. LINDELL (Uppsala, Universitet, Sweden) IN: Canadian Symposium on Remote Sensing, 10th, Edmonton, Canada, May 5-8, 1986, Proceedings. Volume 1. Ottawa, Canadian Aeronautics and Space Institute, 1987, p. 385-394. Research supported by the Swedish Space Corp. refs

## A87-48848#

### SNOWPACK DEPLETION MONITORING IN ALBERTA USING COMPUTER-PROCESSED NOAA IMAGERY

I. SUTHERLAND (Alberta Remote Sensing Centre, Edmonton, Canada) and SAINT FERNER (Alberta Environment, River Forecast Centre, Edmonton, Canada) IN: Canadian Symposium on Remote Sensing, 10th, Edmonton, Canada, May 5-8, 1986, Proceedings. Volume 1. Ottawa, Canadian Aeronautics and Space Institute, 1987, p. 463-471. refs

## A87-48856#

### INDICES OF CLIMATOLOGICAL AND HYDROLOGICAL VARIABILITY DERIVED FROM SATELLITE IMAGERY FOR THE SOUTH SASKATCHEWAN RIVER BASIN

E. LEDREW, P. HOWARTH, J. GARDNER, and B. RUSSON (Waterloo, University, Canada) IN: Canadian Symposium on Remote Sensing, 10th, Edmonton, Canada, May 5-8, 1986, Proceedings. Volume 2. Ottawa, Canadian Aeronautics and Space Institute, 1987, p. 545-557. Research supported by the Royal Canadian Geographical Society and NSERC. refs

## A87-48871#

### INDEXING SMALL CATCHMENTS IN JAVA, INDONESIA, WITH RESPECT TO THEIR RELATIVE SUSCEPTIBILITY TO EROSION

A. E. A. SCHUMACHER (Monenco Consultants, Ltd., Calgary, Canada) IN: Canadian Symposium on Remote Sensing, 10th, Edmonton, Canada, May 5-8, 1986, Proceedings. Volume 2. Ottawa, Canadian Aeronautics and Space Institute, 1987, p. 705-714. refs

A simplified relative erodability rating was developed for the rapid qualitative ranking of small catchments in the Lower Solo River Basin in East Java. This is based on the principles of the Universal Soil Loss Equation (USLE), but requires the delineation on aerial photographs of readily identifiable topographic and land use features contributing to or reflecting potential soil erodability. These were: the characteristic amplitude and slopes within specific terrain units, the degree of dissection of the surface and the land use. The simplicity of this approach allowed inexperienced staff to be very rapidly trained to identify, categorize and delineate these factors through a combination of field surveys and photointerpretation. Classes were established within each of the topographic and land use categories and a score assigned to each class in accordance with its relative contribution to the potential erodability of the land. A simple formula was devised to combine these scores for each delineated terrain/land use unit. The weighted average of these unit scores provided an index for each catchment. Author

## A87-48875#

### HYDROLOGIC APPLICATIONS OF WEATHER RADAR DATA

N. KOUWEN, G. ROSSEEL (Waterloo, University, Canada), and G. GARLAND (Proctor and Redfern Group, Kitchener, Canada) IN: Canadian Symposium on Remote Sensing, 10th, Edmonton, Canada, May 5-8, 1986, Proceedings. Volume 2. Ottawa, Canadian Aeronautics and Space Institute, 1987, p. 749-756. Research supported by the Alberta Research Council. refs (Contract NSERC-A-7982)

Remotely-sensed precipitation data is becoming readily available in various formats for selected areas in Canada and elsewhere. This information, whether available as graphical CAPRI images, its numerical equivalents, or detailed digitized RADAR data can aid hydrologic modelers and flood forecasters in their work. This paper reports on the application of weather RADAR data to the simulation of flood events on two watersheds: the Grand River in Ontario and the Red Deer River in Alberta. A square grid hydrologic simulation model called SIMPLE, developed at the University of Waterloo, was used to perform the hydrologic calculations. This model is designed to take maximum advantage of RADAR generated precipitation data. It is shown that RADAR information can significantly improve hydrologic simulation, and therefore flood forecasting. It is also shown that so-called gray scale or degraded radar data yields hydrologic results nearly as



accurate as more elaborate techniques based on full resolution adjusted radar data. Author

#### A87-48880#

##### A METHODOLOGY FOR AUTOMATED EXTRACTION OF DRAINAGE NETWORKS FROM SATELLITE IMAGERY

J. F. WANG and P. J. HOWARTH (Waterloo, University, Canada) IN: Canadian Symposium on Remote Sensing, 10th, Edmonton, Canada, May 5-8, 1986, Proceedings. Volume 2. Ottawa, Canadian Aeronautics and Space Institute, 1987, p. 811-817. (Contract NSERC-A-0766)

#### A87-53204

##### SUSPENDED SEDIMENT CONCENTRATIONS ESTIMATED FROM LANDSAT MSS

JERRY C. RITCHIE (USDA, Hydrology Laboratory, Beltsville, MD) and CHARLES M. COOPER (USDA, Sedimentation Laboratory, Oxford, MS) IN: IGARSS '87 - International Geoscience and Remote Sensing Symposium, Ann Arbor, MI, May 18-21, 1987, Digest. Volume 2. New York, Institute of Electrical and Electronics Engineers, Inc., 1987, p. 865-869. refs

Good estimates of the concentration of suspended sediments between 50 and 250 mg/l are obtainable using simple regression equations based on Landsat MSS data. Data based on these regression equations may facilitate the development of a computer-based detection system that can classify Landsat MSS data and locate bodies of water with significant suspended sedimentation. Any body of water identified as having a suspended sediment concentration greater than 200 mg/l is a potential target for the development of plans to conserve upland soils. O.C.

#### A87-53215

##### DEVELOPMENT OF EOS-AIDED PROCEDURES FOR THE DETERMINATION OF THE WATER BALANCE OR HYDROLOGIC BUDGET OF A LARGE WATERSHED

RUSSELL CONGALTON, RANDALL THOMAS, PAUL ZINKE, JOHN HELMS, and GEORGE SMOOT (California, University, Berkeley) IN: IGARSS '87 - International Geoscience and Remote Sensing Symposium, Ann Arbor, MI, May 18-21, 1987, Digest. Volume 2. New York, Institute of Electrical and Electronics Engineers, Inc., 1987, p. 949-954. refs

#### A87-53271\* Wisconsin Univ., Madison.

##### SCATTERING PARAMETERS FOR ASPHERICAL HYDROMETEORS AT MICROWAVE FREQUENCIES

C. KUMMEROW (Wisconsin, University, Madison; Minnesota, University, Minneapolis) and J. A. WEINMAN (Wisconsin, University, Madison) IN: IGARSS '87 - International Geoscience and Remote Sensing Symposium, Ann Arbor, MI, May 18-21, 1987, Digest. Volume 2. New York, Institute of Electrical and Electronics Engineers, Inc., 1987, p. 1443-1446. refs (Contract NAGW-872)

Scattering parameters for ensembles of aspherical ice and liquid hydrometeors were calculated at  $\Psi = 50$  deg for frequencies of 37.0, 50.3, and 85.6 GHz. Hydrometeors were assumed to be oblate spheroids whose semiminor axes were aligned at  $\Psi = 0$  deg. The angle of  $50$  deg is determined by the viewing angle of recent satellite-borne radiometers. Backscattering phase functions and extinction coefficients at  $\Psi = 0$  deg were also computed at 18.0, 37.0, and 85.6 GHz to provide information for future nadir scanning radars. The hydrometeors were assumed to be characterized by Marshall-Palmer (1948) size distributions. The extended boundary condition method was used to calculate the extinction and backscattering coefficients as well as the albedo for single scattering and the asymmetry factor of the phase function. Results are fitted to simple functions of the rainfall rate. Some comparisons intended to illustrate the differences and similarities of these results with those obtained from equal volume spheres are also presented. Author

#### A87-54152

##### COMPARISONS OF GAUGE AND SATELLITE RAIN ESTIMATES FOR THE CENTRAL UNITED STATES DURING AUGUST 1979

CECILIA GIRZ GRIFFITH (NOAA, Environmental Research Laboratories, Boulder, CO) Journal of Geophysical Research (ISSN 0148-0227), vol. 92, Aug. 20, 1987, p. 9551-9566. refs

GOES-East satellite thermal IR channel-based rainfall estimates for August 1979 are presently compared with gage rainfalls over hourly and daily time frames for area-averaged amounts and point values pertaining to a 3.6-million sq km region in the central U.S. It is found that while the timing of rain events is comparable for daily area-averaged satellite and gage data, hourly area-averaged gage data exhibit much more short-term fluctuation than the hourly satellite data. For the two satellite algorithms tested, the streamlined technique requires the least computational time and shows a small difference in its comparisons with the gages. O.C.

A87-54153\* National Aeronautics and Space Administration. Goddard Space Flight Center, Greenbelt, Md.

##### SAMPLING ERRORS IN SATELLITE ESTIMATES OF TROPICAL RAIN

ALAN MCCONNELL (Pixel Analysis, Silver Spring, MD) and GERALD R. NORTH (NASA, Goddard Space Flight Center, Greenbelt, MD) Journal of Geophysical Research (ISSN 0148-0227), vol. 92, Aug. 20, 1987, p. 9567-9570.

The GATE rainfall data set is used in a statistical study to estimate the sampling errors that might be expected for the type of snapshot sampling that a low earth-orbiting satellite makes. For averages over the entire 400-km square and for the duration of several weeks, strong evidence is found that sampling errors less than 10 percent can be expected in contributions from each of four rain rate categories which individually account for about one quarter of the total rain. Author

#### A87-54154#

##### COKRIGING RADAR-RAINFALL AND RAIN GAGE DATA

WITOLD F. KRAJEWSKI (NOAA, Hydrologic Research Laboratory, Silver Spring, MD) Journal of Geophysical Research (ISSN 0148-0227), vol. 92, Aug. 20, 1987, p. 9571-9580. Research sponsored by the U.S. National Research Council and NOAA. refs

An ordinary cokriging procedure has been developed to optimally merge rainfall data from radars and standard rain gages. The radar-rainfall data are given in digitized form. The covariance matrices required to perform cokriging are computed from single realization data, using the ergodicity assumption. Since the ground truth and the error structure of the radar data are unknown, parameterization of the covariance between radar data and the true rainfall is required. The sensitivity of the procedure to that parameterization is analyzed within a controlled simulation experiment. The experiment is based on a hypothesized error structure for the rainfall measurements. The effect of measurement noise and network density is examined. The usefulness of the procedure to remove the bias in radar is tested. Daily data are used. Author

#### A87-54155\* Pennsylvania State Univ., University Park.

##### ESTIMATION OF SURFACE MOISTURE AVAILABILITY FROM REMOTE TEMPERATURE MEASUREMENTS

ALBERTO L. FLORES and TOBY N. CARLSON (Pennsylvania State University, University Park) Journal of Geophysical Research (ISSN 0148-0227), vol. 92, Aug. 20, 1987, p. 9581-9585. refs (Contract NAG5-184)

Analysis of moisture availability, determined from GOES IR surface temperature measurements and a boundary layer model, and antecedent precipitation are presented for data taken over Texas and Argentina. Correlations between antecedent precipitation and moisture availability are high where the spatial variation in moisture availability is much larger than an inherent uncertainty in the method, which is judged to be about  $\pm 0.2$  for the moisture availability parameter. In regions where there are large gradients of precipitation, the IR method can provide useful



information on variations in soil moisture availability and, by implication, in precipitation. Author

**A87-54157\*#** National Aeronautics and Space Administration. Goddard Space Flight Center, Greenbelt, Md.

### **A SPACE-TIME STOCHASTIC MODEL OF RAINFALL FOR SATELLITE REMOTE-SENSING STUDIES**

THOMAS L. BELL (NASA, Goddard Space Flight Center, Greenbelt, MD) Journal of Geophysical Research (ISSN 0148-0227), vol. 92, Aug. 20, 1987, p. 9631-9643. refs

A model of the spatial and temporal distribution of rainfall is described that produces random spatial rainfall patterns with these characteristics: (1) the model is defined on a grid with each grid point representing the average rain rate over the surrounding grid box, (2) rain occurs at any one grid point, on average, a specified percentage of the time and has a lognormal probability distribution, (3) spatial correlation of the rainfall can be arbitrarily prescribed, and (4) time stepping is carried out so that large-scale features persist longer than small-scale features. Rain is generated in the model from the portion of a correlated Gaussian random field that exceeds a threshold. The portion of the field above the threshold is rescaled to have a lognormal probability distribution. Sample output of the model designed to mimic radar observations of rainfall during the Global Atmospheric Research Program Atlantic Tropical Experiment (GATE), is shown. The model is intended for use in evaluating sampling strategies for satellite remote-sensing of rainfall and for development of algorithms for converting radiant intensity received by an instrument from its field of view into rainfall amount. Author

**N87-28123#** Helsinki Univ. of Technology, Espoo (Finland). Radio Lab.

### **MONITORING OF SNOW COVER FROM SATELLITE**

MARTTI HALLIKAINEN, PETRI JOLMA, MARTTI TIURI, and RISTO KUITTINEN (Technical Research Centre of Finland, Espoo.) In ESA Proceedings of the ESA/EARSel Europe from Space Symposium p 49-52 Dec. 1986

Avail: NTIS HC A14/MF A01

Monitoring of snow cover using spaceborne microwave radiometers is examined. Discrimination of snow-covered terrain (dry/wet snow) from snowfree terrain is discussed. Retrieval of the water equivalent of snow cover is based on the decrease of the brightness temperature with increasing snow depth, which is due to volume scattering of microwave emission by dry snow particles. For wet snow conditions, the brightness temperature is practically independent of snow depth. Retrieval accuracy is affected by short-term and annual variations in the properties of the topmost snow layers and by land-cover categories. ESA

**N87-28139#** Ruhr Univ., Bochum (West Germany).

### **SATELLITE REMOTE SENSING FOR WATER RESOURCES MANAGEMENT: SOME ENGINEERING AND ECONOMIC ASPECTS**

GERT A. SCHULTZ In ESA Proceedings of the ESA/EARSel Europe from Space Symposium p 171-177 Dec. 1986

Avail: NTIS HC A14/MF A01

The use of satellite imagery to identify changes of land use in a river catchment is described. If this information is entered into mathematical rainfall-runoff models, it is possible to show the effect of land use change on flood and low flow conditions quantitatively. A model which allows the determination of monthly river runoff values with the aid of satellite imagery is presented. It transforms temperature weighted cloud cover index values into runoff. Economic components influencing remote sensing applications are mentioned. ESA

**N87-28150#** Copenhagen Univ. (Denmark). Inst. of Geography. **SNOW MAPPING IN WESTERN GREENLAND** HENRIK SOEGAARD In ESA Proceedings of the ESA/EARSel Europe from Space Symposium p 245-249 Dec. 1986 Sponsored by the Commission for Scientific Research in Greenland Avail: NTIS HC A14/MF A01

Snow mapping in Greenland based on NOAA AVHRR data is presented. Based on data from two major drainage basins, methods for mapping snow cover and water equivalent were elaborated, and validated by field observations and hydrological simulation. It is shown that accuracy in snow cover mapping is greatly increased when a correction for terrain effects is applied and that a linear relationship between snow cover and water equivalent can be established. Applications of the results in snow-hydrology modeling, and the integration of the procedure on a microcomputer based image processing system are discussed. ESA

**N87-28152#** Ministere de l'Environnement et du Cadre de Vie, Neuilly (France).

### **PRESENT STATE, CHANGES, AND QUALITY OF SOLOGNE AND BRENNÉ, TWO FRENCH LARGE WETLANDS, STUDIED WITH LANDSAT MSS AND TM DATA**

MICHEL LENCO and JEAN-PIERRE DEDIEU In ESA Proceedings of the ESA/EARSel Europe from Space Symposium p 259-261 Dec. 1986

Avail: NTIS HC A14/MF A01

Using LANDSAT TM and MSS data, cartographical (1:50,000 scale) and numerical information in 23 classes on the present state and the late 1975/84 changes of the watershed land cover to two large wetlands were obtained. The LANDSAT TM data processing in supervised classification mapped information about depth, aquatic vegetation, turbidity and outer temperature of the ponds in ascertaining thresholds in channels 5, 1, 2, 3, and 6. ESA

**N87-28196#** National Oceanic and Atmospheric Administration, Boulder, Colo.

### **CATALOG OF SUBMARINE VOLCANOES AND HYDROLOGICAL PHENOMENA ASSOCIATED WITH VOLCANIC EVENTS, JANUARY 1, 1900 TO DECEMBER 31, 1959**

P. HEDERVARI Oct. 1986 45 p Prepared in cooperation with Georgiana Observatory, Budapest, Hungary (PB87-183943; SE-42) Avail: NTIS HC A03/MF A01 CSCL 08K

Volume II is the second part of a comprehensive catalog of hydrological phenomena associated with volcanoes. Discussed are phenomena occurring from January 1, 1900 to December 31, 1959. GRA

**N87-29906#** Army Cold Regions Research and Engineering Lab., Hanover, N. H.

### **USE OF LANDSAT DIGITAL DATA FOR SNOW COVER MAPPING IN THE UPPER SAINT JOHN RIVER BASIN, MAINE**

CAROLYN J. MERRY and MICHAEL S. MILLER Jun. 1987

77 p (AD-A183213; CRREL-87-8) Avail: NTIS HC A05/MF A01 CSCL 08L

Measurements of snow depth and its water equivalent were obtained at 11 snow courses in the Allagash, Maine, area in conjunction with acquisition of five LANDSAT-2 and -3 images during the 1977 to 1978 and 1978 to 1979 winters. To test a hypothesis that LANDSAT reflected radiance values on a regional scale do change, histograms of the LANDSAT MSS band 7 reflected radiance values for a 300- x 300-pixel (420 sq km) area near Allagash were evaluated to quantify the change. A statistical description (skewness and kurtosis) of the histogram for each scene was developed and then correlated with ground measurements of snow depth. The LANDSAT data were then re-examined and corrections made for solar elevation and MSS sensor calibration. Reflected radiance from open areas showed a consistent increase in intensity with increasing snow depth. Forested land cover classes did not change with snow depth. Digital imagery data acquired 31 May 1978 when the land was

snow-free was used to classify land cover categories. Ground truth measurements of water equivalent of the snow cover were area-weighted using the land cover classification to derive regional values on each of the five LANDSAT winter scenes. The 1 March 1978 snow measurement of 19.46 cm of water equivalent was used as an input value to the SSARR model. The SSARR prediction for the 1 March to 31 May 1978 period was within 78% of the measured runoff for the initial baseflow period and within 66% of that measured for the spring melt recession period. GRA

## 07

## DATA PROCESSING AND DISTRIBUTION SYSTEMS

Includes film processing, computer technology, satellite and aircraft hardware, and imagery.

**A87-42659\*** Jet Propulsion Lab., California Inst. of Tech., Pasadena.

### OPTICAL IMAGE SUBTRACTION TECHNIQUES, 1975-1985

HUA-KUANG LIU and TIEN-HSIN CHAO (California Institute of Technology, Jet Propulsion Laboratory, Pasadena) IN: Hybrid image processing; Proceedings of the Meeting, Orlando, FL, Apr. 1, 2, 1986. Bellingham, WA, Society of Photo-Optical Instrumentation Engineers, 1986, p. 55-65. refs.

Real- and nonreal-time optical image subtraction (OIS) techniques are reviewed. Real-time OIS techniques include source encoding, polarization modulation, pseudocolor image difference detection, the holographic shear lens technique, and nonlinear optics. Included in the nonreal-time category are speckle diffuser encoding, speckle-pattern encoding, halftone screen encoding, and polarization-shifted encoding. It is concluded that the most useful techniques are the real-time operations. It is noted that some nonreal-time optical techniques can be applied directly while others may be converted into real-time ones through the use of advance real-time spatial light modulators or electrooptic devices. K.K.

**A87-42935**

### A STUDY OF MODERN LANDSCAPE FORMATION IN LOWER MESOPOTAMIA FROM SPACE PHOTOGRAPHS [IZUCHENIE FORMIROVANIYA SOVREMENNYKH LANDSHAFTOV NIZHNEI MESOPOTAMII PO KOSMICHESKIM SNIMKAM]

E. V. GLUSHKO and I. N. MASLENNIKOVA (Moskovskii Gosudarstvennyi Universitet, Moscow, USSR) Issledovanie Zemli iz Kosmosa (ISSN 0205-9614), Jan.-Feb. 1987, p. 51-58. In Russian. refs

**A87-43261**

### THE CCRS SAR/MSS ANDERSON RIVER DATA SET

DAVID G. GOODENOUGH, BERT GUINDON, PHILIPPE M. TEILLET, ALAIN MENARD (Canada Centre for Remote Sensing, Ottawa), and JOHN ZELEK (Intera Technologies, Ltd., Ottawa, Canada) (International Association for Pattern Recognition and IBM France, S.A., Workshop on Analytical Methods in Remote Sensing for Geographic Information Systems, Ecole Nationale Supérieure des Telecommunications, Paris, France, Oct. 23, 24, 1986) IEEE Transactions on Geoscience and Remote Sensing (ISSN 0196-2892), vol. GE-25, May 1987, p. 360-367. refs

Technical Committee no. 7 of the International Association of Pattern Recognition is seeking test data sets that would further research into pattern recognition for remote sensing. Such data sets are usually expensive to acquire and are rarely made available. The Canada Centre for Remote Sensing (CCRS) has chosen to make the SAR/MSS Data Set for Anderson River available. This paper describes the contents and structure of the data set. Several major studies were conducted using these data by the authors and their colleagues. This paper also summarizes the results of these investigations conducted over four years. Studies included classification accuracies with and without terrain slope and aspect

corrections, optimum sensor and feature selection, texture features, and multisensor data integration. Finally, the authors describe the procedure whereby other scientists can gain access to the data set. Author

**A87-44244**

### SECOND GENERATION HIGH-RESOLUTION SPACE SYSTEMS - FIRST RESULTS OF THE SPOT-1 SATELLITE [LA SECONDE GENERATION DES SYSTEMES SPATIAUX A HAUTE RESOLUTION - PREMIERS RESULTATS DU SATELLITE SPOT-1]

GERARD BRACHET (SPOT Image, Toulouse, France) (Societe Internationale de Photogrammetrie et de Teledetection, Symposium sur l'Utilisation de la Teledetection pour le Developpement des Ressources et la Gestion de l'Environnement, Enschede, Netherlands, Aug. 25-29, 1986) Societe Francaise de Photogrammetrie et de Teledetection, Bulletin (ISSN 0244-6014), no. 104, 1986, p. 17-22. In French.

Evaluation of the quality of images received by the SPOT-1 satellite, launched on February 22, 1986, and the commercial distribution of images from the Toulouse/Aussaguel and Kiruna, Sweden receiving stations, are discussed. Signal-to-noise ratios were equal or better than specifications for most of the bands of the two HRV instruments aboard SPOT. Good geometric quality of the images was found with respect to position precision, image deformation, superposition of spectral bands, and altitude determination in the stereoscopic mode. Two direct readout stations in Canada provide real-time coverage of Canada and the United States. The high-resolution, excellent radiometric accuracy, and frequent coverage provided by this system make it useful for applications including cartography, land use and vegetation mapping, and coastal studies. R.R.

**A87-44301**

### DETERMINATION OF THE EXTERNAL-ORIENTATION ELEMENTS OF AERIAL AND SPACE PHOTOGRAPHS [OB OPREDELENIY ELEMENTOV VNESHNEGO ORIENTIROVANIYA AEROKOSMICHESKIKH SNIMKOV]

V. I. KRASNOV and M. K. FURSOV Geodeziya i Kartografiya (ISSN 0016-7126), Feb. 1987, p. 36-42. In Russian. refs

A new system of external-orientation elements (EOEs) is proposed which makes it possible to express them in the form of finite dependences on precise measurements of the reference-point coordinates. The EOE determination is shown to be nonunique when three (and in some cases even more) points are used. In the case of measurement errors, the proposed system makes it possible to reduce the solution of the problem to the determination of only two elements; knowledge of their initial values is not required and constraints on the values of the elements are not imposed. B.J.

**A87-44864\*** National Aeronautics and Space Administration. Goddard Space Flight Center, Greenbelt, Md.

### RADIOMETRIC PROPERTIES OF U.S. PROCESSED LANDSAT MSS DATA

BRIAN L. MARKHAM and JOHN L. BARKER (NASA, Goddard Space Flight Center, Greenbelt, MD) Remote Sensing of Environment (ISSN 0034-4257), vol. 22, June 1987, p. 39-71. refs

The accuracy of radiometric data obtained from Landsat MSS data is examined. The equations and parameters for converting MSS data to physical units, such as radiance, are presented. The basic design and operation of the MSS sensor, its calibration system, and various U.S. ground processing systems are described. The accuracy of radiance data is analyzed in terms of prelaunch radiometric standards and procedures, sensor effects, and processing effects. The consistency of the calibrations between different MSS sensors is evaluated by comparing their responses to the same earth targets under similar conditions. It is observed that there is some correlation between the sensor calibrations; however, the calibrations tend to degrade as the sensors age. I.F.

A87-46540

**CLASSIFICATION OF GEOMORPHIC FEATURES AND LANDSCAPE STABILITY IN NORTHWESTERN NEW MEXICO USING SIMULATED SPOT IMAGERY**

KATHRYN F. CONNORS, THOMAS W. GARDNER, and GARY W. PETERSEN (Pennsylvania State University, University Park) Remote Sensing of Environment (ISSN 0034-4257), vol. 22, July 1987, p. 187-207. refs  
(Contract DE-AC02-83ER-60182)

Euclidean-distance analysis of simulated SPOT data is used to distinguish among geomorphic units that influence surface hydrology, erosion potential, and landscape stability in a semiarid portion of the San Juan Basin, northwestern New Mexico. Geomorphic units are distinguished on the ground by landscape position, geomorphic process type and rate, soil type, vegetation cover, and slope. Level III (Anderson et al., 1976) land cover classification (Level IV classification in two classes) of geomorphic units that are important in inferring landscape stability is attainable with the high spatial resolution of the data (20 m in the multispectral bands and 10 m in the panchromatic band). Classification accuracy is directly related to geomorphic feature homogeneity. Euclidean-distance analysis of the multispectral bands identifies eolian-mantled uplands, surface exposures of B-horizon, coppice dunes, poorly vegetated silty and fine sandy areas, salt pans, sandy areas vegetated with shrubbery, and well-vegetated fine-grained areas. Landscape-stability maps are generated from landscape component age and rates of fluvial or eolian processes on each spectrally distinct geomorphic unit. The panchromatic band discriminates among a 7-13-m-wide arroyo, active and inactive tributary headcuts, and the stable portions of the valley floor.

Author

A87-46745

**AN MTF ANALYSIS OF LANDSAT CLASSIFICATION ERROR AT FIELD BOUNDARIES**

JESS GRUNBLATT (Ministry of Planning and National Development, Kenya Rangeland Ecological Monitoring Unit, Nairobi) Photogrammetric Engineering and Remote Sensing (ISSN 0099-1112), vol. 53, June 1987, p. 639-643. refs

The purpose of this study was to evaluate image classification error as affected by the performance characteristics of the Landsat multispectral scanner (MSS). The MSS modulation transfer function (MTF) was chosen as a means of defining the ability of the MSS sensor to transfer spectral variations in the intensity of reflected radiation (modulation), received at the satellite sensor, to the image data. The MSS MTF was used to predict the degradation of image quality (blur) at field boundaries. A study area of large, homogeneous, agricultural fields of various crop types was selected from a Landsat-2 image and classified. Classification error at field boundaries was compared to the boundary blur predicted by the MSS MTF analysis. A postclassification algorithm employing field boundary information was used to minimize boundary blur impacts on classification accuracy.

Author

A87-47046

**INFORMATION CONTENT ANALYSIS OF LANDSAT IMAGE DATA FOR COMPRESSION**

THOMAS M. CHEN (California, University, Berkeley), DAVID H. STAELIN (MIT, Cambridge, MA), and RONALD B. ARPS (IBM Almaden Research Center, San Jose, CA) IEEE Transactions on Geoscience and Remote Sensing (ISSN 0196-2892), vol. GE-25, July 1987, p. 499-501. refs

This paper investigates information-preserving compression of Landsat image data based on an entropy study. Measurements of the statistical information in actual Landsat-4 images indicate a 3:1 compression ratio can be achieved with a simple real-time compression scheme.

Author

A87-47506

**DETERMINATION OF THE INITIAL MOTION CONDITIONS OF EARTH-RESOURCES SATELLITES ACCORDING TO THE PHOTOGRAMMETRIC PROCESSING OF TOPOGRAPHIC PHOTOGRAPHS ORIENTED IN INERTIAL SPACE [OPREDELENIE NACHAL'NYKH USLOV'II DVIZHENIIA RESURS'NYKH ISZ PO RESUL'TATAM FOTOGRAMMETRICHESKOI OBRABOTKI TOPOGRAFIKESKIKH SNIMKOV, ORIENTIROVANNYKH V INERTSIAL'NOM PROSTRANSTVE]****INERTSIAL'NOM PROSTRANSTVE]**

M. S. URMAEV and G. G. STARORUSSKAIA (Moskovskii Institut Inzhenerov Geodezii, Aerofotos'emki i Kartografii, Moscow, USSR) Geodeziia i Aerofotos'emka (ISSN 0536-101X), no. 1, 1987, p. 60-70. In Russian.

The paper examines a method for determining the initial motion conditions of earth-resources and mapping satellites in LEO according to the photogrammetric processing of topographic photographs of the earth surface oriented in inertial space. At least two photographs must be used, each of which has two fixed points with geodetic coordinates in the coordinate system of the common terrestrial ellipsoid. The collinearity equations serve as the initial equations for the differential refinement of the orbit.

B.J.

A87-48193

**MULTISTAGE PRINCIPAL-COMPONENTS ANALYSIS OF CORRELATIONS [MNOGOSHAGOVYI KOMPONENTNYI ANALIZ KORRELIATSIONNYKH SVIAZEI]**

V. A. KOTTSOV and E. A. GORBUSHINA (AN SSSR, Institut Kosmicheskikh Issledovani, Moscow, USSR) Issledovanie Zemli iz Kosmosa (ISSN 0205-9614), Mar.-Apr. 1987, p. 118-122. In Russian. refs

The feasibility of using the principal-components method to select optimal combinations of spectral channels in the multispectral remote sensing of the earth is discussed. The optimization procedure employs differences in the indeterminacies of correlation matrix elements and eliminates them successively by comparison with a given accuracy threshold. The potential of the method is demonstrated by analysis of multispectral imagery obtained with the MKF-6 camera on Soyuz-22.

B.J.

A87-48359

**SIZE DISTRIBUTIONS OF CLOUDS IN REAL TIME FROM SATELLITE IMAGERY**

D. M. O'BRIEN (CSIRO, Div. of Atmospheric Research, Aspendale, Australia) International Journal of Remote Sensing (ISSN 0143-1161), vol. 8, June 1987, p. 817-837. refs

The estimation of cloud size from an image of a broken cloud is examined. The algorithms of sizing by openings, sizing by area, and sizing by circumscribing circles are analyzed in order to determine which algorithm provides the best definition for cloud size. It is determined that the sizing by opening algorithm is the most accurate for sizing clouds, and the applicability of the algorithm is illustrated by the analysis of a Landsat image of a cumulus cloud field. An instrument for digitizing the image on board the satellite and for processing the image in real time is proposed. The instrument is a scanning radiometer with broadband channels in the visible at 600 nm and in the IR at 11 microns. The operation of the instrument is described, and its performance is evaluated in terms of speed and power. It is concluded that the instrument is useful for estimating cloud size in real time from an image of a broken cloud.

I.F.

A87-48361

**CLOUD SCREENING FOR DETERMINATION OF LAND SURFACE CHARACTERISTICS IN A REDUCED RESOLUTION SATELLITE DATA SET**

G. GUTMAN, D. TARPLEY, and G. OHRING (NOAA, National Environmental Satellite, Data, and Information Service, Washington, DC) International Journal of Remote Sensing (ISSN 0143-1161), vol. 8, June 1987, p. 859-870. refs

A spatial coherence method is developed for cloud screening of a reduced resolution data set over the U.S. Great Plains. The

method is based upon a comparison of the spatial standard deviation of scene radiance for a particular observation time with that for clear sky conditions (the background variability). The procedure relies on the assumption that the presence of partial cloudiness increases spatial variability. The standard deviation thresholds are tabulated functions of space and time and are presented as the background variability maps. Complete cloud covers are screened by testing the computed skin temperatures and albedos against constant thresholds, whereas night-time cirrus and low levels of cloudiness are detected using the 3.7-11 microns brightness temperature differences. The cloud-screening scheme is tested on daytime and nighttime data of July 1986. Author

**A87-48365****AGRICULTURAL, HYDROLOGIC AND OCEANOGRAPHIC STUDIES IN BANGLADESH WITH NOAA AVHRR DATA**

A. ALI, D. A. QUADIR (Bangladesh Space Research and Remote Sensing Organization, Dhaka), and O. K. HUH (Louisiana State University, Baton Rouge) International Journal of Remote Sensing (ISSN 0143-1161), vol. 8, June 1987, p. 917-925. refs

**A87-48655****GEOMETRIC QUALITY OF THEMATIC MAPPER DATA OF THE UNITED KINGDOM**

JOHN R. HARDY (Reading, University, England) IN: Earth remote sensing using the Landsat Thematic Mapper and SPOT sensor systems; Proceedings of the Meeting, Innsbruck, Austria, Apr. 15-17, 1986. Bellingham, WA, Society of Photo-Optical Instrumentation Engineers, 1986, p. 18-24. refs (Contract NERC-F60/G6/03)

Raw TM data of a single scene of southern England without payload or mirror-scan correction data have been transformed to British National Grid coordinates using 101 ground control points. For a whole scene in one transformation, third order is the minimum acceptable for raw data of this state. The standard deviation of the residuals was reduced to subpixel level using third- or fourth-order polynomial transformations, but the 90-percent level is about 40 m or 1.3 pixels, allowing accurate planimetric mapping to scales of 1/100,000 and smaller. System-corrected data have been shown to be marginally better, and under the most favorable conditions both raw and corrected data may be marginally suitable for mapping at 1/50,000. Author

**A87-48656****WITHIN-SCENE RADIOMETRIC CORRECTION OF LANDSAT THEMATIC MAPPER (TM) DATA IN CANADIAN PRODUCTION SYSTEMS**

JENNIFER M. MURPHY (Canada Centre for Remote Sensing, Ottawa) IN: Earth remote sensing using the Landsat Thematic Mapper and SPOT sensor systems; Proceedings of the Meeting, Innsbruck, Austria, Apr. 15-17, 1986. Bellingham, WA, Society of Photo-Optical Instrumentation Engineers, 1986, p. 25-34. refs

**A87-48658****A CONTRIBUTION TO THE OPTIMUM SELECTION OF GROUND CONTROL POINTS IN HIGH RESOLUTION IMAGES**

U. FREI and L. FUSCO (ESA, Earthnet Programme Office, Frascati, Italy) IN: Earth remote sensing using the Landsat Thematic Mapper and SPOT sensor systems; Proceedings of the Meeting, Innsbruck, Austria, Apr. 15-17, 1986. Bellingham, WA, Society of Photo-Optical Instrumentation Engineers, 1986, p. 45-53.

A multitemporal TM data set has been analyzed in order to determine the best image chip characteristics for use in a ground control point (GCP) library. An attempt has been made to identify the optimum selection of image features, bands, chip size, and season of the year for the reference image. The value of correlation coefficient between chips (small subimages centered at the GCP) of the same feature, but acquired at different times, is taken as a component to measure chip quality. Also, the high contrast in a chip is taken to indicate better quality of the GCP. The 'Optimum Chip Factor' (OCF) is a measure of these two aspects of GCP quality. To determine the optimum bands, chip size and features, the OCF was computed in different spectral bands, over different

window sizes and for different features. The best season was found by taking each acquisition date as a reference image and comparing the number of successfully relocated GCPs in all other images. It is found that the best band is band 5, the best features are features with land/water boundaries, and the best chip size is 15 pixels square. To determine the best season of the year, some further investigations will be necessary. Author

**A87-48661****SPOT RADIOMETRIC RESOLUTION PERFORMANCE EVALUATION - PRELIMINARY RESULTS**

G. BEGNI, M. LEROY (CNES, Toulouse, France), and M. DINGUIRARD (ONERA, Centre d'Etudes et de Recherches de Toulouse, France) IN: Earth remote sensing using the Landsat Thematic Mapper and SPOT sensor systems; Proceedings of the Meeting, Innsbruck, Austria, Apr. 15-17, 1986. Bellingham, WA, Society of Photo-Optical Instrumentation Engineers, 1986, p. 77-82. refs

The radiometric resolution capabilities of SPOT are analyzed. SNRs for the three spectral bands and the panchromatic (PA) band of each HRV instrument of SPOT are measured and compared with specifications. It is observed that in the multispectral and HRV1 PA mode specifications are met; however, specifications are not met in the HRV2 PA mode. Structural noise in the HRV2 PA band and the multispectral bands are examined. A procedure for detector normalization is described, and detector normalization coefficients are estimated. It is detected that the residual effects of the detector modulation are less visible than the instrumental noise, and some spurious effects appear at very low radiances and in the XS + P mode. I.F.

**A87-48662****SPOT LOCALIZATION ACCURACY AND GEOMETRIC IMAGE QUALITY**

B. BOISSIN (CNES, Toulouse, France) and JP. GARDELLE (MATRA, S.A., Division Espace, Toulouse, France) IN: Earth remote sensing using the Landsat Thematic Mapper and SPOT sensor systems; Proceedings of the Meeting, Innsbruck, Austria, Apr. 15-17, 1986. Bellingham, WA, Society of Photo-Optical Instrumentation Engineers, 1986, p. 83-92.

This paper presents the method used to check the viewing geometry of the SPOT satellite after the launch. Moreover, the results obtained during the first part of the postlaunch assessment period are given for the various parameters which specify the geometric image quality. The relevant estimation methods are also described, and the specifications are recalled. Author

**A87-48663****SPOT MTF PERFORMANCE EVALUATION**

D. LEGER, M. LEROY, and J. PERBOS (CNES, Toulouse, France) IN: Earth remote sensing using the Landsat Thematic Mapper and SPOT sensor systems; Proceedings of the Meeting, Innsbruck, Austria, Apr. 15-17, 1986. Bellingham, WA, Society of Photo-Optical Instrumentation Engineers, 1986, p. 93-97.

The SPOT MTF is tested during the postlaunch performance assessment using a photointerpretative method. To this end an image catalog is prepared before launch. This catalog is based on high-resolution aerial photographs of 20 cities in the southern part of France in the panchromatic band. Each photograph is subsequently digitized and sampled at 10-m resolution, and for each original photograph a series of 9 images with various and known MTF is obtained through parametric convolution. SPOT MTF is then estimated from a visual comparison between SPOT images and images from the reference catalog. Moreover, an algorithm of evaluation of high-spatial-frequency content is applied to a set of suitable SPOT images, when the two HRV instruments are in parallel viewing, to allow direct comparison between the two instruments' MTF in the panchromatic band. This paper presents a detailed description of these methods and their results. Author

A87-48664

**IMPROVING SPOT IMAGES SIZE AND MULTISPECTRAL RESOLUTION**

D. PRADINES (CNES, Toulouse, France) IN: Earth remote sensing using the Landsat Thematic Mapper and SPOT sensor systems; Proceedings of the Meeting, Innsbruck, Austria, Apr. 15-17, 1986. Bellingham, WA, Society of Photo-Optical Instrumentation Engineers, 1986, p. 98-102.

In order to take advantage of all the capabilities of the SPOT system, new methods for mosaicking SPOT images and increasing the ground resolution of multispectral data have been developed. The mosaicking method uses the capability of acquiring data with HRV instruments in twin mode of operation to obtain an image size of approximately 117 by 110 kilometers. To reduce the processing time, a general mosaicking method is not used, but rather a simplified one which takes into account the radiometric and geometric performance of the SPOT satellite. One of the major SPOT advantages is to provide data with 10-m resolution. In order to take full advantage of this capability, a process which can produce multispectral SPOT images with 10-m resolution was designed. To achieve this goal, special geometric corrections which can insure a perfect superimposability of the panchromatic and multispectral data were designed. Author

A87-48665

**PHOTOGRAMMETRY FROM SPOT WITH MATRA TRASTER ANALYTICAL PLOTTER**

CHRISTIAN VIGNERON and JEAN-LUCIEN SELIGMANN (MATRA, S.A., Saint-Quentin-en-Yvelines, France) IN: Earth remote sensing using the Landsat Thematic Mapper and SPOT sensor systems; Proceedings of the Meeting, Innsbruck, Austria, Apr. 15-17, 1986. Bellingham, WA, Society of Photo-Optical Instrumentation Engineers, 1986, p. 103, 104.

The analytical stereoplotter, TRASTER, for photogrammetry from SPOT, is described. TRASTER provides screen projection of two images and has software for plotting nonconical imageries. The TRASTER software can be utilized for data input, model generation, and data output. The capabilities of TRASTER were evaluated, and it is determined that it is possible to produce accurate 1/50,000 scale maps using TRASTER. I.F.

A87-48669

**THE AUTOMATIC GENERATION OF DIGITAL TERRAIN MODELS FROM SATELLITE IMAGES BY STEREO**

PAUL R. COOPER, DANIEL E. FRIEDMANN, and SCOTT WOOD, A. (MacDonald, Dettwiler and Associates, Ltd., Richmond, Canada) IN: Earth remote sensing using the Landsat Thematic Mapper and SPOT sensor systems; Proceedings of the Meeting, Innsbruck, Austria, Apr. 15-17, 1986. Bellingham, WA, Society of Photo-Optical Instrumentation Engineers, 1986, p. 124-135. Research supported by the National Research Council of Canada. refs  
(Contract NSF DCR-83-20136)

A computer system which automates the process of stereo matching and generates a digital terrain map (DTM) directly from digital satellite images is described. The difficulties of stereo matching are discussed. The basic operation of the system involves: image preparation, boundary extraction, boundary matching, geometric modeling, and product generation. The performance of the system is tested, and it is determined that the system has the ability to derive DTMs of reasonable accuracy from a variety of real imagery. Examples displaying the usefulness of this system are presented. I.F.

A87-48805#

**SPATIAL FILTERING OF DIGITAL LANDSAT DATA FOR THE EXTRACTION OF MAPPING INFORMATION**

S. H. PAINE and M. P. MEPHAM (Calgary, University, Canada) IN: Canadian Symposium on Remote Sensing, 10th, Edmonton, Canada, May 5-8, 1986, Proceedings. Volume 1. Ottawa, Canadian Aeronautics and Space Institute, 1987, p. 27-40. refs

The applicability of five spatial filtering techniques is evaluated using a segment of a 600 x 600 pixel Landsat image of Calgary,

Canada. The five spatial filters are; (1) mean, (2) median, (3) mode, (4) nearest values, and (5) minimum variance. The operations of these filters are described. The data are analyzed in terms of the degree of generalization, the amount of information loss, the sharpness of the edges, and the maintenance of the original data shapes. It is observed that the mean filter introduces errors due to its nonselective smoothing; the median filter removes some variation, but smears the data; the mode filter is useful for removing local variance, but does not smooth the data; the nearest value filter is the most effective; and the minimum variance filter introduces the least amount of error and produces a significant degree of smoothing. I.F.

A87-48807#

**EVALUATION OF ALGORITHMS FOR THE GEOMETRIC CORRECTION OF THEMATIC MAPPER DATA**

B. GUINDON (Canada Centre for Remote Sensing, Ottawa, Canada) IN: Canadian Symposium on Remote Sensing, 10th, Edmonton, Canada, May 5-8, 1986, Proceedings. Volume 1. Ottawa, Canadian Aeronautics and Space Institute, 1987, p. 47-54. refs

Over the past two years, research has been underway at the Canada Centre for Remote Sensing into the evaluation of algorithms which are applicable to the geometric correction of Thematic Mapper (TM) imagery. The results of this effort are being incorporated into a flexible correction capability on the Landsat Digital Image Analysis System (LDIAS). When the software package is complete, it will allow researchers to correct imagery to a variety of map projections and a range of sampling intervals and to apply corrections for terrain relief. This paper describes the details of the processing flow which has been implemented to date. The major topics include processing of ancillary data, acquisition and utilization of ground control points and image resampling. A series of correction experiments have been carried out in which a raw TM scene of the Guelph, Ontario region has been rectified to a UTM map projection. Rectification accuracies of 16 to 17 meters have been achieved using a simplified control point processing scheme. Author

A87-48808#

**APPLICATION OF ACCURACY ASSESSMENT TECHNIQUES TO IMAGE CLASSIFICATION**

B. GUINDON (Canada Centre for Remote Sensing, Ottawa, Canada) and S. NEEMAN (Intera Technologie, Ltd., Ottawa, Canada) IN: Canadian Symposium on Remote Sensing, 10th, Edmonton, Canada, May 5-8, 1986, Proceedings. Volume 1. Ottawa, Canadian Aeronautics and Space Institute, 1987, p. 55-63. refs

The use of Congalton et al. (1983) k statistics for image classification is evaluated by comparing its performance with standard feature selection techniques. Particular attention is given to training area selection and classification performance measurements. The k statistic is a measure of the population level of the diagonal elements of a confusion matrix compared to random occupancy given the marginal column and row proportions. The three features selection techniques studied are average pairwise divergence, average transformed divergence, and minimum pairwise divergence. The gray level means and standard deviations for the images of surface cover types, acquired on July 29, 1984, were computed in each of the high resolution bands. The performance of the k ranking is compared with that of the feature selection techniques. It is observed that none of the selection methods correctly identify all of the optical feature sets and the best results are obtained with k statistics and the average transformed divergence. I.F.

A87-48812#

**AN EVALUATION OF SUN ANGLE COMPUTATION ALGORITHMS**

P. M. TEILLET, M. LASSERE, and C. G. VIGNEAULT (Canada Centre for Remote Sensing, Ottawa) IN: Canadian Symposium on Remote Sensing, 10th, Edmonton, Canada, May 5-8, 1986, Proceedings. Volume 1. Ottawa, Canadian Aeronautics and Space Institute, 1987, p. 91-100. refs

Sun angle computations were studied in the context of remote sensing. For general-purpose use involving readily available, low-precision formulas, errors due to the choice of algorithm are very much less than errors due to location uncertainty and seasonal variations. High-precision determinations of solar illumination angles become important if accurate shadow areas are to be derived from digital terrain information. An error analysis was carried out to assess and rank the principal sources of uncertainty in the solar position as they might occur in the framework of Landsat image data. The concept of uncertainty ellipses is used to illustrate errors in sun angle due to finite solar diameter, finite scene acquisition time, within-scene location variations, and the use of values from an inappropriate epoch. Using a digital elevation model for the Anderson River area in British Columbia, an analysis was carried out to show the strong effect of errors in sun angle on the determination of shadow regions. Issues dealing with computer implementation of sun angle algorithms, solar information provided with image data tapes, and the influence of atmospheric refraction on apparent solar position are also examined. Author

A87-48825#

**PROCESSING OF SEASAT ALTIMETRY DATA ON A DIGITAL IMAGE ANALYSIS SYSTEM**

R. YAZDANI, N. CHRISTOU, and E. DERENYI (New Brunswick, University, Fredericton, Canada) IN: Canadian Symposium on Remote Sensing, 10th, Edmonton, Canada, May 5-8, 1986, Proceedings. Volume 1. Ottawa, Canadian Aeronautics and Space Institute, 1987, p. 233-241. Research supported by the Department of Supply and Services. refs

Digital image analysis systems were used for the processing and displaying geoidal heights and sea surface heights. Three sets of data were experimented with. Each set was rasterized and transformed into image file. Black and white and colour density slicing and pseudo colour display techniques were employed to enhance these surfaces. An analytical relief shading program was developed to make the small, local undulations in height visible. The shape and orientation of the various surfaces were compared by a differencing program specifically written for this purpose. The processing and display techniques employed were of significant assistance to the geodesy group at UNB in their study of the figure of the earth. Author

A87-48826#

**VALIDATION OF STAR-1 SAR IMAGERY COLLECTED OVER MOULD BAY, N.W.T., APRIL 1984**

M. A. CAMERON (Carleton University, Ottawa, Canada), D. J. LAPP (Norland Science and Engineering, Ltd., Ottawa, Canada), and M. E. KIRBY (Intera Technologies, Ltd., Ottawa, Canada) IN: Canadian Symposium on Remote Sensing, 10th, Edmonton, Canada, May 5-8, 1986, Proceedings. Volume 1. Ottawa, Canadian Aeronautics and Space Institute, 1987, p. 243-252. refs

On March 3rd, 1984, Intera Technologies Ltd. flew their STAR-1 Synthetic Aperture Radar (SAR) over Mould Bay N.W.T. in support of the joint AES/NRC experiments conducted between mid March and April. Part of the experiment objective was to determine the minimum size and height of targets detected by the SAR and to observe their relationship to the surrounding ice cover. Visual observations and detailed photography were acquired of specific areas imaged containing different signatures. Several enlargements of the imagery were utilized to compare field measured data with manual measurements of the size and separation of targets in the field which were visible on the imagery. The field work was followed by an analysis of the digital SAR data supplied by Intera Technologies. The work was carried out at the Ice Centre in Ottawa using their DIPIX Image Analysis System. Point target sizes and separation distances between features were determined on a pixel-by-pixel basis and standard filters were applied to the data to determine enhancement value. The data was also degraded to poorer resolutions to simulate other operational systems and determine relative loss of ice feature detail. Author

A87-48847#

**RADIOMETRIC CORRECTIONS OF TOPOGRAPHIC EFFECTS FOR SIMULATED RADARSAT IMAGERY IN A REGION OF MODERATE RELIEF**

M. HINSE, Q. H. J. GWYN, and F. BONN (Sherbrooke, Université, Canada) IN: Canadian Symposium on Remote Sensing, 10th, Edmonton, Canada, May 5-8, 1986, Proceedings. Volume 1. Ottawa, Canadian Aeronautics and Space Institute, 1987, p. 449-462. In French. Research supported by the Fond pour la Formation de Chercheurs et l'Aide à la Recherche du Québec. refs

A87-48857#

**RADIATION MODELLING IN A HIGH RELIEF ENVIRONMENT USING A DIGITAL TERRAIN MODEL AND LANDSAT - TM IMAGERY**

E. LEDREW and C. DUGUAY (Waterloo, University, Canada) IN: Canadian Symposium on Remote Sensing, 10th, Edmonton, Canada, May 5-8, 1986, Proceedings. Volume 2. Ottawa, Canadian Aeronautics and Space Institute, 1987, p. 559-564. refs

For a high relief environment in the Front Range of the Colorado Rockies, spectral maps of surface albedo are produced. The

A87-48818#

**FORECAST OF HURRICANE CHARACTERISTICS FROM GOES IMAGERY**

M. T. A. MAKHDOOM and S. I. SOLOMON (Waterloo, University, Canada) IN: Canadian Symposium on Remote Sensing, 10th, Edmonton, Canada, May 5-8, 1986, Proceedings. Volume 1. Ottawa, Canadian Aeronautics and Space Institute, 1987, p. 163-170. NSERC-supported research. refs

This paper investigates the possibility of using Geostationary Operational Environmental Satellite (GOES) imagery for predicting three major hurricane characteristics, namely, maximum wind velocity, and speed and direction of displacement. The methodology is based on a pattern recognition technique combined with regression analysis in which the independent variables are selected using a physical-mathematical model. Once the hurricane is identified on a photographic image, it is transposed onto a binary feature which is used to identify its type. The variation of the diameter of the cloud pattern of a hurricane and of its type during the last time interval is then related to the variation of maximum wind velocity and speed of displacement over the subsequent time interval. It is concluded that, with respect to maximum wind velocity, both diameter and the type of a cloud pattern are physically important and statistically significant parameters. However, diameter is the only statistically significant parameter in the prediction of speed of displacement, although physical analysis indicates that hurricane type is also important. The binary feature is also used, employing a search and correlation technique, to predict from the variation in the position of the hurricane in the last time interval the direction of the displacement during the next time interval. A fully automated technique has also been used to predict the direction of displacement. Results obtained indicate that prediction of hurricane characteristics, which could be of practical use, may be made from GOES using these models and techniques. Author



upwelling radiance is calculated from Landsat - 5 TM digital data. The downwelling irradiance is calculated for the Landsat spectral bands from the two-stream model of Bruhl and Zdunkowski. Irradiance is corrected for slope, aspect and shading from adjacent mountain peaks using a 30 meter resolution Digital Elevation Model. This is the first phase in a project directed towards mapping net radiation with high spatial resolution. This type of map is of interest in studies of mountain microclimate, ecosystem dynamics, hydrology and geomorphology. Author

### A87-48866#

#### APPLICATIONS OF SATELLITE DERIVED DIGITAL ELEVATION MODELS FOR RESOURCE MAPPING

D. R. ROSE (McDonald Dettwiler and Associates, Ltd., Richmond, Canada) and F. HEGYI (British Columbia Ministry of Forests, Planning and Inventory Branch, Victoria, Canada) IN: Canadian Symposium on Remote Sensing, 10th, Edmonton, Canada, May 5-8, 1986, Proceedings. Volume 2. Ottawa, Canadian Aeronautics and Space Institute, 1987, p. 655-660.

The use of digitally-derived satellite imagery to derive digital elevation models (DEMs) is examined. The cost, production time, and accuracy requirements for satellite-derived DEMs are described. The application of satellite-derived DEMs to topographic mapping, in particular for base and thematic mapping, is discussed. I.F.

### A87-48870#

#### CUSTOM-ENHANCED LANDSAT IMAGERY IN NEAR REAL-TIME

G. J. BURGER and J. M. MILLER (Alaska, University, Fairbanks) IN: Canadian Symposium on Remote Sensing, 10th, Edmonton, Canada, May 5-8, 1986, Proceedings. Volume 2. Ottawa, Canadian Aeronautics and Space Institute, 1987, p. 699-703. refs

The Geophysical Institute operates the Landsat Quick-Look Program which routinely collects MSS data from Alaska, portions of Canada and eastern Siberia. These data can be enhanced to customer specifications and distributed as photographic products to users within hours of the satellite pass. The timeliness of 'near real-time' distribution of full-resolution images, in color or monochrome, increases the value of the data for monitoring dynamic events such as forest fires, volcanic eruptions, river break-up, sea-ice movement, and navigation hazards. Applications of Landsat data since 1980 in the form of quick-look products in the arctic and subarctic regions of western North America are illustrated. Author

### A87-48883#

#### VALIDATION AND SIMULATION OF RADARSAT IMAGERY

G. J. WESSELS, R. T. LOWRY (Intera Technologies, Ltd., Ottawa, Canada), and R. K. RANEY (Radarsat Project Office, Ottawa, Canada) IN: Canadian Symposium on Remote Sensing, 10th, Edmonton, Canada, May 5-8, 1986, Proceedings. Volume 2. Ottawa, Canadian Aeronautics and Space Institute, 1987, p. 841-854. Sponsorship: Department of Supply and Services. refs (Contract DSS-13ST-23413-3-5008)

The SRSIM software package developed to generate simulated spaceborne SAR imagery is described. SRSIM allows users of radar data to evaluate the impact of radar parameter changes on data utility and design engineers to simulate design trade-offs at the image level. Simulations are produced by generating radar reflectivity maps, thermal noise, and speckle consistent with the system being studied. An SAR image simulation generated from the Canada Centre for Remote Sensing SAR-580 airborne radar data is compared with NASA SIR-B data collected over a test site near Montreal, Canada. It is observed that the simulation is accurate and the type of sensor, processor, target scene, and display used affects the spaceborne SAR imagery. Diagrams of the SRSIM are presented. I.F.

### A87-48884#

#### SULPHUR DIOXIDE DAMAGE ASSESSMENT USING COLOUR INFRARED AERIAL PHOTOGRAPHY

M. POLET (Gulf Canada Resources, Calgary, Canada), R. V. DAMS (Intera Technologies, Ltd., Calgary, Canada), and J. WELLS (Integrated Environments, Calgary, Canada) IN: Canadian Symposium on Remote Sensing, 10th, Edmonton, Canada, May 5-8, 1986, Proceedings. Volume 2. Ottawa, Canadian Aeronautics and Space Institute, 1987, p. 855-860. refs

Vegetation damage that resulted from a July 14, 1985 fire at a sour gas plant in Alberta, Canada was assessed using color IR (CIR) aerial photographs and ground transect data. The CIR photographs, which were obtained on July 25, 1985, were at a scale of 1:10,000. The SO<sub>2</sub>-affected forest vegetation appeared bright yellow on the CIR photographs. Estimates of damage by vegetation type/stress level were developed. It is noted that CIR mosaics and digitized area estimates provide accurate area damage delineation that is useful for insurance claim settlements, public hearings, and government regulatory agency meetings. I.F.

### A87-48885#

#### MULTIPLE-LOOK EFFECTS ON SAR CLASSIFICATION ACCURACIES

C. GOSSELIN (Intera Technologies, Ltd., Ottawa, Canada) and R. J. BROWN (Canada Centre for Remote Sensing, Ottawa) IN: Canadian Symposium on Remote Sensing, 10th, Edmonton, Canada, May 5-8, 1986, Proceedings. Volume 2. Ottawa, Canadian Aeronautics and Space Institute, 1987, p. 861-865. refs

At present, there is no available spaceborne radar imagery that can effectively simulate the expected performance of the Radarsat C-band SAR that will be launched in 1990. Indeed, Seasat and SIR A/B acquired only L-band data during their missions. Therefore, airborne C-band SAR data become the best data source for this type of simulation. This process requires a decrease in spatial resolution achieved through pixel averaging and results in a smoothed image no longer representative of raw spaceborne data. In order to simulate more realistic satellite data the Radarsat SAR Simulation Package (RSSP) developed at the Canada Centre for Remote Sensing was used. This software package can introduce additive thermal noise and multiplicative speckle in order to simulate the expected data from a satellite SAR. Four-, eight- and sixteen-look speckles were thus generated and applied to a CVV image of Melfort, Saskatchewan acquired on July 31, 1983. This paper attempts to evaluate the expected performance of the Radarsat SAR for crop-type determination by comparing the results of a maximum-likelihood classification using both a pixel and a field classifier. In particular, the changes in classification accuracy are assessed as a function of the number of looks in the imagery. Author

### A87-48889#

#### NEW SYSTEM FOR THE ORDERING, ARCHIVING AND RETRIEVAL OF DATA FROM EARTH'S RESOURCE SATELLITES

J. CIHLAR and F. GUERTIN (Canada Centre for Remote Sensing, Ottawa) IN: Canadian Symposium on Remote Sensing, 10th, Edmonton, Canada, May 5-8, 1986, Proceedings. Volume 2. Ottawa, Canadian Aeronautics and Space Institute, 1987, p. 895-901.

An earth's resources satellite system that includes satellite reference tracks, a data acquisition planning package, and an archived data catalog is proposed. The main uses of a satellite data reference system are: (1) requests for new data, (2) data acquisition planning and scheduling, (3) archiving raw or processed data, and (4) requests for archived data. The functions of the components of the earth's resources satellite system are described. The implementation of this proposed system and its interfacing with other systems are discussed. Flow charts revealing the method by which the availability of existing satellite data is determined and how data can be ordered and delivered are presented. I.F.

**A87-48896#**

**THE ERS-1/RADARSAT SAR CANADIAN GROUND SEGMENT**  
 M. SACK (McDonald Dettwiler Associates, Ltd., Richmond, Canada) and G. J. PRINCZ (Canada Centre for Remote Sensing, Ottawa)  
 IN: Canadian Symposium on Remote Sensing, 10th, Edmonton, Canada, May 5-8, 1986, Proceedings. Volume 2. Ottawa, Canadian Aeronautics and Space Institute, 1987, p. 957-969. Sponsorship: Department of Supply and Services.  
 (Contract DSS-13SR-23413-4-9041)

As part of the Canadian Microwave Remote Sensing programme requirement, a ground segment is being designed to handle satellite SAR data. The ground segment under consideration will consist of facilities to acquire, process and disseminate SAR data from both the ERS-1 and RADARSAT satellites which will be launched in 1989 and 1991, respectively. The SAR Data Acquisition and Processing Facilities (SARDAPF) will consist of two Data Acquisition Facilities (DAFs) and a single SAR Data Processing Facility (DPF). The two remote DAFs will collect the SAR data from the satellites and will transmit it to the DPF for processing. The DPF will process the data into SAR digital imagery at 1/4 of real-time. The products generated will consist of high resolution (25 meters) and low resolution (100 meters) SAR image data. This data will be disseminated to the user community in digital form (CCT, high speed communications link) and photographic imagery (240 mm film). The data, depending on the type and level of corrections, will be available at a minimum of 3 hours after data acquisition. Author

**A87-48904#**

**A REVOLUTION IN THE PRODUCTION OF SMALL-SCALE AND MEDIUM-SCALE MAPS [UNE REVOLUTION DANS LA PRODUCTION CARTOGRAPHIQUE DE BASE A PETITE ET MOYENNE ECHELLES]**

G. ROCHON, A. LECLERC, S. R. HAJA, and TH. TOUTIN (DIGIM /1983/ Inc., Montreal, Canada) IN: Canadian Symposium on Remote Sensing, 10th, Edmonton, Canada, May 5-8, 1986, Proceedings. Volume 2. Ottawa, Canadian Aeronautics and Space Institute, 1987, p. 1029-1037. In French. refs

The system components and main information processing steps of a semiautomated system for the production of small-scale and medium-scale maps from GPS position data and stereoscopic SPOT images are described, and the system performance is evaluated. It is suggested that the system will reduce production delays and will provide cost reductions of the order of 50 percent for 1:50,000 maps, and of the order of 75 percent for orthoimages. The system also offers the possibility of integrating various digital products such as DTMs. R.R.

**A87-48905#**

**DEVELOPMENT OF A MATHEMATICAL MODEL FOR THE SPATIAL TRIANGULATION OF SPOT IMAGES [DEVELOPEMENT D'UN MODELE MATHEMATIQUE POUR LA SPATIO-TRIANGULATION D'IMAGES SPOT]**

TH. TOUTIN (DIGIM /1983/ Inc., Montreal, Canada) IN: Canadian Symposium on Remote Sensing, 10th, Edmonton, Canada, May 5-8, 1986, Proceedings. Volume 2. Ottawa, Canadian Aeronautics and Space Institute, 1987, p. 1039-1047. In French. refs

A mathematical model which is based on physical and dynamic celestial mechanics is developed for the spatial triangulation of remote sensing images. For the case of the SPOT satellite, results for orders of magnitude of various parameters relating to the motion geometry are given. The evolution laws for the independent parameters which define the vector-sensor unit are first formulated, following which observation and error equations are developed. The model is then extended to formulate a simplified general equation which can be applied to any points used in the resolution of the model by the variation of certain parameters. The spatial triangulation procedure results in a homogeneous network of control points distributed across the observed area, with a relative precision between points of better than 10 m. R.R.

**A87-48906#**

**THE OPERATIONAL USE OF RADARSAT PRODUCTS BY THE ICE CENTRE ENVIRONMENT CANADA**

J. C. FALKINGHAM and B. R. RAMSAY (Ice Centre Environment Canada, Ottawa) IN: Canadian Symposium on Remote Sensing, 10th, Edmonton, Canada, May 5-8, 1986, Proceedings. Volume 2. Ottawa, Canadian Aeronautics and Space Institute, 1987, p. 1049-1053. refs

The AES Ice Centre, situated in Ottawa, will be the heaviest operational user of data from RADARSAT. The data will provide coverage of Canadian ice-infested waters for integration into daily ice charts and forecasts, and for turn-around to users of tactical ice information. The required daily coverage of Arctic and East Coast regions will mean that the Ice Centre will receive up to 135 SAR georeferenced coarse resolution products per day, as well as a much smaller selection of other SAR digital provide daytime, high-resolution optical data in the visible band which will supplement the RADARSAT SAR data, and other remotely sensed data received by the Ice Centre. The AVHRR sensor on board RADARSAT will be viewed as a back-up, in the event of a failure, of the two NOAA AVHRR sensors presently operating. No requirement is foreseen for the RADARSAT Scatterometer data (R-SCAT). RADARSAT digital products will be received by the Ice Centre in near-real time via land-line from the RADARSAT processing facility in Ottawa. They will be a major data input to the VAX-based Ice Data Integration and Analysis System (IDIAS), due to be installed at the Ice Centre prior to the launch of RADARSAT. The proposed methodologies for geocoding, processing, analyzing, and integrating these data will be discussed. IDIAS products derived from RADARSAT data, along with the planned methods of distribution to ice information users, will be also described. Author

**A87-51174**

**AUTOMATED EVALUATION OF LINEAR NETWORKS ON SPOT IMAGES [RECHERCHE AUTOMATIQUE DES RESEAUX LINEAIRES SUR LES IMAGES SPOT]**

ISABELLE DESTIVAL (Institut Geographique National, Saint-Mande, France) Societe Francaise de Photogrammetrie et de Teledetection, Bulletin (ISSN 0244-6014), no. 105, 1987, p. 5-16. In French. refs

SPOT images of the Beauce region are used to demonstrate a two-part automated technique for the extraction of roads and villages from high-resolution satellite imagery. Two different approaches to the detection step, leading to the construction of an image of candidate points, are discussed: (1) the use of morphological transformations to extract from grey-tint images information concerning the narrow (roads) or textured (villages) objects; and (2) a digital method which reduces the number of parameters selected by the operator. Comparison of various operators shows the 'high-form hat' to be the most effective. It is noted that the second step, the reconstructing of objects based on the previous selection of information, cannot be automated. The application of expert systems to the reconstruction of linear networks is also considered. R.R.

**A87-51175**

**GEOMETRIC CORRECTION OF SPACE IMAGES BY THE COLINEARITY-EQUATION METHOD [RESTITUTION GEOMETRIQUE DES IMAGES SPATIALES PAR LA METHODE DE L'EQUATION DE COLINEARITE]**

NING SHU (Wuhan College of Geodesy, Photogrammetry and Cartography, People's Republic of China) Societe Francaise de Photogrammetrie et de Teledetection, Bulletin (ISSN 0244-6014), no. 105, 1987, p. 27-40. In French.

Application of the colinearity-equation method to the geometric correction of remote-sensing imagery is considered, and a technique for the determination of the colinearity-equation parameters using control points and the least-squares method is discussed. The universal equations governing sensor observation are derived, and specific equations for sensors including aerial photography cameras, panoramic photographic cameras, and multispectral scanners are presented. A study is then made of



the colinearity equation for the case when the field reference system is the earth's center. It is noted that this solution permits a more rigorous correction of satellite images. R.R.

### A87-51179

#### FIRST NEW ZEALAND IMAGE FROM THE FRENCH SPOT SATELLITE

S. E. BELLIS (Department of Scientific and Industrial Research, Div. of Information Technology, Lower Hutt, New Zealand) *Journal of Technology* (ISSN 0112-3890), vol. 2, no. 3, 1986, p. 139-142.

It is shown that a SPOT satellite scene of the New Zealand port city of Wellington is of a scale that facilitates the detailed updating of maps and the monitoring of specific sites. Although SPOT has a 26-day repeat cycle, a mirror-based canting system that varies the line-of-sight allows scanners to image a given region for 11 of the 26 days; this pointing/visit capability allows stereo imagery to be generated, a resource which is also very useful in cartography. O.C.

### A87-52795#

#### INTERPRETING METEOROLOGICAL SATELLITE IMAGES USING A COLOR-COMPOSITE TECHNIQUE

ROBERT P. D'ENTREMONT and LARRY W. THOMASON (USAF, Geophysics Laboratory, Hanscom AFB, MA) *American Meteorological Society, Bulletin* (ISSN 0003-0007), vol. 68, July 1987, p. 762-768. refs

An image-display technique is described that simultaneously combines three meteorological satellite images into a color-image product. The technique reveals many features of meteorological interest. It is frequently noted that interpretations of black-and-white 'infrared' nighttime imagery are difficult to make when attempting to distinguish low clouds and fog from cloud-free land and ocean, thin from thick cirrus, and thick nonprecipitating clouds from nimbostratus clouds. It is found that a more-confident discrimination can be obtained between such features when the National Oceanic and Atmospheric Administration (NOAA) Advanced Very High Resolution Radiometer (AVHRR) or Nimbus Scanning Multifrequency Microwave Radiometer (SMMR) data are combined into color-image products. Author

**A87-53018\*** Jet Propulsion Lab., California Inst. of Tech., Pasadena.

#### COLOR ENHANCEMENT OF HIGHLY CORRELATED IMAGES. II - CHANNEL RATIO AND 'CHROMATICITY' TRANSFORMATION TECHNIQUES

ALAN R. GILLESPIE, ANNE B. KAHLE, and RICHARD E. WALKER (California Institute of Technology, Jet Propulsion Laboratory, Pasadena) *Remote Sensing of Environment* (ISSN 0034-4257), vol. 22, Aug. 1987, p. 343-365. refs

Two techniques for enhancing the color of multispectral images are described; both involve ratioing of data from different image channels. In the first technique, the ratioed data are assigned the primary color for display as color ratio pictures, and in the second method, image data are transformed to RGB chromaticity coordinates by ratioing the data acquired in three channels to the sum of their intensities. The two techniques are applied to a NASA Thermal-IR Multispectral Scanner (TIMS) image of Death Valley and to a Landsat MSS image of the Mojave Desert. The basic principles of ratioing are discussed, and the effects of atmospheric path radiances on the interpretation of ratioed images are investigated. It is observed that the color pictures produced using these two enhancement techniques are similar to the pictures enhanced by decorrelation and hue-saturation-intensity methods. I.F.

### A87-53103

#### IMPROVED CLOUD ANALYSIS USING VISIBLE, NEAR-INFRARED, INFRARED, AND MICROWAVE IMAGERY

ROBERT P. D'ENTREMONT, JAMES T. BUNTING, GERALD W. FELDE, and LARRY W. THOMASON (USAF, Geophysics Laboratory, Hanscom AFB, MA) *IN: IGARSS '87 - International Geoscience and Remote Sensing Symposium, Ann Arbor, MI, May 18-21, 1987, Digest. Volume 1.* New York, Institute of Electrical and Electronics Engineers, Inc., 1987, p. 51-56. refs

Automated cloud analysis models such as the Air Force Real-time Nephelanalysis (RTNEPH) currently use visible (0.4-1.1 micron) and infrared (10-12 micron) satellite data during the day, and only infrared data at night. In visible imagery, snow cover is often confused with clouds because both surfaces reflect sunlight well. In infrared imagery, low clouds are frequently confused with cloudfree land and oceans because the cloud and surface temperatures are nearly equal. These problems reduce the accuracy and quality of cloud analysis, such as the RTNEPH, that use satellite imagery as a primary source of cloud observations. However, the quality of cloud analyses can be improved if data from near-infrared (1.6 micron), shorter-wavelength infrared (3.7 micron), and microwave (e.g., 37 GHz) channels are used in conjunction with the visible and infrared data. The processing of this meteorological data will help alleviate many problems in automated cloud analysis models. Author

### A87-53110

#### HIERARCHICAL CLASSIFICATION WITH KNOWLEDGE BASED BINARY DECISION

K. STAENZ, P. MEYER, and K. I. ITTEN (Zuerich, Universitaet, Zurich, Switzerland) *IN: IGARSS '87 - International Geoscience and Remote Sensing Symposium, Ann Arbor, MI, May 18-21, 1987, Digest. Volume 1.* New York, Institute of Electrical and Electronics Engineers, Inc., 1987, p. 97-102. refs

A stepwise hierarchical classification approach based on binary decisions (BDs) was tested in a first attempt in view of possible solutions towards expert systems. A geocoded TM data set was involved in this study to prepare the images for monitoring forest damages. BDs at three classification levels were then necessary to extract the different target types mainly using a standardized density slicing procedure. A classification accuracy of 67 to 91 percent for the various land use classes could be achieved with the proposed classification model. For that purpose, ground truth maps were used for each of the targets investigated. Author

### A87-53112

#### EXPLORING THE SPATIAL DOMAIN

JACQUES H. T. STAKENBORG (CEC, Joint Research Centre, Ispra, Italy) *IN: IGARSS '87 - International Geoscience and Remote Sensing Symposium, Ann Arbor, MI, May 18-21, 1987, Digest. Volume 1.* New York, Institute of Electrical and Electronics Engineers, Inc., 1987, p. 125-130. refs

The use of spatial analysis of remote sensing data to improve the classification of remotely sensed images is studied. A knowledge-based classification method is applied to digitized aerial photographs of Bangkok, Thailand in order to classify housing using form parameters. In a second example, TM images of an area near Freiburg, FRG are segmented by contouring the filtered images in order to divide the images into zones with a homogeneous macrostructure. The procedures for extracting data from digital images using edge segmentation and some properties of the extracted regions are described. I.F.

**A87-53131\*** Department of Agriculture, Beltsville, Md.  
**ROUGHNESS MEASUREMENTS WITH MULTIPOLARIZATION AIRCRAFT DATA**

E. T. ENGMAN (USDA, Agricultural Research Service, Beltsville, MD) and J. R. WANG (NASA, Goddard Space Flight Center, Greenbelt, MD) IN: IGARSS '87 - International Geoscience and Remote Sensing Symposium, Ann Arbor, MI, May 18-21, 1987, Digest. Volume 1. New York, Institute of Electrical and Electronics Engineers, Inc., 1987, p. 273-275. refs

Multipolarization SAR data were collected over the SIR-B target area near Fresno, California, a few days before the Shuttle flight. Attempts to use these data to evaluate roughness models were unsuccessful. It is speculated that the processing of those data to give good total swath and target contrast resulted in very little variation among the bare fields. Special processing to provide adequate contrast among the targets of interest and to account for a large incidence angle variation may be necessary to make these data useful for this type of study. Author

**A87-53139**  
**AN EXPERT SYSTEM FOR PLANIMETRIC FEATURE EXTRACTION**

BEN YEE (MacDonald, Dettwiler and Associates, Ltd., Richmond, Canada) IN: IGARSS '87 - International Geoscience and Remote Sensing Symposium, Ann Arbor, MI, May 18-21, 1987, Digest. Volume 1. New York, Institute of Electrical and Electronics Engineers, Inc., 1987, p. 321-325. Research supported by the National Research Council of Canada.

This paper describes an expert system for extracting planimetric features from multispectral satellite imagery. Visual planimetric feature extraction by human operators is a labor intensive operation. Automated feature extraction offers a potential for substantial time and labor savings as well as for improvements in the accuracy and consistency of planimetric data. The expert system draws on methods from image processing, remote sensing, and Artificial Intelligence (AI). Image processing operations are applied to extract a symbolic description of the image. The symbolic image description is matched against knowledge-based models of planimetric features, resulting in feature recognition and extraction. Promising results have been obtained in exciting features from Landsat Thematic Mapper (TM) and SPOT imagery, demonstrating the potential of knowledge-based techniques in planimetric feature extraction. Author

**A87-53140**  
**SEQUENTIAL THINNING ALGORITHMS FOR REMOTE SENSING APPLICATION**

J. F. WANG (Waterloo, University, Canada) IN: IGARSS '87 - International Geoscience and Remote Sensing Symposium, Ann Arbor, MI, May 18-21, 1987, Digest. Volume 1. New York, Institute of Electrical and Electronics Engineers, Inc., 1987, p. 337-342. Research supported by the Peking University.

In this paper some sequential thinning algorithms have been proposed. It has been proved that these thinning algorithms keep the connectivity of the figures on the images. They can not create holes. They produce very little or even no contraction at the ends of the figures. With some smoothing process, most noises, such as prickles, have been removed. The examples are given of drainage patterns from Landsat images. The results are very satisfactory. Author

**A87-53142**  
**DIGITAL ELEVATION MODEL EXTRACTION FROM STEREO SATELLITE IMAGES**

DAVID S. KAUFFMAN and SCOTT A. WOOD (MacDonald Dettwiler and Associates, Ltd., Richmond, Canada) IN: IGARSS '87 - International Geoscience and Remote Sensing Symposium, Ann Arbor, MI, May 18-21, 1987, Digest. Volume 1. New York, Institute of Electrical and Electronics Engineers, Inc., 1987, p. 349-352. Research supported by the National Research Council of Canada. refs

Two digital technologies have now been combined to allow development of an accurate, robust and fast system for deriving

digital elevation models (DEMs) from stereo satellite images. The system is highly automatic, accurate, and does not require a stereoplotter, greatly reducing the cost of deriving height information. An edge-based hierarchical matching algorithm, resulting from computational vision research, has been used to extract and match corresponding image features in stereo image pairs. This paper describes some of the photogrammetric problems peculiar to satellite-based imaging systems, particularly those problems resulting from the off-nadir viewing introduced by the SPOT satellite. Author

**A87-53143\*** Jet Propulsion Lab., California Inst. of Tech., Pasadena.

**AUTOMATED RECTIFICATION AND GEOCODING OF SAR IMAGERY**

R. KWOK and J. C. CURLANDER (California Institute of Technology, Jet Propulsion Laboratory, Pasadena) IN: IGARSS '87 - International Geoscience and Remote Sensing Symposium, Ann Arbor, MI, May 18-21, 1987, Digest. Volume 1. New York, Institute of Electrical and Electronics Engineers, Inc., 1987, p. 353-358. refs

An automated post-processing system has been developed for rectification and geocoding of SAR (Synthetic Aperture Radar) imagery. The system uses as input a raw uncorrected image from the operational SAR correlator, and produces as a standard output a rectified and geocoded product. The accurate geolocation of SAR image pixels is provided by a spatial transformation model which maps the slant range-azimuth SAR image pixels into their location on a prespecified map grid. This model predicts the geodetic location of each pixel by utilizing: the sensor platform position; a geoid model; the parameters of the data collection system and the processing parameters used in the SAR correlator. Based on their geodetic locations, the pixels are mapped by using the desired cartographic projection equations. This rectification and geocoding technique has been tested with Seasat and SIR-B images. The test results demonstrate absolute location uncertainty of less than 50 m and relative distortion (scale factor and skew) of less than 0.1 percent relative to local variations from the assumed geoid. Author

**A87-53148\*** Jet Propulsion Lab., California Inst. of Tech., Pasadena.

**SPACEBORNE IMAGING RADAR ON EOS**

CHARLES ELACHI and J. B. CIMINO (California Institute of Technology, Jet Propulsion Laboratory, Pasadena) IN: IGARSS '87 - International Geoscience and Remote Sensing Symposium, Ann Arbor, MI, May 18-21, 1987, Digest. Volume 1. New York, Institute of Electrical and Electronics Engineers, Inc., 1987, p. 383-385.

A multiparameter synthetic aperture imaging radar is planned as a facility instrument for the Earth Orbiting System (EOS). This sensor will operate at L, C, and X and at all possible polarizations (HH, VV, HV, VH), thus allowing the acquisition of detailed information about the surface physical and electrical properties. When combined with the visible and IR imaging spectrometry data and the surface topography, a full description of the surface structure, composition, thermal properties and physical properties could then be extracted. Author

**A87-53154**  
**REMOTE SENSING AND LANDSCAPE APPROACHES TO EARTH RESOURCES**

H. GULINCK and P. JANSSENS (Leuven, Katholieke Universiteit, Louvain, Belgium) IN: IGARSS '87 - International Geoscience and Remote Sensing Symposium, Ann Arbor, MI, May 18-21, 1987, Digest. Volume 1. New York, Institute of Electrical and Electronics Engineers, Inc., 1987, p. 467-472. refs

This paper aims at the construction of a framework for the extraction of landscape information from remote sensing data. Distinction is made between the concepts landscape and landscape approach. The latter is relevant to many research fields and planning applications. This framework consists of an analytical and asynthetic stage. Satellite Remote Sensing data, as well as

## 07 DATA PROCESSING AND DISTRIBUTION SYSTEMS

various image processing techniques, can be implemented in this framework. Three landscape investigation issues are discussed.

Author

**A87-53183\*** Purdue Univ., West Lafayette, Ind.  
**SPECTRAL FEATURE DESIGN FOR DATA COMPRESSION IN HIGH DIMENSIONAL MULTISPECTRAL DATA**

C.-C. THOMAS CHEN and DAVID A. LANDGREBE (Purdue University, West Lafayette, IN) IN: IGARSS '87 - International Geoscience and Remote Sensing Symposium, Ann Arbor, MI, May 18-21, 1987, Digest. Volume 1. New York, Institute of Electrical and Electronics Engineers, Inc., 1987, p. 685-690. refs (Contract NAGW-925)

Data transmission loads of high dimensional remote sensor systems can be greatly reduced by applying generalized Karhunen-Loeve transform as a feature design technique. Two spectral feature design approaches based upon the generalized K-L transform are developed to compress information effectively. Six sets of field data from Kansas and North Dakota on three different dates each are used to test the methods. Spatially, temporally and spatially/temporally combined data sets are formed in this paper to test the robustness property of the schemes. The probability of correct classification using Landsat MSS, Thematic Mapper bands and the proposed bands are found and compared. The comparison shows that the results are improved by the proposed methods, and they appear to be satisfactorily robust. The overall data compression ratio in this paper is about 100/16, i.e., about 6 to 1 with no loss in classification accuracy. Author

**A87-53207\*** Woods Hole Oceanographic Institution, Mass.  
**A SYSTEMS-APPROACH TO THE DESIGN OF THE EOS DATA AND INFORMATION SYSTEM**

ROBERT R. P. CHASE (Woods Hole Oceanographic Institution, MA) IN: IGARSS '87 - International Geoscience and Remote Sensing Symposium, Ann Arbor, MI, May 18-21, 1987, Digest. Volume 2. New York, Institute of Electrical and Electronics Engineers, Inc., 1987, p. 887-891. (Contract NAGW-946)

The task of designing a data and information system responsive to the needs of Eos users is stratified by level and approached with contemporary systems design practices. Appropriate systems design principles are applied at the conceptual design level in this paper. A functional, architectural design is described in terms of elemental composition, top-level functions, and external and internal interfaces. The functional validity of this design has been tested and verified through the use of realistic user scenarios consistent with existing plans for the 1990s, the Space Station era. Technologic and management impediments to the development of the requisite data and information system for Eos are examined and a consistent methodology for developing this system is discussed. Author

**A87-53209**  
**DATA CORRECTION FOR AUTOMATED REMOTE SENSING IMAGE INTERPRETATION**

FANGJU WANG and ROSS NEWKIRK (Waterloo, University, Canada) IN: IGARSS '87 - International Geoscience and Remote Sensing Symposium, Ann Arbor, MI, May 18-21, 1987, Digest. Volume 1. New York, Institute of Electrical and Electronics Engineers, Inc., 1987, p. 909-912. Research supported by the International Development and Research Center, National Research Council of Canada, and the Board of Industrial Leadership of Ontario. refs

In building an automated remote sensing image interpretation system, data uncertainty is a key issue which causes some major difficulties. Artificial intelligence techniques provide some methods to deal with data uncertainty but limitations exist. To achieve accurate interpretation, data correction is required prior to analysis. Of the factors which degrade and distort remotely sensed data, atmospheric effects have the largest and most changeable influence. Therefore, it is important to remove or reduce the atmospheric effects to produce corrected data which are as close as possible to the original object radiant energy distribution. This

paper describes a simplified atmospheric correction algorithm and discusses some aspects of a correction system for automated systems. Author

**A87-53213**  
**AUTOMATIC FOCUSING OF SYNTHETIC APERTURE RADAR IMAGES OF DIFFUSE TARGETS**

CHRISTOPHER C. WACKERMAN and DAVID R. LYZENGA (Michigan, Environmental Research Institute, Ann Arbor) IN: IGARSS '87 - International Geoscience and Remote Sensing Symposium, Ann Arbor, MI, May 18-21, 1987, Digest. Volume 2. New York, Institute of Electrical and Electronics Engineers, Inc., 1987, p. 937-940. refs (Contract N00014-81-C-0692)

A method is proposed for the location of the peak of the cross-correlation function when SAR images have only diffuse targets, by averaging correlation functions that are derived from various azimuth lines, followed by a calculation of the correlation peak and of the error in focusing. The determination of when such an image is focused is undertaken by maximizing contrast, maximizing spectral density, or eliminating shifts between images with disjoint bandpasses. Tests using synthetically generated SAR images are presented, together with the implementation of the algorithm on an actual SAR image that contains only ocean gravity waves. O.C.

**A87-53230\*** National Aeronautics and Space Administration. Goddard Space Flight Center, Greenbelt, Md.

**THE LAND ANALYSIS SYSTEM (LAS) - A GENERAL PURPOSE SYSTEM FOR MULTISPECTRAL IMAGE PROCESSING**

STEPHEN W. WHARTON and YUN-CHI LU (NASA, Goddard Space Flight Center, Greenbelt, MD) IN: IGARSS '87 - International Geoscience and Remote Sensing Symposium, Ann Arbor, MI, May 18-21, 1987, Digest. Volume 2. New York, Institute of Electrical and Electronics Engineers, Inc., 1987, p. 1081-1086. refs

The present, general-purpose Land Analysis System (LAS) for image processing furnishes a comprehensive set of functions for the manipulation of MSS data; the initial version has more than 240 functions and utilities ranging from pixel manipulation to complex classification. A LAS user's guide describes each such function in terms of purpose, input parameters, illustrative examples, algorithms, error messages, and user codes. The LAS source code is so distributed as to simplify system maintenance; the Transportable Application Executive is employed as the user interface, thereby accommodating both expert and novice users by means of menus and tutored prompting. O.C.

**A87-53233**  
**A HIGH SPEED DIGITAL PROCESSOR FOR REAL-TIME SYNTHETIC APERTURE RADAR IMAGING**

RALPH FABRIZIO (ESL, Inc., Sunnyvale, CA) IN: IGARSS '87 - International Geoscience and Remote Sensing Symposium, Ann Arbor, MI, May 18-21, 1987, Digest. Volume 2. New York, Institute of Electrical and Electronics Engineers, Inc., 1987, p. 1099-1103. refs (Contract N00014-86-C-0840)

A high speed and reconfigurable digital synthetic aperture radar (SAR) image processing architecture has been identified. This architecture is built around an existing full-custom Very Large Scale Integration (VLSI) FFT chip set and existing systolic processor architecture design capabilities. These technologies have created the opportunity to develop a low-risk, low-cost, and flexible SAR imaging processor. The flexible, advanced digital design meets the real-time image processing requirements for current and anticipated SAR and SAR-like processing systems. Author

A87-53253

**GEOMETRIC DISTORTION CORRECTION WITH HIGH ACCURACY FOR NOAA SATELLITE IMAGES**

WEIDONG SUN and MIKIO TAKAGI (Tokyo, University, Japan) IN: IGARSS '87 - International Geoscience and Remote Sensing Symposium, Ann Arbor, MI, May 18-21, 1987, Digest. Volume 2. New York, Institute of Electrical and Electronics Engineers, Inc., 1987, p. 1257-1262. refs

A geometric distortion correction method employing an ellipsoidal model of the earth is used to improve the accuracy of corrections for the NOAA satellite's images. Geometric distortions can by these means be reduced to between zero and 3 pixels; the method's computation time is, moreover, about four times faster than that of a spherical model's system correction. In order to further reduce the residual geometric distortions of ellipsoidal model corrections, a two-step correction method has been developed for small area analyses that require greater accuracy. The second step of the method uses ground control point template matching correction. O.C.

A87-53254

**ATMOSPHERIC EFFECTS ON LANDSAT TM THERMAL IR DATA**

LUIS A. BARTOLUCCI, MAO CHANG, and MARK R. GRAVES (Murray State University, KY) IN: IGARSS '87 - International Geoscience and Remote Sensing Symposium, Ann Arbor, MI, May 18-21, 1987, Digest. Volume 2. New York, Institute of Electrical and Electronics Engineers, Inc., 1987, p. 1263-1268. Research supported by Murray State University. refs

The components of atmospherically attenuated target radiance and the path radiance emitted by the atmosphere are calculated to explain the fact that for certain meteorological conditions, properly calibrated thermal IR data gathered from aircraft and spacecraft altitudes provide accurate temperature measurements of surface water bodies even when atmospheric corrections are not applied. Results show that although the 8-14-microns atmospheric window is far from being transparent (less than 50 percent transmission), the amount of atmospheric path radiance may be equal to the amount of attenuated target radiance. Errors in remotely sensed temperatures introduced by atmospheric effects are shown to be smaller than those caused by sensor noise and the effects of applying a cubic convolution during the process of converting the TM data from A-tape to geometrically corrected P-tape data format. Author

A87-53259

**STATISTICAL MODELLING AND SUPPRESSION OF SPECKLE IN SYNTHETIC APERTURE RADAR IMAGES**

JONG-SEN LEE (U.S. Navy, Naval Research Laboratory, Washington, DC) IN: IGARSS '87 - International Geoscience and Remote Sensing Symposium, Ann Arbor, MI, May 18-21, 1987, Digest. Volume 2. New York, Institute of Electrical and Electronics Engineers, Inc., 1987, p. 1331-1339. refs

Speckle appearing in SAR images is generated by coherent interference of radar echoes from target scatterers. In this paper the author's research in the area of statistical modeling and suppression of speckles in SAR images is reviewed. Comments are also made to recent papers of other researchers. Speckles are modeled with a multiplicative noise model and verified with Seasat SAR and SIR-B data. Using the statistical noise model, two multiplicative noise-smoothing algorithms are presented. These two algorithms are computationally efficient and have the potential of achieving real-time or near-real-time processing. Several SAR images are used for illustration. Author

A87-53260

**SPATIAL CONSIDERATIONS IN SPECKLE SIMULATION**

R. K. RANEY (Radarsat Project Office, Ottawa, Canada) and G. J. WESSELS (Intera Technologies, Ltd., Ottawa, Canada) IN: IGARSS '87 - International Geoscience and Remote Sensing Symposium, Ann Arbor, MI, May 18-21, 1987, Digest. Volume 2. New York, Institute of Electrical and Electronics Engineers, Inc., 1987, p. 1341-1347. refs

An approach to simulation of SAR image products is described that departs from most other simulation algorithms in the method of speckle generation. Speckle is prepared corresponding to the frequency weightings and look sum strategy of the radar processor combination desired, and then multiplied by the source scene data pre-conditioned by the desired resolution. The method allows output pixel spacings to be specified independent of more fundamental system parameters, and is accomplished efficiently. The approach is described, and typical results are presented. Author

A87-53262

**STATISTICAL MODELING OF INTENSITY DISTRIBUTIONS ON AIRBORNE SAR IMAGERY**

ERIC S. KASISCHKE, ANDREW L. MAFFETT, and RICHARD W. LARSON (Michigan, Environmental Research Institute, Ann Arbor) IN: IGARSS '87 - International Geoscience and Remote Sensing Symposium, Ann Arbor, MI, May 18-21, 1987, Digest. Volume 2. New York, Institute of Electrical and Electronics Engineers, Inc., 1987, p. 1357-1362. USAF-supported research. refs (Contract N00014-81-C-0692)

Three statistical models were evaluated to describe the distribution of image intensities from a multifrequency SAR system: the Gamma distribution, the inverse Gaussian distribution, and the log normal distribution. For  $N = 1-9$  (where  $N$  is the number of independent samples averaged to generate a pixel within the data set), it was found that all three distributions matched the observed SAR image intensity distribution. A linear correlation was found between the  $c$  parameter of the Gamma distribution and  $N$ . It was determined that this correlation could be used to estimate the scene texture. Author

A87-53273\* Jet Propulsion Lab., California Inst. of Tech., Pasadena.

**SPECKLE NOISE REDUCTION OF 1-LOOK SAR IMAGERY**

KRISHNA S. NATHAN and JOHN C. CURLANDER (California Institute of Technology, Jet Propulsion Laboratory, Pasadena) IN: IGARSS '87 - International Geoscience and Remote Sensing Symposium, Ann Arbor, MI, May 18-21, 1987, Digest. Volume 2. New York, Institute of Electrical and Electronics Engineers, Inc., 1987, p. 1457-1462. NASA-supported research. refs

Speckle noise is inherent to synthetic aperture radar (SAR) imagery. Since the degradation of the image due to this noise results in uncertainties in the interpretation of the scene and in a loss of apparent resolution, it is desirable to filter the image to reduce this noise. In this paper, an adaptive algorithm based on the calculation of the local statistics around a pixel is applied to 1-look SAR imagery. The filter adapts to the nonstationarity of the image statistics since the size of the blocks is very small compared to that of the image. The performance of the filter is measured in terms of the equivalent number of looks (ENL) of the filtered image and the resulting resolution degradation. The results are compared to those obtained from different techniques applied to similar data. The local adaptive filter (LAF) significantly increases the ENL of the final image. The associated loss of resolution is also lower than that for other commonly used speckle reduction techniques. Author

**A87-53274**

## **TEXTURAL SEGMENTATION OF SAR IMAGES USING FIRST ORDER STATISTICAL PARAMETERS**

H. LAUR, T. LE TOAN, and A. LOPES (Centre d'Etude Spatiale des Rayonnements, Toulouse, France) IN: IGARSS '87 - International Geoscience and Remote Sensing Symposium, Ann Arbor, MI, May 18-21, 1987, Digest. Volume 2. New York, Institute of Electrical and Electronics Engineers, Inc., 1987, p. 1463-1468. refs

A method of segmentation of SAR images is developed taking into consideration the two components of SAR image texture: intrinsic texture and fading texture. First-order statistical parameters are used as textural parameters; among these, the coefficient of variation is proved the most efficient. The segmentation method starts with a textural transformation by the coefficient of variation computed from a suitable window size. Then different operations are applied on the transformed image to improve the segmentation. Final results permit to separate large units of land cover (cropland, woodland, built-up areas) with a good accuracy. Author

**A87-53289**

## **A PATTERN ANALYSIS TECHNIQUE FOR DISTINGUISHING SURFACE AND CLOUD TYPES IN THE POLAR REGIONS**

ELIZABETH EBERT (Wisconsin, University, Madison) IN: IGARSS '87 - International Geoscience and Remote Sensing Symposium, Ann Arbor, MI, May 18-21, 1987, Digest. Volume 2. New York, Institute of Electrical and Electronics Engineers, Inc., 1987, p. 1611-1616. refs

An algorithm is presented which uses a pattern recognition method for the identification of regions of various surface and cloud types at high latitudes from visible, near-IR and IR Advanced Very High Resolution Radiometer satellite data. The algorithm has been able to classify 870 training samples with a skill score of 84 percent; 1800 artificial samples created by a Monte Carlo technique were classified with an accuracy of 92 percent, representing the theoretical limit of class separability using the given features. O.C.

**A87-53999\*** Science Applications Research, Lanham, Md.

## **A METHODOLOGY FOR EVALUATION OF AN INTERACTIVE MULTISPECTRAL IMAGE PROCESSING SYSTEM**

WILLIAM M. KOVALICK, JEFFREY A. NEWCOMER (Science Applications Research, Lanham, MD), and STEPHEN W. WHARTON (NASA, Goddard Space Flight Center, Greenbelt, MD) Photogrammetric Engineering and Remote Sensing (ISSN 0099-1112), vol. 53, Aug. 1987, p. 1087-1092. refs

Because of the considerable cost of an interactive multispectral image processing system, an evaluation of a prospective system should be performed to ascertain if it will be acceptable to the anticipated users. Evaluation of a developmental system indicated that the important system elements include documentation, user friendliness, image processing capabilities, and system services. The criteria and evaluation procedures for these elements are described herein. The following factors contributed to the success of the evaluation of the developmental system: (1) careful review of documentation prior to program development, (2) construction and testing of macromodules representing typical processing scenarios, (3) availability of other image processing systems for referral and verification, and (4) use of testing personnel with an applications perspective and experience with other systems. This evaluation was done in addition to and independently of program testing by the software developers of the system. Author

**N87-26569\*** ST Systems Corp., Hampton, Va.

## **DATA ANALYSIS AND SOFTWARE SUPPORT FOR THE EARTH RADIATION BUDGET EXPERIMENT**

W. EDMONDS and S. NATARAJAN Aug. 1987 91 p (Contract NAS1-17851)

(NASA-CR-178350; NAS 1.26:178350) Avail: NTIS HC A05/MF A01 CSCL 09B

Computer programming and data analysis efforts were performed in support of the Earth Radiation Budget Experiment (ERBE) at NASA/Langley. A brief description of the ERBE followed

by sections describing software development and data analysis for both prelaunch and postlaunch instrument data are presented. Author

**N87-26697\*** Hawaii Univ., Hilo. Dept. of Geography.

## **DIGITAL DATA FROM SHUTTLE PHOTOGRAPHY: THE EFFECTS OF PLATFORM VARIABLES**

BRUCE E. DAVIS IN NASA. Lyndon B. Johnson Space Center, National Aeronautics and Space Administration (NASA)/American Society for Engineering Education (ASEE) Summer Faculty Fellowship Program, 1986, Volume 1 38 p Jun. 1987

Avail: NTIS HC A16/MF A01 CSCL 05A

Two major criticisms of using Shuttle hand held photography as an Earth science sensor are that it is nondigital, nonquantitative and that it has inconsistent platform characteristics, e.g., variable look angles, especially as compared to remote sensing satellites such as LANDSAT and SPOT. However, these criticisms are assumptions and have not been systematically investigated. The spectral effects of off-nadir views of hand held photography from the Shuttle and their role in interpretation of lava flow morphology on the island of Hawaii are studied. Digitization of photography at JSC and use of LIPS image analysis software in obtaining data is discussed. Preliminary interpretative results of one flow are given. Most of the time was spent in developing procedures and overcoming equipment problems. Preliminary data are satisfactory for detailed analysis. Author

**N87-27352#** National Geophysical Data Center, Boulder, Colo.

## **SOLID EARTH GEOPHYSICS: DATA SERVICES**

Jan. 1987 23 p

(PB87-184107; KGRD-22) Avail: NTIS HC A02/MF A01 CSCL 08G

The National Oceanic and Atmospheric Administration (NOAA) collects, manages, and disseminates many kinds of scientific data that result from the inquiry into the environment. The National Geophysical Data Center (NGDC), one of the several data-management centers of NOAA, is responsible for data activities in the fields of seismology, gravity, topography, geomagnetism, geothermics, marine geology and geophysics, and solar-terrestrial physics. The pamphlet briefly describes the principal products and services NGDC provides through its Solid Earth (SEG) division. Among the most important activities of SEG are acquiring and archiving data, processing and formatting data into standard sets, developing useful data products for customers, and advertising and disseminating data to the scientific, academic, and industrial communities. GRA

**N87-27859#** Norwegian Defence Research Establishment, Kjeller.

## **SAR DETECTION OF SHIPS AND SHIP WAKES**

T. WAHL, K. ELDHUSET, and K. AKSNES IN ESA Proceedings of the SAR Applications Workshop p 61-65 Dec. 1986

Avail: NTIS HC A06/MF A01

Over 200 SAR images of ship wakes were analyzed. Digital techniques for wake detection and analysis are described. Detection of ships and ship wakes from orbiting SAR seems feasible under a wide range of environmental conditions. The state of wake modeling is not sufficient to utilize all the ship information hidden in the wake, although speed and direction of motion can be determined quite straightforwardly. ESA

**N87-27860#** Marconi Co. Ltd., Chelmsford (England).

## **THIN LINE DETECTION IN SAR IMAGES Abstract Only**

J. SKINGLEY and S. QUEGAN IN ESA Proceedings of the SAR Applications Workshop p 67-68 Dec. 1986 Sponsored by the RAE, Farnborough, England, and the Royal Signals and Radar Establishment

Avail: NTIS HC A06/MF A01

The use of local operators (masks), global transforms, and dynamic programming to detect thin lines in SAR images is summarized. Relevance to ship wake detection, SAR data simulation (from the investigation of the nature of thin lines in

SAR imagery), and land use feature extraction from SAR images is mentioned. ESA

**N87-27861#** Lund Univ. (Sweden).

**GEOLOGICAL FEATURE ENHANCEMENT IN SAR IMAGERY**

P. ULRIKSEN and C. SVENSSON /in ESA Proceedings of the SAR Applications Workshop p 69-79 Dec. 1986 (Contract ESA-6692/86-F-FL(SC))

Avail: NTIS HC A06/MF A01

Image enhancement techniques, geological screening of SAR imagery to find test sites, and results from test runs on an image analysis system built to analyze texture are summarized. Work needed on speckle smoothing, shape from shading, human visual response, edge detection, sharpness of magnified images, and computerized classification is discussed. ESA

**N87-27863#** Hunting Geology and Geophysics Ltd., Boreham Wood (England).

**LAND USE FEATURE DETECTION IN SAR IMAGES**

G. C. DEANE, S. QUEGAN, P. N. CHURCHILL, A. HENDRY (Marconi Co. Ltd., Chelmsford, England), R. EVANS, and J. W. TREVETT /in ESA Proceedings of the SAR Applications Workshop p 95-102 Dec. 1986

Avail: NTIS HC A06/MF A01

Segmentation, speckle reduction, and feature detection techniques for automatic interpretation of SAR images are discussed. A quantitative approach for assessing their performance is described. A method for comparing algorithms using filtering followed by edge-detection followed by bonding was developed. Using this method to optimize an algorithm based on the Frost filter suggests that the Frost filter is better replaced by the mean filter. Work on feature detection using correlation led to a method for comparing correlations. It is shown that the mean-square correlator is of no use in the presence of Rayleigh speckle. ESA

**N87-27864#** Ball (Roy) Associates Ltd., Ottawa (Ontario).

**AN ALGORITHM FOR AUTOMATICALLY ACQUIRING GROUND CONTROL POINTS IN SAR IMAGERY**

J. WEILER, M. BRULE, K. LIM, R. BALL, and T. TURNER (Gregory Geoscience Ltd., Ottawa, Ontario) /in ESA Proceedings of the SAR Applications Workshop p 103-110 Dec. 1986

Avail: NTIS HC A06/MF A01

Research into fully automated techniques for acquiring ground control points (GCPs) in SAR imagery is presented. An algorithm whose performance in acquiring GCPs in test imagery is comparable to that of a human operator is described. ESA

**N87-28124#** Technical Univ. of Denmark, Lyngby. Inst. of Electromagnetics.

**CLOUD DETECTION IN NOAA IMAGES**

JOHN SKELMOSE JENSEN /in ESA Proceedings of the ESA/EARSel Europe from Space Symposium p 53-57 Dec. 1986 Sponsored by the Commission for Scientific Research in Greenland, and the Danish Space Research Committee

Avail: NTIS HC A14/MF A01

A technique for cloud detection in NOAA satellite images is described. It operates with only one infrared channel (Ch 4) of NOAA AVHRR data and it is composed of two parts: a segmentation of the image into uniform areas and a classification of these uniform areas into water, ice, and clouds. The technique was evaluated over a test area of the East Greenland coast, and the detection of clouds over water gives good results. But the technique fails to distinguish between ice and clouds. ESA

**N87-28142#** Kingston Polytechnic, Kingston-Upon-Thames (England). School of Computing.

**TOWARDS THE AUTOMATIC RECOGNITION AND VECTORISED DESCRIPTION OF LINEAR FEATURES IN LANDSAT TM IMAGES BY ARTIFICIAL INTELLIGENCE METHODS**

G. PEACEGOOD, G. G. WILKINSON, and P. F. FISHER /in ESA Proceedings of the ESA/EARSel Europe from Space Symposium p 195-198 Dec. 1986

Avail: NTIS HC A14/MF A01

A method for extracting linear features in LANDSAT Thematic Mapper images, representing them, and improving the quality of the results is given. Low-level feature extraction involves: image convolution with 5 X 5 neighborhood masks in 6 directions; thresholding and thinning of the gradient image derived from each maximum value associated with a given direction; formation of arrays containing information about the location and direction of neighbors to edge points, limiting the maximum number to 4 (2 in front of, and 2 behind the edge point, where the terms in front of and behind are defined by the direction of the edge point); linking of neighboring edge points in 3 passes: starting from end points; starting from junctions; and tracing closed shapes; bridging of segments separated by only 1 pixel; and vectorization of segments by fitting polylines to them, using an iterative end-point fit method. ESA

**N87-28143#** Technische Univ., Graz (Austria). Inst. for Image Processing and Computer Graphics.

**INTEGRATED SYSTEMS FOR REMOTE SENSING**

M. F. BUCHROITHNER /in ESA Proceedings of the ESA/EARSel Europe from Space Symposium p 199-203 Dec. 1986

Avail: NTIS HC A14/MF A01

Modular software systems for evaluation of remote sensing data are described. The importance of synergism for the applied systems is pointed out and examples of practical use are given. ESA

**N87-28144#** Technical Univ. of Denmark, Lyngby.

**COMPARISON OF VISUAL AND AUTOMATED LINEAMENT ANALYSES ON LANDSAT MSS IMAGE FROM SOUTH GREENLAND**

KNUT CONRADSEN, BJARNE K. MIELSEN, JOHN L. PETERSEN, and TAGE THYRSTED /in ESA Proceedings of the ESA/EARSel Europe from Space Symposium p 205-211 Dec. 1986 (Contract EXU-041-DK(G); MSM-114-DK(AD))

Avail: NTIS HC A14/MF A01

A procedure for automated identification of linear features in digital imagery is described. It consists of a filtering of the image followed by a local direction estimation for each pixel. Based on these, density maps of the occurrence of linear features can be estimated for given directions. The density maps from the two procedures are compared, and the overall agreement is very high. ESA

**N87-28165#** Instituto de Pesquisas Espaciais, Sao Jose dos Campos (Brazil).

**ENHANCEMENT OF COLORS IN REMOTE SENSING IMAGES USING ROTATION OF THE MATRIX AT THE IHS COORDINATES [REALCE DE CORES EM IMAGENS DE SENSORIAMENTO REMOTO UTILIZANDO ROTACAO DE MATIZ NO ESPACO IHS]**

LUCIANO VIEIRADUTRA and PAULO ROBERTO MENESES Jul. 1987 15 p In PORTUGUESE; ENGLISH summary Presented at the 5th Brazilian Symposium of Telecommunication, Campinas, Brazil, 8-10 Sep. 1987

(INPE-4207-PRE/1088) Avail: NTIS HC A02/MF A01

The multispectral color composite imagery, obtained by digital processing and displayed on video monitors through the combination of the fundamental colors red, green, and blue, consists in an efficient form of presentation. The visual or psychophysiologic perception of the brain to the stimulus of particular colors, tends to combine independently the quantitative components of the fundamental colors, the intensity (I), hue (H)

and saturation (S), and so it is possible to perceive each one of these attributes of color, separately. A method is presented to increase the contrast of the colors, using a transformation to the IHS coordinates which permits individual manipulation in each of these components, in order to obtain a better control about the color composite generated in the video display. The basic procedure is a manipulation of the histograms of the components, I, H, and S, in order to increase, decrease, or offset the range of possible values of the components, by linear transformations. Test of this procedure using LANDSAT-TM scene of a region covered by geological research showed the different component manipulations resulted in different enhancements of lithologic units, formerly not distinguished in the original color composition, which allowed an easier photogeologic interpretation. Author

**N87-28197\*** # Florida State Univ., Tallahassee. Dept. of Meteorology.

**INVESTIGATING THE ROLE OF THE LAND SURFACE IN EXPLAINING THE INTERANNUAL VARIATION OF THE NET RADIATION BALANCE OVER THE WESTERN SAHARA AND SUB-SAHARA** Semiannual Report, 1 Oct. 1986 - 31 May 1987  
ERIC A. SMITH and SHARON NICHOLSON Jul. 1987 19 p  
(Contract NAG5-849)  
(NASA-CR-181183; NAS 1.26:181183) Avail: NTIS HC A02/MF A01 CSDL 04A

The status of the data sets is discussed. Progress was made in both data analysis and modeling areas. The atmospheric and land surface contributions to the net radiation budget over the Sahara-Sahel region is being decoupled. The interannual variability of these two processes was investigated and this variability related to seasonal rainfall fluctuations. A modified Barnes objective analysis scheme was developed which uses an elliptic scan pattern and a 3-pass iteration of the difference fields.

**N87-28374#** Instituto de Pesquisas Espaciais, Sao Jose dos Campos (Brazil). Ministerio da Ciencia e Tecnologia.

**BRIEF INTRODUCTION IN STATISTICAL PATTERN RECOGNITION [BREVE INTRODUCAO AO RECONHECIMENTO ESTATISTICO DE PADROES]**

NELSON DELFINODAVILAMASCARENHAS Jul. 1987 14 p  
In PORTUGUESE; ENGLISH summary Presented at the 39th Annual Conference of SBPC, Symposium on Artificial Intelligence, Brasilia, Jul. 1987  
(INPE-4206-PRE/1087) Avail: NTIS HC A02/MF A01

A brief description of the main techniques of statistical pattern recognition is presented. The discussed topics comprise: feature extraction, statistical classification, learning methods, and clustering. The main problems tackled presently in the area of natural resources detection are also presented. Author

**N87-29575#** Joint Publications Research Service, Arlington, Va.  
**ANALYSIS OF DIRECTIONS OF LINEAR IMAGE ELEMENTS BY STRUCTURE-ZONAL METHOD** Abstract Only

V. A. KOTTSOV In its JPRS Report: Science and Technology. USSR: Space p 118 19 Aug. 1987 Transl. into ENGLISH from Issledovaniye Zemli iz Kosmosa (Moscow, USSR), no. 6, Nov. - Dec. 1986 p 97-100  
Avail: NTIS HC A08/MF A01

The method of structure-zone transformation of video information is one possible means of increasing the effectiveness of studying the Earth from space. The essence of the method is analysis of the characteristics of the spatial structure of an object onboard the spacecraft, with formation of images which code changes in structural characteristics over the field of vision. Here, the specifics of one particular case, structural analysis of the directions of linear elements, as in analysis of the directions of a wide wave action on water surfaces, are studied. Author

**N87-29722#** Environmental Research Inst. of Michigan, Ann Arbor.

**CALIBRATED L-BAND TERRAIN MEASUREMENTS AND ANALYSIS PROGRAM** Final Report, Apr. 1984 - Jan. 1987

R. W. LARSON, E. S. KASISCHKE, and A. L. MAFFETT 1 Mar. 1987 106 p  
(Contract F19628-84-C-0081)  
(AD-A182917; ERIM-174200-16-F) Avail: NTIS HC A06/MF A01 CSDL 171

This report discusses the final year's activities of a program to generate and analyze L-band clutter data. The L-band radar data used throughout this study were derived from airborne synthetic aperture radar imagery. Radar cross section measurements from a variety of distributed targets are presented, including sea surface, sea ice, agricultural fields and forests. Both HH and VV polarized data are presented. Models are presented which describe the intensity distribution of the SAR data as well as describe L-band scattering from rough surfaces. The density distribution models describe the observed SAR intensity distributions quite well, whereas the radar scattering models in some cases overpredict the SAR-observed values. Author (GRA)

**N87-29905#** Woods Hole Oceanographic Institution, Mass.

**SATELLITE IMAGE PROCESSING FOR THE AGULHAS RETROFLEXION REGION**

KELLY LUETKEMEYER Jul. 1987 83 p  
(Contract N00014-82-C-0019; N00014-87-K-0007)  
(AD-A183012; WHOI-87-27) Avail: NTIS HC A05/MF A01 CSDL 08C

In order to analyze the Advanced Very High Resolution Radiometer satellite data from South Africa, a software package has been written. Methodology and algorithms are described which create geometrically corrected registered satellite images over the Agulhas Retroflexion region. Also discussed are programs to overlay latitude and longitude lines, ship tracks, and ancillary data. A method of masking the land and compositing images for cloud removal is also described. GRA

## 08

### INSTRUMENTATION AND SENSORS

Includes data acquisition and camera systems and remote sensors.

**A87-41435**

**THE APPLICATION OF REMOTE SENSING TECHNIQUES IN CHINA**

SHI-REN YANG (Chinese Academy of Sciences, Institute of Remote Sensing Application, Beijing, People's Republic of International Journal of Remote Sensing (ISSN 0143-1161), vol. 8, April 1987, p. 651-658.

The current status of the application of remote sensing techniques in China is described. The Chinese Landsat ground station was recently put into operation, and more than thirty low and medium altitude aircraft for remote sensing applications are now operational. Digital image processing systems are now widely used in remote sensing applications, while new instruments and sensors have been developed and are now in use. Applications of remote sensing in China for land resource surveys, urban pollution detection and environmental monitoring, agriculture, forestry, hydrology, geology, coal mining, uranium exploration, glaciology and cryopedology are discussed. Author



**A87-43262\*** National Aeronautics and Space Administration. Goddard Space Flight Center, Greenbelt, Md.

**MULTIPLE-ANGLE OBSERVATIONS OF REFLECTANCE ANISOTROPY FROM AN AIRBORNE LINEAR ARRAY SENSOR**  
JAMES R. IRONS, BERTRAND L. JOHNSON, JR. (NASA, Goddard Space Flight Center, Greenbelt, MD), and GREGORY H. LINEBAUGH (Science Applications Research, Lanham, MD) IEEE Transactions on Geoscience and Remote Sensing (ISSN 0196-2892), vol. GE-25, May 1987, p. 372-383. NASA-supported research. refs

An airborne pointable imaging multispectral linear array sensor has been developed for the multidirectional observation of surface reflectance anisotropy. The sensor design permits observations up to 45 deg off-nadir in three spectral bands (green, red, and near-infrared). Calibration permits the conversion of sensor data to radiance units with an absolute uncertainty of 6 percent. Observations of five field plots from seven view directions are discussed. Calibration and atmospheric corrections are used to derive hemispherical-directional reflectance factors. A three-term reflectance model is fit to the reflectance factors for each plot to represent the continuous distribution of reflectance factors with view direction. The reflectance model is integrated over all view directions to calculate bihemispherical reflectance factors. The calculated bihemispherical factors differed by 1 to 25 percent from values based on an assumption of isotropic reflectance depending on spectral band and field plot. These calculations demonstrate the technologic and scientific capabilities required for the remote characterization of surface reflectance anisotropy. Remote multidirectional observations are both feasible and needed to fully evaluate land reflectance characteristics. Author

**A87-43302**

**HYBRID POWER AMPLIFIER MODULE FOR X-BAND**

DEVENDAR S. BAINS and HAROLD BALSHEM (Microwave Semiconductor Corp., Somerset, NJ) Microwave Journal (ISSN 0026-2897), vol. 30, May 1987, p. 273, 274, 276 (4 ff.).

The design and development of a compact (30 x 15 x 5 mm size) hybrid amplifier module for X-band applications are discussed. The design steps to obtain the desired performance, the device modeling and stability, the circuit designs, and the performance of the module are examined. It is demonstrated that the radar amplifier module built in hybrid form can achieve 3 W power at 30 dB gain with a 1 dB bandwidth of 10 percent. The hybrid design can be converted to the monolithic form to obtain a monolithic power amplifier. I.S.

**A87-44184\*** National Aeronautics and Space Administration. Goddard Space Flight Center, Greenbelt, Md.

**EARTH RESOURCES INSTRUMENTATION FOR THE SPACE STATION POLAR PLATFORM**

MARTIN J. DONOHOE (NASA, Goddard Space Flight Center, Greenbelt, MD) and DEBORAH VANE (California Institute of Technology, Jet Propulsion Laboratory, Pasadena) IN: Remote sensing; Proceedings of the Meeting, Orlando, FL, Apr. 3, 4, 1986. Bellingham, WA, Society of Photo-Optical Instrumentation Engineers, 1986, p. 76-81. NOAA-sponsored research. refs

The spacecraft and payloads of the Space Station Polar Platform program are described in a brief overview. Present plans call for one platform in a descending morning-equator-crossing orbit at 824 km and two or three platforms in ascending afternoon-crossing orbits at 542-824 km. The components of the NASA Earth Observing System (EOS) and NOAA payloads are listed in tables and briefly characterized, and data-distribution requirements and the mission development schedule are discussed. A drawing of the platform, a graph showing the spectral coverage of the EOS instruments, and a glossary of acronyms are provided. T.K.

**A87-44863\*** Arizona Univ., Tucson.

**REFLECTANCE- AND RADIANCE-BASED METHODS FOR THE IN-FLIGHT ABSOLUTE CALIBRATION OF MULTISPECTRAL SENSORS**

P. N. SLATER, S. F. BIGGAR, R. G. HOLM, R. D. JACKSON, Y. MAO (Arizona, University, Tucson; USDA, Water Conservation Laboratory, Phoenix) et al. Remote Sensing of Environment (ISSN 0034-4257), vol. 22, June 1987, p. 11-37. refs (Contract NAS5-27382)

Variations reported in the in-flight absolute radiometric calibration of the Coastal Zone Color Scanner (CZCS) and the Thematic Mapper (TM) on Landsat 4 are reviewed. At short wavelengths these sensors exhibited a gradual reduction in response, while in the midinfrared the TM showed oscillatory variations, according to the results of TM internal calibration. The methodology and results are presented for five reflectance-based calibrations of the Landsat 5 TM at White Sands, NM, in the period July 1984 to November 1985. These show a + or - 2.8 percent standard deviation for the six solar-reflective bands. Analysis and preliminary results of a second, independent calibration method, based on radiance measurements from a helicopter at White Sands, indicate that this is potentially an accurate method for corroborating the results from the reflectance-based method. Author

**A87-44865\*** California Univ., La Jolla.

**CALIBRATION OF NOAA-7 AVHRR, GOES-5, AND GOES-6 VISSR/VAS SOLAR CHANNELS**

ROBERT FROUIN and CATHERINE GAUTIER (California, University, La Jolla) Remote Sensing of Environment (ISSN 0034-4257), vol. 22, June 1987, p. 73-101. Research supported by the University of California. Previously announced in STAR as N87-16062. refs (Contract NAGW-697)

The NOAA-7, GOES-5 and GOES-6 Visible Infrared Spin Scan Radiometer/Vertical Atmospheric Sounder (VISSR/VAS) solar channels were calibrated. The White Sands Monument area in New Mexico, whose reflectance properties are well known, and space are used as calibration targets. The shortwave reflected terrestrial irradiance that is measured at satellite altitude is computed using a fairly accurate radiative transfer model which accounts for multiple scattering and bidirectional effects. The ground target reflectance and relevant characteristics of the overlying atmosphere are estimated from climatological data and observation at the nearest meteorological sites. The approach is believed to produce accuracies of 8 to 13 percent depending on the channel considered. Author

**A87-44868\*** National Aeronautics and Space Administration. Goddard Space Flight Center, Greenbelt, Md.

**PRACTICAL ASPECTS OF ACHIEVING ACCURATE RADIOMETRIC FIELD MEASUREMENTS**

B. GUENTHER (NASA, Goddard Space Flight Center, Greenbelt, MD) Remote Sensing of Environment (ISSN 0034-4257), vol. 22, June 1987, p. 131-143. refs

This paper provides practical advice for investigators new to the field of high accuracy radiometric experiments. Sources typically used for calibrating land reflectance measurement instruments are identified, and some special considerations for their use are highlighted. The physical nature of the processes determining the output of these sources is emphasized, and an estimate of the typical calibration accuracies achieved with these sources is described. Several techniques for the validation and verification of instrument characterization are reviewed. Experiment design of the Backscattered Ultraviolet Spectrometer (BUV) and the Earth Radiation Budget Experiment (ERBE) are introduced as successful mission designs for accomplishing high accuracy radiation measurements from space. The goal of this paper is to introduce reasoning developed in other missions to experiments devoted to sensing the earth's surface and near surface. Author

**A87-45044**

## **AVERAGING OF RADAR ALTIMETER PULSE RETURNS WITH THE INTERPOLATION TRACKER**

LARS M. H. ULANDER (Chalmers Tekniska Hogskola, Goteborg, Sweden) International Journal of Remote Sensing (ISSN 0143-1161), vol. 8, May 1987, p. 705-721. Research supported by the Swedish Board for Space Activities. refs

Radar altimeters have tracking systems which measure the range to the surface and produce averages of the radar pulse returns. Besides the range measurement, additional geophysical information can be extracted from the average pulse return. This paper describes and analyses a novel tracking and averaging algorithm, the interpolation tracker. It produces undistorted estimates of the mean pulse return in the presence of frequent gaps in the data stream. The theoretical analysis is confirmed by calculated first-order statistics from experimental data. Author

**A87-47173**

## **REMOTE SENSING APPLICATIONS OF THE EARTH'S SURFACE - AN OUTLOOK INTO THE FUTURE**

HERMAN TH. VERSTAPPEN (International Institute for Aerospace Survey and Earth Sciences, Enschede, Netherlands) Photogrammetria (ISSN 0031-8663), vol. 41, April 1987, p. 59-71.

Developments in remote sensing are examined by comparing the equipment of 1962 with that presently utilized for remote sensing. The future roles of high-resolution satellites, low-resolution satellites, and various types of aircraft in resource surveying are assessed. Consideration is given to recording systems in the photographic, thermographic, and microwave bands. The interpretation of the images, and the importance of optimal organization and utilization of the data collected by geographic information systems are discussed. I.F.

**A87-47174**

## **PHOTOGRAMMETRY - THE LARGEST OPERATIONAL APPLICATION OF REMOTE SENSING**

GUY DUCHER (Institut Geographique National, Saint-Mande, France) Photogrammetria (ISSN 0031-8663), vol. 41, April 1987, p. 72-82. refs

The development of remote sensing from aircraft and spacecraft is in full swing in many places and can be expected to lead to many operational applications. By way of comparison, this article highlights the numerous applications of photogrammetry currently in operation in almost every country in the world. A glimpse of future methodology based on space and digital data processing is also provided. Author

**A87-47175**

## **SOME RESULTS OF THE METRIC CAMERA (MC) MISSION-1 ON SPACELAB**

G. TOGLIATTI (Milano, Politecnico, Milan, Italy) Photogrammetria (ISSN 0031-8663), vol. 41, April 1987, p. 83-93. refs

The data provided by the Metric Camera (MC) Experiment flown on the Spacelab mission of November 28-December 8, 1983 are discussed. The experiment was to test the mapping capability of high-resolution space photography. The Spacelab orbited every 90 minutes at an altitude of 250 km, and an area of 11 million sq km was photographed. The results from workshops concerned with mapping and thematic applications of the MC images are described. It is noted that, despite the limitations of the MC images, they have been favorably accepted by the user community. I.F.

**A87-47257\***

Jet Propulsion Lab., California Inst. of Tech., Pasadena.

## **MULTIFREQUENCY AND MULTIPOLARIZATION RADAR SCATTEROMETRY OF SAND DUNES AND COMPARISON WITH SPACEBORNE AND AIRBORNE RADAR IMAGES**

RONALD BLOM and CHARLES ELACHI (California Institute of Technology, Jet Propulsion Laboratory, Pasadena) Journal of Geophysical Research (ISSN 0148-0227), vol. 92, July 10, 1987, p. 7877-7889. NASA-sponsored research. refs

Airborne radar scatterometer data on sand dunes, acquired at multiple frequencies and polarizations, are reported. Radar

backscatter from sand dunes is very sensitive to the imaging geometry. At small incidence angles the radar return is mainly due to quasi-specular reflection from dune slopes favorably oriented toward the radar. A peak return usually occurs at the incidence angle equal to the angle of repose for the dunes. The peak angle is the same at all frequencies as computed from specular reflection theory. At larger angles the return is significantly weaker. The scatterometer measurements verified observations made with airborne and spaceborne radar images acquired over a number of dune fields in the U.S., central Africa, and the Arabian peninsula. The imaging geometry constraints indicate that possible dunes on other planets, such as Venus, will probably not be detected in radar images unless the incidence angle is less than the angles of repose of such dunes and the radar look direction is approximately orthogonal to the dune trends. Author

**A87-48189**

## **FEATURES OF A STATISTICAL MODEL FOR THE INTERACTION BETWEEN ELECTROMAGNETIC WAVES AND REMOTELY SENSED NATURAL OBJECTS [OSOBENOSTI STATISTICHESKOI MODELI PROTSSESA VZAIMODEISTVIA ELEKTROMAGNITNYKH VOLN S ZONDIRUEMYMI PRIRODNYMI OB'EKTAMI]**

V. V. EGOROV (AN SSSR, Institut Kosmicheskikh Issledovani, Moscow, USSR) Issledovanie Zemli iz Kosmosa (ISSN 0205-9614), Mar.-Apr. 1987, p. 90-95. In Russian. refs

An empirical model is proposed for the channel of electromagnetic wave propagation from the radiation source to the sensor with allowance for absorption and scattering in the remotely sensed objects. An impulse transfer function for the channel is derived which is shown to be similar to the bidirectional reflectance function and to be related to the spectral radiance of the sensed object. It is noted that the results obtained are of interest in connection with environmental monitoring and geological studies. B.J.

**A87-48652**

## **EARTH REMOTE SENSING USING THE LANDSAT THEMATIC MAPPER AND SPOT SENSOR SYSTEMS; PROCEEDINGS OF THE MEETING, INNSBRUCK, AUSTRIA, APR. 15-17, 1986**

PHILIP N. SLATER, ED. (Arizona, University, Tucson) Meeting organized by SPIE and Association Nationale de la Recherche Technique. Bellingham, WA, Society of Photo-Optical Instrumentation Engineers (SPIE Proceedings, Volume 660), 1986, 183 p. For individual items see A87-48653 to A87-48676. (SPIE-660)

Papers are presented on absolute radiometric calibration of the Landsat TM; scene-to-scene radiometric normalization for the reflected bands of the Landsat TM; EAS-Earthnet experience in high resolution sensor performance; and TM sensor performance derived from the Earthnet quality control data base. Topics discussed include absolute calibration of the SPOT-1 HRV cameras; SPOT localization accuracy and geometric image quality; improving SPOT images size and multispectral resolution; photogrammetry from SPOT with an analytical plotter; and lithologic discrimination using geobotanical and Landsat TM spectral data. Consideration is given to automatic generation of digital terrain models from satellite images by stereo; shallow water bathymetry and bottom classification by means of Landsat and SPOT optical scanners; the use of color vision principles in the processing of remote sensing imagery; and the use of the modular optoelectronic multispectral scanner for earth observations. I.F.

A87-48654

**SCENE TO SCENE RADIOMETRIC NORMALIZATION OF THE REFLECTED BANDS OF THE LANDSAT THEMATIC MAPPER**

WILLIAM J. VOLCHOK and JOHN R. SCHOTT (Rochester Institute of Technology, NY) IN: Earth remote sensing using the Landsat Thematic Mapper and SPOT sensor systems; Proceedings of the Meeting, Innsbruck, Austria, Apr. 15-17, 1986. Bellingham, WA, Society of Photo-Optical Instrumentation Engineers, 1986, p. 9-17. refs

A technique for radiometric normalization of images of the same area acquired on different dates is discussed. The technique accounts for illumination and atmospheric variations between the scenes. Statistical analysis of segmented scene elements is used to generate band-by-band transformation functions. Examples are presented where Thematic Mapper subscenes (512 x 512 pixels) from 1982 and 1984 are normalized for each reflective band. Analysis of the transformed images indicates that the residual radiometric error after the transform is of the order of one reflectance value. Examples of the utility of the technique for change detection, environmental assessment, and as a general preprocessing technique for scene classification and analysis are discussed.

Author

A87-48659

**TM SENSOR PERFORMANCE AS OBTAINED FROM EARTHNET QUALITY CONTROL DATA BASE**

G. MARK DOHERTY and E. ORIOL-PIBERNAT (ESA, Earthnet Programme Office, Frascati, Italy) IN: Earth remote sensing using the Landsat Thematic Mapper and SPOT sensor systems; Proceedings of the Meeting, Innsbruck, Austria, Apr. 15-17, 1986. Bellingham, WA, Society of Photo-Optical Instrumentation Engineers, 1986, p. 54-63. refs

An operational quality-control system has been implemented at the European Space Agency Landsat stations, Earthnet Programme Office. This automatically checks the characteristics of every single TM product before distribution to users. A record of the results of quality control is kept in order to trace back any problem identified and define statistically the performance of the sensors. Examples of the behavior of some of these parameters are presented, and the benefits of such an approach are discussed.

Author

A87-48660

**ABSOLUTE CALIBRATION OF THE SPOT-1 HRV CAMERAS**

G. BEGNI (CNES, Toulouse, France), M. C. DINGUIRARD (ONERA, Centre d'Etudes et de Recherches de Toulouse, France), R. D. JACKSON (USDA, Water Conservation Laboratory, Phoenix, AZ), and P. N. SLATER (Arizona, University, Tucson) IN: Earth remote sensing using the Landsat Thematic Mapper and SPOT sensor systems; Proceedings of the Meeting, Innsbruck, Austria, Apr. 15-17, 1986. Bellingham, WA, Society of Photo-Optical Instrumentation Engineers, 1986, p. 66-76. refs (Contract CNES-5022)

The preflight and onboard in-flight absolute radiometric calibrations of the two HRV cameras on SPOT-1 are briefly described. The results of the in-flight calibrations at White Sands, New Mexico are presented in detail and compared to the other methods. The ratio of calibration coefficients for the two SPOT-1 HRVs was obtained from a histogram match of a scene imaged simultaneously by the two cameras. This was compared to the ratio of the calibration coefficients from the White Sands results. The ratios are in good agreement, less than or equal to 3 percent in three bands; the exception is multispectral band 2, which shows a 7-percent difference. The histogram result and a comparison with spectral radiances measured from an altitude of 3000 m indicate that, at the time and under the conditions of the calibrations, the specification for a + or - 10-percent rms absolute calibration uncertainty for the SPOT-1 HRVs had been met. The White Sands and histogram ratio results were used to update the calibration of the onboard sun-calibrator system for the HRVs.

Author

A87-48674\*

Ludwig-Maximilians-Universitaet, Munich (West Germany).

**COMPARATIVE ANALYSIS OF DIFFERENT SENSOR DATA (LANDSAT-TM AND MOMS) FOR EARTH OBSERVATION AND IMPACT ON FUTURE SENSOR DEVELOPMENT**

J. BODECHTEL, J. ZILGER (Muenchen, Universitaet, Munich, West Germany), and V. V. SALOMONSON (NASA, Goddard Space Flight Center, Greenbelt, MD) IN: Earth remote sensing using the Landsat Thematic Mapper and SPOT sensor systems; Proceedings of the Meeting, Innsbruck, Austria, Apr. 15-17, 1986. Bellingham, WA, Society of Photo-Optical Instrumentation Engineers, 1986, p. 152-158. refs

The missions of the German Modular Optoelectronic Multispectral Scanner (MOMS) aboard two STS flights demonstrated the feasibility of a novel concept with regard to both technical and scientific objectives. On account of the successful missions, a cooperation was agreed between the German Federal Minister for Research and Technology and NASA for comparing MOMS observations with the more familiar operational Landsat-TM data over selected test sites, as a means of obtaining some relative measure of performance. This paper summarizes the results obtained and presents the MOMS-02, a further experimental representative of the MOMS program aiming at the realization of an operational system for the mid-nineties.

Author

A87-48675

**DIFFERENT SCANNING INSTRUMENTS COMPARISON - MOMS AND TM**

L. FUSCO and A. HSU (ESA, Earthnet Programme Office, Frascati, Italy) IN: Earth remote sensing using the Landsat Thematic Mapper and SPOT sensor systems; Proceedings of the Meeting, Innsbruck, Austria, Apr. 15-17, 1986. Bellingham, WA, Society of Photo-Optical Instrumentation Engineers, 1986, p. 159-168. refs

The Modular Optoelectronic Multispectral Scanner (MOMS), a CCD-type sensor, was flown on two Shuttle missions, STS-7 and STS-11, for experimental purpose. Two MOMS scenes from STS-11 mission were given to the Earthnet Program Office, European Space Agency for image quality analysis; however, the TM data from Landsat 5, which represent state-of-the-art remote-sensing technology, are the only available auxiliary data. Based on some primitive analyses using the TM data as reference, it is concluded that: (1) the registration accuracy between the two MOMS spectral bands is good; however, the algorithm for the radiometric calibration of MOMS detectors must be improved to remove the striping pattern caused by the inappropriate adjustment of radiometric values; and (2) the projected ground pixel size of 20 x 20 m was degraded by some unknown factors, and the actual resolution of the MOMS data is much larger than the projected 20 m ground size. For the time being, the geoscientific applications of the MOMS data are rather limited.

Author

A87-48676

**THE LAND SATELLITE (LANDSAT) SYSTEM - EARTH OBSERVATION SATELLITE COMPANY (EOSAT'S) PLANS FOR LANDSAT-6 AND BEYOND**

JACK ENGEL (Santa Barbara Research Center, Goleta, CA) IN: Earth remote sensing using the Landsat Thematic Mapper and SPOT sensor systems; Proceedings of the Meeting, Innsbruck, Austria, Apr. 15-17, 1986. Bellingham, WA, Society of Photo-Optical Instrumentation Engineers, 1986, p. 169-174.

This paper describes Eosat plans for operating the Landsat system in the Landsat-6,7 era (1985 to 1995). The paper provides background information relative to Eosat and an overview of the planned configurations of both the space segment (spacecraft and Enhanced Thematic Mapper), and the ground segment (Spacecraft Operations Center, Data Capture Site, and Eosat Processing Center) for Landsats 6 and 7. The planned enhancements to the Landsat-6/7 TMs are described in some detail, including the implementation of a panchromatic band of detectors providing 15-m spatial resolution on both ETM sensors and the possible inclusion on the Landsat-7 ETM of as many as five bands of thermal detectors with 120/60-m spatial resolution.

Author

**A87-48801****CANADIAN SYMPOSIUM ON REMOTE SENSING, 10TH, EDMONTON, CANADA, MAY 5-8, 1986, PROCEEDINGS. VOLUME 1 & 2**

M. DIANE THOMPSON, ED. (Intera Technologies, Ltd., Calgary, Canada) and RONALD J. BROWN, ED. (Canada Centre for Remote Sensing, Ottawa, Canada) Symposium sponsored by the Canadian Remote Sensing Society, Canada Centre for Remote Sensing, and Canadian Institute of Surveying. Ottawa, Canadian Aeronautics and Space Institute, 1987. Vol. 1, 607 p.; vol. 2, 565 p. In English and French. For individual items see A87-48802 to A87-48907.

Topics discussed include spatial filtering of digital Landsat data for the extraction of mapping information; the application of accuracy assessment techniques to image classification; the inventory of wetlands with the Landsat TM; an airborne programmable imaging spectrometer for geobotanical applications; and spectral and textural segmentation of multispectral aerial images. Papers are presented on a high-throughput system for bulk processing of multispectral imagery; the influence of melting conditions on the interpretation of radar imagery of sea ice; the application of low altitude sample photography to national land use mapping; the use of satellite derived digital elevation models for resource mapping; and mapping effluent plumes with digitally enhanced and classified aerial photography. Consideration is given to the optimization of seismic vessel deployment using side looking airborne radar; validation and simulation of Radarsat imagery; remote sensing and agricultural resource inventory; the classification of TM data; and the Canadian SPOT program. I.F.

**A87-48835#****BARRIERS TO THE OPERATIONAL USE OF SATELLITE REMOTE SENSING IN CANADA**

D. W. EPP (SED Systems, Inc., Remote Sensing Dept., Saskatoon, Canada) IN: Canadian Symposium on Remote Sensing, 10th, Edmonton, Canada, May 5-8, 1986, Proceedings. Volume 1. Ottawa, Canadian Aeronautics and Space Institute, 1987, p. 331-335.

While Landsat data have been available for use in Canadian applications since 1972, the volume of data applied to ongoing operational programs remains low. The barriers responsible for this limited use are identified and discussed from the perspective of the operations contractor (since 1972) of the Prince Albert Satellite Station. Specific reference is made to the capabilities of remote sensing, data availability, the extraction of information, and the utility of remote sensing in the Canadian context. The paper concludes that, while remote sensing data contain valuable information which can be extracted with increasing proficiency, operational use will only increase when resource managers are convinced that a stable program will consistently provide timely, cost-effective data and information in the variety of forms dictated by their needs. Author

**A87-48836#****A HIGH-THROUGHPUT SYSTEM FOR BULK PROCESSING OF MULTISPECTRAL IMAGERY**

A. J. M. BAILLIE (Canadian Astronautics, Ltd., Ottawa, Canada) IN: Canadian Symposium on Remote Sensing, 10th, Edmonton, Canada, May 5-8, 1986, Proceedings. Volume 1. Ottawa, Canadian Aeronautics and Space Institute, 1987, p. 337-348.

A new processing subsystem for Canada's Landsat Digital Image Analysis System, the Fast Multidimensional Processing System (FMPS), is described. The role of the FMPS is to perform high-speed bulk processing of multispectral imagery data, preprocessed to correct for radiometric and geometric errors; one component of the FMPS is an array processor capable of executing 100 million floating-point operations per second. The FMPS system performs eight image processing functions in the categories of image enhancement, image analysis, and image classification, with each of the functions performed on a per-pixel basis, each pixel consisting of up to 21 channels of spectral information. Using the FMPS, a maximum likelihood classification of a 512 line by 6100 pixel by 20 band image into 11 classes was completed in 18

minutes (as compared to 10 hours by the previous processing method). I.S.

**A87-48844#****ANALYSIS OF DATA FROM THE DFO FLUORESCENCE LINE IMAGER**

G. A. BORSTAD (G.A. Borstad Associates, Ltd., Sidney, Canada), J. F. R. GOWER (Institute of Ocean Sciences, Sidney, Canada), and D. N. TRUAX (Apocalypse Enterprises, Ltd., Victoria, Canada) IN: Canadian Symposium on Remote Sensing, 10th, Edmonton, Canada, May 5-8, 1986, Proceedings. Volume 1. Ottawa, Canadian Aeronautics and Space Institute, 1987, p. 413-422. refs

The DFO Fluorescence Line Imager (FLI) is an imaging spectrometer designed to provide high-spectral-resolution images of low-radiance targets such as water, but with a large dynamic range and extreme flexibility in band definition. These characteristics make it very useful for a wide variety of terrestrial applications as well. Imaging spectrometers will be the next generation of remote sensors. This paper briefly describes the spectral imaging concept upon which the FLI system is based and compares the FLI to other imaging systems. The procedures developed for calibration of the five cameras and 554,000 sensing elements are outlined and evaluated, and the successes and remaining problems summarized. Examples of data presented include evidence of *in vivo* fluorescence and absorption by phytoplankton chlorophyll and comparison to *in situ* data, as well as from benthic plants. Author

**A87-48852#****CCRS AIRBORNE ELECTRO-OPTICAL FACILITY**

S. TILL, W. D. MCCOLL, and R. A. NEVILLE (Canada Centre for Remote Sensing, Ottawa, Canada) IN: Canadian Symposium on Remote Sensing, 10th, Edmonton, Canada, May 5-8, 1986, Proceedings. Volume 1. Ottawa, Canadian Aeronautics and Space Institute, 1987, p. 497-503. refs

The Electrooptical Facility of the Canada Centre for Remote Sensing, designed to provide state-of-the-art multispectral digital image data for remote sensing research and operational applications, is described. The Facility consists of a planning and tasking function, a data acquisition remote sensing aircraft (which carries an MEIS, an MSS, an irradiance spectrometer, a GPS, an inertial navigation/MAID, and a camera), and a digital data processing capability for the production of computer-compatible tapes (CCTs) and hardcopy imagery. The paper discusses the requirements for the mission planning and tasking; provides current specifications for and descriptions of the integrated sensor systems; and detail procedures for data processing and the production of CCTs and hardcopy imagery. Examples of recent applications, including geometrically corrected stereo data, are presented. I.S.

**A87-48865#****MEIS II IMAGERY FOR ENVIRONMENTAL STRESS ANALYSIS**

R. V. DAMS, M. D. THOMPSON (Intera Technologies, Ltd., Calgary, Canada), I. SUTHERLAND, and G. REICHERT (Alberta Remote Sensing Centre, Edmonton, Canada) IN: Canadian Symposium on Remote Sensing, 10th, Edmonton, Canada, May 5-8, 1986, Proceedings. Volume 2. Ottawa, Canadian Aeronautics and Space Institute, 1987, p. 643-653. Research supported by the Alberta Remote Sensing Centre. refs

The use of the airborne multidetector electrooptical imaging scanner (MEIS) II to identify the areal extent and severity of sulfur-related vegetation stress is evaluated. MEIS II imagery for the Ram River and Strachan areas in Alberta, Canada were acquired in July 1983; the techniques for data acquisition and processing are described. Pseudo-CIR photographs, unsupervised classifications, and supervised classifications for the areas are analyzed. Vegetation cover and stress classification at three altitudes are examined. The effects of shadows on the images are investigated. The data reveal that in the Ram River area numerous vegetation types and stress categories are identified; in the Strachan area, forest composition is observed, but vegetation

stress data is not detected. It is noted that the MEIS II data is useful for vegetation stress analysis. I.F.

#### A87-48873#

##### **MULTISPECTRAL VIDEO SYSTEM FOR AIRBORNE REMOTE SENSING - SENSITIVITY, CALIBRATIONS AND CORRECTION**

A. ROBERTS (Simon Fraser University, Burnaby, Canada) and D. J. EVANS IN: Canadian Symposium on Remote Sensing, 10th, Edmonton, Canada, May 5-8, 1986, Proceedings. Volume 2. Ottawa, Canadian Aeronautics and Space Institute, 1987, p. 729-737. refs

A four camera multispectral video system including aircraft installation and image processing interface is described. An RCA Newvicon and three Sony XC-37 CCD video cameras fitted with four matched variable focal length lenses and filter mounts were installed in a turbo-charged Cessna 185C with two camera ports. A wide variety of optical filters can be used to divide the photographic spectrum (360-1100 nm) for multispectral imaging. Video image analysis is achieved through an International Imaging System Model 70/F4 graphics system with a time base corrector and video digitizer for image input from the four video cassette recorders used for data collection. The camera-lens-filter systems were tested for radiometric response distortions and vignetting problems. Characteristics curves were constructed for 9 point locations in each camera's field of view. Camera sensitivity and vignetting characteristics were examined. This information was used in developing suitable exposure and image correction preprocessing procedures. Author

#### A87-48874#

##### **DISCRIMINATION OF SUSPENDED SEDIMENT AND LITTORAL FEATURES USING MULTISPECTRAL VIDEO IMAGERY**

J. LIEDTKE, A. ROBERTS, and D. EVANS (Simon Fraser University, Burnaby, Canada) IN: Canadian Symposium on Remote Sensing, 10th, Edmonton, Canada, May 5-8, 1986, Proceedings. Volume 2. Ottawa, Canadian Aeronautics and Space Institute, 1987, p. 739-747. refs

A multispectral video system containing four low-light sensitive video cameras with narrow band optical filters (bluegreen 420-495 nm, green 510-585 nm, red 620-740 nm, and near-IR 735-1100 nm) was utilized to obtain spectral data for four areas over the Fraser River sediment plume in the Strait of Georgia, Canada. Images were recorded at 2000, 4000, 8000, and 12,000 ft. and color IR aerial photographs and water quality samples were collected. The use of template correction procedures and exposure calculations to correct image quality is discussed. Images of the relative reflectivity changes for the IR, red, and green along a transect across varying sediment concentration conditions were recorded, and the relation between reflectivity values and sediment concentration is studied. It is observed that the video system provided good separation for sediment values of 5 mg/l, and that a low-cost multispectral video system can provide useful and reliable remote sensing data for water quality research. I.F.

#### A87-48890#

##### **THE RADARSAT RMOMS OPTICAL SENSOR**

S. M. TILL, F. J. AHERN (Canada Centre for Remote Sensing, Ottawa), H. WERSTIUK (RADARSAT Project Technical Office, Ottawa, Canada), and D. MEISSNER (Messerschmitt-Boelkow-Blohm GmbH, Ottobrunn, West Germany) IN: Canadian Symposium on Remote Sensing, 10th, Edmonton, Canada, May 5-8, 1986, Proceedings. Volume 2. Ottawa, Canadian Aeronautics and Space Institute, 1987, p. 903-908. refs

The RADARSAT satellite is proposed to carry a complement of sensors, including the synthetic aperture radar and an optical sensor RMOMS. MOMS is the acronym for 'modular optoelectronic multispectral scanner' and is an imaging pushbroom sensor. MOMS-01, the first one of this family, has been flown twice on a space platform (SPAS-01) as part of the Shuttle missions STS-7 and STS-11. It consists of two spectral channels, with each channel comprising spectral filter, lens assembly and linear (charge-coupled device) multi-element arrays. The sensor uses optical butting of

the linear arrays, by means of a double-lens system, in order to generate wide swath coverage. The proposed RMOMS sensor consists of four spectral channels, and offers excellent coverage (400 km swath width), with 30 m spatial resolution, and 10-bit data encoding. Several design features are included to optimize the radiometric resolution, and to enhance the dynamic range. The performance specifications have been carefully matched to user requirements for renewable and non-renewable resource applications. Author

#### A87-48893#

##### **REMOTE SENSING IN THE SAHEL - A TOOL FOR THE INVENTORY AND MONITORING OF RESOURCES [LA TELEDETECTION AU SAHEL - UN OUTIL D'INVENTAIRE ET DE SURVEILLANCE DES RESSOURCES]**

C. PREVOST (Canada Centre for Remote Sensing, Ottawa) and M. YERGEAU (Sherbrooke, Universite, Canada) IN: Canadian Symposium on Remote Sensing, 10th, Edmonton, Canada, May 5-8, 1986, Proceedings. Volume 2. Ottawa, Canadian Aeronautics and Space Institute, 1987, p. 927-936. In French. refs

Applications of remote sensing for the inventorying of natural resources and the identification and prediction of natural disasters in the Sahel are discussed. An approach is discussed and illustrated with images in which daily NOAA-AVHRR data are used to obtain local and global area maps, and in which problem or potential problem areas can be identified using the longer-time-frame MSS and TM systems. Application of the large-format camera used in 1984 on the Space Shuttle to land-use and hydrographic studies is also discussed. It is suggested that the integration of data from these various satellites can significantly reduce the risk of famine in the Sahel. R.R.

#### A87-50226

##### **POINT POSITIONING AND MAPPING WITH LARGE FORMAT CAMERA DATA**

A. GRUEN and E. SPIESS (Zuerich, Eidgenoessische Technische Hochschule, Zurich, Switzerland) Geocarto International (ISSN 1010-6049), vol. 2, June 1987, p. 3-15.

Space borne image data at high spatial and radiometric resolution is becoming increasingly available. The Large Format Camera (LFC) photographs are of unmatched spatial resolution and thus of great interest for an ever increasing user community. This paper investigates the point positioning and mapping capabilities of the LFC system. Point positioning accuracy is explored for planimetry and height with respect to strip triangulation and single stereomodel processing. Identification and interpretation of map features, and the map updating capabilities are analyzed in relation to the map standards of a topographic map 1:100,000. Experiences with Digital Terrain Model generation and orthophoto production are reported. Author

#### A87-53101

##### **IGARSS '87 - INTERNATIONAL GEOSCIENCE AND REMOTE SENSING SYMPOSIUM, UNIVERSITY OF MICHIGAN, ANN ARBOR, MAY 18-21, 1987, DIGEST. VOLUMES 1 & 2**

Symposium sponsored by IEEE, URSI, NASA, et al. New York, Institute of Electrical and Electronics Engineers, Inc., 1987, p. Vol. 1, 793 p.; vol. 2, 893 p. For individual items see A87-53102 to A87-53290.

Papers are presented on geophysical tomography; atmospheric retrieval techniques and analysis; classification techniques for multispectral images; the objectives and instruments of the proposed EOS; scatterometers and altimeters; vegetation and land use studies; microwave surface scattering; microwave remote sensing of rain; and image processing techniques for remotely sensed images. Topics discussed include subsurface sensing and inversion; calibration of SAR systems; microwave measurement systems and techniques; remote sensing of tropospheric phenomena; coding and feature extraction of remotely sensed images; oceanographic remote sensing; correction techniques for remotely sensed images; single and multiple scattering models; and sea ice models and algorithms. Consideration is given to image analysis and processing systems; geological remote sensing;

optical sensors and calibration; passive microwave observation techniques; speckle reduction in SAR images; and cartography and radargrammetry. I.F.

**A87-53108****REMOTE SENSING OF GEOMAGNETIC FIELD AND APPLICATIONS TO CLIMATE PREDICTION**

A. MARY SELVAM (Indian Institute of Tropical Meteorology, Pune, India) IN: IGARSS '87 - International Geoscience and Remote Sensing Symposium, Ann Arbor, MI, May 18-21, 1987, Digest. Volume 1. New York, Institute of Electrical and Electronics Engineers, Inc., 1987, p. 81-86. refs

A gravity wave feedback mechanism for the troposphere-ionosphere coupling is proposed. The mechanism reveals that the global geomagnetic field, atmospheric electric field, and weather system are caused by a semipermanent, scale-invariant atmospheric eddy continuum. The scale-invariant energy structure for the atmospheric eddy continuum is examined. The quantum mechanical nature of the eddy energy structure and the distribution characteristics of the eddy energy perturbation field are analyzed. It is observed that the full continuum of atmospheric eddies exist as a unified whole and originate from buoyant energy supplied from frictional turbulence at the planetary source. A model for atmospheric electric and geomagnetic fields is presented. It is noted that geomagnetic field variations, which are easily monitored using satellite sensors, are applicable to weather and climate predictions. I.F.

**A87-53116****INVESTIGATION OF DESIGN PARAMETERS FOR ERS-1 WIND SCATTEROMETER**

C. C. LIN, H. EICHENHERR, H. R. SCHULTE, R. KUELZER, and A. KOPPE (Dornier System GmbH, Friedrichshafen, West Germany) IN: IGARSS '87 - International Geoscience and Remote Sensing Symposium, Ann Arbor, MI, May 18-21, 1987, Digest. Volume 1. New York, Institute of Electrical and Electronics Engineers, Inc., 1987, p. 167-172. ESA-sponsored research. refs

A certain number of important engineering performance parameters of the ERS-1 wind scatterometer are defined in terms of its impulse response and modulation transfer functions. In this paper, the results of further investigations of scatterometer performance figures are presented. The basic tool used to predict the performance is the impulse response modeling software. The validation of this simulation software was carried out through extensive analyses of all possible errors involved in the mathematical models and their software implementation. The confidence gained through the software validation process forms the basis for the performance sensitivity analysis with respect to the design parameters. Also analyzed are the impacts of the design parameter uncertainties on the overall performance. This includes the effects of the system imperfections such as antenna pointing errors and Doppler compensation error. Author

**A87-53117****AN ADVANCED WIND SCATTEROMETER FOR THE COLUMBUS POLAR PLATFORM PAYLOAD**

M. LANGEMANN and R. W. ZAHN (Dornier System GmbH, Friedrichshafen, West Germany) IN: IGARSS '87 - International Geoscience and Remote Sensing Symposium, Ann Arbor, MI, May 18-21, 1987, Digest. Volume 1. New York, Institute of Electrical and Electronics Engineers, Inc., 1987, p. 175-178.

In 1986, ESA/ESTEC performed a study of a payload for the Columbus Polar Platform to be launched in 1995, which shall carry various earth observation instruments. One core instrument is the wind scatterometer, an upgraded version of the ERS-1 wind scatterometer. This paper will describe the instrument design in terms of instrument configuration, electrical design, and on-board data processing. Author

**A87-53118\*** Jet Propulsion Lab., California Inst. of Tech., Pasadena.

**SELECTION OF EXTENDED AREA LAND TARGET SITES FOR THE CALIBRATION OF SPACEBORNE SCATTEROMETERS**

R. G. KENNETT and F. K. LI (California Institute of Technology, Jet Propulsion Laboratory, Pasadena) IN: IGARSS '87 - International Geoscience and Remote Sensing Symposium, Ann Arbor, MI, May 18-21, 1987, Digest. Volume 1. New York, Institute of Electrical and Electronics Engineers, Inc., 1987, p. 179-184. refs

In order to understand what areas can be used for spaceborne scatterometer calibration and to aid in the design of future land radar systems, the Seasat-1 Scatterometer System (SASS) data on the backscattering coefficient  $\sigma_0$  have been studied. Global images of land and ice backscatter are presented and compared to the terrain type. The global statistics of  $\sigma_0$  for incidence angles between 0 and 70 deg are presented and compared with the Skylab and ground spectrometer results. The brightest land regions are the rain forests. For two such regions, the Amazon Basin and the Congo Basin, detailed images and the variation of  $\sigma_0$  with polarization, angle of incidence, and terrain type are presented. For comparison, a highly nonhomogeneous region, part of the Sahara desert, is studied. Author

**A87-53145\*** Colorado Univ., Boulder.

**THE HIGH RESOLUTION IMAGING SPECTROMETER (HIRIS) FOR EOS**

ALEXANDER F. H. GOETZ (Cooperative Institute for Research in Environmental Sciences, Boulder, CO) and MARK HERRING (California Institute of Technology, Jet Propulsion Laboratory, Pasadena) IN: IGARSS '87 - International Geoscience and Remote Sensing Symposium, Ann Arbor, MI, May 18-21, 1987, Digest. Volume 1. New York, Institute of Electrical and Electronics Engineers, Inc., 1987, p. 367-372. refs

The HIRIS is designed to acquire images in 196 spectral bands simultaneously in the 0.4-2.5 micron wavelength region. HIRIS is a targeting rather than a continuous acquisition instrument and obtains high spatial and spectral resolution images in a 23 km swath with a 30 m GIFOV in vertical viewing. Gimbal pointing is proposed which will allow image acquisition at  $-30 + 60$  deg down-track and  $+ \text{ or } - 25$  deg cross-track. The raw data rate of the instrument is 393 Mbs. The high spectral resolution will make it possible to directly identify surficial materials such as rocks, soils, and suspended matter in water, and HIRIS opens up the possibility of studying biogeochemical processes in vegetation canopies. HIRIS will be used in conjunction with MODIS as a multistage sampling system. Author

**A87-53149****OPERATIONAL INSTRUMENTS ON THE SPACE STATION-POLAR PLATFORMS - CONTRIBUTIONS BY NOAA AND THE INTERNATIONAL COMMUNITY**

BRUCE H. NEEDHAM (NOAA, National Environmental Satellite, Data and Information Service, Washington, DC) IN: IGARSS '87 - International Geoscience and Remote Sensing Symposium, Ann Arbor, MI, May 18-21, 1987, Digest. Volume 1. New York, Institute of Electrical and Electronics Engineers, Inc., 1987, p. 387-392.

In the mid-1990's, the National Aeronautics and Space Administration (NASA) and the European Space Agency (ESA) will combine efforts to launch the Space Station along with two orbiting Polar Platforms. The National Oceanic and Atmospheric Administration (NOAA) will be utilizing the NASA and ESA Polar Platforms to carry its operational instruments for environmental remote sensing as a logical follow on to the current series which ends with the NOAA-K, L, M satellites. This paper will describe the operational instruments that NOAA proposes to fly on the two Polar Platforms, and other international contributions that are under consideration. Author



A87-53163

**MILLIMETER-WAVE POLARIMETRIC MEASUREMENTS OF ARTIFICIAL AND NATURAL TARGETS**

M. W. WHITT and F. T. ULABY (Michigan, University, Ann Arbor)  
 IN: IGARSS '87 - International Geoscience and Remote Sensing Symposium, Ann Arbor, MI, May 18-21, 1987, Digest. Volume 1. New York, Institute of Electrical and Electronics Engineers, Inc., 1987, p. 537-543. refs  
 (Contract DAAG29-85-K-0220)

The millimeter-wave polarimeter is a scatterometer system that uses the HP 8510A vector network analyzer for coherent processing of the received signal. It operates at 35 GHz and 94 GHz, and a third channel at 140 GHz is to be added in 1987. The MMP provides full polarization and phase capabilities to allow measurement of the complete scattering matrix of both distributed and point targets. This paper describes the calibration techniques used at 35 GHz to measure the scattering matrix and presents some sample data. An analysis of the measurement accuracy was performed by comparing the measured values with theoretical calculations for conducting spheres and finite-length conducting cylinders. As an extension of the analysis to natural targets, the scattering matrices of a series of twigs were examined, and preliminary results are presented.

Author

A87-53168

**ON THE ORIGIN OF CROSS-POLARIZATION IN REMOTE SENSING**

S. RIEGGER, W. WIESBECK (Karlsruhe, Universitaet, West Germany), and A. J. SIEBER (CEC, Joint Research Centre, Ispra, Italy) IN: IGARSS '87 - International Geoscience and Remote Sensing Symposium, Ann Arbor, MI, May 18-21, 1987, Digest. Volume 1. New York, Institute of Electrical and Electronics Engineers, Inc., 1987, p. 577-580. refs

The use of cross polarization to identify characteristic signatures in microwave remote sensing is examined. The measurement of the complex scattering matrix using the Vector-Network-Analyzer, and the computation of cross polarization from the matrix are described. The relation between precise cross-polarization measurements and calibration measurements is discussed. The performance of the Vector-Network-Analyzer is evaluated by applying the system to various targets related to remote sensing. Cross-polarization measurements for a lossy dielectric cylinder, a small branch of abies alba, and a circular cut of Yucca and Dieffenbachia leaves were obtained, and it is noted that the system performs well.

I.F.

A87-53179

**REMOTE SENSING BY THE FLUORESCENCE PROPERTY OF THE SCATTERER**

D. B. JADHAV (Indian Institute of Tropical Meteorology, Poona, India) IN: IGARSS '87 - International Geoscience and Remote Sensing Symposium, Ann Arbor, MI, May 18-21, 1987, Digest. Volume 1. New York, Institute of Electrical and Electronics Engineers, Inc., 1987, p. 653-656. refs

Remote sensing according to the fluorescence property of the scattering media is described. The fluorescence emission from crude oil spills, haze, dust, smoke and cloud droplets is considered. The method for eliminating solar radiation background is suggested. The difference between the conventional remote sensing technique and this technique is discussed.

Author

A87-53180\*

National Aeronautics and Space Administration, Goddard Space Flight Center, Greenbelt, Md.

**A MULTIFREQUENCY MICROWAVE RADIOMETER OF THE FUTURE**

D. LE VINE, T. WILHEIT (NASA, Goddard Space Flight Center, Greenbelt, MD), R. MURPHY (NASA, Washington, DC), and C. SWIFT (Massachusetts, University, Amherst) IN: IGARSS '87 - International Geoscience and Remote Sensing Symposium, Ann Arbor, MI, May 18-21, 1987, Digest. Volume 1. New York, Institute of Electrical and Electronics Engineers, Inc., 1987, p. 661-666. refs

The design of the High-Resolution Multifrequency Microwave Radiometer (HMMR), which is to be installed on EOS, is described. The HMMR is to consist of the Advanced Microwave Sounding Unit (AMSU), the Advanced Mechanically Scanned Radiometer (AMSR), and the Electronically Scanned Thinned Array Radiometer (ESTAR). The AMSU is a 20-channel microwave radiometer system designed to measure profiles of atmospheric temperature and humidity and the AMSR is a microwave imager with channels at 6, 10, 18, 21, 37, and 90 GHz for measuring snow cover over land, the age and areal extent of sea ice, the intensity of precipitation over oceans and land, and the amount of water in the atmosphere. ESTAR is an imaging radiometer operating near 1.4 GHz capable of obtaining global maps of surface soil moisture with a spatial resolution of about 10 km. The antenna and signal processing utilized in the ESTAR to achieve the real aperture resolution are examined.

I.F.

A87-53195\*

Jet Propulsion Lab., California Inst. of Tech., Pasadena.

**WIND MEASUREMENTS FOR NON-UNIFORM WIND FIELDS FROM SPACEBORNE SCATTEROMETERS**

CHONG-YUNG CHI and FUK K. LI (California Institute of Technology, Jet Propulsion Laboratory, Pasadena) IN: IGARSS '87 - International Geoscience and Remote Sensing Symposium, Ann Arbor, MI, May 18-21, 1987, Digest. Volume 2. New York, Institute of Electrical and Electronics Engineers, Inc., 1987, p. 765-768. refs

Radar backscattering coefficient measurements by spaceborne scatterometers are presently simulated for the case of nonuniform wind fields, by means of a detailed numerical integration of the radar equation. The winds thus estimated are then compared with a nominal field which is defined as the average wind vector over the wind cell. The simulation results obtained for the NASA scatterometer are presented for cases of random wind fields whose spectra are consistent with the Seasat scatterometer sea surface wind spectrum. When the nonuniformity is small, system noise dominates the wind error; wind error degradation is therefore small for both perfect and imperfect coregistration cases. When it is relatively large, however, the wind error degradation persistently increases for both perfect and imperfect coregistrations.

O.C.

A87-53216\*

Jet Propulsion Lab., California Inst. of Tech., Pasadena.

**SYNERGISM REQUIREMENTS AND CONCEPTS FOR SAR AND HIRIS ON EOS**

J. B. CIMINO, C. BRUEGGE, D. DINER, J. PARIS (California Institute of Technology, Jet Propulsion Laboratory, Pasadena), C. DOBSON, D. GATES, F. ULABY (Michigan, University, Ann Arbor), N. GOEL (Astra Assoc., La Jolla, CA), D. KIMES (NASA, Goddard Space Flight Center, Greenbelt, MD), V. VANDERBILT (NASA, Ames Research Center, Moffett Field, CA) et al. IN: IGARSS '87 - International Geoscience and Remote Sensing Symposium, Ann Arbor, MI, May 18-21, 1987, Digest. Volume 2. New York, Institute of Electrical and Electronics Engineers, Inc., 1987, p. 955-966. NASA-supported research.

A study is conducted to ascertain the synergistic advantages obtainable by combining, in the EOS orbital instrument platform, instruments for the optical and microwave measurements of biophysical properties important in ecosystem modeling. Attention is given to the comparative coverages of the SAR, HIRIS, TIMS and MODIS instruments that will be carried by the platform, and to the ongoing development of joint inversion algorithms for the



modeling of the ecosystems-related data thus obtained. A three-dimensional characterization of the physical attributes of the vegetation canopy and its background surface will be attempted. O.C.

**A87-53223****PERFORMANCE SENSITIVITY FOR X-SAR**

D. MILLER and C. HEER (Dornier System GmbH, Friedrichshafen, West Germany) IN: IGARSS '87 - International Geoscience and Remote Sensing Symposium, Ann Arbor, MI, May 18-21, 1987, Digest. Volume 2. New York, Institute of Electrical and Electronics Engineers, Inc., 1987, p. 1041-1045. refs

Definitions of X-SAR image performance parameters are given together with the required values. The range Impulse Response Function algorithm is briefly derived showing the sensitivity to quadratic and random phase errors. The need for a clear definition of clutter ambiguities and modeling of earth rotation is demonstrated to avoid pessimistic performance predictions. Author

**A87-53225****REMOTE SENSING OF THE EARTH WITH MICROWAVE RADIOMETRY IN GERMANY - RESULTS AND TRENDS**

W. KEYDEL (DFVLR, Institut fuer Hochfrequenztechnik, Oberpfaffenhofen, West Germany) IN: IGARSS '87 - International Geoscience and Remote Sensing Symposium, Ann Arbor, MI, May 18-21, 1987, Digest. Volume 2. New York, Institute of Electrical and Electronics Engineers, Inc., 1987, p. 1053-1058. refs

**A87-53227\*** Jet Propulsion Lab., California Inst. of Tech., Pasadena.**GLOBAL DIGITAL TOPOGRAPHY MAPPING USING A SCANNING RADAR ALTIMETER**

C. ELACHI, K. E. IM, F. LI, and E. RODRIGUEZ (California Institute of Technology, Jet Propulsion Laboratory, Pasadena) IN: IGARSS '87 - International Geoscience and Remote Sensing Symposium, Ann Arbor, MI, May 18-21, 1987, Digest. Volume 2. New York, Institute of Electrical and Electronics Engineers, Inc., 1987, p. 1063-1067.

The conceptual design of a Scanning Radar Altimeter system capable of collecting less than 300-m spatial and less than 3-m height resolution digital topography data for the entire globe, from an orbital platform, is presented. A 37-GHz frequency SRA system is used to achieve the requisite resolution while reducing antenna length in the along-track dimension. Near-global coverage in a short time period is obtained by scanning the antenna beam cross-track, in a swath of about 100 km. Attention is given to the algorithm that will be used to retrieve pixel height from the return waveform. O.C.

**A87-53228\*** Jet Propulsion Lab., California Inst. of Tech., Pasadena.**THE EOS SAR PROGRAM**

JOBEA CIMINO (California Institute of Technology, Jet Propulsion Laboratory, Pasadena) and KEITH CARVER (Massachusetts, University, Amherst) IN: IGARSS '87 - International Geoscience and Remote Sensing Symposium, Ann Arbor, MI, May 18-21, 1987, Digest. Volume 2. New York, Institute of Electrical and Electronics Engineers, Inc., 1987, p. 1069-1071. refs

The goal of the Spaceborne Imaging Radar (SIR) program is to develop a multipolarization, multifrequency synthetic aperture radar (SAR) with variable imaging geometry which will be ready for flight on the Earth Observing System (EOS) in the mid 1990's. Nominally, this SAR will be a three frequency (L-, C- and X-band) system with quad-polarization available for the L- and C-bands and dual polarization for the X-band system. It will be capable of acquiring multiincidence angle data using electronic beam steering and other imaging geometries by mechanically pitching, yawing and rolling the antenna. The EOS SAR will play a key role along with the other EOS instruments in understanding the earth as a system. Author

**A87-53229**

**SOME RESULTS OF MOS-1 AIRBORNE VERIFICATION EXPERIMENT - MSR (MICROWAVE SCANNING RADIOMETER)** KOREHIRO MAEDA, HIROYUKI WAKABAYASHI, and HIDEO SATO (National Space Development Agency of Japan, Tokyo) IN: IGARSS '87 - International Geoscience and Remote Sensing Symposium, Ann Arbor, MI, May 18-21, 1987, Digest. Volume 2. New York, Institute of Electrical and Electronics Engineers, Inc., 1987, p. 1073-1078. refs

Airborne verification experiments undertaken to develop methods for processing sensor data from the Marine Observation Satellite (MOS-1) are described. An airborne microwave scanning radiometer (MSR) was developed by modifying the engineering model of the MOS-1 instrument. Airborne MSR data were collected over various locations in Japan in order to observe atmospheric water vapor, liquid water, sea surface winds, drifting ice, and dry snow. Attention is given to radiometric and geometric distortion correction items, as well as to geophysical retrieval methods. O.C.

**A87-53232\*** Jet Propulsion Lab., California Inst. of Tech., Pasadena.**SPACECRAFT ON-BOARD SAR IMAGE GENERATION FOR EOS-TYPE MISSIONS**

K. Y. LIU, W. E. ARENS (California Institute of Technology, Jet Propulsion Laboratory, Pasadena), H. M. ASSAL, and J. F. VESECKY (Stanford University, CA) IN: IGARSS '87 - International Geoscience and Remote Sensing Symposium, Ann Arbor, MI, May 18-21, 1987, Digest. Volume 2. New York, Institute of Electrical and Electronics Engineers, Inc., 1987, p. 1091-1097. refs

Spacecraft on-board synthetic aperture radar (SAR) image generation is an extremely difficult problem because of the requirements for high computational rates (usually on the order of Giga-operations per second), high reliability (some missions last up to 10 years), and low power dissipation and mass (typically less than 500 watts and 100 Kilograms). Recently, a JPL study was performed to assess the feasibility of on-board SAR image generation for EOS-type missions. This paper summarizes the results of that study. Specifically, it proposes a processor architecture using a VLSI time-domain parallel array for azimuth correlation. Using available space qualifiable technology to implement the proposed architecture, an on-board SAR processor having acceptable power and mass characteristics appears feasible for EOS-type applications. Author

**A87-53251****MATCHING INSTRUMENT DESIGN AND SIGNAL PROCESSING FOR A SCANNING RADIOMETER**

BERND BAUCHE and DETLEF HENNINGS (Koeln, Universitaet, Cologne, West Germany) IN: IGARSS '87 - International Geoscience and Remote Sensing Symposium, Ann Arbor, MI, May 18-21, 1987, Digest. Volume 2. New York, Institute of Electrical and Electronics Engineers, Inc., 1987, p. 1245-1249.

An account is given of the instrument design and signal processing features used by the 'Airborne Version of the Conical Scanning Radiometer' in order to minimize blurring and aliasing errors in radiation budget measurements. Attention is given to the interrelations among modulation transfer characteristics, optical chopping, scan patterns, and sampling rates; their effects on blurring and aliasing are then analyzed. A sophisticated algorithm was developed in order to achieve the retrieval of measured data at a chopper frequency lying below the regular Nyquist limit. O.C.

A87-53268

**A CROSS ANTENNA FOR PASSIVE MICROWAVE REMOTE SENSING**

ANDREW S. MILMAN (Michigan, Environmental Research Institute, Ann Arbor) IN: IGARSS '87 - International Geoscience and Remote Sensing Symposium, Ann Arbor, MI, May 18-21, 1987, Digest. Volume 2. New York, Institute of Electrical and Electronics Engineers, Inc., 1987, p. 1423-1427. Research supported by the Environmental Research Institute of Michigan. refs

Many applications of passive microwave remote sensing from space require the use of long wavelengths (1 to 5 cm), good spatial resolution (1 to 5 km), and good radiometric sensitivity. A cross antenna that meets these goals is described; it needs only 10 percent of the collecting area of a solid scanning antenna that has the same spatial resolution, but has superior noise performance. The cross antenna has no moving parts. Author

A87-53279

**A COMBINED SAR AND SCATTEROMETER SYSTEM**

P. W. WAGGETT and I. A. WARD (General Electric Co., PLC, Marconi Research Centre, Baddow, England) IN: IGARSS '87 - International Geoscience and Remote Sensing Symposium, Ann Arbor, MI, May 18-21, 1987, Digest. Volume 2. New York, Institute of Electrical and Electronics Engineers, Inc., 1987, p. 1507-1509.

The 'SCATTAR' airborne radar concept can simultaneously act as a three-beam wind scatterometer and a SAR; it is here proposed primarily as a validation tool for all the operational modes of the Active Microwave Instrument to be carried by the ESA earth resources satellite ERS-1. Attention is presently given to the SCATTAR three-lobed pattern-generating antenna, its beam discrimination, time lining behavior, and ground range resolution capabilities. O.C.

A87-53280

**DERIVATION OF THE TECHNICAL SPECIFICATION OF THE ERS-1 ACTIVE MICROWAVE INSTRUMENT TO MEET THE SAR-IMAGE QUALITY REQUIREMENTS**

DIETER PIERSCHL (Dornier System GmbH, Friedrichshafen, West Germany) and DAVID HOUNAM (ESA, European Space Research and Technology Centre, Noordwijk, Netherlands) IN: IGARSS '87 - International Geoscience and Remote Sensing Symposium, Ann Arbor, MI, May 18-21, 1987, Digest. Volume 2. New York, Institute of Electrical and Electronics Engineers, Inc., 1987, p. 1511-1516.

A major part of the first European Remote Sensing Satellite (ERS-1) is the so-called Active Microwave Instrument (AMI). The AMI operates in two modes, the Synthetic Aperture Radar (SAR) mode and the Wind Scatterometer mode. This paper describes the philosophy behind the SAR requirement specification, established between the industrial consortium and the European Space Agency, and how the image quality parameters are broken down into sets of verifiable technical parameters. When defining the requirements particular consideration had to be given to the need for their verification after launch. It proved to be necessary to provide detailed definitions of these parameters and develop algorithms for their derivation. As the purpose of the requirements is to constrain the performance of the on-board instrument alone, the characteristics of the on-ground processor and other influences external to the instrument were assumed to be fixed. Author

A87-53283

**THEORETICAL FEASIBILITY OF SAR INTERFEROMETRY**

J. M. DURAND (CNES, Toulouse, France) IN: IGARSS '87 - International Geoscience and Remote Sensing Symposium, Ann Arbor, MI, May 18-21, 1987, Digest. Volume 2. New York, Institute of Electrical and Electronics Engineers, Inc., 1987, p. 1541-1544. refs

SAR technical requirements for the conduct of interferometry that will yield digital terrain models by means of phase measurements are identified, and the limits of the altitude resolution achievable are ascertained, noting phase error sources and selecting several for further investigation. These error sources include random sensor position variation, the random-phase

addition of individual scatterers within an extensive target, and the misregistration of the compared pixels. It is found that orbit repeatability is a critical parameter, and the use of a large wavelength is recommended. The ERS-1 satellite's SAR is judged a feasible but low-resolution basis for radar interferometry. O.C.

N87-25382# Centre National d'Etudes Spatiales, Toulouse (France).

**PRECISE ORBIT DETERMINATION WITH THE DOPPLER ORBITOGRAPHY AND RADIO POSITIONING INTEGRATED BY SATELLITE (DORIS) SYSTEM AND THE ASSOCIATED ZEALOUS FOR ORBIT OBSERVATION METHODS (ZOOM) SOFTWARE**

Y. LABRUNE, FRANCOIS NOUEL, and C. JAYLES IN: ESA Proceedings of the Second International Symposium on Spacecraft Flight Dynamics p 227-231 Dec. 1986

Avail: NTIS HC A22/MF A01

In support of radar altimetry for oceanographic missions by satellites, Doppler Orbitography and Radio-positioning Integrated by Satellite will provide measurements, by a spaceborne receiver, of the Doppler shift of radio signals transmitted from a ground network of a large number of orbit-devoted beacons. A software (Zealous for Orbit Observation Methods) system for orbit extrapolation, covariance analysis, and orbit determination, which is suitable for precise orbits was developed. User friendliness is achieved with screen oriented pre- and post-processors on a microcomputer. The whole system (hardware and software) is conceived for the TOPEX/POSEIDON mission, but it will be tested on the SPOT 2 platform. ESA

N87-25560# National Oceanic and Atmospheric Administration, Washington, D. C. Special Projects Div.

**PLANNING FOR FUTURE OPERATIONAL SENSORS AND OTHER PRIORITIES**

JAMES C. FISCHER, ed., WALTER PLANET, LARRY STOWE, and WILLIAM L. SMITH Jun. 1987 50 p  
(NOAA-NESDIS-30) Avail: NTIS HC A03/MF A01

The study programs established by the National Environmental Satellite, Data, and Information Service (NESDIS) Office of Systems Development for polar orbiting and geostationary platform sensors are defined. The main thrust of the studies is to prepare an operational payload for the polar platform portion of the space station program. The Advanced Medium Resolution Infrared Radiometer (AMRIR) will be a replacement for the Advanced Very High Resolution Radiometer (AVHRR) and the High Resolution Infrared Radiometer Sounder (HIRS), now operational on the NOAA series of polar orbiters. The Global Ozone Monitoring Radiometer (GOMR) will replace the Solar Backscatter Ultraviolet (SBUV) on the polar platform as the operational ozone monitor. A series of geostationary environmental satellites, beginning with GOES-I, will offer improved image products and operate the first operational sounder from a geostationary satellite. Plans directed towards the development of other sensors are discussed and programs to support microwave science investigations are described. M.G.

N87-26264\*# Jet Propulsion Lab., California Inst. of Tech., Pasadena.

**MILLIMETER-WAVE IMAGING SENSOR DATA EVALUATION**

WILLIAM J. WILSON and ANTHONY C. IBBOTT 1 May 1987 81 p Prepared in cooperation with Harry Diamond Labs., Adelphi, Md.

(Contract NAS7-918)

(NASA-CR-181159; NAS 1.26:181159; JPL-PUB-87-16) Avail: NTIS HC A05/MF A01 CSCL 17B

A passive 3-mm radiometer system with a mechanically scanned antenna was built for use on a small aircraft or an Unmanned Aerial Vehicle to produce real near-real-time, moderate-resolution (0.5) images of the ground. One of the main advantages of this passive imaging sensor is that it is able to provide surveillance information through dust, smoke, fog and clouds when visual and IR systems are unusable. It can also be used for a variety of remote sensing applications, such as measurements of surface moisture, surface temperature, vegetation extent and snow cover.

It is also possible to detect reflective objects under vegetation cover. Author

**N87-27310#** Naval Air Development Center, Warminster, Pa.  
**THE FEASIBILITY OF DETECTING A MAGNETIC FIELD FROM A DISTANT PLATFORM Final Report**

MARTIN SQUICCIARINI 15 May 1987 15 p  
 (AD-A180635) Avail: NTIS HC A02/MF A01 CSCL 17F

The long term objective of the Remote Magnetic Sensing (REMAS) project is to study the feasibility of detecting a magnetic field from a distant platform. This can be contrasted with the current method of magnetic sensing that employs an ASQ-81 helium magnetometer housed in a P-3 aircraft. The ASQ-81 must be located within close proximity of the target in order to detect a field but the presence of the P-3 introduces the possibility of distorting the field and thereby invalidating the measurement. However, this dilemma can be circumvented if a remote sensing device is employed to accomplish the field measurements. The platform is removed from the target area and therefore cannot influence the field. An added advantage of remote sensing is its ability to generate a two dimensional field map of the ocean's surface. These features make the study of systems capable of remotely sensing a magnetic field both a provocative and potentially profitable endeavor. GRA

**N87-27311#** Massachusetts Inst. of Tech., Lexington. Lincoln Lab.

**SPACE SURVEILLANCE APPLICATION POTENTIAL OF SCHOTTKY BARRIER IR SENSORS**

MICHAEL J. CANTELLA 9 Apr. 1987 42 p  
 (Contract F19628-85-C-0002)  
 (AD-A180848; TR-772; ESD-TR-86-142) Avail: NTIS HC A03/MF A01 CSCL 17E

Schottky Barrier IR detection is based on the principle of internal photoemission at the surface between a Si substrate and a deposited metal. In a multi-element focal plane array (FPA), this phenomenon provides very high pixel-to-pixel uniformity, so the requirement for corrective signal processing is minimal. The use of standard silicon design and fabrication techniques simplifies detector readout and multiplexing functions and permits practical realization of sensors that contain very large staring focal planes. This report summarizes the status of FPA and camera development and includes typical imagery. For surveillance applications, the high sensitivity obtainable with these large staring arrays offers both signature and background phenomenology opportunities in the medium wavelength (MWIR) band which could not be exploited previously with scanning-type sensors. Examples of predicted surveillance sensor performance include (1) a near-term ground-based system for Day/Night detection of low-altitude space objects and (2) a future space-borne system for space missions. GRA

**N87-27314#** Office of Naval Research, London (England).  
**THE INTERNATIONAL SYMPOSIUM ON MICROWAVE SIGNATURES AND REMOTE SENSING HELD IN GOTHENBURG (SWEDEN) ON 19-22 JANUARY 1987**

JEROME WILLIAMS 28 May 1987 13 p Symposium held in Gothenburg, Sweden, 19-22 Jan. 1987  
 (AD-A181334; ONRL-7-010-C) Avail: NTIS HC A02/MF A01 CSCL 17I

Discussions covered signatures from snow and ice, solid ground, ocean surfaces, and vegetation and considered systems and radar altimetry, interactions and modeling, and new methods. GRA

**N87-27316#** National Aeronautics and Space Administration, Washington, D.C.

**HMMR (HIGH-RESOLUTION MULTIFREQUENCY MICROWAVE RADIOMETER) EARTH OBSERVING SYSTEM, VOLUME 2E. INSTRUMENT PANEL REPORT**

1987 70 p Original contains color illustrations  
 (NASA-TM-89625; NAS 1.15:89625) Avail: NTIS HC A04/MF A01 CSCL 14B

Recommendations and background are provided for a passive microwave remote sensing system of the future designed to meet the observational needs of Earth scientist in the next decade. This system, called the High Resolution Multifrequency Microwave Radiometer (HMMR), is to be part of a complement of instruments in polar orbit. Working together, these instruments will form an Earth Observing System (EOS) to provide the information needed to better understand the fundamental, global scale processes which govern the Earth's environment. Measurements are identified in detail which passive observations in the microwave portion of the spectrum could contribute to an Earth Observing System in polar orbit. Requirements are established, e.g., spatial and temporal resolution, for these measurements so that, when combined with the other instruments in the Earth Observing System, they would yield a data set suitable for understanding the fundamental processes governing the Earth's environment. Existing and/or planned sensor systems are assessed in the light of these requirements, and additional sensor hardware needed to meet these observational requirements are defined. Author

**N87-27854#** European Space Agency, Paris (France).  
**PROCEEDINGS OF THE SAR APPLICATIONS WORKSHOP**

T. D. GUYENNE, comp. and J. J. HUNT, comp. Dec. 1986  
 123 p Workshop held in Frascati, Italy, 16-18 Sep. 1986  
 (ESA-SP-264; ISSN-079-6566; ETN-87-90156) Avail: NTIS HC A06/MF A01

Active microwave observations of sea ice and icebergs; the potential of SAR in a snow and glacier monitoring system; simulation of SAR data products; SAR detection of ships and ship wakes; line detection in SAR images; geological feature enhancement in SAR imagery; use of SAR data for agriculture and forestry; land use feature detection in SAR images; an algorithm for automatically acquiring ground control points in SAR imagery; and SAR instrument studies were discussed. ESA

**N87-27865#** European Space Agency. European Space Research and Technology Center, ESTEC, Noordwijk (Netherlands).

**SUMMARY OF RECENT SAR INSTRUMENT STUDIES**  
 D. R. JANSSEN *In its* Proceedings of the SAR Applications Workshop p 111-119 Dec. 1986  
 Avail: NTIS HC A06/MF A01

Synthetic aperture radar SAR swath widening techniques were studied. Advanced SAR instruments were designed to cover altitudes up to 900 km incidence angular ranges between 20 and 45 deg providing high image quality with dual frequency or twin SAR's. Broadside looking instruments with dual beam capability are favored. An instrument was sized to fit on the Columbus Polar Platform, which required a reduction of image quality and had to be limited to C-band. Detailed SAR instrument definition is in progress to introduce digital techniques for pulse expansion/compression, and to provide antenna designs with dual beam capability with an optimum technology. ESA

**N87-28118#** Politecnico di Milano (Italy).  
**LARGE FORMAT CAMERA: THE SECOND GENERATION PHOTOGRAMMETRIC CAMERA FOR SPACE CARTOGRAPHY**

G. TOGLIATTI and A. MORIONDO *In* ESA Proceedings of the ESA/EARSel Europe from Space Symposium p 15-18 Dec. 1986  
 Avail: NTIS HC A14/MF A01

The shuttle-borne Large Format Camera (LFC) gave high quality photogrammetric images due to three mechanical features: image motion compensator, stellar cameras, and reseau. Images were

tested to evaluate their semantic contents, the plano-altimetric accuracy of the stereomodels, and usefulness for map revision and for new line maps and orthophotos. The contents of the LFC images is exceptionally high, far more than in any 1:50,000 map. The identification of details depends more on contrast with background than on size. The mean square error in planimetric measures is 5 m, in elevation it is 5 to 7 m, according to procedures. The photomaps and orthophotomaps derived from LFC stereomodels are very good and preserve the high level of information. ESA

**N87-28221#** National Climate Program Office, Rockville, Md.  
**NATIONAL CLIMATE PROGRAM Annual Report, 1985**

Jan. 1987 50 p

(PB87-190518) Avail: NTIS HC A03/MF A01 CSCI 04B

African rainfall monitored; drought detection techniques used to assess African crop condition; World Agriculture Outlook Board monitors African crops; climate assessment technology developed for less-developed countries. U.S. heating bills estimated from monthly temperatures, data handling modernized and user serviced expanded; agribusiness use of climate data evaluated; second volume of climate data catalog published; climate products available; scope of satellite products increased; and regional climate centers and states test climate delivery systems are examined. GRA

**N87-28809#** University Coll., London (England). Dept. of Electronic and Electrical Engineering.

**A STUDY OF ANTENNA SIGNAL PROCESSING TECHNIQUES FOR RADAR ALTERNATIVES Final Report**

H. D. GRIFFITHS, C. G. RAPLEY, K. MILNE, and D. J. WINGHAM Paris, France ESA Dec. 1985 166 p  
(Contract ESA-6001/84-NL-GM)

(ESA-CR(P)-2370; ETN-87-90473) Avail: NTIS HC A08/MF A01

The achievements and limitations of Seasat class altimeters are reviewed; performance requirements for more advanced instruments are outlined. Extensions of the altimeter concept involving the use of antenna signal processing techniques are described, and are assessed with regard to observations of the open ocean and topographic surfaces. Activities which ESA should consider supporting as part of a program of advanced altimeter development are discussed. ESA

**N87-28951#** Technical Univ. of Denmark, Lyngby. Inst. of Electromagnetics.

**MICROWAVE RADIOMETRY STUDY CONCERNING PUSHBROOM SYSTEMS. VOLUME 1: A SEA SALINITY/SOIL-MOISTURE PUSHBROOM RADIOMETER SYSTEM**

NIELS SKOU Paris, France ESA Jun. 1986 81 p

(Contract ESTEC-6374/85-NL-GM(SC))

(R-322; ESA-CR(P)-2359-VOL-1; ETN-87-90459) Avail: NTIS HC A05/MF A01

A sea salinity/soil moisture satellite-borne sensor with a 1.4 GHz pushbroom radiometer system as the prime instrument is described. The system can measure sea salinity, to better than 1 per mil provided that sea surface temperature is known to within 0.5 C and wind speed to 0.5 m/sec. These requirements are incompatible with planned ocean missions. However, the parameters can be measured satisfactorily by a companion 2.7 GHz, dual polarized pushbroom radiometer system. The 1.4 GHz radiometer is also ideal for soil moisture measurements. The radiometric resolution is ample, but good moisture estimates require correction for soil temperature, vegetation density, and soil roughness. ESA

**N87-28956#** Instituto de Pesquisas Espaciais, Sao Jose dos Campos (Brazil).

**DETERMINATION OF TRANSFER FUNCTIONS FROM THE THEMATIC MAPPER (TM) SENSOR OF THE LANDSAT-5 SATELLITE [DETERMINACAO DA FUNCAO DE TRANSFERENCIA DO SENSOR TM DO SATELITE LANDSAT-5]**

LEILA MARIA GARCIAFONSECA and NELSON D. A. MASCARENHAS Jul. 1987 8 p In PORTUGUESE Presented at the 10th National Congress of Applied Mathematics and Computation, Gramado, Brazil, 21-25 Sep. 1987 (INPE-4213-PRE/1094) Avail: NTIS HC A02/MF A01

A theoretical model of the Thematic Mapper (TM) sensor of the LANDSAT-5 satellite is presented. The model is constructed for each component separately (optics, detector, electronics). The results of the sampling process are also included. Author

**N87-28957\*#** Massachusetts Inst. of Tech., Cambridge. Research Lab. of Electronics.

**REMOTE SENSING OF EARTH TERRAIN Semiannual Report, 1 Mar. - 31 Aug. 1987**

J. A. KONG 15 Oct. 1987 13 p

(Contract NAG5-270)

(NASA-CR-181370; NAS 1.26:181370) Avail: NTIS HC A02/MF A01 CSCI 08B

A systematic approach for the identification of terrain media such as vegetation canopy, forest, and snow covered fields is developed using the optimum polarimetric classifier. The covariance matrices for the various terrain cover are computed from theoretical models of random medium by evaluating the full polarimetric scattering matrix elements. The optimal classification scheme makes use of a quadratic distance measure and is applied to classify a vegetation canopy consisting of both trees and grass. Experimentally measured data are used to validate the classification scheme. Theoretical probability of classification error using the full polarimetric matrix are compared with classification based on single features including the phase difference between the VV and HH polarization returns. It is shown that the full polarimetric results are optimal and provide better classification performance than single feature measurements. Author

**N87-29904#** Technische Hogeschool, Delft (Netherlands). Afdeling der Geodesie.

**THE ESTIMATION OF VARIANCE COMPONENTS IN GEODETIC NETWORKS Thesis [HET SCHATTEN VAN VARIANTIECOMPONENTEN IN GEODETISCHE NETWERKEN]**

CORNELIS BOS Aug. 1986 63 p In DUTCH

(B8681154; ETN-87-90171) Avail: NTIS HC A04/MF A01

Estimates for variance components, in the framework of the adjustment procedure in geodetic networks, were investigated. The fixed effects model, random effects model and mixed model, as well as several algorithms are treated. The Minguet theory is explained. Applications of variance components estimates are presented. Results of calculations on three test networks are discussed. ESA

**N87-29909#** Army Engineer Topographic Labs., Fort Belvoir, Va.

**A USER'S GUIDE FOR THE ANALYTICAL PHOTOGRAMMETRIC POSITIONING SYSTEM (APPS)**

GEORGE E. NEWBURY Nov. 1986 46 p

(AD-A183773; ETL-0446) Avail: NTIS HC A03/MF A01 CSCI 08B

The Analytical Photogrammetric Positioning System (APPS) and the Automated Geographic Information System (AUTOGIS) are described. The report discusses the recommended approach for using the hardware and software, and gives some examples of projects that may make use of the systems. GRA

## GENERAL

Includes economic analysis.

**A87-43260****AN EXPERT SYSTEM FOR REMOTE SENSING**

DAVID G. GOODENOUGH, GORDON PLUNKETT (Canada Centre for Remote Sensing, Ottawa), MORRIS GOLDBERG (Ottawa, University, Canada), and JOHN ZELEK (Intera Technologies, Ltd., Ottawa, Canada) (International Association for Pattern Recognition and IBM France, S.A., Workshop on Analytical Methods in Remote Sensing for Geographic Information Systems, Ecole Nationale Supérieure des Telecommunications, Paris, France, Oct. 23, 24, 1986) IEEE Transactions on Geoscience and Remote Sensing (ISSN 0196-2892), vol. GE-25, May 1987, p. 349-359. refs

The Canada Centre for Remote Sensing (CCRS) has developed two hierarchical expert systems, the Analyst Advisor and the Map Image Congruency Evaluation (MICE) advisor. The paper describes the architecture of the expert system to compare maps and images (MICE) and the expert system to advise on the extraction of resource information from remotely sensed data, the Analyst Advisor. Details are given concerning the structure of RESHELL (Remote Sensing Shell) and methods of interfacing symbolic reasoning in PROLOG on the AI VAX stations with numeric processing in FORTRAN on several different computers. The first prototype of the Analyst Advisor will be released for internal use at CCRS in March 1987. Author

**A87-48810#****MULTISTAGE REMOTE SENSING WITH GRADE FOUR STUDENTS**

P. A. GYAN IN: Canadian Symposium on Remote Sensing, 10th, Edmonton, Canada, May 5-8, 1986, Proceedings. Volume 1. Ottawa, Canadian Aeronautics and Space Institute, 1987, p. 73-80. refs

Research in the use of remote sensing materials for teaching geography has been primarily restricted to black and white vertical aerial photographs and Landsat C1 imagery (Color 1 composite satellite images from Bands 4, 5 and 7). In such studies, the ability of students to interpret the remote sensing material and learn certain geographic concepts, and the ability of teachers to determine the best teaching method, have been the focus of the major efforts. This paper describes the use of a multistage remote sensing design: the combined use of ground-observed, aircraft, and satellite data in the form of a road map, color infrared vertical aerial photographs, and Landsat C1 imagery to teach grade four elementary school students social studies. The multistage remote sensing study discussed allows these students to learn a variety of geographic concepts and mapping skills from up-to-date materials consequently helping them to better understand the world around them at a local, regional, and even at a global level.

Author

**A87-51143****MOSCOW SEEN BY SATELLITE - ANOTHER IMAGE OF SOVIET URBAN GEOGRAPHY [MOSCOU VUE PAR SATELLITE - UNE AUTRE IMAGE DE LA GEOGRAPHIE URBAINE SOVIETIQUE]**

GALIA BURGEL and GUY BURGEL (Paris X, Université, Nanterre, France) Photo Interpretation (ISSN 0031-8523), vol. 24, Sept.-Oct. 1985, p. 41-45, 47. In French, English, and Spanish.

A Landsat image obtained in May 1981 and processed by color IR methods is analyzed in conjunction with existing information, such as urban features established by surveys and previous remote sensing analyses, in order to investigate the urban texture of Moscow. It is noted that the image scale and the size of the pixels cannot be confirmed, and that only limited verification of the satellite response is possible. The Landsat data confirm the previously suggested hypertrophy of the downtown area and minimization of the outskirts. Also noted are variations in

construction density, the arrangement and structure of pixels of clearly identifiable architectural types, and the relationships between residential, industrial, and green areas. R.R.

**A87-51320****SPOT'S FIRST YEAR**

BOB JAUQUES Space Markets (ISSN 0258-4212), Spring 1987, p. 36-38.

The main features and capabilities of SPOT are described. The objectives of the Preliminary Evaluation Program are discussed. The marketability of SPOT images is examined. I.F.

**A87-51324****EURIMAGE SETS UP SHOP**

CHRIS BULLOCH Space Markets (ISSN 0258-4212), Summer 1987, p. 95-98.

The structure and functions of Eurimage, a group concerned with the distribution of image data obtained from earth observation satellites, are described. Providing the data to the users as quickly as possible is the primary objective of the group; the principal users of the satellite images are national organizations and government agencies concerned with agriculture, soil analysis, and land use. Various applications for Landsat images are discussed. I.F.

**A87-53084****STATUS OF AND PROGNOSIS FOR SPACE REMOTE SENSING**

C. P. WILLIAMS (Earth Observation Satellite Co., Lanham, MD) IN: The human quest in space; Proceedings of the Twenty-fourth Goddard Memorial Symposium, Greenbelt, MD, Mar. 20, 21, 1986. San Diego, CA, Univelt, Inc., 1987, p. 29-33; Discussion, p. 34, 35. (AAS PAPER 86-104)

Current space remote sensing capabilities and future prospects for space remote sensing are discussed. Consideration is given to the capabilities of Landsat and SPOT and the proposed ESA and Japanese remote sensing projects. Due to time and budget constraints, it is suggested that further developments in remote sensing be researched and developed jointly. Various types of platforms and instruments needed for improving remote sensing capabilities, such as low polar orbiting platforms and a worldwide Ka-band satellite communications net with intersatellite laser communication links, are described. I.F.

**A87-53235****THE SPOT PROGRAM - COMMERCIALIZATION OF REMOTE SENSING**

PIERRE BESCOND (SPOT Image Corp., Reston, VA) IN: IGARSS '87 - International Geoscience and Remote Sensing Symposium, Ann Arbor, MI, May 18-21, 1987, Digest. Volume 2. New York, Institute of Electrical and Electronics Engineers, Inc., 1987, p. 1115-1118.

The SPOT 1 remote sensing satellite generates 10-m-resolution panchromatic and 20-m-resolution multispectral images, and in addition offers an off-nadir viewing capability on which the acquisition of stereoscopic images may be based. The SPOT system's ground component consists of a global network of control centers, receiving stations, image processing facilities, and data distributors. SPOT's commercial approach has been the basis for considerable news media applications, concerning such events as large-scale environmental pollution accidents. The long-term plans for the program involve the launching of three additional satellites to ensure continuous image production. O.C.

**A87-53742****THE FUTURE GENERATION OF RESOURCES SATELLITES**

CAESAR VOUTE (International Institute for Aerospace Survey and Earth Sciences, Enschede, Netherlands) ITC Journal (ISSN 0303-2434), no. 4, 1986, p. 307-317. refs

Current trends in remote sensing are considered. A number of national and regional satellite remote sensing programs and projects are described. The requirements for remote sensing and

the distribution of the data are discussed. The commercialization of remote sensing systems and images is examined. I.F.

**A87-53987**

**INTERNATIONAL COOPERATION IN SPACE - ENHANCING THE WORLD'S COMMON SECURITY**

GEORGE BROWN (U.S. House of Representatives, Washington, DC) Space Policy (ISSN 0265-9646), vol. 3, Aug. 1987, p. 166-174.

Instead of preparing for space warfare, the USA could make tremendous use of space activities to enhance global security. Arms control verification, environmental monitoring and international cooperation on space missions are important examples. International space year, 1992, could be the time to launch a triumphant effort such as an international mission to Mars. Author

**N87-29900\*#** Lunar and Planetary Inst., Houston, Tex.

**WORKSHOP ON THE EARTH AS A PLANET**

LEWIS ASHWAL, ed., KEVIN BURKE, ed., MAARTEN DEWIT, ed., and GORDON WELLS, ed. 1986 39 p Workshop held in Orlando, Fla., 27 Oct. 1985

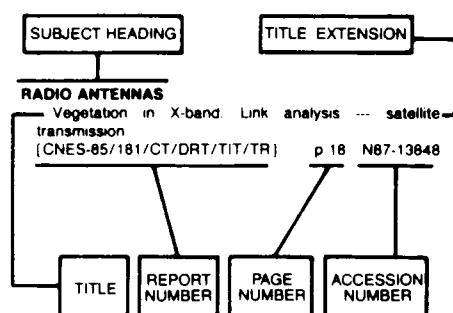
(Contract NASW-4066)

(NASA-CR-180543; NAS 1.26:180543; LPI-TR-86-08) Avail:

NTIS HC A03/MF A01 CSCL 08E

Topics addressed include: remote sensing; petrology; imaging spectroscopy; structural properties; thermal evolution; Earth mantle; early Earth; and megageomorphology. B.G.

## Typical Subject Index Listing



The subject heading is a key to the subject content of the document. The title is used to provide a description of the subject matter. When the title is insufficiently descriptive of the document content, the title extension is added, separated from the title by three hyphens. The (NASA or AIAA) accession number and the page number are included in each entry to assist the user in locating the abstract in the abstract section. If applicable, a report number is also included as an aid in identifying the document. Under any one subject heading, the accession numbers are arranged in sequence with the AIAA accession numbers appearing first.

## A

### ACCURACY

- Radiometric properties of U.S. processed Landsat MSS data p 55 A87-44864
- Maximum accuracy of satellite-borne scatterometer measurements of wind velocity above the ocean p 33 A87-48184
- SPOT localization accuracy and geometric image quality p 57 A87-48662

### ACOUSTIC SCATTERING

- Design study of remote sensing for ocean surface and interior activity [AD-A180578] p 44 N87-25610

### ACOUSTICS

- Design study of remote sensing for ocean surface and interior activity [AD-A180578] p 44 N87-25610
- Wave-theory modelling of convergence zone propagation in the ocean [AD-A183607] p 50 N87-30020

### ADAPTIVE FILTERS

- Speckle noise reduction of 1-look SAR imagery p 65 A87-53273

### ADRIATIC SEA

- Monitoring and modeling of the Adriatic Sea p 46 N87-28133
- ADRIA 84: Airborne investigations of Gelbstoff by optical radiometry and fluorescence lidar --- Adriatic Sea p 46 N87-28154

### ADVECTION

- Large scale ocean-atmosphere interaction in the summer monsoon - The influence of oceanic upwelling and advection on eastern Arabian Sea offshore convection p 36 A87-51585

### AERIAL PHOTOGRAPHY

- Stereoscopic visualization of aerial and space photographs in thematic mapping p 23 A87-42937
- Determination of the external-orientation elements of aerial and space photographs p 55 A87-44301

Color aerial photography in the plant sciences and related fields; Proceedings of the Tenth Biennial Workshop, University of Michigan, Ann Arbor, May 21-24, 1985 p 1 A87-45100

Small format aerial photography for analyzing urban housing problems - A case study in the Bangkok metropolitan region p 17 A87-46309

Multisensor comparison of ice concentration estimates in the marginal ice zone p 31 A87-47295

Possibility of evaluating reservoir influx from aerial and satellite photographs p 51 A87-47577

Analysis of airborne infrared data for interpretative geological mapping of the Brookfield area, Nova Scotia p 24 A87-48804

Large-scale black and white and natural color photographs for the measurement of tree crown areas p 3 A87-48815

Spectral and textural segmentation of multispectral aerial images p 5 A87-48831

Integrated multi-temporal aerial photography and digital mapping for coastal monitoring, Cape Breton Island, Nova Scotia p 34 A87-48837

Colour infrared aerial photography for herbicide drift damage assessment p 6 A87-48864

Indexing small catchments in Java, Indonesia, with respect to their relative susceptibility to erosion p 52 A87-48871

Multispectral video system for airborne remote sensing - Sensitivity, calibrations and correction p 73 A87-48873

Discrimination of suspended sediment and littoral features using multispectral video imagery p 73 A87-48874

Sulphur dioxide damage assessment using colour infrared aerial photography p 60 A87-48884

A trial of oblique imagery from a low cost video camera system for defoliation assessment p 7 A87-48892

Environmental monitoring of Alpine Meadows with large scale aerial photography in Banff National Park p 18 A87-48898

First New Zealand image from the French SPOT satellite p 62 A87-51179

Remote-sensing and geological-geophysical studies of closed platform territories --- Russian book p 26 A87-51875

Sampling semiarid vegetation with large-scale aerial photography p 14 A87-53741

Color infrared video mapping of upland and wetland communities [DE87-010202] p 15 N87-28109

Integration of remote sensing and geophysical data-application to exploration of pyrite ore facies in SW Spain p 27 N87-28119

Evaluation of the range and degradation of mangroves in Southern Sergipe with remote sensing techniques [INPE-4196-PRE/1080] p 16 N87-28160

### AERIAL RECONNAISSANCE

Aircraft microwave radiometry of land p 13 A87-53269

Millimeter-wave imaging sensor data evaluation [NASA-CR-181159] p 77 N87-26264

### AEROMAGNETISM

Remote sensing of deep potential sources over the Nile Delta area p 26 A87-53150

### AEROSPACE ENVIRONMENTS

Space surveillance application potential of Schottky barrier IR sensors [AD-A180848] p 78 N87-27311

### AFRICA

National Climate Program [PB87-190518] p 79 N87-28221

### AFRICAN RIFT SYSTEM

Characteristics of the Gregory Rift (Kenya) dynamics, ground structural analysis, and remote sensing p 23 A87-43353

### AGRICULTURE

Agricultural, hydrologic and oceanographic studies in Bangladesh with NOAA AVHRR data p 57 A87-48365

Stratification of satellite imagery by Uniform Productivity Areas p 5 A87-48840

Comparison of Landsat Thematic Mapper and Multispectral Scanner information content for agricultural applications in Western Canada p 6 A87-48863

Colour infrared aerial photography for herbicide drift damage assessment p 6 A87-48864

Landsat Thematic Mapper data - A useful tool for mapping agricultural areas in Quebec p 6 A87-48867

Spectral studies of dryland agricultural salinity in Western Australia p 8 A87-48901

Effect of resolution on texture application to nearly simultaneous AVHRR and MSS images of an agricultural region p 9 A87-53111

The European Campaign 'AGRISAR '86' p 13 A87-53249

Evaluation of MOMS (Modular Optoelectronic Multispectral Scanner) data for land use/land cover studies - Test site: Piracicaba region, Sao Paulo State, Brazil p 13 A87-53252

A statistical and geometrical edge detector for SAR image segmentation p 13 A87-53275

Study on the use of SAR data for agriculture and forestry p 15 N87-27862

ERAFIS: A computer information system for agriculture and forestry in Spain p 16 N87-28140

### AIR POLLUTION

Biomonitoring plots at the ozone monitoring stations at Great Smoky Mountains National Park, 1985 survey results [PB87-172078] p 19 N87-26464

Effects of ozone on forests in the northeastern United States [DE87-010887] p 16 N87-28190

### AIR QUALITY

Effects of ozone on forests in the northeastern United States [DE87-010887] p 16 N87-28190

### AIR SEA ICE INTERACTIONS

Mesoscale eddies in the Fram Strait marginal ice zone during the 1983 and 1984 Marginal Zone Experiments p 31 A87-47291

On the relationship between atmospheric circulation and the fluctuations in the sea ice extents of the Bering and Okhotsk Seas p 32 A87-47298

### AIR WATER INTERACTIONS

Response of marine atmospheric boundary layer height to sea surface temperature changes - Mixed-layer theory p 34 A87-50277

Large scale ocean-atmosphere interaction in the summer monsoon - The influence of oceanic upwelling and advection on eastern Arabian Sea offshore convection p 36 A87-51585

Moisture transports and budgets of 'moisture bursts' --- of oceanic areas of tropical and subtropical latitudes p 36 A87-51593

Monitoring equatorial Pacific sea level with Geosat p 39 A87-52512

An advanced wind scatterometer for the Columbus Polar Platform payload p 74 A87-53117

The effects of wind-wave coupling on scatterometer wind measurement accuracy p 41 A87-53196

Labrador wind and wave environments [AD-A183218] p 48 N87-29907

### AIRBORNE EQUIPMENT

Multiple-angle observations of reflectance anisotropy from an airborne linear array sensor p 69 A87-43262

Airborne video - Applied to route location studies for electrical power transmission facilities p 17 A87-48802

CCRS airborne Electro-Optical Facility p 72 A87-48852

Using airborne middle-infrared (1.45-2.0 microns) video imagery for distinguishing plant species and soil conditions p 9 A87-53023

Method development and experiences in application of airborne MSS data for forest damage detection p 12 A87-53247

Processing of airborne SAR images of ocean waves p 43 A87-53264

Airborne SAR imaging of azimuthally travelling ocean surface waves - The LEWEX experimental plan p 44 A87-53266



**AIRBORNE LASERS**

Remote sensing of suspended matter in the ocean by airborne lasers and satellite radiometers --- coastal zone color scanner  
[GKSS-86/E/49] p 45 N87-26405

**AIRBORNE SURVEILLANCE RADAR**

Comparison of space and airborne L-HH radar imagery in an agricultural environment p 4 A87-48819  
Iceberg detection using SLAR p 34 A87-48876

**ALBEDO**

Radiation modelling in a high relief environment using a digital terrain model and Landsat - TM imagery p 59 A87-48857

**ALGAE**

Satellite color observations of spring blooming in Bering Sea shelf waters during the ice edge retreat in 1980 p 32 A87-47297

**ALGERIA**

Geomorphological interpretation of the SPOT image of February 23, 1986 concerning Djebel Amour (Algeria) and its border with the Sahara p 25 A87-51145

**ALGORITHMS**

Radiance-ratio algorithm wavelengths for remote oceanic chlorophyll determination p 29 A87-44812  
A microwave radiometer weather-correcting sea ice algorithm p 29 A87-45024  
Evaluation of algorithms for the geometric correction of Thematic Mapper data p 58 A87-48807  
Sequential thinning algorithms for remote sensing application p 63 A87-53140  
Investigation of multi-dimensional algorithms using active and passive microwave data for ice concentration determination p 43 A87-53241  
An algorithm for automatically acquiring ground control points in SAR imagery p 67 N87-27864  
Crop discrimination by means of radar and infrared images p 15 N87-28128  
Brief introduction in statistical pattern recognition [INPE-4206-PRE/1087] p 68 N87-28374  
Satellite image processing for the Agulhas Retroflexion region [AD-A183012] p 68 N87-29905  
NASA sea ice and snow validation plan for the Defense Meteorological Satellite Program special sensor microwave/imager [NASA-TM-100683] p 49 N87-30018

**ALTIMETERS**

Oceanographic and geophysical applications of satellite altimetry p 30 A87-46690  
Global digital topography mapping using a scanning radar altimeter p 76 A87-53227

**ALTIMETRY**

Airborne multibeam radar altimetry --- of oceans p 40 A87-53115  
Deconvolution of sea state parameters from altimeter waveforms p 41 A87-53198

**AMAZON REGION (SOUTH AMERICA)**

The contribution of AVHRR data for measuring and understanding global processes - Large-scale deforestation in the Amazon basin p 11 A87-53151  
Analysis of forest and forest clearings in Amazonia with Landsat and Shuttle Imaging Radar-A data p 13 A87-53250

**AMPLIFIER DESIGN**

Hybrid power amplifier module for X-band p 69 A87-43302

**ANISOTROPIC MEDIA**

Radar polarization signatures of vegetated areas p 11 A87-53202

**ANNUAL VARIATIONS**

Visual interpretation of Landsat MSS quick-look images for the study of the annual swelling of the Niger river in its interior delta, in Mali p 50 A87-44245  
The variability of the North Atlantic marine atmosphere and its relevance to remote sensing p 33 A87-48362

**ANTARCTIC REGIONS**

Antarctic ice streams - A review p 37 A87-51943  
Recent glacial history and rapid ice stream retreat in the Amundsen Sea p 37 A87-51944  
The morphology of ice streams A, B, and C, West Antarctica and their environs p 37 A87-51945  
Ice dynamics at the mouth of ice stream B, Antarctica p 37 A87-51946  
Velocity of ice streams B and C, Antarctica p 37 A87-51947  
Till beneath ice stream B. I - Properties derived from seismic travel times. II - Structure and continuity. III - Till deformation - Evidence and implications. IV - A coupled ice-till flow model --- glacial deposits p 37 A87-51948  
Glaciological studies on Rutford ice stream, Antarctica p 38 A87-51950

**ANTENNAS**

Millimeter-wave imaging sensor data evaluation [NASA-CR-181159] p 77 N87-26264

**APPLICATIONS PROGRAMS (COMPUTERS)**

Data analysis and software support for the Earth radiation budget experiment p 66 N87-26569  
[NASA-CR-178350]  
Satellite image processing for the Agulhas Retroflexion region [AD-A183012] p 68 N87-29905

**AQUATIC PLANTS**

Remote sensing of submerged aquatic vegetation in lower Chesapeake Bay - A comparison of Landsat MSS to TM imagery p 30 A87-46542

**ARCHIPELAGOES**

Remote sensing in Indonesia - A review of the available technology and its applications for resources surveys p 17 A87-46310

**ARCHITECTURE (COMPUTERS)**

A high-throughput system for bulk processing of multispectral imagery p 72 A87-48836

**ARCTIC OCEAN**

Divergent redistribution of ice in the Arctic Ocean (Analysis of space imagery) p 33 A87-48180

**ARCTIC REGIONS**

Operational use of remote sensing for commercial Arctic class vessel navigation p 33 A87-48829  
The influence of melting conditions on the interpretation of radar imagery of sea ice p 34 A87-48849  
Theoretical and experimental study of the radar backscatter of Arctic sea ice p 43 A87-53237  
Vegetation and a LANDSAT-derived land cover map of the Beechey Point quadrangle, Arctic Coastal Plain, Alaska [AD-A180931] p 15 N87-27312  
Arctic drifting buoy data 1979 - 1985 [AD-A182967] p 50 N87-30019  
Satellite-derived ice data sets no. 2: Arctic monthly average microwave brightness temperatures and sea ice concentrations, 1973-1976 [NASA-TM-87825] p 50 N87-30021

**ARGOS SYSTEM**

Interpolation, analysis and archival of data on sea ice trajectories and ocean currents obtained from satellite-linked instruments [PB87-201430] p 48 N87-30010

**ARID LANDS**

Formation of natural underground-water resources in arid regions with special reference to the Dolinoozerskii artesian basin in Mongolia --- Russian book p 50 A87-42911  
Remote sensing in the Sahel - A tool for the inventory and monitoring of resources p 73 A87-48893  
Spectral studies of dryland agricultural salinity in Western Australia p 8 A87-48901  
Sampling semiarid vegetation with large-scale aerial photography p 14 A87-53741

**ARRAYS**

Space surveillance application potential of Schottky barrier IR sensors [AD-A180848] p 78 N87-27311

**ARTIFICIAL INTELLIGENCE**

An expert system for planimetric feature extraction p 63 A87-53139  
Towards the automatic recognition and vectorised description of linear features in LANDSAT TM images by artificial intelligence methods p 67 N87-28142

**ARTIFICIAL SATELLITES**

Data telemetry, assimilation and ocean modeling [AD-A181899] p 47 N87-28239

**ASSIMILATION**

Data telemetry, assimilation and ocean modeling [AD-A181899] p 47 N87-28239

**ASTRODYNAMICS**

Determination of the initial motion conditions of earth-resources satellites according to the photogrammetric processing of topographic photographs oriented in inertial space p 56 A87-47506

**ATLANTIC OCEAN**

Seasat altimetry and the South Atlantic geoid. I - Spectral analysis p 21 A87-45743  
The variability of the North Atlantic marine atmosphere and its relevance to remote sensing p 33 A87-48362  
The dynamics of the northern border of the Gulf Stream revealed by a Tiro-N AVHRR image from October 22, 1980 p 35 A87-51147  
Investigations of relative plate motions in the South Atlantic using Seasat altimeter data p 38 A87-51963  
REX and Geosat - Progress in the first year p 39 A87-52511  
Major morphologic features of the Atlantic Ocean surface p 48 N87-29573  
Proceedings of Atlantic Outer Continental Shelf Region Information Transfer Meeting (ITM) (2nd), January 28-29, 1987 [PB87-200168] p 48 N87-30009

Proceedings of Atlantic Outer Continental Shelf Region Information Transfer Meeting (ITM) (1st), September 4-6, 1985

[PB87-194361] p 48 N87-30011  
Study of physical processes on the US mid-Atlantic continental slope and rise. Volume 1: Executive summary p 48 N87-30012  
[PB87-200515]  
Study of physical processes on the US mid-Atlantic continental slope and rise. Volume 2: Technical presentation p 49 N87-30013  
[PB87-200523]  
Study of physical processes on the US mid-Atlantic continental slope and rise. Volume 3: Appendix p 49 N87-30014  
[PB87-200531]  
Physical oceanographic study of Florida's Atlantic Coast region: Florida Atlantic Coast Transport Study (FACTS). Volume 3: Appendices p 49 N87-30017  
[PB87-201018]  
Wave-theory modelling of convergence zone propagation in the ocean p 50 N87-30020  
[AD-A183607]

**ATMOSPHERIC ATTENUATION**

Scattering parameters for aspherical hydrometeors at microwave frequencies p 53 A87-53271

**ATMOSPHERIC BOUNDARY LAYER**

Response of marine atmospheric boundary layer height to sea surface temperature changes - Mixed-layer theory p 34 A87-50277  
A comparison of the significant features of the marine boundary layers over the Arabian Sea and the Bay of Bengal during Monex 79 p 36 A87-51594

**ATMOSPHERIC CIRCULATION**

Moisture bursts over the tropical Pacific Ocean p 28 A87-43345  
On the relationship between atmospheric circulation and the fluctuations in the sea ice extents of the Bering and Okhotsk Seas p 32 A87-47298  
Observing systems experiments for the onset vortex during Summer Monex p 35 A87-51552  
Use of IR satellite rainfall estimates in diagnosing thermally forced circulations in the Pacific during FGGE SOP-1 p 36 A87-51580

**ATMOSPHERIC COMPOSITION**

Successes of Cosmos-1500 satellite, SLR system p 45 N87-27696

**ATMOSPHERIC CORRECTION**

Multiple-angle observations of reflectance anisotropy from an airborne linear array sensor p 69 A87-43262  
Atmospheric correction of data measured by a flying platform over the sea - Elements of a model and its experimental validation p 35 A87-50292

**ATMOSPHERIC EFFECTS**

Atmospheric effects on Landsat TM thermal IR data p 65 A87-53254

**ATMOSPHERIC MODELS**

A space-time stochastic model of rainfall for satellite remote-sensing studies p 54 A87-54157

**ATMOSPHERIC MOISTURE**

Moisture bursts over the tropical Pacific Ocean p 28 A87-43345  
Estimation of errors in the determination of sea surface temperature and atmospheric moisture content from satellite measurements of outgoing IR radiation in the 10.5-12.5 micron range p 33 A87-48178  
Wintertime disturbances in the tropical Pacific - FGGE IIb and satellite comparisons p 36 A87-51560  
Moisture transports and budgets of 'moisture bursts' --- of oceanic areas of tropical and subtropical latitudes p 36 A87-51593

**ATMOSPHERIC RADIATION**

Radiation modelling in a high relief environment using a digital terrain model and Landsat - TM imagery p 59 A87-48857

**ATMOSPHERIC SOUNDING**

Calibration of NOAA-7 AVHRR, GOES-5, and GOES-6 VISSR/VAS solar channels p 69 A87-44865

**AUTOMATION**

The automatic generation of digital terrain models from satellite images by stereo p 58 A87-48669  
Automatic focusing of synthetic aperture radar images of diffuse targets p 64 A87-53213

**AZIMUTH**

Azimuthal dependence in the gravity field induced by recent and past cryospheric forcings p 35 A87-51487

**B****BACKSCATTERING**

The detection of wetlands on radar imagery p 6 A87-48855  
Estimation of X-band scattering properties of tree components p 13 A87-53277

**BANGLADESH**

Agricultural, hydrologic and oceanographic studies in Bangladesh with NOAA AVHRR data p 57 A87-48365

**BATHYMETERS**

Shallow water bathymetry and bottom classification by means of the Landsat and SPOT optical scanners p 52 A87-48670

An operational multispectral scanner for bathymetric surveys - The ABS NORDA scanner p 42 A87-53199

**BATHYTHERMOGRAPHS**

REX and Geosat - Progress in the first year p 39 A87-52511

**BAYS (TOPOGRAPHIC FEATURES)**

Comparison of numerical simulations with SAR images of ocean surface waves in the New York Bight p 44 A87-53287

**BEARING (DIRECTION)**

Arctic drifting buoy data 1979 - 1985 [AD-A182967] p 50 N87-30019

**BEAUFORT SEA (NORTH AMERICA)**

Beaufort-Chukchi ice margin data from Seasat - Ice motion p 32 A87-47299  
Using NOAA AVHRR in studies of sea ice motion in the Beaufort Sea p 34 A87-48842

**BEDROCK**

Application of remote sensing data to bedrock geological interpretation, Black River-Matheson area, Northern Ontario, Canada p 24 A87-48832

**BERING SEA**

Satellite color observations of spring blooming in Bering Sea shelf waters during the ice edge retreat in 1980 p 32 A87-47297

On the relationship between atmospheric circulation and the fluctuations in the sea ice extents of the Bering and Okhotsk Seas p 32 A87-47298

**BIOCHEMISTRY**

Estimating key forest ecosystem parameters through remote sensing p 12 A87-53245

**BIOMASS**

Potential application of multipolarization SAR for pine-plantation biomass estimation p 1 A87-43263  
Detecting forest structure and biomass with C-band multipolarization radar - Physical model and field tests p 2 A87-46543

**BIOSPHERE**

The closed ecology project - Agricultural and life sciences background [AAS PAPER 86-120] p 9 A87-53093

**BRAZIL**

Evaluation of the range and degradation of mangroves in Southern Sergipe with remote sensing techniques [INPE-4196-PRE/1080] p 16 N87-28160

**BRIGHTNESS TEMPERATURE**

Satellite-derived ice data sets no. 2: Arctic monthly average microwave brightness temperatures and sea ice concentrations, 1973-1976 [NASA-TM-57825] p 50 N87-30021

**BUOYS**

Upwelling filaments and motion of a satellite-tracked drifter along the west coast of North America p 29 A87-45023

Measurement of currents according to the drift of subsatellite buoys p 32 A87-48177

Interpolation, analysis and archival of data on sea ice trajectories and ocean currents obtained from satellite-linked instruments [PB87-201430] p 48 N87-30010

Arctic drifting buoy data 1979 - 1985 [AD-A182967] p 50 N87-30019

**C****C BAND**

Detecting forest structure and biomass with C-band multipolarization radar - Physical model and field tests p 2 A87-46543

Comparison of C-band synthetic aperture radar (SAR) data according to two different depression angles for agricultural applications p 4 A87-48820

**CALDERAS**

Use of TM Landsat data as a support to classical ground-based methodologies in the investigation of a volcanic site in central Italy - The Caldera of Latara p 26 A87-53244

**CALIBRATING**

Reflectance- and radiance-based methods for the in-flight absolute calibration of multispectral sensors p 69 A87-44863

Calibration of NOAA-7 AVHRR, GOES-5, and GOES-6 VISSR/VAS solar channels p 69 A87-44865

Calibration requirements and methodology for remote sensors viewing the ocean in the visible p 29 A87-44866

Practical aspects of achieving accurate radiometric field measurements p 69 A87-44868

Absolute calibration of the SPOT-1 HRV cameras p 71 A87-48660

Correction of the sensor degradation of the Coastal Zone Color Scanner on NIMBUS-7 p 46 N87-28153

Calibrated L-band terrain measurements and analysis program [AD-A182917] p 68 N87-29722

Use of LANDSAT digital data for snow cover mapping in the upper Saint John River Basin, Maine [AD-A183213] p 54 N87-29906

**CALIFORNIA**

Vegetation mapping and stress detection in the Santa Monica Mountains, California p 12 A87-53246

**CAMERAS**

Some results of the Metric Camera (MC) Mission-1 on Spacelab p 70 A87-47175

Absolute calibration of the SPOT-1 HRV cameras p 71 A87-48660

A trial of oblique imagery from a low cost video camera system for defoliation assessment p 7 A87-48892

Point positioning and mapping with large format camera data p 73 A87-50226

**CANADA**

Within-scene radiometric correction of Landsat Thematic Mapper (TM) data in Canadian production systems p 57 A87-48656

**CANOPIES (VEGETATION)**

Radar observations of terrestrial vegetation covers in the 3-cm range p 1 A87-42936

Color aerial photography in the plant sciences and related fields; Proceedings of the Tenth Biennial Workshop, University of Michigan, Ann Arbor, May 21-24, 1985 p 1 A87-45100

Monte Carlo calculation of the dependence of the spectral radiance of vegetation cover on the illumination conditions p 2 A87-48190

Monitoring wheat canopies with a high spectral resolution radiometer p 8 A87-53019

Thematic Mapper response to heavy metal related changes in Canopy LAI of a mixed forest p 12 A87-53248

Modeling gap probability in discontinuous vegetation canopies p 13 A87-53276

Remote sensing of earth terrain [NASA-CR-181370] p 79 N87-28957

**CELESTIAL GEODESY**

New possibilities for the use of gravity data in the realization of geodetic coordinate systems p 21 A87-42939

Earth gravity model improvement - An alternative method for Doppler-tracked satellites p 21 A87-45817

**CENTIMETER WAVES**

Radar observations of terrestrial vegetation covers in the 3-cm range p 1 A87-42936

**CHANGE DETECTION**

The role of remote sensing in the Canada Land Use Monitoring Program (CLUMP) p 18 A87-48895

Thematic Mapper response to heavy metal related changes in Canopy LAI of a mixed forest p 12 A87-53248

**CHARACTERIZATION**

Characterizing the Chesapeake Bay ecosystem and lessons learned [PB87-166930] p 19 N87-26463

**CHESAPEAKE BAY (US)**

Characterizing the Chesapeake Bay ecosystem and lessons learned [PB87-166930] p 19 N87-26463

**CHLOROPHYLLS**

Multiplatform sampling (ship, aircraft, and satellite) of a Gulf Stream warm core ring p 29 A87-44811

Radiance-ratio algorithm wavelengths for remote oceanic chlorophyll determination p 29 A87-44812

Evaluation of the potential of the Thematic Mapper for marine application p 46 N87-28134

**CHUKCHI SEA**

Beaufort-Chukchi ice margin data from Seasat - Ice motion p 32 A87-47299

Interpolation, analysis and archival of data on sea ice trajectories and ocean currents obtained from satellite-linked instruments [PB87-201430] p 48 N87-30010

**CITIES**

Small format aerial photography for analyzing urban housing problems - A case study in the Bangkok metropolitan region p 17 A87-46309

Moscow seen by satellite - Another image of Soviet urban geography p 80 A87-51143

Analysis of environmental information of urban areas using Landsat TM data p 19 A87-53187

**CLASSIFICATIONS**

Discrimination of natural and cultivated vegetation using Thematic Mapper spectral data p 2 A87-48673

Digital image classification approach for estimating forest clearing and regrowth rates and trends p 10 A87-53123

Vegetation and a LANDSAT-derived land cover map of the Beechey Point quadrangle, Arctic Coastal Plain, Alaska [AD-A180931] p 15 N87-27312

Rural land use inventory and mapping in the Ardeche area (France). Improvement of automatic classification by multitemporal analysis of TM data p 15 N87-28127

Brief introduction in statistical pattern recognition [INPE-4206-PRE/1087] p 68 N87-28374

**CLIMATOLOGY**

Indices of climatological and hydrological variability derived from satellite imagery for the South Saskatchewan River Basin p 52 A87-48856

The global forest ecosystem as viewed by ERS-1, SIR-C and EOS p 12 A87-53217

The First ISLSCP Field Experiment (FIFE) p 12 A87-53218

Investigating the role of the land surface in explaining the interannual variation of the net radiation balance over the Western Sahara and sub-Sahara [NASA-CR-181183] p 68 N87-28197

National Climate Program [PB87-190518] p 79 N87-28221

Labrador wind and wave environments [AD-A183218] p 48 N87-29907

**CLOSED ECOLOGICAL SYSTEMS**

The closed ecology project - Agricultural and life sciences background [AAS PAPER 86-120] p 9 A87-53093

Investigation of causes of hydrogen sulfide formation in reclaimed water p 14 N87-23136

**CLOUD COVER**

Analysis of Cosmos-1500 radar images of the ocean surface in a zone of cyclones and mesoscale cloud formations p 32 A87-48176

Cloud screening for determination of land surface characteristics in a reduced resolution satellite data set p 56 A87-48361

Cloud and moisture fields derived from the GLA retrievals of HIRS2/MSU data p 36 A87-51579

Improved cloud analysis using visible, near-infrared, infrared, and microwave imagery p 62 A87-53103

How useful is Landsat monitoring? p 14 A87-54089

**CLOUD PHOTOGRAPHY**

Cloud detection in NOAA images p 67 N87-28124

**CLOUDS (METEOROLOGY)**

Moisture bursts over the tropical Pacific Ocean p 28 A87-43345

Size distributions of clouds in real time from satellite imagery p 56 A87-48359

The effect of subpixel clouds on remote sensing p 2 A87-48360

A pattern analysis technique for distinguishing surface and cloud types in the polar regions p 66 A87-53289

**CLUSTER ANALYSIS**

Cluster based segmentation of multi-temporal Thematic Mapper data as preparation of region-based agricultural land-cover analysis p 9 A87-53109

**CLUTTER**

Calibrated L-band terrain measurements and analysis program [AD-A182917] p 68 N87-29722

**COASTAL CURRENTS**

Physical oceanographic study of Florida's Atlantic Coast region: Florida Atlantic Coast Transport Study (FACTS). Volume 1: Executive summary [PB87-200994] p 49 N87-30015

Physical oceanographic study of Florida's Atlantic Coast region: Florida Atlantic Coast Transport Study (FACTS), volume 2 [PB87-201000] p 49 N87-30016

**COASTAL ECOLOGY**

Integrated multi-temporal aerial photography and digital mapping for coastal monitoring, Cape Breton Island, Nova Scotia p 34 A87-48837

**COASTAL PLAINS**

Vegetation and a LANDSAT-derived land cover map of the Beechey Point quadrangle, Arctic Coastal Plain, Alaska [AD-A180931] p 15 N87-27312

**COASTAL WATER**

Upwelling filaments and motion of a satellite-tracked drifter along the west coast of North America p 29 A87-45023

Monitoring and modeling of the Adriatic Sea p 46 N87-28133

Physical oceanographic study of Florida's Atlantic Coast region: Florida Atlantic Coast Transport Study (FACTS). Volume 3: Appendices [PB87-201018] p 49 N87-30017

**COASTAL ZONE COLOR SCANNER**

Reflectance- and radiance-based methods for the in-flight absolute calibration of multispectral sensors p 69 A87-44863

Remote observations of the marine environment - Spatial heterogeneity of the mesoscale ocean color field in CZCS imagery of California near-coastal waters

p 30 A87-46539

Remote sensing of suspended matter in the ocean by airborne lasers and satellite radiometers --- coastal zone color scanner

[GKSS-86/E/49] p 45 N87-26405

Coastal Zone Color Scanner (CZCS) images and ocean dynamics. Application to the Northwest African upwelling area

p 46 N87-28146

Correction of the sensor degradation of the Coastal Zone Color Scanner on NIMBUS-7

p 46 N87-28153

## COASTS

Remote sensing of coastal wetlands

p 1 A87-40944

Vegetation and a LANDSAT-derived land cover map of the Beechey Point quadrangle, Arctic Coastal Plain, Alaska

[AD-A180931] p 15 N87-27312

Comparison of satellite-derived ocean velocities with observations in the California coastal region

[AD-A182291] p 47 N87-28242

## COLLINEARITY

Geometric correction of space images by the collinearity-equation method

p 61 A87-51175

## COLOR

Enhancement of colors in remote sensing images using rotation of the matrix at the IHS coordinates

[INPE-4207-PRE/1088] p 67 N87-28165

## COLOR CODING

Interpreting meteorological satellite images using a color-composite technique

p 62 A87-52795

Color enhancement of highly correlated images. II - Channel ratio and 'chromaticity' transformation techniques

p 62 A87-53018

## COLOR INFRARED PHOTOGRAPHY

Analysis of airborne infrared data for interpretative geological mapping of the Brookfield area, Nova Scotia

p 24 A87-48804

Colour infrared aerial photography for herbicide drift damage assessment

p 6 A87-48864

Sulphur dioxide damage assessment using colour infrared aerial photography

p 60 A87-48884

## COLOR PHOTOGRAPHY

Color aerial photography in the plant sciences and related fields; Proceedings of the Tenth Biennial Workshop, University of Michigan, Ann Arbor, May 21-24, 1985

p 1 A87-45100

Airborne video - Applied to route location studies for electrical power transmission facilities

p 17 A87-48802

Discrimination of suspended sediment and littoral features using multispectral video imagery

p 73 A87-48874

## COMMERCIAL SPACECRAFT

The SPOT program - Commercialization of remote sensing

p 80 A87-53235

## COMPUTATION

Calculation and accuracy of ERBE scanner measurement locations

[NASA-TP-2670] p 47 N87-28471

## COMPUTER AIDED MAPPING

Snowpack depletion monitoring in Alberta using computer-processed NOAA imagery

p 52 A87-48848

Remote sensing and the agricultural resource inventory

p 8 A87-48899

A revolution in the production of small-scale and medium-scale maps

p 61 A87-48904

Computer-assisted map analysis - Extending the utility of GIS technology

p 18 A87-48907

Integration of topographic data with synthetic aperture radar data for determining forest properties in mountainous terrain

p 14 A87-53278

A methodology for evaluation of an interactive multispectral image processing system

p 66 A87-53999

## COMPUTER GRAPHICS

Regional geobotany with TM - A Sudbury case study

p 25 A87-48861

## COMPUTER PROGRAMMING

Data analysis and software support for the Earth radiation budget experiment

[NASA-CR-178350] p 66 N87-26569

## COMPUTER PROGRAMS

A program for the combined adjustment of VLBI observing sessions

p 22 A87-52766

The Land Analysis System (LAS) - A general purpose system for multispectral image processing

p 64 A87-53230

## COMPUTER SYSTEMS DESIGN

A high-throughput system for bulk processing of multispectral imagery

p 72 A87-48836

## COMPUTER SYSTEMS PERFORMANCE

Comparison of visual and automated lineament analyses on LANDSAT MSS image from south Greenland

p 67 N87-28144

## COMPUTER SYSTEMS PROGRAMS

Precise orbit determination with the Doppler Orbitography and Radio positioning Integrated by Satellite (DORIS) system and the associated Zealous for Orbit Observation Methods (ZOOM) software

p 77 N87-25382

Integrated systems for remote sensing

p 67 N87-28143

## COMPUTER TECHNIQUES

Satellite image processing for the Agulhas Retroflexion region

[AD-A183012] p 68 N87-29905

## COMPUTER VISION

Data correction for automated remote sensing image interpretation

p 64 A87-53209

## CONFERENCES

Color aerial photography in the plant sciences and related fields; Proceedings of the Tenth Biennial Workshop, University of Michigan, Ann Arbor, May 21-24, 1985

p 1 A87-45100

Earth remote sensing using the Landsat Thematic Mapper and SPOT sensor systems; Proceedings of the Meeting, Innsbruck, Austria, Apr. 15-17, 1986

[SPIE-660] p 70 A87-48652

Canadian Symposium on Remote Sensing, 10th, Edmonton, Canada, May 5-8, 1986, Proceedings. Volume 1 & 2

p 72 A87-48801

IGARSS '87 - International Geoscience and Remote Sensing Symposium, University of Michigan, Ann Arbor, May 18-21, 1987, Digest. Volumes 1 & 2

p 73 A87-53101

The International Symposium on Microwave Signatures and Remote Sensing held in Gothenburg (Sweden) on 19-22 January 1987

[AD-A181334] p 78 N87-27314

Proceedings of the SAR Applications Workshop --- Synthetic Aperture Radar

[ESA-SP-264] p 78 N87-27854

Proceedings of the ESA-EARSel Europe from Space Symposium

[ESA-SP-258] p 19 N87-28115

Workshop on The Earth as a Planet

[NASA-CR-180543] p 81 N87-29900

Proceedings of Atlantic Outer Continental Shelf Region Information Transfer Meeting (ITM) (2nd), January 28-29, 1987

[PB87-200168] p 48 N87-30009

Proceedings of Atlantic Outer Continental Shelf Region Information Transfer Meeting (ITM) (1st), September 4-6, 1985

[PB87-194361] p 48 N87-30011

## CONIFERS

Potential application of multipolarization SAR for pine-plantation biomass estimation

p 1 A87-43263

Relationship of Thematic Mapper simulator data to leaf area index of temperate coniferous forests

p 8 A87-53017

## CONTINENTAL SHELVES

Proceedings of Atlantic Outer Continental Shelf Region Information Transfer Meeting (ITM) (2nd), January 28-29, 1987

[PB87-200168] p 48 N87-30009

Proceedings of Atlantic Outer Continental Shelf Region Information Transfer Meeting (ITM) (1st), September 4-6, 1985

[PB87-194361] p 48 N87-30011

Study of physical processes on the US mid-Atlantic continental slope and rise. Volume 1: Executive summary

[PB87-200515] p 48 N87-30012

Study of physical processes on the US mid-Atlantic continental slope and rise. Volume 2: Technical presentation

[PB87-200523] p 49 N87-30013

Study of physical processes on the US mid-Atlantic continental slope and rise. Volume 3: Appendix

[PB87-200531] p 49 N87-30014

## CONTOUR SENSORS

Observations of and a new model for fetch-limited wave growth

p 43 A87-53263

## CONVECTION CLOUDS

Satellite observations of convection during the summer monsoon of 1979

p 36 A87-51587

## CONVECTIVE FLOW

Large scale ocean-atmosphere interaction in the summer monsoon - The influence of oceanic upwelling and advection on eastern Arabian Sea offshore convection

p 36 A87-51585

## CONVERGENCE

Wave-theory modelling of convergence zone propagation in the ocean

[AD-A183607] p 50 N87-30020

## CORAL REEFS

Coral reef survey method for verification of Landsat MSS image data

p 30 A87-46311

Managing coral reefs - Operational benefits of remote sensing in Marine Park planning

p 34 A87-48851

## COSMOS SATELLITES

Successes of Cosmos-1500 satellite, SLR system

p 45 N87-27696

## COVARIANCE

Estimation and modelling of the local empirical covariance function using gravity and satellite altimeter data

p 22 A87-54325

## CROP IDENTIFICATION

Use of rice response characteristics in classification using Landsat MSS digital data

p 1 A87-45046

Monitoring rice areas using Landsat MSS data

p 1 A87-45047

Discrimination of natural and cultivated vegetation using Thematic Mapper spectral data

p 2 A87-48673

Operational, province wide crop area estimation for Manitoba

p 3 A87-48811

Comparison of C-band synthetic aperture radar (SAR) data according to two different depression angles for agricultural applications

p 4 A87-48820

Effects of surface geometry of agricultural fields on radar airborne imagery in X- and C-bands

p 5 A87-48846

An evaluation of Landsat TM and MSS data for crop identification in Manitoba

p 6 A87-48859

Ground targets for the radiometric correction of AVHRR imagery for crop monitoring

p 7 A87-48887

Cluster based segmentation of multi-temporal Thematic Mapper data as preparation of region-based agricultural land-cover analysis

p 9 A87-53109

How useful is Landsat monitoring?

p 14 A87-54089

Crop discrimination by means of radar and infrared images

p 15 N87-28128

## CROP INVENTORIES

Operational, province wide crop area estimation for Manitoba

p 3 A87-48811

Application of image segmentation algorithms to the inventory of crops in Canada

p 3 A87-48813

Using AVHRR data to evaluate the greenness variability within monitoring polygons

p 4 A87-48828

National land use mapping - The application of low altitude sample photography

p 17 A87-48858

Technological feasibility to mobilization for operations - The NOAA crop monitoring case

p 6 A87-48878

Remote sensing and the agricultural resource inventory

p 8 A87-48899

Crop inventorying of small-parcelled areas using SPOT- and TM-data in conjunction with field radiometric measurements

p 10 A87-53126

Rural land use inventory and mapping in the Ardeche area (France). Improvement of automatic classification by multitemporal analysis of TM data

p 15 N87-28127

National Climate Program

[PB87-190518] p 79 N87-28221

## CROPS

The European Campaign 'AGRISAR '86'

p 13 A87-53249

## CROSS POLARIZATION

On the origin of cross-polarization in remote sensing

p 75 A87-53168

## CRUSTAL FRACTURES

Geoid anomalies across Ascension fracture zone and the cooling of the lithosphere

p 21 A87-44352

Mechanisms of crustal deformation in the western US

[NASA-CR-181230] p 27 N87-28200

## CYCLOGENESIS

Analysis of Cosmos-1500 radar images of the ocean surface in a zone of cyclones and mesoscale cloud formations

p 32 A87-48176

## CYCLOONES

Latent heat and cyclone activity in the South Pacific, 10-18 January 1979

p 37 A87-51603

**D**

## DAMAGE ASSESSMENT

Colour infrared aerial photography for herbicide drift damage assessment

p 6 A87-48864

Sulphur dioxide damage assessment using colour infrared aerial photography

p 60 A87-48884

Method development and experiences in application of airborne MSS data for forest damage detection

p 12 A87-53247

Monitoring and inventorying of forest damages by use of LANDSAT TM data

p 16 N87-28138

## DATA ACQUISITION

Study of physical processes on the US mid-Atlantic continental slope and rise. Volume 1: Executive summary

[PB87-200515] p 48 N87-30012

## SUBJECT INDEX

- Satellite-derived ice data sets no. 2: Arctic monthly average microwave brightness temperatures and sea ice concentrations, 1973-1976  
[NASA-TM-87825] p 50 N87-30021
- DATA BASES**  
The CCRS SAR/MSS Anderson River data set p 55 A87-43261  
TM sensor performance as obtained from Earthnet quality control data base p 71 A87-48659
- DATA COMPRESSION**  
Information content analysis of Landsat image data for compression p 56 A87-47046  
Spectral feature design for data compression in high dimensional multispectral data p 64 A87-53183
- DATA MANAGEMENT**  
Solid earth geophysics: Data services [PB87-184107] p 66 N87-27352
- DATA PROCESSING**  
A program for the combined adjustment of VLBI observing sessions p 22 A87-52766  
Data analysis and software support for the Earth radiation budget experiment [NASA-CR-178350] p 66 N87-26569  
Investigating the role of the land surface in explaining the interannual variation of the net radiation balance over the Western Sahara and sub-Sahara [NASA-CR-181183] p 68 N87-28197
- DATA REDUCTION**  
Integration of radiometric and Landsat digital data for geologic investigation and exploration, Guysborough area, Nova Scotia p 24 A87-48803
- DATA RETRIEVAL**  
Cloud and moisture fields derived from the GLA retrievals of HIRS/MSU data p 36 A87-51579
- DATA SIMULATION**  
Classification of geomorphic features and landscape stability in northwestern New Mexico using simulated SPOT imagery p 56 A87-46540  
Validation and simulation of Radarsat imagery p 60 A87-48883  
Relationship of Thematic Mapper simulator data to leaf area index of temperate coniferous forests p 8 A87-53017  
Some results of MOS-1 airborne verification experiment - MSR (microwave scanning radiometer) p 76 A87-53229
- DATA SMOOTHING**  
Spatial filtering of digital Landsat data for the extraction of mapping information p 58 A87-48805  
Smoothing vegetation index profiles - An alternative method for reducing radiometric disturbance in NOAA-AVHRR data p 14 A87-53996
- DATA SYSTEMS**  
New system for the ordering, archiving and retrieval of data from earth's resource satellites p 60 A87-48889  
A systems approach to the design of the Eos data and information system p 64 A87-53207
- DATA TRANSFER (COMPUTERS)**  
An application for the testing and use of the standard data transfer format -- for remotely sensed classified information transmission to GIS center p 18 A87-48886
- DAYTIME**  
Space surveillance application potential of Schottky barrier IR sensors [AD-A180848] p 78 N87-27311
- DEATH VALLEY (CA)**  
Kinematics at the intersection of the Garlock and Death Valley fault zones, California: Integration of TM data and field studies. LANDSAT TM investigation proposal TM-019 [NASA-CR-180666] p 27 N87-28208
- DECISION THEORY**  
Hierarchical classification with knowledge based binary decision -- for thematic mapping image interpretation p 62 A87-53110
- DEFENSE PROGRAM**  
NASA sea ice and snow validation plan for the Defense Meteorological Satellite Program special sensor microwave/imager [NASA-TM-100683] p 49 N87-30018
- DEFOLIATION**  
A trial of oblique imagery from a low cost video camera system for defoliation assessment p 7 A87-48892
- DEFORESTATION**  
Digital image classification approach for estimating forest clearing and regrowth rates and trends p 10 A87-53123  
The contribution of AVHRR data for measuring and understanding global processes - Large-scale deforestation in the Amazon basin p 11 A87-53151  
Analysis of forest and forest clearings in Amazonia with Landsat and Shuttle Imaging Radar-A data p 13 A87-53250

- DEFORMATION**  
Mechanisms of crustal deformation in the western US [NASA-CR-181230] p 27 N87-28200
- DELTA**  
Visual interpretation of Landsat MSS quick-look images for the study of the annual swelling of the Niger river in its interior delta, in Mali p 50 A87-44245
- DEPTH MEASUREMENT**  
Shallow water bathymetry and bottom classification by means of the Landsat and SPOT optical scanners p 52 A87-48670  
An operational multispectral scanner for bathymetric surveys - The ABS NORDA scanner p 42 A87-53199
- DESERTS**  
Selection of extended area land target sites for the calibration of spaceborne scatterometers p 74 A87-53118  
Science synergism study for EOS on evolution of desert surfaces p 12 A87-53214
- DESIGN ANALYSIS**  
Investigation of design parameters for ERS-1 wind scatterometer p 74 A87-53116
- DETECTION**  
The feasibility of detecting a magnetic field from a distant platform [AD-A180635] p 78 N87-27310  
Space surveillance application potential of Schottky barrier IR sensors [AD-A180848] p 78 N87-27311
- DIAMAGNETISM**  
Meissner effect in high-Tc superconductive thin films p 35 A87-51532
- DICTIONARIES**  
Geodetic glossary [PB87-181210] p 22 N87-26562
- DIELECTRIC PROPERTIES**  
The potential of SAR in a snow and glacier monitoring system p 45 N87-27856
- DIFFUSE RADIATION**  
Automatic focusing of synthetic aperture radar images of diffuse targets p 64 A87-53213
- DIGITAL DATA**  
Integration of radiometric and Landsat digital data for geologic investigation and exploration, Guysborough area, Nova Scotia p 24 A87-48803  
Spatial filtering of digital Landsat data for the extraction of mapping information p 58 A87-48805  
Evaluation of algorithms for the geometric correction of Thematic Mapper data p 58 A87-48807  
Processing of Seasat altimetry data on a digital image analysis system p 59 A87-48825  
A high-throughput system for bulk processing of multispectral imagery p 72 A87-48836  
CCRS airborne Electro-Optical Facility p 72 A87-48852  
Digital SAR-Landsat combination for geologic mapping p 24 A87-48853  
Applications of satellite derived digital elevation models for resource mapping p 60 A87-48866  
Digital image classification approach for estimating forest clearing and regrowth rates and trends p 10 A87-53123  
Global digital topography mapping using a scanning radar altimeter p 76 A87-53227  
Digital data from shuttle photography: The effects of platform variables p 66 N87-26697
- DIGITAL RADAR SYSTEMS**  
The operational use of RADARSAT products by the ice centre environment Canada p 61 A87-48906  
A high speed digital processor for real-time synthetic aperture radar imaging p 64 A87-53233
- DIGITAL SIMULATION**  
Digital elevation model extraction from stereo satellite images p 63 A87-53142
- DIGITAL SYSTEMS**  
Use of LANDSAT digital data for snow cover mapping in the upper Saint John River Basin, Maine [AD-A183213] p 54 N87-29906
- DIGITAL TECHNIQUES**  
Progress on digital algorithms for deriving sea ice parameters from SAR data p 43 A87-53238  
Enhancement of colors in remote sensing images using rotation of the matrix at the IHS coordinates [INPE-4207-PRE/1088] p 67 N87-28165
- DISASTERS**  
Contribution of space technology to disaster preparedness, warning, and relief p 20 N87-28130  
The role and perspective of remote sensing for disaster management in the European community p 20 N87-28137
- DISPERSIONS**  
Remote sensing of suspended matter in the ocean by airborne lasers and satellite radiometers -- coastal zone color scanner [GKSS-86/E/49] p 45 N87-26405

## EARTH OBSERVATIONS (FROM SPACE)

- DISPLAY DEVICES**  
Space surveillance application potential of Schottky barrier IR sensors [AD-A180848] p 78 N87-27311  
A user's guide for the Analytical Photogrammetric Positioning System (APPS) [AD-A183773] p 79 N87-29909
- DISTRIBUTION (PROPERTY)**  
Divergent redistribution of ice in the Arctic Ocean (Analysis of space imagery) p 33 A87-48180
- DOPPLER RADAR**  
Inverse synthetic aperture radar imaging techniques for sea-surface targets p 41 A87-53189
- DRAINAGE**  
A methodology for automated extraction of drainage networks from satellite imagery p 53 A87-48880  
Remote sensing as a tool for Alberta Agricultural Wetlands Drainage Inventory p 6 A87-48882  
Sequential thinning algorithms for remote sensing application p 63 A87-53140
- DRAINAGE PATTERNS**  
The detection of soil drainage by using Landsat MSS and TM (Belgian test zones) p 11 A87-53205  
Detection of soil drainage in Pays de Herve, Belgium, on LANDSAT MSS imagery p 15 N87-28129
- DRIFT RATE**  
Measurement of currents according to the drift of subsatellite buoys p 32 A87-48177
- DROUGHT**  
Comparison of NOAA AVHRR data to meteorologic drought indices p 14 A87-53997  
National Climate Program [PB87-190518] p 79 N87-28221
- DUNES**  
Multifrequency and multipolarization radar scatterometry of sand dunes and comparison with spaceborne and airborne radar images p 70 A87-47257
- E**
- EARTH ATMOSPHERE**  
The variability of the North Atlantic marine atmosphere and its relevance to remote sensing p 33 A87-48362  
A pattern analysis technique for distinguishing surface and cloud types in the polar regions p 66 A87-53289  
Calculation and accuracy of ERBE scanner measurement locations [NASA-TP-2670] p 47 N87-28471
- EARTH HYDROSPHERE**  
Remote sensing techniques for the study of hydrological elements p 51 A87-47576  
Water-cycle processes in geosystems and the possibility of the remote sensing of the moisture content of the underlying surface p 51 A87-47580  
Remote-sensing evaluation of the spatial variability of evaporation p 52 A87-47583  
Remote-sensing techniques for investigating the structure of radiation-heat fluxes and the moisture content of geosystems in connection with the problem of monitoring the water component p 52 A87-47584
- EARTH MANTLE**  
Azimuthal dependence in the gravity field induced by recent and past cryospheric forcings p 35 A87-51487  
Workshop on The Earth as a Planet [NASA-CR-180543] p 81 N87-29900
- EARTH MOVEMENTS**  
Pleistocene earth movements in Peninsular India - Evidences from Landsat MSS and Thematic Mapper data p 26 A87-53242
- EARTH OBSERVATIONS (FROM SPACE)**  
Second generation high-resolution space systems - First results of the SPOT-1 satellite p 55 A87-44244  
The Land Satellite (Landsat) system - Earth Observation Satellite Company (Eosat's) plans for Landsat-6 and beyond p 71 A87-48676  
Eurimage sets up shop p 80 A87-51324  
Status of and prognosis for space remote sensing [AAS PAPER 86-104] p 80 A87-53084  
IGARSS '87 - International Geoscience and Remote Sensing Symposium, University of Michigan, Ann Arbor, May 18-21, 1987, Digest, Volumes 1 & 2 p 73 A87-53101  
MODIS - Advanced facility instrument for studies of the earth as a system -- Moderate Resolution Imaging Spectrometer p 40 A87-53144  
European dissemination of Marine Observation Satellite (MOS-1) data p 44 A87-53925  
The Bakerian Lecture, 1986 - Ships from space -- wakes behind surface vessels observed from space p 44 A87-54301  
Digital data from shuttle photography: The effects of platform variables p 66 N87-26697  
Contribution of space technology to disaster preparedness, warning, and relief p 20 N87-28130

- Monitoring and modeling of the Adriatic Sea p 46 N87-28133
- EARTH OBSERVING SYSTEM (EOS)**
- Earth resources instrumentation for the Space Station Polar Platform p 69 A87-44184
- The high resolution imaging spectrometer (HIRIS) for EOS p 74 A87-53145
- Spaceborne laser ranging from EOS p 22 A87-53146
- Spaceborne imaging radar on EOS p 63 A87-53148
- A systems-approach to the design of the Eos data and information system p 64 A87-53207
- Science synergism study for EOS on evolution of desert surfaces p 12 A87-53214
- Development of EOS-aided procedures for the determination of the water balance or hydrologic budget of a large watershed p 53 A87-53215
- Synergism requirements and concepts for SAR and HIRIS on EOS p 75 A87-53216
- The global forest ecosystem as viewed by ERS-1, SIR-C and EOS p 12 A87-53217
- The EOS SAR program p 76 A87-53228
- Spacecraft on-board SAR image generation for EOS-type missions p 76 A87-53232
- HMMR (High-Resolution Multifrequency Microwave Radiometer) Earth observing system, volume 2e. Instrument panel report [NASA-TM-89625] p 78 N87-27316
- EARTH ORBITS**
- A method for the optimization of orbits and structures of satellite systems for the periodic round-the-clock survey of the earth p 21 A87-42938
- EARTH RADIATION BUDGET**
- Matching instrument design and signal processing for a scanning radiometer p 76 A87-53251
- EARTH RADIATION BUDGET EXPERIMENT**
- Data analysis and software support for the Earth radiation budget experiment [NASA-CR-178350] p 66 N87-26569
- Calculation and accuracy of ERBE scanner measurement locations [NASA-TP-2670] p 47 N87-28471
- EARTH RESOURCES**
- The application of remote sensing techniques in China p 68 A87-41435
- Radar observations of terrestrial vegetation covers in the 3-cm range p 1 A87-42936
- Earth resources instrumentation for the Space Station Polar Platform p 69 A87-44184
- Features of a statistical model for the interaction between electromagnetic waves and remotely sensed natural objects p 70 A87-48189
- Canadian Symposium on Remote Sensing, 10th, Edmonton, Canada, May 5-8, 1986, Proceedings. Volume 1 & 2 p 72 A87-48801
- Airborne video - Applied to route location studies for electrical power transmission facilities p 17 A87-48802
- New system for the ordering, archiving and retrieval of data from earth's resource satellites p 60 A87-48889
- Remote sensing and landscape approaches to earth resources p 63 A87-53154
- EARTH RESOURCES INFORMATION SYSTEM**
- Remote sensing in Indonesia - A review of the available technology and its applications for resources surveys p 17 A87-46310
- EARTH RESOURCES SURVEY PROGRAM**
- Using AVHRR data to evaluate the greenness variability within monitoring polygons p 4 A87-48828
- EARTH ROTATION**
- Snow load effect on earth's rotation and gravitational field, 1979-1985 p 22 A87-51964
- EARTH SURFACE**
- Stereoscopic visualization of aerial and space photographs in thematic mapping p 23 A87-42937
- Remote sensing applications of the earth's surface - An outlook into the future p 70 A87-47173
- Water-cycle processes in geosystems and the possibility of the remote sensing of the moisture content of the underlying surface p 51 A87-47580
- Multistage principal-components analysis of correlations --- of spectral channels for multispectral remote sensing image processing p 56 A87-48193
- Cloud screening for determination of land surface characteristics in a reduced resolution satellite data set p 56 A87-48361
- Satellite microwave radiometry of forest and surface types p 9 A87-53120
- Roughness measurements with multipolarization aircraft data p 63 A87-53131
- The First ISLSCP Field Experiment (FIFE) p 12 A87-53218
- Remote sensing of earth terrain [NASA-CR-181370] p 79 N87-28957

**EARTH TIDES**

- The determination of Love numbers from the results of earth-tide observations in the Dnieper-Donets basin (DDB) region p 21 A87-46139
- Tidal and secular tilt from an earthquake zone - Thresholds for detection of regional anomalies p 26 A87-53733

**EARTHNET**

- TM sensor performance as obtained from Earthnet quality control data base p 71 A87-48659

**EARTHQUAKES**

- Tidal and secular tilt from an earthquake zone - Thresholds for detection of regional anomalies p 26 A87-53733
- Mechanisms of crustal deformation in the western US [NASA-CR-181230] p 27 N87-28200

**ECOLOGICAL**

- The impact of LANDSAT Thematic Mapper Data for ecological mapping purposes. A case study at the northern margin of the Alps p 20 N87-28147

**ECONOMIC DEVELOPMENT**

- Mapping of vegetation types in SW Greenland p 16 N87-28149

**ECOSYSTEMS**

- The use of old-field stands of loblolly pine in studies of the potential use of active microwave remote sensors for monitoring forest ecosystems p 11 A87-53153
- Synergism requirements and concepts for SAR and HIRIS on EOS p 75 A87-53216
- The global forest ecosystem as viewed by ERS-1, SIR-C and EOS p 12 A87-53217
- Estimating key forest ecosystem parameters through remote sensing p 12 A87-53245
- Characterizing the Chesapeake Bay ecosystem and lessons learned [PB87-166930] p 19 N87-26463

**EDUCATION**

- Multistage remote sensing with grade four students p 80 A87-48810

**ELECTRO-OPTICS**

- CCRS airborne Electro-Optical Facility p 72 A87-48852
- MEIS II imagery for environmental stress analysis --- Multi-detector Electro-optical Imaging Scanner p 72 A87-48865
- Preliminary results from modelling vegetation spectra derived from MEIS data, Algonquin Park, Ontario p 7 A87-48891
- Evaluation of MOMS (Modular Optoelectronic Multispectral Scanner) data for land use/land cover studies - Test site: Piracicaba region, Sao Paulo State, Brazil p 13 A87-53252

**ELECTROMAGNETIC INTERACTIONS**

- Features of a statistical model for the interaction between electromagnetic waves and remotely sensed natural objects p 70 A87-48189

**ELECTROMAGNETIC NOISE**

- European dissemination of Marine Observation Satellite (MOS-1) data p 44 A87-53925

**ELECTROMAGNETIC PULSES**

- Averaging of radar altimeter pulse returns with the interpolation tracker p 70 A87-45044

**ELECTROMAGNETIC SCATTERING**

- Remote sensing by the fluorescence property of the scatterer p 75 A87-53179

**ELEVATION**

- Digital elevation model extraction from stereo satellite images p 63 A87-53142

**ENERGY BUDGETS**

- Latent heat and cyclone activity in the South Pacific, 10-18 January 1979 p 37 A87-51603

**ENGLAND**

- Geometric quality of Thematic Mapper data of the United Kingdom p 57 A87-48655

**ENVIRONMENT EFFECTS**

- Review of control strategies for ozone and their effects on other environmental issues [PB87-171195] p 19 N87-25634

**ENVIRONMENT MODELS**

- MEIS II imagery for environmental stress analysis --- Multi-detector Electro-optical Imaging Scanner p 72 A87-48865

**ENVIRONMENT POLLUTION**

- Monitoring the background pollution of natural environments, No. 3 p 19 A87-52241
- Remote sensing by the fluorescence property of the scatterer p 75 A87-53179
- Vegetation mapping and stress detection in the Santa Monica Mountains, California p 12 A87-53246

**ENVIRONMENTAL CONTROL**

- The closed ecology project - Agricultural and life sciences background [AAS PAPER 86-120] p 9 A87-53093

**ENVIRONMENTAL ENGINEERING**

- The closed ecology project - Agricultural and life sciences background [AAS PAPER 86-120] p 9 A87-53093

**ENVIRONMENTAL MONITORING**

- Remote sensing techniques for the study of hydrological elements p 51 A87-47576
- Integrated multi-temporal aerial photography and digital mapping for coastal monitoring, Cape Breton Island, Nova Scotia p 34 A87-48837
- Monitoring the fire-danger hazard of Nebraska rangelands with AVHRR data p 17 A87-48838
- Operational water quality surveillance in Sweden using Landsat MSS data p 52 A87-48841
- MEIS II imagery for environmental stress analysis --- Multi-detector Electro-optical Imaging Scanner p 72 A87-48865
- Environmental monitoring of Alpine Meadows with large scale aerial photography in Banff National Park p 18 A87-48898
- The evaluation of TM analysis as a tool in monitoring land use and agricultural stress in Egypt p 18 A87-48903

- Monitoring the background pollution of natural environments, No. 3 p 19 A87-52241
- Problems in the background monitoring of the environment, No. 4 --- Russian book p 19 A87-52242
- How useful is Landsat monitoring? p 14 A87-54089
- Review of control strategies for ozone and their effects on other environmental issues p 19 N87-25634

- [PB87-171195] p 19 N87-25634
- Characterizing the Chesapeake Bay ecosystem and lessons learned [PB87-166930] p 19 N87-26463

- Biomonitoring plots at the ozone monitoring stations at Great Smoky Mountains National Park, 1985 survey results [PB87-172078] p 19 N87-26464

- Proceedings of the ESA-EARSeL Europe from Space Symposium [ESA-SP-258] p 19 N87-28115

- On the use of AVHRR channel-3 data for environmental studies p 20 N87-28135
- Environmental information and cartography p 20 N87-28141

- Proceedings of Atlantic Outer Continental Shelf Region Information Transfer Meeting (ITM) (2nd), January 28-29, 1987 [PB87-200168] p 48 N87-30009

**ENVIRONMENTAL SURVEYS**

- Effects of ozone on forests in the northeastern United States [DE87-010887] p 16 N87-28190

**EQUATORIAL REGIONS**

- Monitoring equatorial Pacific sea level with Geosat p 39 A87-52512

**EROS (SATELLITES)**

- The future generation of resources satellites p 80 A87-53742

**ERROR ANALYSIS**

- An MTF analysis of Landsat classification error at field boundaries p 56 A87-46745
- Estimation of errors in the determination of sea surface temperature and atmospheric moisture content from satellite measurements of outgoing IR radiation in the 10.5-12.5 micron range p 33 A87-48178
- Sampling errors in satellite estimates of tropical rain p 53 A87-54153

**ERROR CORRECTING CODES**

- Data correction for automated remote sensing image interpretation p 64 A87-53209

**ERS-1 (ESA SATELLITE)**

- The ERS-1/RADARSAT SAR Canadian ground segment p 61 A87-48896
- Derivation of the technical specification of the ERS-1 active microwave instrument to meet the SAR-image quality requirements p 77 A87-53280
- Study on the use of SAR data for agriculture and forestry p 15 N87-27862

**ESA SATELLITES**

- The future generation of resources satellites p 80 A87-53742

**ESTIMATES**

- The estimation of variance components in geodetic networks [B8681154] p 79 N87-29904

**ETHIOPIA**

- Remote sensing in the Sahel - A tool for the inventory and monitoring of resources p 73 A87-48893

**EUROPE**

- The role and perspective of remote sensing for disaster management in the European community p 20 N87-28137

**EUROPEAN SPACE PROGRAMS**

- Science synergism study for EOS on evolution of desert surfaces p 12 A87-53214

**EVAPORATION**

- Remote-sensing evaluation of the spatial variability of evaporation p 52 A87-47583

**EVOLUTION (DEVELOPMENT)**

- Workshop on The Earth as a Planet [NASA-CR-180543] p 81 N87-29900

**EXPERIMENT DESIGN**

- Measurement of spectral signatures in Less Favored Areas (LFA): A contribution to the definition of a remote sensing multitemporal experiment p 20 N87-28145

**EXPERT SYSTEMS**

- An expert system for remote sensing p 80 A87-43260  
Hierarchical classification with knowledge based binary decision --- for thematic mapping image interpretation p 62 A87-53110  
A system for knowledge-based segmentation of remotely-sensed images p 11 A87-53136  
An expert system for planimetric feature extraction p 63 A87-53139

**F****FARM CROPS**

- Remote-sensing evaluation of moisture supply to crops according to the leaf-surface thermal regime p 2 A87-47582

- The evaluation of TM analysis as a tool in monitoring land use and agricultural stress in Egypt p 18 A87-48903

- How useful is Landsat monitoring? p 14 A87-54089

**FARMLANDS**

- Mapping of vegetation types in SW Greenland p 16 N87-28149

**FEASIBILITY ANALYSIS**

- Technological feasibility to mobilization for operations - The NOAA crop monitoring case p 6 A87-48878  
SPOT, a satellite for oceanography? p 41 A87-53194

- The feasibility of detecting a magnetic field from a distant platform [AD-A180635] p 78 N87-27310

**FIRES**

- Airborne multispectral observations over burned and unburned prairies p 10 A87-53122

**FLORIDA**

- Physical oceanographic study of Florida's Atlantic Coast region: Florida Atlantic Coast Transport Study (FACTS). Volume 1: Executive summary [PB87-200994] p 49 N87-30015

- Physical oceanographic study of Florida's Atlantic Coast region: Florida Atlantic Coast Transport Study (FACTS), volume 2 [PB87-201000] p 49 N87-30016

- Physical oceanographic study of Florida's Atlantic Coast region: Florida Atlantic Coast Transport Study (FACTS). Volume 3: Appendices [PB87-201018] p 49 N87-30017

**FLOW GEOMETRY**

- Rheology of the 1983 Royal Gardens basalt flows, Kilauea Volcano, Hawaii p 26 A87-51725

**FLOW MEASUREMENT**

- Measurement of currents according to the drift of subsatellite buoys p 32 A87-48177

**FLOW VELOCITY**

- Comparison of satellite-derived ocean velocities with observations in the California coastal region [AD-A182291] p 47 N87-28242

**FLUID DYNAMICS**

- Features of the water dynamics of Lake Ladoga according to remote sensing data p 50 A87-44296

**FLUORESCENCE**

- Analysis of data from the DFO fluorescence line imager p 72 A87-48844

- Remote sensing by the fluorescence property of the scatterer p 75 A87-53179

- Theory of fluorescent irradiance fields in lakes and seas [PB87-196465] p 47 N87-28954

**FLYING PLATFORMS**

- Atmospheric correction of data measured by a flying platform over the sea - Elements of a model and its experimental validation p 35 A87-50292

**FOAMS**

- Foam activity on the sea surface as a Markov random process p 28 A87-44289

**FOCUSING**

- Modeling of focus effects in SAR images of the ocean surface p 42 A87-53212

- Automatic focusing of synthetic aperture radar images of diffuse targets p 64 A87-53213

**FOOD**

- Whitetail deer food availability maps from Thematic Mapper data p 14 A87-53998

**FOREST FIRE DETECTION**

- Monitoring the fire-danger hazard of Nebraska rangelands with AVHRR data p 17 A87-48838

**FOREST MANAGEMENT**

- Comparison of classification and enhancement techniques using Landsat imagery for the northern coniferous forest p 4 A87-48821

- Use of Thematic Mapper satellite images for disturbance updating of timber/range maps p 4 A87-48822

- The use of multi-spectral and radar remote sensing data for monitoring forest clearcut and regeneration sites on Vancouver Island p 5 A87-48834

- The role of Landsat multi-spectral scanner data in the analysis of northern spotted owl habitat p 7 A87-48894

- Thermographic remote sensing of northern forest areas in regeneration after clear or strip cutting - Preliminary observations p 8 A87-48897

- Digital image classification approach for estimating forest clearing and regrowth rates and trends p 10 A87-53123

- Study on the use of SAR data for agriculture and forestry p 15 N87-27862

- ERAFIS: A computer information system for agriculture and forestry in Spain p 16 N87-28140

- Evaluation of the range and degradation of mangroves in Southern Sergipe with remote sensing techniques [INPE-4196-PRE/1080] p 16 N87-28160

**FORESTS**

- Potential application of multipolarization SAR for pine-plantation biomass estimation p 1 A87-43263

- Detecting forest structure and biomass with C-band multipolarization radar - Physical model and field tests p 2 A87-46543

- Spectral and textural segmentation of multispectral aerial images p 5 A87-48831

- Thematic Mapper information about Canadian forests - Early results from across the country p 6 A87-48869

- A trial of oblique imagery from a low cost video camera system for defoliation assessment p 7 A87-48892

- TM and MEIS data for future Alberta forest inventories p 8 A87-48900

- Relationship of Thematic Mapper simulator data to leaf area index of temperate coniferous forests p 8 A87-53017

- Using remotely sensed Landsat MSS data to assess groundwater influence on the Barmah-Millewa Forest p 10 A87-53124

- The use of old-field stands of loblolly pine in studies of the potential use of active microwave remote sensors for monitoring forest ecosystems p 11 A87-53153

- Landscape pattern and successional dynamics in the boreal forest p 11 A87-53155

- Automatic classification of forestal areas by remote sensing techniques p 12 A87-53211

- Development of EOS-aided procedures for the determination of the water balance or hydrologic budget of a large watershed p 53 A87-53215

- Estimating key forest ecosystem parameters through remote sensing p 12 A87-53245

- Method development and experiences in application of airborne MSS data for forest damage detection p 12 A87-53247

- Thematic Mapper response to heavy metal related changes in Canopy LAI of a mixed forest p 12 A87-53248

- Analysis of forest and forest clearings in Amazonia with Landsat and Shuttle Imaging Radar-A data p 13 A87-53250

- Integration of topographic data with synthetic aperture radar data for determining forest properties in mountainous terrain p 14 A87-53278

- Color infrared video mapping of upland and wetland communities [DE87-010202] p 15 N87-28109

- Monitoring and inventoring of forest damages by use of LANDSAT TM data p 16 N87-28138

- Effects of ozone on forests in the northeastern United States [DE87-010887] p 16 N87-28190

**FOURIER ANALYSIS**

- Approximating SIR-B response characteristics and estimating wave height and wavelength for ocean imagery p 44 A87-53288

**FRANCE**

- Present state, changes, and quality of Sologne and Brenne, two French large wetlands, studied with LANDSAT MSS and TM data p 54 N87-28152

**FROST**

- Thermal infrared images from satellites compared to shelter temperature. Application to frost nowcasting in a citrus orchard p 15 N87-28136

- A model of thermal inertia for frost forecasting in agricultural areas --- satellite imagery p 16 N87-28151

**G****GARP ATLANTIC TROPICAL EXPERIMENT**

- Sampling errors in satellite estimates of tropical rain p 53 A87-54153

**GEOBOTANY**

- Lithologic discrimination using geobotanical and Landsat TM spectral data p 23 A87-48667

- Spectral discrimination of geobotanical anomalies using Landsat Thematic Mapper data p 2 A87-48668

- A geobotanic approach to the study of the geology of Cape Smith using Landsat-MSS data p 25 A87-48860

- Regional geobotany with TM - A Sudbury case study p 25 A87-48861

**GEOCHRONOLOGY**

- Application of space photographs to geomorphological investigations in southwestern Tadzhikistan p 23 A87-48186

**GEODESY**

- Snow load effect on earth's rotation and gravitational field, 1979-1985 p 22 A87-51964

**GEODETC COORDINATES**

- New possibilities for the use of gravity data in the realization of geodetic coordinate systems p 21 A87-42939

- The estimation of variance components in geodetic networks [B8681154] p 79 N87-29904

**GEODETC SATELLITES**

- The Navy Geosat mission - An overview p 38 A87-52501

- Determination of ocean geodetic data from Geosat p 38 A87-52506

- Preliminary results from the processing of a limited set of Geosat radar altimeter data p 22 A87-52507

- Comparison of Geosat and ground-truth wind and wave observations - Preliminary results p 38 A87-52509

- Validation of Geosat altimeter-derived wind speeds and significant wave heights using buoy data p 39 A87-52510

- REX and Geosat - Progress in the first year p 39 A87-52511

- Monitoring equatorial Pacific sea level with Geosat p 39 A87-52512

- Ice measurements by Geosat radar altimetry p 39 A87-52513

- Waveform analysis for Geosat day 96 p 39 A87-52514

- Design of Geosat Exact Repeat Mission p 39 A87-52515

**GEODETC SURVEYS**

- New instrumentation techniques in geodesy p 22 A87-46692

- A program for the combined adjustment of VLBI observing sessions p 22 A87-52766

- Spaceborne laser ranging from EOS p 22 A87-53146

- Geodetic glossary [PB87-181210] p 22 N87-25652

**GEOGRAPHIC INFORMATION SYSTEMS**

- An application for the testing and use of the standard data transfer format --- for remotely sensed classified information transmission to GIS center p 18 A87-48886

- Computer-assisted map analysis - Extending the utility of GIS technology p 18 A87-48907

- Solid earth geophysics: Data services [PB87-184107] p 66 N87-27352

- A user's guide for the Analytical Photogrammetric Positioning System (APPS) [AD-A183773] p 79 N87-29909

**GEOGRAPHY**

- Multistage remote sensing with grade four students p 80 A87-48810

- Moscow seen by satellite - Another image of Soviet urban geography p 80 A87-51143

**GEOIDS**

- Geoid anomalies across Ascension fracture zone and the cooling of the lithosphere p 21 A87-44352

- Seasat altimetry and the South Atlantic geoid. I - Spectral analysis p 21 A87-45743

- Satellite altimeter measurements of the geoid in sea ice zones p 30 A87-45816

**GEOLOGICAL FAULTS**

- Tidal and secular tilt from an earthquake zone - Thresholds for detection of regional anomalies p 26 A87-53733

- Kinematics at the intersection of the Garlock and Death Valley fault zones, California: Integration of TM data and field studies. LANDSAT TM investigation proposal TM-019 [NASA-CR-180666] p 27 N87-28208

**GEOLOGICAL SURVEYS**

- Space photographs of the Onega-Ladoga isthmus and the prediction of mineral finds p 23 A87-48185



- Pleistocene earth movements in Peninsular India -  
Evidences from Landsat MSS and Thematic Mapper  
data p 26 A87-53242
- Study on the use and characteristics of SAR systems  
for geological applications  
[ESA-CR(P)-2342] p 27 N87-26467
- Integration of remote sensing and geophysical  
data-application to exploration of pyrite ore facies in SW  
Spain p 27 N87-28119
- Requirements on radar data for geological application:  
A case study by use of multistage data of the test site  
Sardagna/Italy p 27 N87-28120
- SPOT: How good for geology? A comparison with  
LANDSAT MSS p 27 N87-28121
- GEOLOGY**
- Remote-sensing and geological-geophysical studies of  
closed platform territories --- Russian book  
p 26 A87-51875
- Mechanisms of crustal deformation in the western US  
[NASA-CR-181230] p 27 N87-28200
- GEOMAGNETISM**
- Remote sensing of geomagnetic field and applications  
to climate prediction p 74 A87-53108
- Geomagnetic intersection of tectonic structures seen  
in space photographs p 28 N87-29574
- GEOMETRIC RECTIFICATION (IMAGERY)**
- Geometric quality of Thematic Mapper data of the United  
Kingdom p 57 A87-48655
- A contribution to the optimum selection of ground control  
points in high resolution images p 57 A87-48658
- SPOT localization accuracy and geometric image  
quality p 57 A87-48662
- Evaluation of algorithms for the geometric correction  
of Thematic Mapper data p 58 A87-48807
- Automated evaluation of linear networks on SPOT  
images p 61 A87-51174
- Geometric correction of space images by the  
colinearity-equation method p 61 A87-51175
- Automated rectification and geocoding of SAR  
imagery p 63 A87-53143
- Geometric distortion correction with high accuracy for  
NOAA satellite images p 65 A87-53253
- GEOMORPHOLOGY**
- Remote sensing of the geomorphologic formations and  
vegetation in the eastern High Atlas region of Morocco  
from SPOT satellite data p 23 A87-45048
- Classification of geomorphic features and landscape  
stability in northwestern New Mexico using simulated SPOT  
imagery p 56 A87-46540
- Application of space photographs to geomorphological  
investigations in southwestern Tadzhikistan  
p 23 A87-48186
- Analysis of airborne infrared data for interpretative  
geological mapping of the Brookfield area, Nova Scotia  
p 24 A87-48804
- Shuttle imaging Radar-A (SIR-A) scenes from Iran and  
China p 25 A87-48854
- A geobotanic approach to the study of the geology of  
Cape Smith using Landsat-MSS data p 25 A87-48860
- Applications of satellite derived digital elevation models  
for resource mapping p 60 A87-48866
- A structural analysis of the Mabou Basin, Cape Breton  
Island using enhanced Landsat MSS imagery  
p 25 A87-48879
- Geomorphological interpretation of the SPOT image of  
February 23, 1986 concerning Djebel Amour (Algeria) and  
its border with the Sahara p 25 A87-51145
- Morphostructure and geological patterns in  
central-southern Norway according to a Landsat image  
p 25 A87-51146
- Science synergism study for EOS on evolution of desert  
surfaces p 12 A87-53214
- Workshop on The Earth as a Planet  
[NASA-CR-180543] p 81 N87-29900
- GEOLOGICAL FLUIDS**
- Rheology of the 1983 Royal Gardens basalt flows,  
Kilauea Volcano, Hawaii p 26 A87-51725
- GEOPHYSICS**
- Radio interferometry p 21 A87-46688
- Oceanographic and geophysical applications of satellite  
altimetry p 30 A87-46690
- IGARSS '87 - International Geoscience and Remote  
Sensing Symposium, University of Michigan, Ann Arbor,  
May 18-21, 1987, Digest. Volumes 1 & 2  
p 73 A87-53101
- Solid earth geophysics: Data services  
[PB87-184107] p 66 N87-27352
- GEOPOTENTIAL**
- New possibilities for the use of gravity data in the  
realization of geodetic coordinate systems  
p 21 A87-42939
- GEOSAT SATELLITES**
- The Navy Geosat mission - An overview  
p 38 A87-52501
- The Geosat radar altimeter p 38 A87-52502

- Preliminary determination of the Geosat radar altimeter  
noise spectrum p 38 A87-52503
- Determination of ocean geodetic data from Geosat  
p 38 A87-52506
- Preliminary results from the processing of a limited set  
of Geosat radar altimeter data p 22 A87-52507
- Comparison of Geosat and ground-truth wind and wave  
observations - Preliminary results p 38 A87-52509
- Validation of Geosat altimeter-derived wind speeds and  
significant wave heights using buoy data  
p 39 A87-52510
- REX and Geosat - Progress in the first year  
p 39 A87-52511
- Monitoring equatorial Pacific sea level with Geosat  
p 39 A87-52512
- Ice measurements by Geosat radar altimetry  
p 39 A87-52513
- Waveform analysis for Geosat day 96  
p 39 A87-52514
- Design of Geosat Exact Repeat Mission  
p 39 A87-52515
- Wind and wave statistics as derived from the Geosat  
radar altimeter and with comparisons with in situ  
measurements p 40 A87-53127
- GEOSTROPHIC WIND**
- Comparison of satellite-derived ocean velocities with  
observations in the California coastal region  
[AD-A182291] p 47 N87-28242
- Arctic drifting buoy data 1979 - 1985  
[AD-A182967] p 50 N87-30019
- GEOTEMPERATURE**
- Remote-sensing evaluation of the spatial variability of  
evaporation p 52 A87-47583
- GLACIAL DRIFT**
- Recent glacial history and rapid ice stream retreat in  
the Amundsen Sea p 37 A87-51944
- Till beneath ice stream B. I - Properties derived from  
seismic travel times. II - Structure and continuity. III - Till  
deformation - Evidence and implications. IV - A coupled  
ice-till flow model --- glacial deposits p 37 A87-51948
- GLACIERS**
- Azimuthal dependence in the gravity field induced by  
recent and past cryospheric forcings p 35 A87-51487
- The potential of SAR in a snow and glacier monitoring  
system p 45 N87-27856
- GLACIOLOGY**
- Antarctic ice streams - A review p 37 A87-51943
- Recent glacial history and rapid ice stream retreat in  
the Amundsen Sea p 37 A87-51944
- The morphology of ice streams A, B, and C, West  
Antarctica and their environs p 37 A87-51945
- Ice dynamics at the mouth of ice stream B, Antarctica  
p 37 A87-51946
- Velocity of ice streams B and C, Antarctica  
p 37 A87-51947
- Till beneath ice stream B. I - Properties derived from  
seismic travel times. II - Structure and continuity. III - Till  
deformation - Evidence and implications. IV - A coupled  
ice-till flow model --- glacial deposits p 37 A87-51948
- Glaciological studies on Rutford ice stream, Antarctica  
p 38 A87-51950
- GLOBAL ATMOSPHERIC RESEARCH PROGRAM**
- Some aspects of the surface circulation south of 20  
deg S revealed by First GARP Global Experiment drifters  
p 28 A87-42748
- GLOBAL POSITIONING SYSTEM**
- New instrumentation techniques in geodesy  
p 22 A87-46692
- GOES SATELLITES**
- Forecast of hurricane characteristics from GOES  
imagery p 59 A87-48818
- Planning for future operational sensors and other  
priorities  
[NOAA-NESDIS-30] p 77 N87-25560
- GRASSLANDS**
- Effectiveness of the Thematic Mapper for the range  
condition assessment in fescue grasslands of  
Southwestern Alberta p 6 A87-48850
- Interpretation of prairie land cover types from SIR-B  
data p 7 A87-48888
- Airborne multispectral observations over burned and  
unburned prairies p 10 A87-53122
- Results from the pushbroom microwave radiometer  
flights over the Konza Prairie in 1985 p 11 A87-53206
- Detection of soil drainage in Pays de Herve, Belgium,  
on LANDSAT MSS imagery p 15 N87-28129
- GRAVIMETRY**
- Estimation and modelling of the local empirical  
covariance function using gravity and satellite altimeter  
data p 22 A87-54325
- GRAVITATIONAL FIELDS**
- New possibilities for the use of gravity data in the  
realization of geodetic coordinate systems  
p 21 A87-42939
- Earth gravity model improvement - An alternative method  
for Doppler-tracked satellites p 21 A87-45817

- Azimuthal dependence in the gravity field induced by  
recent and past cryospheric forcings p 35 A87-51487
- Snow load effect on earth's rotation and gravitational  
field, 1979-1985 p 22 A87-51964
- Remote sensing of deep potential sources over the Nile  
Delta area p 26 A87-53150
- GRAVITY ANOMALIES**
- Solid earth geophysics: Data services  
[PB87-184107] p 66 N87-27352
- GRAVITY WAVES**
- Foam activity on the sea surface as a Markov random  
process p 28 A87-44289
- Radar signatures of oil films floating on the sea  
surface p 41 A87-53192
- GREAT SMOKY MOUNTAINS (NC-TN)**
- Biomonitoring plots at the ozone monitoring stations at  
Great Smoky Mountains National Park, 1985 survey  
results  
[PB87-172078] p 19 N87-26464
- GREENLAND**
- Boundary layer, upper ocean, and ice observations in  
the Greenland Sea marginal ice zone p 31 A87-47296
- Mapping of vegetation types in SW Greenland  
p 16 N87-28149
- Snow mapping in western Greenland  
p 54 N87-28150
- GROUND TRUTH**
- A contribution to the optimum selection of ground control  
points in high resolution images p 57 A87-48658
- Integration of radiometric and Landsat digital data for  
geologic investigation and exploration, Guysborough area,  
Nova Scotia p 24 A87-48803
- Landsat-based wildlife habitat mapping - A study of  
collaboration between analyst and user  
p 3 A87-48809
- Comparison of Geosat and ground-truth wind and wave  
observations - Preliminary results p 38 A87-52509
- Aircraft microwave radiometry of land  
p 13 A87-53269
- Modeling gap probability in discontinuous vegetation  
canopies p 13 A87-53276
- Whitetail deer food availability maps from Thematic  
Mapper data p 14 A87-53998
- An algorithm for automatically acquiring ground control  
points in SAR imagery p 67 N87-27864
- Evaluation of the range and degradation of mangroves  
in Southern Sergipe with remote sensing techniques  
[INPE-4196-PRE/1080] p 16 N87-28160
- GROUND WATER**
- Formation of natural underground-water resources in  
arid regions with special reference to the Dolinoozerskii  
artesian basin in Mongolia --- Russian book  
p 50 A87-42911
- Using remotely sensed Landsat MSS data to assess  
groundwater influence on the Barmah-Millewa Forest  
p 10 A87-53124
- GULF OF ALASKA**
- Gulf of Alaska: Physical environment and biological  
resources  
[PB87-103230] p 47 N87-29033
- GULF STREAM**
- Multiplatform sampling (ship, aircraft, and satellite) of  
a Gulf Stream warm core ring p 29 A87-44811
- The dynamics of the northern border of the Gulf Stream  
revealed by a Tiros-N AVHRR image from October 22,  
1980 p 35 A87-51147
- Study of physical processes on the US mid-Atlantic  
continental slope and rise. Volume 1: Executive  
summary  
[PB87-200515] p 48 N87-30012
- Physical oceanographic study of Florida's Atlantic Coast  
region: Florida Atlantic Coast Transport Study (FACTS).  
Volume 3: Appendices  
[PB87-201018] p 49 N87-30017
- H**
- HABITATS**
- Inventory of wetlands with Landsat's Thematic Mapper  
p 3 A87-48817
- Landsat thematic mapper data in wildlife habitat  
management - Reference to deer wintering habitat  
p 5 A87-48845
- The role of Landsat multi-spectral scanner data in the  
analysis of northern spotted owl habitat  
p 7 A87-48894
- HAWAII**
- Rheology of the 1983 Royal Gardens basalt flows,  
Kilauea Volcano, Hawaii p 26 A87-51725
- HEAT BALANCE**
- Boundary layer, upper ocean, and ice observations in  
the Greenland Sea marginal ice zone p 31 A87-47296



**HERBICIDES**

- Colour infrared aerial photography for herbicide drift damage assessment p 6 A87-48864

**HIERARCHIES**

- Hierarchical classification with knowledge based binary decision --- for thematic mapping image interpretation p 62 A87-53110

**HIGH RESOLUTION**

- Second generation high-resolution space systems - First results of the SPOT-1 satellite p 55 A87-44244

**HUMAN PERFORMANCE**

- Comparison of visual and automated lineament analyses on LANDSAT MSS image from south Greenland p 67 N87-28144

**HUMIDITY**

- Cloud and moisture fields derived from the GLA retrievals of HIRS2/MSU data p 36 A87-51579

**HURRICANES**

- Forecast of hurricane characteristics from GOES imagery p 59 A87-48818

**HYDROGEN SULFIDE**

- Investigation of causes of hydrogen sulfide formation in reclaimed water p 14 N87-23136

**HYDROGEOLOGY**

- Formation of natural underground-water resources in arid regions with special reference to the Dolinoozerskii artesian basin in Mongolia --- Russian book p 50 A87-42911

- Geomagnetic intersection of tectonic structures seen in space photographs p 28 N87-29574

**HYDROGRAPHY**

- Comparison of satellite-derived ocean velocities with observations in the California coastal region [AD-A182291] p 47 N87-28242

- Study of physical processes on the US mid-Atlantic continental slope and rise. Volume 1: Executive summary [PB87-200515] p 48 N87-30012

**HYDROLOGICAL CYCLE**

- Water-cycle processes in geosystems and the possibility of the remote sensing of the moisture content of the underlying surface p 51 A87-47580

- Indices of climatological and hydrological variability derived from satellite imagery for the South Saskatchewan River Basin p 52 A87-48856

**HYDROLOGY**

- Remote sensing techniques for the study of hydrological elements p 51 A87-47576

- Agricultural, hydrologic and oceanographic studies in Bangladesh with NOAA AVHRR data p 57 A87-48365

- Using remotely sensed Landsat MSS data to assess groundwater influence on the Barmah-Millewa Forest p 10 A87-53124

- Development of EOS-aided procedures for the determination of the water balance or hydrologic budget of a large watershed p 53 A87-53215

- Catalog of submarine volcanoes and hydrological phenomena associated with volcanic events, January 1, 1900 to December 31, 1959 p 54 N87-28196

**HYDROLOGY MODELS**

- Parameterization of models of runoff formation in simple catchment areas using remote-sensing data p 51 A87-47579

- Hydrologic applications of weather radar data p 52 A87-48875

- Use of LANDSAT digital data for snow cover mapping in the upper Saint John River Basin, Maine [AD-A183213] p 54 N87-29906

**HYDROMETEOROLOGY**

- Possibility of evaluating reservoir influx from aerial and satellite photographs p 51 A87-47577

- Modeling the snowmelt runoff in mountain catchment areas using satellite data p 51 A87-47578

- Remote-sensing evaluation of moisture supply to crops according to the leaf-surface thermal regime p 2 A87-47582

- Evaluation of the effect of hydrometeors on the characteristics of radar images of sea ice p 33 A87-48181

- Satellite microwave radiometry of snow water equivalent p 52 A87-48823

- Snowpack depletion monitoring in Alberta using computer-processed NOAA imagery p 52 A87-48848

- Comparisons of gauge and satellite rain estimates for the central United States during August 1979 p 53 A87-54152

- Cokriging radar-rainfall and rain gage data p 53 A87-54154

**ICE**

- The operational use of RADARSAT products by the ice centre environment Canada p 61 A87-48906

- Scattering parameters for aspherical hydrometeors at microwave frequencies p 53 A87-53271

- The International Symposium on Microwave Signatures and Remote Sensing held in Gothenburg (Sweden) on 19-22 January 1987 [AD-A181334] p 78 N87-27314

**ICE FLOES**

- Recent glacial history and rapid ice stream retreat in the Amundsen Sea p 37 A87-51944

- Ice dynamics at the mouth of ice stream B, Antarctica p 37 A87-51946

- Velocity of ice streams B and C, Antarctica p 37 A87-51947

- Till beneath ice stream B, I - Properties derived from seismic travel times. II - Structure and continuity. III - Till deformation - Evidence and implications. IV - A coupled ice-till flow model --- glacial deposits p 37 A87-51948

- Glaciological studies on Rutford ice stream, Antarctica p 38 A87-51950

- Tracking of ice floes p 46 N87-28155

- Interpolation, analysis and archival of data on sea ice trajectories and ocean currents obtained from satellite-linked instruments [PB87-201430] p 48 N87-30010

**ICE FORMATION**

- Labrador wind and wave environments [AD-A183218] p 48 N87-29907

**ICE MAPPING**

- Use of synthetic aperture radar-derived kinematics in mapping mesoscale ocean structure within the interior marginal ice zone p 31 A87-47294

- Validation of STAR-1 SAR imagery collected over Mould Bay, N.W.T., April 1984 p 59 A87-48826

- The morphology of ice streams A, B, and C, West Antarctica and their environs p 37 A87-51945

- Ice measurements by Geosat radar altimetry p 39 A87-52513

- Theoretical and experimental study of the radar backscatter of Arctic sea ice p 43 A87-53237

- Observing rotation and deformation of sea ice with synthetic aperture radar p 43 A87-53239

- Investigation of multi-dimensional algorithms using active and passive microwave data for ice concentration determination p 43 A87-53241

- Active microwave observations of sea ice and icebergs p 45 N87-27855

- Satellite-derived ice data sets no. 2: Arctic monthly average microwave brightness temperatures and sea ice concentrations, 1973-1976 [NASA-TM-87825] p 50 N87-30021

**ICE REPORTING**

- Evolution of microwave sea ice signatures during early summer and midsummer in the marginal ice zone p 31 A87-47293

- Progress on digital algorithms for deriving sea ice parameters from SAR data p 43 A87-53238

- Active microwave observations of sea ice and icebergs p 45 N87-27855

- The potential of SAR in a snow and glacier monitoring system p 45 N87-27856

- Large scale sea ice studies based on Scanning Multichannel Microwave Radiometers (SMMR) data p 16 N87-28148

- Sea ice observations by SAR --- satellite observation p 47 N87-28156

**ICEBERGS**

- Iceberg detection using SLAR p 34 A87-48876

**IDENTIFYING**

- Remote sensing of earth terrain [NASA-CR-181370] p 79 N87-28957

**ILLUMINANCE**

- Monte Carlo calculation of the dependence of the spectral radiance of vegetation cover on the illumination conditions p 2 A87-48190

**IMAGE ANALYSIS**

- An expert system for remote sensing p 80 A87-43260

- The CCRS SAR/MSS Anderson River data set p 55 A87-43261

- Climatological implications of a satellite-borne SAR imaging the sea surface p 30 A87-46403

- Information content analysis of Landsat image data for compression p 56 A87-47046

- Investigation of the relief of ore-containing regions on the basis of space photographs (with reference to eastern Yakutia) p 23 A87-48188

- The automatic generation of digital terrain models from satellite images by stereo p 58 A87-48669

- Application of accuracy assessment techniques to image classification --- photointerpretation and scene analysis p 58 A87-48808

- Landsat-based wildlife habitat mapping - A study of collaboration between analyst and user p 3 A87-48809

- Operational, province wide crop area estimation for Manitoba p 3 A87-48811

- An evaluation of sun angle computation algorithms p 59 A87-48812

- Application of image segmentation algorithms to the inventory of crops in Canada p 3 A87-48813

- Processing of Seasat altimetry data on a digital image analysis system p 59 A87-48825

- Spectral and textural segmentation of multispectral aerial images p 5 A87-48831

- The influence of melting conditions on the interpretation of radar imagery of sea ice p 34 A87-48849

- Geological interpretations from Landsat of the Troodos Massive, Cyprus p 25 A87-48862

- Interpreting meteorological satellite images using a color-composite technique p 62 A87-52795

- Cluster based segmentation of multi-temporal Thematic Mapper data as preparation of region-based agricultural land-cover analysis p 9 A87-53109

- Digital image classification approach for estimating forest clearing and regrowth rates and trends p 10 A87-53123

- A system for knowledge-based segmentation of remotely-sensed images p 11 A87-53136

- Analysis of environmental information of urban areas using Landsat TM data p 19 A87-53187

- Automatic classification of forestal areas by remote sensing techniques p 12 A87-53211

- Textural segmentation of SAR images using first order statistical parameters p 66 A87-53274

- Integration of topographic data with synthetic aperture radar data for determining forest properties in mountainous terrain p 14 A87-53278

- A pattern analysis technique for distinguishing surface and cloud types in the polar regions p 66 A87-53289

- Digital data from shuttle photography: The effects of platform variables p 66 N87-26697

- SAR detection of ships and ship wakes p 66 N87-27859

- Thin line detection in SAR images p 66 N87-27860

- Land use feature detection in SAR images p 67 N87-27863

- Cloud detection in NOAA images p 67 N87-28124

- Rural land use inventory and mapping in the Ardeche area (France). Improvement of automatic classification by multitemporal analysis of TM data p 15 N87-28127

- Integrated systems for remote sensing p 67 N87-28143

- Studies of tidal flat environments with LANDSAT MSS data p 47 N87-28157

- Spectral characteristics and the extent of paleosols of the Palouse formation [NASA-CR-181208] p 17 N87-28195

- Kinematics at the intersection of the Garlock and Death Valley fault zones, California: Integration of TM data and field studies. LANDSAT TM investigation proposal TM-019 [NASA-CR-180666] p 27 N87-28208

- Brief introduction in statistical pattern recognition [INPE-4206-PRE/1087] p 68 N87-28374

**IMAGE ENHANCEMENT**

- Comparison of classification and enhancement techniques using Landsat imagery for the northern coniferous forest p 4 A87-48821

- Custom-enhanced Landsat imagery in near real-time p 60 A87-48870

- A methodology for automated extraction of drainage networks from satellite imagery p 53 A87-48880

- Color enhancement of highly correlated images. II - Channel ratio and 'chromaticity' transformation techniques p 62 A87-53018

- Geological feature enhancement in SAR imagery p 67 N87-27861

- IMAGE FILTERS**

- Automated evaluation of linear networks on SPOT images p 61 A87-51174

- Crop discrimination by means of radar and infrared images p 15 N87-28128

- IMAGE INTENSIFIERS**

- Statistical modeling of intensity distributions on airborne SAR imagery p 65 A87-53262

- IMAGE PROCESSING**

- Optical image subtraction techniques, 1975-1985 p 55 A87-42659

- Remote sensing of submerged aquatic vegetation in lower Chesapeake Bay - A comparison of Landsat MSS to TM imagery p 30 A87-46542
- A contribution to the optimum selection of ground control points in high resolution images p 57 A87-48658
- An evaluation of sun angle computation algorithms p 59 A87-48812
- Evaluation of MEIS-II multispectral scanner data for quaternary geological mapping in the Chatham area, southwestern Ontario p 24 A87-48816
- Satellite microwave radiometry of snow water equivalent p 52 A87-48823
- A high-throughput system for bulk processing of multispectral imagery p 72 A87-48836
- Digital SAR-Landsat combination for geologic mapping p 24 A87-48853
- An evaluation of Landsat TM and MSS data for crop identification in Manitoba p 6 A87-48859
- Multispectral video system for airborne remote sensing - Sensitivity, calibrations and correction p 73 A87-48873
- A revolution in the production of small-scale and medium-scale maps p 61 A87-48904
- Development of a mathematical model for the spatial triangulation of SPOT images p 61 A87-48905
- Remote-sensing and geological-geophysical studies of closed platform territories --- Russian book p 26 A87-51875
- Effect of resolution on texture application to nearly simultaneous AVHRR and MSS images of an agricultural region p 9 A87-53111
- Exploring the spatial domain --- analysis of remote sensing data p 62 A87-53112
- An expert system for planimetric feature extraction p 63 A87-53139
- Sequential thinning algorithms for remote sensing application p 63 A87-53140
- Automated rectification and geocoding of SAR imagery p 63 A87-53143
- Performance sensitivity for X-SAR p 76 A87-53223
- The production of real time wave spectra from the SIR-C SAR p 42 A87-53224
- The Land Analysis System (LAS) - A general purpose system for multispectral image processing p 64 A87-53230
- Spacecraft on-board SAR image generation for EOS-type missions p 76 A87-53232
- A high speed digital processor for real-time synthetic aperture radar imaging p 64 A87-53233
- Processing of airborne SAR images of ocean waves p 43 A87-53264
- A methodology for evaluation of an interactive multispectral image processing system p 66 A87-53999
- Digital data from shuttle photography: The effects of platform variables p 66 A87-26697
- Proceedings of the SAR Applications Workshop --- Synthetic Aperture Radar p 78 A87-27854
- [ESA-SP-264]
- An algorithm for automatically acquiring ground control points in SAR imagery p 67 A87-27864
- Cloud detection in NOAA images p 67 A87-28124
- Analysis of directions of linear image elements by structure-zonal method p 68 A87-29575
- Satellite image processing for the Agulhas Retroflexion region p 68 A87-29905
- [AD-A183012]
- Use of LANDSAT digital data for snow cover mapping in the upper Saint John River Basin, Maine p 54 A87-29906
- [AD-A183213]
- IMAGE RESOLUTION**
- Second generation high-resolution space systems - First results of the SPOT-1 satellite p 55 A87-44244
- Improving SPOT images size and multispectral resolution p 58 A87-48664
- Comparison of Landsat Thematic Mapper and Multispectral Scanner information content for agricultural applications in Western Canada p 6 A87-48863
- Thematic Mapper information about Canadian forests - Early results from across the country p 6 A87-48869
- Contribution of improved resolution to morphological analysis - The example of the Rhone delta p 25 A87-51144
- Speckle noise reduction of 1-look SAR imagery p 65 A87-53273
- IMAGES**
- Millimeter-wave imaging sensor data evaluation [NASA-CR-181159] p 77 A87-26264
- Analysis of directions of linear image elements by structure-zonal method p 68 A87-29575
- IMAGING RADAR**
- Spaceborne imaging radar on EOS p 63 A87-53148
- IMAGING SPECTROMETERS**
- Remote sensing of coastal wetlands p 1 A87-40944

- Analysis of data from the DFO fluorescence line imager p 72 A87-48844
- MODIS - Advanced facility instrument for studies of the earth as a system --- Moderate Resolution Imaging Spectrometer p 40 A87-53144
- IMAGING TECHNIQUES**
- Preliminary results from modelling vegetation spectra derived from MEIS data, Algonquin Park, Ontario p 7 A87-48891
- The high resolution imaging spectrometer (HIRIS) for EOS p 74 A87-53145
- Millimeter-wave imaging sensor data evaluation [NASA-CR-181159] p 77 A87-26264
- INDUCTANCE**
- Meissner effect in high-Tc superconductive thin films p 35 A87-51532
- INERTIA**
- Determination of the initial motion conditions of earth-resources satellites according to the photogrammetric processing of topographic photographs oriented in inertial space p 56 A87-47506
- A model of thermal inertia for frost forecasting in agricultural areas --- satellite imagery p 16 A87-28151
- INFORMATION DISSEMINATION**
- New system for the ordering, archiving and retrieval of data from earth's resource satellites p 60 A87-48889
- INFORMATION SYSTEMS**
- A systems-approach to the design of the Eos data and information system p 64 A87-53207
- ERAFIS: A computer information system for agriculture and forestry in Spain p 16 A87-28140
- INFORMATION TRANSFER**
- Data telemetry, assimilation and ocean modeling [AD-A181899] p 47 A87-28239
- Proceedings of Atlantic Outer Continental Shelf Region Information Transfer Meeting (ITM) (2nd), January 28-29, 1987 p 48 A87-30009
- [PB87-200168]
- Proceedings of Atlantic Outer Continental Shelf Region Information Transfer Meeting (ITM) (1st), September 4-6, 1985 p 48 A87-30011
- [PB87-194361]
- INFRARED DETECTORS**
- Use of IR satellite rainfall estimates in diagnosing thermally forced circulations in the Pacific during FGGE SOP-1 p 36 A87-51580
- Space surveillance application potential of Schottky barrier IR sensors [AD-A180848] p 78 A87-27311
- INFRARED IMAGERY**
- Studies of the wavelike process in the surface temperature field of the equatorial Pacific using Meteor-satellite IR measurements p 28 A87-42931
- A multispectral study of the St. Louis area under snow-covered conditions using NOAA-7 AVHRR data p 51 A87-46538
- Calibration of Thematic Mapper thermal data for water surface temperature mapping - Case study on the Great Lakes p 51 A87-46545
- The dynamics of the northern border of the Gulf Stream revealed by a Tiros-N AVHRR image from October 22, 1980 p 35 A87-51147
- Satellite observations of surface temperatures and flow patterns, Sea of Japan and East China Sea, late March 1979 p 40 A87-53020
- Using airborne middle-infrared (1.45-2.0 microns) video imagery for distinguishing plant species and soil conditions p 9 A87-53023
- Improved cloud analysis using visible, near-infrared, infrared, and microwave imagery p 62 A87-53103
- Color infrared video mapping of upland and wetland communities p 15 A87-28109
- [DE87-010202]
- Crop discrimination by means of radar and infrared images p 15 A87-28128
- Thermal infrared images from satellites compared to shelter temperature. Application to frost nowcasting in a citrus orchard p 15 A87-28136
- Application of satellite data to tropic-subtropic moisture coupling [NASA-CR-4092] p 48 A87-29067
- [AD-A183012]
- Satellite image processing for the Agulhas Retroflexion region p 68 A87-29905
- INFRARED PHOTOGRAPHY**
- Comparison of satellite-derived ocean velocities with observations in the California coastal region [AD-A182291] p 47 A87-28242
- INFRARED RADAR**
- Aircraft microwave radiometry of land p 13 A87-53269
- Estimation of surface moisture availability from remote temperature measurements p 53 A87-54155

**INFRARED RADIATION**

- Estimation of errors in the determination of sea surface temperature and atmospheric moisture content from satellite measurements of outgoing IR radiation in the 10.5-12.5 micron range p 33 A87-48178
- Atmospheric effects on Landsat TM thermal IR data p 65 A87-53254

**INFRARED RADIOMETERS**

- Effect of resolution on texture application to nearly simultaneous AVHRR and MSS images of an agricultural region p 9 A87-53111
- HMMR (High-Resolution Multifrequency Microwave Radiometer) Earth observing system, volume 2e. Instrument panel report [NASA-TM-89625] p 78 A87-27316

**INFRARED REFLECTION**

- Measurement of leaf relative water content by infrared reflectance p 9 A87-53024

**INLAND WATERS**

- Remote-sensing evaluation of the spatial variability of evaporation p 52 A87-47583
- Remote-sensing techniques for investigating the structure of radiation-heat fluxes and the moisture content of geosystems in connection with the problem of monitoring the water component p 52 A87-47584

**INSTRUMENT ERRORS**

- Correction of the sensor degradation of the Coastal Zone Color Scanner on NIMBUS-7 p 46 A87-28153

**INSTRUMENT PACKAGES**

- HMMR (High-Resolution Multifrequency Microwave Radiometer) Earth observing system, volume 2e. Instrument panel report [NASA-TM-89625] p 78 A87-27316

**INTENSITY**

- Enhancement of colors in remote sensing images using rotation of the matrix at the IHS coordinates [INPE-4207-PRE/1086] p 67 A87-28165

**INTERFEROMETRY**

- Theoretical feasibility of SAR interferometry p 77 A87-53283
- Interferometric radar measurement of ocean surface currents p 44 A87-54107

**INTERNAL WAVES**

- Features of the water dynamics of Lake Ladoga according to remote sensing data p 50 A87-44296

**INTERNATIONAL COOPERATION**

- Operational instruments on the Space Station-Polar Platforms - Contributions by NOAA and the international community p 74 A87-53149
- International cooperation in space - Enhancing the world's common security p 81 A87-53987

**INTERTROPICAL CONVERGENT ZONES**

- Use of IR satellite rainfall estimates in diagnosing thermally forced circulations in the Pacific during FGGE SOP-1 p 36 A87-51580

**IRRIGATION**

- Extent of saline/waterlogged lands within irrigated Alberta. I - Inventory and preliminary evaluation of existing mapping data p 5 A87-48830

**ISTHMUSES**

- Space photographs of the Onega-Ladoga isthmus and the prediction of mineral finds p 23 A87-48185

**J****JAPANESE SPACECRAFT**

- Some results of MOS-1 airborne verification experiment - MSR (microwave scanning radiometer) p 76 A87-53229

**K****KARHUNEN-LOEVE EXPANSION**

- Spectral feature design for data compression in high dimensional multispectral data p 64 A87-53183

**KINEMATICS**

- Use of synthetic aperture radar-derived kinematics in mapping mesoscale ocean structure within the interior marginal ice zone p 31 A87-47294

**KRIGING**

- Cokriging radar-rainfall and rain gage data p 53 A87-54154

**L****LABRADOR**

- Labrador wind and wave environments [AD-A183218] p 48 A87-29907

**LAKES**

- Features of the water dynamics of Lake Ladoga according to remote sensing data p 50 A87-44296
- Theory of fluorescent irradiance fields in lakes and seas [PB87-196465] p 47 A87-28954

## LAND ICE

- Antarctic ice streams - A review p 37 A87-51943  
 The morphology of ice streams A, B, and C, West Antarctica and their environs p 37 A87-51945  
 Velocity of ice streams B and C, Antarctica p 37 A87-51947  
 Glaciological studies on Rutford ice stream, Antarctica p 38 A87-51950  
 Ice measurements by Geosat radar altimetry p 39 A87-52513

## LAND MANAGEMENT

- Technological feasibility to mobilization for operations - The NOAA crop monitoring case p 6 A87-48878  
 Computer-assisted map analysis - Extending the utility of GIS technology p 18 A87-48907

## LAND USE

- National land use mapping - The application of low altitude sample photography p 17 A87-48858  
 Rural land use classification using Landsat Thematic Mapper data p 18 A87-48868  
 Indexing small catchments in Java, Indonesia, with respect to their relative susceptibility to erosion p 52 A87-48871  
 The role of remote sensing in the Canada Land Use Monitoring Program (CLUMP) p 18 A87-48895  
 The evaluation of TM analysis as a tool in monitoring land use and agricultural stress in Egypt p 18 A87-48903  
 Land cover classification using SPOT data p 18 A87-50227  
 Evaluation of MOMS (Modular Optoelectronic Multispectral Scanner) data for land use/land cover studies - Test site: Piracicaba region, Sao Paulo State, Brazil p 13 A87-53252  
 Land use feature detection in SAR images p 67 N87-27863  
 Urban development planning using thematic mapper data of Munich (FRG) p 20 N87-28117

## LANDFORMS

- A study of modern landscape formation in Lower Mesopotamia from space photographs p 55 A87-42935

## LANDMARKS

- Determination of the external-orientation elements of aerial and space photographs p 55 A87-44301

## LANDSAT SATELLITES

- Remote sensing of coastal wetlands p 1 A87-40944  
 Visual interpretation of Landsat MSS quick-look images for the study of the annual swelling of the Niger river in its interior delta, in Mali p 50 A87-44245  
 Radiometric properties of U.S. processed Landsat MSS data p 55 A87-44864  
 Use of rice response characteristics in classification using Landsat MSS digital data p 1 A87-45046  
 Monitoring rice areas using Landsat MSS data p 1 A87-45047  
 Coral reef survey method for verification of Landsat MSS image data p 30 A87-46311  
 Remote sensing of submerged aquatic vegetation in lower Chesapeake Bay - A comparison of Landsat MSS to TM imagery p 30 A87-46542  
 Updating maps of climax vegetation cover with Landsat MSS data in Queensland, Australia p 2 A87-46744  
 An MTF analysis of Landsat classification error at field boundaries p 56 A87-46745  
 Information content analysis of Landsat image data for compression p 56 A87-47046  
 Earth remote sensing using the Landsat Thematic Mapper and SPOT sensor systems; Proceedings of the Meeting, Innsbruck, Austria, Apr. 15-17, 1986 [SPIE-660] p 70 A87-48652  
 Scene to scene radiometric normalization of the reflected bands of the Landsat Thematic Mapper p 71 A87-48654  
 Within-scene radiometric correction of Landsat Thematic Mapper (TM) data in Canadian production systems p 57 A87-48656  
 TM sensor performance as obtained from Earthnet quality control data base p 71 A87-48659  
 Evaluation of Landsat Thematic Mapper - Imagery for geological exploration p 23 A87-48666  
 Lithologic discrimination using geobotanical and Landsat TM spectral data p 23 A87-48667  
 Spectral discrimination of geobotanical anomalies using Landsat Thematic Mapper data p 2 A87-48668  
 Shallow water bathymetry and bottom classification by means of the Landsat and SPOT optical scanners p 52 A87-48670  
 Significance of TM data as a tool to support regional planning activities p 17 A87-48671  
 Discrimination of natural and cultivated vegetation using Thematic Mapper spectral data p 2 A87-48673  
 Comparative analysis of different sensor data (Landsat-TM and MOMS) for earth observation and impact on future sensor development p 71 A87-48674

Different scanning instruments comparison - MOMS and TM --- Modular Optoelectronic Multispectral Scanner p 71 A87-48675

The Land Satellite (Landsat) system - Earth Observation Satellite Company (Eosat's) plans for Landsat-6 and beyond p 71 A87-48676  
 Integration of radiometric and Landsat digital data for geologic investigation and exploration, Guysborough area, Nova Scotia p 24 A87-48803  
 Spatial filtering of digital Landsat data for the extraction of mapping information p 58 A87-48805  
 Landsat-based wildlife habitat mapping - A study of collaboration between analyst and user p 3 A87-48809

Inventory of wetlands with Landsat's Thematic Mapper p 3 A87-48817

Comparison of classification and enhancement techniques using Landsat imagery for the northern coniferous forest p 4 A87-48821

Application of remote sensing data to bedrock geological interpretation, Black River-Matheson area, Northern Ontario, Canada p 24 A87-48832

A high-throughput system for bulk processing of multispectral imagery p 72 A87-48836

Effectiveness of the Thematic Mapper for the range condition assessment in fescue grasslands of Southwestern Alberta p 6 A87-48850

Managing coral reefs - Operational benefits of remote sensing in Marine Park planning p 34 A87-48851

Digital SAR-Landsat combination for geologic mapping p 24 A87-48853

An evaluation of Landsat TM and MSS data for crop identification in Manitoba p 6 A87-48859

A geobotanic approach to the study of the geology of Cape Smith using Landsat-MSS data p 25 A87-48860

Geological interpretations from Landsat of the Troodos Massive, Cyprus p 25 A87-48862

Comparison of Landsat Thematic Mapper and Multispectral Scanner information content for agricultural applications in Western Canada p 6 A87-48863

Landsat Thematic Mapper data - A useful tool for mapping agricultural areas in Quebec p 6 A87-48867

Custom-enhanced Landsat imagery in near real-time p 60 A87-48870

A structural analysis of the Mabou Basin, Cape Breton Island using enhanced Landsat MSS imagery p 25 A87-48879

The role of Landsat multi-spectral scanner data in the analysis of northern spotted owl habitat p 7 A87-48894

Morphostructure and geological patterns in central-southern Norway according to a Landsat image p 25 A87-51146

Status of and prognosis for space remote sensing [AAS PAPER 86-104] p 80 A87-53084

Using remotely sensed Landsat MSS data to assess groundwater influence on the Barmah-Millewa Forest p 10 A87-53124

A multi-source image set for the study of soil texture and drainage as observed from Thematic Mapper data in Northern Belgium p 10 A87-53125

Analysis of environmental information of urban areas using Landsat TM data p 19 A87-53187

Suspended sediment concentrations estimated from Landsat MSS p 53 A87-53204

Use of TM Landsat data as a support to classical ground-based methodologies in the investigation of a volcanic site in central Italy - The Caldera of Latara p 26 A87-53244

Thematic Mapper response to heavy metal related changes in Canopy LAI of a mixed forest p 12 A87-53248

Atmospheric effects on Landsat TM thermal IR data p 65 A87-53254

Application of TM imagery to mapping volcanic rock assemblages at tertiary calderas of the basin and range province p 26 A87-53257

The future generation of resources satellites p 80 A87-53742

Whitetail deer food availability maps from Thematic Mapper data p 14 A87-53998

How useful is Landsat monitoring? p 14 A87-54089

Urban development planning using thematic mapper data of Munich (FRG) p 20 N87-28117

Integration of remote sensing and geophysical data-application to exploration of pyrite ore facies in SW Spain p 27 N87-28119

SPOT: How good for geology? A comparison with LANDSAT MSS p 27 N87-28121

Detection of soil drainage in Pays de Herve, Belgium, on LANDSAT MSS imagery p 15 N87-28129

Evaluation of the potential of the Thematic Mapper for marine application p 46 N87-28134

Monitoring and inventoring of forest damages by use of LANDSAT TM data p 16 N87-28138

Towards the automatic recognition and vectorised description of linear features in LANDSAT TM images by artificial intelligence methods p 67 N87-28142

The impact of LANDSAT Thematic Mapper Data for ecological mapping purposes. A case study at the northern margin of the Alps p 20 N87-28147

Studies of tidal flat environments with LANDSAT MSS data p 47 N87-28157

Determination of transfer functions from the Thematic Mapper (TM) sensor of the LANDSAT-5 satellite [INPE-4213-PRE/1094] p 79 N87-28956

Use of LANDSAT digital data for snow cover mapping in the upper Saint John River Basin, Maine [AD-A183213] p 54 N87-29906

Reflectance- and radiance-based methods for the in-flight absolute calibration of multispectral sensors p 69 A87-44863

Calibration of Thematic Mapper thermal data for water surface temperature mapping - Case study on the Great Lakes p 51 A87-46545

Rural land use classification using Landsat Thematic Mapper data p 18 A87-48868

Rural land use inventory and mapping in the Ardeche area (France). Improvement of automatic classification by multitemporal analysis of TM data p 15 N87-28127

Spaceborne laser ranging from EOS p 22 A87-53146

Latent heat and cyclone activity in the South Pacific, 10-18 January 1979 p 37 A87-51603

Rheology of the 1983 Royal Gardens basalt flows, Kilauea Volcano, Hawaii p 26 A87-51725

Relationship of Thematic Mapper simulator data to leaf area index of temperate coniferous forests p 8 A87-53017

Thematic Mapper response to heavy metal related changes in Canopy LAI of a mixed forest p 12 A87-53248

Remote-sensing evaluation of moisture supply to crops according to the leaf-surface thermal regime p 2 A87-47582

Relationship of Thematic Mapper simulator data to leaf area index of temperate coniferous forests p 8 A87-53017

Measurement of leaf relative water content by infrared reflectance p 9 A87-53024

Millimeter-wave polarimetric measurements of artificial and natural targets p 75 A87-53163

Polarization utilization in the microwave inversion of leaf angle distributions p 11 A87-53201

Optical image subtraction techniques, 1975-1985 p 55 A87-42659

Estimating key forest ecosystem parameters through remote sensing p 12 A87-53245

Automated evaluation of linear networks on SPOT images p 61 A87-51174

Thin line detection in SAR images p 66 N87-27860

Mesoscale eddies in the Fram Strait marginal ice zone during the 1983 and 1984 Marginal Zone Experiments p 31 A87-47291

Lithological discrimination in central Snowdonia using airborne multispectral scanner imagery p 23 A87-48358

Lithologic discrimination using geobotanical and Landsat TM spectral data p 23 A87-48667

A study of the potential application of SPOT imagery in structural geology p 24 A87-48827

Application of TM imagery to mapping volcanic rock assemblages at tertiary calderas of the basin and range province p 26 A87-53257

Enhancement of colors in remote sensing images using rotation of the matrix at the IHS coordinates [INPE-4207-PRE/1088] p 67 N87-28165

Kinematics at the intersection of the Garlock and Death Valley fault zones, California: Integration of TM data and field studies. LANDSAT TM investigation proposal TM-019 [NASA-CR-180666] p 27 N87-28208

Geoid anomalies across Ascension fracture zone and the cooling of the lithosphere p 21 A87-44352

An evaluation of sun angle computation algorithms p 59 A87-48812

- Comparison of C-band synthetic aperture radar (SAR) data according to two different depression angles for agricultural applications p 4 A87-48820
- LOVE WAVES**  
The determination of Love numbers from the results of earth-tide observations in the Dnieper-Donets basin (DDB) region p 21 A87-46139
- LOW ALTITUDE**  
National land use mapping - The application of low altitude sample photography p 17 A87-48858

## M

- MAGNETIC ANOMALIES**  
Tidal and secular tilt from an earthquake zone - Thresholds for detection of regional anomalies p 26 A87-53733
- MAGNETIC FIELDS**  
Remote sensing of deep potential sources over the Nile Delta area p 26 A87-53150  
The feasibility of detecting a magnetic field from a distant platform [AD-A180635] p 78 A87-27310
- MAGNETIC FLUX**  
Meissner effect in high-Tc superconductive thin films p 35 A87-51532
- MAGNETIC TAPES**  
Satellite-derived ice data sets no. 2: Arctic monthly average microwave brightness temperatures and sea ice concentrations, 1973-1976 [NASA-TM-87825] p 50 A87-30021
- MAINE**  
Use of LANDSAT digital data for snow cover mapping in the upper Saint John River Basin, Maine [AD-A183213] p 54 A87-29906
- MAN ENVIRONMENT INTERACTIONS**  
Problems in the background monitoring of the environment, No. 4 --- Russian book p 19 A87-52242
- MAN MACHINE SYSTEMS**  
Tracking of ice floes p 46 A87-28155
- MANAGEMENT INFORMATION SYSTEMS**  
The role and perspective of remote sensing for disaster management in the European community p 20 A87-28137
- MAPPING**  
Automated rectification and geocoding of SAR imagery p 63 A87-53143  
Global digital topography mapping using a scanning radar altimeter p 76 A87-53227  
Vegetation and a LANDSAT-derived land cover map of the Beechey Point quadrangle, Arctic Coastal Plain, Alaska [AD-A180931] p 15 A87-27312  
Color infrared video mapping of upland and wetland communities [DE87-010202] p 15 A87-28109  
Environmental information and cartography p 20 A87-28141  
Use of LANDSAT digital data for snow cover mapping in the upper Saint John River Basin, Maine [AD-A183213] p 54 A87-29906
- MAPS**  
Multistage remote sensing with grade four students p 80 A87-48810  
Stratification of satellite imagery by Uniform Productivity Areas p 5 A87-48840  
Vegetation and a LANDSAT-derived land cover map of the Beechey Point quadrangle, Arctic Coastal Plain, Alaska [AD-A180931] p 15 A87-27312
- MARANGONI CONVECTION**  
Radar signatures of oil films floating on the sea surface p 41 A87-53192
- MARINE BIOLOGY**  
Gulf of Alaska: Physical environment and biological resources [PB87-103230] p 47 A87-29033
- MARINE ENVIRONMENTS**  
Remote observations of the marine environment - Spatial heterogeneity of the mesoscale ocean color field in CZCS imagery of California near-coastal waters p 30 A87-46539  
Managing coral reefs - Operational benefits of remote sensing in Marine Park planning p 34 A87-48851  
Gulf of Alaska: Physical environment and biological resources [PB87-103230] p 47 A87-29033  
Proceedings of Atlantic Outer Continental Shelf Region Information Transfer Meeting (ITM) (2nd), January 28-29, 1987 [PB87-200168] p 48 A87-30009
- MARINE METEOROLOGY**  
From satellite orbit into the eye of the typhoon --- Russian book p 29 A87-44679

- The variability of the North Atlantic marine atmosphere and its relevance to remote sensing p 33 A87-48362  
Response of marine atmospheric boundary layer height to sea surface temperature changes - Mixed-layer theory p 34 A87-50277  
Observing systems experiments for the onset vortex during Summer Monex p 35 A87-51552  
Sea surface temperature retrieval from the Tiros-N AVHRR instrument for the FGGE period (Dec. 1978-Nov. 1979) p 35 A87-51553  
Comparisons of FGGE IIb and IIb winds in a tropical synoptic system p 35 A87-51559  
Wintertime disturbances in the tropical Pacific - FGGE IIb and satellite comparisons p 36 A87-51560  
Moisture transports and budgets of 'moisture bursts' --- of oceanic areas of tropical and subtropical latitudes p 36 A87-51593  
A comparison of the significant features of the marine boundary layers over the Arabian Sea and the Bay of Bengal during Monex 79 p 36 A87-51594  
Latent heat and cyclone activity in the South Pacific, 10-18 January 1979 p 37 A87-51603  
Labrador wind and wave environments [AD-A183218] p 48 A87-29907
- MARINE RESOURCES**  
Gulf of Alaska: Physical environment and biological resources [PB87-103230] p 47 A87-29033
- MARITIME SATELLITES**  
Operational use of remote sensing for commercial Arctic class vessel navigation p 33 A87-48829  
Some results of MOS-1 airborne verification experiment - MSR (microwave scanning radiometer) p 76 A87-53229  
European dissemination of Marine Observation Satellite (MOS-1) data p 44 A87-53925
- MARKETING**  
SPOT's first year p 80 A87-51320  
Eurimage sets up shop p 80 A87-51324
- MARKOV PROCESSES**  
Foam activity on the sea surface as a Markov random process p 28 A87-44289
- MARSHLANDS**  
The detection of vegetative stress utilizing remotely sensed data and soil sampling p 8 A87-50231
- MATHEMATICAL MODELS**  
Features of a statistical model for the interaction between electromagnetic waves and remotely sensed natural objects p 70 A87-48189  
Development of a mathematical model for the spatial triangulation of SPOT images p 61 A87-48905  
Statistical modeling of intensity distributions on airborne SAR imagery p 65 A87-53262  
A model of thermal inertia for frost forecasting in agricultural areas --- satellite imagery p 16 A87-28151  
Investigating the role of the land surface in explaining the interannual variation of the net radiation balance over the Western Sahara and sub-Sahara [NASA-CR-181183] p 68 A87-28197  
Mechanisms of crustal deformation in the western US [NASA-CR-181230] p 27 A87-28200
- MEASURING INSTRUMENTS**  
New instrumentation techniques in geodesy p 22 A87-46692
- MELTING**  
The influence of melting conditions on the interpretation of radar imagery of sea ice p 34 A87-48849
- MESOMETEOROLOGY**  
A comparison of the significant features of the marine boundary layers over the Arabian Sea and the Bay of Bengal during Monex 79 p 36 A87-51594
- MESOSCALE PHENOMENA**  
Climatological implications of a satellite-borne SAR imaging the sea surface p 30 A87-46403  
Remote observations of the marine environment - Spatial heterogeneity of the mesoscale ocean color field in CZCS imagery of California near-coastal waters p 30 A87-46539  
Mesoscale eddies in the Fram Strait marginal ice zone during the 1983 and 1984 Marginal Zone Experiments p 31 A87-47291  
Variations of mesoscale and large-scale sea ice morphology in the 1984 Marginal Ice Zone Experiment as observed by microwave remote sensing p 31 A87-47292  
Use of synthetic aperture radar-derived kinematics in mapping mesoscale ocean structure within the interior marginal ice zone p 31 A87-47294  
Altimetric data assimilation for ocean dynamics and forecasting p 39 A87-52516
- METALS**  
Thematic Mapper response to heavy metal related changes in Canopy LAI of a mixed forest p 12 A87-53248

- METEOROLOGICAL RADAR**  
Hydrologic applications of weather radar data p 52 A87-48875  
Cokriging radar-rainfall and rain gage data p 53 A87-54154
- METEOROLOGICAL SATELLITES**  
From satellite orbit into the eye of the typhoon --- Russian book p 29 A87-44679  
Forecast of hurricane characteristics from GOES imagery p 59 A87-48818  
Cloud and moisture fields derived from the GLA retrievals of HIRS2/MSU data p 36 A87-51579  
Interpreting meteorological satellite images using a color-composite technique p 62 A87-52795  
Comparisons of gauge and satellite rain estimates for the central United States during August 1979 p 53 A87-54152
- METEOROLOGY**  
Improved cloud analysis using visible, near-infrared, infrared, and microwave imagery p 62 A87-53103  
Successes of Cosmos-1500 satellite, SLR system p 45 A87-27696  
NASA sea ice and snow validation plan for the Defense Meteorological Satellite Program special sensor microwave/imager [NASA-TM-100683] p 49 A87-30018
- METRIC PHOTOGRAPHY**  
Some results of the Metric Camera (MC) Mission-1 on Spacelab p 70 A87-47175  
Large Format Camera: The second generation photogrammetric camera for space cartography p 78 A87-28118
- MICROWAVE AMPLIFIERS**  
Hybrid power amplifier module for X-band p 69 A87-43302
- MICROWAVE ANTENNAS**  
A cross antenna for passive microwave remote sensing p 77 A87-53268
- MICROWAVE IMAGERY**  
Variations of mesoscale and large-scale sea ice morphology in the 1984 Marginal Ice Zone Experiment as observed by microwave remote sensing p 31 A87-47292  
Multisensor comparison of ice concentration estimates in the marginal ice zone p 31 A87-47295  
Improved cloud analysis using visible, near-infrared, infrared, and microwave imagery p 62 A87-53103  
The International Symposium on Microwave Signatures and Remote Sensing held in Gothenburg (Sweden) on 19-22 January 1987 [AD-A181334] p 78 A87-27314  
NASA sea ice and snow validation plan for the Defense Meteorological Satellite Program special sensor microwave/imager [NASA-TM-100683] p 49 A87-30018
- MICROWAVE RADIOMETERS**  
A microwave radiometer weather-correcting sea ice algorithm p 29 A87-45024  
Shuttle Imaging Radar B (SIR-B) Weddell Sea ice observations - A comparison of SIR-B and scanning multichannel microwave radiometer ice concentrations p 32 A87-47300  
Satellite microwave radiometry of snow water equivalent p 52 A87-48823  
Satellite microwave radiometry of forest and surface types p 9 A87-53120  
A multifrequency microwave radiometer of the future p 75 A87-53180  
Results from the pushbroom microwave radiometer flights over the Konza Prairie in 1985 p 11 A87-53206  
Remote sensing of the earth with microwave radiometry in Germany - Results and trends p 76 A87-53225  
Some results of MOS-1 airborne verification experiment - MSR (microwave scanning radiometer) p 76 A87-53229  
Optimum use of dual frequency passive microwave measurements for ice/ocean interactions p 43 A87-53240  
Matching instrument design and signal processing for a scanning radiometer p 76 A87-53251  
Aircraft microwave radiometry of land p 13 A87-53269  
HMMR (High-Resolution Multifrequency Microwave Radiometer) Earth observing system, volume 2e. Instrument panel report [NASA-TM-89625] p 78 A87-27316  
Monitoring of snow cover from satellite p 54 A87-28123  
Large scale sea ice studies based on Scanning Multichannel Microwave Radiometers (SMMR) data p 16 A87-28148  
Microwave radiometry study concerning pushbroom systems. Volume 1: A sea salinity/soil-moisture pushbroom radiometer system [R-322] p 79 A87-28951

- Satellite-derived ice data sets no. 2: Arctic monthly average microwave brightness temperatures and sea ice concentrations, 1973-1976 [NASA-TM-87825] p 50 N87-30021
- MICROWAVE SCATTERING**  
Scattering parameters for aspherical hydrometeors at microwave frequencies p 53 A87-53271  
Estimation of X-band scattering properties of tree components p 13 A87-53277
- MICROWAVE SENSORS**  
Evolution of microwave sea ice signatures during early summer and midsummer in the marginal ice zone p 31 A87-47293  
The use of old-field stands of loblolly pine in studies of the potential use of active microwave remote sensors for monitoring forest ecosystems p 11 A87-53153  
Theoretical models for microwave remote sensing of snow-covered sea ice p 42 A87-53236  
Investigation of multi-dimensional algorithms using active and passive microwave data for ice concentration determination p 43 A87-53241
- MICROWAVE SOUNDING**  
A multifrequency microwave radiometer of the future p 75 A87-53180  
The effects of wind-wave coupling on scatterometer wind measurement accuracy p 41 A87-53196  
Polarization utilization in the microwave inversion of leaf angle distributions p 11 A87-53201  
Results from the pushbroom microwave radiometer flights over the Konza Prairie in 1985 p 11 A87-53206
- MIDLATITUDE ATMOSPHERE**  
Comparisons of gauge and satellite rain estimates for the central United States during August 1979 p 53 A87-54152
- MILITARY SPACECRAFT**  
The Navy Geosat mission - An overview p 38 A87-52501
- MILLIMETER WAVES**  
Millimeter-wave polarimetric measurements of artificial and natural targets p 75 A87-53163  
Millimeter-wave imaging sensor data evaluation [NASA-CR-181159] p 77 N87-26264
- MINERAL DEPOSITS**  
Space photographs of the Onega-Ladoga isthmus and the prediction of mineral finds p 23 A87-48185  
Investigation of the relief of ore-containing regions on the basis of space photographs (with reference to eastern Yakutia) p 23 A87-48188
- MINERAL EXPLORATION**  
Integration of remote sensing and geophysical data-application to exploration of pyrite ore facies in SW Spain p 27 N87-28119
- MODULATION TRANSFER FUNCTION**  
An MTF analysis of Landsat classification error at field boundaries p 56 A87-46745  
SPOT MTF performance evaluation p 57 A87-48663  
Modulation transfer function of radar return power from the ocean p 42 A87-53219
- MOISTURE CONTENT**  
Remote sensing techniques for the study of hydrological elements p 51 A87-47576  
Water-cycle processes in geosystems and the possibility of the remote sensing of the moisture content of the underlying surface p 51 A87-47580  
Measurement of leaf relative water content by infrared reflectance p 9 A87-53024  
Application of satellite data to tropic-subtropic moisture coupling [NASA-CR-4092] p 48 N87-29067
- MONSOONS**  
Large scale ocean-atmosphere interaction in the summer monsoon - The influence of oceanic upwelling and advection on eastern Arabian Sea offshore convection p 36 A87-51585  
Satellite observations of convection during the summer monsoon of 1979 p 36 A87-51587
- MONTE CARLO METHOD**  
Monte Carlo calculation of the dependence of the spectral radiance of vegetation cover on the illumination conditions p 2 A87-48190
- MORPHOLOGY**  
Contribution of improved resolution to morphological analysis - The example of the Rhone delta p 25 A87-51144  
Major morphologic features of the Atlantic Ocean surface p 48 N87-29573
- MOUNTAINS**  
Modeling the snowmelt runoff in mountain catchment areas using satellite data p 51 A87-47578  
Environmental monitoring of Alpine Meadows with large scale aerial photography in Banff National Park p 18 A87-48898  
Vegetation mapping and stress detection in the Santa Monica Mountains, California p 12 A87-53246
- MULTISENSOR APPLICATIONS**  
Multisensor comparison of ice concentration estimates in the marginal ice zone p 31 A87-47295
- MULTISPECTRAL BAND SCANNERS**  
The CCRS SAR/MSS Anderson River data set p 55 A87-43261  
Visual interpretation of Landsat MSS quick-look images for the study of the annual swelling of the Niger river in its interior delta, in Mali p 50 A87-44245  
Radiometric properties of U.S. processed Landsat MSS data p 55 A87-44864  
A multispectral study of the St. Louis area under snow-covered conditions using NOAA-7 AVHRR data p 51 A87-46538  
Remote sensing of submerged aquatic vegetation in lower Chesapeake Bay - A comparison of Landsat MSS to TM imagery p 30 A87-46542  
Updating maps of climax vegetation cover with Landsat MSS data in Queensland, Australia p 2 A87-46744  
Lithological discrimination in central Snowdonia using airborne multispectral scanner imagery p 23 A87-48358  
Scene to scene radiometric normalization of the reflected bands of the Landsat Thematic Mapper p 71 A87-48654  
Comparative analysis of different sensor data (Landsat-TM and MOMS) for earth observation and impact on future sensor development p 71 A87-48674  
Different scanning instruments comparison - MOMS and TM --- Modular Optoelectronic Multispectral Scanner p 71 A87-48675  
Evaluation of MEIS-II multispectral scanner data for quaternary geological mapping in the Chatham area, southwestern Ontario p 24 A87-48816  
Application of remote sensing data to bedrock geological interpretation, Black River-Matheson area, Northern Ontario, Canada p 24 A87-48832  
The use of multi-spectral and radar remote sensing data for monitoring forest clearcut and regeneration sites on Vancouver Island p 5 A87-48834  
A high-throughput system for bulk processing of multispectral imagery p 72 A87-48836  
Operational water quality surveillance in Sweden using Landsat MSS data p 52 A87-48841  
An evaluation of Landsat TM and MSS data for crop identification in Manitoba p 6 A87-48859  
A geobotanic approach to the study of the geology of Cape Smith using Landsat-MSS data p 25 A87-48860  
Geological interpretations from Landsat of the Troodos Massive, Cyprus p 25 A87-48862  
Comparison of Landsat Thematic Mapper and Multispectral Scanner information content for agricultural applications in Western Canada p 6 A87-48863  
MEIS II imagery for environmental stress analysis --- Multi-detector Electro-optical Imaging Scanner p 72 A87-48865  
Custom-enhanced Landsat imagery in near real-time p 60 A87-48870  
A structural analysis of the Mabou Basin, Cape Breton Island using enhanced Landsat MSS imagery p 25 A87-48879  
An application for the testing and use of the standard data transfer format --- for remotely sensed classified information transmission to GIS center p 18 A87-48886  
Preliminary results from modelling vegetation spectra derived from MEIS data, Algonquin Park, Ontario p 7 A87-48891  
The role of Landsat multi-spectral scanner data in the analysis of northern spotted owl habitat p 7 A87-48894  
TM and MEIS data for future Alberta forest inventories p 8 A87-48900  
Spectral studies of dryland agricultural salinity in Western Australia p 8 A87-48901  
Color enhancement of highly correlated images. II - Channel ratio and 'chromaticity' transformation techniques p 62 A87-53018  
Effect of resolution on texture application to nearly simultaneous AVHRR and MSS images of an agricultural region p 9 A87-53111  
Airborne multispectral observations over burned and unburned prairies p 10 A87-53122  
Using remotely sensed Landsat MSS data to assess groundwater influence on the Barmah-Millewa Forest p 10 A87-53124  
Spectral feature design for data compression in high dimensional multispectral data p 64 A87-53183  
An operational multispectral scanner for bathymetric surveys - The ABS NORDA scanner p 42 A87-53199  
Suspended sediment concentrations estimated from Landsat MSS p 53 A87-53204  
Analysis of Eocene depositional environments - Preliminary TM and TIMS results, Wind River Basin, Wyoming p 26 A87-53243
- Method development and experiences in application of airborne MSS data for forest damage detection p 12 A87-53247  
Evaluation of MOMS (Modular Optoelectronic Multispectral Scanner) data for land use/land cover studies - Test site: Piracicaba region, Sao Paulo State, Brazil p 13 A87-53252  
Vegetation and a LANDSAT-derived land cover map of the Beechey Point quadrangle, Arctic Coastal Plain, Alaska [AD-A180931] p 15 N87-27312  
SPOT: How good for geology? A comparison with LANDSAT MSS p 27 N87-28121  
Sea surface temperatures and the detection of ocean circulation patterns and fronts from AVHRR imagery p 45 N87-28125  
Present state, changes, and quality of Sologne and Brenne, two French large wetlands, studied with LANDSAT MSS and TM data p 54 N87-28152  
Studies of tidal flat environments with LANDSAT MSS data p 47 N87-28157
- MULTISPECTRAL LINEAR ARRAYS**  
Multiple-angle observations of reflectance anisotropy from an airborne linear array sensor p 69 A87-43262  
The RADARSAT RMOMS optical sensor --- Modular Optoelectronic Multispectral Scanner p 73 A87-48890
- MULTISPECTRAL PHOTOGRAPHY**  
Multistage principal-components analysis of correlations --- of spectral channels for multispectral remote sensing image processing p 56 A87-48193  
Absolute calibration of the SPOT-1 HRV cameras p 71 A87-48660  
Improving SPOT images size and multispectral resolution p 58 A87-48664  
Spectral and textural segmentation of multispectral aerial images p 5 A87-48831  
Multispectral video system for airborne remote sensing - Sensitivity, calibrations and correction p 73 A87-48873  
Discrimination of suspended sediment and littoral features using multispectral video imagery p 73 A87-48874  
The Land Analysis System (LAS) - A general purpose system for multispectral image processing p 64 A87-53230  
A methodology for evaluation of an interactive multispectral image processing system p 66 A87-53999  
Detection of soil drainage in Pays de Herve, Belgium, on LANDSAT MSS imagery p 15 N87-28129
- N**
- NATIONAL PARKS**  
Environmental monitoring of Alpine Meadows with large scale aerial photography in Banff National Park p 18 A87-48898
- NAVIGATION SATELLITES**  
Operational use of remote sensing for commercial Arctic class vessel navigation p 33 A87-48829
- NEPHANALYSIS**  
Size distributions of clouds in real time from satellite imagery p 56 A87-48359  
Improved cloud analysis using visible, near-infrared, infrared, and microwave imagery p 62 A87-53103
- NIGHT**  
Space surveillance application potential of Schottky barrier IR sensors [AD-A180848] p 78 N87-27311
- NIMBUS 7 SATELLITE**  
Large scale sea ice studies based on Scanning Multichannel Microwave Radiometers (SMMR) data p 16 N87-28148  
Correction of the sensor degradation of the Coastal Zone Color Scanner on NIMBUS-7 p 46 N87-28153
- NOAA SATELLITES**  
Agricultural, hydrologic and oceanographic studies in Bangladesh with NOAA AVHRR data p 57 A87-48365  
Technological feasibility to mobilization for operations - The NOAA crop monitoring case p 6 A87-48878  
Operational instruments on the Space Station-Polar Platforms - Contributions by NOAA and the international community p 74 A87-53149  
Geometric distortion correction with high accuracy for NOAA satellite images p 65 A87-53253  
Smoothing vegetation index profiles - An alternative method for reducing radiometric disturbance in NOAA/AVHRR data p 14 A87-53996  
Comparison of NOAA AVHRR data to meteorologic drought indices p 14 A87-53997  
Cloud detection in NOAA images p 67 N87-28124  
On the use of AVHRR channel-3 data for environmental studies p 20 N87-28135  
Snow mapping in western Greenland p 54 N87-28150

## NOAA 7 SATELLITE

A multispectral study of the St. Louis area under snow-covered conditions using NOAA-7 AVHRR data p 51 A87-46538

## NOAA 8 SATELLITE

Sea surface temperatures and the detection of ocean circulation patterns and fronts from AVHRR imagery p 45 N87-28125

## NOISE REDUCTION

Preliminary determination of the Geosat radar altimeter noise spectrum p 38 A87-52503  
Speckle noise reduction of 1-look SAR imagery p 65 A87-53273

## NOISE SPECTRA

Preliminary determination of the Geosat radar altimeter noise spectrum p 38 A87-52503

## NORTH AMERICA

Upwelling filaments and motion of a satellite-tracked drifter along the west coast of North America p 29 A87-45023

## NORWAY

Morphostructure and geological patterns in central-southern Norway according to a Landsat image p 25 A87-51146

## NOWCASTING

Thermal infrared images from satellites compared to shelter temperature. Application to frost nowcasting in a citrus orchard p 15 N87-28136

## NUMERICAL WEATHER FORECASTING

Altmetric data assimilation for ocean dynamics and forecasting p 39 A87-52516

## O

## OCEAN BOTTOM

Satellite altimeter measurements of the geoid in sea ice zones p 30 A87-45816  
Morphometric studies of world ocean p 45 N87-28077

Catalog of submarine volcanoes and hydrological phenomena associated with volcanic events, January 1, 1900 to December 31, 1959 p 54 N87-28196

Major morphologic features of the Atlantic Ocean surface p 48 N87-29573

Study of physical processes on the US mid-Atlantic continental slope and rise. Volume 2: Technical presentation [PB87-200523] p 49 N87-30013

Study of physical processes on the US mid-Atlantic continental slope and rise. Volume 3: Appendix [PB87-200531] p 49 N87-30014

## OCEAN COLOR SCANNER

Remote sensing in support of ecological studies of the bowhead whale p 34 A87-48843  
Analysis of data from the DFO fluorescence line imager p 72 A87-48844

## OCEAN CURRENTS

Some aspects of the surface circulation south of 20 deg S revealed by First GARP Global Experiment drifters p 28 A87-42748

Measurement of currents according to the drift of subsatellite buoys p 32 A87-48177

Satellite observations of surface temperatures and flow patterns, Sea of Japan and East China Sea, late March 1979 p 40 A87-53020

Interferometric radar measurement of ocean surface currents p 44 A87-54107

Sea surface temperatures and the detection of ocean circulation patterns and fronts from AVHRR imagery p 45 N87-28125

Comparison of satellite-derived ocean velocities with observations in the California coastal region [AD-A182291] p 47 N87-28242

Satellite image processing for the Agulhas Retroflexion region [AD-A183012] p 68 N87-29905

Physical oceanographic study of Florida's Atlantic Coast region: Florida Atlantic Coast Transport Study (FACTS). Volume 3: Appendices [PB87-201018] p 49 N87-30017

## OCEAN DYNAMICS

Some aspects of the surface circulation south of 20 deg S revealed by First GARP Global Experiment drifters p 28 A87-42748

Studies of the wavelike process in the surface temperature field of the equatorial Pacific using Meteor-satellite IR measurements p 28 A87-42931

Introduction to sea-surface topography from satellite altimetry p 38 A87-52508

Altmetric data assimilation for ocean dynamics and forecasting p 39 A87-52516

Poseidon radar altimeter description and signal processing p 40 A87-53114

Airborne multibeam radar altimetry --- of oceans p 40 A87-53115

Coastal Zone Color Scanner (CZCS) images and ocean dynamics. Application to the Northwest African upwelling area p 46 N87-28146

Comparison of satellite-derived ocean velocities with observations in the California coastal region [AD-A182291] p 47 N87-28242

## OCEAN MODELS

Introduction to sea-surface topography from satellite altimetry p 38 A87-52508

REX and Geosat - Progress in the first year p 39 A87-52511

Design of Geosat Exact Repeat Mission p 39 A87-52515

Comparison of numerical simulations with SAR images of ocean surface waves in the New York Bight p 44 A87-53287

Design study of remote sensing for ocean surface and interior activity [AD-A180578] p 44 N87-25610

Monitoring and modeling of the Adriatic Sea p 46 N87-28133

Data telemetry, assimilation and ocean modeling [AD-A181899] p 47 N87-28239

## OCEAN SURFACE

Radar scattering and equilibrium ranges in wind-generated waves with application to scatterometry p 28 A87-42746

Some aspects of the surface circulation south of 20 deg S revealed by First GARP Global Experiment drifters p 28 A87-42748

Studies of the wavelike process in the surface temperature field of the equatorial Pacific using Meteor-satellite IR measurements p 28 A87-42931

Foam activity on the sea surface as a Markov random process p 28 A87-44289

Radiance-ratio algorithm wavelengths for remote oceanic chlorophyll determination p 29 A87-44812

Climatological implications of a satellite-borne SAR imaging the sea surface p 30 A87-46403

Analysis of Cosmos-1500 radar images of the ocean surface in a zone of cyclones and mesoscale cloud formations p 32 A87-48176

Measurement of currents according to the drift of subsatellite buoys p 32 A87-48177

Maximum accuracy of satellite-borne scatterometer measurements of wind velocity above the ocean p 33 A87-48184

Ocean wave parameter measurement using a dual-radar system - A simulation study p 33 A87-48363

The Navy Geosat mission - An overview p 38 A87-52501

The Geosat radar altimeter p 38 A87-52502

Determination of ocean geodetic data from Geosat p 38 A87-52506

Introduction to sea-surface topography from satellite altimetry p 38 A87-52508

Comparison of Geosat and ground-truth wind and wave observations - Preliminary results p 38 A87-52509

Validation of Geosat altimeter-derived wind speeds and significant wave heights using buoy data p 39 A87-52510

REX and Geosat - Progress in the first year p 39 A87-52511

Poseidon radar altimeter oceanographic remote sensing p 40 A87-53113

Airborne multibeam radar altimetry --- of oceans p 40 A87-53115

Investigation of design parameters for ERS-1 wind scatterometer p 74 A87-53116

An advanced wind scatterometer for the Columbus Polar Platform payload p 74 A87-53117

A spaceborne LFM scatterometer for ocean surface wind vector measurement - A time domain approach --- Linearly Frequency Modulated p 40 A87-53119

Wind and wave statistics as derived from the Geosat radar altimeter and with comparisons with in situ measurements p 40 A87-53127

Inverse synthetic aperture radar imaging techniques for sea-surface targets p 41 A87-53189

Radar signatures of oil films floating on the sea surface p 41 A87-53192

Deconvolution of sea state parameters from altimeter waveforms p 41 A87-53198

Modeling of focus effects in SAR images of the ocean surface p 42 A87-53212

Automatic focusing of synthetic aperture radar images of diffuse targets p 64 A87-53213

Modulation transfer function of radar return power from the ocean p 42 A87-53219

The production of real time wave spectra from the SIR-C SAR p 42 A87-53224

Real time global ocean wave spectra from SIR-C - Systems design p 42 A87-53234

Optimum use of dual frequency passive microwave measurements for ice/ocean interactions p 43 A87-53240

Observations of and a new model for fetch-limited wave growth p 43 A87-53263

The comparison of ocean-wave spectra recovered from SIR-B and Seasat observations with simultaneous buoy data p 43 A87-53265

The response of SAR imagery to azimuth travelling ocean surface waves as determined from shuttle SAR imagery p 44 A87-53286

Comparison of numerical simulations with SAR images of ocean surface waves in the New York Bight p 44 A87-53287

European dissemination of Marine Observation Satellite (MOS-1) data p 44 A87-53925

Interferometric radar measurement of ocean surface currents p 44 A87-54107

The Bakerian Lecture, 1986 - Ships from space --- wakes behind surface vessels observed from space p 44 A87-54301

Design study of remote sensing for ocean surface and interior activity [AD-A180578] p 44 N87-25610

The International Symposium on Microwave Signatures and Remote Sensing held in Gothenburg (Sweden) on 19-22 January 1987 [AD-A181334] p 78 N87-27314

Major morphologic features of the Atlantic Ocean surface p 48 N87-29573

Labrador wind and wave environments [AD-A183218] p 48 N87-29907

Wave-theory modelling of convergence zone propagation in the ocean [AD-A183607] p 50 N87-30020

## OCEANOGRAPHIC PARAMETERS

Boundary layer, upper ocean, and ice observations in the Greenland Sea marginal ice zone p 31 A87-47296

Waveform analysis for Geosat day 96 p 39 A87-52514

Poseidon radar altimeter oceanographic remote sensing p 40 A87-53113

The determination of sea-state bias and non-linear wave parameters from satellite altimeter data p 46 N87-28132

Data telemetry, assimilation and ocean modeling [AD-A181899] p 47 N87-28239

Microwave radiometry study concerning pushbroom systems. Volume 1: A sea salinity/soil-moisture pushbroom radiometer system [R-322] p 79 N87-28951

Study of physical processes on the US mid-Atlantic continental slope and rise. Volume 1: Executive summary [PB87-200515] p 48 N87-30012

## OCEANOGRAPHY

Calibration requirements and methodology for remote sensors viewing the ocean in the visible p 29 A87-44866

Oceanographic and geophysical applications of satellite altimetry p 30 A87-46690

Agricultural, hydrologic and oceanographic studies in Bangladesh with NOAA AVHRR data p 57 A87-48365

SPOT, a satellite for oceanography? p 41 A87-53194

Approximating SIR-B response characteristics and estimating wave height and wavelength for ocean imagery p 44 A87-53288

Remote sensing of suspended matter in the ocean by airborne lasers and satellite radiometers --- coastal zone color scanner [GKSS-86/E/49] p 45 N87-26405

Successes of Cosmos-1500 satellite, SLR system p 45 N87-27696

Study of physical processes on the US mid-Atlantic continental slope and rise. Volume 1: Executive summary [PB87-200515] p 48 N87-30012

Study of physical processes on the US mid-Atlantic continental slope and rise. Volume 2: Technical presentation [PB87-200523] p 49 N87-30013

Physical oceanographic study of Florida's Atlantic Coast region: Florida Atlantic Coast Transport Study (FACTS). Volume 1: Executive summary [PB87-200994] p 49 N87-30015

Physical oceanographic study of Florida's Atlantic Coast region: Florida Atlantic Coast Transport Study (FACTS), volume 2 [PB87-201000] p 49 N87-30016

Physical oceanographic study of Florida's Atlantic Coast region: Florida Atlantic Coast Transport Study (FACTS). Volume 3: Appendices [PB87-201018] p 49 N87-30017



**OCEANS**

- Processing of airborne SAR images of ocean waves  
p 43 A87-53264
- Airborne SAR imaging of azimuthally travelling ocean surface waves - The LEWEX experimental plan  
p 44 A87-53266

**OIL POLLUTION**

- Observation of oil slicks on the ocean by X-band SLAR  
p 41 A87-53191
- Radar signatures of oil films floating on the sea surface  
p 41 A87-53192

**OIL SLICKS**

- Arctic drifting buoy data 1979 - 1985  
[AD-A182967] p 50 N87-30019

**ONBOARD DATA PROCESSING**

- The ERS-1/RADARSAT SAR Canadian ground segment  
p 61 A87-48896
- The operational use of RADARSAT products by the ice centre environment Canada  
p 61 A87-48906

**OPTICAL CORRECTION PROCEDURE**

- Correction of the sensor degradation of the Coastal Zone Color Scanner on NIMBUS-7  
p 46 N87-28153

**OPTICAL DATA PROCESSING**

- Optical image subtraction techniques, 1975-1985  
p 55 A87-42659

**OPTICAL RADAR**

- ADRIA 84: Airborne investigations of Gelbstoff by optical radiometry and fluorescence lidar --- Adriatic Sea  
p 46 N87-28154

**OPTOELECTRONIC DEVICES**

- Different scanning instruments comparison - MOMS and TM --- Modular Optoelectronic Multispectral Scanner  
p 71 A87-48675
- MEIS II imagery for environmental stress analysis --- Multi-detector Electro-optical Imaging Scanner  
p 72 A87-48865

- The RADARSAT RMOMS optical sensor --- Modular Optoelectronic Multispectral Scanner  
p 73 A87-48890

**ORBIT CALCULATION**

- Precise orbit determination with the Doppler Orbitography and Radio positioning Integrated by Satellite (DORIS) system and the associated Zealous for Orbit Observation Methods (ZOOM) software  
p 77 N87-25382

**ORBIT SPECTRUM UTILIZATION**

- A method for the optimization of orbits and structures of satellite systems for the periodic round-the-clock survey of the earth  
p 21 A87-42938

**ORBITAL MANEUVERS**

- Design of Geosat Exact Repeat Mission  
p 39 A87-52515

**ORBITAL MECHANICS**

- Design of Geosat Exact Repeat Mission  
p 39 A87-52515

**ORCHARDS**

- Thermal infrared images from satellites compared to shelter temperature. Application to frost nowcasting in a citrus orchard  
p 15 N87-28136

**ORGANIC MATERIALS**

- ADRIA 84: Airborne investigations of Gelbstoff by optical radiometry and fluorescence lidar --- Adriatic Sea  
p 46 N87-28154

**OROGRAPHY**

- Remote sensing of the geomorphologic formations and vegetation in the eastern High Atlas region of Morocco from SPOT satellite data  
p 23 A87-45048
- Modeling the snowmelt runoff in mountain catchment areas using satellite data  
p 51 A87-47578

**OZONE**

- Review of control strategies for ozone and their effects on other environmental issues  
[PB87-171195] p 19 N87-25634
- Biomonitoring plots at the ozone monitoring stations at Great Smoky Mountains National Park, 1985 survey results  
[PB87-172078] p 19 N87-26464
- Effects of ozone on forests in the northeastern United States  
[DE87-010887] p 16 N87-28190

**P****PACIFIC OCEAN**

- Moisture bursts over the tropical Pacific Ocean  
p 28 A87-43345
- Use of IR satellite rainfall estimates in diagnosing thermally forced circulations in the Pacific during FGGE SOP-1  
p 36 A87-51580
- Monitoring equatorial Pacific sea level with Geosat  
p 39 A87-52512
- Application of satellite data to tropic-subtropical moisture coupling  
[NASA-CR-4092] p 48 N87-29067

**PALEONTOLOGY**

- Application of space photographs to paleoseismological investigations (with reference to the Mongolian Altai)  
p 23 A87-48187

**PARAMETER IDENTIFICATION**

- The determination of sea-state bias and non-linear wave parameters from satellite altimeter data  
p 46 N87-28132
- Sea ice observations by SAR --- satellite observation  
p 47 N87-28156

**PATTERN RECOGNITION**

- Spectral and textural segmentation of multispectral aerial images  
p 5 A87-48831
- Hierarchical classification with knowledge based binary decision --- for thematic mapping image interpretation  
p 62 A87-53110
- A system for knowledge-based segmentation of remotely-sensed images  
p 11 A87-53136
- An expert system for planimetric feature extraction  
p 63 A87-53139
- Remote sensing of deep potential sources over the Nile Delta area  
p 26 A87-53150
- Data correction for automated remote sensing image interpretation  
p 64 A87-53209
- Towards the automatic recognition and vectorised description of linear features in LANDSAT TM images by artificial intelligence methods  
p 67 N87-28142
- Comparison of visual and automated lineament analyses on LANDSAT MSS image from south Greenland  
p 67 N87-28144
- Brief introduction in statistical pattern recognition [INPE-4206-PRE/1087]  
p 68 N87-28374

**PERFORMANCE PREDICTION**

- SPOT MTF performance evaluation  
p 57 A87-48663
- Investigation of design parameters for ERS-1 wind scatterometer  
p 74 A87-53116

**PERIODIC VARIATIONS**

- Variations of mesoscale and large-scale sea ice morphology in the 1984 Marginal Ice Zone Experiment as observed by microwave remote sensing  
p 31 A87-47292

**PHASE ERROR**

- Theoretical feasibility of SAR interferometry  
p 77 A87-53283

**PHOSPHORESCENCE**

- ADRIA 84: Airborne investigations of Gelbstoff by optical radiometry and fluorescence lidar --- Adriatic Sea  
p 46 N87-28154

**PHOTOELECTRIC EMISSION**

- Space surveillance application potential of Schottky barrier IR sensors  
[AD-A180848] p 78 N87-27311

**PHOTO GEOLOGY**

- Characteristics of the Gregory Rift (Kenya) dynamics, ground structural analysis, and remote sensing  
p 23 A87-43353
- Lithological discrimination in central Snowdonia using airborne multispectral scanner imagery  
p 23 A87-48358
- Evaluation of Landsat Thematic Mapper - Imagery for geological exploration  
p 23 A87-48666
- Integration of radiometric and Landsat digital data for geologic investigation and exploration, Guysborough area, Nova Scotia  
p 24 A87-48803
- Analysis of airborne infrared data for interpretative geological mapping of the Brookfield area, Nova Scotia  
p 24 A87-48804
- Evaluation of MEIS-II multispectral scanner data for quaternary geological mapping in the Chatham area, southwestern Ontario  
p 24 A87-48816
- Application of remote sensing data to bedrock geological interpretation, Black River-Matheson area, Northern Ontario, Canada  
p 24 A87-48832
- Digital SAR-Landsat combination for geologic mapping  
p 24 A87-48853
- Shuttle imaging Radar-A (SIR-A) scenes from Iran and China  
p 25 A87-48854
- Pleistocene earth movements in Peninsular India - Evidences from Landsat MSS and Thematic Mapper data  
p 26 A87-53242

**PHOTOGRAMMETRY**

- Photogrammetry - The largest operational application of remote sensing  
p 70 A87-47174
- Determination of the initial motion conditions of earth-resources satellites according to the photogrammetric processing of topographic photographs oriented in inertial space  
p 56 A87-47506
- Photogrammetry from SPOT with Matra TRASTER analytical plotter  
p 58 A87-48865
- Point positioning and mapping with large format camera data  
p 73 A87-50226
- Digital elevation model extraction from stereo satellite images  
p 63 A87-53142
- Sampling semiarid vegetation with large-scale aerial photography  
p 14 A87-53741

- Study on the use and characteristics of SAR for geological applications. Part 2: Radargrammetry aspects [ESA-CR(P)-2325-PT-2]  
p 27 N87-26466

- Vegetation and a LANDSAT-derived land cover map of the Beechey Point quadrangle, Arctic Coastal Plain, Alaska  
[AD-A180931] p 15 N87-27312

- Large Format Camera: The second generation photogrammetric camera for space cartography  
p 78 N87-28118

- A user's guide for the Analytical Photogrammetric Positioning System (APPS)  
[AD-A183773] p 79 N87-29909

**PHOTOINTERPRETATION**

- A study of modern landscape formation in Lower Mesopotamia from space photographs  
p 55 A87-42935
- Use of rice response characteristics in classification using Landsat MSS digital data  
p 1 A87-45046
- Analysis of airborne infrared data for interpretative geological mapping of the Brookfield area, Nova Scotia  
p 24 A87-48804
- Application of accuracy assessment techniques to image classification --- photointerpretation and scene analysis  
p 58 A87-48808
- An evaluation of sun angle computation algorithms  
p 59 A87-48812
- Large-scale black and white and natural color photographs for the measurement of tree crown areas  
p 3 A87-48815
- Evaluation of MEIS-II multispectral scanner data for quaternary geological mapping in the Chatham area, southwestern Ontario  
p 24 A87-48816
- National land use mapping - The application of low altitude sample photography  
p 17 A87-48858
- Indexing small catchments in Java, Indonesia, with respect to their relative susceptibility to erosion  
p 52 A87-48871

- A methodology for automated extraction of drainage networks from satellite imagery  
p 53 A87-48880
- Development of a mathematical model for the spatial triangulation of SPOT images  
p 61 A87-48905
- Land cover classification using SPOT data  
p 18 A87-50227

- Geomorphological interpretation of the SPOT image of February 23, 1986 concerning Djebel Amour (Algeria) and its border with the Sahara  
p 25 A87-51145
- Morphostructure and geological patterns in central-southern Norway according to a Landsat image  
p 25 A87-51146

- Data correction for automated remote sensing image interpretation  
p 64 A87-53209
- Automatic classification of forestal areas by remote sensing techniques  
p 12 A87-53211
- Geomagnetic intersection of tectonic structures seen in space photographs  
p 28 N87-29574

**PHOTOMAPPING**

- An expert system for remote sensing  
p 80 A87-43260
- Lithological discrimination in central Snowdonia using airborne multispectral scanner imagery  
p 23 A87-48358
- Spatial filtering of digital Landsat data for the extraction of mapping information  
p 58 A87-48805
- Landsat-based wildlife habitat mapping - A study of collaboration between analyst and user  
p 3 A87-48809

- Multistage remote sensing with grade four students  
p 80 A87-48810

- Application of remote sensing data to bedrock geological interpretation, Black River-Matheson area, Northern Ontario, Canada  
p 24 A87-48832

- Stratification of satellite imagery by Uniform Productivity Areas  
p 5 A87-48840

- Digital SAR-Landsat combination for geologic mapping  
p 24 A87-48853

- Remote sensing as a tool for Alberta Agricultural Wetlands Drainage Inventory  
p 6 A87-48882
- A revolution in the production of small-scale and medium-scale maps  
p 61 A87-48904
- Point positioning and mapping with large format camera data  
p 73 A87-50226
- Large Format Camera: The second generation photogrammetric camera for space cartography  
p 78 N87-28118

**PLANKTON**

- Coastal Zone Color Scanner (CZCS) images and ocean dynamics. Application to the Northwest African upwelling area  
p 46 N87-28146

**PLANT STRESS**

- MEIS II imagery for environmental stress analysis --- Multi-detector Electro-optical Imaging Scanner  
p 72 A87-48865
- Sulphur dioxide damage assessment using colour infrared aerial photography  
p 60 A87-48884



- Preliminary results from modelling vegetation spectra derived from MEIS data, Algonquin Park, Ontario p 7 A87-48891
- The evaluation of TM analysis as a tool in monitoring land use and agricultural stress in Egypt p 18 A87-48903
- The detection of vegetative stress utilizing remotely sensed data and soil sampling p 8 A87-50231
- Measurement of leaf relative water content by infrared reflectance p 9 A87-53024
- Vegetation mapping and stress detection in the Santa Monica Mountains, California p 12 A87-53246
- PLANTS (BOTANY)**
- Color aerial photography in the plant sciences and related fields; Proceedings of the Tenth Biennial Workshop, University of Michigan, Ann Arbor, May 21-24, 1985 p 1 A87-45100
- Using airborne middle-infrared (1.45-2.0 microns) video imagery for distinguishing plant species and soil conditions p 9 A87-53023
- PLATES (TECTONICS)**
- Geoid anomalies across Ascension fracture zone and the cooling of the lithosphere p 21 A87-44352
- Investigations of relative plate motions in the South Atlantic using Seasat altimeter data p 38 A87-51963
- PLOTTERS**
- Photogrammetry from SPOT with Matra TRASTER analytical plotter p 58 A87-48665
- POLAR METEOROLOGY**
- A pattern analysis technique for distinguishing surface and cloud types in the polar regions p 66 A87-53289
- POLAR ORBITS**
- Earth resources instrumentation for the Space Station Polar Platform p 69 A87-44184
- POLARIMETRY**
- Millimeter-wave polarimetric measurements of artificial and natural targets p 75 A87-53163
- Remote sensing of earth terrain [NASA-CR-181370] p 79 N87-28957
- POLARIZATION (WAVES)**
- Polarization utilization in the microwave inversion of leaf angle distributions p 11 A87-53201
- Radar polarization signatures of vegetated areas p 11 A87-53202
- POLLUTION CONTROL**
- Review of control strategies for ozone and their effects on other environmental issues [PB87-171195] p 19 N87-25634
- POLLUTION MONITORING**
- Monitoring the background pollution of natural environments, No. 3 p 19 A87-52241
- Problems in the background monitoring of the environment, No. 4 --- Russian book p 19 A87-52242
- Monitoring and modeling of the Adriatic Sea p 46 N87-28133
- POLLUTION TRANSPORT**
- Problems in the background monitoring of the environment, No. 4 --- Russian book p 19 A87-52242
- Monitoring and modeling of the Adriatic Sea p 46 N87-28133
- Physical oceanographic study of Florida's Atlantic Coast region: Florida Atlantic Coast Transport Study (FACTS). Volume 1: Executive summary [PB87-200994] p 49 N87-30015
- Physical oceanographic study of Florida's Atlantic Coast region: Florida Atlantic Coast Transport Study (FACTS), volume 2 [PB87-201000] p 49 N87-30016
- POSEIDON SATELLITE**
- Poseidon radar altimeter description and signal processing p 40 A87-53114
- POSITION (LOCATION)**
- Calculation and accuracy of ERBE scanner measurement locations [NASA-TP-2670] p 47 N87-28471
- POSITIONING**
- A user's guide for the Analytical Photogrammetric Positioning System (APPS) [AD-A183773] p 79 N87-29909
- POTABLE WATER**
- Investigation of causes of hydrogen sulfide formation in reclaimed water p 14 N87-23136
- POWER AMPLIFIERS**
- Hybrid power amplifier module for X-band p 69 A87-43302
- PRECIPITATION (METEOROLOGY)**
- Hydrologic applications of weather radar data p 52 A87-48875
- PRESSURE MEASUREMENT**
- Upwelling filaments and motion of a satellite-tracked drifter along the west coast of North America p 29 A87-45023
- PRINCIPAL COMPONENTS ANALYSIS**
- Multistage principal-components analysis of correlations --- of spectral channels for multispectral remote sensing image processing p 56 A87-48193

**PROBABILITY DENSITY FUNCTIONS**

- Deconvolution of sea state parameters from altimeter waveforms p 41 A87-53198

**PROJECT PLANNING**

- Planning for future operational sensors and other priorities [NOAA-NESDIS-30] p 77 N87-25560

**PROVING**

- NASA sea ice and snow validation plan for the Defense Meteorological Satellite Program special sensor microwave/imager [NASA-TM-100683] p 49 N87-30018

**PUSHBROOM SENSOR MODES**

- The RADARSAT RMOMS optical sensor --- Modular Optoelectronic Multispectral Scanner p 73 A87-48890
- Results from the pushbroom microwave radiometer flights over the Konza Prairie in 1985 p 11 A87-53206
- Microwave radiometry study concerning pushbroom systems. Volume 1: A sea salinity/soil-moisture pushbroom radiometer system [R-322] p 79 N87-28951

**Q****QUALITY CONTROL**

- TM sensor performance as obtained from Earthnet quality control data base p 71 A87-48659

**R****RADAR CROSS SECTIONS**

- Calibrated L-band terrain measurements and analysis program [AD-A182917] p 68 N87-29722

**RADAR DATA**

- Comparison of C-band synthetic aperture radar (SAR) data according to two different depression angles for agricultural applications p 4 A87-48820
- Optimization of seismic vessel deployment using side looking airborne radar p 34 A87-48881
- Validation and simulation of Radarsat imagery p 60 A87-48883
- Interpretation of prairie land cover types from SIR-B data p 7 A87-48888
- The operational use of RADARSAT products by the ice centre environment Canada p 61 A87-48906
- Roughness measurements with multipolarization aircraft data p 63 A87-53131
- Cokriging radar-rainfall and rain gage data p 53 A87-54154
- Requirements on radar data for geological application: A case study by use of multistage data of the test site Sardegna/Italy p 27 N87-28120

**RADAR DETECTION**

- Iceberg detection using SLAR p 34 A87-48876

**RADAR ECHOES**

- Statistical modelling and suppression of speckle in synthetic aperture radar images p 65 A87-53259

**RADAR EQUIPMENT**

- Hybrid power amplifier module for X-band p 69 A87-43302

**RADAR GEOLOGY**

- Study on the use and characteristics of SAR for geological applications. Part 2: Radargrammetry aspects [ESA-CR(P)-2325-PT-2] p 27 N87-26466
- Study on the use and characteristics of SAR systems for geological applications [ESA-CR(P)-2342] p 27 N87-26467
- Geological feature enhancement in SAR imagery p 67 N87-27861
- Requirements on radar data for geological application: A case study by use of multistage data of the test site Sardegna/Italy p 27 N87-28120

**RADAR IMAGERY**

- Radar observations of terrestrial vegetation covers in the 3-cm range p 1 A87-42936
- Potential application of multipolarization SAR for pine-plantation biomass estimation p 1 A87-43263
- Climatological implications of a satellite-borne SAR imaging the sea surface p 30 A87-46403
- Detecting forest structure and biomass with C-band multipolarization radar - Physical model and field tests p 2 A87-46543
- Multifrequency and multipolarization radar scatterometry of sand dunes and comparison with spaceborne and airborne radar images p 70 A87-47257
- Use of synthetic aperture radar-derived kinematics in mapping mesoscale ocean structure within the interior marginal ice zone p 31 A87-47294
- Multisensor comparison of ice concentration estimates in the marginal ice zone p 31 A87-47295
- Beaufort-Chukchi ice margin data from Seasat - Ice motion p 32 A87-47299

- Analysis of Cosmos-1500 radar images of the ocean surface in a zone of cyclones and mesoscale cloud formations p 32 A87-48176
- Evaluation of the effect of hydrometeors on the characteristics of radar images of sea ice p 33 A87-48181
- Comparison of space and airborne L-HH radar imagery in an agricultural environment p 4 A87-48819
- Validation of STAR-1 SAR imagery collected over Mould Bay, N.W.T., April 1984 p 59 A87-48826
- The use of multi-spectral and radar remote sensing data for monitoring forest clearcut and regeneration sites on Vancouver Island p 5 A87-48834
- Effects of surface geometry of agricultural fields on radar airborne imagery in X- and C-bands p 5 A87-48846
- Radiometric corrections of topographic effects for simulated RADARSAT imagery in a region of moderate relief p 59 A87-48847
- The influence of melting conditions on the interpretation of radar imagery of sea ice p 34 A87-48849
- The detection of wetlands on radar imagery p 6 A87-48855
- Multiple-look effects on SAR classification accuracies p 60 A87-48885
- Inverse synthetic aperture radar imaging techniques for sea-surface targets p 41 A87-53189
- Modeling of focus effects in SAR images of the ocean surface p 42 A87-53212
- Automatic focusing of synthetic aperture radar images of diffuse targets p 64 A87-53213
- Global digital topography mapping using a scanning radar altimeter p 76 A87-53227
- A high speed digital processor for real-time synthetic aperture radar imaging p 64 A87-53233
- The European Campaign 'AGRISAR '86' p 13 A87-53249
- Statistical modelling and suppression of speckle in synthetic aperture radar images p 65 A87-53259
- Spatial considerations in speckle simulation --- of spaceborne synthetic aperture radar imagery p 65 A87-53260
- Statistical modeling of intensity distributions on airborne SAR imagery p 65 A87-53262
- Speckle noise reduction of 1-look SAR imagery p 65 A87-53273
- Textural segmentation of SAR images using first order statistical parameters p 66 A87-53274
- A statistical and geometrical edge detector for SAR image segmentation p 13 A87-53275
- Derivation of the technical specification of the ERS-1 active microwave instrument to meet the SAR-image quality requirements p 77 A87-53280
- The response of SAR imagery to azimuth travelling ocean surface waves as determined from shuttle SAR imagery p 44 A87-53286
- Comparison of numerical simulations with SAR images of ocean surface waves in the New York Bight p 44 A87-53287
- Study on the use and characteristics of SAR for geological applications. Part 2: Radargrammetry aspects [ESA-CR(P)-2325-PT-2] p 27 N87-26466
- Study on the use and characteristics of SAR systems for geological applications [ESA-CR(P)-2342] p 27 N87-26467
- Proceedings of the SAR Applications Workshop --- Synthetic Aperture Radar [ESA-SP-264] p 78 N87-27854
- SAR detection of ships and ship wakes p 66 N87-27859
- Thin line detection in SAR images p 66 N87-27860
- Geological feature enhancement in SAR imagery p 67 N87-27861
- Land use feature detection in SAR images p 67 N87-27863
- An algorithm for automatically acquiring ground control points in SAR imagery p 67 N87-27864
- Crop discrimination by means of radar and infrared images p 15 N87-28128
- RADAR MAPS**
- Observations of and a new model for fetch-limited wave growth p 43 A87-53263
- Study on the use and characteristics of SAR for geological applications. Part 2: Radargrammetry aspects [ESA-CR(P)-2325-PT-2] p 27 N87-26466
- RADAR MEASUREMENT**
- Ocean wave parameter measurement using a dual-radar system - A simulation study p 33 A87-48363
- Airborne multibeam radar altimetry --- of oceans p 40 A87-53115
- Wind and wave statistics as derived from the Geosat radar altimeter and with comparisons with in situ measurements p 40 A87-53127
- Radar polarization signatures of vegetated areas p 11 A87-53202
- Progress on digital algorithms for deriving sea ice parameters from SAR data p 43 A87-53238

- Interferometric radar measurement of ocean surface currents p 44 A87-54107
- Calibrated L-band terrain measurements and analysis program [AD-A182917] p 68 N87-29722
- RADAR PHOTOGRAPHY**
- Study on the use and characteristics of SAR for geological applications. Part 2: Radargrammetry aspects [ESA-CR(P)-2325-PT-2] p 27 N87-26466
- Study on the use and characteristics of SAR systems for geological applications [ESA-CR(P)-2342] p 27 N87-26467
- RADAR SCATTERING**
- Radar scattering and equilibrium ranges in wind-generated waves with application to scatterometry p 28 A87-42746
- Multifrequency and multipolarization radar scatterometry of sand dunes and comparison with spaceborne and airborne radar images p 70 A87-47257
- Retrieval of surface roughness parameters from dual-frequency measurements of radar backscattering coefficients p 10 A87-53130
- The use of old-field stands of loblolly pine in studies of the potential use of active microwave remote sensors for monitoring forest ecosystems p 11 A87-53153
- On the origin of cross-polarization in remote sensing p 75 A87-53168
- Modulation transfer function of radar return power from the ocean p 42 A87-53219
- Theoretical and experimental study of the radar backscatter of Arctic sea ice p 43 A87-53237
- Statistical modelling and suppression of speckle in synthetic aperture radar images p 65 A87-53259
- Calibrated L-band terrain measurements and analysis program [AD-A182917] p 68 N87-29722
- RADAR SIGNATURES**
- Observation of oil slicks on the ocean by X-band SLAR p 41 A87-53191
- Radar signatures of oil films floating on the sea surface p 41 A87-53192
- The potential of SAR in a snow and glacier monitoring system p 45 A87-27856
- RADAR TARGETS**
- Calibration of NOAA-7 AVHRR, GOES-5, and GOES-6 VISSR/VAS solar channels p 69 A87-44865
- Statistical modelling and suppression of speckle in synthetic aperture radar images p 65 A87-53259
- SAR detection of ships and ship wakes p 66 N87-27859
- RADAR TRACKING**
- Averaging of radar altimeter pulse returns with the interpolation tracker p 70 A87-45044
- RADARSAT**
- Radiometric corrections of topographic effects for simulated RADARSAT imagery in a region of moderate relief p 59 A87-48847
- Validation and simulation of Radarsat imagery p 60 A87-48883
- Multiple-look effects on SAR classification accuracies p 60 A87-48885
- The RADARSAT RMOMS optical sensor --- Modular Optoelectronic Multispectral Scanner p 73 A87-48890
- The ERS-1/RADARSAT SAR Canadian ground segment p 61 A87-48896
- The operational use of RADARSAT products by the ice centre environment Canada p 61 A87-48906
- RADIANCE**
- Radiance-ratio algorithm wavelengths for remote oceanic chlorophyll determination p 29 A87-44812
- Monte Carlo calculation of the dependence of the spectral radiance of vegetation cover on the illumination conditions p 2 A87-48190
- Cloud and moisture fields derived from the GLA retrievals of HIRS2/MSU data p 36 A87-51579
- Use of LANDSAT digital data for snow cover mapping in the upper Saint John River Basin, Maine [AD-A183213] p 54 N87-29906
- RADIATION DISTRIBUTION**
- Radiation modelling in a high relief environment using a digital terrain model and Landsat - TM imagery p 59 A87-48857
- RADIATIVE HEAT TRANSFER**
- A microwave radiometer weather-correcting sea ice algorithm p 29 A87-45024
- Remote-sensing techniques for investigating the structure of radiation-heat fluxes and the moisture content of geosystems in connection with the problem of monitoring the water component p 52 A87-47584
- Theory of fluorescent irradiance fields in lakes and seas [PB87-196465] p 47 N87-28954

**RADIATIVE TRANSFER**

Investigating the role of the land surface in explaining the interannual variation of the net radiation balance over the Western Sahara and sub-Sahara

[NASA-CR-181183] p 68 N87-28197

**RADIO ALTIMETERS**

Averaging of radar altimeter pulse returns with the interpolation tracker p 70 A87-45044

The Geosat radar altimeter p 38 A87-52502

Preliminary determination of the Geosat radar altimeter noise spectrum p 38 A87-52503

Determination of ocean geodetic data from Geosat p 38 A87-52506

Preliminary results from the processing of a limited set of Geosat radar altimeter data p 22 A87-52507

Ice measurements by Geosat radar altimetry p 39 A87-52513

Poseidon radar altimeter oceanographic remote sensing p 40 A87-53113

Active microwave observations of sea ice and icebergs p 45 N87-27855

A study of antenna signal processing techniques for radar alternatives [ESA-CR(P)-2370] p 79 N87-28809

**RADIO INTERFEROMETERS**

Radio interferometry p 21 A87-46688

**RADIO METEOROLOGY**

Satellite microwave radiometry of snow water equivalent p 52 A87-48823

**RADIO SCATTERING**

Estimation of X-band scattering properties of tree components p 13 A87-53277

**RADIOMETERS**

Integration of radiometric and Landsat digital data for geologic investigation and exploration, Guysborough area, Nova Scotia p 24 A87-48803

Sea surface temperature retrieval from the Tiros-N AVHRR instrument for the FGGE period (Dec. 1978-Nov. 1979) p 35 A87-51553

Millimeter-wave imaging sensor data evaluation [NASA-CR-181159] p 77 N87-26264

On the use of AVHRR channel-3 data for environmental studies p 20 N87-28135

**RADIOMETRIC CORRECTION**

Reflectance- and radiance-based methods for the in-flight absolute calibration of multispectral sensors p 69 A87-44863

Radiometric properties of U.S. processed Landsat MSS data p 55 A87-44864

Practical aspects of achieving accurate radiometric field measurements p 69 A87-44868

Scene to scene radiometric normalization of the reflected bands of the Landsat Thematic Mapper p 71 A87-48654

Within-scene radiometric correction of Landsat Thematic Mapper (TM) data in Canadian production systems p 57 A87-48656

Absolute calibration of the SPOT-1 HRV cameras p 71 A87-48660

Radiometric corrections of topographic effects for simulated RADARSAT imagery in a region of moderate relief p 59 A87-48847

Ground targets for the radiometric correction of AVHRR imagery for crop monitoring p 7 A87-48887

Smoothing vegetation index profiles - An alternative method for reducing radiometric disturbance in NOAA/AVHRR data p 14 A87-53996

**RADIOMETRIC RESOLUTION**

SPOT radiometric resolution performance evaluation - Preliminary results p 57 A87-48661

Using AVHRR data to evaluate the greenness variability within monitoring polygons p 4 A87-48828

Monitoring the fire-danger hazard of Nebraska rangelands with AVHRR data p 17 A87-48838

Using NOAA AVHRR in studies of sea ice motion in the Beaufort Sea p 34 A87-48842

Monitoring wheat canopies with a high spectral resolution radiometer p 8 A87-53019

The contribution of AVHRR data for measuring and understanding global processes - Large-scale deforestation in the Amazon basin p 11 A87-53151

A cross antenna for passive microwave remote sensing p 77 A87-53268

**RAIN**

Use of IR satellite rainfall estimates in diagnosing thermally forced circulations in the Pacific during FGGE SOP-1 p 36 A87-51580

Scattering parameters for aspherical hydrometeors at microwave frequencies p 53 A87-53271

Comparisons of gauge and satellite rain estimates for the central United States during August 1979 p 53 A87-54152

Sampling errors in satellite estimates of tropical rain p 53 A87-54153

Cokriging radar-rainfall and rain gage data p 53 A87-54154

A space-time stochastic model of rainfall for satellite remote-sensing studies p 54 A87-54157

National Climate Program [PB87-190518] p 79 N87-28221

**RAIN FORESTS**

Selection of extended area land target sites for the calibration of spaceborne scatterometers p 74 A87-53118

Evaluation of the range and degradation of mangroves in Southern Sergipe with remote sensing techniques [INPE-4196-PRE/1080] p 16 N87-28160

**RAIN GAGES**

Cokriging radar-rainfall and rain gage data p 53 A87-54154

**RANGELANDS**

Monitoring the fire-danger hazard of Nebraska rangelands with AVHRR data p 17 A87-48838

Effectiveness of the Thematic Mapper for the range condition assessment in fescue grasslands of Southwestern Alberta p 6 A87-48850

**READOUT**

Space surveillance application potential of Schottky barrier IR sensors [AD-A180848] p 78 N87-27311

**REAL TIME OPERATION**

Optical image subtraction techniques, 1975-1985 p 55 A87-42659

Custom-enhanced Landsat imagery in near real-time p 60 A87-48870

The production of real time wave spectra from the SIR-C SAR p 42 A87-53224

Real time global ocean wave spectra from SIR-C - Systems design p 42 A87-53234

**REFLECTANCE**

Monitoring wheat canopies with a high spectral resolution radiometer p 8 A87-53019

Investigation of design parameters for ERS-1 wind scatterometer p 74 A87-53116

**REFLECTION**

Use of LANDSAT digital data for snow cover mapping in the upper Saint John River Basin, Maine [AD-A183213] p 54 N87-29906

**REFORESTATION**

Digital image classification approach for estimating forest clearing and regrowth rates and trends p 10 A87-53123

**REGIONAL PLANNING**

Significance of TM data as a tool to support regional planning activities p 17 A87-48671

**REGRESSION ANALYSIS**

Comparison of NOAA AVHRR data to meteorologic drought indices p 14 A87-53997

**RELIEF MAPS**

Investigation of the relief of ore-containing regions on the basis of space photographs (with reference to eastern Yakutia) p 23 A87-48188

Radiometric corrections of topographic effects for simulated RADARSAT imagery in a region of moderate relief p 59 A87-48847

**REMOTE SENSING**

Remote sensing of coastal wetlands p 1 A87-40944

The application of remote sensing techniques in China p 68 A87-41435

Formation of natural underground-water resources in arid regions with special reference to the Dolinoozerskii artesian basin in Mongolia --- Russian book p 50 A87-42911

A study of modern landscape formation in Lower Mesopotamia from space photographs p 55 A87-42935

An expert system for remote sensing p 80 A87-43260

The CCRS SAR/MSS Anderson River data set p 55 A87-43261

Multiple-angle observations of reflectance anisotropy from an airborne linear array sensor p 69 A87-43262

Characteristics of the Gregory Rift (Kenya) dynamics, ground structural analysis, and remote sensing p 23 A87-43353

Foam activity on the sea surface as a Markov random process p 28 A87-44289

Features of the water dynamics of Lake Ladoga according to remote sensing data p 50 A87-44296

Multiparameter sampling (ship, aircraft, and satellite) of a Gulf Stream warm core ring p 29 A87-44811

Radiance-ratio algorithm wavelengths for remote oceanic chlorophyll determination p 29 A87-44812

Practical aspects of achieving accurate radiometric field measurements p 69 A87-44868

Remote sensing in Indonesia - A review of the available technology and its applications for resources surveys p 17 A87-46310

Remote observations of the marine environment - Spatial heterogeneity of the mesoscale ocean color field in CZCS imagery of California near-coastal waters p 30 A87-46539

Remote sensing of submerged aquatic vegetation in lower Chesapeake Bay - A comparison of Landsat MSS to TM imagery p 30 A87-46542

Remote sensing applications of the earth's surface - An outlook into the future p 70 A87-47173

Photogrammetry - The largest operational application of remote sensing p 70 A87-47174

Multifrequency and multipolarization radar scatterometry of sand dunes and comparison with spaceborne and airborne radar images p 70 A87-47257

Variations of mesoscale and large-scale sea ice morphology in the 1984 Marginal Ice Zone Experiment as observed by microwave remote sensing p 31 A87-47292

Evolution of microwave sea ice signatures during early summer and midsummer in the marginal ice zone p 31 A87-47293

Multisensor comparison of ice concentration estimates in the marginal ice zone p 31 A87-47295

Remote sensing techniques for the study of hydrological elements p 51 A87-47576

Parameterization of models of runoff formation in simple catchment areas using remote-sensing data p 51 A87-47579

Remote-sensing evaluation of moisture supply to crops according to the leaf-surface thermal regime p 2 A87-47582

Remote-sensing evaluation of the spatial variability of evaporation p 52 A87-47583

Remote-sensing techniques for investigating the structure of radiation-heat fluxes and the moisture content of geosystems in connection with the problem of monitoring the water component p 52 A87-47584

Evaluation of the effect of hydrometeors on the characteristics of radar images of sea ice p 33 A87-48181

Features of a statistical model for the interaction between electromagnetic waves and remotely sensed natural objects p 70 A87-48189

Multistage principal-components analysis of correlations --- of spectral channels for multispectral remote sensing image processing p 56 A87-48193

Lithological discrimination in central Snowdonia using airborne multispectral scanner imagery p 23 A87-48358

The effect of subpixel clouds on remote sensing p 2 A87-48360

The variability of the North Atlantic marine atmosphere and its relevance to remote sensing p 33 A87-48362

Agricultural, hydrologic and oceanographic studies in Bangladesh with NOAA AVHRR data p 57 A87-48365

Earth remote sensing using the Landsat Thematic Mapper and SPOT sensor systems; Proceedings of the Meeting, Innsbruck, Austria, Apr. 15-17, 1986 [SPIE-660] p 70 A87-48652

Geometric quality of Thematic Mapper data of the United Kingdom p 57 A87-48655

Evaluation of Landsat Thematic Mapper - Imagery for geological exploration p 23 A87-48666

Lithological discrimination using geobotanical and Landsat TM spectral data p 23 A87-48667

Shallow water bathymetry and bottom classification by means of the Landsat and SPOT optical scanners p 52 A87-48670

The Land Satellite (Landsat) system - Earth Observation Satellite Company (Eosat's) plans for Landsat-6 and beyond p 71 A87-48676

Canadian Symposium on Remote Sensing, 10th, Edmonton, Canada, May 5-8, 1986, Proceedings. Volume 1 & 2 p 72 A87-48801

Multistage remote sensing with grade four students p 80 A87-48810

Operational, province wide crop area estimation for Manitoba p 3 A87-48811

Application of image segmentation algorithms to the inventory of crops in Canada p 3 A87-48813

Operational use of remote sensing for commercial Arctic class vessel navigation p 33 A87-48829

Application of remote sensing data to bedrock geological interpretation, Black River-Matheson area, Northern Ontario, Canada p 24 A87-48832

The use of multi-spectral and radar remote sensing data for monitoring forest clearcut and regeneration sites on Vancouver Island p 5 A87-48834

Barriers to the operational use of satellite remote sensing in Canada p 72 A87-48835

Operational water quality surveillance in Sweden using Landsat MSS data p 52 A87-48841

Remote sensing in support of ecological studies of the bowhead whale p 34 A87-48843

Analysis of data from the DFO fluorescence line imager p 72 A87-48844

Snowpack depletion monitoring in Alberta using computer-processed NOAA imagery p 52 A87-48848

The influence of melting conditions on the interpretation of radar imagery of sea ice p 34 A87-48849

Effectiveness of the Thematic Mapper for the range condition assessment in fescue grasslands of Southwestern Alberta p 6 A87-48850

Managing coral reefs - Operational benefits of remote sensing in Marine Park planning p 34 A87-48851

CCRS airborne Electro-Optical Facility p 72 A87-48852

Shuttle imaging Radar-A (SIR-A) scenes from Iran and China p 25 A87-48854

The detection of wetlands on radar imagery p 6 A87-48855

Regional geobotany with TM - A Sudbury case study p 25 A87-48861

Multispectral video system for airborne remote sensing - Sensitivity, calibrations and correction p 73 A87-48873

Discrimination of suspended sediment and littoral features using multispectral video imagery p 73 A87-48874

Optimization of seismic vessel deployment using side looking airborne radar p 34 A87-48881

Remote sensing as a tool for Alberta Agricultural Wetlands Drainage Inventory p 6 A87-48882

Multiple-look effects on SAR classification accuracies p 60 A87-48885

An application for the testing and use of the standard data transfer format --- for remotely sensed classified information transmission to GIS center p 18 A87-48886

Interpretation of prairie land cover types from SIR-B data p 7 A87-48888

New system for the ordering, archiving and retrieval of data from earth's resource satellites p 60 A87-48889

Preliminary results from modelling vegetation spectra derived from MEIS data, Algonquin Park, Ontario p 7 A87-48891

A trial of oblique imagery from a low cost video camera system for defoliation assessment p 7 A87-48892

Remote sensing in the Sahel - A tool for the inventory and monitoring of resources p 73 A87-48893

The role of remote sensing in the Canada Land Use Monitoring Program (CLUMP) p 18 A87-48895

The ERS-1/RADARSAT SAR Canadian ground segment p 61 A87-48896

Thermographic remote sensing of northern forest areas in regeneration after clear or strip cutting - Preliminary observations p 8 A87-48897

Environmental monitoring of Alpine Meadows with large scale aerial photography in Banff National Park p 18 A87-48898

Remote sensing and the agricultural resource inventory p 8 A87-48899

TM and MEIS data for future Alberta forest inventories p 8 A87-48900

Spectral studies of dryland agricultural salinity in Western Australia p 8 A87-48901

Development of a mathematical model for the spatial triangulation of SPOT images p 61 A87-48905

The detection of vegetative stress utilizing remotely sensed data and soil sampling p 8 A87-50231

Atmospheric correction of data measured by a flying platform over the sea - Elements of a model and its experimental validation p 35 A87-50292

SPOT's first year p 80 A87-51320

Eurimage sets up shop p 80 A87-51324

Remote-sensing and geological-geophysical studies of closed platform territories --- Russian book p 26 A87-51875

Color enhancement of highly correlated images. II - Channel ratio and 'chromaticity' transformation techniques p 62 A87-53018

Monitoring wheat canopies with a high spectral resolution radiometer p 8 A87-53019

Using airborne middle-infrared (1.45-2.0 microns) video imagery for distinguishing plant species and soil conditions p 9 A87-53023

Measurement of leaf relative water content by infrared reflectance p 9 A87-53024

Status of and prognosis for space remote sensing [AAS PAPER 86-104] p 80 A87-53084

IGARSS '87 - International Geoscience and Remote Sensing Symposium, University of Michigan, Ann Arbor, May 18-21, 1987, Digest. Volumes 1 & 2 p 73 A87-53101

Improved cloud analysis using visible, near-infrared, infrared, and microwave imagery p 62 A87-53103

Remote sensing of geomagnetic field and applications to climate prediction p 74 A87-53108

Cluster based segmentation of multi-temporal Thematic Mapper data as preparation of region-based agricultural land-cover analysis p 9 A87-53109

Exploring the spatial domain --- analysis of remote sensing data p 62 A87-53112

Poseidon radar altimeter oceanographic remote sensing p 40 A87-53113

Airborne multibeam radar altimetry --- of oceans p 40 A87-53115

Airborne multispectral observations over burned and unburned prairies p 10 A87-53122

Using remotely sensed Landsat MSS data to assess groundwater influence on the Barmah-Millewa Forest p 10 A87-53124

Retrieval of surface roughness parameters from dual-frequency measurements of radar backscattering coefficients p 10 A87-53130

A system for knowledge-based segmentation of remotely-sensed images p 11 A87-53136

Sequential thinning algorithms for remote sensing application p 63 A87-53140

Remote sensing of deep potential sources over the Nile Delta area p 26 A87-53150

Remote sensing and landscape approaches to earth resources p 63 A87-53154

Millimeter-wave polarimetric measurements of artificial and natural targets p 75 A87-53163

On the origin of cross-polarization in remote sensing p 75 A87-53168

Remote sensing by the fluorescence property of the scatterer p 75 A87-53179

Spectral feature design for data compression in high dimensional multispectral data p 64 A87-53183

Analysis of environmental information of urban areas using Landsat TM data p 19 A87-53187

Observation of oil slicks on the ocean by X-band SLAR p 41 A87-53191

SPOT, a satellite for oceanography? p 41 A87-53194

Wind measurements for non-uniform wind fields from spaceborne scatterometers p 75 A87-53195

An operational multispectral scanner for bathymetric surveys - The ABS NORDA scanner p 42 A87-53199

Polarization utilization in the microwave inversion of leaf angle distributions p 11 A87-53201

Radar polarization signatures of vegetated areas p 11 A87-53202

Results from the pushbroom microwave radiometer flights over the Konza Prairie in 1985 p 11 A87-53206

Data correction for automated remote sensing image interpretation p 64 A87-53209

Automatic classification of forestal areas by remote sensing techniques p 12 A87-53211

Synergism requirements and concepts for SAR and HIRIS on EOS p 75 A87-53216

The global forest ecosystem as viewed by ERS-1, SIR-C and EOS p 12 A87-53217

The First ISLSCP Field Experiment (FIFE) p 12 A87-53218

Remote sensing of the earth with microwave radiometry in Germany - Results and trends p 76 A87-53225

The Land Analysis System (LAS) - A general purpose system for multispectral image processing p 64 A87-53230

The SPOT program - Commercialization of remote sensing p 80 A87-53235

Theoretical models for microwave remote sensing of snow-covered sea ice p 42 A87-53236

Observing rotation and deformation of sea ice with synthetic aperture radar p 43 A87-53239

Optimum use of dual frequency passive microwave measurements for ice/ocean interactions p 43 A87-53240

Analysis of Eocene depositional environments - Preliminary TM and TIMS results, Wind River Basin, Wyoming p 26 A87-53243

Estimating key forest ecosystem parameters through remote sensing p 12 A87-53245

The European Campaign 'AGRISAR '86' p 13 A87-53249

Geometric distortion correction with high accuracy for NOAA satellite images p 65 A87-53253

Spatial considerations in speckle simulation --- of spaceborne synthetic aperture radar imagery p 65 A87-53260

A cross antenna for passive microwave remote sensing p 77 A87-53268

Textural segmentation of SAR images using first order statistical parameters p 66 A87-53274

Modeling gap probability in discontinuous vegetation canopies p 13 A87-53276

Estimation of X-band scattering properties of tree components p 13 A87-53277

Integration of topographic data with synthetic aperture radar data for determining forest properties in mountainous terrain p 14 A87-53278

A combined SAR and scatterometer system p 77 A87-53279

Derivation of the technical specification of the ERS-1 active microwave instrument to meet the SAR-image quality requirements p 77 A87-53280

The future generation of resources satellites p 80 A87-53742

European dissemination of Marine Observation Satellite (MOS-1) data p 44 A87-53925

Smoothing vegetation index profiles - An alternative method for reducing radiometric disturbance in NOAA-AVHRR data p 14 A87-53996

Comparison of NOAA AVHRR data to meteorologic drought indices p 14 A87-53997

A methodology for evaluation of an interactive multispectral image processing system p 66 A87-53999

Estimation of surface moisture availability from remote temperature measurements p 53 A87-54155

A space-time stochastic model of rainfall for satellite remote-sensing studies p 54 A87-54157

Millimeter-wave imaging sensor data evaluation [NASA-CR-181159] p 77 A87-26264

Remote sensing of suspended matter in the ocean by airborne lasers and satellite radiometers --- coastal zone color scanner [GKSS-86/E/49] p 45 N87-26405

HMMR (High-Resolution Multifrequency Microwave Radiometer) Earth observing system, volume 2e. Instrument panel report [NASA-TM-89625] p 78 N87-27316

Proceedings of the ESA-EARSeL Europe from Space Symposium [ESA-SP-258] p 19 N87-28115

Integration of remote sensing and geophysical data-application to exploration of pyrite ore facies in SW Spain p 27 N87-28119

Contribution of space technology to disaster preparedness, warning, and relief p 20 N87-28130

Monitoring and modeling of the Adriatic Sea p 46 N87-28133

The role and perspective of remote sensing for disaster management in the European community p 20 N87-28137

Satellite remote sensing for water resources management: Some engineering and economic aspects p 54 N87-28139

ERAFIS: A computer information system for agriculture and forestry in Spain p 16 N87-28140

Environmental information and cartography p 20 N87-28141

Integrated systems for remote sensing p 67 N87-28143

Measurement of spectral signatures in Less Favored Areas (LFA): A contribution to the definition of a remote sensing multitemporal experiment p 20 N87-28145

ADRIA 84: Airborne investigations of Gelbstoff by optical radiometry and fluorescence lidar --- Adriatic Sea p 46 N87-28154

Spectral characteristics and the extent of paleosols of the Palouse formation [NASA-CR-181208] p 17 N87-28195

Calculation and accuracy of ERBE scanner measurement locations [NASA-TP-2670] p 47 N87-28471

Theory of fluorescent irradiance fields in lakes and seas [PB87-196465] p 47 N87-28954

Remote sensing of earth terrain [NASA-CR-181370] p 79 N87-28957

Workshop on The Earth as a Planet [NASA-CR-180543] p 81 N87-29900

**REMOTE SENSORS**

Calibration requirements and methodology for remote sensors viewing the ocean in the visible p 29 A87-44866

TM sensor performance as obtained from Earthnet quality control data base p 71 A87-48659

Comparative analysis of different sensor data (Landsat-TM and MOMS) for earth observation and impact on future sensor development p 71 A87-48674

Different scanning instruments comparison - MOMS and TM --- Modular Optoelectronic Multispectral Scanner p 71 A87-48675

Selection of extended area land target sites for the calibration of spaceborne scatterometers p 74 A87-53118

MODIS - Advanced facility instrument for studies of the earth as a system --- Moderate Resolution Imaging Spectrometer p 40 A87-53144

A multifrequency microwave radiometer of the future p 75 A87-53180

Planning for future operational sensors and other priorities [NOAA-NESDIS-30] p 77 N87-25560

The feasibility of detecting a magnetic field from a distant platform [AD-A180635] p 78 N87-27310

Data telemetry, assimilation and ocean modeling [AD-A181899] p 47 N87-28239

Comparison of satellite-derived ocean velocities with observations in the California coastal region [AD-A182291] p 47 N87-28242

Labrador wind and wave environments [AD-A183218] p 48 N87-29907

**RESEARCH**

Arctic drifting buoy data 1979 - 1985 [AD-A182967] p 50 N87-30019

**RESERVOIRS**

Possibility of evaluating reservoir influx from aerial and satellite photographs p 51 A87-47577

Suspended sediment concentrations estimated from Landsat MSS p 53 A87-53204

**RESIDENTIAL AREAS**

Small format aerial photography for analyzing urban housing problems - A case study in the Bangkok metropolitan region p 17 A87-46309

**RESOURCES MANAGEMENT**

Barriers to the operational use of satellite remote sensing in Canada p 72 A87-48835

Proceedings of the ESA-EARSeL Europe from Space Symposium [ESA-SP-258] p 19 N87-28115

**RHEOLOGY**

Rheology of the 1983 Royal Gardens basalt flows, Kilauea Volcano, Hawaii p 26 A87-51725

**RHONE DELTA (FRANCE)**

Contribution of improved resolution to morphological analysis - The example of the Rhone delta p 25 A87-51144

**RICE**

Use of rice response characteristics in classification using Landsat MSS digital data p 1 A87-45046

Monitoring rice areas using Landsat MSS data p 1 A87-45047

**RIVER BASINS**

The determination of Love numbers from the results of earth-tide observations in the Dnieper-Donets basin (DDB) region p 21 A87-46139

Indices of climatological and hydrological variability derived from satellite imagery for the South Saskatchewan River Basin p 52 A87-48856

Analysis of Eocene depositional environments - Preliminary TM and TIMS results, Wind River Basin, Wyoming p 26 A87-53243

Use of LANDSAT digital data for snow cover mapping in the upper Saint John River Basin, Maine [AD-A183213] p 54 N87-29906

**ROCKS**

Millimeter-wave polarimetric measurements of artificial and natural targets p 75 A87-53163

Application of TM imagery to mapping volcanic rock assemblages at tertiary calderas of the basin and range province p 26 A87-53257

**ROCKY MOUNTAINS (NORTH AMERICA)**

Radiation modelling in a high relief environment using a digital terrain model and Landsat - TM imagery p 59 A87-48857

**ROSS ICE SHELF**

Antarctic ice streams - A review p 37 A87-51943

**RURAL AREAS**

Rural land use classification using Landsat Thematic Mapper data p 18 A87-48868

A model of thermal inertia for frost forecasting in agricultural areas --- satellite imagery p 16 N87-28151

**RURAL LAND USE**

Spectral studies of dryland agricultural salinity in Western Australia p 8 A87-48901

Rural land use inventory and mapping in the Ardeche area (France). Improvement of automatic classification by multitemporal analysis of TM data p 15 N87-28127

## S

**SAHARA DESERT (AFRICA)**

Geomorphological interpretation of the SPOT image of February 23, 1986 concerning Djebel Amour (Algeria) and its border with the Sahara p 25 A87-51145

Investigating the role of the land surface in explaining the interannual variation of the net radiation balance over the Western Sahara and sub-Sahara [NASA-CR-181183] p 68 N87-28197

**SALINITY**

The detection of vegetative stress utilizing remotely sensed data and soil sampling p 8 A87-50231

Microwave radiometry study concerning pushbroom systems. Volume 1: A sea salinity/soil-moisture pushbroom radiometer system [R-322] p 79 N87-28951

**SATELLITE ALTIMETRY**

Geoid anomalies across Ascension fracture zone and the cooling of the lithosphere p 21 A87-44352

Seasat altimetry and the South Atlantic geoid. I - Spectral analysis p 21 A87-45743

Satellite altimeter measurements of the geoid in sea ice zones p 30 A87-45816

Earth gravity model improvement - An alternative method for Doppler-tracked satellites p 21 A87-45817

Oceanographic and geophysical applications of satellite altimetry p 30 A87-46690

Processing of Seasat altimetry data on a digital image analysis system p 59 A87-48825

Investigations of relative plate motions in the South Atlantic using Seasat altimeter data p 38 A87-51963

The Navy Geosat mission - An overview p 38 A87-52501

The Geosat radar altimeter p 38 A87-52502

Preliminary determination of the Geosat radar altimeter noise spectrum p 38 A87-52503

Determination of ocean geodetic data from Geosat p 38 A87-52506

Preliminary results from the processing of a limited set of Geosat radar altimeter data p 22 A87-52507

Introduction to sea-surface topography from satellite altimetry p 38 A87-52508

Validation of Geosat altimeter-derived wind speeds and significant wave heights using buoy data p 39 A87-52510

Ice measurements by Geosat radar altimetry p 39 A87-52513

Waveform analysis for Geosat day 96 p 39 A87-52514

Design of Geosat Exact Repeat Mission p 39 A87-52515

Altimetric data assimilation for ocean dynamics and forecasting p 39 A87-52516

Poseidon radar altimeter description and signal processing p 40 A87-53114

Wind and wave statistics as derived from the Geosat radar altimeter and with comparisons with in situ measurements p 40 A87-53127

Estimation and modelling of the local empirical covariance function using gravity and satellite altimeter data p 22 A87-54325

Active microwave observations of sea ice and icebergs p 45 N87-27855

The determination of sea-state bias and non-linear wave parameters from satellite altimeter data p 46 N87-28132

A study of antenna signal processing techniques for radar alternatives [ESA-CR(P)-2370] p 79 N87-28809

**SATELLITE ANTENNAS**

A cross antenna for passive microwave remote sensing p 77 A87-53268

Summary of recent SAR instrument studies p 78 N87-27865

**SATELLITE DOPPLER POSITIONING**

Earth gravity model improvement - An alternative method for Doppler-tracked satellites p 21 A87-45817

Precise orbit determination with the Doppler Orbitography and Radio positioning Integrated by Satellite (DORIS) system and the associated Zealous for Orbit Observation Methods (ZOOM) software p 77 N87-25382

**SATELLITE IMAGERY**

The application of remote sensing techniques in China p 68 A87-41435

Studies of the wavelike process in the surface temperature field of the equatorial Pacific using Meteor-satellite IR measurements p 28 A87-42931

Characteristics of the Gregory Rift (Kenya) dynamics, ground structural analysis, and remote sensing p 23 A87-43353

Second generation high-resolution space systems - First results of the SPOT-1 satellite p 55 A87-44244

Visual interpretation of Landsat MSS quick-look images for the study of the annual swelling of the Niger river in its interior delta, in Mali p 50 A87-44245

Use of rice response characteristics in classification using Landsat MSS digital data p 1 A87-45046

Remote sensing of the geomorphologic formations and vegetation in the eastern High Atlas region of Morocco from SPOT satellite data p 23 A87-45048

Coral reef survey method for verification of Landsat MSS image data p 30 A87-46311

Classification of geomorphic features and landscape stability in northwestern New Mexico using simulated SPOT imagery p 56 A87-46540

Information content analysis of Landsat image data for compression p 56 A87-47046

Modeling the snowmelt runoff in mountain catchment areas using satellite data p 51 A87-47578

Space photographs of the Omega-Ladoga isthmus and the prediction of mineral finds p 23 A87-48185

Size distributions of clouds in real time from satellite imagery p 56 A87-48359

The effect of subpixel clouds on remote sensing p 2 A87-48360

Cloud screening for determination of land surface characteristics in a reduced resolution satellite data set p 56 A87-48361

Scene to scene radiometric normalization of the reflected bands of the Landsat Thematic Mapper p 71 A87-48654

Geometric quality of Thematic Mapper data of the United Kingdom p 57 A87-48655

Within-scene radiometric correction of Landsat Thematic Mapper (TM) data in Canadian production systems p 57 A87-48656

A contribution to the optimum selection of ground control points in high resolution images p 57 A87-48658

SPOT radiometric resolution performance evaluation - Preliminary results p 57 A87-48661

SPOT localization accuracy and geometric image quality p 57 A87-48662

SPOT MTF performance evaluation p 57 A87-48663

Improving SPOT images size and multispectral resolution p 58 A87-48664

Evaluation of Landsat Thematic Mapper - Imagery for geological exploration p 23 A87-48666

Lithological discrimination using geobotanical and Landsat TM spectral data p 23 A87-48667

Spectral discrimination of geobotanical anomalies using Landsat Thematic Mapper data p 2 A87-48668

The automatic generation of digital terrain models from satellite images by stereo p 58 A87-48669

Significance of TM data as a tool to support regional planning activities p 17 A87-48671

Discrimination of natural and cultivated vegetation using Thematic Mapper spectral data p 2 A87-48673

Comparative analysis of different sensor data (Landsat-TM and MOMS) for earth observation and impact on future sensor development p 71 A87-48674

Different scanning instruments comparison - MOMS and TM --- Modular Optoelectronic Multispectral Scanner p 71 A87-48675

Operational, province wide crop area estimation for Manitoba p 3 A87-48811

Forecast of hurricane characteristics from GOES imagery p 59 A87-48818

Comparison of classification and enhancement techniques using Landsat imagery for the northern coniferous forest p 4 A87-48821

Use of Thematic Mapper satellite images for disturbance updating of timber/range maps p 4 A87-48822

Satellite microwave radiometry of snow water equivalent p 52 A87-48823

A study of the potential application of SPOT imagery in structural geology p 24 A87-48827

Barriers to the operational use of satellite remote sensing in Canada p 72 A87-48835

Stratification of satellite imagery by Uniform Productivity Areas p 5 A87-48840

Using NOAA AVHRR in studies of sea ice motion in the Beaufort Sea p 34 A87-48842

Landsat thematic mapper data in wildlife habitat management - Reference to deer wintering habitat p 5 A87-48845

Snowpack depletion monitoring in Alberta using computer-processed NOAA imagery p 52 A87-48848

Effectiveness of the Thematic Mapper for the range condition assessment in fescue grasslands of Southwestern Alberta p 6 A87-48850

Managing coral reefs - Operational benefits of remote sensing in Marine Park planning p 34 A87-48851

The detection of wetlands on radar imagery p 6 A87-48855

Indices of climatological and hydrological variability derived from satellite imagery for the South Saskatchewan River Basin p 52 A87-48856

Radiation modelling in a high relief environment using a digital terrain model and Landsat - TM imagery p 59 A87-48857

Comparison of Landsat Thematic Mapper and Multispectral Scanner information content for agricultural applications in Western Canada p 6 A87-48863

Applications of satellite derived digital elevation models for resource mapping p 60 A87-48866

Landsat Thematic Mapper data - A useful tool for mapping agricultural areas in Quebec p 6 A87-48867

Rural land use classification using Landsat Thematic Mapper data p 18 A87-48868

Thematic Mapper information about Canadian forests - Early results from across the country p 6 A87-48869

Custom-enhanced Landsat imagery in near real-time p 60 A87-48870

Technological feasibility to mobilization for operations - The NOAA crop monitoring case p 6 A87-48878

A structural analysis of the Mabou Basin, Cape Breton Island using enhanced Landsat MSS imagery p 25 A87-48879

A methodology for automated extraction of drainage networks from satellite imagery p 53 A87-48880

Validation and simulation of Radarsat imagery p 60 A87-48883

An application for the testing and use of the standard data transfer format --- for remotely sensed classified information transmission to GIS center p 18 A87-48886

Ground targets for the radiometric correction of AVHRR imagery for crop monitoring p 7 A87-48887

New system for the ordering, archiving and retrieval of data from earth's resource satellites p 60 A87-48889

The RADARSAT RMOMS optical sensor --- Modular Optoelectronic Multispectral Scanner p 73 A87-48890

The role of Landsat multi-spectral scanner data in the analysis of northern spotted owl habitat p 7 A87-48894

The role of remote sensing in the Canada Land Use Monitoring Program (CLUMP) p 18 A87-48895

The ERS-1/RADARSAT SAR Canadian ground segment p 61 A87-48896

Remote sensing and the agricultural resource inventory p 8 A87-48899

TM and MEIS data for future Alberta forest inventories p 8 A87-48900

Spectral studies of dryland agricultural salinity in Western Australia p 8 A87-48901

A revolution in the production of small-scale and medium-scale maps p 61 A87-48904

The operational use of RADARSAT products by the ice centre environment Canada p 61 A87-48906

Land cover classification using SPOT data p 18 A87-50227

Moscow seen by satellite - Another image of Soviet urban geography p 80 A87-51143

The dynamics of the northern border of the Gulf Stream revealed by a Tiro-N AVHRR image from October 22, 1980 p 35 A87-51147

Automated evaluation of linear networks on SPOT images p 61 A87-51174

SPOT's first year p 80 A87-51320

Eurimage sets up shop p 80 A87-51324

Interpreting meteorological satellite images using a color-composite technique p 62 A87-52795

Improved cloud analysis using visible, near-infrared, infrared, and microwave imagery p 62 A87-53103

Cluster based segmentation of multi-temporal Thematic Mapper data as preparation of region-based agricultural land-cover analysis p 9 A87-53109

Effect of resolution on texture application to nearly simultaneous AVHRR and MSS images of an agricultural region p 9 A87-53111

Digital image classification approach for estimating forest clearing and regrowth rates and trends p 10 A87-53123

Using remotely sensed Landsat MSS data to assess groundwater influence on the Barmah-Millewa Forest p 10 A87-53124

An expert system for planimetric feature extraction p 63 A87-53139

Sequential thinning algorithms for remote sensing application p 63 A87-53140

Digital elevation model extraction from stereo satellite images p 63 A87-53142

Remote sensing and landscape approaches to earth resources p 63 A87-53154

Suspended sediment concentrations estimated from Landsat MSS p 53 A87-53204

The detection of soil drainage by using Landsat MSS and TM (Belgian test zones) p 11 A87-53205

Pleistocene earth movements in Peninsular India - Evidences from Landsat MSS and Thematic Mapper data p 26 A87-53242

Analysis of Eocene depositional environments - Preliminary TM and TIMS results, Wind River Basin, Wyoming p 26 A87-53243

Use of TM Landsat data as a support to classical ground-based methodologies in the investigation of a volcanic site in central Italy - The Caldera of Latera p 26 A87-53244

Analysis of forest and forest clearings in Amazonia with Landsat and Shuttle Imaging Radar-A data p 13 A87-53250

Geometric distortion correction with high accuracy for NOAA satellite images p 65 A87-53253

Application of TM imagery to mapping volcanic rock assemblages at tertiary calderas of the basin and range province p 26 A87-53257

A pattern analysis technique for distinguishing surface and cloud types in the polar regions p 66 A87-53289

Smoothing vegetation index profiles - An alternative method for reducing radiometric disturbance in NOAA/AVHRR data p 14 A87-53396

Comparisons of gauge and satellite rain estimates for the central United States during August 1979 p 53 A87-54152

The Bakerian Lecture, 1986 - Ships from space --- wakes behind surface vessels observed from space p 44 A87-54301

Sea surface temperatures and the detection of ocean circulation patterns and fronts from AVHRR imagery p 45 N87-28125

Thermal infrared images from satellites compared to shelter temperature. Application to frost nowcasting in a citrus orchard p 15 N87-28136

Satellite remote sensing for water resources management: Some engineering and economic aspects p 54 N87-28139

Coastal Zone Color Scanner (CZCS) images and ocean dynamics. Application to the Northwest African upwelling area p 46 N87-28146

Snow mapping in western Greenland p 54 N87-28150

A model of thermal inertia for frost forecasting in agricultural areas --- satellite imagery p 16 N87-28151

Tracking of ice floes p 46 N87-28155

Spectral characteristics and the extent of paleosols of the Palouse formation p 17 N87-28195

[NASA-CR-181208] p 17 N87-28195

Investigating the role of the land surface in explaining the interannual variation of the net radiation balance over the Western Sahara and sub-Sahara p 68 N87-28197

[NASA-CR-181183] p 68 N87-28197

National Climate Program p 79 N87-28221

[PB87-190518] p 79 N87-28221

Application of satellite data to tropic-subtropical moisture coupling p 48 N87-29067

[NASA-CR-4092] p 48 N87-29067

Satellite image processing for the Agulhas Retroflexion region p 68 N87-29905

[AD-A183012] p 68 N87-29905

Use of LANDSAT digital data for snow cover mapping in the upper Saint John River Basin, Maine p 54 N87-29906

[AD-A183213] p 54 N87-29906

Physical oceanographic study of Florida's Atlantic Coast region: Florida Atlantic Coast Transport Study (FACTS). Volume 1: Executive summary p 49 N87-30015

[PB87-200994] p 49 N87-30015

Physical oceanographic study of Florida's Atlantic Coast region: Florida Atlantic Coast Transport Study (FACTS), volume 2 p 49 N87-30016

[PB87-201000] p 49 N87-30016

**SATELLITE OBSERVATION**

Radar scattering and equilibrium ranges in wind-generated waves with application to scatterometry p 28 A87-42746

Some aspects of the surface circulation south of 20 deg S revealed by First GARP Global Experiment drifters p 28 A87-42748

A method for the optimization of orbits and structures of satellite systems for the periodic round-the-clock survey of the earth p 21 A87-42938

From satellite orbit into the eye of the typhoon --- Russian book p 29 A87-44679

Satellite color observations of spring blooming in Bering Sea shelf waters during the ice edge retreat in 1980 p 32 A87-47297

On the relationship between atmospheric circulation and the fluctuations in the sea ice extents of the Bering and Okhotsk Seas p 32 A87-47298

Beaufort-Chukchi ice margin data from Seasat - Ice motion p 32 A87-47299

Shuttle Imaging Radar B (SIR-B) Weddell Sea ice observations - A comparison of SIR-B and scanning multichannel microwave radiometer ice concentrations p 32 A87-47300

Measurement of currents according to the drift of subsatellite buoys p 32 A87-48177

The variability of the North Atlantic marine atmosphere and its relevance to remote sensing p 33 A87-48362

Canadian Symposium on Remote Sensing, 10th, Edmonton, Canada, May 5-8, 1986, Proceedings. Volume 1 & 2 p 72 A87-48801

A geobotanic approach to the study of the geology of Cape Smith using Landsat-MSS data p 25 A87-48860

The evaluation of TM analysis as a tool in monitoring land use and agricultural stress in Egypt p 18 A87-48903

Wintertime disturbances in the tropical Pacific - FGGE IIb and satellite comparisons p 36 A87-51560

Satellite observations of convection during the summer monsoon of 1979 p 36 A87-51587

Satellite observations of surface temperatures and flow patterns, Sea of Japan and East China Sea, late March 1979 p 40 A87-53020

Satellite microwave radiometry of forest and surface types p 9 A87-53120

Landscape pattern and successional dynamics in the boreal forest p 11 A87-53155

Science synergism study for EOS on evolution of desert surfaces p 12 A87-53214

- The First ISLSCP Field Experiment (FIFE) p 12 A87-53218
- Tidal and secular tilt from an earthquake zone - Thresholds for detection of regional anomalies p 26 A87-53733
- A space-time stochastic model of rainfall for satellite remote-sensing studies p 54 A87-54157
- Proceedings of the ESA-EARSeL Europe from Space Symposium [ESA-SP-258] p 19 N87-28115
- Urban development planning using thematic mapper data of Munich (FRG) p 20 N87-28117
- Monitoring of snow cover from satellite p 54 N87-28123
- Satellite remote sensing for water resources management: Some engineering and economic aspects p 54 N87-28139
- Large scale sea ice studies based on Scanning Multichannel Microwave Radiometers (SMMR) data p 16 N87-28148
- Sea ice observations by SAR --- satellite observation p 47 N87-28156
- Comparison of satellite-derived ocean velocities with observations in the California coastal region [AD-A182291] p 47 N87-28242
- SATELLITE ORBITS**
- From satellite orbit into the eye of the typhoon --- Russian book p 29 A87-44679
- Determination of the initial motion conditions of earth-resources satellites according to the photogrammetric processing of topographic photographs oriented in inertial space p 56 A87-47506
- Design of Geosat Exact Repeat Mission p 39 A87-52515
- SATELLITE ORIENTATION**
- Determination of the initial motion conditions of earth-resources satellites according to the photogrammetric processing of topographic photographs oriented in inertial space p 56 A87-47506
- SATELLITE SOUNDING**
- Estimation of errors in the determination of sea surface temperature and atmospheric moisture content from satellite measurements of outgoing IR radiation in the 10.5-12.5 micron range p 33 A87-48178
- Maximum accuracy of satellite-borne scatterometer measurements of wind velocity above the ocean p 33 A87-48184
- Remote sensing in the Sahel - A tool for the inventory and monitoring of resources p 73 A87-48893
- Use of IR satellite rainfall estimates in diagnosing thermally forced circulations in the Pacific during FGGE SOP-1 p 36 A87-51580
- Sampling errors in satellite estimates of tropical rain p 53 A87-54153
- Estimation and modelling of the local empirical covariance function using gravity and satellite altimeter data p 22 A87-54325
- SATELLITE TRACKING**
- Upwelling filaments and motion of a satellite-tracked drifter along the west coast of North America p 29 A87-45023
- Earth gravity model improvement - An alternative method for Doppler-tracked satellites p 21 A87-45817
- Precise orbit determination with the Doppler Orbitography and Radio positioning Integrated by Satellite (DORIS) system and the associated Zealous for Orbit Observation Methods (ZOOM) software p 77 N87-25382
- Tracking of ice floes p 46 N87-28155
- Arctic drifting buoy data 1979 - 1985 [AD-A182967] p 50 N87-30019
- SATELLITE-BORNE INSTRUMENTS**
- Some results of the Metric Camera (MC) Mission-1 on Spacelab p 70 A87-47175
- Maximum accuracy of satellite-borne scatterometer measurements of wind velocity above the ocean p 33 A87-48184
- Poseidon radar altimeter oceanographic remote sensing p 40 A87-53113
- Investigation of design parameters for ERS-1 wind scatterometer p 74 A87-53116
- An advanced wind scatterometer for the Columbus Polar Platform payload p 74 A87-53117
- Selection of extended area land target sites for the calibration of spaceborne scatterometers p 74 A87-53118
- A spaceborne LFM scatterometer for ocean surface wind vector measurement - A time domain approach --- Linearly Frequency Modulated p 40 A87-53119
- A multifrequency microwave radiometer of the future p 75 A87-53180
- Wind measurements for non-uniform wind fields from spaceborne scatterometers p 75 A87-53195
- A comparative study of several wind estimation algorithms for spaceborne scatterometers p 41 A87-53197
- Performance sensitivity for X-SAR p 76 A87-53223
- Scattering parameters for aspherical hydrometeors at microwave frequencies p 53 A87-53271
- A combined SAR and scatterometer system p 77 A87-53279
- The future generation of resources satellites p 80 A87-53742
- Planning for future operational sensors and other priorities [NOAA-NESDIS-30] p 77 N87-25560
- Summary of recent SAR instrument studies p 78 N87-27865
- Evaluation of the potential of the Thematic Mapper for marine application p 46 N87-28134
- Microwave radiometry study concerning pushbroom systems. Volume 1: A sea salinity/soil-moisture pushbroom radiometer system [R-322] p 79 N87-28951
- Interpolation, analysis and archival of data on sea ice trajectories and ocean currents obtained from satellite-linked instruments [PB87-201430] p 48 N87-30010
- SATELLITE-BORNE PHOTOGRAPHY**
- A study of modern landscape formation in Lower Mesopotamia from space photographs p 55 A87-42935
- Stereoscopic visualization of aerial and space photographs in thematic mapping p 23 A87-42937
- Monitoring rice areas using Landsat MSS data p 1 A87-45047
- Determination of the initial motion conditions of earth-resources satellites according to the photogrammetric processing of topographic photographs oriented in inertial space p 56 A87-47506
- Possibility of evaluating reservoir influx from aerial and satellite photographs p 51 A87-47577
- Divergent redistribution of ice in the Arctic Ocean (Analysis of space imagery) p 33 A87-48180
- Multistage principal-components analysis of correlations --- of spectral channels for multispectral remote sensing image processing p 56 A87-48193
- Development of a mathematical model for the spatial triangulation of SPOT images p 61 A87-48905
- Point positioning and mapping with large format camera data p 73 A87-50226
- Remote-sensing and geological-geophysical studies of closed platform territories --- Russian book p 26 A87-51875
- Comparison of satellite-derived ocean velocities with observations in the California coastal region [AD-A182291] p 47 N87-28242
- SATELLITE-BORNE RADAR**
- Climatological implications of a satellite-borne SAR imaging the sea surface p 30 A87-46403
- Analysis of Cosmos-1500 radar images of the ocean surface in a zone of cyclones and mesoscale cloud formations p 32 A87-48176
- Evaluation of the effect of hydrometeors on the characteristics of radar images of sea ice p 33 A87-48181
- Multiple-look effects on SAR classification accuracies p 60 A87-48885
- Poseidon radar altimeter description and signal processing p 40 A87-53114
- Wind and wave statistics as derived from the Geosat radar altimeter and with comparisons with in situ measurements p 40 A87-53127
- Synergism requirements and concepts for SAR and HIRIS on EOS p 75 A87-53216
- Derivation of the technical specification of the ERS-1 active microwave instrument to meet the SAR-image quality requirements p 77 A87-53280
- Study on the use and characteristics of SAR systems for geological applications [ESA-CR(P)-2342] p 27 N87-26467
- Successes of Cosmos-1500 satellite, SLR system p 45 N87-27696
- SAR detection of ships and ship wakes p 66 N87-27859
- Study on the use of SAR data for agriculture and forestry p 15 N87-27862
- Requirements on radar data for geological application: A case study by use of multistage data of the testsite Sardegna/Italy p 27 N87-28120
- Sea ice observations by SAR --- satellite observation p 47 N87-28156
- SCALE EFFECT**
- Sampling semiarid vegetation with large-scale aerial photography p 14 A87-53741
- SCANNING**
- Calculation and accuracy of ERBE scanner measurement locations [NASA-TP-2670] p 47 N87-28471
- SCATTEROMETERS**
- Radar scattering and equilibrium ranges in wind-generated waves with application to scatterometry p 28 A87-42746
- Maximum accuracy of satellite-borne scatterometer measurements of wind velocity above the ocean p 33 A87-48184
- Investigation of design parameters for ERS-1 wind scatterometer p 74 A87-53116
- An advanced wind scatterometer for the Columbus Polar Platform payload p 74 A87-53117
- Selection of extended area land target sites for the calibration of spaceborne scatterometers p 74 A87-53118
- A spaceborne LFM scatterometer for ocean surface wind vector measurement - A time domain approach --- Linearly Frequency Modulated p 40 A87-53119
- Wind measurements for non-uniform wind fields from spaceborne scatterometers p 75 A87-53195
- The effects of wind-wave coupling on scatterometer wind measurement accuracy p 41 A87-53196
- A comparative study of several wind estimation algorithms for spaceborne scatterometers p 41 A87-53197
- A combined SAR and scatterometer system p 77 A87-53279
- Derivation of the technical specification of the ERS-1 active microwave instrument to meet the SAR-image quality requirements p 77 A87-53280
- SCENE ANALYSIS**
- Scene to scene radiometric normalization of the reflected bands of the Landsat Thematic Mapper p 71 A87-48654
- A contribution to the optimum selection of ground control points in high resolution images p 57 A87-48658
- Application of accuracy assessment techniques to image classification --- photointerpretation and scene analysis p 58 A87-48808
- Landsat-based wildlife habitat mapping - A study of collaboration between analyst and user p 3 A87-48809
- Thematic Mapper information about Canadian forests - Early results from across the country p 6 A87-48869
- A methodology for automated extraction of drainage networks from satellite imagery p 53 A87-48880
- Towards the automatic recognition and vectorised description of linear features in LANDSAT TM images by artificial intelligence methods p 67 N87-28142
- Comparison of visual and automated lineament analyses on LANDSAT MSS image from south Greenland p 67 N87-28144
- SCHOTTKY DIODES**
- Space surveillance application potential of Schottky barrier IR sensors [AD-A180848] p 78 N87-27311
- SEA ICE**
- A microwave radiometer weather-correcting sea ice algorithm p 29 A87-45024
- Satellite altimeter measurements of the geoid in sea ice zones p 30 A87-45816
- Variations of mesoscale and large-scale sea ice morphology in the 1984 Marginal Ice Zone Experiment as observed by microwave remote sensing p 31 A87-47292
- Evolution of microwave sea ice signatures during early summer and midsummer in the marginal ice zone p 31 A87-47293
- Use of synthetic aperture radar-derived kinematics in mapping mesoscale ocean structure within the interior marginal ice zone p 31 A87-47294
- Multisensor comparison of ice concentration estimates in the marginal ice zone p 31 A87-47295
- Boundary layer, upper ocean, and ice observations in the Greenland Sea marginal ice zone p 31 A87-47296
- Satellite color observations of spring blooming in Bering Sea shelf waters during the ice edge retreat in 1980 p 32 A87-47297
- On the relationship between atmospheric circulation and the fluctuations in the sea ice extents of the Bering and Okhotsk Seas p 32 A87-47298
- Beaufort-Chukchi ice margin data from Seasat - Ice motion p 32 A87-47299
- Shuttle Imaging Radar B (SIR-B) Weddell Sea ice observations - A comparison of SIR-B and scanning multichannel microwave radiometer ice concentrations p 32 A87-47300
- Divergent redistribution of ice in the Arctic Ocean (Analysis of space imagery) p 33 A87-48180
- Evaluation of the effect of hydrometeors on the characteristics of radar images of sea ice p 33 A87-48181
- Operational use of remote sensing for commercial Arctic class vessel navigation p 33 A87-48829
- Using NOAA AVHRR in studies of sea ice motion in the Beaufort Sea p 34 A87-48842



- The influence of melting conditions on the interpretation of radar imagery of sea ice p 34 A87-48849
- Optimization of seismic vessel deployment using side looking airborne radar p 34 A87-48881
- Antarctic ice streams - A review p 37 A87-51943
- Recent glacial history and rapid ice stream retreat in the Amundsen Sea p 37 A87-51944
- The morphology of ice streams A, B, and C, West Antarctica and their environs p 37 A87-51945
- Ice dynamics at the mouth of ice stream B, Antarctica p 37 A87-51946
- Velocity of ice streams B and C, Antarctica p 37 A87-51947
- Till beneath ice stream B. I - Properties derived from seismic travel times. II - Structure and continuity. III - Till deformation - Evidence and implications. IV - A coupled ice-till flow model --- glacial deposits p 37 A87-51948
- Glaciological studies on Rutford ice stream, Antarctica p 38 A87-51950
- Theoretical models for microwave remote sensing of snow-covered sea ice p 42 A87-53236
- Theoretical and experimental study of the radar backscatter of Arctic sea ice p 43 A87-53237
- Progress on digital algorithms for deriving sea ice parameters from SAR data p 43 A87-53238
- Observing rotation and deformation of sea ice with synthetic aperture radar p 43 A87-53239
- Optimum use of dual frequency passive microwave measurements for ice/ocean interactions p 43 A87-53240
- Investigation of multi-dimensional algorithms using active and passive microwave data for ice concentration determination p 43 A87-53241
- Active microwave observations of sea ice and icebergs p 45 A87-27855
- Large scale sea ice studies based on Scanning Multichannel Microwave Radiometers (SMMR) data p 16 A87-28148
- Sea ice observations by SAR --- satellite observation p 47 A87-28156
- Labrador wind and wave environments [AD-A183218] p 48 A87-29907
- Interpolation, analysis and archival of data on sea ice trajectories and ocean currents obtained from satellite-linked instruments [PB87-201430] p 48 A87-30010
- NASA sea ice and snow validation plan for the Defense Meteorological Satellite Program special sensor microwave/imager [NASA-TM-100683] p 49 A87-30018
- Satellite-derived ice data sets no. 2: Arctic monthly average microwave brightness temperatures and sea ice concentrations, 1973-1976 [NASA-TM-87825] p 50 A87-30021
- SEA LEVEL**
- Monitoring equatorial Pacific sea level with Geosat p 39 A87-52512
- Waveform analysis for Geosat day 96 p 39 A87-52514
- Poseidon radar altimeter description and signal processing p 40 A87-53114
- SEA OF OKHOTSK**
- On the relationship between atmospheric circulation and the fluctuations in the sea ice extents of the Bering and Okhotsk Seas p 32 A87-47298
- SEA STATES**
- Deconvolution of sea state parameters from altimeter waveforms p 41 A87-53198
- The determination of sea-state bias and non-linear wave parameters from satellite altimeter data p 46 A87-28132
- SEA SURFACE TEMPERATURE**
- Studies of the wavelike process in the surface temperature field of the equatorial Pacific using Meteor-satellite IR measurements p 28 A87-42931
- Multiparameter sampling (ship, aircraft, and satellite) of a Gulf Stream warm core ring p 29 A87-44811
- A microwave radiometer weather-correcting sea ice algorithm p 29 A87-45024
- Calibration of Thematic Mapper thermal data for water surface temperature mapping - Case study on the Great Lakes p 51 A87-46545
- Estimation of errors in the determination of sea surface temperature and atmospheric moisture content from satellite measurements of outgoing IR radiation in the 10.5-12.5 micron range p 33 A87-48178
- Response of marine atmospheric boundary layer height to sea surface temperature changes - Mixed-layer theory p 34 A87-50277
- Sea surface temperature retrieval from the Tiros-N AVHRR instrument for the FGGE period (Dec. 1978-Nov. 1979) p 35 A87-51553
- Satellite observations of surface temperatures and flow patterns, Sea of Japan and East China Sea, late March 1979 p 40 A87-53020

Sea surface temperatures and the detection of ocean circulation patterns and fronts from AVHRR imagery p 45 A87-28125

**SEA TRUTH**

- Coral reef survey method for verification of Landsat MSS image data p 30 A87-46311
- Comparison of Geosat and ground-truth wind and wave observations - Preliminary results p 38 A87-52509
- Validation of Geosat altimeter-derived wind speeds and significant wave heights using buoy data p 39 A87-52510

**SEA WATER**

- Atmospheric correction of data measured by a flying platform over the sea - Elements of a model and its experimental validation p 35 A87-50292

**SEAS**

- Theory of fluorescent irradiance fields in lakes and seas [PB87-196465] p 47 A87-28954

**SEASAT SATELLITES**

- Seasat altimetry and the South Atlantic geoid. I - Spectral analysis p 21 A87-45743
- Processing of Seasat altimetry data on a digital image analysis system p 59 A87-48825
- The detection of wetlands on radar imagery p 6 A87-48855
- Investigations of relative plate motions in the South Atlantic using Seasat altimeter data p 38 A87-51963
- Processing of airborne SAR images of ocean waves p 43 A87-53264
- The comparison of ocean-wave spectra recovered from SIR-B and Seasat observations with simultaneous buoy data p 43 A87-53265

**SECULAR VARIATIONS**

- Azimuthal dependence in the gravity field induced by recent and past cryospheric forcings p 35 A87-51487
- Tidal and secular tilt from an earthquake zone - Thresholds for detection of regional anomalies p 26 A87-53733

**SEDIMENTS**

- Discrimination of suspended sediment and littoral features using multispectral video imagery p 73 A87-48874
- Suspended sediment concentrations estimated from Landsat MSS p 53 A87-53204
- Analysis of Eocene depositional environments - Preliminary TM and TIMS results, Wind River Basin, Wyoming p 26 A87-53243
- Evaluation of the potential of the Thematic Mapper for marine application p 46 A87-28134
- Studies of tidal flat environments with LANDSAT MSS data p 47 A87-28157

**SEISMOLOGY**

- Application of space photographs to paleoseismological investigations (with reference to the Mongolian Altai) p 23 A87-48187
- Optimization of seismic vessel deployment using side looking airborne radar p 34 A87-48881
- Till beneath ice stream B. I - Properties derived from seismic travel times. II - Structure and continuity. III - Till deformation - Evidence and implications. IV - A coupled ice-till flow model --- glacial deposits p 37 A87-51948

**SENSORS**

- Determination of transfer functions from the Thematic Mapper (TM) sensor of the LANDSAT-5 satellite [INPE-4213-PRE/1094] p 79 A87-28956

**SHALLOW WATER**

- Shallow water bathymetry and bottom classification by means of the Landsat and SPOT optical scanners p 52 A87-48670
- An operational multispectral scanner for bathymetric surveys - The ABS NORDA scanner p 42 A87-53199

**SHIPS**

- Operational use of remote sensing for commercial Arctic class vessel navigation p 33 A87-48829
- The Bakerian Lecture, 1986 - Ships from space --- wakes behind surface vessels observed from space p 44 A87-54301
- SAR detection of ships and ship wakes p 66 A87-27859

**SHUTTLE IMAGING RADAR**

- Shuttle Imaging Radar B (SIR-B) Weddell Sea ice observations - A comparison of SIR-B and scanning multichannel microwave radiometer ice concentrations p 32 A87-47300
- Comparison of space and airborne L-HH radar imagery in an agricultural environment p 4 A87-48819
- Shuttle imaging Radar-A (SIR-A) scenes from Iran and China p 25 A87-48854
- Interpretation of prairie land cover types from SIR-B data p 7 A87-48888
- The production of real time wave spectra from the SIR-C SAR p 42 A87-53224
- Real time global ocean wave spectra from SIR-C - Systems design p 42 A87-53234

Analysis of forest and forest clearings in Amazonia with Landsat and Shuttle Imaging Radar-A data p 13 A87-53250

- The response of SAR imagery to azimuth travelling ocean surface waves as determined from shuttle SAR imagery p 44 A87-53286
- Approximating SIR-B response characteristics and estimating wave height and wavelength for ocean imagery p 44 A87-53288

Requirements on radar data for geological application: A case study by use of multistage data of the test site Sardegna/Italy p 27 A87-28120

**SIDE-LOOKING RADAR**

- Iceberg detection using SLAR p 34 A87-48876
- Optimization of seismic vessel deployment using side looking airborne radar p 34 A87-48881
- Observation of oil slicks on the ocean by X-band SLAR p 41 A87-53191

**SIGNAL DETECTION**

- Design study of remote sensing for ocean surface and interior activity [AD-A180578] p 44 A87-25610

**SIGNAL DETECTORS**

- Design study of remote sensing for ocean surface and interior activity [AD-A180578] p 44 A87-25610

**SIGNAL PROCESSING**

- Poseidon radar altimeter description and signal processing p 40 A87-53114
- Matching instrument design and signal processing for a scanning radiometer p 76 A87-53251
- Space surveillance application potential of Schottky barrier IR sensors [AD-A180848] p 78 A87-27311
- A study of antenna signal processing techniques for radar alternatives [ESA-CR(P)-2370] p 79 A87-28809

**SIGNATURE ANALYSIS**

- Evolution of microwave sea ice signatures during early summer and midsummer in the marginal ice zone p 31 A87-47293

**SIRS B SATELLITE**

- The comparison of ocean-wave spectra recovered from SIR-B and Seasat observations with simultaneous buoy data p 43 A87-53265

**SIZE DISTRIBUTION**

- Size distributions of clouds in real time from satellite imagery p 56 A87-48359

**SLOPES**

- Study of physical processes on the US mid-Atlantic continental slope and rise. Volume 1: Executive summary [PB87-200515] p 48 A87-30012
- Study of physical processes on the US mid-Atlantic continental slope and rise. Volume 2: Technical presentation [PB87-200523] p 49 A87-30013
- Study of physical processes on the US mid-Atlantic continental slope and rise. Volume 3: Appendix [PB87-200531] p 49 A87-30014

**SNOW**

- Glaciological studies on Rutford ice stream, Antarctica p 38 A87-51950
- Snow load effect on earth's rotation and gravitational field, 1979-1985 p 22 A87-51964
- The International Symposium on Microwave Signatures and Remote Sensing held in Gothenburg (Sweden) on 19-22 January 1987 [AD-A181334] p 78 A87-27314
- The potential of SAR in a snow and glacier monitoring system p 45 A87-27856
- NASA sea ice and snow validation plan for the Defense Meteorological Satellite Program special sensor microwave/imager [NASA-TM-100683] p 49 A87-30018

**SNOW COVER**

- A multispectral study of the St. Louis area under snow-covered conditions using NOAA-7 AVHRR data p 51 A87-46538
- Satellite microwave radiometry of snow water equivalent p 52 A87-48823
- Snowpack depletion monitoring in Alberta using computer-processed NOAA imagery p 52 A87-48848
- Theoretical models for microwave remote sensing of snow-covered sea ice p 42 A87-53236
- Monitoring of snow cover from satellite p 54 A87-28123
- Snow mapping in western Greenland p 54 A87-28150
- Remote sensing of earth terrain [NASA-CR-181370] p 79 A87-28957
- Use of LANDSAT digital data for snow cover mapping in the upper Saint John River Basin, Maine [AD-A183213] p 54 A87-29906



**SOFTWARE ENGINEERING**

- Data analysis and software support for the Earth radiation budget experiment  
[NASA-CR-178350] p 66 N87-26569

**SOIL EROSION**

- Indexing small catchments in Java, Indonesia, with respect to their relative susceptibility to erosion p 52 N87-48871

**SOIL MAPPING**

- Evaluation of MEIS-II multispectral scanner data for quaternary geological mapping in the Chatham area, southwestern Ontario p 24 A87-48816  
Extent of saline/waterlogged lands within irrigated Alberta. I - Inventory and preliminary evaluation of existing mapping data p 5 A87-48830  
Integrated multi-temporal aerial photography and digital mapping for coastal monitoring, Cape Breton Island, Nova Scotia p 34 A87-48837  
Effects of surface geometry of agricultural fields on radar airborne imagery in X- and C-bands p 5 A87-48846  
The detection of vegetative stress utilizing remotely sensed data and soil sampling p 8 A87-50231  
Detection of soil drainage in Pays de Herve, Belgium, on LANDSAT MSS imagery p 15 N87-28129  
Spectral characteristics and the extent of paleosols of the Palouse formation  
[NASA-CR-181208] p 17 N87-28195

**SOIL MOISTURE**

- Remote-sensing evaluation of moisture supply to crops according to the leaf-surface thermal regime p 2 A87-47582  
Using airborne middle-infrared (1.45-2.0 microns) video imagery for distinguishing plant species and soil conditions p 9 A87-53023  
Retrieval of surface roughness parameters from dual-frequency measurements of radar backscattering coefficients p 10 A87-53130  
The detection of soil drainage by using Landsat MSS and TM (Belgian test zones) p 11 A87-53205  
Results from the pushbroom microwave radiometer flights over the Konza Prairie in 1985 p 11 A87-53206  
Estimation of surface moisture availability from remote temperature measurements p 53 A87-54155  
Microwave radiometry study concerning pushbroom systems. Volume 1: A sea salinity/soil-moisture pushbroom radiometer system p 79 N87-28951

**SOIL SCIENCE**

- A multi-source image set for the study of soil texture and drainage as observed from Thematic Mapper data in Northern Belgium p 10 A87-53125

**SOILS**

- Spectral characteristics and the extent of paleosols of the Palouse formation  
[NASA-CR-181208] p 17 N87-28195

**SOLAR POSITION**

- An evaluation of sun angle computation algorithms p 59 A87-48812

**SOLAR SENSORS**

- An evaluation of sun angle computation algorithms p 59 A87-48812

**SOLAR TERRESTRIAL INTERACTIONS**

- Solid earth geophysics: Data services  
[PB87-184107] p 66 N87-27352

**SONAR**

- Design study of remote sensing for ocean surface and interior activity  
[AD-A180578] p 44 N87-25610

**SOUND TRANSMISSION**

- Wave-theory modelling of convergence zone propagation in the ocean  
[AD-A183607] p 50 N87-30020

**SOUTHERN HEMISPHERE**

- Seasat altimetry and the South Atlantic geoid. I - Spectral analysis p 21 A87-45743

**SPACE BASED RADAR**

- The Geosad radar altimeter p 38 A87-52502  
Spaceborne imaging radar on EOS p 63 A87-53148  
Modulation transfer function of radar return power from the ocean p 42 A87-53219  
The EOS SAR program p 76 A87-53228  
Spacecraft on-board SAR image generation for EOS-type missions p 76 A87-53232  
Spatial considerations in speckle simulation --- of spaceborne synthetic aperture radar imagery p 65 A87-53260

**SPACE COMMERCIALIZATION**

- Eurimage sets up shop p 80 A87-51324  
Status of and prognosis for space remote sensing  
[AAS PAPER 86-104] p 80 A87-53084

**SPACE LAW**

- International cooperation in space - Enhancing the world's common security p 81 A87-53987

**SPACE NAVIGATION**

- Arctic drifting buoy data 1979 - 1985  
[AD-A182967] p 50 N87-30019

**SPACE PLATFORMS**

- Earth resources instrumentation for the Space Station Polar Platform p 69 A87-44184

**SPACE SHUTTLE MISSION 31-C**

- Different scanning instruments comparison - MOMS and TM --- Modular Optoelectronic Multispectral Scanner p 71 A87-48675

**SPACE SHUTTLE MISSION 41-B**

- Different scanning instruments comparison - MOMS and TM --- Modular Optoelectronic Multispectral Scanner p 71 A87-48675

**SPACE SHUTTLE PAYLOADS**

- Comparative analysis of different sensor data (Landsat-TM and MOMS) for earth observation and impact on future sensor development p 71 A87-48674  
Large Format Camera: The second generation photogrammetric camera for space cartography p 78 N87-28118

**SPACE STATION POLAR PLATFORMS**

- Earth resources instrumentation for the Space Station Polar Platform p 69 A87-44184

**SPACE STATIONS**

- Operational instruments on the Space Station-Polar Platforms - Contributions by NOAA and the international community p 74 A87-53149

**SPACE SURVEILLANCE (SPACEBORNE)**

- Space surveillance application potential of Schottky barrier IR sensors  
[AD-A180848] p 78 N87-27311

**SPACEBORNE LASERS**

- Spaceborne laser ranging from EOS p 22 A87-53146

**SPACEBORNE PHOTOGRAPHY**

- Determination of the external-orientation elements of aerial and space photographs p 55 A87-44301  
Space photographs of the Onega-Ladoga isthmus and the prediction of mineral finds p 23 A87-48185  
Application of space photographs to geomorphological investigations in southwestern Tadzhikistan p 23 A87-48186  
Application of space photographs to paleoseismological investigations (with reference to the Mongolian Altai) p 23 A87-48187  
Investigation of the relief of ore-containing regions on the basis of space photographs (with reference to eastern Yakutia) p 23 A87-48188  
Absolute calibration of the SPOT-1 HRV cameras p 71 A87-48660  
National land use mapping - The application of low altitude sample photography p 17 A87-48858  
First New Zealand image from the French SPOT satellite p 62 A87-51179  
Digital data from shuttle photography: The effects of platform variables p 66 N87-26697  
Large Format Camera: The second generation photogrammetric camera for space cartography p 78 N87-28118

- Geomagnetic intersection of tectonic structures seen in space photographs p 26 N87-23574

**SPACECRAFT INSTRUMENTS**

- Earth resources instrumentation for the Space Station Polar Platform p 69 A87-44184  
Operational instruments on the Space Station-Polar Platforms - Contributions by NOAA and the international community p 74 A87-53149

**SPACELAB PAYLOADS**

- Some results of the Metric Camera (MC) Mission-1 on Spacelab p 70 A87-47175

**SPAIN**

- ERAFIS: A computer information system for agriculture and forestry in Spain p 16 N87-28140

**SPATIAL DISTRIBUTION**

- Analysis of environmental information of urban areas using Landsat TM data p 19 A87-53187  
Studies of tidal flat environments with LANDSAT MSS data p 47 N87-28157

- Arctic drifting buoy data 1979 - 1985  
[AD-A182967] p 50 N87-30019

**SPATIAL FILTERING**

- Spatial filtering of digital Landsat data for the extraction of mapping information p 58 A87-48805

**SPATIAL RESOLUTION**

- Geometric correction of space images by the colinearity-equation method p 61 A87-51175  
Exploring the spatial domain --- analysis of remote sensing data p 62 A87-53112  
Spatial considerations in speckle simulation --- of spaceborne synthetic aperture radar imagery p 65 A87-53260

**SPECKLE PATTERNS**

- Statistical modelling and suppression of speckle in synthetic aperture radar images p 65 A87-53259  
Spatial considerations in speckle simulation --- of spaceborne synthetic aperture radar imagery p 65 A87-53260

- Speckle noise reduction of 1-look SAR imagery p 65 A87-53273

- Approximating SIR-B response characteristics and estimating wave height and wavelength for ocean imagery p 44 A87-53288

**SPECTRAL CORRELATION**

- Multistage principal-components analysis of correlations --- of spectral channels for multispectral remote sensing image processing p 56 A87-48193

**SPECTRAL REFLECTANCE**

- Multiple-angle observations of reflectance anisotropy from an airborne linear array sensor p 69 A87-43262  
Calibration of NOAA-7 AVHRR, GOES-5, and GOES-6 VISSR/VAS solar channels p 69 A87-44865  
Monte Carlo calculation of the dependence of the spectral radiance of vegetation cover on the illumination conditions p 2 A87-48190  
Spectral and textural segmentation of multispectral aerial images p 5 A87-48831  
Preliminary results from modelling vegetation spectra derived from MEIS data, Algonquin Park, Ontario p 7 A87-48891

- Measurement of leaf relative water content by infrared reflectance p 9 A87-53024

- Method development and experiences in application of airborne MSS data for forest damage detection p 12 A87-53247

- Studies of tidal flat environments with LANDSAT MSS data p 47 N87-28157

- Spectral characteristics and the extent of paleosols of the Palouse formation  
[NASA-CR-181208] p 17 N87-28195

**SPECTRAL RESOLUTION**

- Improving SPOT images size and multispectral resolution p 58 A87-48664  
Monitoring wheat canopies with a high spectral resolution radiometer p 8 A87-53019  
Remote sensing by the fluorescence property of the scatterer p 75 A87-53179

**SPECTRAL SENSITIVITY**

- Correction of the sensor degradation of the Coastal Zone Color Scanner on NIMBUS-7 p 46 N87-28153

**SPECTRAL SIGNATURES**

- The International Symposium on Microwave Signatures and Remote Sensing held in Gothenburg (Sweden) on 19-22 January 1987  
[AD-A181334] p 78 N87-27314

- Measurement of spectral signatures in Less Favored Areas (LFA): A contribution to the definition of a remote sensing multitemporal experiment p 20 N87-28145

**SPECTRUM ANALYSIS**

- Seasat altimetry and the South Atlantic geoid. I - Spectral analysis p 21 A87-45743

**SPOT (FRENCH SATELLITE)**

- Remote sensing of coastal wetlands p 1 A87-40944

- Second generation high-resolution space systems - First results of the SPOT-1 satellite p 55 A87-44244

- Remote sensing of the geomorphologic formations and vegetation in the eastern High Atlas region of Morocco from SPOT satellite data p 23 A87-45048

- Classification of geomorphic features and landscape stability in northwestern New Mexico using simulated SPOT imagery p 56 A87-46540

- Earth remote sensing using the Landsat Thematic Mapper and SPOT sensor systems; Proceedings of the Meeting, Innsbruck, Austria, Apr. 15-17, 1986  
[SPIE-660] p 70 A87-48652

- Absolute calibration of the SPOT-1 HRV cameras p 71 A87-48660

- SPOT radiometric resolution performance evaluation - Preliminary results p 57 A87-48661

- SPOT localization accuracy and geometric image quality p 57 A87-48662

- SPOT MTF performance evaluation p 57 A87-48663

- Improving SPOT images size and multispectral resolution p 58 A87-48664

- Photogrammetry from SPOT with Matra TRASTER analytical plotter p 58 A87-48665

- Shallow water bathymetry and bottom classification by means of the Landsat and SPOT optical scanners p 52 A87-48670

- A study of the potential application of SPOT imagery in structural geology p 24 A87-48827

- Land cover classification using SPOT data p 18 A87-50227

- Geomorphological interpretation of the SPOT image of February 23, 1986 concerning Djebel Amour (Algeria) and its border with the Sahara p 25 A87-51145

- Automated evaluation of linear networks on SPOT images p 61 A87-51174

- SPOT's first year p 80 A87-51320

- Crop inventories of small-parcelled areas using SPOT- and TM-data in conjunction with field radiometric measurements p 10 A87-53126

- SPOT, a satellite for oceanography?  
p 41 A87-53194
- The SPOT program - Commercialization of remote sensing  
p 80 A87-53235
- The future generation of resources satellites  
p 80 A87-53742
- SPOT: How good for geology? A comparison with LANDSAT MSS  
p 27 A87-28121
- SPRING (SEASON)**  
Satellite color observations of spring blooming in Bering Sea shelf waters during the ice edge retreat in 1980  
p 32 A87-47297
- STATISTICAL ANALYSIS**  
Features of a statistical model for the interaction between electromagnetic waves and remotely sensed natural objects  
p 70 A87-48189
- Textural segmentation of SAR images using first order statistical parameters  
p 66 A87-53274
- STATISTICAL CORRELATION**  
Modeling gap probability in discontinuous vegetation canopies  
p 13 A87-53276
- STATISTICAL DISTRIBUTIONS**  
Statistical modeling of intensity distributions on airborne SAR imagery  
p 65 A87-53262
- STEREOPHOTOGRAPHY**  
Stereoscopic visualization of aerial and space photographs in thematic mapping  
p 23 A87-42937
- Photogrammetry from SPOT with Matra TRASTER analytical plotter  
p 58 A87-48665
- Digital elevation model extraction from stereo satellite images  
p 63 A87-53142
- STEREOSCOPY**  
The automatic generation of digital terrain models from satellite images by stereo  
p 58 A87-48669
- A user's guide for the Analytical Photogrammetric Positioning System (APPS)  
[AD-A183773]  
p 79 A87-29909
- STOCHASTIC PROCESSES**  
A space-time stochastic model of rainfall for satellite remote-sensing studies  
p 54 A87-54157
- STRAITS**  
Mesoscale eddies in the Fram Strait marginal ice zone during the 1983 and 1984 Marginal Zone Experiments  
p 31 A87-47291
- STRATIFICATION**  
Stratification of satellite imagery by Uniform Productivity Areas  
p 5 A87-48840
- STRATIGRAPHY**  
Geological interpretations from Landsat of the Troodos Massive, Cyprus  
p 25 A87-48862
- STRESS ANALYSIS**  
Mechanisms of crustal deformation in the western US [NASA-CR-181230]  
p 27 A87-28200
- STRUCTURAL ANALYSIS**  
Analysis of directions of linear image elements by structure-zonal method  
p 68 A87-29575
- STRUCTURAL BASINS**  
Formation of natural underground-water resources in arid regions with special reference to the Dolinoozerskii artesian basin in Mongolia --- Russian book  
p 50 A87-42911
- STRUCTURAL PROPERTIES (GEOLOGY)**  
Characteristics of the Gregory Rift (Kenya) dynamics, ground structural analysis, and remote sensing  
p 23 A87-43353
- Investigation of the relief of ore-containing regions on the basis of space photographs (with reference to eastern Yakutia)  
p 23 A87-48188
- A study of the potential application of SPOT imagery in structural geology  
p 24 A87-48827
- A structural analysis of the Mabou Basin, Cape Breton Island using enhanced Landsat MSS imagery  
p 25 A87-48879
- Elements of lineament tectonics --- Russian book  
p 27 A87-53954
- Comparison of visual and automated lineament analyses on LANDSAT MSS image from south Greenland  
p 67 A87-28144
- Kinematics at the intersection of the Garlock and Death Valley fault zones, California: Integration of TM data and field studies. LANDSAT TM investigation proposal TM-019  
[NASA-CR-180666]  
p 27 A87-28208
- Workshop on The Earth as a Planet  
[NASA-CR-180543]  
p 81 A87-29900
- SUBTRACTION**  
Optical image subtraction techniques, 1975-1985  
p 55 A87-42659
- SULFUR DIOXIDES**  
Sulphur dioxide damage assessment using colour infrared aerial photography  
p 60 A87-48884
- SUMMER**  
Evolution of microwave sea ice signatures during early summer and midsummer in the marginal ice zone  
p 31 A87-47293

- Boundary layer, upper ocean, and ice observations in the Greenland Sea marginal ice zone  
p 31 A87-47296
- Observing systems experiments for the onset vortex during Summer Monex  
p 35 A87-51552
- Comparisons of gauge and satellite rain estimates for the central United States during August 1979  
p 53 A87-54152
- SUPERCONDUCTIVITY**  
Meissner effect in high-Tc superconductive thin films  
p 35 A87-51532
- SUPERHIGH FREQUENCIES**  
Hybrid power amplifier module for X-band  
p 69 A87-43302
- Observation of oil slicks on the ocean by X-band SLAR  
p 41 A87-53191
- SURFACE GEOMETRY**  
Effects of surface geometry of agricultural fields on radar airborne imagery in X- and C-bands  
p 5 A87-48846
- SURFACE NAVIGATION**  
Operational use of remote sensing for commercial Arctic class vessel navigation  
p 33 A87-48829
- SURFACE PROPERTIES**  
Water-cycle processes in geosystems and the possibility of the remote sensing of the moisture content of the underlying surface  
p 51 A87-47580
- SURFACE ROUGHNESS**  
Retrieval of surface roughness parameters from dual-frequency measurements of radar backscattering coefficients  
p 10 A87-53130
- Roughness measurements with multipolarization aircraft data  
p 63 A87-53131
- SURFACE TEMPERATURE**  
Thermographic remote sensing of northern forest areas in regeneration after clear or strip cutting - Preliminary observations  
p 8 A87-48897
- Atmospheric effects on Landsat TM thermal IR data  
p 65 A87-53254
- Estimation of surface moisture availability from remote temperature measurements  
p 53 A87-54155
- SURFACE WAVES**  
Processing of airborne SAR images of ocean waves  
p 43 A87-53264
- Airborne SAR imaging of azimuthally travelling ocean surface waves - The LEWEX experimental plan  
p 44 A87-53266
- Comparison of numerical simulations with SAR images of ocean surface waves in the New York Bight  
p 44 A87-53287
- SURVEILLANCE**  
Millimeter-wave imaging sensor data evaluation [NASA-CR-181159]  
p 77 A87-26264
- SWATH WIDTH**  
Summary of recent SAR instrument studies  
p 78 A87-27865
- SYNCHRONOUS SATELLITES**  
First New Zealand image from the French SPOT satellite  
p 62 A87-51179
- SYNOPTIC METEOROLOGY**  
Comparisons of FGGE IIb and IIb winds in a tropical synoptic system  
p 35 A87-51559
- SYNTHETIC APERTURE RADAR**  
The CCRS SAR/MSS Anderson River data set  
p 55 A87-43261
- Potential application of multipolarization SAR for pine-plantation biomass estimation  
p 1 A87-43263
- Climatological implications of a satellite-borne SAR imaging the sea surface  
p 30 A87-46403
- Detecting forest structure and biomass with C-band multipolarization radar - Physical model and field tests  
p 2 A87-46543
- Use of synthetic aperture radar-derived kinematics in mapping mesoscale ocean structure within the interior marginal ice zone  
p 31 A87-47294
- Comparison of space and airborne L-HH radar imagery in an agricultural environment  
p 4 A87-48819
- Comparison of C-band synthetic aperture radar (SAR) data according to two different depression angles for agricultural applications  
p 4 A87-48820
- Validation of STAR-1 SAR imagery collected over Mould Bay, N.W.T., April 1984  
p 59 A87-48826
- Digital SAR-Landsat combination for geologic mapping  
p 24 A87-48853
- Multiple-look effects on SAR classification accuracies  
p 60 A87-48885
- The RADARSAT RMOMS optical sensor --- Modular Optoelectronic Multispectral Scanner  
p 73 A87-48890
- The ERS-1/RADARSAT SAR Canadian ground segment  
p 61 A87-48896
- Roughness measurements with multipolarization aircraft data  
p 63 A87-53131
- Automated rectification and geocoding of SAR imagery  
p 63 A87-53143
- Spaceborne imaging radar on EOS  
p 63 A87-53148
- Inverse synthetic aperture radar imaging techniques for sea-surface targets  
p 41 A87-53189

- Observation of oil slicks on the ocean by X-band SLAR  
p 41 A87-53191
- Modeling of focus effects in SAR images of the ocean surface  
p 42 A87-53212
- Automatic focusing of synthetic aperture radar images of diffuse targets  
p 64 A87-53213
- Synergism requirements and concepts for SAR and HIRIS on EOS  
p 75 A87-53216
- Performance sensitivity for X-SAR  
p 76 A87-53223
- The production of real time wave spectra from the SIR-C SAR  
p 42 A87-53224
- The EOS SAR program  
p 76 A87-53228
- Spacecraft on-board SAR image generation for EOS-type missions  
p 76 A87-53232
- A high speed digital processor for real-time synthetic aperture radar imaging  
p 64 A87-53233
- Real time global ocean wave spectra from SIR-C - Systems design  
p 42 A87-53234
- Progress on digital algorithms for deriving sea ice parameters from SAR data  
p 43 A87-53238
- Observing rotation and deformation of sea ice with synthetic aperture radar  
p 43 A87-53239
- The European Campaign 'AGRISAR '86'  
p 13 A87-53249
- Statistical modelling and suppression of speckle in synthetic aperture radar images  
p 65 A87-53259
- Spatial considerations in speckle simulation --- of spaceborne synthetic aperture radar imagery  
p 65 A87-53260
- Statistical modeling of intensity distributions on airborne SAR imagery  
p 65 A87-53262
- Processing of airborne SAR images of ocean waves  
p 43 A87-53264
- The comparison of ocean-wave spectra recovered from SIR-B and Seasat observations with simultaneous buoy data  
p 43 A87-53265
- Airborne SAR imaging of azimuthally travelling ocean surface waves - The LEWEX experimental plan  
p 44 A87-53266
- Speckle noise reduction of 1-look SAR imagery  
p 65 A87-53273
- Textural segmentation of SAR images using first order statistical parameters  
p 66 A87-53274
- A statistical and geometrical edge detector for SAR image segmentation  
p 13 A87-53275
- Integration of topographic data with synthetic aperture radar data for determining forest properties in mountainous terrain  
p 14 A87-53278
- A combined SAR and scatterometer system  
p 77 A87-53279
- Derivation of the technical specification of the ERS-1 active microwave instrument to meet the SAR-image quality requirements  
p 77 A87-53280
- Theoretical feasibility of SAR interferometry  
p 77 A87-53283
- The response of SAR imagery to azimuth travelling ocean surface waves as determined from shuttle SAR imagery  
p 44 A87-53286
- Comparison of numerical simulations with SAR images of ocean surface waves in the New York Bight  
p 44 A87-53287
- Study on the use and characteristics of SAR for geological applications. Part 2: Radargrammetry aspects [ESA-CR(P)-2325-PT-2]  
p 27 A87-26466
- Study on the use and characteristics of SAR systems for geological applications [ESA-CR(P)-2342]  
p 27 A87-26467
- Proceedings of the SAR Applications Workshop --- Synthetic Aperture Radar [ESA-SP-264]  
p 78 A87-27854
- Active microwave observations of sea ice and icebergs  
p 45 A87-27855
- The potential of SAR in a snow and glacier monitoring system  
p 45 A87-27856
- SAR detection of ships and ship wakes  
p 66 A87-27859
- Thin line detection in SAR images  
p 66 A87-27860
- Geological feature enhancement in SAR imagery  
p 67 A87-27861
- Study on the use of SAR data for agriculture and forestry  
p 15 A87-27862
- Land use feature detection in SAR images  
p 67 A87-27863
- An algorithm for automatically acquiring ground control points in SAR imagery  
p 67 A87-27864
- Summary of recent SAR instrument studies  
p 78 A87-27865
- Crop discrimination by means of radar and infrared images  
p 15 A87-28128
- Sea ice observations by SAR --- satellite observation  
p 47 A87-28156
- Calibrated L-band terrain measurements and analysis program [AD-A182917]  
p 68 A87-29722

## SYNTHETIC APERTURES

The global forest ecosystem as viewed by ERS-1, SIR-C and EOS p 12 A87-53217

## SYSTEMS ENGINEERING

An advanced wind scatterometer for the Columbus Polar Platform payload p 74 A87-53117  
A systems-approach to the design of the Eos data and information system p 64 A87-53207  
Real time global ocean wave spectra from SIR-C - Systems design p 42 A87-53234

## T

## TARGET ACQUISITION

Inverse synthetic aperture radar imaging techniques for sea-surface targets p 41 A87-53189

## TARGET RECOGNITION

Crop inventorying of small-parcelled areas using SPOT- and TM-data in conjunction with field radiometric measurements p 10 A87-53126  
SAR detection of ships and ship wakes p 66 A87-27859

## TECHNOLOGY ASSESSMENT

Photogrammetry - The largest operational application of remote sensing p 70 A87-47174  
Remote sensing of the earth with microwave radiometry in Germany - Results and trends p 76 A87-53225  
Study on the use of SAR data for agriculture and forestry p 15 A87-27862  
Requirements on radar data for geological application: A case study by use of multistage data of the test site Sardegna/Italy p 27 A87-28120  
SPOT: How good for geology? A comparison with LANDSAT MSS p 27 A87-28121

## TECHNOLOGY UTILIZATION

Remote sensing in Indonesia - A review of the available technology and its applications for resources surveys p 17 A87-46310  
Radio interferometry p 21 A87-46688  
Oceanographic and geophysical applications of satellite altimetry p 30 A87-46690  
Remote sensing applications of the earth's surface - An outlook into the future p 70 A87-47173  
Canadian Symposium on Remote Sensing, 10th, Edmonton, Canada, May 5-8, 1986, Proceedings. Volume 1 & 2 p 72 A87-48801  
Using airborne middle-infrared (1.45-2.0 microns) video imagery for distinguishing plant species and soil conditions p 9 A87-53023  
Contribution of space technology to disaster preparedness, warning, and relief p 20 A87-28130  
The role and perspective of remote sensing for disaster management in the European community p 20 A87-28137

## TECTONICS

Geological interpretations from Landsat of the Troodos Massif, Cyprus p 25 A87-48862  
Elements of lineament tectonics - Russian book p 27 A87-53954  
Kinematics at the intersection of the Garlock and Death Valley fault zones, California: Integration of TM data and field studies. LANDSAT TM investigation proposal TM-019 p 27 A87-28208  
[NASA-CR-180666] p 27 A87-28208  
Geomagnetic intersection of tectonic structures seen in space photographs p 28 A87-29574

## TELEMETRY

Data telemetry, assimilation and ocean modeling [AD-A181899] p 47 A87-28239

## TEMPERATURE MEASUREMENT

Studies of the wavelike process in the surface temperature field of the equatorial Pacific using Meteor-satellite IR measurements p 28 A87-42931  
Estimation of surface moisture availability from remote temperature measurements p 53 A87-54155  
Millimeter-wave imaging sensor data evaluation [NASA-CR-181159] p 77 A87-26264  
Thermal infrared images from satellites compared to shelter temperature. Application to frost nowcasting in a citrus orchard p 15 A87-28136

## TERMINOLOGY

Geodetic glossary [PB87-181210] p 22 A87-25652

## TERRAIN

Classification of geomorphic features and landscape stability in northwestern New Mexico using simulated SPOT imagery p 56 A87-46540  
Remote sensing and landscape approaches to earth resources p 63 A87-53154  
Landscape pattern and successional dynamics in the boreal forest p 11 A87-53155  
Remote sensing of earth terrain [NASA-CR-181370] p 79 A87-28957

## TERRAIN ANALYSIS

The automatic generation of digital terrain models from satellite images by stereo p 58 A87-48669  
Calibrated L-band terrain measurements and analysis program [AD-A182917] p 68 A87-29722

## TEXTURES

Textural segmentation of SAR images using first order statistical parameters p 66 A87-53274

## THEMATIC MAPPERS (LANDSAT)

Remote sensing of submerged aquatic vegetation in lower Chesapeake Bay - A comparison of Landsat MSS to TM imagery p 30 A87-46542  
Calibration of Thematic Mapper thermal data for water surface temperature mapping - Case study on the Great Lakes p 51 A87-46545  
Earth remote sensing using the Landsat Thematic Mapper and SPOT sensor systems; Proceedings of the Meeting, Innsbruck, Austria, Apr. 15-17, 1986 [SPIE-660] p 70 A87-48652  
Scene to scene radiometric normalization of the reflected bands of the Landsat Thematic Mapper p 71 A87-48654  
Geometric quality of Thematic Mapper data of the United Kingdom p 57 A87-48655  
Within-scene radiometric correction of Landsat Thematic Mapper (TM) data in Canadian production systems p 57 A87-48656  
TM sensor performance as obtained from Earthnet quality control data base p 71 A87-48659  
Evaluation of Landsat Thematic Mapper - Imagery for geological exploration p 23 A87-48666  
Lithologic discrimination using geobotanical and Landsat TM spectral data p 23 A87-48667  
Spectral discrimination of geobotanical anomalies using Landsat Thematic Mapper data p 2 A87-48668  
Significance of TM data as a tool to support regional planning activities p 17 A87-48671  
Discrimination of natural and cultivated vegetation using Thematic Mapper spectral data p 2 A87-48673  
Comparative analysis of different sensor data (Landsat-TM and MOMS) for earth observation and impact on future sensor development p 71 A87-48674  
Different scanning instruments comparison - MOMS and TM - Modular Optoelectronic Multispectral Scanner p 71 A87-48675  
Evaluation of algorithms for the geometric correction of Thematic Mapper data p 58 A87-48807  
Inventory of wetlands with Landsat's Thematic Mapper p 3 A87-48817  
Use of Thematic Mapper satellite images for disturbance updating of timber/range maps p 4 A87-48822  
Landsat thematic mapper data in wildlife habitat management - Reference to deer wintering habitat p 5 A87-48845  
Effectiveness of the Thematic Mapper for the range condition assessment in fescue grasslands of Southwestern Alberta p 6 A87-48850  
Radiation modelling in a high relief environment using a digital terrain model and Landsat - TM imagery p 59 A87-48857  
An evaluation of Landsat TM and MSS data for crop identification in Manitoba p 6 A87-48859  
Regional geobotany with TM - A Sudbury case study p 25 A87-48861  
Comparison of Landsat Thematic Mapper and Multispectral Scanner information content for agricultural applications in Western Canada p 6 A87-48863  
Landsat Thematic Mapper data - A useful tool for mapping agricultural areas in Quebec p 6 A87-48867  
Rural land use classification using Landsat Thematic Mapper data p 18 A87-48868  
Thematic Mapper information about Canadian forests - Early results from across the country p 6 A87-48869  
TM and MEIS data for future Alberta forest inventories p 8 A87-48900  
The evaluation of TM analysis as a tool in monitoring land use and agricultural stress in Egypt p 18 A87-48903  
Urban development planning using thematic mapper data of Munich (FRG) p 20 A87-28117  
Rural land use inventory and mapping in the Ardeche area (France). Improvement of automatic classification by multitemporal analysis of TM data p 15 A87-28127  
Evaluation of the potential of the Thematic Mapper for marine application p 46 A87-28134  
Monitoring and inventoring of forest damages by use of LANDSAT TM data p 16 A87-28138  
Towards the automatic recognition and vectorised description of linear features in LANDSAT TM images by artificial intelligence methods p 67 A87-28142  
The impact of LANDSAT Thematic Mapper Data for ecological mapping purposes. A case study at the northern margin of the Alps p 20 A87-28147

Present state, changes, and quality of Sologne and Brenne, two French large wetlands, studied with LANDSAT MSS and TM data p 54 A87-28152  
Kinematics at the intersection of the Garlock and Death Valley fault zones, California: Integration of TM data and field studies. LANDSAT TM investigation proposal TM-019 [NASA-CR-180666] p 27 A87-28208  
Determination of transfer functions from the Thematic Mapper (TM) sensor of the LANDSAT-5 satellite [INPE-4213-PRE/1094] p 79 A87-28956

## THEMATIC MAPPING

Stereoscopic visualization of aerial and space photographs in thematic mapping p 23 A87-42937  
Reflectance- and radiance-based methods for the in-flight absolute calibration of multispectral sensors p 69 A87-48863  
Remote sensing of submerged aquatic vegetation in lower Chesapeake Bay - A comparison of Landsat MSS to TM imagery p 30 A87-46542  
Calibration of Thematic Mapper thermal data for water surface temperature mapping - Case study on the Great Lakes p 51 A87-46545  
Updating maps of climax vegetation cover with Landsat MSS data in Queensland, Australia p 2 A87-46744  
Earth remote sensing using the Landsat Thematic Mapper and SPOT sensor systems; Proceedings of the Meeting, Innsbruck, Austria, Apr. 15-17, 1986 [SPIE-660] p 70 A87-48652  
Scene to scene radiometric normalization of the reflected bands of the Landsat Thematic Mapper p 71 A87-48654  
Geometric quality of Thematic Mapper data of the United Kingdom p 57 A87-48655  
Within-scene radiometric correction of Landsat Thematic Mapper (TM) data in Canadian production systems p 57 A87-48656  
A contribution to the optimum selection of ground control points in high resolution images p 57 A87-48658  
TM sensor performance as obtained from Earthnet quality control data base p 71 A87-48659  
Evaluation of Landsat Thematic Mapper - Imagery for geological exploration p 23 A87-48666  
Lithologic discrimination using geobotanical and Landsat TM spectral data p 23 A87-48667  
Spectral discrimination of geobotanical anomalies using Landsat Thematic Mapper data p 2 A87-48668  
Significance of TM data as a tool to support regional planning activities p 17 A87-48671  
Discrimination of natural and cultivated vegetation using Thematic Mapper spectral data p 2 A87-48673  
Comparative analysis of different sensor data (Landsat-TM and MOMS) for earth observation and impact on future sensor development p 71 A87-48674  
Different scanning instruments comparison - MOMS and TM - Modular Optoelectronic Multispectral Scanner p 71 A87-48675  
Evaluation of algorithms for the geometric correction of Thematic Mapper data p 58 A87-48807  
Application of accuracy assessment techniques to image classification - photointerpretation and scene analysis p 58 A87-48808  
Application of image segmentation algorithms to the inventory of crops in Canada p 3 A87-48813  
Evaluation of MEIS-II multispectral scanner data for quaternary geological mapping in the Chatham area, southwestern Ontario p 24 A87-48816  
Inventory of wetlands with Landsat's Thematic Mapper p 3 A87-48817  
Use of Thematic Mapper satellite images for disturbance updating of timber/range maps p 4 A87-48822  
Landsat thematic mapper data in wildlife habitat management - Reference to deer wintering habitat p 5 A87-48845  
Effectiveness of the Thematic Mapper for the range condition assessment in fescue grasslands of Southwestern Alberta p 6 A87-48850  
Radiation modelling in a high relief environment using a digital terrain model and Landsat - TM imagery p 59 A87-48857  
An evaluation of Landsat TM and MSS data for crop identification in Manitoba p 6 A87-48859  
Regional geobotany with TM - A Sudbury case study p 25 A87-48861  
Comparison of Landsat Thematic Mapper and Multispectral Scanner information content for agricultural applications in Western Canada p 6 A87-48863  
Landsat Thematic Mapper data - A useful tool for mapping agricultural areas in Quebec p 6 A87-48867  
Rural land use classification using Landsat Thematic Mapper data p 18 A87-48868  
Thematic Mapper information about Canadian forests - Early results from across the country p 6 A87-48869  
TM and MEIS data for future Alberta forest inventories p 8 A87-48900

The evaluation of TM analysis as a tool in monitoring land use and agricultural stress in Egypt

p 18 A87-48903

Relationship of Thematic Mapper simulator data to leaf area index of temperate coniferous forests

p 8 A87-53017

Cluster based segmentation of multi-temporal Thematic Mapper data as preparation of region-based agricultural land-cover analysis

p 9 A87-53109

Hierarchical classification with knowledge based binary decision --- for thematic mapping image interpretation

p 62 A87-53110

A multi-source image set for the study of soil texture and drainage as observed from Thematic Mapper data in Northern Belgium

p 10 A87-53125

Analysis of environmental information of urban areas using Landsat TM data

p 19 A87-53187

The detection of soil drainage by using Landsat MSS and TM (Belgian test zones)

p 11 A87-53205

Pleistocene earth movements in Peninsular India - Evidences from Landsat MSS and Thematic Mapper data

p 26 A87-53242

Analysis of Eocene depositional environments - Preliminary TM and TIMS results, Wind River Basin, Wyoming

p 26 A87-53243

Vegetation mapping and stress detection in the Santa Monica Mountains, California

p 12 A87-53246

Method development and experiences in application of airborne MSS data for forest damage detection

p 12 A87-53247

Thematic Mapper response to heavy metal related changes in Canopy LAI of a mixed forest

p 12 A87-53248

Evaluation of MOMS (Modular Optoelectronic Multispectral Scanner) data for land use/land cover studies - Test site: Piracicaba region, Sao Paulo State, Brazil

p 13 A87-53252

Atmospheric effects on Landsat TM thermal IR data

p 65 A87-53254

Application of TM imagery to mapping volcanic rock assemblages at tertiary calderas of the basin and range province

p 26 A87-53257

Whitetail deer food availability maps from Thematic Mapper data

p 14 A87-53998

Urban development planning using thematic mapper data of Munich (FRG)

p 20 A87-28117

Integration of remote sensing and geophysical data-application to exploration of pyrite ore facies in SW Spain

p 27 A87-28119

Rural land use inventory and mapping in the Ardeche area (France). Improvement of automatic classification by multitemporal analysis of TM data

p 15 A87-28127

Evaluation of the potential of the Thematic Mapper for marine application

p 46 A87-28134

Monitoring and inventoring of forest damages by use of LANDSAT TM data

p 16 A87-28138

Towards the automatic recognition and vectorised description of linear features in LANDSAT TM images by artificial intelligence methods

p 67 A87-28142

The impact of LANDSAT Thematic Mapper Data for ecological mapping purposes. A case study at the northern margin of the Alps

p 20 A87-28147

Mapping of vegetation types in SW Greenland

p 16 A87-28149

Snow mapping in western Greenland

p 54 A87-28150

Present state, changes, and quality of Sologne and Brenne, two French large wetlands, studied with LANDSAT MSS and TM data

p 54 A87-28152

Enhancement of colors in remote sensing images using rotation of the matrix at the IHS coordinates

[INPE-4207-PRE/1088] p 67 A87-28165

Spectral characteristics and the extent of paleosols of the Palouse formation

[NASA-CR-181208] p 17 A87-28195

Determination of transfer functions from the Thematic Mapper (TM) sensor of the LANDSAT-5 satellite

[INPE-4213-PRE/1094] p 79 A87-28956

**THERMAL MAPPING**

Remote-sensing evaluation of moisture supply to crops according to the leaf-surface thermal regime

p 2 A87-47582

A model of thermal inertia for frost forecasting in agricultural areas --- satellite imagery

p 16 A87-28151

**THERMOGRAPHY**

Thermographic remote sensing of northern forest areas in regeneration after clear or strip cutting - Preliminary observations

p 8 A87-48897

**THIN FILMS**

Meissner effect in high-Tc superconductive thin films

p 35 A87-51532

**TIDAL FLATS**

Studies of tidal flat environments with LANDSAT MSS data

p 47 A87-28157

## TIMBER IDENTIFICATION

Comparison of classification and enhancement techniques using Landsat imagery for the northern coniferous forest

p 4 A87-48821

Automatic classification of forestal areas by remote sensing techniques

p 12 A87-53211

**TIMBER INVENTORY**

Large-scale black and white and natural color photographs for the measurement of tree crown areas

p 3 A87-48815

Use of Thematic Mapper satellite images for disturbance updating of timber/range maps

p 4 A87-48822

TM and MEIS data for future Alberta forest inventories

p 8 A87-48900

Monitoring and inventoring of forest damages by use of LANDSAT TM data

p 16 A87-28138

**TIMBER VIGOR**

Large-scale black and white and natural color photographs for the measurement of tree crown areas

p 3 A87-48815

A trial of oblique imagery from a low cost video camera system for defoliation assessment

p 7 A87-48892

**TIROS N SERIES SATELLITES**

The dynamics of the northern border of the Gulf Stream revealed by a Tiros-N AVHRR image from October 22, 1980

p 35 A87-51147

Sea surface temperature retrieval from the Tiros-N AVHRR instrument for the FGGE period (Dec. 1978-Nov. 1979)

p 35 A87-51553

**TOPOGRAPHY**

Satellite altimeter measurements of the geoid in sea ice zones

p 30 A87-45816

Classification of geomorphic features and landscape stability in northwestern New Mexico using simulated SPOT imagery

p 56 A87-46540

Radiometric corrections of topographic effects for simulated RADARSAT imagery in a region of moderate relief

p 59 A87-48847

Introduction to sea-surface topography from satellite altimetry

p 38 A87-52508

Remote sensing and landscape approaches to earth resources

p 63 A87-53154

Landscape pattern and successional dynamics in the boreal forest

p 11 A87-53155

Global digital topography mapping using a scanning radar altimeter

p 76 A87-53227

Observations of and a new model for fetch-limited wave growth

p 43 A87-53263

Integration of topographic data with synthetic aperture radar data for determining forest properties in mountainous terrain

p 14 A87-53278

Theoretical feasibility of SAR interferometry

p 77 A87-53283

Solid earth geophysics: Data services

[PB87-184107] p 66 A87-27352

Morphometric studies of world ocean

p 45 A87-28077

Major morphologic features of the Atlantic Ocean surface

p 48 A87-29573

Study of physical processes on the US mid-Atlantic continental slope and rise. Volume 1: Executive summary

[PB87-200515] p 48 A87-30012

Study of physical processes on the US mid-Atlantic continental slope and rise. Volume 2: Technical presentation

[PB87-200523] p 49 A87-30013

**TRACKING (POSITION)**

Design study of remote sensing for ocean surface and interior activity

[AD-A180578] p 44 A87-25610

**TRAINING EVALUATION**

Multistage remote sensing with grade four students

p 80 A87-48810

**TRAJECTORIES**

Arctic drifting buoy data 1979 - 1985

[AD-A182967] p 50 A87-30019

**TRAJECTORY ANALYSIS**

Tracking of ice floes

p 46 A87-28155

Interpolation, analysis and archival of data on sea ice trajectories and ocean currents obtained from satellite-linked instruments

[PB87-201430] p 48 A87-30010

**TRAJECTORY OPTIMIZATION**

A method for the optimization of orbits and structures of satellite systems for the periodic round-the-clock survey of the earth

p 21 A87-42938

**TRANSFER FUNCTIONS**

Determination of transfer functions from the Thematic Mapper (TM) sensor of the LANDSAT-5 satellite

[INPE-4213-PRE/1094] p 79 A87-28956

**TRANSFERRING**

Data telemetry, assimilation and ocean modeling

[AD-A181899] p 47 A87-28239

## TRANSFORMATIONS (MATHEMATICS)

Brief introduction in statistical pattern recognition

[INPE-4206-PRE/1087] p 68 A87-28374

**TRANSPORT PROPERTIES**

Moisture transports and budgets of 'moisture bursts' --- of oceanic areas of tropical and subtropical latitudes

p 36 A87-51593

**TRANSPORT THEORY**

Physical oceanographic study of Florida's Atlantic Coast region: Florida Atlantic Coast Transport Study (FACTS). Volume 3: Appendices

[PB87-201018] p 49 A87-30017

**TREES (PLANTS)**

Estimation of X-band scattering properties of tree components

p 13 A87-53277

Effects of ozone on forests in the northeastern United States

[DE87-010887] p 16 A87-28190

**TRIANGULATION**

Development of a mathematical model for the spatial triangulation of SPOT images

p 61 A87-48905

**TROPICAL METEOROLOGY**

Moisture bursts over the tropical Pacific Ocean

p 28 A87-43345

Comparisons of FGGE IIb and IIb winds in a tropical synoptic system

p 35 A87-51559

Wintertime disturbances in the tropical Pacific - FGGE IIb and satellite comparisons

p 36 A87-51560

Moisture transports and budgets of 'moisture bursts' --- of oceanic areas of tropical and subtropical latitudes

p 36 A87-51593

Sampling errors in satellite estimates of tropical rain

p 53 A87-54153

**TROPICAL REGIONS**

Application of satellite data to tropic-subtropical moisture coupling

[NASA-CR-4092] p 48 A87-29067

**TROPOSPHERE**

Application of satellite data to tropic-subtropical moisture coupling

[NASA-CR-4092] p 48 A87-29067

**TURBULENT BOUNDARY LAYER**

Boundary layer, upper ocean, and ice observations in the Greenland Sea marginal ice zone

p 31 A87-47296

A comparison of the significant features of the marine boundary layers over the Arabian Sea and the Bay of Bengal during Monex 79

p 36 A87-51594

**TYPHOONS**

From satellite orbit into the eye of the typhoon --- Russian book

p 29 A87-44679

## U

### ULTRAHIGH FREQUENCIES

Comparison of space and airborne L-HH radar imagery in an agricultural environment

p 4 A87-48819

Calibrated L-band terrain measurements and analysis program

[AD-A182917] p 68 A87-29722

**ULTRAVIOLET SPECTROMETERS**

The high resolution imaging spectrometer (HIRIS) for EOS

p 74 A87-53145

**UNDERWATER ACOUSTICS**

Wave-theory modelling of convergence zone propagation in the ocean

[AD-A183607] p 50 A87-30020

**UNITED STATES**

Mechanisms of crustal deformation in the western US

[NASA-CR-181230] p 27 A87-28200

National Climate Program

[PB87-190518] p 79 A87-28221

Study of physical processes on the US mid-Atlantic continental slope and rise. Volume 2: Technical presentation

[PB87-200523] p 49 A87-30013

Study of physical processes on the US mid-Atlantic continental slope and rise. Volume 3: Appendix

[PB87-200531] p 49 A87-30014

**UPWELLING WATER**

Large scale ocean-atmosphere interaction in the summer monsoon - The influence of oceanic upwelling and advection on eastern Arabian Sea offshore convection

p 36 A87-51585

Coastal Zone Color Scanner (CZCS) images and ocean dynamics. Application to the Northwest African upwelling area

p 46 A87-28146

**URBAN DEVELOPMENT**

Urban development planning using thematic mapper data of Munich (FRG)

p 20 A87-28117

**URBAN PLANNING**

Urban development planning using thematic mapper data of Munich (FRG)

p 20 A87-28117

## URBAN RESEARCH

Small format aerial photography for analyzing urban housing problems - A case study in the Bangkok metropolitan region p 17 A87-46309

An application for the testing and use of the standard data transfer format --- for remotely sensed classified information transmission to GIS center p 18 A87-48886

## USER MANUALS (COMPUTER PROGRAMS)

A user's guide for the Analytical Photogrammetric Positioning System (APPS) [AD-A183773] p 79 N87-29909

## USER REQUIREMENTS

A methodology for evaluation of an interactive multispectral image processing system p 66 A87-53999

## V

## VARIANCE (STATISTICS)

The estimation of variance components in geodetic networks [B8681154] p 79 N87-29904

## VEGETATION

Remote sensing of the geomorphologic formations and vegetation in the eastern High Atlas region of Morocco from SPOT satellite data p 23 A87-45048

Discrimination of natural and cultivated vegetation using Thematic Mapper spectral data p 2 A87-48673

Shuttle imaging Radar-A (SIR-A) scenes from Iran and China p 25 A87-48854

On the origin of cross-polarization in remote sensing p 75 A87-53168

Polarization utilization in the microwave inversion of leaf angle distributions p 11 A87-53201

Radar polarization signatures of vegetated areas p 11 A87-53202

Vegetation mapping and stress detection in the Santa Monica Mountains, California p 12 A87-53246

Vegetation and a LANDSAT-derived land cover map of the Beechey Point quadrangle, Arctic Coastal Plain, Alaska [AD-A180931] p 15 N87-27312

The International Symposium on Microwave Signatures and Remote Sensing held in Gothenburg (Sweden) on 19-22 January 1987 [AD-A181334] p 78 N87-27314

Mapping of vegetation types in SW Greenland p 16 N87-28149

## VEGETATION GROWTH

Updating maps of climax vegetation cover with Landsat MSS data in Queensland, Australia p 2 A87-46744

Sampling semiarid vegetation with large-scale aerial photography p 14 A87-53741

## VEGETATIVE INDEX

The effect of subpixel clouds on remote sensing p 2 A87-48360

Comparison of space and airborne L-HH radar imagery in an agricultural environment p 4 A87-48819

Aircraft microwave radiometry of land p 13 A87-53269

Smoothing vegetation index profiles - An alternative method for reducing radiometric disturbance in NOAA/AVHRR data p 14 A87-53996

Comparison of NOAA AVHRR data to meteorologic drought indices p 14 A87-53997

Whitetail deer food availability maps from Thematic Mapper data p 14 A87-53998

## VELOCITY MEASUREMENT

Comparison of satellite-derived ocean velocities with observations in the California coastal region [AD-A182291] p 47 N87-28242

## VERY LONG BASE INTERFEROMETRY

Radio interferometry p 21 A87-46688

A program for the combined adjustment of VLBi observing sessions p 22 A87-52766

## VIDEO DATA

Airborne video - Applied to route location studies for electrical power transmission facilities p 17 A87-48802

Color infrared video mapping of upland and wetland communities [DE87-010202] p 15 N87-28109

Analysis of directions of linear image elements by structure-zonal method p 68 N87-29575

## VIDEO EQUIPMENT

Multispectral video system for airborne remote sensing - Sensitivity, calibrations and correction p 73 A87-48873

## VISCOELASTICITY

Azimuthal dependence in the gravity field induced by recent and past cryospheric forcings p 35 A87-51487

## VISIBLE INFRARED SPIN SCAN RADIOMETER

Calibration of NOAA-7 AVHRR, GOES-5, and GOES-6 VISSR/VAS solar channels p 69 A87-44865

## VISIBLE SPECTRUM

Calibration requirements and methodology for remote sensors viewing the ocean in the visible p 29 A87-44866

## VISUAL PERCEPTION

Enhancement of colors in remote sensing images using rotation of the matrix at the IHS coordinates [INPE-4207-PRE/1088] p 67 N87-28165

## VOLCANOES

Rheology of the 1983 Royal Gardens basalt flows, Kilauea Volcano, Hawaii p 26 A87-51725

Use of TM Landsat data as a support to classical ground-based methodologies in the investigation of a volcanic site in central Italy - The Caldera of Latera p 26 A87-53244

Application of TM imagery to mapping volcanic rock assemblages at tertiary calderas of the basin and range province p 26 A87-53257

Catalog of submarine volcanoes and hydrological phenomena associated with volcanic events, January 1, 1900 to December 31, 1959 [PB87-183943] p 54 N87-28196

## VORTICES

Features of the water dynamics of Lake Ladoga according to remote sensing data p 50 A87-44296

Mesoscale eddies in the Fram Strait marginal ice zone during the 1983 and 1984 Marginal Zone Experiments p 31 A87-47291

Observing systems experiments for the onset vortex during Summer Monex p 35 A87-51552

Physical oceanographic study of Florida's Atlantic Coast region: Florida Atlantic Coast Transport Study (FACTS), Volume 3: Appendices [PB87-201018] p 49 N87-30017

## W

## WAKES

The Bakerian Lecture, 1986 - Ships from space --- wakes behind surface vessels observed from space p 44 A87-54301

SAR detection of ships and ship wakes p 66 N87-27859

## WATER COLOR

Satellite color observations of spring blooming in Bering Sea shelf waters during the ice edge retreat in 1980 p 32 A87-47297

## WATER CURRENTS

Features of the water dynamics of Lake Ladoga according to remote sensing data p 50 A87-44296

ADRIA 84: Airborne investigations of Gelbstoff by optical radiometry and fluorescence lidar --- Adriatic Sea p 46 N87-28154

Physical oceanographic study of Florida's Atlantic Coast region: Florida Atlantic Coast Transport Study (FACTS), Volume 1: Executive summary [PB87-200994] p 49 N87-30015

Physical oceanographic study of Florida's Atlantic Coast region: Florida Atlantic Coast Transport Study (FACTS), volume 2 [PB87-201000] p 49 N87-30016

Physical oceanographic study of Florida's Atlantic Coast region: Florida Atlantic Coast Transport Study (FACTS), Volume 3: Appendices [PB87-201018] p 49 N87-30017

## WATER MANAGEMENT

Satellite remote sensing for water resources management: Some engineering and economic aspects p 54 N87-28139

## WATER POLLUTION

Monitoring and modeling of the Adriatic Sea p 46 N87-28133

## WATER QUALITY

Operational water quality surveillance in Sweden using Landsat MSS data p 52 A87-48841

Investigation of causes of hydrogen sulfide formation in reclaimed water p 14 N87-23136

## WATER RECLAMATION

Investigation of causes of hydrogen sulfide formation in reclaimed water p 14 N87-23136

## WATER RESOURCES

Formation of natural underground-water resources in arid regions with special reference to the Dolinoozerskii artesian basin in Mongolia --- Russian book p 50 A87-42911

## WATER RUNOFF

Possibility of evaluating reservoir inflow from aerial and satellite photographs p 51 A87-47577

Modeling the snowmelt runoff in mountain catchment areas using satellite data p 51 A87-47578

Parameterization of models of runoff formation in simple catchment areas using remote-sensing data p 51 A87-47579

Snowpack depletion monitoring in Alberta using computer-processed NOAA imagery p 52 A87-48848

Development of EOS-aided procedures for the determination of the water balance or hydrologic budget of a large watershed p 53 A87-53215

## WATER TEMPERATURE

Upwelling filaments and motion of a satellite-tracked drifter along the west coast of North America p 29 A87-45023

Calibration of Thematic Mapper thermal data for water surface temperature mapping - Case study on the Great Lakes p 51 A87-46545

## WATER VAPOR

A microwave radiometer weather-correcting sea ice algorithm p 29 A87-45024

Moisture transports and budgets of 'moisture bursts' --- of oceanic areas of tropical and subtropical latitudes p 36 A87-51593

## WATER WAVES

Radar scattering and equilibrium ranges in wind-generated waves with application to scatterometry p 28 A87-42746

Ocean wave parameter measurement using a dual-radar system - A simulation study p 33 A87-48363

Comparison of Geosat and ground-truth wind and wave observations - Preliminary results p 38 A87-52509

Validation of Geosat altimeter-derived wind speeds and significant wave heights using buoy data p 39 A87-52510

Wind and wave statistics as derived from the Geosat radar altimeter and with comparisons with in situ measurements p 40 A87-53127

The effects of wind-wave coupling on scatterometer wind measurement accuracy p 41 A87-53196

The production of real time wave spectra from the SIR-C SAR p 42 A87-53224

Real time global ocean wave spectra from SIR-C - Systems design p 42 A87-53234

Observations of and a new model for fetch-limited wave growth p 43 A87-53263

The comparison of ocean-wave spectra recovered from SIR-B and Seasat observations with simultaneous buoy data p 43 A87-53265

The response of SAR imagery to azimuth travelling ocean surface waves as determined from shuttle SAR imagery p 44 A87-53286

Approximating SIR-B response characteristics and estimating wave height and wavelength for ocean imagery p 44 A87-53288

The determination of sea-state bias and non-linear wave parameters from satellite altimeter data p 46 N87-28132

Analysis of directions of linear image elements by structure-zonal method p 68 N87-29575

Labrador wind and wave environments [AD-A183218] p 48 N87-29907

## WATERSHEDS

Indexing small catchments in Java, Indonesia, with respect to their relative susceptibility to erosion p 52 A87-48871

Hydrologic applications of weather radar data p 52 A87-48875

Airborne multispectral observations over burned and unburned prairies p 10 A87-53122

Development of EOS-aided procedures for the determination of the water balance or hydrologic budget of a large watershed p 53 A87-53215

## WAVE GENERATION

Radar scattering and equilibrium ranges in wind-generated waves with application to scatterometry p 28 A87-42746

## WAVE PROPAGATION

Observations of and a new model for fetch-limited wave growth p 43 A87-53263

Wave-theory modelling of convergence zone propagation in the ocean [AD-A183607] p 50 N87-30020

## WAVEFORMS

Waveform analysis for Geosat day 96 p 39 A87-52514

## WEATHER FORECASTING

Forecast of hurricane characteristics from GOES imagery p 59 A87-48818

Hydrologic applications of weather radar data p 52 A87-48875

Remote sensing of geomagnetic field and applications to climate prediction p 74 A87-53108

A model of thermal inertia for frost forecasting in agricultural areas --- satellite imagery p 16 N87-28151

National Climate Program [PB87-190518] p 79 N87-28221

## WETLANDS

Remote sensing of coastal wetlands p 1 A87-40944

Inventory of wetlands with Landsat's Thematic Mapper p 3 A87-48817

- Extent of saline/waterlogged lands within irrigated Alberta. I - Inventory and preliminary evaluation of existing mapping data p 5 A87-48830
- The detection of wetlands on radar imagery p 6 A87-48855
- Remote sensing as a tool for Alberta Agricultural Wetlands Drainage Inventory p 6 A87-48882
- Color infrared video mapping of upland and wetland communities [DE87-010202] p 15 N87-28109
- Present state, changes, and quality of Sologne and Brenne, two French large wetlands, studied with LANDSAT MSS and TM data p 54 N87-28152

**WHALES**

- Remote sensing in support of ecological studies of the bowhead whale p 34 A87-48843

**WHEAT**

- Monitoring wheat canopies with a high spectral resolution radiometer p 8 A87-53019

**WILDLIFE**

- Landsat-based wildlife habitat mapping - A study of collaboration between analyst and user p 3 A87-48809
- Landsat thematic mapper data in wildlife habitat management - Reference to deer wintering habitat p 5 A87-48845

**WIND (METEOROLOGY)**

- Optimum use of dual frequency passive microwave measurements for ice/ocean interactions p 43 A87-53240
- Labrador wind and wave environments [AD-A183218] p 48 N87-29907
- Arctic drifting buoy data 1979 - 1985 [AD-A182967] p 50 N87-30019

**WIND EFFECTS**

- Coastal Zone Color Scanner (CZCS) images and ocean dynamics. Application to the Northwest African upwelling area p 46 N87-28146

**WIND MEASUREMENT**

- An advanced wind scatterometer for the Columbus Polar Platform payload p 74 A87-53117
- A spaceborne LFM scatterometer for ocean surface wind vector measurement - A time domain approach --- Linearly Frequency Modulated p 40 A87-53119
- Wind and wave statistics as derived from the Geosat radar altimeter and with comparisons with in situ measurements p 40 A87-53127
- Wind measurements for non-uniform wind fields from spaceborne scatterometers p 75 A87-53195
- The effects of wind-wave coupling on scatterometer wind measurement accuracy p 41 A87-53196

**WIND VELOCITY**

- Validation of Geosat altimeter-derived wind speeds and significant wave heights using buoy data p 39 A87-52510
- A comparative study of several wind estimation algorithms for spaceborne scatterometers p 41 A87-53197

**WIND VELOCITY MEASUREMENT**

- Maximum accuracy of satellite-borne scatterometer measurements of wind velocity above the ocean p 33 A87-48184

**Y****YTTRIUM COMPOUNDS**

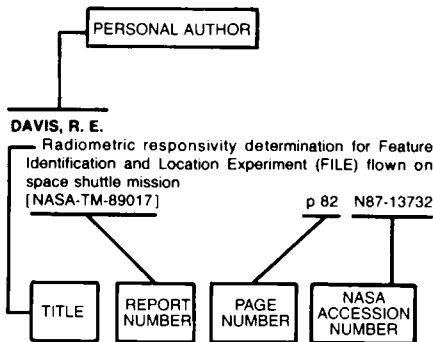
- Meissner effect in high-Tc superconductive thin films p 35 A87-51532

# PERSONAL AUTHOR INDEX

EARTH RESOURCES / A Continuing Bibliography (Issue 56)

FEBRUARY 1988

## Typical Personal Author Index Listing



Listings in this index are arranged alphabetically by personal author. The title of the document provides the user with a brief description of the subject matter. The report number helps to indicate the type of document listed (e.g., NASA report, translation, NASA contractor report). The page and accession numbers are located beneath and to the right of the title. Under any one author's name the accession numbers are arranged in sequence with the AIAA accession numbers appearing first.

## A

- ABADIE, J.**  
Poseidon radar altimeter description and signal processing p 40 A87-53114
- ABER, JOHN D.**  
Estimating key forest ecosystem parameters through remote sensing p 12 A87-53245
- ABRAMS, MICHAEL**  
Kinematics at the intersection of the Garlock and Death Valley fault zones, California: Integration of TM data and field studies. LANDSAT TM investigation proposal TM-019 [NASA-CR-180666] p 27 N87-28208
- ACEVEDO, WILLIAM**  
Vegetation and a LANDSAT-derived land cover map of the Beechey Point quadrangle, Arctic Coastal Plain, Alaska [AD-A180931] p 15 N87-27312
- ACKERMAN, STEVEN A.**  
Satellite observations of convection during the summer monsoon of 1979 p 36 A87-51587
- ACKLESOM, S. G.**  
Remote sensing of submerged aquatic vegetation in lower Chesapeake Bay - A comparison of Landsat MSS to TM imagery p 30 A87-46542
- ADAMS, B. W.**  
Effectiveness of the Thematic Mapper for the range condition assessment in fescue grasslands of Southwestern Alberta p 6 A87-48850
- ADAMS, M. B.**  
Effects of ozone on forests in the northeastern United States [DE87-010887] p 16 N87-28190
- AGREEN, RUSSELL W.**  
Monitoring equatorial Pacific sea level with Geosat p 39 A87-52512
- AHERN, F. J.**  
Thematic Mapper information about Canadian forests - Early results from across the country p 6 A87-48869  
The RADARSAT RMOMS optical sensor p 39 A87-48890
- AHMAD, Z.**  
Sea surface temperature retrieval from the Tiros-N AVHRR instrument for the FGGE period (Dec. 1978-Nov. 1979) p 35 A87-51553

- AKHAVI, M. S.**  
Integration of radiometric and Landsat digital data for geologic investigation and exploration, Guysborough area, Nova Scotia p 24 A87-48803  
Analysis of airborne infrared data for interpretative geological mapping of the Brookfield area, Nova Scotia p 24 A87-48804  
The detection of vegetative stress utilizing remotely sensed data and soil sampling p 8 A87-50231
- AKSNES, K.**  
SAR detection of ships and ship wakes p 66 N87-27859
- ALANIZ, M. A.**  
Using airborne middle-infrared (1.45-2.0 microns) video imagery for distinguishing plant species and soil conditions p 9 A87-53023
- ALEKSANDROV, V. I.**  
Evaluation of the effect of hydrometeors on the characteristics of radar images of sea ice p 33 A87-48181
- ALEXANDER, DAVID P.**  
Using remotely sensed Landsat MSS data to assess groundwater influence on the Barmah-Millewa Forest p 10 A87-53124
- ALI, A.**  
Agricultural, hydrologic and oceanographic studies in Bangladesh with NOAA AVHRR data p 57 A87-48365
- ALLEY, R. B.**  
Till beneath ice stream B. I - Properties derived from seismic travel times. II - Structure and continuity. III - Till deformation - Evidence and implications. IV - A coupled ice-till flow model p 37 A87-51948
- ALPERS, WERNER**  
Radar signatures of oil films floating on the sea surface p 41 A87-53192
- AMMANN, V.**  
ADRIA 84: Airborne investigations of Gelbstoff by optical radiometry and fluorescence lidar p 46 N87-28154
- ANAN'EV, I. P.**  
Remote-sensing evaluation of the spatial variability of evaporation p 52 A87-47583
- ANDERSON, L. L., JR.**  
Wintertime disturbances in the tropical Pacific - FGGE IIb and satellite comparisons p 36 A87-51560
- ANDREOLI, G.**  
Measurement of spectral signatures in Less Favored Areas (LFA): A contribution to the definition of a remote sensing multitemporal experiment p 20 N87-28145
- ANDREOTTI, YURIY**  
Successes of Cosmos-1500 satellite, SLR system p 45 N87-27696
- ANTONOVA, I. B.**  
Space photographs of the Onega-Ladoga isthmus and the prediction of mineral finds p 23 A87-48185
- ARCHIBALD, P. D.**  
Thematic Mapper information about Canadian forests - Early results from across the country p 6 A87-48869
- ARENS, W. E.**  
Spacecraft on-board SAR image generation for EOS-type missions p 76 A87-53232
- ARPS, RONALD B.**  
Information content analysis of Landsat image data for compression p 56 A87-47046
- ASHWAL, LEWIS**  
Workshop on The Earth as a Planet [NASA-CR-180543] p 81 N87-29900
- ASRAR, G.**  
Airborne multispectral observations over burned and unburned prairies p 10 A87-53122
- ASSAL, H. M.**  
Spacecraft on-board SAR image generation for EOS-type missions p 76 A87-53232

## B

- BADHWAR, G. D.**  
Estimation of X-band scattering properties of tree components p 13 A87-53277
- BAGROVA, Z. A.**  
Space photographs of the Onega-Ladoga isthmus and the prediction of mineral finds p 23 A87-48185

- BAIBAKOV, SERGEI NIKOLAEVICH**  
From satellite orbit into the eye of the typhoon p 29 A87-44679
- BAILLIE, A. J. M.**  
A high-throughput system for bulk processing of multispectral imagery p 72 A87-48836
- BAIN, D.**  
Stratification of satellite imagery by Uniform Productivity Areas p 5 A87-48840
- BAINS, DEVENDAR S.**  
Hybrid power amplifier module for X-band p 69 A87-43302
- BAKANOV, K. G.**  
Possibility of evaluating reservoir influx from aerial and satellite photographs p 51 A87-47577
- BAKER, KAREN S.**  
Multiplatform sampling (ship, aircraft, and satellite) of a Gulf Stream warm core ring p 29 A87-44811
- BALANDIN, V. A.**  
Investigation of the relief of ore-containing regions on the basis of space photographs (with reference to eastern Yakutia) p 23 A87-48188
- BALENKO, V. G.**  
The determination of Love numbers from the results of earth-tide observations in the Dnieper-Donets basin (DDB) region p 21 A87-46139
- BALL, R.**  
An algorithm for automatically acquiring ground control points in SAR imagery p 67 N87-27864
- BALSHEM, HAROLD**  
Hybrid power amplifier module for X-band p 69 A87-43302
- BANNINGER, C.**  
Spectral discrimination of geobotanical anomalies using Landsat Thematic Mapper data p 2 A87-48668  
Thematic Mapper response to heavy metal related changes in Canopy LAI of a mixed forest p 12 A87-53248
- BARALE, VITTORIO**  
Remote observations of the marine environment - Spatial heterogeneity of the mesoscale ocean color field in CZCS imagery of California near-coastal waters p 30 A87-46539
- BARDSLEY, K. L.**  
How useful is Landsat monitoring? p 14 A87-54089
- BARET, F.**  
Monitoring wheat canopies with a high spectral resolution radiometer p 8 A87-53019
- BARKER, JOHN L.**  
Radiometric properties of U.S. processed Landsat MSS data p 55 A87-44864
- BARNES, W.**  
MODIS - Advanced facility instrument for studies of the earth as a system p 40 A87-53144
- BARTOLUCCI, LUIS A.**  
Atmospheric effects on Landsat TM thermal IR data p 65 A87-53254
- BATH, A. C.**  
Application of remote sensing data to bedrock geological interpretation, Black River-Matheson area, Northern Ontario, Canada p 24 A87-48832
- BAUCHE, BERNARD**  
Matching instrument design and signal processing for a scanning radiometer p 76 A87-53251
- BEAUBIEN, J.**  
A geobotanic approach to the study of the geology of Cape Smith using Landsat-MSS data p 25 A87-48860
- BEAUMONT, CHRISTOPHER**  
Tidal and secular tilt from an earthquake zone - Thresholds for detection of regional anomalies p 26 A87-53733
- BEGNI, G.**  
Absolute calibration of the SPOT-1 HRV cameras p 71 A87-48660  
SPOT radiometric resolution performance evaluation - Preliminary results p 57 A87-48661
- BEKHTEREV, I. I.**  
Measurement of currents according to the drift of subsatellite buoys p 32 A87-48177
- BELL, THOMAS L.**  
A space-time stochastic model of rainfall for satellite remote-sensing studies p 54 A87-54157



**BELLISS, S. E.**

First New Zealand image from the French SPOT satellite p 62 A87-51179

**BENELLI, G.**

Crop discrimination by means of radar and infrared images p 15 N87-28128

**BENIE, G. P.**

Application of image segmentation algorithms to the inventory of crops in Canada p 3 A87-48813

**BENNETT, JOHN R.**

Comparison of numerical simulations with SAR images of ocean surface waves in the New York Bight p 44 A87-53287

**BENTLEY, C. R.**

Till beneath ice stream B. I - Properties derived from seismic travel times. II - Structure and continuity. III - Till deformation - Evidence and implications. IV - A coupled ice-till flow model p 37 A87-51948

**BENTLEY, CHARLES R.**

Antarctic ice streams - A review p 37 A87-51943  
The morphology of ice streams A, B, and C, West Antarctica and their environs p 37 A87-51945

**BERKOWITZ, RAYMOND S.**

Inverse synthetic aperture radar imaging techniques for sea-surface targets p 41 A87-53189

**BERNIER, M.**

Effectiveness of the Thematic Mapper for the range condition assessment in fescue grasslands of Southwestern Alberta p 6 A87-48850  
Landsat Thematic Mapper data - A useful tool for mapping agricultural areas in Quebec p 6 A87-48867

**BERNSTEIN, RALPH**

Discrimination of natural and cultivated vegetation using Thematic Mapper spectral data p 2 A87-48673

**BERRY, J. K.**

Computer-assisted map analysis - Extending the utility of GIS technology p 18 A87-48907

**BESCOND, PIERRE**

The SPOT program - Commercialization of remote sensing p 80 A87-53235

**BIANCALE, R.**

Earth gravity model improvement - An alternative method for Doppler-tracked satellites p 21 A87-45817

**BIANCHI, ALEJANDRO A.**

Some aspects of the surface circulation south of 20 deg S revealed by First GARP Global Experiment drifters p 28 A87-42748

**BIGGAR, S. F.**

Reflectance- and radiance-based methods for the in-flight absolute calibration of multispectral sensors p 69 A87-44863

**BIGGS, R. B.**

Characterizing the Chesapeake Bay ecosystem and lessons learned [PB87-166930] p 19 N87-26463

**BINDSCHADLER, R. A.**

Ice dynamics at the mouth of ice stream B, Antarctica p 37 A87-51946

**BINDSCHADLER, ROBERT A.**

Ice measurements by Geosat radar altimetry p 39 A87-52513

**BIRNIE, RICHARD W.**

Lithologic discrimination using geobotanical and Landsat TM spectral data p 23 A87-48667

**BLANKENSHIP, D. D.**

Till beneath ice stream B. I - Properties derived from seismic travel times. II - Structure and continuity. III - Till deformation - Evidence and implications. IV - A coupled ice-till flow model p 37 A87-51948

**BLOM, RONALD**

Multifrequency and multipolarization radar scatterometry of sand dunes and comparison with spaceborne and airborne radar images p 70 A87-47257

**BODECHTEL, J.**

Comparative analysis of different sensor data (Landsat-TM and MOMS) for earth observation and impact on future sensor development p 71 A87-48674

**BOGOSLOVSKII, VADIM ALEKSANDROVICH**

Remote-sensing and geological-geophysical studies of closed platform territories p 26 A87-51875

**BOISSIN, B.**

SPOT localization accuracy and geometric image quality p 57 A87-48662

**BOLZAN, J.**

Velocity of ice streams B and C, Antarctica p 37 A87-51947

**BONHAM-CARTER, G. F.**

Preliminary results from modelling vegetation spectra derived from MEIS data, Algonquin Park, Ontario p 7 A87-48891

**BONN, F.**

Landsat thematic mapper data in wildlife habitat management - Reference to deer wintering habitat p 5 A87-48845

Effects of surface geometry of agricultural fields on radar airborne imagery in X- and C-bands p 5 A87-48846

Radiometric corrections of topographic effects for simulated RADARSAT imagery in a region of moderate relief p 59 A87-48847

Thermographic remote sensing of northern forest areas in regeneration after clear or strip cutting - Preliminary observations p 8 A87-48897

**BONSIGNORI, R.**

Aircraft microwave radiometry of land p 13 A87-53269

**BORN, GEORGE H.**

Design of Geosat Exact Repeat Mission p 39 A87-52515

**BORSTAD, G. A.**

Remote sensing in support of ecological studies of the bowhead whale p 34 A87-48843  
Analysis of data from the DFO fluorescence line imager p 72 A87-48844

**BOS, CORNELIS**

The estimation of variance components in geodetic networks [B8681154] p 79 N87-29904

**BOSCHI, ENZO**

Azimuthal dependence in the gravity field induced by recent and past cryospheric forcings p 35 A87-51487

**BOTKIN, DANIEL B.**

Landscape pattern and successional dynamics in the boreal forest p 11 A87-53155

**BOUSQUET, P.**

A statistical and geometrical edge detector for SAR image segmentation p 13 A87-53275

**BOWLEY, B. R.**

Integrated multi-temporal aerial photography and digital mapping for coastal monitoring, Cape Breton Island, Nova Scotia p 34 A87-48837

**BOYD, P.**

Optimization of seismic vessel deployment using side looking airborne radar p 34 A87-48881

**BRACEWELL, R. N.**

Observing rotation and deformation of sea ice with synthetic aperture radar p 43 A87-53239

**BRACHET, GERARD**

Second generation high-resolution space systems - First results of the SPOT-1 satellite p 55 A87-44244

**BRAEDT, J.**

Significance of TM data as a tool to support regional planning activities p 17 A87-48671

**BRAMM, R. G.**

Rural land use classification using Landsat Thematic Mapper data p 18 A87-48868

**BRENNER, ANITA C.**

Ice measurements by Geosat radar altimetry p 39 A87-52513

**BREWER, L. W.**

The role of Landsat multi-spectral scanner data in the analysis of northern spotted owl habitat p 7 A87-48894

**BROWN, GEORGE**

International cooperation in space - Enhancing the world's common security p 81 A87-53987

**BROWN, O.**

Study of physical processes on the US mid-Atlantic continental slope and rise. Volume 1: Executive summary [PB87-200515] p 48 N87-30012

Study of physical processes on the US mid-Atlantic continental slope and rise. Volume 2: Technical presentation [PB87-200523] p 49 N87-30013

Study of physical processes on the US mid-Atlantic continental slope and rise. Volume 3: Appendix [PB87-200531] p 49 N87-30014

**BROWN, OTIS B.**

Multiplatform sampling (ship, aircraft, and satellite) of a Gulf Stream warm core ring p 29 A87-44811

**BROWN, R.**

The global forest ecosystem as viewed by ERS-1, SIR-C and EOS p 12 A87-53217

**BROWN, R. J.**

Comparison of space and airborne L-HH radar imagery in an agricultural environment p 4 A87-48819

Comparison of C-band synthetic aperture radar (SAR) data according to two different depression angles for agricultural applications p 4 A87-48820

The use of multi-spectral and radar remote sensing data for monitoring forest clearcut and regeneration sites on Vancouver Island p 5 A87-48834

Comparison of Landsat Thematic Mapper and Multispectral Scanner information content for agricultural applications in Western Canada p 6 A87-48863

Technological feasibility to mobilization for operations - The NOAA crop monitoring case p 6 A87-48878

Multiple-look effects on SAR classification accuracies p 60 A87-48885

Ground targets for the radiometric correction of AVHRR imagery for crop monitoring p 7 A87-48887

**BROWN, RONALD J.**

Canadian Symposium on Remote Sensing, 10th, Edmonton, Canada, May 5-8, 1986, Proceedings. Volume 1 & 2 p 72 A87-48801

**BRUCE, B.**

Regional geobotany with TM - A Sudbury case study p 25 A87-48861

Geological interpretations from Landsat of the Troodos Massive, Cyprus p 25 A87-48862

**BRUEGGE, C.**

Synergism requirements and concepts for SAR and HIRIS on EOS p 75 A87-53216

**BRULE, M.**

An algorithm for automatically acquiring ground control points in SAR imagery p 67 N87-27864

**BUCHROITHNER, M. F.**

Integrated systems for remote sensing p 67 N87-28143

**BULLARD, RICHARD K.**

Environmental information and cartography p 20 N87-28141

**BULLOCH, CHRIS**

Eurimage sets up shop p 80 A87-51324

**BUNTING, JAMES T.**

Improved cloud analysis using visible, near-infrared, infrared, and microwave imagery p 62 A87-53103

**BURGEL, GALIA**

Moscow seen by satellite - Another image of Soviet urban geography p 80 A87-51143

**BURGEL, GUY**

Moscow seen by satellite - Another image of Soviet urban geography p 80 A87-51143

**BURGER, G. J.**

Custom-enhanced Landsat imagery in near real-time p 60 A87-48870

**BURKE, KEVIN**

Workshop on The Earth as a Planet [NASA-CR-180543] p 81 N87-29900

**BURLESHIN, M. I.**

Geomagnetic intersection of tectonic structures seen in space photographs p 28 N87-29574

**BURNS, B. A.**

Use of synthetic aperture radar-derived kinematics in mapping mesoscale ocean structure within the interior marginal ice zone p 31 A87-47294

Multisensor comparison of ice concentration estimates in the marginal ice zone p 31 A87-47295

Progress on digital algorithms for deriving sea ice parameters from SAR data p 43 A87-53238

**BURNS, BARBARA A.**

Investigation of multi-dimensional algorithms using active and passive microwave data for ice concentration determination p 43 A87-53241

**BUSACCA, ALAN**

Spectral characteristics and the extent of paleosols of the Palouse formation [NASA-CR-181208] p 17 N87-28195

**C****CALDWELL, P.**

Inventory of wetlands with Landsat's Thematic Mapper p 3 A87-48817

**CALLIS, SUSAN L.**

Smoothing vegetation index profiles - An alternative method for reducing radiometric disturbance in NOAA/AVHRR data p 14 A87-53996

**CALMAN, JACK**

Introduction to sea-surface topography from satellite altimetry p 38 A87-52508

**CAMERLYNCK, CHRISTIAN**

Geoid anomalies across Ascension fracture zone and the cooling of the lithosphere p 21 A87-44352

**CAMERON, M. A.**

Validation of STAR-1 SAR imagery collected over Mould Bay, N.W.T., April 1984 p 59 A87-48826

**CAMPBELL, W. J.**

Variations of mesoscale and large-scale sea ice morphology in the 1984 Marginal Ice Zone Experiment as observed by microwave remote sensing p 31 A87-47292

Multisensor comparison of ice concentration estimates in the marginal ice zone p 31 A87-47295

**CANTELLA, MICHAEL J.**

Space surveillance application potential of Schottky barrier IR sensors [AD-A180848] p 78 N87-27311

**CAPPA, C.**

Climatological implications of a satellite-borne SAR imaging the sea surface p 30 A87-46403

**CAPPELLINI, V.**

Crop discrimination by means of radar and infrared images p 15 N87-28128

**CARLSON, TOBY N.**

Estimation of surface moisture availability from remote temperature measurements p 53 A87-54155

**CARR, FREDERICK H.**

Observing systems experiments for the onset vortex during Summer Monex p 35 A87-51552

**CARSEY, FRANK**

Beaufort-Chukchi ice margin data from Seasat - Ice motion p 32 A87-47299

**CARVER, KEITH**

The EOS SAR program p 76 A87-53228

**CASAGRANDE, C.**

Study of physical processes on the US mid-Atlantic continental slope and rise. Volume 1: Executive summary [PB87-200515] p 48 A87-30012

Study of physical processes on the US mid-Atlantic continental slope and rise. Volume 2: Technical presentation [PB87-200523] p 49 A87-30013

Study of physical processes on the US mid-Atlantic continental slope and rise. Volume 3: Appendix [PB87-200531] p 49 A87-30014

**CASELLES, V.**

Thermal infrared images from satellites compared to shelter temperature. Application to frost nowcasting in a citrus orchard p 15 N87-28136

**CAVALIERI, D. J.**

A model of thermal inertia for frost forecasting in agricultural areas p 16 N87-28151

**CAVALIERI, DONALD J.**

Multisensor comparison of ice concentration estimates in the marginal ice zone p 31 A87-47295

On the relationship between atmospheric circulation and the fluctuations in the sea ice extents of the Bering and Okhotsk Seas p 32 A87-47298

**CAVALIERI, DONALD J.**

Shuttle Imaging Radar B (SIR-B) Weddell Sea ice observations - A comparison of SIR-B and scanning multichannel microwave radiometer ice concentrations p 32 A87-47300

Investigation of multi-dimensional algorithms using active and passive microwave data for ice concentration determination p 43 A87-53241

NASA sea ice and snow validation plan for the Defense Meteorological Satellite Program special sensor microwave/imager [NASA-TM-100683] p 49 N87-30018

**CAVAYAS, F.**

Study on the use of SAR data for agriculture and forestry p 15 N87-27862

**CHAMPION, I.**

Monitoring wheat canopies with a high spectral resolution radiometer p 8 A87-53019

**CHANG, ALFRED T. C.**

Snow load effect on earth's rotation and gravitational field, 1979-1985 p 22 A87-51964

**CHANG, C.**

Extent of saline/waterlogged lands within irrigated Alberta. I - Inventory and preliminary evaluation of existing mapping data p 5 A87-48830

**CHANG, MAO**

Atmospheric effects on Landsat TM thermal IR data p 65 A87-53254

**CHANOND, CHANTANA**

Small format aerial photography for analyzing urban housing problems - A case study in the Bangkok metropolitan region p 17 A87-46309

**CHAO, B. FONG**

Snow load effect on earth's rotation and gravitational field, 1979-1985 p 22 A87-51964

**CHAO, TIEN-HSIN**

Optical image subtraction techniques, 1975-1985 p 55 A87-42659

**CHAPMAN, BRUCE**

Deconvolution of sea state parameters from altimeter waveforms p 41 A87-53198

**CHASE, ROBERT R. P.**

A systems-approach to the design of the Eos data and information system p 64 A87-53207

**CHAUHAN, N. S.**

Polarization utilization in the microwave inversion of leaf angle distributions p 11 A87-53201

**CHEN, C.-C. THOMAS**

Spectral feature design for data compression in high dimensional multispectral data p 64 A87-53183

**CHEN, THOMAS M.**

Information content analysis of Landsat image data for compression p 56 A87-47046

**CHEN, YIN-WU**

Inverse synthetic aperture radar imaging techniques for sea-surface targets p 41 A87-53189

**CHENEY, R. E.**

Oceanographic and geophysical applications of satellite altimetry p 30 A87-46690

**CHENEY, ROBERT E.**

Monitoring equatorial Pacific sea level with Geosat p 39 A87-52512

**CHENG, YAAN**

Spectral characteristics and the extent of paleosols of the Palouse formation [NASA-CR-181208] p 17 N87-28195

**CHERNIAWSKY, J. Y.**

Using NOAA AVHRR in studies of sea ice motion in the Beaufort Sea p 34 A87-48842

**CHHABRA, B. M.**

Observing systems experiments for the onset vortex during Summer Monex p 35 A87-51552

**CHI, CHONG-YUNG**

Wind measurements for non-uniform wind fields from spaceborne scatterometers p 75 A87-53195

A comparative study of several wind estimation algorithms for spaceborne scatterometers p 41 A87-53197

Deconvolution of sea state parameters from altimeter waveforms p 41 A87-53198

**CHIARANTINI, L.**

Aircraft microwave radiometry of land p 13 A87-53269

**CHIZHOV, S. V.**

Investigation of causes of hydrogen sulfide formation in reclaimed water p 14 N87-23136

**CHOTIROS, NICHOLAS P.**

Design study of remote sensing for ocean surface and interior activity [AD-A180578] p 44 N87-25610

**CHOY, LAWRENCE W.**

Comparison of Geosat and ground-truth wind and wave observations - Preliminary results p 35 A87-52509

**CHRISTENSEN, NORMAN C., JR.**

The use of old-field stands of loblolly pine in studies of the potential use of active microwave remote sensors for monitoring forest ecosystems p 11 A87-53153

**CHRISTENSEN, PETER RANDRUP**

Tracking of ice floes p 46 N87-28155

**CHRISTOU, N.**

Processing of Seasat altimetry data on a digital image analysis system p 59 A87-48825

**CHURCHILL, P. N.**

Land use feature detection in SAR images p 67 N87-27863

**CIHLAR, J.**

Interpretation of prairie land cover types from SIR-B data p 7 A87-48888

New system for the ordering, archiving and retrieval of data from earth's resource satellites p 60 A87-48889

The global forest ecosystem as viewed by ERS-1, SIR-C and EOS p 12 A87-53217

**CIMINO, J. B.**

Spaceborne imaging radar on EOS p 63 A87-53148

Synergism requirements and concepts for SAR and HIRIS on EOS p 75 A87-53216

The global forest ecosystem as viewed by ERS-1, SIR-C and EOS p 12 A87-53217

**CIMINO, JOBEA**

The EOS SAR program p 76 A87-53228

**CLARK, DENNIS K.**

Satellite color observations of spring blooming in Bering Sea shelf waters during the ice edge retreat in 1980 p 32 A87-47297

**COHEN, STEVEN C.**

Spaceborne laser ranging from EOS p 22 A87-53146

**COKER, J.**

Sea surface temperatures and the detection of ocean circulation patterns and fronts from AVHRR imagery p 45 N87-28125

**COLEMAN, K.**

Landsat-based wildlife habitat mapping - A study of collaboration between analyst and user p 3 A87-48809

**COMISO, J. C.**

Satellite-derived ice data sets no. 2: Arctic monthly average microwave brightness temperatures and sea ice concentrations, 1973-1976 [NASA-TM-87825] p 50 N87-30021

**CONESE, C.**

Automatic classification of forestal areas by remote sensing techniques p 12 A87-53211

**CONGALTON, RUSSELL**

Development of EOS-aided procedures for the determination of the water balance or hydrologic budget of a large watershed p 53 A87-53215

**CONNORS, KATHRYN F.**

Classification of geomorphic features and landscape stability in northwestern New Mexico using simulated SPOT imagery p 56 A87-46540

**CONRADSEN, KNUT**

Comparison of visual and automated lineament analyses on LANDSAT MSS image from south Greenland p 67 N87-28144

**COOPER, CHARLES M.**

Suspended sediment concentrations estimated from Landsat MSS p 53 A87-53204

**COOPER, PAUL R.**

The automatic generation of digital terrain models from satellite images by stereo p 58 A87-48669

**CORDEY, R. A.**

The comparison of ocean-wave spectra recovered from SIR-B and Seasat observations with simultaneous buoy data p 43 A87-53265

**CORR, D. G.**

A system for knowledge-based segmentation of remotely-sensed images p 11 A87-53136

**COSOLI, P.**

A system for knowledge-based segmentation of remotely-sensed images p 11 A87-53136

**COURTILLOT, VINCENT**

Geoid anomalies across Ascension fracture zone and the cooling of the lithosphere p 21 A87-44352

Seasat altimetry and the South Atlantic geoid. I - Spectral analysis p 21 A87-45743

**COX, STEPHEN K.**

Satellite observations of convection during the summer monsoon of 1979 p 36 A87-51587

**CRACKNELL, A. P.**

On the use of AVHRR channel-3 data for environmental studies p 20 N87-28135

**CROSS, A.**

A system for knowledge-based segmentation of remotely-sensed images p 11 A87-53136

**CROWN, P. H.**

Spectral studies of dryland agricultural salinity in Western Australia p 8 A87-48901

**CUEVAS, J. M.**

ERAFIS: A computer information system for agriculture and forestry in Spain p 16 N87-28140

**CURLANDER, J. C.**

Automated rectification and geocoding of SAR imagery p 63 A87-53143

**CURLANDER, JOHN C.**

Speckle noise reduction of 1-look SAR imagery p 65 A87-53273

**CURREY, B.**

How useful is Landsat monitoring? p 14 A87-54089

**D****D'ENTREMONT, ROBERT P.**

Interpreting meteorological satellite images using a color-composite technique p 62 A87-52795

Improved cloud analysis using visible, near-infrared, infrared, and microwave imagery p 62 A87-53103

**DAIDA, J. M.**

Observing rotation and deformation of sea ice with synthetic aperture radar p 43 A87-53239

**DAMS, R. V.**

Colour infrared aerial photography for herbicide drift damage assessment p 6 A87-48864

MEIS II imagery for environmental stress analysis p 72 A87-48865

Remote sensing as a tool for Alberta Agricultural Wetlands Drainage Inventory p 6 A87-48882

Sulphur dioxide damage assessment using colour infrared aerial photography p 60 A87-48884

**DAVIS, BRUCE E.**

Digital data from shuttle photography: The effects of platform variables p 66 N87-26697

**DAVIS, M. R.**

Using airborne middle-infrared (1.45-2.0 microns) video imagery for distinguishing plant species and soil conditions p 9 A87-53023

**DE BRUM FERREIRA, D.**

The dynamics of the northern border of the Gulf Stream revealed by a Tiros-N AVHRR image from October 22, 1980 p 35 A87-51147

**DE CHATEAU-THIERRY, P.**

Poseidon radar altimeter oceanographic remote sensing p 40 A87-53113

**DEANE, G. C.**

Land use feature detection in SAR images p 67 N87-27863

**DEBEKKERING, J. A.**

Monitoring and modeling of the Adriatic Sea p 46 N87-28133

**DECKER, WAYNE L.**

Smoothing vegetation index profiles - An alternative method for reducing radiometric disturbance in NOAA/AVHRR data p 14 A87-53996

**DEDIEU, JEAN-PIERRE**

Present state, changes, and quality of Sologne and Brenne, two French large wetlands, studied with LANDSAT MSS and TM data p 54 N87-28152

**DEER, D.**

Operational use of remote sensing for commercial Arctic class vessel navigation p 33 A87-48829

- DEFEO, NANCY J.**  
Lithologic discrimination using geobotanical and Landsat TM spectral data p 23 A87-48667
- DEGLORIA, STEPHEN D.**  
Discrimination of natural and cultivated vegetation using Thematic Mapper spectral data p 2 A87-48673
- DEGNAN, JOHN J.**  
Spaceborne laser ranging from EOS p 22 A87-53146
- DELEGIDO, J.**  
A model of thermal inertia for frost forecasting in agricultural areas p 16 N87-28151
- DELFINODAVILAMASCARENHAS, NELSON**  
Brief introduction in statistical pattern recognition [INPE-4206-PRE/1087] p 68 N87-28374
- DEMOURAABDON, MYRIAN**  
Evaluation of the range and degradation of mangroves in Southern Sergipe with remote sensing techniques [INPE-4196-PRE/1080] p 16 N87-28160
- DERENYI, E.**  
Processing of Seasat altimetry data on a digital image analysis system p 59 A87-48825
- DERENYI, E. E.**  
Comparison of classification and enhancement techniques using Landsat imagery for the northern coniferous forest p 4 A87-48821
- DESTIVAL, ISABELLE**  
Automated evaluation of linear networks on SPOT images p 61 A87-51174
- DEWIT, MAARTEN**  
Workshop on The Earth as a Planet [NASA-CR-180543] p 81 N87-29900
- DIGBY-ARGUS, S.**  
The detection of wetlands on radar imagery p 6 A87-48855
- DILLINGER, WILLIAM H.**  
A program for the combined adjustment of VLBI observing sessions p 22 A87-52766
- DINER, D.**  
Synergism requirements and concepts for SAR and HIRIS on EOS p 75 A87-53216
- DINGUIRARD, M.**  
SPOT radiometric resolution performance evaluation - Preliminary results p 57 A87-48661
- DINGUIRARD, M. C.**  
Absolute calibration of the SPOT-1 HRV cameras p 11 A87-48660
- DION, L.**  
A geobotanic approach to the study of the geology of Cape Smith using Landsat-MSS data p 25 A87-48860
- DIRKS, R. W. J.**  
Shallow water bathymetry and bottom classification by means of the Landsat and SPOT optical scanners p 52 A87-48670
- DIXON-GOUGH, ROBERT W.**  
Environmental information and cartography p 20 N87-28141
- DIZENZO, SILVANO**  
Discrimination of natural and cultivated vegetation using Thematic Mapper spectral data p 2 A87-48673
- DOAKE, C. S. M.**  
Glaciological studies on Rutford ice stream, Antarctica p 38 A87-51950
- DOBSON, C.**  
Synergism requirements and concepts for SAR and HIRIS on EOS p 75 A87-53216  
The global forest ecosystem as viewed by ERS-1, SIR-C and EOS p 12 A87-53217
- DOBSON, ELLA**  
Validation of Geosat altimeter-derived wind speeds and significant wave heights using buoy data p 39 A87-52510
- DOBSON, ELLA B.**  
Wind and wave statistics as derived from the Geosat radar altimeter and with comparisons with in situ measurements p 40 A87-53127
- DOBSON, M. C.**  
On the use of AVHRR channel-3 data for environmental studies p 20 N87-28135
- DOHERTY, G. MARK**  
TM sensor performance as obtained from Earthnet quality control data base p 71 A87-48659
- DOMIK, G.**  
Study on the use and characteristics of SAR for geological applications. Part 2: Radargrammetry aspects [ESA-CR(P)-2325-PT-2] p 27 N87-26466
- DONELAN, MARK A.**  
Radar scattering and equilibrium ranges in wind-generated waves with application to scatterometry p 28 A87-42746
- DONOHUE, MARTIN J.**  
Earth resources instrumentation for the Space Station Polar Platform p 69 A87-44184

- DONZELI, PEDRO LUIZ**  
Evaluation of MOMS (Modular Optoelectronic Multispectral Scanner) data for land use/land cover studies - Test site: Piracicaba region, Sao Paulo State, Brazil p 13 A87-53252
- DOUGLAS, B. C.**  
Oceanographic and geophysical applications of satellite altimetry p 30 A87-46690
- DOUGLAS, BRUCE C.**  
Monitoring equatorial Pacific sea level with Geosat p 39 A87-52512
- DOWNNEY, I. D.**  
Sea surface temperatures and the detection of ocean circulation patterns and fronts from AVHRR imagery p 45 N87-28125
- DREINI, GIANCARLO**  
Wave-theory modelling of convergence zone propagation in the ocean [AD-A183607] p 50 N87-30020
- DUCHER, GUY**  
Photogrammetry - The largest operational application of remote sensing p 70 A87-47174
- DUGUAY, C.**  
Radiation modelling in a high relief environment using a digital terrain model and Landsat - TM imagery p 59 A87-48857
- DUMONT, J. P.**  
Poseidon radar altimeter description and signal processing p 40 A87-53114
- DUMOULIN, G.**  
Effects of surface geometry of agricultural fields on radar airborne imagery in X- and C-bands p 5 A87-48846
- DUNFORD, CHRISTOPHER**  
Sampling semiarid vegetation with large-scale aerial photography p 14 A87-53741
- DUPONT, O.**  
Effectiveness of the Thematic Mapper for the range condition assessment in fescue grasslands of Southwestern Alberta p 6 A87-48850  
Landsat Thematic Mapper data - A useful tool for mapping agricultural areas in Quebec p 6 A87-48867
- DURAND, J. M.**  
Theoretical feasibility of SAR interferometry p 77 A87-53283
- DUSSEAU, M. B.**  
Evaluation of MEIS-II multispectral scanner data for quaternary geological mapping in the Chatham area, southwestern Ontario p 24 A87-48816

## E

- EBERT, ELIZABETH**  
A pattern analysis technique for distinguishing surface and cloud types in the polar regions p 66 A87-53289
- EBY, J. R.**  
The role of Landsat multi-spectral scanner data in the analysis of northern spotted owl habitat p 7 A87-48894
- EDMONDS, W.**  
Data analysis and software support for the Earth radiation budget experiment [NASA-CR-178350] p 66 N87-26569
- EERENS, H.**  
Crop inventorying of small-parcelled areas using SPOT- and TM-data in conjunction with field radiometric measurements p 10 A87-53126
- EGLME, M.**  
European dissemination of Marine Observation Satellite (MOS-1) data p 44 A87-53925
- EGOROV, V. V.**  
Features of a statistical model for the interaction between electromagnetic waves and remotely sensed natural objects p 70 A87-48189
- EICHENHERR, H.**  
Investigation of design parameters for ERS-1 wind scatterometer p 74 A87-53116
- EL-MOSSELY, E.**  
Remote sensing of deep potential sources over the Nile Delta area p 26 A87-53150
- EL-RAEY, M.**  
Remote sensing of deep potential sources over the Nile Delta area p 26 A87-53150
- EL-SAHARTY, A.**  
Remote sensing of deep potential sources over the Nile Delta area p 26 A87-53150
- ELACHI, C.**  
Global digital topography mapping using a scanning radar altimeter p 76 A87-53227
- ELACHI, CHARLES**  
Multifrequency and multipolarization radar scatterometry of sand dunes and comparison with spaceborne and airborne radar images p 70 A87-47257  
Spaceborne imaging radar on EOS p 63 A87-53148

- ELDHUSE, K.**  
SAR detection of ships and ship wakes p 66 N87-27859
- ELLIS, T. J.**  
Landsat-based wildlife habitat mapping - A study of collaboration between analyst and user p 3 A87-48809
- ENGEL, JACK**  
The Land Satellite (Landsat) system - Earth Observation Satellite Company (Eosat's) plans for Landsat-6 and beyond p 71 A87-48876
- ENGMAN, E. T.**  
Roughness measurements with multipolarization aircraft data p 63 A87-53131
- EPP, D. W.**  
Barriers to the operational use of satellite remote sensing in Canada p 72 A87-48835
- ESCOBAR, D. E.**  
Using airborne middle-infrared (1.45-2.0 microns) video imagery for distinguishing plant species and soil conditions p 9 A87-53023
- ESPINDOLA, CARMEN REGINA S.**  
Evaluation of the range and degradation of mangroves in Southern Sergipe with remote sensing techniques [INPE-4196-PRE/1080] p 16 N87-28160
- EVANS, D.**  
Discrimination of suspended sediment and littoral features using multispectral video imagery p 73 A87-48874
- EVANS, D. J.**  
Multispectral video system for airborne remote sensing - Sensitivity, calibrations and correction p 73 A87-48873
- EVANS, R.**  
Land use feature detection in SAR images p 67 N87-27863  
Study of physical processes on the US mid-Atlantic continental slope and rise. Volume 1: Executive summary [PB87-200515] p 48 N87-30012  
Study of physical processes on the US mid-Atlantic continental slope and rise. Volume 2: Technical presentation [PB87-200523] p 49 N87-30013  
Study of physical processes on the US mid-Atlantic continental slope and rise. Volume 3: Appendix [PB87-200531] p 49 N87-30014
- EVANS, ROBERT H.**  
Multiplatform sampling (ship, aircraft, and satellite) of a Gulf Stream warm core ring p 29 A87-44811
- EVERETT, JOHN R.**  
Evaluation of Landsat Thematic Mapper - Imagery for geological exploration p 23 A87-48666
- EVERITT, J. H.**  
Using airborne middle-infrared (1.45-2.0 microns) video imagery for distinguishing plant species and soil conditions p 9 A87-53023
- EYRE, J. R.**  
The variability of the North Atlantic marine atmosphere and its relevance to remote sensing p 33 A87-48362

## F

- FABBRI, A. G.**  
A structural analysis of the Mabou Basin, Cape Breton Island using enhanced Landsat MSS imagery p 25 A87-48879
- FABRIZIO, RALPH**  
A high speed digital processor for real-time synthetic aperture radar imaging p 64 A87-53233
- FALKINGHAM, J. C.**  
The operational use of RADARSAT products by the ice centre environment Canada p 61 A87-48906
- FARR, TOM G.**  
Science synergism study for EOS on evolution of desert surfaces p 12 A87-53214
- FELDE, GERALD W.**  
Improved cloud analysis using visible, near-infrared, infrared, and microwave imagery p 62 A87-53103
- FERNER, SAINT**  
Snowpack depletion monitoring in Alberta using computer-processed NOAA imagery p 52 A87-48848
- FERRAZZOLI, P.**  
Aircraft microwave radiometry of land p 13 A87-53269
- FIGUEROA, HORACIO A.**  
Some aspects of the surface circulation south of 20 deg S revealed by First GARP Global Experiment drifters p 28 A87-42748
- FILATOV, N. N.**  
Features of the water dynamics of Lake Ladoga according to remote sensing data p 50 A87-44296
- FILLON, M.**  
Application of image segmentation algorithms to the inventory of crops in Canada p 3 A87-48813

- FINK, JONATHAN H.**  
Rheology of the 1983 Royal Gardens basalt flows, Kilauea Volcano, Hawaii p 26 A87-51725
- FISCELLA, B.**  
Climatological implications of a satellite-borne SAR imaging the sea surface p 30 A87-46403
- FISCHER, JAMES C.**  
Planning for future operational sensors and other priorities [NOAA-NESDIS-30] p 77 N87-25560
- FISHER, P. F.**  
Towards the automatic recognition and vectorised description of linear features in LANDSAT TM images by artificial intelligence methods p 67 N87-28142
- FITZE, L. J. D.**  
Colour infrared aerial photography for herbicide drift damage assessment p 6 A87-48864
- FLEMER, D. A.**  
Characterizing the Chesapeake Bay ecosystem and lessons learned [PB87-166930] p 19 N87-26463
- FLORES, ALBERTO L.**  
Estimation of surface moisture availability from remote temperature measurements p 53 A87-54155
- FOLVING, S.**  
Mapping of vegetation types in SW Greenland p 16 N87-28149  
Studies of tidal flat environments with LANDSAT MSS data p 47 N87-28157
- FORD, J.**  
The global forest ecosystem as viewed by ERS-1, SIR-C and EOS p 12 A87-53217
- FOSTER, JAMES L.**  
Snow load effect on earth's rotation and gravitational field, 1979-1985 p 22 A87-51964
- FRASER, A. S.**  
How useful is Landsat monitoring? p 14 A87-54089
- FRAYSSE, G.**  
The European Campaign 'AGRISAR '86' p 13 A87-53249
- FRAZIER, B. E.**  
Spectral characteristics and the extent of paleosols of the Palouse formation [NASA-CR-181208] p 17 N87-28195
- FREEMAN, N. G.**  
Airborne SAR imaging of azimuthally travelling ocean surface waves - The LEWEX experimental plan p 44 A87-53266
- FREI, U.**  
A contribution to the optimum selection of ground control points in high resolution images p 57 A87-48658
- FRIEDMANN, DANIEL E.**  
The automatic generation of digital terrain models from satellite images by stereo p 58 A87-48669
- FROLICH, R. M.**  
Glaciological studies on Rutford ice stream, Antarctica p 38 A87-51950
- FROUIN, ROBERT**  
Calibration of NOAA-7 AVHRR, GOES-5, and GOES-6 VISSR/VAS solar channels p 69 A87-44865
- FRYE, DANIEL E.**  
Data telemetry, assimilation and ocean modeling [AD-A181899] p 47 N87-28239
- FURSOV, M. K.**  
Determination of the external-orientation elements of aerial and space photographs p 55 A87-44301
- FUSCO, L.**  
A contribution to the optimum selection of ground control points in high resolution images p 57 A87-48658  
Different scanning instruments comparison - MOMS and TM p 71 A87-48675  
European dissemination of Marine Observation Satellite (MOS-1) data p 44 A87-53925
- G**
- GALLIDEPARATESI, S. R.**  
The role and perspective of remote sensing for disaster management in the European community p 20 N87-28137
- GANDIA, S.**  
A model of thermal inertia for frost forecasting in agricultural areas p 16 N87-28151
- GARCIAFONSECA, LEILA MARIA**  
Determination of transfer functions from the Thematic Mapper (TM) sensor of the LANDSAT-5 satellite [INPE-4213-PRE/1094] p 79 N87-28956
- GARDELLE, JP.**  
SPOT localization accuracy and geometric image quality p 57 A87-48662
- GARDNER, J.**  
Indices of climatological and hydrological variability derived from satellite imagery for the South Saskatchewan River Basin p 52 A87-48856
- GARDNER, THOMAS W.**  
Classification of geomorphic features and landscape stability in northwestern New Mexico using simulated SPOT imagery p 56 A87-46540
- GARLAND, G.**  
Hydrologic applications of weather radar data p 52 A87-48875
- GASPERINI, PAOLO**  
Azimuthal dependence in the gravity field induced by recent and past cryospheric forcings p 35 A87-51487
- GATES, D.**  
Synergism requirements and concepts for SAR and HIRIS on EOS p 75 A87-53216  
The global forest ecosystem as viewed by ERS-1, SIR-C and EOS p 12 A87-53217
- GAUTIER, CATHERINE**  
Calibration of NOAA-7 AVHRR, GOES-5, and GOES-6 VISSR/VAS solar channels p 69 A87-44865
- GAVRILENKO, A. S.**  
Radar observations of terrestrial vegetation covers in the 3-cm range p 1 A87-42936
- GENDLER, V. E.**  
Stereoscopic visualization of aerial and space photographs in thematic mapping p 23 A87-42937
- GEORGE, H.**  
Evaluation of MEIS-II multispectral scanner data for quaternary geological mapping in the Chatham area, southwestern Ontario p 24 A87-48816
- GETULIOMVIEIRA, ERNESTO**  
Evaluation of the range and degradation of mangroves in Southern Sergipe with remote sensing techniques [INPE-4196-PRE/1080] p 16 N87-28160
- GHIN, A. M.**  
Remote sensing techniques for the study of hydrological elements p 51 A87-47576
- GIBERT, DOMINIQUE**  
Geoid anomalies across Ascension fracture zone and the cooling of the lithosphere p 21 A87-44352  
Seasat altimetry and the South Atlantic geoid. I - Spectral analysis p 21 A87-45743
- GILL, STEVE**  
Spectral characteristics and the extent of paleosols of the Palouse formation [NASA-CR-181208] p 17 N87-28195
- GILLESPIE, ALAN R.**  
Color enhancement of highly correlated images. II - Channel ratio and 'chromaticity' transformation techniques p 62 A87-53018
- GLAZMAN, ROMAN E.**  
The effects of wind-wave coupling on scatterometer wind measurement accuracy p 41 A87-53196
- GLOERSEN, P.**  
Variations of mesoscale and large-scale sea ice morphology in the 1984 Marginal Ice Zone Experiment as observed by microwave remote sensing p 31 A87-47292  
Multisensor comparison of ice concentration estimates in the marginal ice zone p 31 A87-47295
- GLUSHKO, E. V.**  
A study of modern landscape formation in Lower Mesopotamia from space photographs p 55 A87-42935
- GOEL, N.**  
Synergism requirements and concepts for SAR and HIRIS on EOS p 75 A87-53216
- GOETZ, ALEXANDER F. H.**  
The high resolution imaging spectrometer (HIRIS) for EOS p 74 A87-53145
- GOETZ, SCOTT J.**  
Landscape pattern and successional dynamics in the boreal forest p 11 A87-53155
- GOLDBERG, M.**  
Application of image segmentation algorithms to the inventory of crops in Canada p 3 A87-48813
- GOLDBERG, MORRIS**  
An expert system for remote sensing p 80 A87-43260
- GOLDHIRSH, JULIUS**  
Validation of Geosat altimeter-derived wind speeds and significant wave heights using buoy data p 39 A87-52510
- GOLDSTEIN, R. M.**  
Interferometric radar measurement of ocean surface currents p 44 A87-54107
- GOMBEER, R.**  
Crop inventorying of small-parcelled areas using SPOT- and TM-data in conjunction with field radiometric measurements p 10 A87-53126
- GONZALEZ-ALONSO, F.**  
ERAFIS: A computer information system for agriculture and forestry in Spain p 16 N87-28140
- GOODENOUGH, DAVID G.**  
An expert system for remote sensing p 80 A87-43260  
The CCRS SAR/MSS Anderson River data set p 55 A87-43261
- GOOSSENS, R.**  
A multi-source image set for the study of soil texture and drainage as observed from Thematic Mapper data in Northern Belgium p 10 A87-53125  
The detection of soil drainage by using Landsat MSS and TM (Belgian test zones) p 11 A87-53205  
Detection of soil drainage in Pays de Herve, Belgium, on LANDSAT MSS imagery p 15 N87-28129
- GORBUSHINA, E. A.**  
Multistage principal-components analysis of correlations p 56 A87-48193
- GORDON, HOWARD R.**  
Calibration requirements and methodology for remote sensors viewing the ocean in the visible p 29 A87-44866
- GORMAN, R. W.**  
Operational use of remote sensing for commercial Arctic class vessel navigation p 33 A87-48829
- GOSSSELIN, C.**  
Multiple-look effects on SAR classification accuracies p 60 A87-48885  
Study on the use of SAR data for agriculture and forestry p 15 N87-27862
- GOUGEON, F. A.**  
Spectral and textural segmentation of multispectral aerial images p 5 A87-48831
- GOULD, G. J.**  
Proceedings of Atlantic Outer Continental Shelf Region Information Transfer Meeting (ITM) (2nd), January 28-29, 1987 p 48 N87-30009  
Proceedings of Atlantic Outer Continental Shelf Region Information Transfer Meeting (ITM) (1st), September 4-6, 1985 p 48 N87-30011
- GOWER, J. F. R.**  
Using NOAA AVHRR in studies of sea ice motion in the Beaufort Sea p 34 A87-48842  
Analysis of data from the DFO fluorescence line imager p 72 A87-48844
- GOZEBERTIN, B.**  
Study on the use of SAR data for agriculture and forestry p 15 N87-27862
- GRAHAM, D. F.**  
Shuttle imaging Radar-A (SIR-A) scenes from Iran and China p 25 A87-48854
- GRAVES, MARK R.**  
Atmospheric effects on Landsat TM thermal IR data p 65 A87-53254
- GREENBAUM, D.**  
Lithological discrimination in central Snowdonia using airborne multispectral scanner imagery p 23 A87-48358
- GREKU, R. KH.**  
Major morphologic features of the Atlantic Ocean surface p 48 N87-29573
- GRENFELL, T. C.**  
Evolution of microwave sea ice signatures during early summer and midsummer in the marginal ice zone p 31 A87-47293
- GRIFFITH, CECILIA GIRZ**  
Comparisons of gauge and satellite rain estimates for the central United States during August 1979 p 53 A87-54152
- GRIFFITHS, H. D.**  
A study of antenna signal processing techniques for radar alternatives [ESA-CR(P)-2370] p 79 N87-28809
- GROSS, M. F.**  
Remote sensing of coastal wetlands p 1 A87-40944
- GROSSMAN, ROBERT L.**  
Large scale ocean-atmosphere interaction in the summer monsoon - The influence of oceanic upwelling and advection on eastern Arabian Sea offshore convection p 36 A87-51585
- GRUEN, A.**  
Point positioning and mapping with large format camera data p 73 A87-50226
- GRUNBLATT, JESS**  
An MTF analysis of Landsat classification error at field boundaries p 56 A87-46745
- GRUNES, MITCHELL R.**  
Comparison of Geosat and ground-truth wind and wave observations - Preliminary results p 38 A87-52509
- GUDMANDSEN, P.**  
Active microwave observations of sea ice and icebergs p 45 N87-27855
- GUENTHER, B.**  
Practical aspects of achieving accurate radiometric field measurements p 69 A87-44868
- GUERTIN, F.**  
New system for the ordering, archiving and retrieval of data from earth's resource satellites p 60 A87-48889

## GUEST, P. S.

- Variations of mesoscale and large-scale sea ice morphology in the 1984 Marginal Ice Zone Experiment as observed by microwave remote sensing p 31 A87-47292

## GUILLEMOT, J.

- Geomorphological interpretation of the SPOT image of February 23, 1986 concerning Djebel Amour (Algeria) and its border with the Sahara p 25 A87-51145

## GUINDON, B.

- Evaluation of algorithms for the geometric correction of Thematic Mapper data p 58 A87-48807  
Application of accuracy assessment techniques to image classification p 58 A87-48808

## GUINDON, BERT

- The CCRS SAR/MSS Anderson River data set p 55 A87-43261

## GULINCK, H.

- Remote sensing and landscape approaches to earth resources p 63 A87-53154

## GUTMAN, G.

- Cloud screening for determination of land surface characteristics in a reduced resolution satellite data set p 56 A87-48361

## GUY, M.

- Contribution of improved resolution to morphological analysis - The example of the Rhone delta p 25 A87-51144

## GUYENNE, T. D.

- Proceedings of the SAR Applications Workshop [ESA-SP-264] p 78 A87-27854

## GUYMER, T. H.

- The determination of sea-state bias and non-linear wave parameters from satellite altimeter data p 46 A87-28132

## GUYOT, G.

- Monitoring wheat canopies with a high spectral resolution radiometer p 8 A87-53019

## GUYOT, LIONEL

- Visual interpretation of Landsat MSS quick-look images for the study of the annual swelling of the Niger river in its interior delta, in Mali p 50 A87-44245

## GUZZI, RODOLFO

- Atmospheric correction of data measured by a flying platform over the sea - Elements of a model and its experimental validation p 35 A87-50292

## GWYN, Q. H. J.

- Effects of surface geometry of agricultural fields on radar airborne imagery in X- and C-bands p 5 A87-48846  
Radiometric corrections of topographic effects for simulated RADARSAT imagery in a region of moderate relief p 59 A87-48847

## GYAN, P. A.

- Multistage remote sensing with grade four students p 80 A87-48810

## H

## HAIMBACH, STEPHEN P.

- An operational multispectral scanner for bathymetric surveys - The ABS NORDA scanner p 42 A87-53199

## HAJA, S. R.

- A revolution in the production of small-scale and medium-scale maps p 61 A87-48904

## HALL, DOROTHY K.

- Snow load effect on earth's rotation and gravitational field, 1979-1985 p 22 A87-51964

## HALL, FORREST G.

- Landscape pattern and successional dynamics in the boreal forest p 11 A87-53155  
The First ISLSCP Field Experiment (FIFE) p 12 A87-53218

## HALL, J.

- Geological interpretations from Landsat of the Troodos Massive, Cyprus p 25 A87-48862

## HALL, R. J.

- Large-scale black and white and natural color photographs for the measurement of tree crown areas p 3 A87-48815

## HALLIKAINEN, M.

- Satellite microwave radiometry of snow water equivalent p 52 A87-48823

## HALLIKAINEN, MARTTI

- Satellite microwave radiometry of forest and surface types p 9 A87-53120  
Monitoring of snow cover from satellite p 54 A87-28123

## HALLOCK, ZACHARIAH R.

- REX and Geosat - Progress in the first year p 39 A87-52511

## HAMILTON, P.

- Study of physical processes on the US mid-Atlantic continental slope and rise. Volume 1: Executive summary [PB87-200515] p 48 A87-30012

- Study of physical processes on the US mid-Atlantic continental slope and rise. Volume 2: Technical presentation [PB87-200523] p 49 A87-30013

- Study of physical processes on the US mid-Atlantic continental slope and rise. Volume 3: Appendix [PB87-200531] p 49 A87-30014

## HANCOCK, D. W., III

- Observations of and a new model for fetch-limited wave growth p 43 A87-53263

## HANCOCK, DAVID W., III

- Waveform analysis for Geosat day 96 p 39 A87-52514

## HANSON, HOWARD P.

- Response of marine atmospheric boundary layer height to sea surface temperature changes - Mixed-layer theory p 34 A87-50277

## HANZLICK, D. J.

- Interpolation, analysis and archival of data on sea ice trajectories and ocean currents obtained from satellite-linked instruments [PB87-201430] p 48 A87-30010

## HARDISKY, M. A.

- Remote sensing of coastal wetlands p 1 A87-40944

## HARDY, JOHN R.

- Geometric quality of Thematic Mapper data of the United Kingdom p 57 A87-48655

## HARE, E. W.

- Preliminary results from modelling vegetation spectra derived from MEIS data, Algonquin Park, Ontario p 7 A87-48891

## HARIS, J.

- The detection of wetlands on radar imagery p 6 A87-48855

## HARKER, D. B.

- Extent of saline/waterlogged lands within irrigated Alberta. I - Inventory and preliminary evaluation of existing mapping data p 5 A87-48830

## HARRIS, J.

- Shuttle imaging Radar-A (SIR-A) scenes from Iran and China p 25 A87-48854

## HART, JUDY

- Spectral characteristics and the extent of paleosols of the Palouse formation [NASA-CR-181208] p 17 A87-28195

## HATTA, SHIN-ICHIRO

- Meissner effect in high-Tc superconductive thin films p 35 A87-51532

## HAUCK, MARTIN

- Evaluation of MOMS (Modular Optoelectronic Multispectral Scanner) data for land use/land cover studies - Test site: Piracicaba region, Sao Paulo State, Brazil p 13 A87-53252

## HAYDN, R.

- Significance of TM data as a tool to support regional planning activities p 17 A87-48671  
Monitoring and inventoring of forest damages by use of LANDSAT TM data p 16 A87-28138

## HAYNE, GEORGE S.

- Waveform analysis for Geosat day 96 p 39 A87-52514

## HECKER, F.

- Extent of saline/waterlogged lands within irrigated Alberta. I - Inventory and preliminary evaluation of existing mapping data p 5 A87-48830

## HEDERVARI, P.

- Catalog of submarine volcanoes and hydrological phenomena associated with volcanic events, January 1, 1900 to December 31, 1959 [PB87-183943] p 54 A87-28196

## HEER, C.

- Performance sensitivity for X-SAR p 76 A87-53223

## HEGYI, F.

- Applications of satellite derived digital elevation models for resource mapping p 60 A87-48866

## HELMS, JOHN

- Development of EOS-aided procedures for the determination of the water balance or hydrologic budget of a large watershed p 53 A87-53215

## HENDRY, A.

- Land use feature detection in SAR images p 67 A87-27863

## HENNING, DETLEF

- Matching instrument design and signal processing for a scanning radiometer p 76 A87-53251

## HERRING, MARK

- The high resolution imaging spectrometer (HIRIS) for EOS p 74 A87-53145

## HESANY, VAHID

- Modulation transfer function of radar return power from the ocean p 42 A87-53219

## HEWITT, M. J., III

- The role of Landsat multi-spectral scanner data in the analysis of northern spotted owl habitat p 7 A87-48894

## HEYLER, GENE A.

- Design of Geosat Exact Repeat Mission p 39 A87-52515

## HICK, P. T.

- Spectral studies of dryland agricultural salinity in Western Australia p 8 A87-48901

## HICKMAN, G. DANIEL

- An operational pre-mission scanner for bathymetric surveys - The ABS NORDA scanner p 42 A87-53199

## HIGASHINO, HIDETAKA

- Meissner effect in high-Tc superconductive thin films p 35 A87-51532

## HILL, GREG J. E.

- Updating maps of climax vegetation cover with Landsat MSS data in Queensland, Australia p 2 A87-46744

## HILL, JOACHIM

- Cluster based segmentation of multi-temporal Thematic Mapper data as preparation of region-based agricultural land-cover analysis p 9 A87-53109

- Rural land use inventory and mapping in the Ardeche area (France). Improvement of automatic classification by multitemporal analysis of TM data p 15 A87-28127

## HILTON, J. E.

- Use of Thematic Mapper satellite images for disturbance updating of timber/range maps p 4 A87-48822

## HINES, D. E.

- Observations of and a new model for fetch-limited wave growth p 43 A87-53263

## HINSE, M.

- Radiometric corrections of topographic effects for simulated RADARSAT imagery in a region of moderate relief p 59 A87-48847

## HODGES, CARL N.

- The closed ecology project - Agricultural and life sciences background [AAS PAPER 86-120] p 9 A87-53093

## HODGSON, M. E.

- Color infrared video mapping of upland and wetland communities [DE87-010202] p 15 A87-28109

## HOFFMAN, LAWRENCE H.

- Calculation and accuracy of ERBE scanner measurement locations [NASA-TP-2670] p 47 A87-28471

## HOGE, FRANK E.

- Multiplatform sampling (ship, aircraft, and satellite) of a Gulf Stream warm core ring p 29 A87-44811  
Radiance-ratio algorithm wavelengths for remote oceanic chlorophyll determination p 29 A87-44812

## HOGG, D. C.

- A system for knowledge-based segmentation of remotely-sensed images p 11 A87-53136

## HOLM, R. G.

- Reflectance- and radiance-based methods for the in-flight absolute calibration of multispectral sensors p 69 A87-44863

## HOLT, BENJAMIN

- Beaufort-Chukchi ice margin data from Seasat - Ice motion p 32 A87-47299  
Shuttle Imaging Radar B (SIR-B) Weddell Sea ice observations - A comparison of SIR-B and scanning multichannel microwave radiometer ice concentrations p 32 A87-47300

## HOLT, TEDDY

- A comparison of the significant features of the marine boundary layers over the Arabian Sea and the Bay of Bengal during Monex 79 p 36 A87-51594

## HOOD, D. W.

- Gulf of Alaska: Physical environment and biological resources [PB87-103230] p 47 A87-29033

## HORNSBY, J.

- Geological interpretations from Landsat of the Troodos Massive, Cyprus p 25 A87-48862

## HORNSBY, J. K.

- Regional geobotany with TM - A Sudbury case study p 25 A87-48861

## HOSGOOD, B.

- Measurement of spectral signatures in Less Favored Areas (LFA): A contribution to the definition of a remote sensing multitemporal experiment p 20 A87-28145

## HOUNAM, DAVID

- Derivation of the technical specification of the ERS-1 active microwave instrument to meet the SAR-image quality requirements p 77 A87-53280

## HOWARTH, P.

- Indices of climatological and hydrological variability derived from satellite imagery for the South Saskatchewan River Basin p 52 A87-48856

## HOWARTH, P. J.

- A methodology for automated extraction of drainage networks from satellite imagery p 53 A87-48880

## HSU, A.

- Different scanning instruments comparison - MOMS and TM p 71 A87-48675

- Hsu, L. C.**  
Application of TM imagery to mapping volcanic rock assemblages at tertiary calderas of the basin and range province p 26 A87-53257
- HUEHNERFUSS, HEINRICH**  
Radar signatures of oil films floating on the sea surface p 41 A87-53192
- HUH, O. K.**  
Agricultural, hydrologic and oceanographic studies in Bangladesh with NOAA AVHRR data p 57 A87-48365
- HUH, OSCAR K.**  
Satellite observations of surface temperatures and flow patterns, Sea of Japan and East China Sea, late March 1979 p 40 A87-53020
- HUNT, E. RAYMOND, JR.**  
Measurement of leaf relative water content by infrared reflectance p 9 A87-53024
- HUNT, J. J.**  
Proceedings of the SAR Applications Workshop [ESA-SP-264] p 78 A87-27854
- HUTTON, C. A.**  
Comparison of space and airborne L-HH radar imagery in an agricultural environment p 4 A87-48819
- I**
- IAROSLAVSKII, L. P.**  
Stereoscopic visualization of aerial and space photographs in thematic mapping p 23 A87-42937
- IASINSKII, S. V.**  
Parameterization of models of runoff formation in simple catchment areas using remote-sensing data p 51 A87-47579
- IBBOTT, ANTHONY C.**  
Millimeter-wave imaging sensor data evaluation [NASA-CR-181159] p 77 A87-26264
- IL'IN, V. A.**  
Stereoscopic visualization of aerial and space photographs in thematic mapping p 23 A87-42937
- IL'INA, ELENA BORISOVNA**  
Remote-sensing and geological-geophysical studies of closed platform territories p 26 A87-51875
- IM, K. E.**  
Global digital topography mapping using a scanning radar altimeter p 76 A87-53227
- IMAIZUMI, SHIGEYOSHI**  
Analysis of environmental information of urban areas using Landsat TM data p 19 A87-53187
- IMHOFF, M.**  
The global forest ecosystem as viewed by ERS-1, SIR-C and EOS p 12 A87-53217
- IOKICH, D. R.**  
Remote-sensing evaluation of moisture supply to crops according to the leaf-surface thermal regime p 2 A87-47582
- IRONS, JAMES R.**  
Multiple-angle observations of reflectance anisotropy from an airborne linear array sensor p 69 A87-43262
- ISHIHARA, OSAMU**  
Analysis of environmental information of urban areas using Landsat TM data p 19 A87-53187
- ITTEN, K. I.**  
Hierarchical classification with knowledge based binary decision p 62 A87-53110
- IZRAELI, I. A.**  
Monitoring the background pollution of natural environments, No. 3 p 19 A87-52241
- J**
- JACKSON, FREDERICK C.**  
The response of SAR imagery to azimuth travelling ocean surface waves as determined from shuttle SAR imagery p 44 A87-53286
- JACKSON, G.**  
Remote sensing and the agricultural resource inventory p 8 A87-48899
- JACKSON, R. D.**  
Reflectance- and radiance-based methods for the in-flight absolute calibration of multispectral sensors p 69 A87-44863  
Absolute calibration of the SPOT-1 HRV cameras p 71 A87-48660
- JACOBSON, J. E.**  
Inventory of wetlands with Landsat's Thematic Mapper p 3 A87-48817
- JADHAV, D. B.**  
Remote sensing by the fluorescence property of the scatterer p 75 A87-53179
- JANSSSEN, D. R.**  
Summary of recent SAR instrument studies p 78 A87-27865
- JANSSSENS, P.**  
Remote sensing and landscape approaches to earth resources p 63 A87-53154
- JAQUES, BOB**  
SPOT's first year p 80 A87-51320
- JASKOLLA, F.**  
Requirements on radar data for geological application: A case study by use of multistage data of the test site Sardegna/Italy p 27 A87-28120  
The impact of LANDSAT Thematic Mapper Data for ecological mapping purposes. A case study at the northern margin of the Alps p 20 A87-28147
- JAYLES, C.**  
Precise orbit determination with the Doppler Orbitography and Radio positioning Integrated by Satellite (DORIS) system and the associated Zealous for Orbit Observation Methods (ZOOM) software p 77 A87-25382
- JEFFERIES, W. C.**  
Digital SAR-Landsat combination for geologic mapping p 24 A87-48853
- JEKELI, CHRISTOPHER**  
New instrumentation techniques in geodesy p 22 A87-46692
- JENSEN, FINN B.**  
Wave-theory modelling of convergence zone propagation in the ocean [AD-A183607] p 50 A87-30020
- JENSEN, J. R.**  
Color infrared video mapping of upland and wetland communities [DE87-010202] p 15 A87-28109
- JENSEN, JOHN SKELMOSE**  
Cloud detection in NOAA images p 67 A87-28124
- JHA, A. M.**  
A spaceborne LFM scatterometer for ocean surface wind vector measurement - A time domain approach p 40 A87-53119
- JOHANNESSEN, J. A.**  
Mesoscale eddies in the Fram Strait marginal ice zone during the 1983 and 1984 Marginal Zone Experiments p 31 A87-47291
- JOHANNESSEN, O. M.**  
Mesoscale eddies in the Fram Strait marginal ice zone during the 1983 and 1984 Marginal Zone Experiments p 31 A87-47291  
Variations of mesoscale and large-scale sea ice morphology in the 1984 Marginal Ice Zone Experiment as observed by microwave remote sensing p 31 A87-47292
- JOHNSON, BERTRAND L., JR.**  
Multiple-angle observations of reflectance anisotropy from an airborne linear array sensor p 69 A87-43262
- JOLMA, P.**  
Satellite microwave radiometry of snow water equivalent p 52 A87-48823
- JOLMA, PETRI**  
Satellite microwave radiometry of forest and surface types p 9 A87-53120  
Monitoring of snow cover from satellite p 54 A87-28123
- JOLY, F.**  
Geomorphological interpretation of the SPOT image of February 23, 1986 concerning Djebel Amour (Algeria) and its border with the Sahara p 25 A87-51145
- JOSBERGER, E. G.**  
Variations of mesoscale and large-scale sea ice morphology in the 1984 Marginal Ice Zone Experiment as observed by microwave remote sensing p 31 A87-47292
- JOY, RICHARD T.**  
An operational multispectral scanner for bathymetric surveys - The ABS NORDA scanner p 42 A87-53199
- K**
- KAHLE, ANNE B.**  
Color enhancement of highly correlated images. II - Channel ratio and 'chromaticity' transformation techniques p 62 A87-53018
- KALICHARRAN, K. D.**  
Analysis of airborne infrared data for interpretative geological mapping of the Brookfield area, Nova Scotia p 24 A87-48804  
Application of remote sensing data to bedrock geological interpretation, Black River-Matheson area, Northern Ontario, Canada p 24 A87-48832
- KALMYKOV, A. I.**  
Radar observations of terrestrial vegetation covers in the 3-cm range p 1 A87-42936
- KALUGIN, V. V.**  
Studies of the wavelike process in the surface temperature field of the equatorial Pacific using Meteor-satellite IR measurements p 28 A87-42931
- KANEMASU, E. T.**  
Airborne multispectral observations over burned and unburned prairies p 10 A87-53122
- KANN, D. M.**  
Latent heat and cyclone activity in the South Pacific, 10-18 January 1979 p 37 A87-51603
- KAPRALOV, YE. G.**  
Morphometric studies of world ocean p 45 A87-28077
- KARASEV, A. G.**  
Measurement of currents according to the drift of subsatellite buoys p 32 A87-48177
- KASISCHKE, E. S.**  
Calibrated L-band terrain measurements and analysis program [AD-A182917] p 68 A87-29722
- KASISCHKE, ERIC S.**  
The use of old-field stands of loblolly pine in studies of the potential use of active microwave remote sensors for monitoring forest ecosystems p 11 A87-53153  
Statistical modeling of intensity distributions on airborne SAR imagery p 65 A87-53262
- KATS, IAKOV GIRSHEVICH**  
Elements of lineament tectonics p 27 A87-53954
- KAUFFMAN, DAVID S.**  
Digital elevation model extraction from stereo satellite images p 63 A87-53142
- KAUFMAN, YORAM J.**  
The effect of subpixel clouds on remote sensing p 2 A87-48360
- KAUFMANN, H.**  
Urban development planning using thematic mapper data of Munich (FRG) p 20 A87-28117  
Monitoring and inventoring of forest damages by use of LANDSAT TM data p 16 A87-28138
- KELLER, M. R.**  
Multisensor comparison of ice concentration estimates in the marginal ice zone p 31 A87-47295
- KELLOGG, DAVIDA E.**  
Recent glacial history and rapid ice stream retreat in the Amundsen Sea p 37 A87-51944
- KELLOGG, THOMAS B.**  
Recent glacial history and rapid ice stream retreat in the Amundsen Sea p 37 A87-51944
- KELLY, GAIL D.**  
Updating maps of climax vegetation cover with Landsat MSS data in Queensland, Australia p 2 A87-46744
- KENCHINGTON, R. A.**  
Managing coral reefs - Operational benefits of remote sensing in Marine Park planning p 34 A87-48851
- KENNETT, R. G.**  
Selection of extended area land target sites for the calibration of spaceborne scatterometers p 74 A87-53118
- KERR, R. C.**  
Using NOAA AVHRR in studies of sea ice motion in the Beaufort Sea p 34 A87-48842
- KESIK, A. B.**  
Evaluation of MEIS-II multispectral scanner data for quaternary geological mapping in the Chatham area, southwestern Ontario p 24 A87-48816
- KEYDEL, W.**  
Remote sensing of the earth with microwave radiometry in Germany - Results and trends p 76 A87-53225
- KHRISTOFOROV, G. N.**  
Maximum accuracy of satellite-borne scatterometer measurements of wind velocity above the ocean p 33 A87-48184
- KIBLER, JAMES F.**  
Calculation and accuracy of ERBE scanner measurement locations [NASA-TP-2670] p 47 A87-28471
- KIDDER, STANLEY Q.**  
A multispectral study of the St. Louis area under snow-covered conditions using NOAA-7 AVHRR data p 51 A87-46538
- KIENEGGER, E.**  
Study on the use and characteristics of SAR for geological applications. Part 2: Radiogrammetry aspects [ESA-CR(P)-2325-PT-2] p 27 A87-26466
- KIASHCHENKO, N. I.**  
Measurement of currents according to the drift of subsatellite buoys p 32 A87-48177
- KILGUS, CHARLES C.**  
The Navy Geosat mission - An overview p 38 A87-52501
- KIM, CHOEN**  
Method development and experiences in application of airborne MSS data for forest damage detection p 12 A87-53247
- KIMANGA, R. S.**  
National land use mapping - The application of low altitude sample photography p 17 A87-48858
- KIMES, D.**  
Synergism requirements and concepts for SAR and HIRIS on EOS p 75 A87-53216

## KIRBY, M. E.

Validation of STAR-1 SAR imagery collected over Mould Bay, N.W.T., April 1984 p 59 A87-48826

## KLAR, A.

Environmental monitoring of Alpine Meadows with large scale aerial photography in Banff National Park p 18 A87-48898

## KLEMAS, V.

Remote sensing of coastal wetlands p 1 A87-40944

Remote sensing of submerged aquatic vegetation in lower Chesapeake Bay - A comparison of Landsat MSS to TM imagery p 30 A87-46542

## KNEPPECK, I. D.

A trial of oblique imagery from a low cost video camera system for defoliation assessment p 7 A87-48892

## KNUDSEN, PER

Estimation and modelling of the local empirical covariance function using gravity and satellite altimeter data p 22 A87-54325

## KOCH, B.

Monitoring and inventoring of forest damages by use of LANDSAT TM data p 16 A87-28138

## KOCHEGAROV, S. F.

Remote-sensing evaluation of moisture supply to crops according to the leaf-surface thermal regime p 2 A87-47582

## KOELN, G. T.

Inventory of wetlands with Landsat's Thematic Mapper p 3 A87-48817

## KOLESINA, N. B.

Investigation of causes of hydrogen sulfide formation in reclaimed water p 14 A87-23136

## KONDRATEV, K. I. A.

Features of the water dynamics of Lake Ladoga according to remote sensing data p 50 A87-44296

## KONG, J. A.

Theoretical models for microwave remote sensing of snow-covered sea ice p 42 A87-53236

Remote sensing of earth terrain [NASA-CR-181370] p 79 A87-28957

## KONG, XIANG-NING

Effect of resolution on texture application to nearly simultaneous AVHRR and MSS images of an agricultural region p 9 A87-53111

## KOPPE, A.

Investigation of design parameters for ERS-1 wind scatterometer p 74 A87-53116

## KOPROVA, L. I.

Studies of the wavelike process in the surface temperature field of the equatorial Pacific using Meteor-satellite IR measurements p 28 A87-42931

## KORPORAL, K. D.

An application for the testing and use of the standard data transfer format p 18 A87-48886

## KOTLIAROV, V. L.

Measurement of currents according to the drift of subsatellite buoys p 32 A87-48177

## KOTTSOV, V. A.

Multistage principal-components analysis of correlations p 56 A87-48193

Analysis of directions of linear image elements by structure-zonal method p 68 A87-29575

## KOUWEN, N.

Hydrologic applications of weather radar data p 52 A87-48875

## KOVALICK, WILLIAM M.

A methodology for evaluation of an interactive multispectral image processing system p 66 A87-53999

## KOZU, TOSHIKI

Observation of oil slicks on the ocean by X-band SLAR p 41 A87-53191

## KRAJEWSKI, WITOLD F.

Cokriging radar-rainfall and rain gage data p 53 A87-54154

## KRAKOWSKI, E.

Optimization of seismic vessel deployment using side looking airborne radar p 34 A87-48881

## KRASNOV, V. I.

Determination of the external-orientation elements of aerial and space photographs p 55 A87-44301

## KRAUSE-RABE, S.

Monitoring and inventoring of forest damages by use of LANDSAT TM data p 16 A87-28138

## KRISHTALKA, LEONARD

Analysis of Eocene depositional environments - Preliminary TM and TIMS results, Wind River Basin, Wyoming p 26 A87-53243

## KUCHLER, DEBORAH A.

Coral reef survey method for verification of Landsat MSS image data p 30 A87-46311

## KUCHMENT, L. G.

Remote sensing techniques for the study of hydrological elements p 51 A87-47576

## KUELZER, R.

Investigation of design parameters for ERS-1 wind scatterometer p 74 A87-53116

## KUITTINEN, RISTO

Monitoring of snow cover from satellite p 54 A87-28123

## KULIKOV, I. U. N.

Remote sensing techniques for the study of hydrological elements p 51 A87-47576

Parameterization of models of runoff formation in simple catchment areas using remote-sensing data p 51 A87-47579

Remote-sensing techniques for investigating the structure of radiation-heat fluxes and the moisture content of geosystems in connection with the problem of monitoring the water component p 52 A87-47584

## KUMMEROW, C.

Scattering parameters for aspherical hydrometeors at microwave frequencies p 53 A87-53271

## KUX, HERMANN J. H.

Evaluation of MOMS (Modular Optoelectronic Multispectral Scanner) data for land use/land cover studies - Test site: Piracicaba region, Sao Paulo State, Brazil p 13 A87-53252

## KUZ'MINA, E. N.

Remote-sensing and geological-geophysical studies of closed platform territories p 26 A87-51875

## KWOK, R.

Automated rectification and geocoding of SAR imagery p 63 A87-53143

## L

## LABONTE, M.

Thermographic remote sensing of northern forest areas in regeneration after clear or strip cutting - Preliminary observations p 8 A87-48897

## LABRUNE, Y.

Precise orbit determination with the Doppler Orbitography and Radio positioning Integrated by Satellite (DORIS) system and the associated Zealous for Orbit Observation Methods (ZOOM) software p 77 A87-25382

## LACAZE, BERNARD

Remote sensing of the geomorphologic formations and vegetation in the eastern High Atlas region of Morocco from SPOT satellite data p 23 A87-45048

## LAHRAOUI, LANCEN

Remote sensing of the geomorphologic formations and vegetation in the eastern High Atlas region of Morocco from SPOT satellite data p 23 A87-45048

## LAMBOLEY, M.

Poseidon radar altimeter description and signal processing p 40 A87-53114

## LANDGREBE, DAVID A.

Spectral feature design for data compression in high dimensional multispectral data p 64 A87-53183

## LANE, E. M.

Colour infrared aerial photography for herbicide drift damage assessment p 6 A87-48864

## LANG, HAROLD R.

Analysis of Eocene depositional environments - Preliminary TM and TIMS results, Wind River Basin, Wyoming p 26 A87-53243

## LANG, R. H.

Polarization utilization in the microwave inversion of leaf angle distributions p 11 A87-53201

## LANGEMANN, M.

An advanced wind scatterometer for the Columbus Polar Platform payload p 74 A87-53117

## LANSARD, E.

Earth gravity model improvement - An alternative method for Doppler-tracked satellites p 21 A87-45817

## LAPP, D. J.

Validation of STAR-1 SAR imagery collected over Mould Bay, N.W.T., April 1984 p 59 A87-48826

The influence of melting conditions on the interpretation of radar imagery of sea ice p 34 A87-48849

## LARSON, R. W.

Calibrated L-band terrain measurements and analysis program [AD-A182917] p 68 A87-29722

## LARSON, RICHARD W.

Statistical modeling of intensity distributions on airborne SAR imagery p 65 A87-53262

## LASSERE, M.

An evaluation of sun angle computation algorithms p 59 A87-48812

## LATHROP, RICHARD G., JR.

Calibration of Thematic Mapper thermal data for water surface temperature mapping - Case study on the Great Lakes p 51 A87-46545

## LAUR, H.

Textural segmentation of SAR images using first order statistical parameters p 66 A87-53274

## LAWRENCE, G. R.

Digital SAR-Landsat combination for geologic mapping p 24 A87-48853

## LAWRENCE, R. W.

Results from the pushbroom microwave radiometer flights over the Konza Prairie in 1985 p 11 A87-53206

## LAXON, S. W.

Satellite altimeter measurements of the geoid in sea ice zones p 30 A87-45816

## LE TOAN, T.

Textural segmentation of SAR images using first order statistical parameters p 66 A87-53274

## LE VINE, D.

A multifrequency microwave radiometer of the future p 75 A87-53180

## LEAVITT, E. D.

Optimization of seismic vessel deployment using side looking airborne radar p 34 A87-48881

## LEBERL, F.

Study on the use and characteristics of SAR for geological applications. Part 2: Radargrammetry aspects [ESA-CR(P)-2325-PT-2] p 27 A87-26466

## LECKIE, D. G.

A trial of oblique imagery from a low cost video camera system for defoliation assessment p 7 A87-48892

## LECLERC, A.

A revolution in the production of small-scale and medium-scale maps p 61 A87-48904

## LEDREW, E.

Indices of climatological and hydrological variability derived from satellite imagery for the South Saskatchewan River Basin p 52 A87-48856

Radiation modelling in a high relief environment using a digital terrain model and Landsat - TM imagery p 59 A87-48857

## LEE, JONG-SEN

Statistical modelling and suppression of speckle in synthetic aperture radar images p 65 A87-53259

## LEE, T.

Physical oceanographic study of Florida's Atlantic Coast region: Florida Atlantic Coast Transport Study (FACTS). Volume 1: Executive summary p 49 A87-30015

Physical oceanographic study of Florida's Atlantic Coast region: Florida Atlantic Coast Transport Study (FACTS), volume 2 p 49 A87-30016

Physical oceanographic study of Florida's Atlantic Coast region: Florida Atlantic Coast Transport Study (FACTS). Volume 3: Appendices [PB87-201018] p 49 A87-30017

## LEE, WAH T.

Labrador wind and wave environments [AD-A183218] p 48 A87-29907

## LEE, Y. J.

The use of multi-spectral and radar remote sensing data for monitoring forest clearcut and regeneration sites on Vancouver Island p 5 A87-48834

## LEEKHAI, CHAMNIAN

Small format aerial photography for analyzing urban housing problems - A case study in the Bangkok metropolitan region p 17 A87-46309

## LEGER, D.

SPOT MTF performance evaluation p 57 A87-48663

## LEMIEUX, G. H.

Thermographic remote sensing of northern forest areas in regeneration after clear or strip cutting - Preliminary observations p 8 A87-48897

## LENCO, MICHEL

Present state, changes, and quality of Sologne and Brenne, two French large wetlands, studied with LANDSAT MSS and TM data p 54 A87-28152

## LONDON, C.

Spectral studies of dryland agricultural salinity in Western Australia p 38 A87-48901

## LENG, D.

Sea surface temperatures and the detection of ocean circulation patterns and fronts from AVHRR imagery p 45 A87-28125

## LEROY, M.

SPOT radiometric resolution performance evaluation - Preliminary results p 57 A87-48661

SPOT MTF performance evaluation p 57 A87-48663

## LESCHACK, A. RICHARD

Preliminary determination of the Geosat radar altimeter noise spectrum p 38 A87-52503

## LEWKI, L.

Extent of saline/waterlogged lands within irrigated Alberta. I - Inventory and preliminary evaluation of existing mapping data p 5 A87-48830

## LI, F.

Global digital topography mapping using a scanning radar altimeter p 76 A87-53227



## M

- LI, F. K.**  
Selection of extended area land target sites for the calibration of spaceborne scatterometers p 74 A87-53118
- LI, FUK K.**  
Wind measurements for non-uniform wind fields from spaceborne scatterometers p 75 A87-53195  
A comparative study of several wind estimation algorithms for spaceborne scatterometers p 41 A87-53197
- LI, XIAOWEN**  
Modeling gap probability in discontinuous vegetation canopies p 13 A87-53276
- LIEDTKE, J.**  
Discrimination of suspended sediment and littoral features using multispectral video imagery p 73 A87-48874
- LILLESAND, THOMAS M.**  
Calibration of Thematic Mapper thermal data for water surface temperature mapping - Case study on the Great Lakes p 51 A87-46545
- LIM, K.**  
An algorithm for automatically acquiring ground control points in SAR imagery p 67 N87-27864
- LIN, C. C.**  
Investigation of design parameters for ERS-1 wind scatterometer p 74 A87-53116
- LIN, F. C.**  
Theoretical models for microwave remote sensing of snow-covered sea ice p 42 A87-53236
- LINDELL, L. T.**  
Operational water quality surveillance in Sweden using Landsat MSS data p 52 A87-48841
- LINEBAUGH, GREGORY H.**  
Multiple-angle observations of reflectance anisotropy from an airborne linear array sensor p 69 A87-43262
- LIU, ERIC**  
Deconvolution of sea state parameters from altimeter waveforms p 41 A87-53198
- LIU, HUA-KUANG**  
Optical image subtraction techniques, 1975-1985 p 55 A87-42659
- LIU, K. Y.**  
Spacecraft on-board SAR image generation for EOS-type missions p 76 A87-53232
- LIVINGSTONE, C. E.**  
Airborne SAR imaging of azimuthally traveling ocean surface waves - The LEWEX experimental plan p 44 A87-53266
- LOMBARDINI, P. P.**  
Climatological implications of a satellite-borne SAR imaging the sea surface p 30 A87-46403
- LOPES, A.**  
Textural segmentation of SAR images using first order statistical parameters p 66 A87-53274  
A statistical and geometrical edge detector for SAR image segmentation p 13 A87-53275
- LOWRY, R. T.**  
The influence of melting conditions on the interpretation of radar imagery of sea ice p 34 A87-48849  
Validation and simulation of Radarsat imagery p 60 A87-48883
- LOZIEV, V. P.**  
Application of space photographs to geomorphological investigations in southwestern Tadzhikistan p 23 A87-48186
- LU, YUN-CHI**  
The Land Analysis System (LAS) - A general purpose system for multispectral image processing p 64 A87-53230
- LUCE, M. P.**  
Operational use of remote sensing for commercial Arctic class vessel navigation p 33 A87-48829
- LUETKEMEYER, KELLY**  
Satellite image processing for the Agulhas Retroflexion region [AD-A183012] p 68 N87-29905
- LUNETTA, ROSS S.**  
Whitetail deer food availability maps from Thematic Mapper data p 14 A87-53998
- LUTHER, C. A.**  
Evolution of microwave sea ice signatures during early summer and midsummer in the marginal ice zone p 31 A87-47293
- LYDEN, J. D.**  
Progress on digital algorithms for deriving sea ice parameters from SAR data p 43 A87-53238
- LYZENGA, DAVID R.**  
Modeling of focus effects in SAR images of the ocean surface p 42 A87-53212  
Automatic focusing of synthetic aperture radar images of diffuse targets p 64 A87-53213  
Comparison of numerical simulations with SAR images of ocean surface waves in the New York Bight p 44 A87-53287
- MACARTHUR, J. L.**  
Real time global ocean wave spectra from SIR-C - Systems design p 42 A87-53234
- MACARTHUR, JOHN L.**  
The Geosat radar altimeter p 38 A87-52502
- MACAYEAL, D. R.**  
Ice dynamics at the mouth of ice stream B, Antarctica p 37 A87-51946
- MACK, A. R.**  
Stratification of satellite imagery by Uniform Productivity Areas p 5 A87-48840  
An evaluation of Landsat TM and MSS data for crop identification in Manitoba p 6 A87-48859
- MACKEY, H. E., JR.**  
Color infrared video mapping of upland and wetland communities [DE87-010202] p 15 N87-28109
- MACKIERNAN, G. B.**  
Characterizing the Chesapeake Bay ecosystem and lessons learned [PB87-166930] p 19 N87-26463
- MACKLIN, J. T.**  
The comparison of ocean-wave spectra recovered from SIR-B and Seasat observations with simultaneous buoy data p 43 A87-53265
- MAEDA, KOREHIRO**  
Some results of MOS-1 airborne verification experiment - MSR (microwave scanning radiometer) p 76 A87-53229
- MAETZER, C.**  
The potential of SAR in a snow and glacier monitoring system p 45 N87-27856
- MAFFETT, A. L.**  
Calibrated L-band terrain measurements and analysis program [AD-A182917] p 68 N87-29722
- MAFFETT, ANDREW L.**  
Statistical modeling of intensity distributions on airborne SAR imagery p 65 A87-53262
- MAGAHAY, L.**  
Operational, province wide crop area estimation for Manitoba p 47 A87-48811
- MAGUIRE, CHRISTINE**  
Coral reef survey method for verification of Landsat MSS image data p 30 A87-46311
- MAJOR, JUDY A.**  
Ice measurements by Geosat radar altimetry p 39 A87-52513
- MAKHDOOM, M. T. A.**  
Forecast of hurricane characteristics from GOES imagery p 59 A87-48818
- MALINGREAU, J. P.**  
The contribution of AVHRR data for measuring and understanding global processes - Large-scale deforestation in the Amazon basin p 11 A87-53151
- MALINGREAU, JEAN-PAUL**  
Remote sensing in Indonesia - A review of the available technology and its applications for resources surveys p 17 A87-46310
- MALYEVAC, CAROL W.**  
Determination of ocean geodetic data from Geosat p 38 A87-52506
- MANDYCH, A. F.**  
Possibility of evaluating reservoir influx from aerial and satellite photographs p 51 A87-47577  
Water-cycle processes in geosystems and the possibility of the remote sensing of the moisture content of the underlying surface p 51 A87-47580
- MANLEY, T.**  
Mesoscale eddies in the Fram Strait marginal ice zone during the 1983 and 1984 Marginal Zone Experiments p 31 A87-47291
- MANLEY, T. O.**  
Use of synthetic aperture radar-derived kinematics in mapping mesoscale ocean structure within the interior marginal ice zone p 31 A87-47294
- MANORE, M.**  
Technological feasibility to mobilization for operations - The NOAA crop monitoring case p 6 A87-48878
- MANORE, M. J.**  
An application for the testing and use of the standard data transfer format p 18 A87-48886  
Ground targets for the radiometric correction of AVHRR imagery for crop monitoring p 7 A87-48887
- MANTRIPP, D. R.**  
Glaciological studies on Rutford ice stream, Antarctica p 38 A87-51950
- MAO, Y.**  
Reflectance- and radiance-based methods for the in-flight absolute calibration of multispectral sensors p 69 A87-44863
- MARACCHI, G.**  
Automatic classification of forestal areas by remote sensing techniques p 12 A87-53211
- MARACCI, G.**  
Measurement of spectral signatures in Less Favored Areas (LFA): A contribution to the definition of a remote sensing multimaterial experiment p 20 N87-28145
- MARKHAM, BRIAN L.**  
Radiometric properties of U.S. processed Landsat MSS data p 55 A87-44864
- MARSHAK, A. L.**  
Monte Carlo calculation of the dependence of the spectral radiance of vegetation cover on the illumination conditions p 2 A87-48190
- MARTH, PAUL C., JR.**  
The Geosat radar altimeter p 38 A87-52502
- MARTIN, SEELYE**  
Shuttle Imaging Radar B (SIR-B) Weddell Sea ice observations - A comparison of SIR-B and scanning multichannel microwave radiometer ice concentrations p 32 A87-47300
- MARTYNOV, ALEKSANDR IVANOVICH**  
From satellite orbit into the eye of the typhoon p 29 A87-44679
- MASCARENHAS, NELSON D. A.**  
Determination of transfer functions from the Thematic Mapper (TM) sensor of the LANDSAT-5 satellite [INPE-4213-PRE/1094] p 79 N87-28956
- MASELLI, F.**  
Automatic classification of forestal areas by remote sensing techniques p 12 A87-53211
- MASLENNIKOVA, I. N.**  
A study of modern landscape formation in Lower Mesopotamia from space photographs p 55 A87-42935
- MASUKO, HARUNOBU**  
Observation of oil slicks on the ocean by X-band SLAR p 41 A87-53191
- MATZLER, C.**  
Evolution of microwave sea ice signatures during early summer and midsummer in the marginal ice zone p 31 A87-47293
- MAYKUT, GARY A.**  
Boundary layer, upper ocean, and ice observations in the Greenland Sea marginal ice zone p 31 A87-47296
- MAYNARD, NANCY G.**  
Satellite color observations of spring blooming in Bering Sea shelf waters during the ice edge retreat in 1980 p 32 A87-47297
- MCADOO, D. C.**  
Oceanographic and geophysical applications of satellite altimetry p 30 A87-46690
- MCCLOY, K. R.**  
Use of rice response characteristics in classification using Landsat MSS digital data p 1 A87-45046  
Monitoring rice areas using Landsat MSS data p 1 A87-45047
- MCCOLL, W. D.**  
CCRS airborne Electro-Optical Facility p 72 A87-48852
- MCCONATHY, DONALD R.**  
The Navy Geosat mission - An overview p 38 A87-52501
- MCCONNELL, ALAN**  
Sampling errors in satellite estimates of tropical rain p 53 A87-54153
- MCCOURT, M. L.**  
Integrated multi-temporal aerial photography and digital mapping for coastal monitoring, Cape Breton Island, Nova Scotia p 34 A87-48837
- MCGUIRK, J. P.**  
Comparisons of FGGE IIb and IIIb winds in a tropical synoptic system p 35 A87-51559  
Wintertime disturbances in the tropical Pacific - FGGE IIb and satellite comparisons p 36 A87-51560  
Moisture transports and budgets of 'moisture bursts' p 36 A87-51593
- MCGUIRK, JAMES P.**  
Moisture bursts over the tropical Pacific Ocean p 28 A87-43345  
Application of satellite data to tropic-subtropical moisture coupling [NASA-CR-4092] p 48 N87-29067
- MCINNIS, T. R.**  
Integration of radiometric and Landsat digital data for geologic investigation and exploration, Guysborough area, Nova Scotia p 24 A87-48803
- MCKENNA, ANTHONY**  
Coral reef survey method for verification of Landsat MSS image data p 30 A87-46311
- MCLEOD, J. C.**  
Effectiveness of the Thematic Mapper for the range condition assessment in fescue grasslands of Southwestern Alberta p 6 A87-48850
- MCPHEE, MILES G.**  
Boundary layer, upper ocean, and ice observations in the Greenland Sea marginal ice zone p 31 A87-47296

**MEGIER, JACQUES**

- Cluster based segmentation of multi-temporal Thematic Mapper data as preparation of region-based agricultural land-cover analysis p 9 A87-53109
- Rural land use inventory and mapping in the Ardeche area (France). Improvement of automatic classification by multitemporal analysis of TM data p 15 N87-28127

**MEISSNER, D.**

- The RADARSAT RMOMS optical sensor p 73 A87-48890

**MELIA, J.**

- Thermal infrared images from satellites compared to shelter temperature. Application to frost nowcasting in a citrus orchard p 15 N87-28136

**MELITA, OLGA**

- Proceedings of the ESA-EARSeL Europe from Space Symposium [ESA-SP-258] p 19 N87-28115

**MELLING, H.**

- Using NOAA AVHRR in studies of sea ice motion in the Beaufort Sea p 34 A87-48842

**MELLOR, JOHN R.**

- Coral reef survey method for verification of Landsat MSS image data p 30 A87-46311

**MENARD, ALAIN**

- The CCRS SAR/MSS Anderson River data set p 55 A87-43261

**MENESES, PAULO ROBERTO**

- Enhancement of colors in remote sensing images using rotation of the matrix at the IHS coordinates [INPE-4207-PRE/1088] p 67 N87-28165

**MEPHAM, M. P.**

- Spatial filtering of digital Landsat data for the extraction of mapping information p 58 A87-48805

**MERRY, CAROLYN J.**

- Use of LANDSAT digital data for snow cover mapping in the upper Saint John River Basin, Maine [AD-A183213] p 54 N87-29906

**MESHCHENIN, I. G.**

- Water-cycle processes in geosystems and the possibility of the remote sensing of the moisture content of the underlying surface p 51 A87-47580

**MEYER, E. L.**

- Review of control strategies for ozone and their effects on other environmental issues [PB87-171195] p 19 N87-25634

**MEYER, P.**

- Hierarchical classification with knowledge based binary decision p 62 A87-53110

**MIELSEN, BJARNE K.**

- Comparison of visual and automated lineament analyses on LANDSAT MSS image from south Greenland p 67 N87-28144

**MILFORD, J. C.**

- A structural analysis of the Mabou Basin, Cape Breton Island using enhanced Landsat MSS imagery p 25 A87-48879

**MILLER, B. L.**

- Latent heat and cyclone activity in the South Pacific, 10-18 January 1979 p 37 A87-51603

**MILLER, D.**

- Operational use of remote sensing for commercial Arctic class vessel navigation p 33 A87-48829
- Performance sensitivity for X-SAR p 76 A87-53223

**MILLER, J. M.**

- Custom-enhanced Landsat imagery in near real-time p 60 A87-48870

**MILLER, J. R.**

- Preliminary results from modelling vegetation spectra derived from MEIS data, Algonquin Park, Ontario p 7 A87-48891

**MILLER, LAURY L.**

- Monitoring equatorial Pacific sea level with Geosat p 39 A87-52512

**MILLER, MICHAEL S.**

- Use of LANDSAT digital data for snow cover mapping in the upper Saint John River Basin, Maine [AD-A183213] p 54 N87-29906

**MILMAN, ANDREW S.**

- A cross antenna for passive microwave remote sensing p 77 A87-53268

**MILNE, K.**

- A study of antenna signal processing techniques for radar alternatives [ESA-CR(P)-2370] p 79 N87-28809

**MINNETT, P. J.**

- The variability of the North Atlantic marine atmosphere and its relevance to remote sensing p 33 A87-48362

**MISRA, TAPAN**

- A spaceborne LFM scatterometer for ocean surface wind vector measurement - A time domain approach p 40 A87-53119

**MITCHELL, JIM L.**

- REX and Geosat - Progress in the first year p 39 A87-52511

**Design of Geosat Exact Repeat Mission**

p 39 A87-52515

**MITCHELL, W.**

- Sea surface temperature retrieval from the Tiros-N AVHRR instrument for the FGGE period (Dec. 1978-Nov. 1979) p 35 A87-51553

**MO, TSAN**

- Retrieval of surface roughness parameters from dual-frequency measurements of radar backscattering coefficients p 10 A87-53130

**MONALDO, FRANK**

- Validation of Geosat altimeter-derived wind speeds and significant wave heights using buoy data p 39 A87-52510

**MONALDO, FRANK M.**

- The production of real time wave spectra from the SIR-C SAR p 42 A87-53224
- The response of SAR imagery to azimuth travelling ocean surface waves as determined from shuttle SAR imagery p 44 A87-53286

**MONTGOMERY, H.**

- MODIS - Advanced facility instrument for studies of the earth as a system p 40 A87-53144

**MOORE, D. G.**

- Using AVHRR data to evaluate the greenness variability within monitoring polygons p 4 A87-48828

**MOORE, RICHARD K.**

- Modulation transfer function of radar return power from the ocean p 42 A87-53219

**MORIN, R. L.**

- Comparison of classification and enhancement techniques using Landsat imagery for the northern coniferous forest p 4 A87-48821

**MORIONDO, A.**

- Large Format Camera: The second generation photogrammetric camera for space cartography p 78 A87-28118

**MORISON, JAMES H.**

- Boundary layer, upper ocean, and ice observations in the Greenland Sea marginal ice zone p 31 A87-47296

**MORO, J.**

- ERAFIS: A computer information system for agriculture and forestry in Spain p 16 N87-28140

**MORTON, R. J.**

- Large-scale black and white and natural color photographs for the measurement of tree crown areas p 3 A87-48815

**MOTYZHEV, S. V.**

- Measurement of currents according to the drift of subsatellite buoys p 32 A87-48177

**MUKOUYAMA, YUJI**

- Land cover classification using SPOT data p 18 A87-50227

**MUNK, W. H.**

- The Bakerian Lecture, 1986 - Ships from space p 44 A87-54301

**MURPHY, JENNIFER M.**

- Within-scene radiometric correction of Landsat Thematic Mapper (TM) data in Canadian production systems p 57 A87-48656

**MURPHY, R.**

- A multifrequency microwave radiometer of the future p 75 A87-53180

**MURPHY, ROBERT E.**

- The First ISLSCP Field Experiment (FIFE) p 12 A87-53218

**MUZYLEV, E. L.**

- Modeling the snowmelt runoff in mountain catchment areas using satellite data p 51 A87-47578

**N****NATARAJAN, S.**

- Data analysis and software support for the Earth radiation budget experiment [NASA-CR-178350] p 66 N87-26569

**NATHAN, KRISHNA S.**

- Speckle noise reduction of 1-look SAR imagery p 65 A87-53273

**NAZIROV, M.**

- Divergent redistribution of ice in the Arctic Ocean (Analysis of space imagery) p 33 A87-48180

**NEEDHAM, BRUCE H.**

- Operational instruments on the Space Station-Polar Platforms - Contributions by NOAA and the international community p 74 A87-53149

**NEEMAN, S.**

- Application of accuracy assessment techniques to image classification p 58 A87-48808

**NEHLSSEN, W.**

- Characterizing the Chesapeake Bay ecosystem and lessons learned [PB87-166930] p 19 N87-26463

**NESBY, R. K.**

- Large-scale black and white and natural color photographs for the measurement of tree crown areas p 3 A87-48815
- TM and MEIS data for future Alberta forest inventories p 8 A87-48900

**NEVILLE, R. A.**

- CCRS Airborne Electro-Optical Facility p 72 A87-48852

**NEWBURY, GEORGE E.**

- A user's guide for the Analytical Photogrammetric Positioning System (APPS) [AD-A183773] p 79 N87-29909

**NEWCOMER, JEFFREY A.**

- A methodology for evaluation of an interactive multispectral image processing system p 66 A87-53999

**NEWKIRK, ROSS**

- Data correction for automated remote sensing image interpretation p 64 A87-53209

**NICHOLSON, SHARON**

- Investigating the role of the land surface in explaining the interannual variation of the net radiation balance over the Western Sahara and sub-Saharan [NASA-CR-181183] p 68 N87-28197

**NIGRO, L.**

- Crop discrimination by means of radar and infrared images p 15 N87-28128

**NOBEL, PARK S.**

- Measurement of leaf relative water content by infrared reflectance p 9 A87-53024

**NORTH, GERALD R.**

- Sampling errors in satellite estimates of tropical rain p 53 A87-54153

**NOUEL, FRANCOIS**

- Precise orbit determination with the Doppler Orbitography and Radio positioning Integrated by Satellite (DORIS) system and the associated Zealous for Orbit Observation Methods (ZOOM) software p 77 N87-25382

**NYKJAER, L.**

- Coastal Zone Color Scanner (CZCS) images and ocean dynamics. Application to the Northwest African upwelling area p 46 N87-28146

**O****O'BRIEN, D. M.**

- Size distributions of clouds in real time from satellite imagery p 56 A87-48359

**O'CONNOR, WILLIAM P.**

- Snow load effect on earth's rotation and gravitational field, 1979-1985 p 22 A87-51964

**OB'EDKOV, IURII LEONIDOVICH**

- Formation of natural underground-water resources in arid regions with special reference to the Dolinoozerskii artesian basin in Mongolia p 50 A87-42911

**OCULINN, K. W.**

- Color infrared video mapping of upland and wetland communities [DE87-010202] p 15 N87-28109

**ODEN, S. F.**

- Real time global ocean wave spectra from SIR-C - Systems design p 42 A87-53234

**OGIL'VI, A. A.**

- Remote-sensing and geological-geophysical studies of closed platform territories p 26 A87-51875

**OHARA, JOHN F.**

- Comparison of satellite-derived ocean velocities with observations in the California coastal region [AD-A182291] p 47 N87-28242

**OHLEN, D. O.**

- Using AVHRR data to evaluate the greenness variability within monitoring polygons p 4 A87-48828

**OHRING, G.**

- Cloud screening for determination of land surface characteristics in a reduced resolution satellite data set p 56 A87-48361

**OJIMA, TAKEYUKI**

- Observation of oil slicks on the ocean by X-band SLAR p 41 A87-53191

**OLSON, CHARLES E., JR.**

- Color aerial photography in the plant sciences and related fields: Proceedings of the Tenth Biennial Workshop, University of Michigan, Ann Arbor, May 21-24, 1985 p 1 A87-45100

**ONORATI, G.**

- Use of TM Landsat data as a support to classical ground-based methodologies in the investigation of a volcanic site in central Italy - The Caldera of Latera p 26 A87-53244

**ONSTOTT, R. G.**

- Evolution of microwave sea ice signatures during early summer and midsummer in the marginal ice zone p 31 A87-47293

- Progress on digital algorithms for deriving sea ice parameters from SAR data p 43 A87-53238
- ONSTOTT, ROBERT G.**  
Theoretical and experimental study of the radar backscatter of Arctic sea ice p 43 A87-53237  
Investigation of multi-dimensional algorithms using active and passive microwave data for ice concentration determination p 43 A87-53241
- ORIOU-PIERNAT, E.**  
TM sensor performance as obtained from Earthnet quality control data base p 71 A87-48659
- ORMSBY, JAMES P.**  
Whitetail deer food availability maps from Thematic Mapper data p 14 A87-53998
- OSTROW, H.**  
MODIS - Advanced facility instrument for studies of the earth as a system p 40 A87-53144

## P

- PAINE, S. H.**  
Spatial filtering of digital Landsat data for the extraction of mapping information p 58 A87-48805
- PALANIYELU, R.**  
Pleistocene earth movements in Peninsular India - Evidences from Landsat MSS and Thematic Mapper data p 26 A87-53242
- PALOSCIA, S.**  
Aircraft microwave radiometry of land p 13 A87-53269  
Crop discrimination by means of radar and infrared images p 15 N87-28128
- PAMPALONI, P.**  
Aircraft microwave radiometry of land p 13 A87-53269  
Crop discrimination by means of radar and infrared images p 15 N87-28128
- PANCHANATHAN, S.**  
Pleistocene earth movements in Peninsular India - Evidences from Landsat MSS and Thematic Mapper data p 26 A87-53242
- PAPADAKIS, JOHN E.**  
Upwelling filaments and motion of a satellite-tracked drifter along the west coast of North America p 29 A87-45023
- PARIS, J.**  
Synergism requirements and concepts for SAR and HIRIS on EOS p 75 A87-53216  
The global forest ecosystem as viewed by ERS-1, SIR-C and EOS p 12 A87-53217
- PARIS, JACK F.**  
Detecting forest structure and biomass with C-band multipolarization radar - Physical model and field tests p 2 A87-48543
- PARKINSON, C. L.**  
On the relationship between atmospheric circulation and the fluctuations in the sea ice extents of the Bering and Okhotsk Seas p 32 A87-47208  
Satellite-derived ice data sets no. 2: Arctic monthly average microwave brightness temperatures and sea ice concentrations, 1973-1976 [NASA-TM-87825] p 50 N87-30021
- PARSONS, CHESTER L.**  
Airborne multibeam radar altimetry p 40 A87-53115
- PEACEGOOD, G.**  
Towards the automatic recognition and vectorised description of linear features in LANDSAT TM images by artificial intelligence methods p 67 N87-28142
- PEDERSEN, LEIF TOUDAL**  
Large scale sea ice studies based on Scanning Multichannel Microwave Radiometers (SMMR) data p 16 N87-28148
- PELLINEN, L. P.**  
New possibilities for the use of gravity data in the realization of geodetic coordinate systems p 21 A87-42939
- PERBOS, J.**  
SPOT MTF performance evaluation p 57 A87-48663
- PERRON, S.**  
Thermographic remote sensing of northern forest areas in regeneration after clear or strip cutting - Preliminary observations p 8 A87-48897
- PERTSEV, B. P.**  
The determination of Love numbers from the results of earth-tide observations in the Dnieper-Donets basin (DDB) region p 21 A87-46139
- PESCOD, R. W.**  
The variability of the North Atlantic marine atmosphere and its relevance to remote sensing p 33 A87-48362
- PETERS, JOHN**  
Tidal and secular tilt from an earthquake zone - Thresholds for detection of regional anomalies p 26 A87-53733

- PETERSEN, GARY W.**  
Classification of geomorphic features and landscape stability in northwestern New Mexico using simulated SPOT imagery p 56 A87-46540
- PETERSEN, JOHN L.**  
Comparison of visual and automated lineament analyses on LANDSAT MSS image from south Greenland p 67 N87-28144
- PETERSON, DAVID L.**  
Relationship of Thematic Mapper simulator data to leaf area index of temperate coniferous forests p 8 A87-53017  
Estimating key forest ecosystem parameters through remote sensing p 12 A87-53245
- PEULVAST, J.-P.**  
Morphostructure and geological patterns in central-southern Norway according to a Landsat image p 25 A87-51146
- PIAU, P.**  
SPOT, a satellite for oceanography? p 41 A87-53194  
Processing of airborne SAR images of ocean waves p 43 A87-53264
- PICHUGIN, A. P.**  
Radar observations of terrestrial vegetation covers in the 3-cm range p 1 A87-42936
- PIERCE, R. N.**  
Airborne video - Applied to route location studies for electrical power transmission facilities p 17 A87-48802
- PIERSCHER, DIETER**  
Derivation of the technical specification of the ERS-1 active microwave instrument to meet the SAR-image quality requirements p 77 A87-53280
- PIERSON, WILLARD J., JR.**  
Radar scattering and equilibrium ranges in wind-generated waves with application to scatterometry p 28 A87-42746
- PILLAI, N. S.**  
A spaceborne LFM scatterometer for ocean surface wind vector measurement - A time domain approach p 40 A87-53119
- PIOLA, ALBERTO R.**  
Some aspects of the surface circulation south of 20 deg S revealed by First GARP Global Experiment drifters p 28 A87-42748
- PISARENKO, V. A.**  
Remote-sensing evaluation of moisture supply to crops according to the leaf-surface thermal regime p 2 A87-47582
- PITTS, D. E.**  
Estimation of X-band scattering properties of tree components p 13 A87-53277
- PLANET, WALTER**  
Planning for future operational sensors and other priorities [NOAA-NESDIS-30] p 77 N87-25500
- PLUNKETT, GORDON**  
An expert system for remote sensing p 80 A87-43260
- PODAIRE, A.**  
Monitoring wheat canopies with a high spectral resolution radiometer p 8 A87-53019
- POIRIER, S.**  
Comparison of C-band synthetic aperture radar (SAR) data according to two different depression angles for agricultural applications p 4 A87-48820  
Study on the use of SAR data for agriculture and forestry p 15 N87-27862
- POKRANT, H.**  
Operational, province wide crop area estimation for Manitoba p 3 A87-48811
- POKROVSKAIA, I. V.**  
Foam activity on the sea surface as a Markov random process p 28 A87-44289
- POLET, M.**  
Sulphur dioxide damage assessment using colour infrared aerial photography p 60 A87-48884
- POLETAEV, ANATOLII IVANOVICH**  
Elements of lineament tectonics p 27 A87-53954
- POPLAVSKAIA, L. K.**  
Modeling the snowmelt runoff in mountain catchment areas using satellite data p 51 A87-47578
- POPOV, I. G.**  
Investigation of causes of hydrogen sulfide formation in reclaimed water p 14 N87-23136
- POSCOLIERI, M.**  
Use of TM Landsat data as a support to classical ground-based methodologies in the investigation of a volcanic site in central Italy - The Caldera of Latera p 26 A87-53244
- PRADINES, D.**  
Improving SPOT images size and multispectral resolution p 58 A87-48664

- PREISENDORFER, R. W.**  
Theory of fluorescent irradiance fields in lakes and seas [PB87-196465] p 47 N87-28954
- PREVOST, C.**  
Stratification of satellite imagery by Uniform Productivity Areas p 5 A87-48840  
Interpretation of prairie land cover types from SIR-B data p 7 A87-48888  
Remote sensing in the Sahel - A tool for the inventory and monitoring of resources p 73 A87-48893
- PRICE, CURTIS V.**  
Vegetation mapping and stress detection in the Santa Monica Mountains, California p 12 A87-53246
- PRICE, CURTIS, V.**  
Lithologic discrimination using geobotanical and Landsat TM spectral data p 23 A87-48667
- PRIEST, ROGER**  
Coral reef survey method for verification of Landsat MSS image data p 30 A87-46311
- PRINCZ, G. J.**  
The ERS-1/RADARSAT SAR Canadian ground segment p 61 A87-48896
- PRITCHARD, R. S.**  
Interpolation, analysis and archival of data on sea ice trajectories and ocean currents obtained from satellite-linked instruments [PB87-201430] p 48 N87-30010
- PROUT, N. A.**  
Technological feasibility to mobilization for operations - The NOAA crop monitoring case p 6 A87-48878  
The evaluation of TM analysis as a tool in monitoring land use and agricultural stress in Egypt p 18 A87-48903

## Q

- QUADIR, D. A.**  
Agricultural, hydrologic and oceanographic studies in Bangladesh with NOAA AVHRR data p 57 A87-48365
- QUEGAN, S.**  
Thin line detection in SAR images p 66 N87-27860  
Land use feature detection in SAR images p 67 N87-27863

## R

- RAGGAM, J.**  
Study on the use and characteristics of SAR for geological applications. Part 2: Radargrammetry aspects [ESA-CR(P)-2325-PT-2] p 27 N87-26466
- RAIZONVILLE, P.**  
Poseidon radar altimeter description and signal processing p 40 A87-53114
- RAMAMURTHY, MOHAN**  
Observing systems experiments for the onset vortex during Summer Monex p 35 A87-51552
- RAMAN, SETHU**  
A comparison of the significant features of the marine boundary layers over the Arabian Sea and the Bay of Bengal during Monex 79 p 36 A87-51594
- RAMASAMY, S. M.**  
Pleistocene earth movements in Peninsular India - Evidences from Landsat MSS and Thematic Mapper data p 26 A87-53242
- RAMSAY, B. R.**  
The operational use of RADARSAT products by the ice centre environment Canada p 61 A87-48906
- RAMSEIER, R. O.**  
Optimum use of dual frequency passive microwave measurements for ice/ocean interactions p 43 A87-53240
- RANEY, R. K.**  
Validation and simulation of Radarsat imagery p 60 A87-48883  
Spatial considerations in speckle simulation p 65 A87-53260
- RAPLEY, C. G.**  
Satellite altimeter measurements of the geoid in sea ice zones p 30 A87-45816  
A study of antenna signal processing techniques for radar alternatives [ESA-CR(P)-2370] p 79 N87-28809
- RAST, M.**  
Requirements on radar data for geological application: A case study by use of multistage data of the test site Sardegna/Italy p 27 N87-28120
- REA, W. A.**  
Spectral studies of dryland agricultural salinity in Western Australia p 8 A87-48901
- REDLINE, ANDREW D.**  
Analysis of Eocene depositional environments - Preliminary TM and TIMS results, Wind River Basin, Wyoming p 26 A87-53243

## REFK, R.

Coastal Zone Color Scanner (CZCS) images and ocean dynamics. Application to the Northwest African upwelling area p 46 A87-28146

## REICHERT, G.

MEIS II imagery for environmental stress analysis p 72 A87-48865

## REICHERT, G. C.

Rural land use classification using Landsat Thematic Mapper data p 18 A87-48868

## RENCZ, A. N.

Preliminary results from modelling vegetation spectra derived from MEIS data, Algonquin Park, Ontario p 7 A87-48891

## REUTER, D.

Cloud and moisture fields derived from the GLA retrievals of HIRS2/MSU data p 36 A87-51579

## REUTER, R.

ADRIA 84: Airborne investigations of Gelbstoff by optical radiometry and fluorescence lidar p 46 A87-28154

## REYNA, E.

Estimation of X-band scattering properties of tree components p 13 A87-53277

## RHEAULT, M.

A study of the potential application of SPOT imagery in structural geology p 24 A87-48827  
Study on the use of SAR data for agriculture and forestry p 15 A87-27862

## RIEGGER, S.

On the origin of cross-polarization in remote sensing p 75 A87-53168

## RINKEL, M.

Physical oceanographic study of Florida's Atlantic Coast region: Florida Atlantic Coast Transport Study (FACTS). Volume 1: Executive summary p 49 A87-30015  
[PB87-200994]

Physical oceanographic study of Florida's Atlantic Coast region: Florida Atlantic Coast Transport Study (FACTS), volume 2 p 49 A87-30016  
[PB87-201000]

Physical oceanographic study of Florida's Atlantic Coast region: Florida Atlantic Coast Transport Study (FACTS). Volume 3: Appendices p 49 A87-30017  
[PB87-201018]

## RITCHIE, JERRY C.

Suspended sediment concentrations estimated from Landsat MSS p 53 A87-53204

## RIZZI, ROLANDO

Atmospheric correction of data measured by a flying platform over the sea - Elements of a model and its experimental validation p 35 A87-50292

## ROBERTS, A.

Multispectral video system for airborne remote sensing - Sensitivity, calibrations and correction p 73 A87-48873

Discrimination of suspended sediment and littoral features using multispectral video imagery p 73 A87-48874

## ROBERTSON, DOUGLAS S.

Radio interferometry p 21 A87-46688  
A program for the combined adjustment of VLBI observing sessions p 22 A87-52766

## ROBERTSON, FRANKLIN R.

Use of IR satellite rainfall estimates in diagnosing thermally forced circulations in the Pacific during FGGE SOP-1 p 36 A87-51580  
Latent heat and cyclone activity in the South Pacific, 10-18 January 1979 p 37 A87-51603

## ROBERTSON, S. L.

TM and MEIS data for future Alberta forest inventories p 8 A87-48900

## ROBINSON, ALLAN R.

Altimetric data assimilation for ocean dynamics and forecasting p 39 A87-52516

## ROBINSON, M. R.

Monitoring rice areas using Landsat MSS data p 1 A87-45047

## ROCHON, G.

A study of the potential application of SPOT imagery in structural geology p 24 A87-48827  
A revolution in the production of small-scale and medium-scale maps p 61 A87-48904  
Study on the use of SAR data for agriculture and forestry p 15 A87-27862

## ROCK, B.

The global forest ecosystem as viewed by ERS-1, SIR-C and EOS p 12 A87-53217

## ROCK, BARRETT N.

Measurement of leaf relative water content by infrared reflectance p 9 A87-53024

## RODRIGUEZ, E.

Global digital topography mapping using a scanning radar altimeter p 76 A87-53227

## RODRIGUEZ, ERNESTO

Deconvolution of sea state parameters from altimeter waveforms p 41 A87-53198

## ROEKAERTS, M.

Crop inventorying of small-parcelled areas using SPOT- and TM-data in conjunction with field radiometric measurements p 10 A87-53126

## ROONEY, S. T.

Till beneath ice stream B. I - Properties derived from seismic travel times. II - Structure and continuity. III - Till deformation - Evidence and implications. IV - A coupled ice-till flow model p 37 A87-51948

## ROSE, D. R.

Applications of satellite derived digital elevation models for resource mapping p 60 A87-48866

## ROSS, I. K.

Monte Carlo calculation of the dependence of the spectral radiance of vegetation cover on the illumination conditions p 2 A87-48190

## ROSSEEL, G.

Hydrologic applications of weather radar data p 52 A87-48875

## ROTT, H.

The potential of SAR in a snow and glacier monitoring system p 45 A87-27856

## ROVINSKII, I. A.

Monitoring the background pollution of natural environments, No. 3 p 19 A87-52241  
Problems in the background monitoring of the environment, No. 4 p 19 A87-52242

## ROZANOVA, E. I.

Estimation of errors in the determination of sea surface temperature and atmospheric moisture content from satellite measurements of outgoing IR radiation in the 10.5-12.5 micron range p 33 A87-48178

## RUBINSTEIN, I. G.

Optimum use of dual frequency passive microwave measurements for ice/ocean interactions p 43 A87-53240

## RUF, C.

A microwave radiometer weather-correcting sea ice algorithm p 29 A87-45024

## RUMIANSEVA, ELIA FEDOROVNA

Elements of lineament tectonics p 27 A87-53954

## RUNNING, STEVEN W.

Relationship of Thematic Mapper simulator data to leaf area index of temperate coniferous forests p 8 A87-53017

## RUSSELL, W. G. R.

Spectral studies of dryland agricultural salinity in Western Australia p 8 A87-48901

## RUSSON, B.

Indices of climatological and hydrological variability derived from satellite imagery for the South Saskatchewan River Basin p 52 A87-48856

## S

## SABADINI, ROBERTO

Azimuthal dependence in the gravity field induced by recent and past cryospheric forcings p 35 A87-51487

## SACK, M.

The ERS-1/RADARSAT SAR Canadian ground segment p 61 A87-48896

## SADER, STEVEN A.

Digital image classification approach for estimating forest clearing and regrowth rates and trends p 10 A87-53123

## SADO, E. V.

Evaluation of MEIS-II multispectral scanner data for quaternary geological mapping in the Chatham area, southwestern Ontario p 24 A87-48816

## SADOWSKI, F. G.

Monitoring the fire-danger hazard of Nebraska rangelands with AVHRR data p 17 A87-48838

## SAIDOV, M. S.

Application of space photographs to geomorphological investigations in southwestern Tadzhikistan p 23 A87-48186

## SAILOR, RICHARD V.

Preliminary determination of the Geosat radar altimeter noise spectrum p 38 A87-52503

## SAITOU, IKUO

Analysis of environmental information of urban areas using Landsat TM data p 19 A87-53187

## SAKAMOTO, CLARENCE M.

Smoothing vegetation index profiles - An alternative method for reducing radiometric disturbance in NOAA-AVHRR data p 14 A87-53996

## SALOM, M. J.

A model of thermal inertia for frost forecasting in agricultural areas p 16 A87-28151

## SALOMONSON, V. V.

Comparative analysis of different sensor data (Landsat-TM and MOMS) for earth observation and impact on future sensor development p 71 A87-48674

MODIS - Advanced facility instrument for studies of the earth as a system p 40 A87-53144

## SALVI, S.

Use of TM Landsat data as a support to classical ground-based methodologies in the investigation of a volcanic site in central Italy - The Caldera of Latara p 26 A87-53244

## SAMADANI, R.

Observing rotation and deformation of sea ice with synthetic aperture radar p 43 A87-53239

## SANCHINI, P. J.

Biomonitoring plots at the ozone monitoring stations at Great Smoky Mountains National Park, 1985 survey results [PB87-172078] p 19 A87-26464

## SATO, HIDEO

Some results of MOS-1 airborne verification experiment - MSR (microwave scanning radiometer) p 76 A87-53229

## SAUL'SKII, V. K.

A method for the optimization of orbits and structures of satellite systems for the periodic round-the-clock survey of the earth p 21 A87-42938

## SCHLITTENHARDT, P.

Coastal Zone Color Scanner (CZCS) images and ocean dynamics. Application to the Northwest African upwelling area p 46 A87-28146

ADRIA 84: Airborne investigations of Gelbstoff by optical radiometry and fluorescence lidar p 46 A87-28154

## SCHMITZ-PEIFFER, A.

Remote sensing of suspended matter in the ocean by airborne lasers and satellite radiometers [GKSS-86/E/49] p 45 A87-26405

## SCHMUGGE, T. J.

Airborne multispectral observations over burned and unburned prairies p 10 A87-53122

Results from the pushbroom microwave radiometer flights over the Konza Prairie in 1985 p 11 A87-53206

## SCHMUGGE, THOMAS J.

Retrieval of surface roughness parameters from dual-frequency measurements of radar backscattering coefficients p 10 A87-53130

## SCHOTT, F.

Physical oceanographic study of Florida's Atlantic Coast region: Florida Atlantic Coast Transport Study (FACTS). Volume 1: Executive summary p 49 A87-30015  
[PB87-200994]

Physical oceanographic study of Florida's Atlantic Coast region: Florida Atlantic Coast Transport Study (FACTS), volume 2 p 49 A87-30016  
[PB87-201000]

Physical oceanographic study of Florida's Atlantic Coast region: Florida Atlantic Coast Transport Study (FACTS). Volume 3: Appendices p 49 A87-30017  
[PB87-201018]

## SCHOTT, JOHN R.

Scene to scene radiometric normalization of the reflected bands of the Landsat Thematic Mapper p 71 A87-48654

## SCHULTE, H. R.

Investigation of design parameters for ERS-1 wind scatterometer p 74 A87-53116

## SCHULTZ, GERT A.

Satellite remote sensing for water resources management: Some engineering and economic aspects p 54 A87-28139

## SCHUMACHER, A. E. A.

Indexing small catchments in Java, Indonesia, with respect to their relative susceptibility to erosion p 52 A87-48871

## SCOTT, J. F.

Observations of and a new model for fetch-limited wave growth p 43 A87-53263

## SCULLY-POWER, P.

The Bakerian Lecture, 1986 - Ships from space p 44 A87-54301

## SELIGMANN, JEAN-LUCIEN

Photogrammetry from SPOT with Matra TRASTER analytical plotter p 58 A87-48665

## SELLERS, PIERIS J.

The First ISLSCP Field Experiment (FIFE) p 12 A87-53218

## SELYAM, A. MARY

Remote sensing of geomagnetic field and applications to climate prediction p 74 A87-53108

## SESOEREN, A.

SPOT: How good for geology? A comparison with Landsat MSS p 27 A87-28121

## SEUTHE, C.

A geobotanic approach to the study of the geology of Cape Smith using Landsat-MSS data p 25 A87-48860

## SHABTAIE, S.

Ice dynamics at the mouth of ice stream B, Antarctica p 37 A87-51946

Velocity of ice streams B and C, Antarctica p 37 A87-51947

- SHABTAIE, SION**  
The morphology of ice streams A, B, and C, West Antarctica and their environs p 37 A87-51945
- SHARKOV, E. A.**  
Foam activity on the sea surface as a Markov random process p 28 A87-44289
- SHAW, PETER R.**  
Investigations of relative plate motions in the South Atlantic using Seasat altimeter data p 38 A87-51963
- SHAW, V. L.**  
Iceberg detection using SLAR p 34 A87-48876
- SHEARN, T. S.**  
Managing coral reefs - Operational benefits of remote sensing in Marine Park planning p 34 A87-48851
- SHIKINA, M. I.**  
Investigation of causes of hydrogen sulfide formation in reclaimed water p 14 A87-23136
- SHIM, TAEBO**  
Satellite observations of surface temperatures and flow patterns, Sea of Japan and East China Sea, late March 1979 p 40 A87-53020
- SHIN, R. T.**  
Theoretical models for microwave remote sensing of snow-covered sea ice p 42 A87-53236
- SHINBEROV, B. L.**  
Remote-sensing evaluation of moisture supply to crops according to the leaf-surface thermal regime p 2 A87-47582
- SHU, NING**  
Geometric correction of space images by the collinearity-equation method p 61 A87-51175
- SHUCHMAN, R.**  
Mesoscale eddies in the Fram Strait marginal ice zone during the 1983 and 1984 Marginal Zone Experiments p 31 A87-47291
- SHUCHMAN, R. A.**  
Use of synthetic aperture radar-derived kinematics in mapping mesoscale ocean structure within the interior marginal ice zone p 31 A87-47294  
Progress on digital algorithms for deriving sea ice parameters from SAR data p 43 A87-53238
- SHUHY, JOSEPH L.**  
Comparison of Geosat and ground-truth wind and wave observations - Preliminary results p 38 A87-52509
- SHUL'GIN, O. V.**  
Analysis of Cosmos-1500 radar images of the ocean surface in a zone of cyclones and mesoscale cloud formations p 32 A87-48176
- SIEBER, A. J.**  
On the origin of cross-polarization in remote sensing p 75 A87-53168  
The global forest ecosystem as viewed by ERS-1, SIR-C and EOS p 12 A87-53217  
The European Campaign 'AGRISAR '86' p 13 A87-53249
- SIMONIN, A.**  
Geomorphological interpretation of the SPOT image of February 23, 1986 concerning Djebel Amour (Algeria) and its border with the Sahara p 25 A87-51145
- SINYAK, YU. YE.**  
Investigation of causes of hydrogen sulfide formation in reclaimed water p 14 A87-23136
- SIROIS, J.**  
Landsat thematic mapper data in wildlife habitat management - Reference to deer wintering habitat p 5 A87-48845
- SKINGLEY, J.**  
Thin line detection in SAR images p 66 A87-27860
- SKORIK, A. V.**  
Water-cycle processes in geosystems and the possibility of the remote sensing of the moisture content of the underlying surface p 51 A87-47580
- SKOU, NIELS**  
Microwave radiometry study concerning pushbroom systems. Volume 1: A sea salinity/soil-moisture pushbroom radiometer system [R-322] p 79 A87-28951
- SKRIVER, H.**  
Active microwave observations of sea ice and icebergs p 45 A87-27855
- SKRIVER, HENNING**  
Sea ice observations by SAR p 47 A87-28156
- SLATER, P. N.**  
Reflectance- and radiance-based methods for the in-flight absolute calibration of multispectral sensors p 69 A87-44863  
Absolute calibration of the SPOT-1 HRV cameras p 71 A87-48660
- SLATER, PHILIP N.**  
Earth remote sensing using the Landsat Thematic Mapper and SPOT sensor systems; Proceedings of the Meeting, Innsbruck, Austria, Apr. 15-17, 1986 [SPIE-660] p 70 A87-48652
- SLOTH, PETER**  
Large scale sea ice studies based on Scanning Multichannel Microwave Radiometers (SMMR) data p 16 A87-28148
- SMITH, A. M.**  
Glaciological studies on Rutford ice stream, Antarctica p 38 A87-51950
- SMITH, ERIC A.**  
Investigating the role of the land surface in explaining the interannual variation of the net radiation balance over the Western Sahara and sub-Sahara [NASA-CR-181183] p 68 A87-28197
- SMITH, F. R.**  
Monitoring rice areas using Landsat MSS data p 1 A87-45047
- SMITH, M. P.**  
Observing rotation and deformation of sea ice with synthetic aperture radar p 43 A87-53239
- SMITH, NEIL R.**  
Moisture bursts over the tropical Pacific Ocean p 28 A87-43345
- SMITH, RAYMOND C.**  
Multiplatform sampling (ship, aircraft, and satellite) of a Gulf Stream warm core ring p 29 A87-44811
- SMITH, SAMUEL L., III**  
Determination of ocean geodetic data from Geosat p 38 A87-52506
- SMITH, WILLIAM L.**  
Planning for future operational sensors and other priorities [NOAA-NESDIS-30] p 77 A87-25560
- SMOLOV, V. E.**  
Maximum accuracy of satellite-borne scatterometer measurements of wind velocity above the ocean p 33 A87-48184
- SMOOT, GEORGE**  
Development of EOS-aided procedures for the determination of the water balance or hydrologic budget of a large watershed p 53 A87-53215
- SNEYD, A. R.**  
Operational use of remote sensing for commercial Arctic class vessel navigation p 33 A87-48829  
The influence of melting conditions on the interpretation of radar imagery of sea ice p 34 A87-48849
- SNYDER, B. A.**  
Comparisons of FGGE IIb and IIb winds in a tropical synoptic system p 35 A87-51559
- SOBRINO, J. A.**  
Thermal infrared images from satellites compared to shelter temperature. Application to frost nowcasting in a citrus orchard p 15 A87-28136
- SOEGAARD, HENRIK**  
Snow mapping in western Greenland p 54 A87-28150
- SOLOMON, S. I.**  
Forecast of hurricane characteristics from GOES imagery p 59 A87-48818
- SOMERFELDT, T. G.**  
Extent of saline/waterlogged lands within irrigated Alberta. I - Inventory and preliminary evaluation of existing mapping data p 5 A87-48830
- SPANNER, MICHAEL A.**  
Relationship of Thematic Mapper simulator data to leaf area index of temperate coniferous forests p 8 A87-53017
- SPATZ, D. M.**  
Application of TM imagery to mapping volcanic rock assemblages at tertiary calderas of the basin and range province p 26 A87-53257
- SPEIGHT, C. A.**  
Integrated multi-temporal aerial photography and digital mapping for coastal monitoring, Cape Breton Island, Nova Scotia p 34 A87-48837
- SPIESS, E.**  
Point positioning and mapping with large format camera data p 73 A87-50226
- SPITZER, D.**  
Shallow water bathymetry and bottom classification by means of the Landsat and SPOT optical scanners p 52 A87-48670
- SQUICCIARINI, MARTIN**  
The feasibility of detecting a magnetic field from a distant platform [AD-A180635] p 78 A87-27310
- SQUIRE, VERNON**  
Shuttle Imaging Radar B (SIR-B) Weddell Sea ice observations - A comparison of SIR-B and scanning multichannel microwave radiometer ice concentrations p 32 A87-47300
- SROKOSZ, M. A.**  
The determination of sea-state bias and non-linear wave parameters from satellite altimeter data p 46 A87-28132
- ST. MARTIN, JOSEPH W.**  
Arctic drifting buoy data 1979 - 1985 [AD-A182967] p 50 A87-30019
- ST-JULIEN, P.**  
A study of the potential application of SPOT imagery in structural geology p 24 A87-48827
- STAELIN, DAVID H.**  
Information content analysis of Landsat image data for compression p 56 A87-47046
- STAENZ, K.**  
Hierarchical classification with knowledge based binary decision p 62 A87-53110
- STAKENBORG, JACQUES H. T.**  
Exploring the spatial domain p 62 A87-53112
- STARORUSSKAIA, G. G.**  
Determination of the initial motion conditions of earth-resources satellites according to the photogrammetric processing of topographic photographs oriented in inertial space p 56 A87-47506
- STEFFENSEN, R.**  
An evaluation of Landsat TM and MSS data for crop identification in Manitoba p 6 A87-48859
- STEIN, S. J.**  
Biomonitoring plots at the ozone monitoring stations at Great Smoky Mountains National Park, 1985 survey results [PB87-172078] p 19 A87-26464
- STEPHENSON, S. N.**  
Ice dynamics at the mouth of ice stream B, Antarctica p 37 A87-51946
- STONE, THOMAS A.**  
Analysis of forest and forest clearings in Amazonia with Landsat and Shuttle Imaging Radar-A data p 13 A87-53250
- STOWE, LARRY**  
Planning for future operational sensors and other priorities [NOAA-NESDIS-30] p 77 A87-25560
- STRAHLER, ALAN H.**  
Modeling gap probability in discontinuous vegetation canopies p 13 A87-53276
- STRATHMANN, F.-W.**  
Urban development planning using thematic mapper data of Munich (FRG) p 20 A87-28117
- STREBEL, DONALD E.**  
Landscape pattern and successional dynamics in the boreal forest p 11 A87-53155
- STROBL, D.**  
The potential of SAR in a snow and glacier monitoring system p 45 A87-27856
- STROM, A. L.**  
Application of space photographs to paleoseismological investigations (with reference to the Mongolian Altai) p 23 A87-48187
- STRONG, A.**  
Sea surface temperature retrieval from the Tiros-N AVHRR instrument for the FGGE period (Dec. 1978-Nov. 1979) p 35 A87-51553
- STUCKY, RICHARD K.**  
Analysis of Eocene depositional environments - Preliminary TM and TIMS results, Wind River Basin, Wyoming p 26 A87-53243
- STURM, B.**  
Correction of the sensor degradation of the Coastal Zone Color Scanner on NIMBUS-7 p 46 A87-28153
- SUITSU, TAKESHI**  
Observation of oil slicks on the ocean by X-band SLAR p 41 A87-53191
- SUN, WEIDONG**  
Geometric distortion correction with high accuracy for NOAA satellite images p 65 A87-53253
- SUSSKIND, J.**  
Cloud and moisture fields derived from the GLA retrievals of HIRS2/MSU data p 36 A87-51579
- SUTANTO**  
Remote sensing in Indonesia - A review of the available technology and its applications for resources surveys p 17 A87-46310
- SUTHERLAND, I.**  
Large-scale black and white and natural color photographs for the measurement of tree crown areas p 3 A87-48815  
Snowpack depletion monitoring in Alberta using computer-processed NOAA imagery p 52 A87-48848  
MEIS II imagery for environmental stress analysis p 72 A87-48865
- SUTOVSKII, V. M.**  
Estimation of errors in the determination of sea surface temperature and atmospheric moisture content from satellite measurements of outgoing IR radiation in the 10.5-12.5 micron range p 33 A87-48178
- SUTTON, J.**  
Technological feasibility to mobilization for operations - The NOAA crop monitoring case p 6 A87-48878  
Sea surface temperature retrieval from the Tiros-N AVHRR instrument for the FGGE period (Dec. 1978-Nov. 1979) p 35 A87-51553

## SUTTON, J. F.

- The evaluation of TM analysis as a tool in monitoring land use and agricultural stress in Egypt  
p 18 A87-48903

## SVENDSEN, E.

- Mesoscale eddies in the Fram Strait marginal ice zone during the 1983 and 1984 Marginal Zone Experiments  
p 31 A87-47291

## SVENDSEN, E. A.

- Evolution of microwave sea ice signatures during early summer and midsummer in the marginal ice zone  
p 31 A87-47293

## SVENSSON, C.

- Geological feature enhancement in SAR imagery  
p 67 N87-27861

## SWIFT, C.

- A multifrequency microwave radiometer of the future  
p 75 A87-53180

## SWIFT, C. T.

- A microwave radiometer weather-correcting sea ice algorithm  
p 29 A87-45024

## SWIFT, CALVIN T.

- NASA sea ice and snow validation plan for the Defense Meteorological Satellite Program special sensor microwave/imager [NASA-TM-100683]  
p 49 N87-30018

## SWIFT, R. N.

- Observations of and a new model for fetch-limited wave growth  
p 43 A87-53263

## SWIFT, ROBERT N.

- Radiance-ratio algorithm wavelengths for remote oceanic chlorophyll determination  
p 29 A87-44812

## T

## TAILOR, A.

- A system for knowledge-based segmentation of remotely-sensed images  
p 11 A87-53136

## TAKAGI, MIKIO

- Geometric distortion correction with high accuracy for NOAA satellite images  
p 65 A87-53253

## TARANIK, J. V.

- Application of TM imagery to mapping volcanic rock assemblages at tertiary calderas of the basin and range province  
p 26 A87-53257

## TARPLEY, D.

- Cloud screening for determination of land surface characteristics in a reduced resolution satellite data set  
p 56 A87-48361

## TASSAN, S.

- Evaluation of the potential of the Thematic Mapper for marine application  
p 46 N87-28134

## TATEISHI, RYUTARO

- Land cover classification using SPOT data  
p 18 A87-50227

## TAYLOR, G. E., JR.

- Effects of ozone on forests in the northeastern United States [DE87-010887]  
p 16 N87-28190

## TEILLET, P. M.

- An evaluation of sun angle computation algorithms  
p 59 A87-48812

## TEILLET, PHILIPPE M.

- The CCRS SAR/MSS Anderson River data set  
p 55 A87-43261

## TEUBER, KURT B.

- Relationship of Thematic Mapper simulator data to leaf area index of temperate coniferous forests  
p 8 A87-53017

## THERRIEN, M.

- Landsat Thematic Mapper data - A useful tool for mapping agricultural areas in Quebec  
p 6 A87-48867

## THOMAS, RANDALL

- Development of EOS-aided procedures for the determination of the water balance or hydrologic budget of a large watershed  
p 53 A87-53215

## THOMASON, LARRY W.

- Interpreting meteorological satellite images using a color-composite technique  
p 62 A87-52795  
Improved cloud analysis using visible, near-infrared, infrared, and microwave imagery  
p 62 A87-53103

## THOMPSON, A. H.

- Comparisons of FGGE IIb and IIb winds in a tropical synoptic system  
p 35 A87-51559  
Wintertime disturbances in the tropical Pacific - FGGE IIb and satellite comparisons  
p 36 A87-51560  
Moisture transports and budgets of 'moisture bursts'  
p 36 A87-51593

## THOMPSON, AYLMER H.

- Moisture bursts over the tropical Pacific Ocean  
p 28 A87-43345

- Application of satellite data to tropic-subtropical moisture coupling [NASA-CR-4092]  
p 48 N87-29067

## THOMPSON, J. DANA

- REX and Geosat - Progress in the first year  
p 39 A87-52511

## THOMPSON, M. D.

- MEIS II imagery for environmental stress analysis  
p 72 A87-48865

- Remote sensing as a tool for Alberta Agricultural Wetlands Drainage Inventory  
p 6 A87-48882

## THOMPSON, M. DIANE

- Canadian Symposium on Remote Sensing, 10th, Edmonton, Canada, May 5-8, 1986, Proceedings. Volume 1 & 2  
p 72 A87-48801

## THOMSON, K. P. B.

- Application of image segmentation algorithms to the inventory of crops in Canada  
p 3 A87-48813  
Comparison of C-band synthetic aperture radar (SAR) data according to two different depression angles for agricultural applications  
p 4 A87-48820  
Study on the use of SAR data for agriculture and forestry  
p 15 N87-27862

## THOMSON, RICHARD E.

- Upwelling filaments and motion of a satellite-tracked drifter along the west coast of North America  
p 29 A87-45023

## THYRSTED, TAGE

- Comparison of visual and automated lineament analyses on LANDSAT MSS image from south Greenland  
p 67 N87-28144

## TILL, S.

- CCRS airborne Electro-Optical Facility  
p 72 A87-48852

## TILL, S. M.

- The RADARSAT RMOMS optical sensor  
p 73 A87-48890

## TILLEY, DAVID G.

- Approximating SIR-B response characteristics and estimating wave height and wavelength for ocean imagery  
p 44 A87-53288

## TIPIE, V. K.

- Characterizing the Chesapeake Bay ecosystem and lessons learned [PB87-166930]  
p 19 N87-26463

## TIURI, MARTTI

- Monitoring of snow cover from satellite  
p 54 N87-28123

## TOGLIATTI, G.

- Some results of the Metric Camera (MC) Mission-1 on Spacelab  
p 70 A87-47175  
Large Format Camera: The second generation photogrammetric camera for space cartography  
p 78 N87-28118

## TOUTIN, TH.

- A revolution in the production of small-scale and medium-scale maps  
p 61 A87-48904  
Development of a mathematical model for the spatial triangulation of SPOT images  
p 61 A87-48905

## TOUZI, R.

- A statistical and geometrical edge detector for SAR image segmentation  
p 13 A87-53275

## TREVETT, J. W.

- Land use feature detection in SAR images  
p 67 N87-27863

## TRIGILA, R.

- Use of TM Landsat data as a support to classical ground-based methodologies in the investigation of a volcanic site in central Italy - The Caldera of Latara  
p 26 A87-53244

## TRIVERO, P.

- Climatological implications of a satellite-borne SAR imaging the sea surface  
p 30 A87-46403

## TROFIMOV, DMITRII MIKHAILOVICH

- Remote-sensing and geological-geophysical studies of closed platform territories  
p 26 A87-51875

## TRUAX, D. N.

- Using NOAA AVHRR in studies of sea ice motion in the Beaufort Sea  
p 34 A87-48842  
Analysis of data from the DFO fluorescence line imager  
p 72 A87-48844

## TUCKER, C. J.

- The contribution of AVHRR data for measuring and understanding global processes - Large-scale deforestation in the Amazon basin  
p 11 A87-53151

## TURCOTTE, DONALD L.

- Mechanisms of crustal deformation in the western US [NASA-CR-181230]  
p 27 N87-28200

## TURNER, T.

- An algorithm for automatically acquiring ground control points in SAR imagery  
p 67 N87-27864

## U

## ULABY, F.

- Synergism requirements and concepts for SAR and HIRIS on EOS  
p 75 A87-53216

## ULABY, F. T.

- Millimeter-wave polarimetric measurements of artificial and natural targets  
p 75 A87-53163

## ULANDER, L.

- Active microwave observations of sea ice and icebergs  
p 45 N87-27855

## ULANDER, LARS M. H.

- Averaging of radar altimeter pulse returns with the interpolation tracker  
p 70 A87-45044

## ULIANA, ENZO A.

- Comparison of Geosat and ground-truth wind and wave observations - Preliminary results  
p 38 A87-52509

## ULRIKSEN, P.

- Geological feature enhancement in SAR imagery  
p 67 N87-27861

## UMEHARA, TOSHIHIKO

- Observation of oil slicks on the ocean by X-band SLAR  
p 41 A87-53191

## URMAEV, M. S.

- Determination of the initial motion conditions of earth-resources satellites according to the photogrammetric processing of topographic photographs oriented in inertial space  
p 56 A87-47506

## USPENSKII, A. B.

- Estimation of errors in the determination of sea surface temperature and atmospheric moisture content from satellite measurements of outgoing IR radiation in the 10.5-12.5 micron range  
p 33 A87-48178

## V

## VACHON, P. W.

- Airborne SAR imaging of azimuthally travelling ocean surface waves - The LEWEX experimental plan  
p 44 A87-53266

## VAN CAMP, L.

- A multi-source image set for the study of soil texture and drainage as observed from Thematic Mapper data in Northern Belgium  
p 10 A87-53125  
The detection of soil drainage by using Landsat MSS and TM (Belgian test zones)  
p 11 A87-53205

## VAN DER GRIENT, C.

- Preliminary results from modelling vegetation spectra derived from MEIS data, Algonquin Park, Ontario  
p 7 A87-48891

## VAN DIJK, ALBERT

- Smoothing vegetation index profiles - An alternative method for reducing radiometric disturbance in NOAA/AVHRR data  
p 14 A87-53996

## VAN HEE, DENNIS H.

- Preliminary results from the processing of a limited set of Geosat radar altimeter data  
p 22 A87-52507

## VAN R. CLAASEN, A.

- Managing coral reefs - Operational benefits of remote sensing in Marine Park planning  
p 34 A87-48851

## VAN ZYL, JAKOB J.

- Radar polarization signatures of vegetated areas  
p 11 A87-53202

## VANCAMP, L.

- Coastal Zone Color Scanner (CZCS) images and ocean dynamics. Application to the Northwest African upwelling area  
p 46 N87-28146

## VANDERBILT, V.

- Synergism requirements and concepts for SAR and HIRIS on EOS  
p 75 A87-53216

## VANE, DEBORAH

- Earth resources instrumentation for the Space Station Polar Platform  
p 69 A87-44184

## VARGO, S.

- Physical oceanographic study of Florida's Atlantic Coast region: Florida Atlantic Coast Transport Study (FACTS). Volume 1: Executive summary  
p 49 N87-30015

- Physical oceanographic study of Florida's Atlantic Coast region: Florida Atlantic Coast Transport Study (FACTS), volume 2  
p 49 N87-30016

- Physical oceanographic study of Florida's Atlantic Coast region: Florida Atlantic Coast Transport Study (FACTS). Volume 3: Appendices  
p 49 N87-30017

- [PB87-201000]  
p 49 N87-30017

## VAUGHAN, D. G.

- Glaciological studies on Rutford ice stream, Antarctica  
p 38 A87-51950

## VAUGHAN, R. A.

- Sea surface temperatures and the detection of ocean circulation patterns and fronts from AVHRR imagery  
p 45 N87-28125

## VEROSUB, KEN

- Kinematics at the intersection of the Garlock and Death Valley fault zones, California: Integration of TM data and field studies. LANDSAT TM investigation proposal TM-019  
p 27 N87-28208

- [NASA-CR-180666]  
p 27 N87-28208

- VERSTAPPEN, HERMAN TH.**  
Remote sensing applications of the earth's surface - An outlook into the future p 70 A87-47173
- VESECKY, J. F.**  
Spacecraft on-board SAR image generation for EOS-type missions p 76 A87-53232  
Observing rotation and deformation of sea ice with synthetic aperture radar p 43 A87-53239
- VICKERS, H.**  
Comparison of Landsat Thematic Mapper and Multispectral Scanner information content for agricultural applications in Western Canada p 6 A87-48863  
Interpretation of prairie land cover types from SIR-B data p 7 A87-48888
- VIDAL-MADJAR, DANIEL**  
Effect of resolution on texture application to nearly simultaneous AVHRR and MSS images of an agricultural region p 9 A87-53111
- VIDAL, GERARD F.**  
Characteristics of the Gregory Rift (Kenya) dynamics, ground structural analysis, and remote sensing p 23 A87-43353
- VIEIRADUTRA, LUCIANO**  
Enhancement of colors in remote sensing images using rotation of the matrix at the LHS coordinates [INPE-4207-PRE/1088] p 67 N87-28165
- VIGNEAULT, C. G.**  
An evaluation of sun angle computation algorithms p 59 A87-48812
- VIGNERON, CHRISTIAN**  
Photogrammetry from SPOT with Matra TRASTER analytical plotter p 58 A87-48665
- VINCENT, D. G.**  
Latent heat and cyclone activity in the South Pacific, 10-18 January 1979 p 37 A87-51603
- VINCENT, P.**  
Study on the use of SAR data for agriculture and forestry p 15 N87-27862
- VINOGRADOVA, L. A.**  
Investigation of causes of hydrogen sulfide formation in reclaimed water p 14 N87-23136
- VITKUS, R. IU.**  
Stereoscopic visualization of aerial and space photographs in thematic mapping p 23 A87-42937
- VLODAVETS, V. V.**  
Investigation of causes of hydrogen sulfide formation in reclaimed water p 14 N87-23136
- VOLCHOK, WILLIAM J.**  
Scene to scene radiometric normalization of the reflected bands of the Landsat Thematic Mapper p 71 A87-48654
- VOLK, P.**  
Significance of TM data as a tool to support regional planning activities p 17 A87-48671  
Integration of remote sensing and geophysical data-application to exploration of pyrite ore facies in SW Spain p 27 N87-28119
- VOUTE, CAESAR**  
The future generation of resources satellites p 80 A87-53742
- W**
- WACKERMAN, C. C.**  
Progress on digital algorithms for deriving sea ice parameters from SAR data p 43 A87-53238
- WACKERMAN, CHRISTOPHER C.**  
Modeling of focus effects in SAR images of the ocean surface p 42 A87-53212  
Automatic focusing of synthetic aperture radar images of diffuse targets p 64 A87-53213
- WADSWORTH, A.**  
SPOT, a satellite for oceanography? p 41 A87-53194
- WAGGETT, P. W.**  
A combined SAR and scatterometer system p 77 A87-53279
- WAHL, T.**  
SAR detection of ships and ship wakes p 66 N87-27859
- WAKABAYASHI, HIROYUKI**  
Some results of MOS-1 airborne verification experiment - MSR (microwave scanning radiometer) p 76 A87-53229
- WALKER, DONALD A.**  
Vegetation and a LANDSAT-derived land cover map of the Beechey Point quadrangle, Arctic Coastal Plain, Alaska [AD-A180931] p 15 N87-27312
- WALKER, RICHARD E.**  
Color enhancement of highly correlated images. II - Channel ratio and 'chromaticity' transformation techniques p 62 A87-53018
- WALL, JOSEPH G.**  
The Geosat radar altimeter p 38 A87-52502
- WALSH, E. J.**  
Observations of and a new model for fetch-limited wave growth p 43 A87-53263
- WALSH, STEPHEN J.**  
Comparison of NOAA AVHRR data to meteorologic drought indices p 14 A87-53997
- WALSTAD, LEONARD J.**  
Altimetric data assimilation for ocean dynamics and forecasting p 39 A87-52516
- WALTER, L.**  
Contribution of space technology to disaster preparedness, warning, and relief p 20 N87-28130
- WALTERS, J. M.**  
A microwave radiometer weather-correcting sea ice algorithm p 29 A87-45024
- WANG, FANGJU**  
Data correction for automated remote sensing image interpretation p 64 A87-53209
- WANG, J. F.**  
A methodology for automated extraction of drainage networks from satellite imagery p 53 A87-48880  
Sequential thinning algorithms for remote sensing application p 63 A87-53140
- WANG, J. R.**  
Roughness measurements with multipolarization aircraft data p 63 A87-53131  
Results from the pushbroom microwave radiometer flights over the Konza Prairie in 1985 p 11 A87-53206
- WANG, JAMES R.**  
Retrieval of surface roughness parameters from dual-frequency measurements of radar backscattering coefficients p 10 A87-53130
- WARD, I. A.**  
A combined SAR and scatterometer system p 77 A87-53279
- WARREN, PETER L.**  
Sampling semiarid vegetation with large-scale aerial photography p 14 A87-53741
- WASA, KIYOTAKA**  
Meissner effect in high-Tc superconductive thin films p 35 A87-51532
- WATTS, R.**  
Study of physical processes on the US mid-Atlantic continental slope and rise. Volume 1: Executive summary [PB87-200515] p 48 N87-30012  
Study of physical processes on the US mid-Atlantic continental slope and rise. Volume 2: Technical presentation [PB87-200523] p 49 N87-30013  
Study of physical processes on the US mid-Atlantic continental slope and rise. Volume 3: Appendix [PB87-200531] p 49 N87-30014
- WEAVER, WILLIAM L.**  
Calculation and accuracy of ERBE scanner measurement locations [NASA-TP-2670] p 47 N87-28471
- WEILER, J.**  
An algorithm for automatically acquiring ground control points in SAR imagery p 67 N87-27864
- WEIN, R. W.**  
Comparison of classification and enhancement techniques using Landsat imagery for the northern coniferous forest p 4 A87-48821
- WEINMAN, J. A.**  
Scattering parameters for aspherical hydrometeors at microwave frequencies p 53 A87-53271
- WELLS, GORDON**  
Workshop on The Earth as a Planet [NASA-CR-180543] p 81 N87-29900
- WELLS, J.**  
Sulphur dioxide damage assessment using colour infrared aerial photography p 60 A87-48884
- WERLE, D.**  
The use of multi-spectral and radar remote sensing data for monitoring forest clearcut and regeneration sites on Vancouver Island p 5 A87-48834
- WERSTIUK, H.**  
The RADARSAT RMOMS optical sensor p 73 A87-48890
- WESLEY, D. E.**  
Inventory of wetlands with Landsat's Thematic Mapper p 3 A87-48817
- WESSELS, G. J.**  
Validation and simulation of Radarsat imagery p 60 A87-48883  
Spatial considerations in speckle simulation p 65 A87-53260
- WESSELS, J.**  
Technological feasibility to mobilization for operations - The NOAA crop monitoring case p 6 A87-48878
- WESSMAN, CAROL A.**  
Estimating key forest ecosystem parameters through remote sensing p 12 A87-53245
- WEST, GLADYS B.**  
Determination of ocean geodetic data from Geosat p 38 A87-52506
- WESTHAVER, A.**  
Environmental monitoring of Alpine Meadows with large scale aerial photography in Banff National Park p 18 A87-48898
- WESTIN, F. C.**  
Using AVHRR data to evaluate the greenness variability within monitoring polygons p 4 A87-48828
- WESTMAN, WALTER E.**  
Detecting forest structure and biomass with C-band multipolarization radar - Physical model and field tests p 2 A87-46543  
Vegetation mapping and stress detection in the Santa Monica Mountains, California p 12 A87-53246
- WESTOVER, D. E.**  
Monitoring the fire-danger hazard of Nebraska rangelands with AVHRR data p 17 A87-48838
- WHARTON, STEPHEN W.**  
The Land Analysis System (LAS) - A general purpose system for multispectral image processing p 64 A87-53230  
A methodology for evaluation of an interactive multispectral image processing system p 66 A87-53999
- WHERRY, DAVID**  
Spectral characteristics and the extent of paleosols of the Palouse formation [NASA-CR-181208] p 17 N87-28195
- WHILLANS, I. M.**  
Velocity of ice streams B and C, Antarctica p 37 A87-51947
- WHILLANS, IAN M.**  
The morphology of ice streams A, B, and C, West Antarctica and their environs p 37 A87-51945
- WHITE, D. B.**  
Landsat-based wildlife habitat mapping - A study of collaboration between analyst and user p 3 A87-48809
- WHITT, M. W.**  
Millimeter-wave polarimetric measurements of artificial and natural targets p 75 A87-53163
- WIESEBECK, W.**  
On the origin of cross-polarization in remote sensing p 75 A87-53168
- WILHEIT, T.**  
A multifrequency microwave radiometer of the future p 75 A87-53180
- WILKERSON, JOHN**  
Validation of Geosat altimeter-derived wind speeds and significant wave heights using buoy data p 39 A87-52510
- WILKINSON, G. G.**  
Towards the automatic recognition and vectorised description of linear features in LANDSAT TM images by artificial intelligence methods p 67 N87-28142
- WILLIAMS, C. P.**  
Status of and prognosis for space remote sensing [AAS PAPER 86-104] p 80 A87-53084
- WILLIAMS, JEROME**  
The International Symposium on Microwave Signatures and Remote Sensing held in Gothenburg (Sweden) on 19-22 January 1987 [AD-A181334] p 78 N87-27314
- WILSON, D. A.**  
The role of remote sensing in the Canada Land Use Monitoring Program (CLUMP) p 18 A87-48895
- WILSON, WILLIAM J.**  
Millimeter-wave imaging sensor data evaluation [NASA-CR-181159] p 77 N87-26264
- WINGHAM, D. J.**  
A study of antenna signal processing techniques for radar alternatives [ESA-CR(P)-2370] p 79 N87-28809
- WONG, A. K. C.**  
Spectral and textural segmentation of multispectral aerial images p 5 A87-48831
- WOOD, SCOTT A.**  
Digital elevation model extraction from stereo satellite images p 63 A87-53142
- WOOD, SCOTT, A.**  
The automatic generation of digital terrain models from satellite images by stereo p 58 A87-48669
- WOODS, KERRY D.**  
Landscape pattern and successional dynamics in the boreal forest p 11 A87-53155
- WOODWELL, GEORGE M.**  
Analysis of forest and forest clearings in Amazonia with Landsat and Shuttle Imaging Radar-A data p 13 A87-53250
- WRIGHT, C. WAYNE**  
Radiance-ratio algorithm wavelengths for remote oceanic chlorophyll determination p 29 A87-44812



## WU, HUEY-TZU

## WU, HUEY-TZU

A multispectral study of the St. Louis area under snow-covered conditions using NOAA-7 AVHRR data  
p 51 A87-46538

## WU, L. K.

Estimation of X-band scattering properties of tree components  
p 13 A87-53277

## WU, SHIH-TSENG

Potential application of multipolarization SAR for pine-plantation biomass estimation p 1 A87-43263  
Integration of topographic data with synthetic aperture radar data for determining forest properties in mountainous terrain p 14 A87-53278

## WYATT, LUCY R.

Ocean wave parameter measurement using a dual-radar system - A simulation study p 33 A87-48363

## Y

## YANG, SHI-REN

The application of remote sensing techniques in China  
p 68 A87-41435

## YATABE, S. M.

A structural analysis of the Mabou Basin, Cape Breton Island using enhanced Landsat MSS imagery  
p 25 A87-48879

## YAZDANI, R.

Comparison of classification and enhancement techniques using Landsat imagery for the northern coniferous forest p 4 A87-48821  
Processing of Seasat altimetry data on a digital image analysis system p 59 A87-48825

## YEE, BEN

An expert system for planimetric feature extraction  
p 63 A87-53139

## YERGEAU, M.

Remote sensing in the Sahel - A tool for the inventory and monitoring of resources p 73 A87-48893

## YUEN, DAVID A.

Azimuthal dependence in the gravity field induced by recent and past cryospheric forcings p 35 A87-51487

## Z

## ZACHARIASEN, F.

The Bakerian Lecture, 1986 - Ships from space  
p 44 A87-54301

## ZAHN, R. W.

An advanced wind scatterometer for the Columbus Polar Platform payload p 74 A87-53117

## ZAITSEV, L. V.

Features of the water dynamics of Lake Ladoga according to remote sensing data p 50 A87-44296

## ZANTOPP, R.

Physical oceanographic study of Florida's Atlantic Coast region: Florida Atlantic Coast Transport Study (FACTS). Volume 1: Executive summary p 49 N87-30015  
[PB87-200994]  
Physical oceanographic study of Florida's Atlantic Coast region: Florida Atlantic Coast Transport Study (FACTS), volume 2 p 49 N87-30016  
[PB87-201000]  
Physical oceanographic study of Florida's Atlantic Coast region: Florida Atlantic Coast Transport Study (FACTS). Volume 3: Appendices p 49 N87-30017  
[PB87-201018]

## ZAPEVALOV, A. S.

Maximum accuracy of satellite-borne scatterometer measurements of wind velocity above the ocean  
p 33 A87-48184

## ZEBKER, H. A.

Interferometric radar measurement of ocean surface currents p 44 A87-54107

## ZEBKER, HOWARD A.

Radar polarization signatures of vegetated areas  
p 11 A87-53202

## ZELEK, JOHN

An expert system for remote sensing p 80 A87-43260  
The CCRS SAR/MSS Anderson River data set p 55 A87-43261

## ZIBORDI, GIUSEPPE

Atmospheric correction of data measured by a flying platform over the sea - Elements of a model and its experimental validation p 35 A87-50292

## ZILGER, J.

Comparative analysis of different sensor data (Landsat-TM and MOMS) for earth observation and impact on future sensor development p 71 A87-48674

## ZIMBELMAN, JAMES R.

Rheology of the 1983 Royal Gardens basalt flows, Kilauea Volcano, Hawaii p 26 A87-51725

## ZIMMERMAN, S. T.

Gulf of Alaska: Physical environment and biological resources  
[PB87-103230] p 47 N87-29033

## ZINKE, PAUL

Development of EOS-aided procedures for the determination of the water balance or hydrologic budget of a large watershed p 53 A87-53215

## ZOUGH, R.

Estimation of X-band scattering properties of tree components p 13 A87-53277

## ZUBENKO, F. S.

Features of the water dynamics of Lake Ladoga according to remote sensing data p 50 A87-44296

## ZUNIGA, A.

Geological interpretations from Landsat of the Troodos Massive, Cyprus p 25 A87-48862

## ZVONAREV, K. A.

Morphometric studies of world ocean  
p 45 N87-28077

## ZWALLY, H. J.

Satellite-derived ice data sets no. 2: Arctic monthly average microwave brightness temperatures and sea ice concentrations, 1973-1976  
[NASA-TM-87825] p 50 N87-30021

## ZWALLY, H. JAY

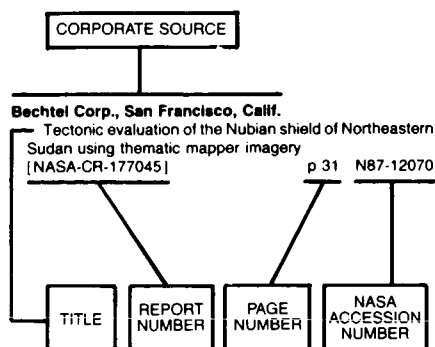
Ice measurements by Geosat radar altimetry  
p 39 A87-52513

# CORPORATE SOURCE INDEX

EARTH RESOURCES / A Continuing Bibliography (Issue 56)

FEBRUARY 1988

## Typical Corporate Source Index Listing



Listings in this index are arranged alphabetically by corporate source. The title of the document is used to provide a brief description of the subject matter. The page number and the accession number are included in each entry to assist the user in locating the abstract in the abstract section. If applicable, a report number is also included as an aid in identifying the document.

## A

- Arbeitsgemeinschaft Geowissenschaftliche Fernerkundung, Munich (West Germany).**  
Study on the use and characteristics of SAR systems for geological applications  
[ESA-CR(P)-2342] p 27 N87-26467
- Arizona State Univ., Tempe.**  
Rheology of the 1983 Royal Gardens basalt flows, Kilauea Volcano, Hawaii p 26 A87-51725
- Arizona Univ., Tucson.**  
Reflectance- and radiance-based methods for the in-flight absolute calibration of multispectral sensors p 69 A87-44863
- Army Cold Regions Research and Engineering Lab., Hanover, N. H.**  
Use of LANDSAT digital data for snow cover mapping in the upper Saint John River Basin, Maine  
[AD-A183213] p 54 N87-29906
- Army Engineer Topographic Lab., Fort Belvoir, Va.**  
A user's guide for the Analytical Photogrammetric Positioning System (APPS)  
[AD-A183773] p 79 N87-29909

## B

- Bail (Roy) Associates Ltd., Ottawa (Ontario).**  
An algorithm for automatically acquiring ground control points in SAR imagery p 67 N87-27864
- Bergen Univ. (Norway).**  
Variations of mesoscale and large-scale sea ice morphology in the 1984 Marginal Ice Zone Experiment as observed by microwave remote sensing p 31 A87-47292
- Evolution of microwave sea ice signatures during early summer and midsummer in the marginal ice zone p 31 A87-47293
- Bern Univ. (Switzerland).**  
Evolution of microwave sea ice signatures during early summer and midsummer in the marginal ice zone p 31 A87-47293

## Bigelow Lab. for Ocean Sciences, West Boothbay Harbor, Maine.

Remote sensing of submerged aquatic vegetation in lower Chesapeake Bay - A comparison of Landsat MSS to TM imagery p 30 A87-46542

## Bologna Univ. (Italy).

Azimuthal dependence in the gravity field induced by recent and past cryospheric forcings p 35 A87-51487

## Butler Univ., Indianapolis, Ind.

Biomonitoring plots at the ozone monitoring stations at Great Smoky Mountains National Park, 1985 survey results  
[PB87-172078] p 19 N87-26464

## C

## California Univ., La Jolla.

Calibration of NOAA-7 AVHRR, GOES-5, and GOES-6 VISSR/VAS solar channels p 69 A87-44865

Satellite color observations of spring blooming in Bering Sea shelf waters during the ice edge retreat in 1980 p 32 A87-47297

## California Univ., Los Angeles.

Measurement of leaf relative water content by infrared reflectance p 9 A87-53024

## California Univ., San Diego.

Multiparameter sampling (ship, aircraft, and satellite) of a Gulf Stream warm core ring p 29 A87-44811

## California Univ., Santa Barbara.

Multiparameter sampling (ship, aircraft, and satellite) of a Gulf Stream warm core ring p 29 A87-44811

Landscape pattern and successional dynamics in the boreal forest p 11 A87-53155

## Cambridge Univ. (England).

Shuttle Imaging Radar B (SIR-B) Weddell Sea ice observations - A comparison of SIR-B and scanning multichannel microwave radiometer ice concentrations p 32 A87-47300

## Canada Centre for Inland Waters, Burlington (Ontario).

Radar scattering and equilibrium ranges in wind-generated waves with application to scatterometry p 28 A87-42746

## Canada Centre for Remote Sensing, Ottawa (Ontario).

The global forest ecosystem as viewed by ERS-1, SIR-C and EOS p 12 A87-53217

## Carnegie Museum of Natural History, Pittsburgh, Pa.

Analysis of Eocene depositional environments - Preliminary TM and TIMS results, Wind River Basin, Wyoming p 26 A87-53243

## Centre National d'Etudes Spatiales, Toulouse (France).

Precise orbit determination with the Doppler Orbitography and Radio positioning Integrated by Satellite (DORIS) system and the associated Zealous for Orbit Observation Methods (ZOOM) software p 77 N87-25382

## Chicago Univ., Ill.

Ice dynamics at the mouth of ice stream B, Antarctica  
[AD-A182967] p 37 A87-51946

## City Coll. of the City Univ. of New York.

Radar scattering and equilibrium ranges in wind-generated waves with application to scatterometry p 28 A87-42746

## Coast Guard Research and Development Center, Groton, Conn.

Arctic drifting buoy data 1979 - 1985  
[AD-A182967] p 50 N87-30019

## Colorado Univ., Boulder.

The high resolution imaging spectrometer (HIRIS) for EOS p 74 A87-53145

Vegetation and a LANDSAT-derived land cover map of the Beechey Point quadrangle, Arctic Coastal Plain, Alaska  
[AD-A180931] p 15 N87-27312

## Commission of the European Communities, Ispra (Italy).

The global forest ecosystem as viewed by ERS-1, SIR-C and EOS p 12 A87-53217

## Computer Sciences Corp., Beltsville, Md.

Retrieval of surface roughness parameters from dual-frequency measurements of radar backscattering coefficients p 10 A87-53130

## Copenhagen Univ. (Denmark).

Coastal Zone Color Scanner (CZCS) images and ocean dynamics. Application to the Northwest African upwelling area p 46 N87-28146

Snow mapping in western Greenland p 54 N87-28150

## Cornell Univ., Ithaca, N.Y.

Mechanisms of crustal deformation in the western US [NASA-CR-181230] p 27 N87-28200

## Corps of Engineers, Detroit, Mich.

Whitetail deer food availability maps from Thematic Mapper data p 14 A87-53998

## Coyote (E.) Enterprises, Inc., Mineral Wells, Tex.

Color infrared video mapping of upland and wetland communities  
[DE87-010202] p 15 N87-28109

## D

## Dartmouth Coll., Hanover, N.H.

Lithologic discrimination using geobotanical and Landsat TM spectral data p 23 A87-48667

## Delaware Univ., Lewes.

Characterizing the Chesapeake Bay ecosystem and lessons learned  
[PB87-166930] p 19 N87-26463

## Delaware Univ., Newark.

Remote sensing of coastal wetlands p 1 A87-40944

Remote sensing of submerged aquatic vegetation in lower Chesapeake Bay - A comparison of Landsat MSS to TM imagery p 30 A87-46542

Characterizing the Chesapeake Bay ecosystem and lessons learned  
[PB87-166930] p 19 N87-26463

## Department of Agriculture, Beltsville, Md.

Retrieval of surface roughness parameters from dual-frequency measurements of radar backscattering coefficients p 10 A87-53130

Roughness measurements with multipolarization aircraft data p 63 A87-53131

Results from the pushbroom microwave radiometer flights over the Konza Prairie in 1985 p 11 A87-53206

## Department of Agriculture, Phoenix, Ariz.

Reflectance- and radiance-based methods for the in-flight absolute calibration of multispectral sensors p 69 A87-44863

## Department of the Navy, Washington, D. C.

Evolution of microwave sea ice signatures during early summer and midsummer in the marginal ice zone p 31 A87-47293

## Deutsche Forschungs- und Versuchsanstalt fuer Luft- und Raumfahrt, Oberpfaffenhofen (West Germany).

ADRIA 84: Airborne investigations of Gelbstoff by optical radiometry and fluorescence lidar p 46 N87-28154

## Digim (1983), Inc. Montreal (Quebec).

Study on the use of SAR data for agriculture and forestry p 15 N87-27862

## Du Pont de Nemours (E. I.) and Co., Alken, S.C.

Color infrared video mapping of upland and wetland communities  
[DE87-010202] p 15 N87-28109

## Dundee Univ. (Scotland).

Sea surface temperatures and the detection of ocean circulation patterns and fronts from AVHRR imagery p 45 N87-28125

On the use of AVHRR channel-3 data for environmental studies p 20 N87-28135

## E

## EG and G Washington Analytical Services Center, Inc., Lanham, Md.

Ice measurements by Geosat radar altimetry p 39 A87-52513

## EG and G Washington Analytical Services Center, Inc., Pocomoke City, Md.

Radiance-ratio algorithm wavelengths for remote oceanic chlorophyll determination p 29 A87-44812

Observations of and a new model for fetch-limited wave growth p 43 A87-53263

**Environmental Protection Agency, Research Triangle Park, N.C.**

Review of control strategies for ozone and their effects on other environmental issues  
[PB87-171195] p 19 N87-25634

**Environmental Research Inst. of Michigan, Ann Arbor.**

Evolution of microwave sea ice signatures during early summer and midsummer in the marginal ice zone  
p 31 A87-47293

Multisensor comparison of ice concentration estimates in the marginal ice zone  
p 31 A87-47295

Theoretical and experimental study of the radar backscatter of Arctic sea ice  
p 43 A87-53237

Investigation of multi-dimensional algorithms using active and passive microwave data for ice concentration determination  
p 43 A87-53241

Comparison of numerical simulations with SAR images of ocean surface waves in the New York Bight  
p 44 A87-53287

Calibrated L-band terrain measurements and analysis program  
[AD-A182917] p 68 N87-29722

**Environmental Research Lab., Gulf Breeze, Fla.**

Characterizing the Chesapeake Bay ecosystem and lessons learned  
[PB87-166930] p 19 N87-26463

**European Space Agency, Paris (France).**

Proceedings of the SAR Applications Workshop  
[ESA-SP-264] p 78 N87-27854

Proceedings of the ESA-EARSel Europe from Space Symposium  
[ESA-SP-258] p 19 N87-28115

**European Space Agency, European Space Research and Technology Center, ESTEC, Noordwijk (Netherlands).**

Summary of recent SAR instrument studies  
p 78 N87-27865

**F****Florence Univ. (Italy).**

Crop discrimination by means of radar and infrared images  
p 15 N87-28128

**Florida State Univ. System, St. Petersburg.**

Physical oceanographic study of Florida's Atlantic Coast region: Florida Atlantic Coast Transport Study (FACTS). Volume 1: Executive summary  
[PB87-200994] p 49 N87-30015

Physical oceanographic study of Florida's Atlantic Coast region: Florida Atlantic Coast Transport Study (FACTS), volume 2  
[PB87-201000] p 49 N87-30016

Physical oceanographic study of Florida's Atlantic Coast region: Florida Atlantic Coast Transport Study (FACTS). Volume 3: Appendices  
[PB87-201018] p 49 N87-30017

**Florida State Univ., Tallahassee.**

Investigating the role of the land surface in explaining the interannual variation of the net radiation balance over the Western Sahara and sub-Sahara  
[NASA-CR-181183] p 68 N87-28197

**G****Geological Survey, Tacoma, Wash.**

Variations of mesoscale and large-scale sea ice morphology in the 1984 Marginal Ice Zone Experiment as observed by microwave remote sensing  
p 31 A87-47292

Multisensor comparison of ice concentration estimates in the marginal ice zone  
p 31 A87-47295

**Geological Survey of the Netherlands, Enschede.**

SPOT: How good for geology? A comparison with LANDSAT MSS  
p 27 N87-28121

**Georgiana Observatory, Budapest (Hungary).**

Catalog of submarine volcanoes and hydrological phenomena associated with volcanic events, January 1, 1900 to December 31, 1959  
[PB87-183943] p 54 N87-28196

**Ghent Univ. (Belgium).**

Detection of soil drainage in Pays de Herve, Belgium, on LANDSAT MSS imagery  
p 15 N87-28129

**GKSS-Forschungszentrum Geesthacht (West Germany).**

Remote sensing of suspended matter in the ocean by airborne lasers and satellite radiometers  
[GKSS-86/E/49] p 45 N87-26405

**H****Harry Diamond Labs., Adelphi, Md.**

Millimeter-wave imaging sensor data evaluation  
[NASA-CR-181159] p 77 N87-26264

**Hawaii Univ., Hilo.**

Digital data from shuttle photography: The effects of platform variables  
p 66 N87-26697

**Helsinki Univ. of Technology, Espoo (Finland).**

Monitoring of snow cover from satellite  
p 54 N87-28123

**Hunter Coll., New York.**

Modeling gap probability in discontinuous vegetation canopies  
p 13 A87-53276

**Hunting Geology and Geophysics Ltd., Boreham Wood (England).**

Land use feature detection in SAR images  
p 67 N87-27863

**I****IBM Italia, Rome.**

Discrimination of natural and cultivated vegetation using Thematic Mapper spectral data  
p 2 A87-48673

**IceCasting, Inc., Seattle, Wash.**

Interpolation, analysis and archival of data on sea ice trajectories and ocean currents obtained from satellite-linked instruments  
[PB87-201430] p 48 N87-30010

**Innsbruck Univ. (Austria).**

The potential of SAR in a snow and glacier monitoring system  
p 45 N87-27856

**Institut fuer Allgemeine und Angewandte Geophysik, Munich (West Germany).**

Requirements on radar data for geological application: A case study by use of multistage data of the test site Sardegna/Italy  
p 27 N87-28120

**Institute of Oceanographic Sciences, Wormley (England).**

The determination of sea-state bias and non-linear wave parameters from satellite altimeter data  
p 46 N87-28132

**Instituto de Pesquisas Espaciais, Sao Jose dos Campos (Brazil).**

Evaluation of the range and degradation of mangroves in Southern Sergipe with remote sensing techniques  
[INPE-4196-PRE/1080] p 16 N87-28160

Enhancement of colors in remote sensing images using rotation of the matrix at the IHS coordinates  
[INPE-4207-PRE/1088] p 67 N87-28165

Brief introduction in statistical pattern recognition  
[INPE-4206-PRE/1087] p 68 N87-28374

Determination of transfer functions from the Thematic Mapper (TM) sensor of the LANDSAT-5 satellite  
[INPE-4213-PRE/1094] p 79 N87-28956

**Instituto Nacional de Investigaciones Agrarias, Madrid (Spain).**

ERAFIS: A computer information system for agriculture and forestry in Spain  
p 16 N87-28140

**International Business Machines Corp., Palo Alto, Calif.**

Discrimination of natural and cultivated vegetation using Thematic Mapper spectral data  
p 2 A87-48673

**Istituto Nazionale di Geofisica, Rome (Italy).**

Azimuthal dependence in the gravity field induced by recent and past cryospheric forcings  
p 35 A87-51487

**J****Jet Propulsion Lab., California Inst. of Tech., Pasadena.**

Optical image subtraction techniques, 1975-1985  
p 55 A87-42659

Earth resources instrumentation for the Space Station Polar Platform  
p 69 A87-44184

Detecting forest structure and biomass with C-band multipolarization radar - Physical model and field tests  
p 2 A87-46543

Multifrequency and multipolarization radar scatterometry of sand dunes and comparison with spaceborne and airborne radar images  
p 70 A87-47257

Beaufort-Chukchi ice margin data from Seasat - Ice motion  
p 32 A87-47299

Shuttle Imaging Radar B (SIR-B) Weddell Sea ice observations - A comparison of SIR-B and scanning multichannel microwave radiometer ice concentrations  
p 32 A87-47300

Color enhancement of highly correlated images. II - Channel ratio and 'chromaticity' transformation techniques  
p 62 A87-53018

Measurement of leaf relative water content by infrared reflectance  
p 9 A87-53024

Selection of extended area land target sites for the calibration of spaceborne scatterometers  
p 74 A87-53118

Automated rectification and geocoding of SAR imagery  
p 63 A87-53143

The high resolution imaging spectrometer (HIRIS) for EOS  
p 74 A87-53145

Spaceborne imaging radar on EOS  
p 63 A87-53148

Wind measurements for non-uniform wind fields from spaceborne scatterometers  
p 75 A87-53195

The effects of wind-wave coupling on scatterometer wind measurement accuracy  
p 41 A87-53196

A comparative study of several wind estimation algorithms for spaceborne scatterometers  
p 41 A87-53197

Deconvolution of sea state parameters from altimeter waveforms  
p 41 A87-53198

Radar polarization signatures of vegetated areas  
p 11 A87-53202

Science synergism study for EOS on evolution of desert surfaces  
p 12 A87-53214

Synergism requirements and concepts for SAR and HIRIS on EOS  
p 75 A87-53216

The global forest ecosystem as viewed by ERS-1, SIR-C and EOS  
p 12 A87-53217

Global digital topography mapping using a scanning radar altimeter  
p 76 A87-53227

The EOS SAR program  
p 76 A87-53228

Spacecraft on-board SAR image generation for EOS-type missions  
p 76 A87-53232

Analysis of Eocene depositional environments - Preliminary TM and TIMS results, Wind River Basin, Wyoming  
p 26 A87-53243

Speckle noise reduction of 1-look SAR imagery  
p 65 A87-53273

Interferometric radar measurement of ocean surface currents  
p 44 A87-54107

Millimeter-wave imaging sensor data evaluation  
[NASA-CR-181159] p 77 N87-26264

Kinematics at the intersection of the Garlock and Death Valley fault zones, California: Integration of TM data and field studies. LANDSAT TM investigation proposal TM-019  
[NASA-CR-180666] p 27 N87-28208

**Johns Hopkins Univ., Laurel, Md.**

The response of SAR imagery to azimuth travelling ocean surface waves as determined from shuttle SAR imagery  
p 44 A87-53286

Approximating SIR-B response characteristics and estimating wave height and wavelength for ocean imagery  
p 44 A87-53288

**Joint Publications Research Service, Arlington, Va.**

Investigation of causes of hydrogen sulfide formation in reclaimed water  
p 14 N87-23136

Successes of Cosmos-1500 satellite, SLR system  
p 45 N87-27696

Morphometric studies of world ocean  
p 45 N87-28077

Major morphologic features of the Atlantic Ocean surface  
p 48 N87-29573

Geomagnetic intersection of tectonic structures seen in space photographs  
p 28 N87-29574

Analysis of directions of linear image elements by structure-zonal method  
p 68 N87-29575

**Joint Research Centre of the European Communities, Ispra (Italy).**

The contribution of AVHRR data for measuring and understanding global processes - Large-scale deforestation in the Amazon basin  
p 11 A87-53151

Rural land use inventory and mapping in the Ardeche area (France). Improvement of automatic classification by multitemporal analysis of TM data  
p 15 N87-28127

Monitoring and modeling of the Adriatic Sea  
p 46 N87-28133

Evaluation of the potential of the Thematic Mapper for marine application  
p 46 N87-28134

The role and perspective of remote sensing for disaster management in the European community  
p 20 N87-28137

Measurement of spectral signatures in Less Favored Areas (LFA): A contribution to the definition of a remote sensing multitemporal experiment  
p 20 N87-28145

Correction of the sensor degradation of the Coastal Zone Color Scanner on NIMBUS-7  
p 46 N87-28153

**K****Kansas Univ. Center for Research, Inc., Lawrence.**

Estimation of X-band scattering properties of tree components  
p 13 A87-53277

**Kington Polytechnic, Kington-Upon-Thames (England).**

Towards the automatic recognition and vectorised description of linear features in LANDSAT TM images by artificial intelligence methods  
p 67 N87-28142

**L****Laval Univ. (Quebec).**

Study on the use of SAR data for agriculture and forestry  
p 15 N87-27862

- Lockheed Engineering and Management Services Co., Inc., Houston, Tex.**  
Estimation of X-band scattering properties of tree components p 13 A87-53277
- Ludwig-Maximilians-Universität, Munich (West Germany).**  
Comparative analysis of different sensor data (Landsat-TM and MOMS) for earth observation and impact on future sensor development p 71 A87-48674  
The impact of LANDSAT Thematic Mapper Data for ecological mapping purposes. A case study at the northern margin of the Alps p 20 N87-28147
- Lunar and Planetary Inst., Houston, Tex.**  
Rheology of the 1983 Royal Gardens basalt flows, Kilauea Volcano, Hawaii p 26 A87-51725  
Workshop on The Earth as a Planet [NASA-CR-180543] p 81 N87-29900
- Lund Univ. (Sweden).**  
Geological feature enhancement in SAR imagery p 67 N87-27861

## M

- Marconi Co. Ltd., Chelmsford (England).**  
Thin line detection in SAR images p 66 N87-27860
- Maryland Univ., College Park.**  
The First ISLSCP Field Experiment (FIFE) p 12 A87-53218  
Characterizing the Chesapeake Bay ecosystem and lessons learned [PB87-166930] p 19 N87-26463
- Massachusetts Inst. of Tech., Cambridge.**  
Theoretical models for microwave remote sensing of snow-covered sea ice p 42 A87-53236  
Remote sensing of earth terrain [NASA-CR-181370] p 79 N87-28957
- Massachusetts Inst. of Tech., Lexington.**  
Space surveillance application potential of Schottky barrier IR sensors [AD-A180848] p 78 N87-27311
- Massachusetts Univ., Amherst.**  
A microwave radiometer weather-correcting sea ice algorithm p 29 A87-45024  
A multifrequency microwave radiometer of the future p 75 A87-53180 p 76 A87-53228
- The EOS SAR program** p 76 A87-53228
- Massachusetts Univ., Boston.**  
NASA sea ice and snow validation plan for the Defense Meteorological Satellite Program special sensor microwave/imager [NASA-TM-100683] p 49 N87-30018
- Miami Univ., Coral Gables, Fla.**  
Calibration requirements and methodology for remote sensors viewing the ocean in the visible p 29 A87-44866
- Miami Univ., Fla.**  
Multiplatform sampling (ship, aircraft, and satellite) of a Gulf Stream warm core ring p 29 A87-44811
- Michigan Univ., Ann Arbor.**  
Synergism requirements and concepts for SAR and HIRIS on EOS p 75 A87-53216  
The global forest ecosystem as viewed by ERS-1, SIR-C and EOS p 12 A87-53217
- Ministère de l'Environnement et du Cadre de Vie, Neuilly (France).**  
Present state, changes, and quality of Sologne and Brenne, two French large wetlands, studied with LANDSAT MSS and TM data p 54 N87-28152
- Minnesota Univ., Minneapolis.**  
Azimuthal dependence in the gravity field induced by recent and past cryospheric forcings p 35 A87-51487  
Scattering parameters for aspherical hydrometeors at microwave frequencies p 53 A87-53271
- Montana Univ., Missoula.**  
Relationship of Thematic Mapper simulator data to leaf area index of temperate coniferous forests p 8 A87-53017
- Montreal Univ. (Quebec).**  
Study on the use of SAR data for agriculture and forestry p 15 N87-27862

## N

- National Aeronautics and Space Administration, Washington, D.C.**  
A multifrequency microwave radiometer of the future p 75 A87-53180  
The First ISLSCP Field Experiment (FIFE) p 12 A87-53218  
HMMR (High-Resolution Multifrequency Microwave Radiometer) Earth observing system, volume 2e. Instrument panel report [NASA-TM-89625] p 78 N87-27316

- National Aeronautics and Space Administration. Ames Research Center, Moffett Field, Calif.**  
Detecting forest structure and biomass with C-band multipolarization radar - Physical model and field tests p 2 A87-46543  
Relationship of Thematic Mapper simulator data to leaf area index of temperate coniferous forests p 8 A87-53017  
Synergism requirements and concepts for SAR and HIRIS on EOS p 75 A87-53216  
Estimating key forest ecosystem parameters through remote sensing p 12 A87-53245  
Vegetation mapping and stress detection in the Santa Monica Mountains, California p 12 A87-53246
- National Aeronautics and Space Administration. Goddard Space Flight Center, Greenbelt, Md.**  
Multiple-angle observations of reflectance anisotropy from an airborne linear array sensor p 69 A87-43262  
Earth resources instrumentation for the Space Station Polar Platform p 69 A87-44184  
Radiometric properties of U.S. processed Landsat MSS data p 55 A87-44864  
Practical aspects of achieving accurate radiometric field measurements p 69 A87-44868  
Variations of mesoscale and large-scale sea ice morphology in the 1984 Marginal Ice Zone Experiment as observed by microwave remote sensing p 31 A87-47292  
Multisensor comparison of ice concentration estimates in the marginal ice zone p 31 A87-47295  
Satellite color observations of spring blooming in Bering Sea shelf waters during the ice edge retreat in 1980 p 32 A87-47297  
On the relationship between atmospheric circulation and the fluctuations in the sea ice extents of the Bering and Okhotsk Seas p 32 A87-47298  
Shuttle Imaging Radar B (SIR-B) Weddell Sea ice observations - A comparison of SIR-B and scanning multichannel microwave radiometer ice concentrations p 32 A87-47300  
The effect of subpixel clouds on remote sensing p 2 A87-48360  
Comparative analysis of different sensor data (Landsat-TM and MOMS) for earth observation and impact on future sensor development p 71 A87-48674  
Cloud and moisture fields derived from the GLA retrievals of HIRS2/MSU data p 36 A87-51579  
Ice dynamics at the mouth of ice stream B, Antarctica p 37 A87-51946  
Snow load effect on earth's rotation and gravitational field, 1979-1985 p 22 A87-51964  
Ice measurements by Geosat radar altimetry p 39 A87-52513  
Retrieval of surface roughness parameters from dual-frequency measurements of radar backscattering coefficients p 10 A87-53130  
Roughness measurements with multipolarization aircraft data p 63 A87-53131  
MODIS - Advanced facility instrument for studies of the earth as a system p 40 A87-53144  
Spaceborne laser ranging from EOS p 22 A87-53146  
The contribution of AVHRR data for measuring and understanding global processes - Large-scale deforestation in the Amazon basin p 11 A87-53151  
Landscape pattern and successional dynamics in the boreal forest p 11 A87-53155  
A multifrequency microwave radiometer of the future p 75 A87-53180  
Results from the pushbroom microwave radiometer flights over the Konza Prairie in 1985 p 11 A87-53206  
Synergism requirements and concepts for SAR and HIRIS on EOS p 75 A87-53216  
The global forest ecosystem as viewed by ERS-1, SIR-C and EOS p 12 A87-53217  
The First ISLSCP Field Experiment (FIFE) p 12 A87-53218  
The Land Analysis System (LAS) - A general purpose system for multispectral image processing p 64 A87-53230  
Investigation of multi-dimensional algorithms using active and passive microwave data for ice concentration determination p 43 A87-53241  
The response of SAR imagery to azimuth travelling ocean surface waves as determined from shuttle SAR imagery p 44 A87-53286  
Whitetail deer food availability maps from Thematic Mapper data p 14 A87-53998  
A methodology for evaluation of an interactive multispectral image processing system p 66 A87-53999  
Sampling errors in satellite estimates of tropical rain p 53 A87-54153  
A space-time stochastic model of rainfall for satellite remote-sensing studies p 54 A87-54157

- Contribution of space technology to disaster preparedness, warning, and relief p 20 N87-28130  
NASA sea ice and snow validation plan for the Defense Meteorological Satellite Program special sensor microwave/imager [NASA-TM-100683] p 49 N87-30018  
Satellite-derived ice data sets no. 2: Arctic monthly average microwave brightness temperatures and sea ice concentrations, 1973-1976 [NASA-TM-87825] p 50 N87-30021
- National Aeronautics and Space Administration. Lyndon B. Johnson Space Center, Houston, Tex.**  
Estimation of X-band scattering properties of tree components p 13 A87-53277
- National Aeronautics and Space Administration. Langley Research Center, Hampton, Va.**  
Results from the pushbroom microwave radiometer flights over the Konza Prairie in 1985 p 11 A87-53206  
Calculation and accuracy of ERBE scanner measurement locations [NASA-TP-2670] p 47 N87-28471
- National Aeronautics and Space Administration. Marshall Space Flight Center, Huntsville, Ala.**  
Use of IR satellite rainfall estimates in diagnosing thermally forced circulations in the Pacific during FGGE SOP-1 p 36 A87-51580  
Latent heat and cyclone activity in the South Pacific, 10-18 January 1979 p 37 A87-51603
- National Aeronautics and Space Administration. National Space Technology Labs., Bay Saint Louis, Miss.**  
Potential application of multipolarization SAR for pine-plantation biomass estimation p 1 A87-43263  
Digital image classification approach for estimating forest clearing and regrowth rates and trends p 10 A87-53123  
An operational multispectral scanner for bathymetric surveys - The ABS NORDA scanner p 42 A87-53199  
Integration of topographic data with synthetic aperture radar data for determining forest properties in mountainous terrain p 14 A87-53278
- National Aeronautics and Space Administration. Wallops Flight Center, Wallops Island, Va.**  
Multiplatform sampling (ship, aircraft, and satellite) of a Gulf Stream warm core ring p 29 A87-44811  
Radiance-ratio algorithm wavelengths for remote oceanic chlorophyll determination p 29 A87-44812  
Waveform analysis for Geosat day 96 p 39 A87-52514  
Airborne multibeam radar altimetry p 40 A87-53115  
Observations of and a new model for fetch-limited wave growth p 43 A87-53263
- National Climate Program Office, Rockville, Md.**  
National Climate Program [PB87-190518] p 79 N87-28221
- National Geodetic Survey, Rockville, Md.**  
Geodetic glossary [PB87-181210] p 22 N87-25652
- National Geophysical Data Center, Boulder, Colo.**  
Solid earth geophysics: Data services [PB87-184107] p 66 N87-27352
- National Marine Fisheries Service, Washington, D.C.**  
Characterizing the Chesapeake Bay ecosystem and lessons learned [PB87-166930] p 19 N87-26463
- National Ocean Service, Anchorage, Alaska.**  
Gulf of Alaska: Physical environment and biological resources [PB87-103230] p 47 N87-29033
- National Oceanic and Atmospheric Administration, Boulder, Colo.**  
Catalog of submarine volcanoes and hydrological phenomena associated with volcanic events, January 1, 1900 to December 31, 1959 [PB87-183943] p 54 N87-28196
- National Oceanic and Atmospheric Administration, Seattle, Wash.**  
Theory of fluorescent irradiance fields in lakes and seas [PB87-196465] p 47 N87-28954
- National Oceanic and Atmospheric Administration, Washington, D.C.**  
Satellite color observations of spring blooming in Bering Sea shelf waters during the ice edge retreat in 1980 p 32 A87-47297  
Planning for future operational sensors and other priorities [NOAA-NESDIS-30] p 77 N87-25560
- Naval Air Development Center, Warminster, Pa.**  
The feasibility of detecting a magnetic field from a distant platform [AD-A180635] p 78 N87-27310
- Naval Ocean Research and Development Activity, Bay St. Louis, Miss.**  
An operational multispectral scanner for bathymetric surveys - The ABS NORDA scanner p 42 A87-53199

**Naval Postgraduate School, Monterey, Calif.**

Variations of mesoscale and large-scale sea ice morphology in the 1984 Marginal Ice Zone Experiment as observed by microwave remote sensing  
p 31 A87-47292

Comparison of satellite-derived ocean velocities with observations in the California coastal region  
[AD-A182291] p 47 N87-28242

**Naval Research Lab., Washington, D.C.**

Multisensor comparison of ice concentration estimates in the marginal ice zone p 31 A87-47295

**Naval Ship Research and Development Center, Bethesda, Md.**

Labrador wind and wave environments  
[AD-A183218] p 48 N87-29907

**North East London Polytechnic, Dagenham (England).**

Environmental information and cartography p 20 N87-28141

**Norwegian Defence Research Establishment, Kjeller.**

SAR detection of ships and ship wakes p 66 N87-27859

**O**

**Oak Ridge National Lab., Tenn.**

Effects of ozone on forests in the northeastern United States  
[DE87-010887] p 16 N87-28190

**Office of Naval Research, London (England).**

The International Symposium on Microwave Signatures and Remote Sensing held in Gothenburg (Sweden) on 19-22 January 1987  
[AD-A181334] p 78 N87-27314

**P**

**Pennsylvania State Univ., University Park.**

Estimation of surface moisture availability from remote temperature measurements p 53 A87-54155

**Politecnico di Milano (Italy).**

Large Format Camera: The second generation photogrammetric camera for space cartography p 78 N87-28118

**Purdue Univ., West Lafayette, Ind.**

Latent heat and cyclone activity in the South Pacific, 10-18 January 1979 p 37 A87-51603  
Spectral feature design for data compression in high dimensional multispectral data p 64 A87-53183

**R**

**Roskilde Univ. (Denmark).**

Mapping of vegetation types in SW Greenland p 16 N87-28149  
Studies of tidal flat environments with LANDSAT MSS data p 47 N87-28157

**Ruhr Univ., Bochum (West Germany).**

Satellite remote sensing for water resources management: Some engineering and economic aspects p 54 N87-28139

**S**

**SACLANT ASW Research Center, La Spezia (Italy).**

Wave-theory modelling of convergence zone propagation in the ocean  
[AD-A183607] p 50 N87-30020

**Sanchini BioResearch, Inc., Aurora, Colo.**

Biomonitoring plots at the ozone monitoring stations at Great Smoky Mountains National Park, 1985 survey results  
[PB87-172078] p 19 N87-26464

**Science Applications International Corp., Newport, R.I.**

Study of physical processes on the US mid-Atlantic continental slope and rise. Volume 1: Executive summary p 48 N87-30012  
Study of physical processes on the US mid-Atlantic continental slope and rise. Volume 2: Technical presentation  
[PB87-200523] p 49 N87-30013  
Study of physical processes on the US mid-Atlantic continental slope and rise. Volume 3: Appendix  
[PB87-200531] p 49 N87-30014

**Science Applications Research, Lanham, Md.**

Multiple-angle observations of reflectance anisotropy from an airborne linear array sensor p 69 A87-43262  
Ice dynamics at the mouth of ice stream B, Antarctica p 37 A87-51946  
Landscape pattern and successional dynamics in the boreal forest p 11 A87-53155

A methodology for evaluation of an interactive multispectral image processing system p 66 A87-53999

**Scranton Univ., Pa.**

Remote sensing of coastal wetlands p 1 A87-40944

**South Carolina Univ., Columbia.**

Color infrared video mapping of upland and wetland communities  
[DE87-010202] p 15 N87-28109

**ST Systems Corp., Hampton, Va.**

Data analysis and software support for the Earth radiation budget experiment  
[NASA-CR-178350] p 66 N87-26569

**Stanford Univ., Calif.**

Spacecraft on-board SAR image generation for EOS-type missions p 76 A87-53232  
Observing rotation and deformation of sea ice with synthetic aperture radar p 43 A87-53239

**T**

**Technical Univ. of Denmark, Lyngby.**

Active microwave observations of sea ice and icebergs p 45 N87-27855  
Cloud detection in NOAA images p 67 N87-28124  
Comparison of visual and automated lineament analyses on LANDSAT MSS image from south Greenland p 67 N87-28144  
Large scale sea ice studies based on Scanning Multichannel Microwave Radiometers (SMMR) data p 16 N87-28148  
Tracking of ice floes p 46 N87-28155  
Sea ice observations by SAR p 47 N87-28156  
Microwave radiometry study concerning pushbroom systems. Volume 1: A sea salinity/soil-moisture pushbroom radiometer system p 79 N87-28951  
[R-322]

**Technicolor Government Services, Inc., Moffett Field, Calif.**

Vegetation mapping and stress detection in the Santa Monica Mountains, California p 12 A87-53246

**Technion - Israel Inst. of Tech., Haifa.**

The effect of subpixel clouds on remote sensing p 2 A87-48360

**Technische Hogeschool, Delft (Netherlands).**

The estimation of variance components in geodetic networks  
[B8681154] p 79 N87-29904

**Technische Univ., Graz (Austria).**

Study on the use and characteristics of SAR for geological applications. Part 2: Radargrammetry aspects  
[ESA-CR(P)-2325-PT-2] p 27 N87-26466  
Integrated systems for remote sensing p 67 N87-28143

**Technische Univ., Munich (West Germany).**

Urban development planning using thematic mapper data of Munich (FRG) p 20 N87-28117  
Integration of remote sensing and geophysical data-application to exploration of pyrite ore facies in SW Spain p 27 N87-28119  
Monitoring and inventoring of forest damages by use of LANDSAT TM data p 16 N87-28138

**Texas A&M Univ., College Station.**

Moisture bursts over the tropical Pacific Ocean p 28 A87-43345  
Comparisons of FGGE IIb and IIb winds in a tropical synoptic system p 35 A87-51559  
Wintertime disturbances in the tropical Pacific - FGGE IIb and satellite comparisons p 36 A87-51560  
Moisture transports and budgets of 'moisture bursts' p 36 A87-51593

Application of satellite data to tropic-subtropic moisture coupling  
[NASA-CR-4092] p 48 N87-29067

**Texas Univ., Austin.**

Design study of remote sensing for ocean surface and interior activity  
[AD-A180578] p 44 N87-25610

**TGS Technology, Inc., Moffett Field, Calif.**

Relationship of Thematic Mapper simulator data to leaf area index of temperate coniferous forests p 8 A87-53017

**U**

**University Coll., London (England).**

A study of antenna signal processing techniques for radar alternatives  
[ESA-CR(P)-2370] p 79 N87-28809

**Utah State Univ., Logan.**

Biomonitoring plots at the ozone monitoring stations at Great Smoky Mountains National Park, 1985 survey results  
[PB87-172078] p 19 N87-26464

**V**

**Valencia Univ. (Spain).**

Thermal infrared images from satellites compared to shelter temperature. Application to frost nowcasting in a citrus orchard p 15 N87-28136  
A model of thermal inertia for frost forecasting in agricultural areas p 16 N87-28151

**W**

**Walcott and Associates, Inc., Alexandria, Va.**

Proceedings of Atlantic Outer Continental Shelf Region Information Transfer Meeting (ITM) (2nd), January 28-29, 1987 p 48 N87-30009

Proceedings of Atlantic Outer Continental Shelf Region Information Transfer Meeting (ITM) (1st), September 4-6, 1985  
[PB87-194361] p 48 N87-30011

**Washington State Univ., Pullman.**

Spectral characteristics and the extent of paleosols of the Palouse formation  
[NASA-CR-181208] p 17 N87-28195

**Washington Univ., Seattle.**

Evolution of microwave sea ice signatures during early summer and midsummer in the marginal ice zone p 31 A87-47293

Shuttle Imaging Radar B (SIR-B) Weddell Sea ice observations - A comparison of SIR-B and scanning multichannel microwave radiometer ice concentrations p 32 A87-47300

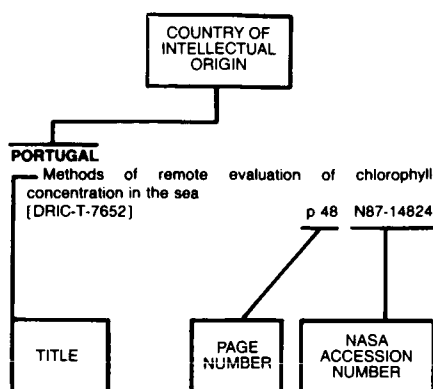
**Wisconsin Univ., Madison.**

Ice dynamics at the mouth of ice stream B, Antarctica p 37 A87-51946  
Estimating key forest ecosystem parameters through remote sensing p 12 A87-53245  
Scattering parameters for aspherical hydrometeors at microwave frequencies p 53 A87-53271

**Woods Hole Oceanographic Institution, Mass.**

A systems-approach to the design of the Eos data and information system p 64 A87-53207  
Analysis of forest and forest clearings in Amazonia with Landsat and Shuttle Imaging Radar-A data p 13 A87-53250  
Data telemetry, assimilation and ocean modeling  
[AD-A181899] p 47 N87-28239  
Satellite image processing for the Agulhas Retroflexion region  
[AD-A183012] p 68 N87-29905

## Typical Foreign Technology Index Listing



Listings in this index are arranged alphabetically by country of intellectual origin. The title of the document is used to provide a brief description of the subject matter. The page number and the accession number are included in each entry to assist the user in locating the citation in the abstract section.

## A

### ARGENTINA

Some aspects of the surface circulation south of 20 deg S revealed by First GARP Global Experiment drifters p 28 A87-42748

### AUSTRALIA

Use of rice response characteristics in classification using Landsat MSS digital data p 1 A87-45046  
Monitoring rice areas using Landsat MSS data p 1 A87-45047  
Updating maps of climax vegetation cover with Landsat MSS data in Queensland, Australia p 2 A87-46744  
Size distributions of clouds in real time from satellite imagery p 56 A87-48359  
Managing coral reefs - Operational benefits of remote sensing in Marine Park planning p 34 A87-48851  
Spectral studies of dryland agricultural salinity in Western Australia p 8 A87-48901  
Using remotely sensed Landsat MSS data to assess groundwater influence on the Barmah-Millewa Forest p 10 A87-53124

### AUSTRIA

Coral reef survey method for verification of Landsat MSS image data p 30 A87-46311  
Spectral discrimination of geobotanical anomalies using Landsat Thematic Mapper data p 2 A87-48668  
Thematic Mapper response to heavy metal related changes in Canopy LAI of a mixed forest p 12 A87-53248  
Study on the use and characteristics of SAR for geological applications. Part 2: Radargrammetry aspects [ESA-CR(P)-2325-PT-2] p 27 A87-26466  
The potential of SAR in a snow and glacier monitoring system p 45 A87-27856  
Integrated systems for remote sensing p 67 A87-28143

## B

### BELGIUM

A multi-source image set for the study of soil texture and drainage as observed from Thematic Mapper data in Northern Belgium p 10 A87-53125  
Crop inventorying of small-parcelled areas using SPOT- and TM-data in conjunction with field radiometric measurements p 10 A87-53126  
Remote sensing and landscape approaches to earth resources p 63 A87-53154  
The detection of soil drainage by using Landsat MSS and TM (Belgian test zones) p 11 A87-53205  
European dissemination of Marine Observation Satellite (MOS-1) data p 44 A87-53925  
Detection of soil drainage in Pays de Herve, Belgium, on LANDSAT MSS imagery p 15 A87-28129

### BRAZIL

Evaluation of MOMS (Modular Optoelectronic Multispectral Scanner) data for land use/land cover studies - Test site: Piracicaba region, Sao Paulo State, Brazil p 13 A87-53252  
Evaluation of the range and degradation of mangroves in Southern Sergipe with remote sensing techniques [INPE-4196-PRE/1080] p 16 A87-28160  
Enhancement of colors in remote sensing images using rotation of the matrix at the IHS coordinates [INPE-4207-PRE/1088] p 67 A87-28165  
Brief introduction in statistical pattern recognition [INPE-4206-PRE/1087] p 68 A87-28374  
Determination of transfer functions from the Thematic Mapper (TM) sensor of the LANDSAT-5 satellite [INPE-4213-PRE/1094] p 79 A87-28956

## C

### CANADA

Radar scattering and equilibrium ranges in wind-generated waves with application to scatterometry p 28 A87-42746  
An expert system for remote sensing p 80 A87-43260  
The CCRS SAR/MSS Anderson River data set p 55 A87-43261  
Upwelling filaments and motion of a satellite-tracked drifter along the west coast of North America p 29 A87-45023  
Within-scene radiometric correction of Landsat Thematic Mapper (TM) data in Canadian production systems p 57 A87-48656  
The automatic generation of digital terrain models from satellite images by stereo p 58 A87-48669  
Canadian Symposium on Remote Sensing, 10th, Edmonton, Canada, May 5-8, 1986, Proceedings, Volume 1 & 2 p 72 A87-48801  
Airborne video - Applied to route location studies for electrical power transmission facilities p 17 A87-48802  
Integration of radiometric and Landsat digital data for geologic investigation and exploration, Guysborough area, Nova Scotia p 24 A87-48803  
Analysis of airborne infrared data for interpretative geological mapping of the Brookfield area, Nova Scotia p 24 A87-48804  
Spatial filtering of digital Landsat data for the extraction of mapping information p 58 A87-48805  
Evaluation of algorithms for the geometric correction of Thematic Mapper data p 58 A87-48807  
Application of accuracy assessment techniques to image classification p 58 A87-48808  
Landsat-based wildlife habitat mapping - A study of collaboration between analyst and user p 3 A87-48809  
Multistage remote sensing with grade four students p 80 A87-48810  
Operational, province wide crop area estimation for Manitoba p 3 A87-48811  
An evaluation of sun angle computation algorithms p 59 A87-48812  
Application of image segmentation algorithms to the inventory of crops in Canada p 3 A87-48813

Large-scale black and white and natural color photographs for the measurement of tree crown areas p 3 A87-48815  
Evaluation of MEIS-II multispectral scanner data for quaternary geological mapping in the Chatham area, southwestern Ontario p 24 A87-48816  
Forecast of hurricane characteristics from GOES imagery p 59 A87-48818  
Comparison of space and airborne L-HH radar imagery in an agricultural environment p 4 A87-48819  
Comparison of C-band synthetic aperture radar (SAR) data according to two different depression angles for agricultural applications p 4 A87-48820  
Comparison of classification and enhancement techniques using Landsat imagery for the northern coniferous forest p 4 A87-48821  
Use of Thematic Mapper satellite images for disturbance updating of timber/range maps p 4 A87-48822  
Processing of Seasat altimetry data on a digital image analysis system p 59 A87-48825  
Validation of STAR-1 SAR imagery collected over Mould Bay, N.W.T., April 1984 p 59 A87-48826  
A study of the potential application of SPOT imagery in structural geology p 24 A87-48827  
Operational use of remote sensing for commercial Arctic class vessel navigation p 33 A87-48829  
Extent of saline/waterlogged lands within irrigated Alberta. I - Inventory and preliminary evaluation of existing mapping data p 5 A87-48830  
Spectral and textural segmentation of multispectral aerial images p 5 A87-48831  
Application of remote sensing data to bedrock geological interpretation, Black River-Matheson area, Northern Ontario, Canada p 24 A87-48832  
The use of multi-spectral and radar remote sensing data for monitoring forest clearcut and regeneration sites on Vancouver Island p 5 A87-48834  
Barriers to the operational use of satellite remote sensing in Canada p 72 A87-48835  
A high-throughput system for bulk processing of multispectral imagery p 72 A87-48836  
Integrated multi-temporal aerial photography and digital mapping for coastal monitoring, Cape Breton Island, Nova Scotia p 34 A87-48837  
Stratification of satellite imagery by Uniform Productivity Areas p 5 A87-48840  
Using NOAA AVHRR in studies of sea ice motion in the Beaufort Sea p 34 A87-48842  
Remote sensing in support of ecological studies of the bowhead whale p 34 A87-48843  
Analysis of data from the DFO fluorescence line imager p 72 A87-48844  
Landsat thematic mapper data in wildlife habitat management - Reference to deer wintering habitat p 5 A87-48845  
Effects of surface geometry of agricultural fields on radar airborne imagery in X- and C-bands p 5 A87-48846  
Radiometric corrections of topographic effects for simulated RADARSAT imagery in a region of moderate relief p 59 A87-48847  
Snowpack depletion monitoring in Alberta using computer-processed NOAA imagery p 52 A87-48848  
The influence of melting conditions on the interpretation of radar imagery of sea ice p 34 A87-48849  
Effectiveness of the Thematic Mapper for the range condition assessment in fescue grasslands of Southwestern Alberta p 6 A87-48850  
CCRS airborne Electro-Optical Facility p 72 A87-48852  
Digital SAR-Landsat combination for geologic mapping p 24 A87-48853  
Shuttle imaging Radar-A (SIR-A) scenes from Iran and China p 25 A87-48854  
The detection of wetlands on radar imagery p 6 A87-48855  
Indices of climatological and hydrological variability derived from satellite imagery for the South Saskatchewan River Basin p 52 A87-48856  
Radiation modelling in a high relief environment using a digital terrain model and Landsat - TM imagery p 59 A87-48857

- National land use mapping - The application of low altitude sample photography p 17 A87-48858
- An evaluation of Landsat TM and MSS data for crop identification in Manitoba p 6 A87-48859
- A geobotanic approach to the study of the geology of Cape Smith using Landsat-MSS data p 25 A87-48860
- Regional geobotany with TM - A Sudbury case study p 25 A87-48861
- Geological interpretations from Landsat of the Troodos Massive, Cyprus p 25 A87-48862
- Comparison of Landsat Thematic Mapper and Multispectral Scanner information content for agricultural applications in Western Canada p 6 A87-48863
- Colour infrared aerial photography for herbicide drift damage assessment p 6 A87-48864
- MEIS II imagery for environmental stress analysis p 72 A87-48865
- Applications of satellite derived digital elevation models for resource mapping p 60 A87-48866
- Landsat Thematic Mapper data - A useful tool for mapping agricultural areas in Quebec p 6 A87-48867
- Rural land use classification using Landsat Thematic Mapper data p 18 A87-48868
- Thematic Mapper information about Canadian forests - Early results from across the country p 6 A87-48869
- Indexing small catchments in Java, Indonesia, with respect to their relative susceptibility to erosion p 52 A87-48871
- Multispectral video system for airborne remote sensing - Sensitivity, calibrations and correction p 73 A87-48873
- Discrimination of suspended sediment and littoral features using multispectral video imagery p 73 A87-48874
- Hydrologic applications of weather radar data p 52 A87-48875
- Iceberg detection using SLAR p 34 A87-48876
- Technological feasibility to mobilization for operations - The NOAA crop monitoring case p 6 A87-48878
- A structural analysis of the Mabou Basin, Cape Breton Island using enhanced Landsat MSS imagery p 25 A87-48879
- A methodology for automated extraction of drainage networks from satellite imagery p 53 A87-48880
- Optimization of seismic vessel deployment using side looking airborne radar p 34 A87-48881
- Remote sensing as a tool for Alberta Agricultural Wetlands Drainage Inventory p 6 A87-48882
- Validation and simulation of Radarsat imagery p 60 A87-48883
- Sulphur dioxide damage assessment using colour infrared aerial photography p 60 A87-48884
- Multiple-look effects on SAR classification accuracies p 60 A87-48885
- An application for the testing and use of the standard data transfer format p 18 A87-48886
- Ground targets for the radiometric correction of AVHRR imagery for crop monitoring p 7 A87-48887
- Interpretation of prairie land cover types from SIR-B data p 7 A87-48888
- New system for the ordering, archiving and retrieval of data from earth's resource satellites p 60 A87-48889
- The RADARSAT RMOMS optical sensor p 73 A87-48890
- Preliminary results from modelling vegetation spectra derived from MEIS data, Algonquin Park, Ontario p 7 A87-48891
- A trial of oblique imagery from a low cost video camera system for defoliation assessment p 7 A87-48892
- Remote sensing in the Sahel - A tool for the inventory and monitoring of resources p 73 A87-48893
- The role of Landsat multi-spectral scanner data in the analysis of northern spotted owl habitat p 7 A87-48894
- The role of remote sensing in the Canada Land Use Monitoring Program (CLUMP) p 18 A87-48895
- The ERS-1/RADARSAT SAR Canadian ground segment p 61 A87-48896
- Thermographic remote sensing of northern forest areas in regeneration after clear or strip cutting - Preliminary observations p 8 A87-48897
- Environmental monitoring of Alpine Meadows with large scale aerial photography in Banff National Park p 18 A87-48898
- Remote sensing and the agricultural resource inventory p 8 A87-48899
- TM and MEIS data for future Alberta forest inventories p 8 A87-48900
- The evaluation of TM analysis as a tool in monitoring land use and agricultural stress in Egypt p 18 A87-48903
- A revolution in the production of small-scale and medium-scale maps p 61 A87-48904
- Development of a mathematical model for the spatial triangulation of SPOT images p 61 A87-48905

- The operational use of RADARSAT products by the ice centre environment Canada p 61 A87-48906
- Computer-assisted map analysis - Extending the utility of GIS technology p 18 A87-48907
- The detection of vegetative stress utilizing remotely sensed data and soil sampling p 8 A87-50231
- An expert system for planimetric feature extraction p 63 A87-53139
- Sequential thinning algorithms for remote sensing application p 63 A87-53140
- Digital elevation model extraction from stereo satellite images p 63 A87-53142
- Data correction for automated remote sensing image interpretation p 64 A87-53209
- Optimum use of dual frequency passive microwave measurements for ice/ocean interactions p 43 A87-53240
- Spatial considerations in speckle simulation p 65 A87-53260
- Airborne SAR imaging of azimuthally travelling ocean surface waves - The LEWEX experimental plan p 44 A87-53266
- Tidal and secular tilt from an earthquake zone - Thresholds for detection of regional anomalies p 26 A87-53733
- Study on the use of SAR data for agriculture and forestry p 15 A87-27862
- An algorithm for automatically acquiring ground control points in SAR imagery p 67 A87-27864
- CHINA, PEOPLE'S REPUBLIC OF**
- The application of remote sensing techniques in China p 68 A87-41435
- Geometric correction of space images by the colinearity-equation method p 61 A87-51175

## D

## DENMARK

- Estimation and modelling of the local empirical covariance function using gravity and satellite altimeter data p 22 A87-54325
- Active microwave observations of sea ice and icebergs p 45 A87-27855
- Cloud detection in NOAA images p 67 A87-28124
- Comparison of visual and automated lineament analyses on LANDSAT MSS image from south Greenland p 67 A87-28144
- Coastal Zone Color Scanner (CZCS) images and ocean dynamics. Application to the Northwest African upwelling area p 46 A87-28146
- Large scale sea ice studies based on Scanning Multichannel Microwave Radiometers (SMMR) data p 16 A87-28148
- Mapping of vegetation types in SW Greenland p 16 A87-28149
- Snow mapping in western Greenland p 54 A87-28150
- Tracking of ice floes p 46 A87-28155
- Sea ice observations by SAR p 47 A87-28156
- Studies of tidal flat environments with LANDSAT MSS data p 47 A87-28157
- Microwave radiometry study concerning pushbroom systems. Volume 1: A sea salinity/soil-moisture pushbroom radiometer system p 79 A87-28951
- [R-322]

## E

## EGYPT

- Remote sensing of deep potential sources over the Nile Delta area p 26 A87-53150

## ESTONIA

- Monte Carlo calculation of the dependence of the spectral radiance of vegetation cover on the illumination conditions p 2 A87-48190

## F

## FINLAND

- Satellite microwave radiometry of snow water equivalent p 52 A87-48823
- Satellite microwave radiometry of forest and surface types p 9 A87-53120
- Monitoring of snow cover from satellite p 54 A87-28123

## FRANCE

- Second generation high-resolution space systems - First results of the SPOT-1 satellite p 55 A87-44244
- Visual interpretation of Landsat MSS quick-look images for the study of the annual swelling of the Niger river in its interior delta, in Mali p 50 A87-44245
- Geoid anomalies across Ascension fracture zone and the cooling of the lithosphere p 21 A87-44352

- Remote sensing of the geomorphologic formations and vegetation in the eastern High Atlas region of Morocco from SPOT satellite data p 23 A87-45048
- Seasat altimetry and the South Atlantic geoid. I - Spectral analysis p 21 A87-45743
- Earth gravity model improvement - An alternative method for Doppler-tracked satellites p 21 A87-45817
- Photogrammetry - The largest operational application of remote sensing p 70 A87-47174
- Absolute calibration of the SPOT-1 HRV cameras p 71 A87-48660
- SPOT radiometric resolution performance evaluation - Preliminary results p 57 A87-48661
- SPOT localization accuracy and geometric image quality p 57 A87-48662
- SPOT MTF performance evaluation p 57 A87-48663
- Improving SPOT images size and multispectral resolution p 58 A87-48664
- Photogrammetry from SPOT with Matra TRASTER analytical plotter p 58 A87-48665
- Moscow seen by satellite - Another image of Soviet urban geography p 80 A87-51143
- Contribution of improved resolution to morphological analysis - The example of the Rhone delta p 25 A87-51144
- Geomorphological interpretation of the SPOT image of February 23, 1986 concerning Djebel Amour (Algeria) and its border with the Sahara p 25 A87-51145
- Morphostructure and geological patterns in central-southern Norway according to a Landsat image p 25 A87-51146
- Automated evaluation of linear networks on SPOT images p 61 A87-51174
- Monitoring wheat canopies with a high spectral resolution radiometer p 8 A87-53019
- Effect of resolution on texture application to nearly simultaneous AVHRR and MSS images of an agricultural region p 9 A87-53111
- Poseidon radar altimeter oceanographic remote sensing p 40 A87-53113
- Poseidon radar altimeter description and signal processing p 40 A87-53114
- SPOT, a satellite for oceanography? p 41 A87-53194
- Processing of airborne SAR images of ocean waves p 43 A87-53264
- Textural segmentation of SAR images using first order statistical parameters p 66 A87-53274
- A statistical and geometrical edge detector for SAR image segmentation p 13 A87-53275
- Theoretical feasibility of SAR interferometry p 77 A87-53283
- Precise orbit determination with the Doppler Orbitography and Radio positioning Integrated by Satellite (DORIS) system and the associated Zealous for Orbit Observation Methods (ZOOM) software p 77 A87-25382
- Proceedings of the SAR Applications Workshop [ESA-SP-264] p 78 A87-27854
- Proceedings of the ESA-EARSel Europe from Space Symposium [ESA-SP-258] p 19 A87-28115
- G**
- GERMANY, FEDERAL REPUBLIC OF**
- Significance of TM data as a tool to support regional planning activities p 17 A87-48671
- Comparative analysis of different sensor data (Landsat-TM and MOMS) for earth observation and impact on future sensor development p 71 A87-48674
- Investigation of design parameters for ERS-1 wind scatterometer p 74 A87-53116
- An advanced wind scatterometer for the Columbus Polar Platform payload p 74 A87-53117
- On the origin of cross-polarization in remote sensing p 75 A87-53168
- Radar signatures of oil films floating on the sea surface p 41 A87-53192
- Performance sensitivity for X-SAR p 76 A87-53223
- Remote sensing of the earth with microwave radiometry in Germany - Results and trends p 76 A87-53225
- Method development and experiences in application of airborne MSS data for forest damage detection p 12 A87-53247
- Matching instrument design and signal processing for a scanning radiometer p 76 A87-53251
- Derivation of the technical specification of the ERS-1 active microwave instrument to meet the SAR-image quality requirements p 77 A87-53280
- Remote sensing of suspended matter in the ocean by airborne lasers and satellite radiometers [GKSS-86/E/49] p 45 A87-26405



- Study on the use and characteristics of SAR systems for geological applications  
[ESA-CR(P)-2342] p 27 N87-26467
- Urban development planning using thematic mapper data of Munich (FRG) p 20 N87-28117
- Integration of remote sensing and geophysical data-application to exploration of pyrite ore facies in SW Spain p 27 N87-28119
- Requirements on radar data for geological application: A case study by use of multistage data of the test site Sardegna/Italy p 27 N87-28120
- Rural land use inventory and mapping in the Ardeche area (France). Improvement of automatic classification by multitemporal analysis of TM data p 15 N87-28127
- Monitoring and inventoring of forest damages by use of LANDSAT TM data p 16 N87-28138
- Satellite remote sensing for water resources management: Some engineering and economic aspects p 54 N87-28139
- The impact of LANDSAT Thematic Mapper Data for ecological mapping purposes. A case study at the northern margin of the Alps p 20 N87-28147
- ADRIA 84: Airborne investigations of Gelbstoff by optical radiometry and fluorescence lidar p 46 N87-28154

## I

## INDIA

- Remote sensing of geomagnetic field and applications to climate prediction p 74 A87-53108
- A spaceborne LFM scatterometer for ocean surface wind vector measurement - A time domain approach p 40 A87-53119
- Remote sensing by the fluorescence property of the scatterer p 75 A87-53179
- Pleistocene earth movements in Peninsular India - Evidences from Landsat MSS and Thematic Mapper data p 26 A87-53242

## INTERNATIONAL ORGANIZATION

- Remote sensing in Indonesia - A review of the available technology and its applications for resources surveys p 17 A87-46310
- Remote sensing applications of the earth's surface - An outlook into the future p 70 A87-47173
- A contribution to the optimum selection of ground control points in high resolution images p 57 A87-48658
- TM sensor performance as obtained from Earthnet quality control data base p 71 A87-48659
- Different scanning instruments comparison - MOMS and TM p 71 A87-48675
- Cluster based segmentation of multi-temporal Thematic Mapper data as preparation of region-based agricultural land-cover analysis p 9 A87-53109
- Exploring the spatial domain p 62 A87-53112
- The contribution of AVHRR data for measuring and understanding global processes - Large-scale deforestation in the Amazon basin p 11 A87-53151
- The global forest ecosystem as viewed by ERS-1, SIR-C and EOS p 12 A87-53217
- The European Campaign 'AGRISAR '86' p 13 A87-53249

## ITALY

- Climatological implications of a satellite-borne SAR imaging the sea surface p 30 A87-46403
- Some results of the Metric Camera (MC) Mission-1 on Spacelab p 70 A87-47175
- Atmospheric correction of data measured by a flying platform over the sea - Elements of a model and its experimental validation p 35 A87-50292
- Automatic classification of forestal areas by remote sensing techniques p 12 A87-53211
- Use of TM Landsat data as a support to classical ground-based methodologies in the investigation of a volcanic site in central Italy - The Caldera of Latara p 26 A87-53244
- Aircraft microwave radiometry of land p 13 A87-53269
- Large Format Camera: The second generation photogrammetric camera for space cartography p 78 N87-28118
- Crop discrimination by means of radar and infrared images p 15 N87-28128
- Monitoring and modeling of the Adriatic Sea p 46 N87-28133
- Evaluation of the potential of the Thematic Mapper for marine application p 46 N87-28134
- The role and perspective of remote sensing for disaster management in the European community p 20 N87-28137
- Measurement of spectral signatures in Less Favored Areas (LFA): A contribution to the definition of a remote sensing multitemporal experiment p 20 N87-28145
- Correction of the sensor degradation of the Coastal Zone Color Scanner on NIMBUS-7 p 46 N87-28153

- Wave-theory modelling of convergence zone propagation in the ocean  
[AD-A183607] p 50 N87-30020

## J

## JAPAN

- Land cover classification using SPOT data p 18 A87-50227
- Meissner effect in high-Tc superconductive thin films p 35 A87-51532
- Analysis of environmental information of urban areas using Landsat TM data p 19 A87-53187
- Observation of oil slicks on the ocean by X-band SLAR p 41 A87-53191
- Some results of MOS-1 airborne verification experiment - MSR (microwave scanning radiometer) p 76 A87-53229
- Geometric distortion correction with high accuracy for NOAA satellite images p 65 A87-53253

## K

## KENYA

- An MTF analysis of Landsat classification error at field boundaries p 56 A87-46745

## N

## NETHERLANDS

- Shallow water bathymetry and bottom classification by means of the Landsat and SPOT optical scanners p 52 A87-48670
- The future generation of resources satellites p 80 A87-53742
- Summary of recent SAR instrument studies p 78 N87-27865
- SPOT: How good for geology? A comparison with LANDSAT MSS p 27 N87-28121
- The estimation of variance components in geodetic networks [B8681154] p 79 N87-29904

## NEW ZEALAND

- First New Zealand image from the French SPOT satellite p 62 A87-51179

## NORWAY

- Mesoscale eddies in the Fram Strait marginal ice zone during the 1983 and 1984 Marginal Zone Experiments p 31 A87-47291
- SAR detection of ships and ship wakes p 66 N87-27859

## O

## OTHER

- Agricultural, hydrologic and oceanographic studies in Bangladesh with NOAA AVHRR data p 57 A87-48365
- How useful is Landsat monitoring? p 14 A87-54089

## P

## PORTUGAL

- The dynamics of the northern border of the Gulf Stream revealed by a Tiros-N AVHRR image from October 22, 1980 p 35 A87-51147

## S

## SPAIN

- Thermal infrared images from satellites compared to shelter temperature. Application to frost nowcasting in a citrus orchard p 15 N87-28136
- ERAFIS: A computer information system for agriculture and forestry in Spain p 16 N87-28140
- A model of thermal inertia for frost forecasting in agricultural areas p 16 N87-28151

## SWEDEN

- Averaging of radar altimeter pulse returns with the interpolation tracker p 70 A87-45044
- Operational water quality surveillance in Sweden using Landsat MSS data p 52 A87-48841
- Geological feature enhancement in SAR imagery p 67 N87-27861

## SWITZERLAND

- Point positioning and mapping with large format camera data p 73 A87-50226
- SPOT's first year p 80 A87-51320
- Eurimage sets up shop p 80 A87-51324
- Hierarchical classification with knowledge based binary decision p 62 A87-53110

## T

## THAILAND

- Small format aerial photography for analyzing urban housing problems - A case study in the Bangkok metropolitan region p 17 A87-46309

## U

## U.S.S.R.

- Formation of natural underground-water resources in arid regions with special reference to the Dolinoozerskii artesian basin in Mongolia p 50 A87-42911
- Studies of the wavelike process in the surface temperature field of the equatorial Pacific using Meteor-satellite IR measurements p 28 A87-42931
- A study of modern landscape formation in Lower Mesopotamia from space photographs p 55 A87-42935
- Radar observations of terrestrial vegetation covers in the 3-cm range p 1 A87-42936
- Stereoscopic visualization of aerial and space photographs in thematic mapping p 23 A87-42937
- A method for the optimization of orbits and structures of satellite systems for the periodic round-the-clock survey of the earth p 21 A87-42938
- New possibilities for the use of gravity data in the realization of geodetic coordinate systems p 21 A87-42939
- Foam activity on the sea surface as a Markov random process p 28 A87-44289
- Features of the water dynamics of Lake Ladoga according to remote sensing data p 50 A87-44296
- Determination of the external-orientation elements of aerial and space photographs p 55 A87-44301
- From satellite orbit into the eye of the typhoon p 29 A87-44679
- The determination of Love numbers from the results of earth-tide observations in the Dnieper-Donets basin (DDB) region p 21 A87-46139
- Determination of the initial motion conditions of earth-resources satellites according to the photogrammetric processing of topographic photographs oriented in inertial space p 56 A87-47506
- Remote sensing techniques for the study of hydrological elements p 51 A87-47576
- Possibility of evaluating reservoir influx from aerial and satellite photographs p 51 A87-47577
- Modeling the snowmelt runoff in mountain catchment areas using satellite data p 51 A87-47578
- Parameterization of models of runoff formation in simple catchment areas using remote-sensing data p 51 A87-47579
- Water-cycle processes in geosystems and the possibility of the remote sensing of the moisture content of the underlying surface p 51 A87-47580
- Remote-sensing evaluation of moisture supply to crops according to the leaf-surface thermal regime p 2 A87-47582
- Remote-sensing evaluation of the spatial variability of evaporation p 52 A87-47583
- Remote-sensing techniques for investigating the structure of radiation-heat fluxes and the moisture content of geosystems in connection with the problem of monitoring the water component p 52 A87-47584
- Analysis of Cosmos-1500 radar images of the ocean surface in a zone of cyclones and mesoscale cloud formations p 32 A87-48176
- Measurement of currents according to the drift of subsatellite buoys p 32 A87-48177
- Estimation of errors in the determination of sea surface temperature and atmospheric moisture content from satellite measurements of outgoing IR radiation in the 10.5-12.5 micron range p 33 A87-48178
- Divergent redistribution of ice in the Arctic Ocean (Analysis of space imagery) p 33 A87-48180
- Evaluation of the effect of hydrometeors on the characteristics of radar images of sea ice p 33 A87-48181
- Maximum accuracy of satellite-borne scatterometer measurements of wind velocity above the ocean p 33 A87-48184
- Space photographs of the Omega-Ladoga isthmus and the prediction of mineral finds p 23 A87-48185
- Application of space photographs to geomorphological investigations in southwestern Tadzhikistan p 23 A87-48186
- Application of space photographs to paleoseismological investigations (with reference to the Mongolian Altai) p 23 A87-48187
- Investigation of the relief of ore-containing regions on the basis of space photographs (with reference to eastern Yakutia) p 23 A87-48188

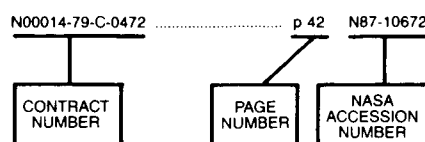
- Features of a statistical model for the interaction between electromagnetic waves and remotely sensed natural objects p 70 A87-48189
- Multistage principal-components analysis of correlations p 56 A87-48193
- Remote-sensing and geological-geophysical studies of closed platform territories p 26 A87-51875
- Monitoring the background pollution of natural environments, No. 3 p 19 A87-52241
- Problems in the background monitoring of the environment, No. 4 p 19 A87-52242
- Elements of lineament tectonics p 27 A87-53954
- Investigation of causes of hydrogen sulfide formation in reclaimed water p 14 N87-23136
- Successes of Cosmos-1500 satellite, SLR system p 45 N87-27696
- Morphometric studies of world ocean p 45 N87-28077
- Major morphologic features of the Atlantic Ocean surface p 48 N87-29573
- Geomagnetic intersection of tectonic structures seen in space photographs p 28 N87-29574
- Analysis of directions of linear image elements by structure-zonal method p 68 N87-29575
- UNITED KINGDOM**
- Satellite altimeter measurements of the geoid in sea ice zones p 30 A87-45816
- Lithological discrimination in central Snowdonia using airborne multispectral scanner imagery p 23 A87-48358
- The variability of the North Atlantic marine atmosphere and its relevance to remote sensing p 33 A87-48362
- Ocean wave parameter measurement using a dual-radar system - A simulation study p 33 A87-48363
- Geometric quality of Thematic Mapper data of the United Kingdom p 57 A87-48655
- Glaciological studies on Rutford ice stream, Antarctica p 38 A87-51950
- A system for knowledge-based segmentation of remotely-sensed images p 11 A87-53136
- The comparison of ocean-wave spectra recovered from SIF-B and Seasat observations with simultaneous buoy data p 43 A87-53265
- A combined SAR and scatterometer system p 77 A87-53279
- Thin line detection in SAR images p 66 N87-27860
- Land use feature detection in SAR images p 67 N87-27863
- Sea surface temperatures and the detection of ocean circulation patterns and fronts from AVHRR imagery p 45 N87-28125
- The determination of sea-state bias and non-linear wave parameters from satellite altimeter data p 46 N87-28132
- On the use of AVHRR channel-3 data for environmental studies p 20 N87-28135
- Environmental information and cartography p 20 N87-28141
- Towards the automatic recognition and vectorised description of linear features in LANDSAT TM images by artificial intelligence methods p 67 N87-28142
- Present state, changes, and quality of Sologne and Brenne, two French large wetlands, studied with LANDSAT MSS and TM data p 54 N87-28152
- A study of antenna signal processing techniques for radar alternatives [ESA-CR(P)-2370] p 79 N87-28809

# CONTRACT NUMBER INDEX

EARTH RESOURCES / A Continuing Bibliography (Issue 56)

FEBRUARY 1988

## Typical Contract Number Index Listing



Listings in this index are arranged alpha-numerically by contract number. Under each contract number, the accession numbers denoting documents that have been produced as a result of research done under that contract are arranged in ascending order with the AIAA accession numbers appearing first. The accession number denotes the number by which the citation is identified in the abstract section. Preceding the accession number is the page number on which the citation may be found.

NAGW-735	p 13	A87-53276	
NAGW-872	p 53	A87-53271	
NAGW-925	p 64	A87-53183	
NAGW-946	p 64	A87-53207	
NAG5-184	p 53	A87-54155	
NAG5-270	p 42	A87-53236	
	p 79	N87-28957	
NAG5-319	p 27	N87-28200	
NAG5-770	p 35	A87-51487	
NAG5-849	p 68	N87-28197	
NASA ORDER W-15085	p 44	A87-53287	
NASA TASK 199-30-72-05	p 12	A87-53246	
NASA TASK 677-21-35-08	p 12	A87-53246	
NASW-3389	p 26	A87-51725	
NASW-4049	p 23	A87-48667	
NASW-4066	p 81	N87-29900	
NAS1-17851	p 66	N87-26569	
NAS5-27377	p 2	A87-48673	
NAS5-27382	p 69	A87-44863	
NAS5-27580	p 30	A87-46542	
NAS5-28758	p 17	N87-28195	
NAS5-28796	p 29	A87-44866	
NAS7-918	p 77	N87-26264	
NAS8-35182	p 28	A87-43345	
	p 35	A87-51559	
	p 36	A87-51560	
	p 36	A87-51593	
	p 48	N87-29067	
NAS8-35187	p 36	A87-51580	
	p 37	A87-51603	
NCA2-OR-475-301	p 8	A87-53017	
NERC-F60/G6/03	p 57	A87-48655	
NOAA PROJECT 144-U824	p 51	A87-46545	
NOAA-NA-800AAD00086	p 51	A87-46545	
NOAA-NA-85AADSG033	p 1	A87-40944	
NPS-PX-0001-5-0823	p 19	N87-26464	
NSERC-A-0766	p 53	A87-48880	
NSERC-A-4201	p 5	A87-48846	
NSERC-A-7982	p 52	A87-48875	
NSF ATM-79-23918	p 35	A87-51552	
NSF ATM-81-19321	p 35	A87-51552	
NSF ATM-82-069004	p 36	A87-51585	
NSF ATM-82-17960	p 36	A87-51594	
NSF ATM-83-05502	p 51	A87-46538	
NSF ATM-84-18472	p 36	A87-51587	
NSF ATM-85-05749	p 37	A87-51603	
NSF BSR-84-02051	p 26	A87-53243	
NSF BSR-84-14455	p 9	A87-53024	
NSF DAR-80-17836	p 1	A87-40944	
NSF DCR-83-20136	p 58	A87-48669	
NSF DPP-80-20000	p 37	A87-51944	
NSF DPP-81-17235	p 37	A87-51947	
NSF DPP-81-20322	p 37	A87-51948	
NSF DPP-81-20332	p 37	A87-51945	
NSF DPP-82-07320	p 37	A87-51946	
NSF DPP-84-05287	p 37	A87-51946	
NSF DPP-84-12404	p 37	A87-51943	
	p 37	A87-51945	
	p 37	A87-51948	
	p 37	A87-51946	
	p 37	A87-51946	
	p 35	A87-51487	
	p 42	A87-53236	
	p 29	A87-44811	
	p 38	A87-51963	
	p 29	A87-44811	
	p 31	A87-47296	
	p 42	A87-53219	
	p 31	A87-47294	
	p 43	A87-53238	
	p 43	A87-53241	
	p 42	A87-53212	
	p 64	A87-53213	
	p 65	A87-53262	
	p 31	A87-47293	
	p 68	N87-29905	
	p 31	A87-47294	
	p 31	A87-47294	
	p 42	A87-53236	
	p 31	A87-47296	
	p 31	A87-47296	
	p 34	A87-50277	
	p 31	A87-47293	
N00014-85-K-0569	p 43	A87-53237	
N00014-86-C-0840	p 44	N87-25610	
N00014-86-K-0751	p 64	A87-53233	
N00014-87-K-0007	p 47	N87-28239	
N0014-85-C-0020	p 68	N87-29905	
USDA-59-2041-1-2-086-0	p 28	A87-42748	
644-11-00-04-74	p 14	A87-53741	
665-45-20-01	p 77	N87-26264	
	p 47	N87-28471	

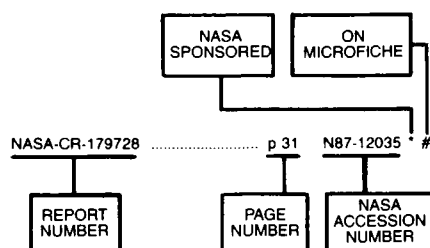
CONTRACT

# REPORT NUMBER INDEX

EARTH RESOURCES / A Continuing Bibliography (Issue 56)

FEBRUARY 1988

## Typical Report Number Index Listing



Listings in this index are arranged alphabetically by report number. The page number indicates the page on which the citation is located. The accession number denotes the number by which the citation is identified. An asterisk (\*) indicates that the item is a NASA report. A pound sign (#) indicates that the item is available on microfiche.

ETN-87-90171	p 79	N87-29904	#	PB87-183943	p 54	N87-28196	#
ETN-87-90459	p 79	N87-28951	#	PB87-184107	p 66	N87-27352	#
ETN-87-90473	p 79	N87-28809	#	PB87-190518	p 79	N87-28221	#
ETN-87-99915	p 45	N87-26405	#	PB87-194361	p 48	N87-30011	#
ETN-87-99980	p 27	N87-26466	#	PB87-196465	p 47	N87-28954	#
ETN-87-99993	p 27	N87-26467	#	PB87-200168	p 48	N87-30009	#
				PB87-200515	p 48	N87-30012	#
GKSS-86/E/49	p 45	N87-26405	#	PB87-200523	p 49	N87-30013	#
HRI-93	p 19	N87-26464	#	PB87-200531	p 49	N87-30014	#
ICI-RPT-87010	p 48	N87-30010	#	PB87-200994	p 49	N87-30015	#
INPE-4196-PRE/1080	p 16	N87-28160	#	PB87-201000	p 49	N87-30016	#
INPE-4206-PRE/1087	p 68	N87-28374	#	PB87-201018	p 49	N87-30017	#
INPE-4207-PRE/1088	p 67	N87-28165	#	PB87-201430	p 48	N87-30010	#
INPE-4213-PRE/1094	p 79	N87-28956	#				
ISSN-0344-9629	p 45	N87-26405	#	R-322	p 79	N87-28951	#
ISSN-0379-6566	p 19	N87-28115	#	REPT-87B0492	p 49	N87-30018 *	#
ISSN-079-6566	p 78	N87-27854	#	SACLANTCEN-SM-194	p 50	N87-30020	#
JPL-PUB-87-16	p 77	N87-26264 *	#	SAIC-86/7539/129-VOL-1	p 48	N87-30012	#
KGRD-22	p 66	N87-27352	#	SAIC-86/7539/129-VOL-2	p 49	N87-30013	#
L-16218	p 47	N87-28471 *	#	SAIC-86/7539/129-VOL-3	p 49	N87-30014	#
LC-86-61105	p 22	N87-25652	#	SE-42	p 54	N87-28196	#
LPI-TR-86-08	p 81	N87-29900 *	#	SPIE-660	p 70	N87-48652	#
NAS 1.15:100683	p 49	N87-30018 *	#	TR-772	p 78	N87-27311	#
NAS 1.15:87825	p 50	N87-30021 *	#	USCG-D-10-87	p 50	N87-30019	#
NAS 1.15:89625	p 78	N87-27316 *	#	WHOI-87-21	p 47	N87-28239	#
NAS 1.26:178350	p 66	N87-26569 *	#	WHOI-87-27	p 68	N87-29905	#
NAS 1.26:180543	p 81	N87-29900 *	#				
NAS 1.26:180666	p 27	N87-28208 *	#				
NAS 1.26:181159	p 77	N87-26264 *	#				
NAS 1.26:181183	p 68	N87-28197 *	#				
NAS 1.26:181208	p 17	N87-28195 *	#				
NAS 1.26:181230	p 27	N87-28200 *	#				
NAS 1.26:181370	p 79	N87-28957 *	#				
NAS 1.26:4092	p 48	N87-29067 *	#				
NAS 1.60:2670	p 47	N87-28471 *	#				
NASA-CR-178350	p 66	N87-26569 *	#				
NASA-CR-180543	p 81	N87-29900 *	#				
NASA-CR-180666	p 27	N87-28208 *	#				
NASA-CR-181159	p 77	N87-26264 *	#				
NASA-CR-181183	p 68	N87-28197 *	#				
NASA-CR-181208	p 17	N87-28195 *	#				
NASA-CR-181230	p 27	N87-28200 *	#				
NASA-CR-181370	p 79	N87-28957 *	#				
NASA-CR-4092	p 48	N87-29067 *	#				
NASA-TM-100683	p 49	N87-30018 *	#				
NASA-TM-87825	p 50	N87-30021 *	#				
NASA-TM-89625	p 78	N87-27316 *	#				
NASA-TP-2670	p 47	N87-28471 *	#				
NOAA-NESDIS-30	p 77	N87-25560	#				
NOAA-TM-ERL-PMEL-70	p 47	N87-28954	#				
OCS/MMS-85/0106	p 48	N87-30011	#				
OCS/MMS-86/0079-VOL-1	p 49	N87-30015	#				
OCS/MMS-86/0079-VOL-2	p 49	N87-30016	#				
OCS/MMS-86/0079-VOL-3	p 49	N87-30017	#				
OCS/MMS-86/0095	p 47	N87-29033	#				
OCS/MMS-87/0024-VOL-1	p 48	N87-30012	#				
OCS/MMS-87/0024-VOL-2	p 49	N87-30013	#				
OCS/MMS-87/0024-VOL-3	p 49	N87-30014	#				
OCS/MMS-87/0033	p 48	N87-30009	#				
ONRL-7-010-C	p 78	N87-27314	#				
PB87-103230	p 47	N87-29033	#				
PB87-166930	p 19	N87-26463	#				
PB87-171195	p 19	N87-25634	#				
PB87-172078	p 19	N87-26464	#				
PB87-181210	p 22	N87-25652	#				

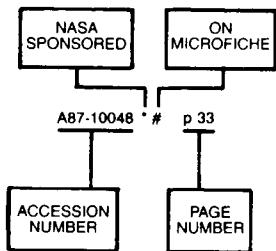
REPORT

# ACCESSION NUMBER INDEX

EARTH RESOURCES / A Continuing Bibliography (Issue 56)

FEBRUARY 1988

## Typical Accession Number Index Listing



Listings in this index are arranged alphabetically by accession number. The page number listed to the right indicates the page on which the citation is located. An asterisk (\*) indicates that the item is a NASA report. A pound sign (#) indicates that the item is available on microfiche.

A87-40944 \* p 1  
A87-41435 p 68  
A87-42659 \* p 55  
A87-42746 \* p 28  
A87-42748 p 28  
A87-42911 p 50  
A87-42931 p 28  
A87-42935 p 55  
A87-42936 p 1  
A87-42937 p 23  
A87-42938 p 21  
A87-42939 p 21  
A87-43260 p 80  
A87-43261 p 55  
A87-43262 \* p 69  
A87-43263 \* # p 1  
A87-43302 p 69  
A87-43345 \* p 28  
A87-43353 \* # p 23  
A87-44184 \* p 69  
A87-44244 p 55  
A87-44245 p 50  
A87-44289 p 28  
A87-44296 p 50  
A87-44301 p 55  
A87-44352 p 21  
A87-44679 p 29  
A87-44811 \* p 29  
A87-44812 \* p 29  
A87-44863 \* p 69  
A87-44864 \* p 55  
A87-44865 \* p 69  
A87-44866 \* p 29  
A87-44868 \* p 69  
A87-45023 p 29  
A87-45024 \* p 29  
A87-45044 p 70  
A87-45046 p 1  
A87-45047 p 1  
A87-45048 p 23  
A87-45100 p 1  
A87-45743 p 21  
A87-45816 p 30  
A87-45817 p 21  
A87-46139 p 21  
A87-46306 p 17  
A87-46310 p 17  
A87-46311 p 30  
A87-46403 p 30  
A87-46538 p 51  
A87-46539 p 30  
A87-46540 p 56  
A87-46542 \* p 30  
A87-46543 \* p 2  
A87-46545 p 51

A87-46688 # p 21  
A87-46690 # p 30  
A87-46692 # p 22  
A87-46744 p 2  
A87-46745 p 56  
A87-47046 p 56  
A87-47173 p 70  
A87-47174 p 70  
A87-47175 p 70  
A87-47257 \* p 70  
A87-47291 p 31  
A87-47292 \* p 31  
A87-47293 \* p 31  
A87-47294 p 31  
A87-47295 \* p 31  
A87-47296 p 31  
A87-47297 \* p 32  
A87-47298 \* # p 32  
A87-47299 \* p 32  
A87-47300 \* p 32  
A87-47506 p 56  
A87-47576 p 51  
A87-47577 p 51  
A87-47578 p 51  
A87-47579 # p 51  
A87-47580 p 51  
A87-47582 p 2  
A87-47583 p 52  
A87-47584 p 52  
A87-48176 p 32  
A87-48177 p 32  
A87-48178 p 33  
A87-48180 p 33  
A87-48181 p 33  
A87-48184 p 33  
A87-48185 p 23  
A87-48186 p 23  
A87-48187 p 23  
A87-48188 p 23  
A87-48189 p 70  
A87-48190 p 2  
A87-48193 p 56  
A87-48358 p 23  
A87-48359 p 56  
A87-48360 \* p 2  
A87-48361 p 56  
A87-48362 p 33  
A87-48363 p 33  
A87-48365 p 57  
A87-48652 p 70  
A87-48654 p 71  
A87-48655 p 57  
A87-48656 p 57  
A87-48658 p 57  
A87-48659 p 71

A87-48660 p 71  
A87-48661 p 57  
A87-48662 p 57  
A87-48663 p 57  
A87-48664 p 58  
A87-48665 p 58  
A87-48666 p 23  
A87-48667 \* p 23  
A87-48668 p 2  
A87-48669 p 58  
A87-48670 p 52  
A87-48671 p 17  
A87-48673 \* p 2  
A87-48674 \* p 71  
A87-48675 p 71  
A87-48676 p 71  
A87-48801 p 72  
A87-48802 # p 17  
A87-48803 # p 24  
A87-48804 # p 24  
A87-48805 # p 58  
A87-48807 # p 58  
A87-48808 # p 58  
A87-48809 # p 3  
A87-48810 # p 80  
A87-48811 # p 3  
A87-48812 # p 59  
A87-48813 # p 3  
A87-48815 # p 3  
A87-48816 # p 24  
A87-48817 # p 3  
A87-48818 # p 59  
A87-48819 # p 4  
A87-48820 # p 4  
A87-48821 # p 4  
A87-48822 # p 4  
A87-48823 # p 52  
A87-48825 # p 59  
A87-48826 # p 59  
A87-48827 # p 24  
A87-48828 # p 4  
A87-48829 # p 33  
A87-48830 # p 5  
A87-48831 # p 5  
A87-48832 # p 24  
A87-48834 # p 5  
A87-48835 # p 72  
A87-48836 # p 72  
A87-48837 # p 34  
A87-48838 # p 17  
A87-48840 # p 5  
A87-48841 # p 52  
A87-48842 # p 34  
A87-48843 # p 34  
A87-48844 # p 72  
A87-48845 # p 5  
A87-48846 # p 5  
A87-48847 # p 59  
A87-48848 # p 52  
A87-48849 # p 34  
A87-48850 # p 6  
A87-48851 # p 34  
A87-48852 # p 72  
A87-48853 # p 24  
A87-48854 # p 25  
A87-48855 # p 6  
A87-48856 # p 52  
A87-48857 # p 59  
A87-48858 # p 17  
A87-48859 # p 6  
A87-48860 # p 25  
A87-48861 # p 25  
A87-48862 # p 25  
A87-48863 # p 6  
A87-48864 # p 6  
A87-48865 # p 72  
A87-48866 # p 60  
A87-48867 # p 6  
A87-48868 # p 18  
A87-48869 # p 6  
A87-48870 # p 60  
A87-48871 # p 52  
A87-48873 # p 73

A87-48874 # p 73  
A87-48875 # p 52  
A87-48876 # p 34  
A87-48878 # p 6  
A87-48879 # p 25  
A87-48880 # p 53  
A87-48881 # p 34  
A87-48882 # p 6  
A87-48883 # p 60  
A87-48884 # p 60  
A87-48885 # p 60  
A87-48886 # p 18  
A87-48887 \* p 7  
A87-48888 # p 7  
A87-48889 # p 60  
A87-48890 # p 73  
A87-48891 # p 7  
A87-48892 # p 7  
A87-48893 # p 73  
A87-48894 # p 7  
A87-48895 # p 18  
A87-48896 # p 61  
A87-48897 # p 8  
A87-48898 # p 18  
A87-48899 # p 8  
A87-48900 # p 8  
A87-48901 # p 8  
A87-48903 # p 18  
A87-48904 # p 61  
A87-48905 # p 61  
A87-48906 # p 61  
A87-48907 # p 18  
A87-50226 p 73  
A87-50227 p 18  
A87-50231 p 8  
A87-50277 p 34  
A87-50292 p 35  
A87-51143 p 80  
A87-51144 p 25  
A87-51145 p 25  
A87-51146 p 25  
A87-51147 p 35  
A87-51174 p 61  
A87-51175 p 61  
A87-51179 p 62  
A87-51220 p 80  
A87-51324 p 80  
A87-51487 \* p 35  
A87-51532 p 35  
A87-51552 p 35  
A87-51553 p 35  
A87-51559 \* p 35  
A87-51560 \* p 36  
A87-51579 \* p 36  
A87-51580 \* p 36  
A87-51585 p 36  
A87-51587 p 36  
A87-51593 \* p 36  
A87-51594 p 36  
A87-51603 \* p 37  
A87-51725 \* p 26  
A87-51875 p 26  
A87-51943 p 37  
A87-51944 p 37  
A87-51945 p 37  
A87-51946 \* p 37  
A87-51947 p 37  
A87-51948 p 37  
A87-51950 p 38  
A87-51963 p 38  
A87-51964 \* # p 22  
A87-52241 p 19  
A87-52242 p 19  
A87-52501 p 38  
A87-52502 p 38  
A87-52503 p 38  
A87-52506 p 38  
A87-52507 p 22  
A87-52508 p 38  
A87-52509 p 38  
A87-52510 p 39  
A87-52511 p 39  
A87-52512 p 39

A87-52513 \* p 39  
A87-52514 \* p 39  
A87-52515 p 39  
A87-52516 p 39  
A87-52766 p 22  
A87-52795 # p 62  
A87-53017 \* p 8  
A87-53018 \* p 62  
A87-53019 p 8  
A87-53020 p 40  
A87-53023 p 9  
A87-53024 \* p 9  
A87-53084 p 80  
A87-53093 p 9  
A87-53101 p 73  
A87-53103 p 62  
A87-53108 p 74  
A87-53109 p 9  
A87-53110 p 62  
A87-53111 p 9  
A87-53112 p 62  
A87-53113 p 40  
A87-53114 p 40  
A87-53115 \* p 40  
A87-53116 p 74  
A87-53117 p 74  
A87-53118 \* p 74  
A87-53119 p 40  
A87-53120 p 9  
A87-53122 p 10  
A87-53123 \* p 10  
A87-53124 p 10  
A87-53125 p 10  
A87-53126 p 10  
A87-53127 p 40  
A87-53130 \* p 10  
A87-53131 \* p 63  
A87-53136 p 11  
A87-53139 p 63  
A87-53140 p 63  
A87-53142 p 63  
A87-53143 \* p 63  
A87-53144 \* p 40  
A87-53145 \* p 74  
A87-53146 \* p 22  
A87-53148 \* p 63  
A87-53149 p 74  
A87-53150 p 26  
A87-53151 \* p 11  
A87-53153 p 11  
A87-53154 p 63  
A87-53155 \* p 11  
A87-53163 p 75  
A87-53168 p 75  
A87-53179 p 75  
A87-53180 \* p 75  
A87-53183 \* p 64  
A87-53187 p 19  
A87-53189 p 41  
A87-53191 p 41  
A87-53192 p 41  
A87-53194 p 41  
A87-53195 \* p 75  
A87-53196 \* p 41  
A87-53197 \* p 41  
A87-53198 \* p 41  
A87-53199 \* p 42  
A87-53201 p 11  
A87-53202 \* p 11  
A87-53204 p 53  
A87-53205 p 11  
A87-53206 \* p 11  
A87-53207 \* p 64  
A87-53209 p 64  
A87-53211 p 12  
A87-53212 p 42  
A87-53213 p 64  
A87-53214 \* p 12  
A87-53215 p 53  
A87-53216 \* p 75  
A87-53217 \* p 12  
A87-53218 \* p 12  
A87-53219 p 42

ACCESSION

A87-53223	p 76	N87-27855	# p 45
A87-53224	p 42	N87-27856	# p 45
A87-53225	p 76	N87-27859	# p 66
A87-53227 *	p 76	N87-27860	# p 66
A87-53228 *	p 76	N87-27861	# p 67
A87-53229	p 76	N87-27862	# p 15
A87-53230 *	p 64	N87-27863	# p 67
A87-53232 *	p 76	N87-27864	# p 67
A87-53233	p 64	N87-27865	# p 78
A87-53234	p 42	N87-28077	# p 45
A87-53235	p 80	N87-28109	# p 15
A87-53236 *	p 42	N87-28115	# p 19
A87-53237 *	p 43	N87-28117	# p 20
A87-53238	p 43	N87-28118	# p 78
A87-53239 *	p 43	N87-28119	# p 27
A87-53240	p 43	N87-28120	# p 27
A87-53241 *	p 43	N87-28121	# p 27
A87-53242	p 26	N87-28123	# p 54
A87-53243 *	p 26	N87-28124	# p 67
A87-53244	p 26	N87-28125	# p 45
A87-53245 *	p 12	N87-28127	# p 15
A87-53246 *	p 12	N87-28128	# p 15
A87-53247	p 12	N87-28129	# p 15
A87-53248	p 12	N87-28130	# p 20
A87-53249	p 13	N87-28132	# p 46
A87-53250 *	p 13	N87-28133	# p 46
A87-53251	p 76	N87-28134	# p 46
A87-53252	p 13	N87-28135	# p 20
A87-53253	p 65	N87-28136	# p 15
A87-53254	p 65	N87-28137	# p 20
A87-53257	p 26	N87-28138	# p 16
A87-53259	p 65	N87-28139	# p 54
A87-53260	p 65	N87-28140	# p 16
A87-53262	p 65	N87-28141	# p 20
A87-53263 *	p 43	N87-28142	# p 67
A87-53264	p 43	N87-28143	# p 67
A87-53265	p 43	N87-28144	# p 67
A87-53266	p 44	N87-28145	# p 20
A87-53268	p 77	N87-28146	# p 46
A87-53269	p 13	N87-28147	# p 20
A87-53271 *	p 53	N87-28148	# p 16
A87-53273 *	p 65	N87-28149	# p 16
A87-53274	p 66	N87-28150	# p 54
A87-53275	p 13	N87-28151	# p 16
A87-53276 *	p 13	N87-28152	# p 54
A87-53277 *	p 13	N87-28153	# p 46
A87-53278 *	p 14	N87-28154	# p 46
A87-53279	p 77	N87-28155	# p 46
A87-53280	p 77	N87-28156	# p 47
A87-53283	p 77	N87-28157	# p 47
A87-53286 *	p 44	N87-28160	# p 16
A87-53287 *	p 44	N87-28165	# p 67
A87-53288 *	p 44	N87-28190	# p 16
A87-53289	p 66	N87-28195 *	# p 17
A87-53733	p 26	N87-28196	# p 54
A87-53741	p 14	N87-28197 *	# p 68
A87-53742	p 80	N87-28200 *	# p 27
A87-53925 #	p 44	N87-28208 *	# p 27
A87-53954	p 27	N87-28221	# p 79
A87-53987	p 81	N87-28239	# p 47
A87-53996	p 14	N87-28242	# p 47
A87-53997	p 14	N87-28374	# p 68
A87-53998 *	p 14	N87-28471 *	# p 47
A87-53999 *	p 66	N87-28809	# p 79
A87-54089	p 14	N87-28951	# p 79
A87-54107 *	p 44	N87-28954	# p 47
A87-54152	p 53	N87-28956	# p 79
A87-54153 *	p 53	N87-28957 *	# p 79
A87-54154 #	p 53	N87-29033	# p 47
A87-54155 *	p 53	N87-29067 *	# p 48
A87-54157 *	p 54	N87-29573	# p 48
A87-54301	p 44	N87-29574	# p 28
A87-54325	p 22	N87-29575	# p 68
		N87-29722	# p 68
		N87-29900 *	# p 81
N87-23136 #	p 14	N87-29904	# p 79
N87-25382 #	p 77	N87-29905	# p 68
N87-25560 #	p 77	N87-29906	# p 54
N87-25610 #	p 44	N87-29907	# p 48
N87-25634 #	p 19	N87-29909	# p 79
N87-25652 #	p 22	N87-30009	# p 48
N87-26264 *	p 77	N87-30010	# p 48
N87-26405 #	p 45	N87-30011	# p 48
N87-26463 #	p 19	N87-30012	# p 48
N87-26464 #	p 19	N87-30013	# p 49
N87-26466 #	p 27	N87-30014	# p 49
N87-26467 #	p 27	N87-30015	# p 49
N87-26569 #	p 66	N87-30016	# p 49
N87-26697 *	p 66	N87-30017	# p 49
N87-27310 #	p 78	N87-30018 *	# p 49
N87-27311 #	p 78	N87-30019	# p 50
N87-27312 #	p 15	N87-30020	# p 50
N87-27314 #	p 78	N87-30021 *	# p 50
N87-27316 *	p 78		
N87-27352 #	p 66		
N87-27696 #	p 45		
N87-27854 #	p 78		

# AVAILABILITY OF CITED PUBLICATIONS

## IAA ENTRIES (A87-10000 Series)

Publications announced in *IAA* are available from the AIAA Technical Information Service as follows: Paper copies of accessions are available at \$10.00 per document (up to 50 pages), additional pages \$0.25 each. Microfiche<sup>(1)</sup> of documents announced in *IAA* are available at the rate of \$4.00 per microfiche on demand. Standing order microfiche are available at the rate of \$1.45 per microfiche for *IAA* source documents and \$1.75 per microfiche for AIAA meeting papers.

Minimum air-mail postage to foreign countries is \$2.50. All foreign orders are shipped on payment of pro-forma invoices.

All inquiries and requests should be addressed to: Technical Information Service, American Institute of Aeronautics and Astronautics, 555 West 57th Street, New York, NY 10019. Please refer to the accession number when requesting publications.

## STAR ENTRIES (N87-10000 Series)

One or more sources from which a document announced in *STAR* is available to the public is ordinarily given on the last line of the citation. The most commonly indicated sources and their acronyms or abbreviations are listed below. If the publication is available from a source other than those listed, the publisher and his address will be displayed on the availability line or in combination with the corporate source line.

Avail: NTIS. Sold by the National Technical Information Service. Prices for hard copy (HC) and microfiche (MF) are indicated by a price code preceded by the letters HC or MF in the *STAR* citation. Current values for the price codes are given in the tables on NTIS PRICE SCHEDULES.

Documents on microfiche are designated by a pound sign (#) following the accession number. The pound sign is used without regard to the source or quality of the microfiche.

Initially distributed microfiche under the NTIS SRIM (Selected Research in Microfiche) is available at greatly reduced unit prices. For this service and for information concerning subscription to NASA printed reports, consult the NTIS Subscription Section, Springfield, Va. 22161.

NOTE ON ORDERING DOCUMENTS: When ordering NASA publications (those followed by the \* symbol), use the N accession number. NASA patent applications (only the specifications are offered) should be ordered by the US-Patent-Appl-SN number. Non-NASA publications (no asterisk) should be ordered by the AD, PB, or other *report* number shown on the last line of the citation, not by the N accession number. It is also advisable to cite the title and other bibliographic identification.

Avail: SOD (or GPO). Sold by the Superintendent of Documents, U.S. Government Printing Office, in hard copy. The current price and order number are given following the availability line. (NTIS will fill microfiche requests, as indicated above, for those documents identified by a # symbol.)

(1) A microfiche is a transparent sheet of film, 105 by 148 mm in size containing as many as 60 to 98 pages of information reduced to micro images (not to exceed 26:1 reduction).



- Avail: BLL (formerly NLL): British Library Lending Division, Boston Spa, Wetherby, Yorkshire, England. Photocopies available from this organization at the price shown. (If none is given, inquiry should be addressed to the BLL.)
- Avail: DOE Depository Libraries. Organizations in U.S. cities and abroad that maintain collections of Department of Energy reports, usually in microfiche form, are listed in *Energy Research Abstracts*. Services available from the DOE and its depositories are described in a booklet, *DOE Technical Information Center - Its Functions and Services* (TID-4660), which may be obtained without charge from the DOE Technical Information Center.
- Avail: ESDU. Pricing information on specific data, computer programs, and details on ESDU topic categories can be obtained from ESDU International Ltd. Requesters in North America should use the Virginia address while all other requesters should use the London address, both of which are on the page titled ADDRESSES OF ORGANIZATIONS.
- Avail: Fachinformationszentrum, Karlsruhe. Sold by the Fachinformationszentrum Energie, Physik, Mathematik GMBH, Eggenstein Leopoldshafen, Federal Republic of Germany, at the price shown in deutschmarks (DM).
- Avail: HMSO. Publications of Her Majesty's Stationery Office are sold in the U.S. by Pendragon House, Inc. (PHI), Redwood City, California. The U.S. price (including a service and mailing charge) is given, or a conversion table may be obtained from PHI.
- Avail: NASA Public Document Rooms. Documents so indicated may be examined at or purchased from the National Aeronautics and Space Administration, Public Documents Room (Room 126), 600 Independence Ave., S.W., Washington, D.C. 20546, or public document rooms located at each of the NASA research centers, the NASA Space Technology Laboratories, and the NASA Pasadena Office at the Jet Propulsion Laboratory.
- Avail: Univ. Microfilms. Documents so indicated are dissertations selected from *Dissertation Abstracts* and are sold by University Microfilms as xerographic copy (HC) and microfilm. All requests should cite the author and the Order Number as they appear in the citation.
- Avail: US Patent and Trademark Office. Sold by Commissioner of Patents and Trademarks, U.S. Patent and Trademark Office, at the standard price of \$1.50 each, postage free. (See discussion of NASA patents and patent applications below.)
- Avail: (US Sales Only). These foreign documents are available to users within the United States from the National Technical Information Service (NTIS). They are available to users outside the United States through the International Nuclear Information Service (INIS) representative in their country, or by applying directly to the issuing organization.
- Avail: USGS. Originals of many reports from the U.S. Geological Survey, which may contain color illustrations, or otherwise may not have the quality of illustrations preserved in the microfiche or facsimile reproduction, may be examined by the public at the libraries of the USGS field offices whose addresses are listed in this Introduction. The libraries may be queried concerning the availability of specific documents and the possible utilization of local copying services, such as color reproduction.
- Avail: Issuing Activity, or Corporate Author, or no indication of availability. Inquiries as to the availability of these documents should be addressed to the organization shown in the citation as the corporate author of the document.

## **PUBLIC COLLECTIONS OF NASA DOCUMENTS**

**DOMESTIC:** NASA and NASA-sponsored documents and a large number of aerospace publications are available to the public for reference purposes at the library maintained by the American Institute of Aeronautics and Astronautics, Technical Information Service, 555 West 57th Street, 12th Floor, New York, New York 10019.

**EUROPEAN:** An extensive collection of NASA and NASA-sponsored publications is maintained by the British Library Lending Division, Boston Spa, Wetherby, Yorkshire, England for public access. The British Library Lending Division also has available many of the non-NASA publications cited in *STAR*. European requesters may purchase facsimile copy or microfiche of NASA and NASA-sponsored documents, those identified by both the symbols # and \* from ESA – Information Retrieval Service European Space Agency, 8-10 rue Mario-Nikis, 75738 CEDEX 15, France.

### **FEDERAL DEPOSITORY LIBRARY PROGRAM**

In order to provide the general public with greater access to U.S. Government publications, Congress established the Federal Depository Library Program under the Government Printing Office (GPO), with 50 regional depositories responsible for permanent retention of material, inter-library loan, and reference services. At least one copy of nearly every NASA and NASA-sponsored publication, either in printed or microfiche format, is received and retained by the 50 regional depositories. A list of the regional GPO libraries, arranged alphabetically by state, appears on the inside back cover. These libraries are *not* sales outlets. A local library can contact a Regional Depository to help locate specific reports, or direct contact may be made by an individual.

## **STANDING ORDER SUBSCRIPTIONS**

NASA SP-7041 and its supplements are available from the National Technical Information Service (NTIS) on standing order subscription as PB 88-903800 at the price of \$15.50 domestic and \$31.00 foreign. Standing order subscriptions do not terminate at the end of a year, as do regular subscriptions, but continue indefinitely unless specifically terminated by the subscriber.

## ADDRESSES OF ORGANIZATIONS

American Institute of Aeronautics and  
Astronautics  
Technical Information Service  
555 West 57th Street, 12th Floor  
New York, New York 10019

British Library Lending Division,  
Boston Spa, Wetherby, Yorkshire,  
England

Commissioner of Patents and  
Trademarks  
U.S. Patent and Trademark Office  
Washington, D.C. 20231

Department of Energy  
Technical Information Center  
P.O. Box 62  
Oak Ridge, Tennessee 37830

ESA-Information Retrieval Service  
ESRIN  
Via Galileo Galilei  
00044 Frascati (Rome) Italy

ESDU International, Ltd.  
1495 Chain Bridge Road  
McLean, Virginia 22101

ESDU International, Ltd.  
251-259 Regent Street  
London, W1R 7AD, England

Fachinformationszentrum Energie, Physik,  
Mathematik GMBH  
7514 Eggenstein Leopoldshafen  
Federal Republic of Germany

Her Majesty's Stationery Office  
P.O. Box 569, S.E. 1  
London, England

NASA Scientific and Technical Information  
Facility  
P.O. Box 8757  
B.W.I. Airport, Maryland 21240

National Aeronautics and Space  
Administration  
Scientific and Technical Information  
Division (NTT-1)  
Washington, D.C. 20546

National Technical Information Service  
5285 Port Royal Road  
Springfield, Virginia 22161

Pendragon House, Inc.  
899 Broadway Avenue  
Redwood City, California 94063

Superintendent of Documents  
U.S. Government Printing Office  
Washington, D.C. 20402

University Microfilms  
A Xerox Company  
300 North Zeeb Road  
Ann Arbor, Michigan 48106

University Microfilms, Ltd.  
Tylers Green  
London, England

U.S. Geological Survey Library  
National Center - MS 950  
12201 Sunrise Valley Drive  
Reston, Virginia 22092

U.S. Geological Survey Library  
2255 North Gemini Drive  
Flagstaff, Arizona 86001

U.S. Geological Survey  
345 Middlefield Road  
Menlo Park, California 94025

U.S. Geological Survey Library  
Box 25046  
Denver Federal Center, MS914  
Denver, Colorado 80225

1. Report No. NASA SP-7041 (56)	2. Government Accession No.	3. Recipient's Catalog No.	
4. Title and Subtitle EARTH RESOURCES A Continuing Bibliography (Issue 56)		5. Report Date February, 1988	
		6. Performing Organization Code	
7. Author(s)		8. Performing Organization Report No.	
		10. Work Unit No.	
9. Performing Organization Name and Address National Aeronautics and Space Administration Washington, DC 20546		11. Contract or Grant No.	
		13. Type of Report and Period Covered	
12. Sponsoring Agency Name and Address		14. Sponsoring Agency Code	
15. Supplementary Notes			
16. Abstract <p>This bibliography lists 547 reports, articles and other documents introduced into the NASA scientific and technical information system between October 1 and December 31, 1987. Emphasis is placed on the use of remote sensing and geophysical instrumentation in spacecraft and aircraft to survey and inventory natural resources and urban areas. Subject matter is grouped according to agriculture and forestry, environmental changes and cultural resources, geodesy and cartography, geology and mineral resources, hydrology and water management, data processing and distribution systems, instrumentation and sensors, and economic analysis.</p>			
17. Key Words (Suggested by Authors(s)) Bibliographies Earth Resources Remote Sensors		18. Distribution Statement Unclassified - Unlimited	
19. Security Classif. (of this report) Unclassified	20. Security Classif. (of this page) Unclassified	21. No. of Pages 152	22. Price * A07/HC

\*For sale by the National Technical Information Service, Springfield, Virginia 22161

NASA-Langley, 1988

# NTIS PRICE SCHEDULES

(Effective January 1, 1988)

## Schedule A STANDARD PRICE DOCUMENTS AND MICROFICHE

PRICE CODE	PAGE RANGE	NORTH AMERICAN PRICE	FOREIGN PRICE
A01	Microfiche	\$ 6.95	\$13.90
A02	001-010	9.95	19.90
A03	011-050	12.95	25.90
A04-A05	051-100	14.95	29.90
A06-A09	101-200	19.95	39.90
A10-A13	201-300	25.95	51.90
A14-A17	301-400	32.95	65.90
A18-A21	401-500	38.95	77.90
A22-A25	501-600	44.95	89.90
A99	601-up	*	*
NO1		49.50	89.90
NO2		48.00	80.00

## Schedule E EXCEPTION PRICE DOCUMENTS AND MICROFICHE

PRICE CODE	NORTH AMERICAN PRICE	FOREIGN PRICE
E01	\$ 8.50	17.00
E02	11.00	22.00
E03	12.00	24.00
E04	14.50	29.00
E05	16.50	33.00
E06	19.00	38.00
E07	21.50	43.00
E08	24.00	48.00
E09	26.50	53.00
E10	29.00	58.00
E11	31.50	63.00
E12	34.00	68.00
E13	36.50	73.00
E14	39.50	79.00
E15	43.00	86.00
E16	47.00	94.00
E17	51.00	102.00
E18	55.00	110.00
E19	61.00	122.00
E20	71.00	142.00
E99	*	*

\*Contact NTIS for price quote.

### IMPORTANT NOTICE

NTIS Shipping and Handling Charges

U.S., Canada, Mexico — ADD \$3.00 per TOTAL ORDER

All Other Countries — ADD \$4.00 per TOTAL ORDER

Exceptions — Does NOT apply to:

ORDERS REQUESTING NTIS RUSH HANDLING  
ORDERS FOR SUBSCRIPTION OR STANDING ORDER PRODUCTS ONLY

NOTE: Each additional delivery address on an order  
requires a separate shipping and handling charge.